Stony Brook University

I. Topochemical Polymerization of Novel Diacetylenes

II. Synthesis and Characterizations of Soluble Polydiacetylenes

A Dissertation Presented

by

Zhong Li

to

The Graduate School

in Partial Fulfillment of the

Requirements

for the Degree of

Doctor of Philosophy

in

Chemistry

Stony Brook University

August 2008

Stony Brook University

The Graduate School

Zhong Li

We, the dissertation committee for the above candidate for the

Doctor of Philosophy degree, hereby recommend

acceptance of this dissertation.

Frank W. Fowler – Dissertation Advisor
Professor, Chemistry

Joseph W. Lauher – Dissertation Advisor
Professor, Chemistry

Dale D. Drueckhammer – Chairperson of Defense
Professor, Chemistry

Michelle M. Millar – Third Member
Professor, Chemistry

Peter W. Stephens – Outside Member
Professor, Physics & Astronomy
Stony Brook University

This dissertation is accepted by the Graduate School

Lawrence Martin

Dean of the Graduate School

Abstract of the Dissertation

I. Topochemical Polymerization of Novel Diacetylenes

II. Synthesis and Characterizations of Soluble Polydiacetylenes

by

Zhong Li

Doctor of Philosophy

in

Chemistry

Stony Brook University

2008

This dissertation includes two major research projects as described in the title.

The goal of the first project was to achieve the long-standing goal of a aryldiacetylene polymerization through a Single-Crystal-to-Single-Crystal transition. By exploring various unsymmetrical aryldiacetylenes, the first example of a poly(aryldiacetylene) single crystal has been successfully obtained for terminal phenyl diacetylene monomers in a supramolecular host-guest salt. The structure of the corresponding polymer has been confirmed by single crystal X-ray diffraction along with other characterization methods. The investigation regarding the polymerization pathway, particularly the aspects of structural changes associated with the reaction transition, reveals an unexpected mechanism. It is found that the entire rigid phenyl rings pivot a dramatic angle along with the large movement involving the diacetylene moieties as the polymerization proceeds. This work also expands the scope of the host-guest strategy to organic salt systems that will allow the topochemical polymerizations of a greater variety of diacetylene monomers.

The second project focused more on the polydiacetylene materials made by the host-guest strategy. Poly(deca-4,6-diynedioic acid), a polydiacetylene soluble in both dimethyl sulfoxide and water, was successfully prepared and characterized. The solubility of this conjugated polymer allows the accurate determination of the molecular weight and polydispersity of the polydiacetylenes made by the host-guest strategy for the first time. These results also demonstrate that polydiacetylene materials with better quality can be synthesized by the host-guest strategy in comparison to any other methods seen in literature. The solution study of this material shows reversible dramatic color changes in response to either concentration or pH variations.

This dissertation is dedicated to my parents:

Dewang Li and Guiqiong Zhong

Table of Contents

Chapter Three
Synthesis and Characterizations of Soluble PDAs

Chapter Four
Experiment Section

List of Figures

Figures **Page**

Chapter One

Chapter Two

Chapter Three

List of Schemes

Scheme **Page**

Chapter One

Chapter two

Chapter Three

List of Tables

Table **Page**

Chapter Two

Chapter Four

List of Abbreviations

Å	angstrom
BPOD	(8-butoxycarbonyl)methylurethanyl)-1-(5-pyrimidyl)octa-1,3-diyne
CD	cyclodextrin
CMC	critical micelle concentration
CP	conjugated polymer
CPE	conjugated polyelectrolyte
CSD	Cambridge Structural Database
d	repeat distance
DBU	1,8-diazabicyclo[5.4.0]undec-7-ene
dc	direct current
DCHD	1,6-di-(*N*-carbazolyl)-2,4-hexadiyne-1,6-diol
DFT	density functional theory
DIEA	N,N-diisopropylethylamine
DMAP	4-dimethylaminopyridine
DMF	dimethylformamide
DMPC	dimyristoylphosphatidylcholine
DMSO	dimethyl sulfoxide
DSC	differential scanning calorimerty
ECL	effective conjugation length
Et	ethyl
FT-IR	Fourier transform infrared
GPC	gel permeation chromatography
H_2OG	oxalamide of glycine
IUPAC	International Union of Pure and Applied Chemistry
LB	Langmuir-Blodgett
LC	liquid-crystalline or liquid crystal
$LiAlH_4$	lithium aluminum hydride
LS	Langmuir–Schaefer
M_n	weight average molar mass
MPA	multi-photon absorption
***n*-BCMU**	*n*-butoxycarbonylmethyl urethane
NBS	*N*-bromosuccinimide
***n*-Bu**	*normal*-butyl
NMR	nuclear magnetic resonance
PA	polyacetylene
PAn	polyaniline
PCDA	10,12-pentacosadiynoic acid
PDA	polydiacetylene
PDI	polydispersity index
Poly(PTS)	poly(hexa-2,4-diyne-1,6-diyl bis(*para*-toluene sulfonate))
PPE	poly(*para*-phenylene ethynylene)
PPP	poly(*para*-phenylene)
PPV	poly(*para*-phenylene vinylene)
PPy	polypyrrole
PTh	polythiophene
3PyO	N,N'-bis(3-pyridylmethyl)oxalamide
4PyO	N,N'-bis(4-pyridylmethyl)oxalamide
3PyU	N,N'-bis(3-pyridylmethyl)urea

4PyU	N,N'-bis(4-pyridylmethyl)urea
$R_{1,4}$	C_1-C_4 contact
SCSC	single-crystal-to-single-crystal
SEC	size exclusion chromatography
SEM	scanning electron microscope
TBAF	tetra-*n*-butylammonium fluoride
TBS	*tert*-butyldimethylsilyl
***t*-Bu**	*tert*-butyl
TCDU	bis-(phenyl)-urethane of 5,7-dodecadiyne-1,2-diol
TEA	triethylamine
TEM	transmission electron microscopy
TES	triethylsilyl
Tf	trifluoromethanesulfonic
TGA	thermogravimetric analysis
THF	tetrahydrofuran
TMEDA	tetramethylethylenediamine
TMS	trimethylsilyl
TPHDDA	1,1,6,6- tetraphenylhexadiynediamin
Ts	tosyl
UV-Vis	ultraviolet-visible
γ	declination angle
$\chi^{(3)}$	third-order susceptibilities

Acknowledgments

I'd like to express my sincere gratefulness to my advisors, Prof. Bill Fowler and Joe Lauher. They really taught me a lot by their own expertise as chemist and their great attitude as excellent educator. Other than education, they always offered me a great amount of freedom and encouraged me to test my own ideas during research; they always cared about my own research interest and future career development; they have also been very considerate, holding parties at Bill's sail boat or Joe's house. I definitely had a lot of great memories with them. Most importantly, these two gentlemen are also always making me feel something I have been taught and appreciating since a kid. There is an old Chinese Saying, "Even if someone is your teacher for just one day, you should regard him like your father for the rest of your life." And I truly believe in this traditional Chinese philosophy. Bill and Joe are exactly this type of teacher. They always make me feel they do care about their students very much. I think I'm really really luck from this point of view because I have two this kind of teacher during the most important 5 years in my life.

I also very much appreciate the great Ph.D. program at Stony Brook Chemistry Department. The entire personnel in this department were fantastic. Just because of all their contributions, one can only finish a Ph.D. study here.

I really need to thank my fellow students and friends in this department too. We were like a big family. We helped each other by sharing not only chemicals, but also experiences, techniques, equipments, frustration as well as excitation. It's been a great pleasured to have such a wonderful group and I am very pound to be alumni here.

Finally, I'd like to thank my family. Without their support, encouragement and love, nothing is possible for me. I would specially thank my wife Lu. We've been through every thing, happiness and unhappiness, together here at Stony Brook. Her company means so much for me, forever.

Chapter One

Introduction

1.1. Background

Since the accidental discovery of metal-like polyacetylenes in the early 1970's,[1] the study of conjugated polymers (CPs) has grown up into a highly disciplinary field featured by a combination of synthetic chemistry, physics of condensed matter and material sciences. On the molecular level, the substantial π-electron delocalization along the highly conjugated polymer backbone made CPs the simplest model of "molecular wire" and thus triggered the explosive research activities in scientific world. One the other hand, the fascinating chemical and physical properties originating from such a unique molecular structure attracted a lot of concerns from industry as well. There are already some established applications and a considerable volume of precommercialization work is in progress, utilizing the novel electroconductivity,[2] semiconducting properties,[3,4] non-linear optical behaviors,[5] electroluminescence,[6,7] exceptional mechanical properties,[8] among many others. These applications are to some degree limited by the low stability towards ambient conditions (H_2O and O_2) and the lack of processability often characterizing these materials. As a result, the preparation of well-defined conjugated polymers with improved processability and stability characteristics is often a much demanded need that requires considerable contributions from chemists.

Indeed, since the very beginning synthetic organic/polymer chemistry has taken the leading role due to the fact that all the other applied and theoretical research activities stem from the new CP materials prepared by chemists. Over the decades, considerable effort has been devoted towards the construction of various polyconjugated molecules and their derivatives with enhanced properties.

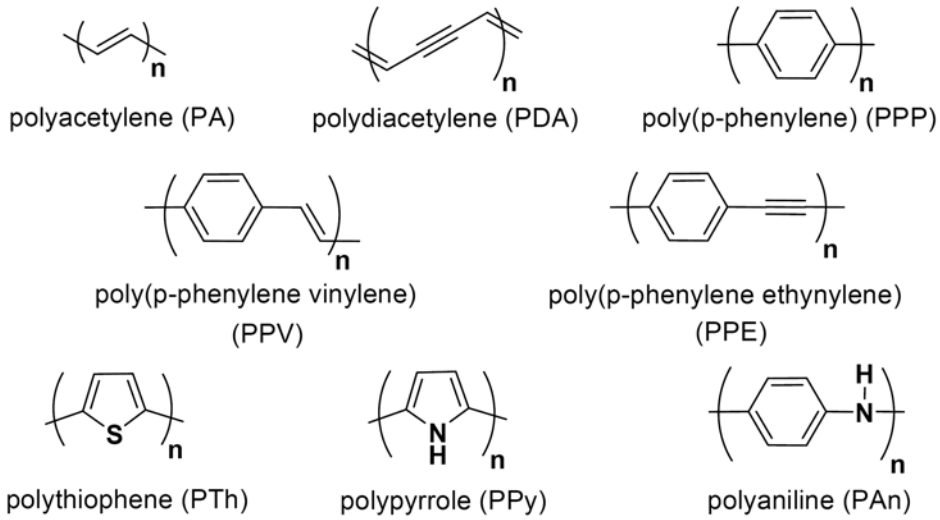

Figure 1.1. Representative structures of organic conjugated π-systems illustrating the most commonly studied building blocks

Figure 1.1 shows the major types of CPs receiving the most concern. Among them, $(CH)_x$, the polyacetylenes (PAs), which consist of alternate single and double carbon-carbon bonds, represent the simplest model of this class of materials and are also the very first polymer materials found to demonstrate surprisingly high electroconductivity (upon doping).[9] Their closest relative is the 1,4-polymer of diacetylene molecules (polydiacetylenes or PDAs), which is generally believed to consist of alternate double and triple bonds. As described in the dissertation title, the synthesis of PDAs has been the central theme of this dissertation. Other hydrocarbon polymers, such as poly(*para*-phenylene) (PPP), as well as the alternating copolymer of phenylene and ethylene,

namely poly(*para*-phenylene vinylene) (PPV), or phenylene and acetylene, namely poly(*para*-phenylene ethynylene) (PPE), are also widely studied as the analogues to the PAs. The heterocyclic cousins of the full carbon polymeric aromatics, such as polythiophene (PTh) and polypyrrole (PPy), plus polyaniline (PAn), are among the popular research objectives as well.

In this chapter, a brief review will be focused on the development of the synthesis, properties and applications of PDA materials only. The vast volume of research activities concerning other CPs mentioned above is beyond the scope of this dissertation. For the detailed discussions of those materials one can be referred to specialized reviews.[10-16]

1.2. Synthesis of PDAs

From the perspective of classical synthetic chemistry, the preparation of PDAs is very challenging due to the fact that the multi-functionalities (4 reactive sp-hybridized carbons) of diacetylene moiety could considerably complicate the polymerization process. Among all the possible reactions, only the 1,4-addition product is desired and literally defined as *polydiacetylenes*. The commonly used methods of making other CPs are generally based on various organometallic systems, such as the Ziegler-Natta catalyst ($Ti(O\textit{t}\text{-}Bu)_4/Et_3Al$)[17] or group VI metal catalyst ($MoCl_5$, WCl_6)[18,19] for PAs, the Lewis acid/oxidant systems[20] or the Grignard cross-coupling of dihalobenzenes in the presence of a nickel catalyst[21] for PPPs, Heck coupling polymerization[22] for PPVs, Sonogashira coupling polymerization[23] or alkyne metathesis[24] for PPEs, and the similar coupling

polymerization for the poly(heteroaromatics) (PThs, PPys, and PAns). However, so far there is no any "wet chemistry" method that seems to be applicable for the diacetylene 1,4-polymerization which demands the ability of discriminating the 1,4-addition from any other competitive side reactions. The most successful way of synthesizing PDAs is known to be the topochemical polymerization. Generally, topochemical polymerizations are reactions that take place in a condensed phase with the structure of the product determined by the prearrangement of the reactant monomers in space. Particularly in the case of diacetylene topochemical polymerization, the diacetylene molecules are preorganized in the molecular assemblies with the C_1 and C_4 carbons of neighboring monomers purposely placed with the closest distance among the contacts of all the sp-hybridized carbons to facilitate 1,4-polymerization and thereby rule out any undesired side reactions (**Scheme 1.1**).

Scheme 1.1

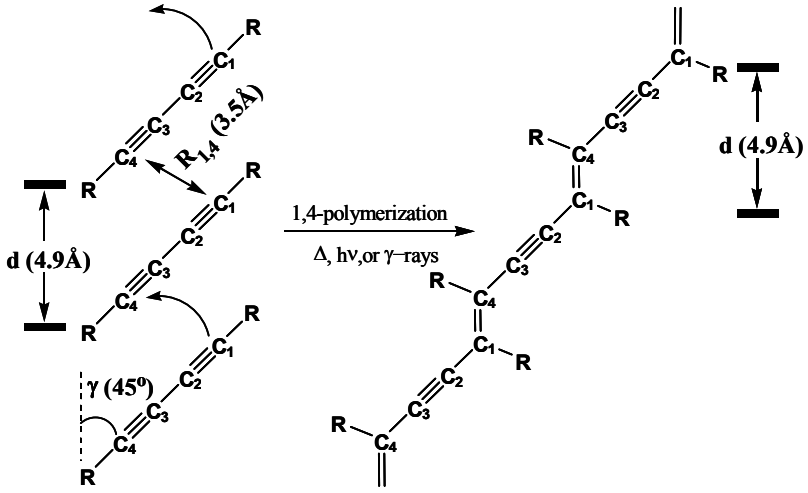

A lot of sophisticate supramolecular architectures satisfying this topochemical arrangement have been developed. Most of them, especially the work done in the early age of this field, focus on the diacetylene 1,4-polymerization in crystalline solid state. There are also many other reports describing the similar topochemical polymerization in

the liquid-crystalline (LC) state, in various super structures formed by diacetylenic lipids, or in many other unique supramolecular assemblies. Before the detailed examples are discussed, a short summary of diacetylene monomer synthesis is given in the following section.

1.2.1. Synthesis of Diacetylenes

Symmetrically disubstituted diacetylenes are usually obtained via Glaser coupling[25] of terminal acetylenes. The reaction is carried out in the presence of a cuprous salt with air (O_2) as oxidant. A modified condition using the copper(I)-TMEDA catalyst system developed by Hay[26,27] is much more popular nowadays since the solubility of the catalyst complex in a wider range of solvents makes the Hay coupling much more versatile.

The most satisfactory procedure for the synthesis of unsymmetrically disubstituted diacetylenes is the Cadiot-Chodkiewicz coupling[28] of a terminal acetylene with a haloacetylene (usually obtained by the halogenation of a different terminal acetylene) in the presence of Cu(I) salts. The Pd(0)-catalyzed coupling of a terminal acetylene with a iodoacetylene in the presence of a Cu(I) salt is also a successful route.[29]

Scheme 1.2

Hay Coupling

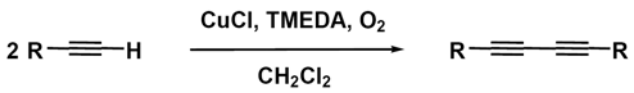

Cadiot-Chodkiewicz Coupling

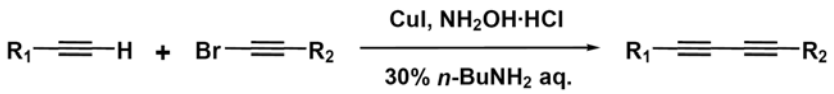

1.2.2. Solid State Topochemical Polymerization

The concept of topochemical polymerization is officially defined in a general sense by IUPAC[30] as reactions in the crystalline phase proceeding under minimal atomic and molecular displacement. The extended application of this concept for the diacetylene topochemical polymerization was first developed by Wegner[31] in 1969 in a case studying the polymerization of 2,4-hexadiyn-1,6-diol derivatives in solid state, although the same term was then borrowed by other "soft" supramolecular assemblies later. Soon after Wegner's pioneering work, Baughman[32] formulated the ideal topochemical structural requirements of the monomer orientation in the molecular crystal of diacetylenes (**Scheme 1.1**). These requirements is useful guidance when one needs to design a diacetylene supramolecular architecture for efficient 1,4-polymerization. Specifically, by spacing the monomeric atomic positions with a proper separation (**d**, ~ 4.9 Å) as found in the corresponding polymer, the molecular motion associated with the polymerization process is minimized if the distance of the reaction sites ($\mathbf{R_{1,4}}$) falls in the range of van der Waals contact (~3.5 Å) between C_1 and C_4. Therefore, the angle (γ) between the axis of the array and the diacetylene rod is desired to be ~ 45 º, as illustrated in **Scheme 1.1**. These parameters are very important for synthesizing high quality PDA materials, as well as for making the defect-free PDA crystals in the cases when the orientation of highly ordered polymer chains is desired. This is because a large molecular motion during the polymerization propagation could cause the accumulation of strain throughout the entire crystal that would eventually destroy the crystal lattice and consequently stop the further polymerization.

1.2.2.1. Homocrystal Strategy

Understanding the topochemical constraints mentioned above does not guarantee that one can easily obtain the exact line-up in any diacetylene crystals. The solid state reactivity is more easily achieved by monomers with large end groups than by those with small end groups. The role of the end groups seems to be critical since the interactions between the end groups determine the lattice structure in the monomer crystals. The flexibility of the end groups attached to the diacetylene unit must also be taken into consideration when designing a polymerizable diacetylene molecule. However, although a vast volume of work has been published concerning the solid state polymerization of various diacetylene monomers, only a few of them naturally crystallize in the manner consistent precisely with the above-mentioned geometric requirements and yield nearly

Scheme 1.3

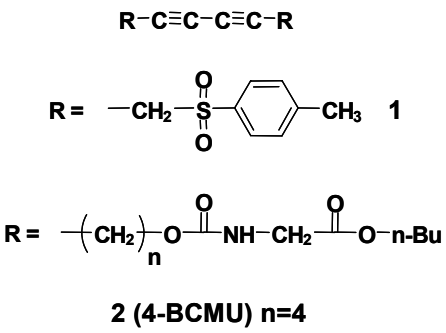

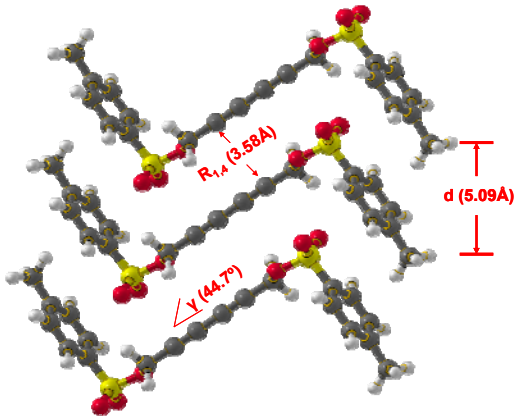

Figure 1.2 Crystal structure of **1**

perfect polymer single crystals upon induction by heating or irradiation. One of the most successful examples is hexa-2,4-diyne-1,6-diyl bis(*p*-toluene sulfonate) **1** (**Scheme 1.3**). Its crystal structure shows nearly perfect packing of the diacetylene units as shown in **Figure 1.2**. As a result, the topochemical polymerization of **1** can be easily driven upon

annealing treatment to provide the corresponding polymer poly(PTS) in the form of macroscopic crystals. The polymerization process is characterized by the occurrence of an induction period, during which time the polymerization rate increases by a factor of up to 200.[33] Bloor *et al.*[34] noted that there is a 10% contraction of the crystal along the chain axis after polymerization, indicating that some degree of lattice strain is generated by the mismatch of the polymer and monomer lattices as the polymerization proceeds. Baughman[35] then proposed that the autocatalytic effects observed during polymerization can be explained quantitatively by a strain-dependent rate of chain initiation and chain propagation. According to his theory, the polymer chain length is probably determined by the crystal strain field. However, due to its poor solubility, the exact molecular weight of poly(PTS) has been difficult to determine by standard methods.

Another extensively studied class of PDAs is *n*-butoxycarbonylmethyl urethane. They are generally abbreviated as *n*-BCMU and the number ***n*** refers to different number of methylene groups between the diacetylene unit and the head group. Among them, 4-BCMU (**2** in **Scheme 1.3**), which topochemically polymerizes much more efficiently by γ-irradiation than by heating,[36] is the most well-documented example among all reported diacetylenes. The excellent solubility of the resulting polymer poly(4-BCMU) in common solvents makes many characterization methods accessible to define its structure and properties. Spagnoli and coworkers[37] reported that by optimizing the γ-irradiation dose the size of poly(4-BCMU) can reach up to $M_n \approx 2.6 \times 10^6$ g/mol (corresponding to 5100 repeat units) with a very narrow molecular weight distribution (polydispersity index or PDI = 1.01 in the best case, and PDI < 1.5 in all of their samples) according to Size Exclusion Chromatography (SEC) measurement.

1.2.2.2. Cocrystal Strategy

Over the past decades, many diacetylene compounds have been synthesized and screened for the possibility of providing the corresponding PDAs in solid state. Unfortunately, most of them do not naturally self-assemble into the crystals compatible with the necessary topochemical parameters.

Using the comprehensive expertise in both synthetic chemistry and structural chemistry characterizing the Fowler/Lauher group,[38-46] we have developed a cocrystal strategy to purposely control the packing of diacetylene monomers in the solid state in order to fulfill the structural requirements for topochemical polymerization.[47-51] This unique approach utilizes the strength of both Supramol. Chem. and crystal engineering to create a host-guest cocrystal system for semi-predictable molecular packing. Particularly, the most important geometric parameter **d** is determined by the repeat distance of certain molecule that can form reliable H-bonding networks in a fashion with a controllable separation of ~ 4.9 Å as above-mentioned. In our own terminology, we call this certain molecule the "host". A library of the host candidates has been built up to collect the information of their H-bonding behaviors as well as the typical repeat distances. As shown in **Figure 1.3**, the ureas or oxalamides seem to be the best host molecules for the diacetylene polymerization due to their close-to-4.9 Å repeat distances determined by their characteristic H-bonding α-networks. The "guest" molecules are the diacetylene monomers, which associate tightly with the hosts through H-bonding inheriting the **d** value from their cocrystal host. Clearly, in the cocrystal systems host and guest molecules each have a role to play. The hosts control the proper intermolecular separations while

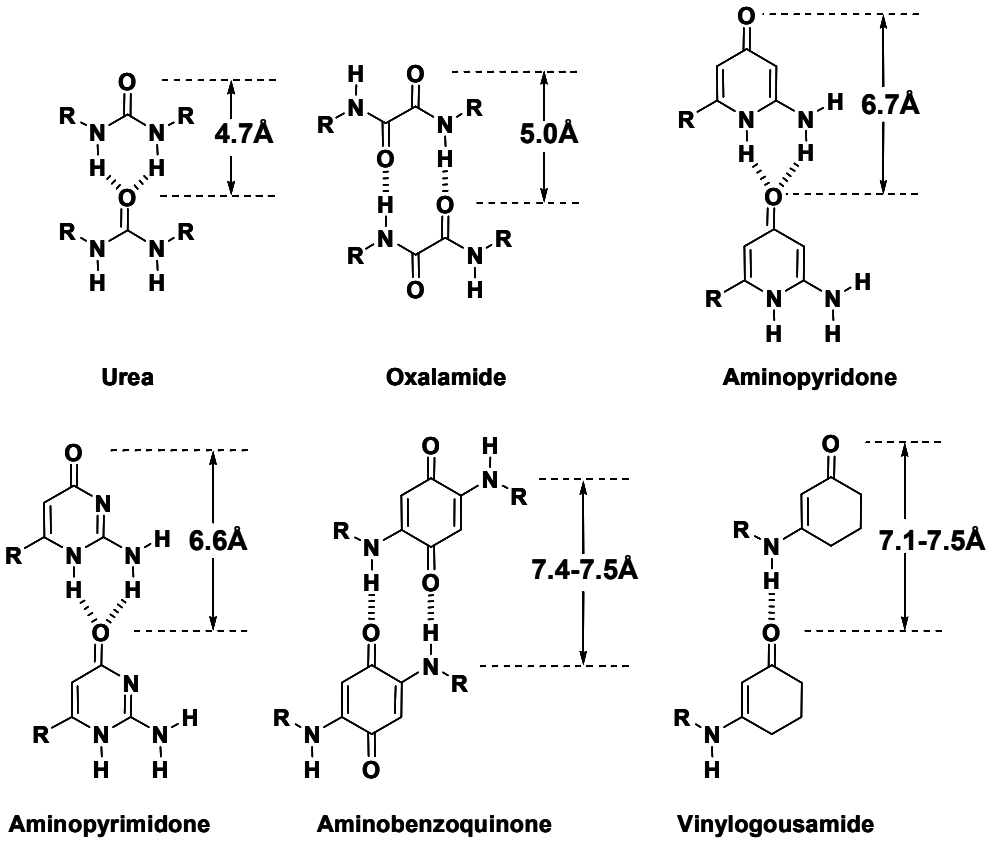

Figure 1.3 The library of host molecules that can form the two-dimensional H-bonding α-networks with controllable repeat distance.

the guests provide the reactive functionalities. The so-called host-guest strategy is essentially a method relying on supramolecular synthons. By this means, the amount of synthetic work needed for developing new polymerizable diacetylenic individuals can be largely reduced by adding more variations and opportunities to all the existing diacetylenes. Another advantage is that the host molecules can be easily removed after polymerization to afford neat PDAs since the connections between hosts and guests are not covalent bonds. More importantly, although this strategy does not guarantee that each host-guest pair could provide perfectly packed cocrystals to generate the corresponding polymer, it does include great intelligence in the sense of molecular design.

By using this creative strategy, we not only succeeded in polymerizing diacetylenes,[47,50-52] but also solved some long-standing problems, such as the polymerization of triacetylenes[53] and trienes[54] (**Figure 1.4**).

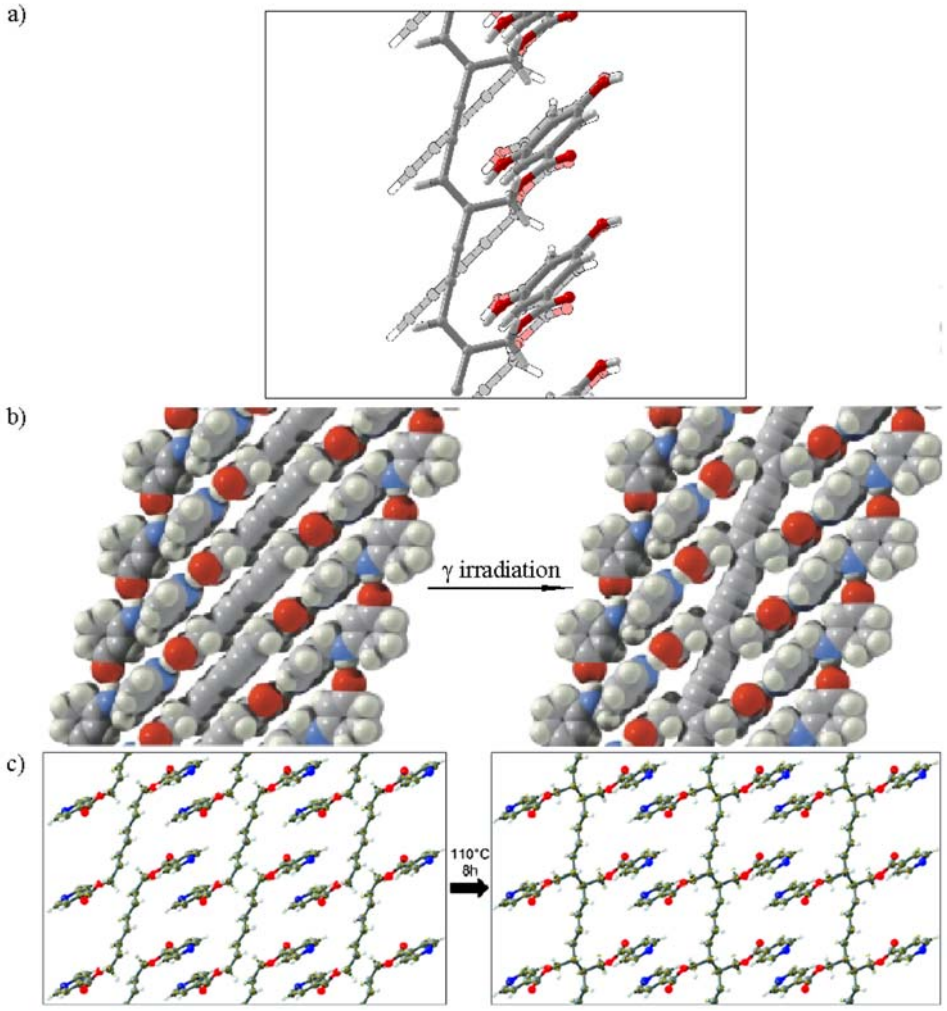

Figure 1.4 The success of host-guest cocrystal strategy. (a) 1,4-Polymerization of terminal diacetylenes. The pale background drawing is the monomers. The bold foreground drawing shows the polymer;[55] (b) Polymerization of triacetylenes induced by γ irradiation;[53] (c) Polymerization of trienes induced by heat.[54]

It is noteworthy that another important factor required by the diacetylene topochemical polymerization, the orientation angle ***γ***, is not efficiently controlled in our strategy. In most cases that we have investigated the control of **d** is fairly reliable by

using the most optimized hosts; unfortunately, the deviation of γ from the ideal 45 º often prevents an otherwise nicely packed cocrystal assembly from polymerizing. Nevertheless, this unique host-guest strategy still clearly demonstrates the power of the supramolecular synthetic chemistry and its great potential in molecular design.

1.2.3. Polymerization in the LC State

It is well known that in a LC state mesogenic molecules are self-organized into ordered arrays, although the degree of order is not as high as in condensed crystals. The diacetylene polymerization in mesophase was first noted by IBM scientists in 1979,[56] but the details about the structure and properties of the polymer material were not revealed. Similar polymerizations were also reported by other groups[57-59] later on, however, this method doesn't seem to be reliable enough to generate neat PDAs since most of the results were not supported by direct evidences that can clarify the polymer structure. On the other hand, there exists some negative evidence. Milbrun and coworkers emphasized that alternative route other than 1,4-polymerization may occur based on the fact that no nonlinear optical activities were observed in the resulting polymers.[60] Nonetheless, LC state still provides an alternate access to PDA materials. Izuoka and coworkers[61] utilized solid state ^{13}C NMR spectra to confirm the PDAs of monomer **3** topochemically polymerized in the nematic phase. While in most of the other work, characterizations such as thermo analysis, X-ray diffraction, FT-IR

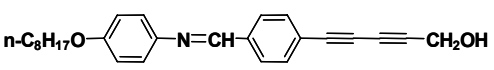

3

and UV-Vis spectroscopy were used to define the structure of the polymers.[52,62-65]

1.2.4. Polymerization in Lipid Assemblies

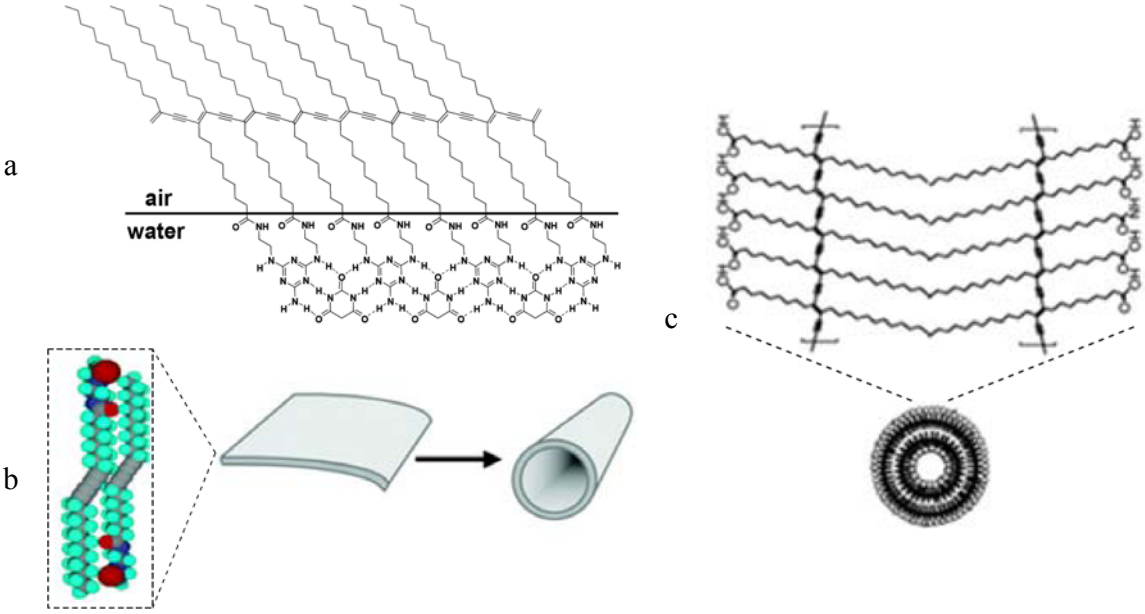

Figure 1.5 PDAs formed in thin films (a);[66] tubules (b);[67] and vesicles (c).[68]

The ability of the amphiphilic lipid molecules to self-assemble into sophisticated supramolecular structures is well known to be the origin of many important biological functions such as molecular recognition, transport, energy conversion, and signal transduction occurring at the cell membrane surface. Various well-organized architectures, such as thin films, vesicles and tubules, can be obtained by natural or synthetic lipids at proper conditions. And almost all of these formations have been found to provide an effective topochemical environment leading to PDAs when the diacetylene functionalities are incorporated into the lipid assemblies (**Figure 1.5**).

1.2.4.1. Langmuir, Langmuir-Blodgett (LB) and Langmuir–Schaefer (LS) films

The spreading of amphiphilic lipid molecules at the air-water interface followed by compressing produces well-organized Langmuir films. These ultrathin films can be transferred onto solid supports to make mono- and multi-layer LB or LS films. Thin films of amphiphilic diacetylene molecules organized by this technique have successfully in produced useful PDA materials. The Leblanc group have made the most contributions to the polydiacetylene Langmuir monolayers. They designed various lipid systems, such as 2-amino-4,6-bis-((10,12-pentacosadiyn amido)ethylamino)-1,3,5-triazine **4** which readily forms a complementary H-bonding self-assembly at the air-water interface with barbituric acid or cyanuric acid,[66] *N*'-di-10,12-pentacosadiynoic urea **5** that forms an abnormal monolayer with the polar moiety suspending in the air phase while one of the hydrophobic tails contacting with water,[69] the amphiphilic dendrimer containing 10,12-pentacosadiynoic acid (PCDA),[70] among many others. In all of these Langmuir films, diacetylenes are readily polymerized upon UV irradiation. Tachinana and coworkers[71] studied the polymerization behaviors of a series amphiphilic diacetylenes in the LB films. The diacetylenes they used have the same number of carbons but different diacetylene locations (**Scheme 1.4**). It is

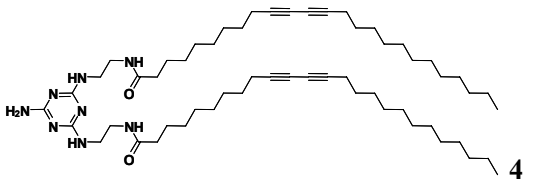

4

barbituric acid

cyanuric acid

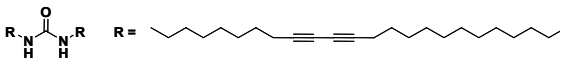

5

Scheme 1.4

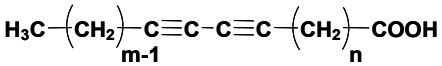

m+n = 20

found that the intermolecular distance **d** is ~ 5 Å for all the LB films. This value is the same as the typical one for solid state topochemical 1,4-polymerization. As for the tilt angle γ, it shows a tendency of approaching to the idea value of 45º desired in solid state when the spacer (**n**) between the diacetylene moiety and the carboxylic acid group increases. Unlike in the highly-ordered compact crystalline state, the diacetylene molecules in these films have enough mobility that even films with a small **n** (corresponding to γ = 17.6º for **n** = 4 and γ = 71.3º for **n** = 2) are polymerizable, although only short polymers or oligomers are believed to form.

1.2.4.2. Vesicles

Vesicles that can be made from either naturally-derived phospholipids or synthetic lipids are broadly defined as any structure composed of amphiphilic molecular bilayers that enclose a volume. Long ago people realized that amphiphilic monomers containing a polymerizable group somewhere along the molecular unit are able to provide vesicles with enhanced stability. A lot of work involving various reactive groups, such as acryloyl, methacryloyl, styryl and butadienyl, has been reported.[72]

The first bilayer vesicles formed from hydrated diacetylenic amphiphiles were reported by Ringsdorf.[73] Sonication of diacetylene monomer **6** produces a colorless, slightly turbid solution. Electron microscopy indicates the

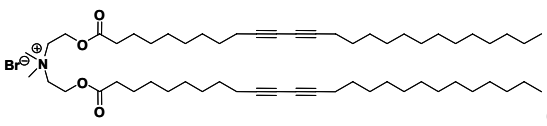

6

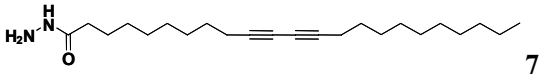

7

presence of multilamellar vesicles with diameters up to 400 nm. Polymerization of these vesicles by UV irradiation initially causes the formation of a blue product that changed to red at the end. Inspired by this work, a lot of other "membrane mimetic" systems containing diacetylene moieties have been developed.[72] Although double-chain lipids are perhaps the most common materials for vesicle formation, many singlechained amphiphiles are also capable of forming multibilayer vesicle structures.[68] For example, vesicles made of hydrazide **7** can be prepared upon hydration and sonication at ~ 65 ºC. The polymerization behavior in these vesicles depends strongly on the pH of the surrounding aqueous medium and the photopolymerization only occurs at low pH. In addition, these polymerized vesicles undergo an unprecedented reversible color change (blue/red) when the pH of the surrounding aqueous medium is cycled between acidic and basic conditions.[74]

1.2.4.3. Tubules

Another representative self-assembled morphology adopted by bilayer-forming lipid molecules is the tubular structure.[75] The variety of the tubules with well-defined diameters (larger than carbon nanotubes), lengths, and wall thicknesses makes them novel host substances in mesoscale host-guest chemistry or perfect templates for creating sophisticate inorganic and organic-inorganic hybrid tubular nanostructures.[76] In addition, the diacetylene lipid nanotubes themselves can be stabilized and directly used as useful functional materials after efficient polymerization enhancement due to the unique

photophysical properties of PDAs. As first reported by Yager and co-workers,[77-79] the synthetic lecithin **8**, 1,2-bis(10,12-tricosadiynoyl)-*sn*-glycero-3-phosphocholine, forms

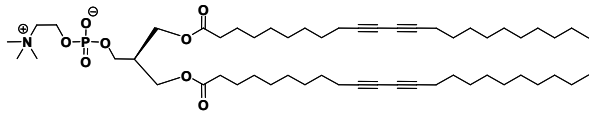

8

multilamellar tubules in ethanolic solutions that are typically tens of micrometer in length and about 0.6 μm in external diameter. These tubules can be polymerized by UV irradiation to give dark red polymer nanotubes, usually associated with the helical rippling on the surface caused by the strain and deformation in the tubule structure during polymerization. Structural modifications of **8** results in analogues which either form tubules closely resembling those obtained from **8** or yield various other related morphologies, such as helixes, ribbons, sheets, braided fibers, and planar platelets.[80-84] Other than these naturally-derived lipids, there are some much simpler synthetic amphiphilic diacetylenes, even achiral ones, that can also self-assemble into polymerizable tubular structures. The achiral

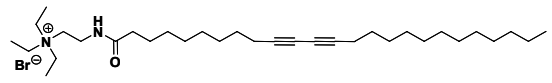

9

diacetylene amine salt **9**, which does not have the handness information usually required for such simple molecular structures to form nanotubes, can still form high quality monodisperse nanotubes through simple supramolecular synthesis.[67]

Mechanistically, these supramolecular assemblies form as the result of favorable H-bonding interactions, hydrophobic-hydrophobic interactions or sometimes both.[85] Additionally, in some special cases the strong π-π interactions can also serve as the

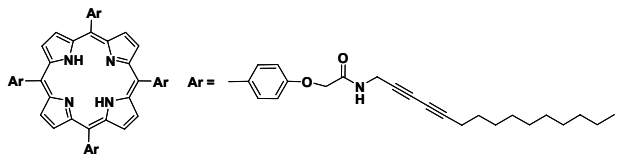

10

driving force leading to the formation of polymerizable one-dimensional structures. For example,

polydiacetylene nanowires up to several tens of micrometers in length can be produced by photopolymerization of the π-stacking column of diacetylene attached porphyrin **10**.[86]

1.2.5. Other Methods

In addition to the assemblies mentioned above that pre-organize the diacetylene moieties in a manner that allows the topochemical polymerization, there are some other impressive supramolecular architectures that have also been designed to achieve the same goal.

Lu *et al.*[87,88] developed a method that combines diacetylenic surfactants with silica precursors to synthesize PDA/silica nanocomposites. The general scheme of this method is as follows (depicted in **Figure 1.6**). The precursors, surfactants and hydrochloride acid

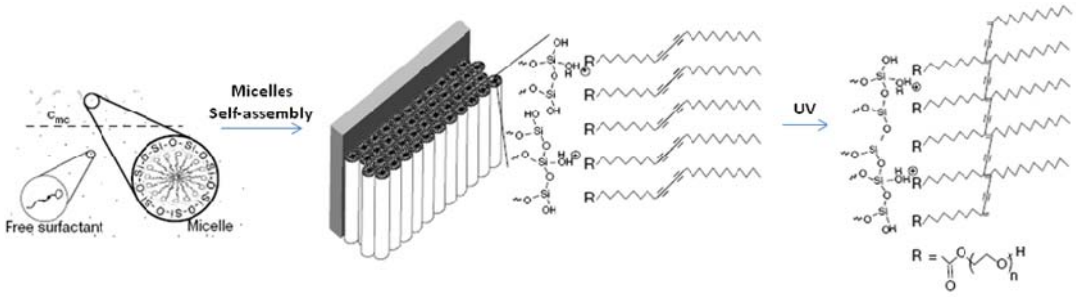

Figure 1.6 Synthesize PDA/silica nanocomposites

(HCl, for the purpose of catalytic hydrolysis to generate silica *in situ*) are mixed in a THF/water solvent to form a homogeneous solution with an initial surfactant concentration C_0 much less than the critical micelle concentration (CMC). The preferential evaporation of THF progressively concentrates the solution to the self-

assembly of diacetylene/silica surfactant micelles and allows their further organization into various ordered three-dimensional LC mesophases. It was confirmed that the diacetylene units in either hexagonal or lamellar mesostructure can successfully polymerize to generate PDA/silica nanocomposite, while the cubic mesophases is not polymerizable. This method was further modified by the same research group using silica-precursor-containing diacetylenic surfactants.[89,90] The modified system demonstrates more tunability on the mesostructures of the nanocomposites.

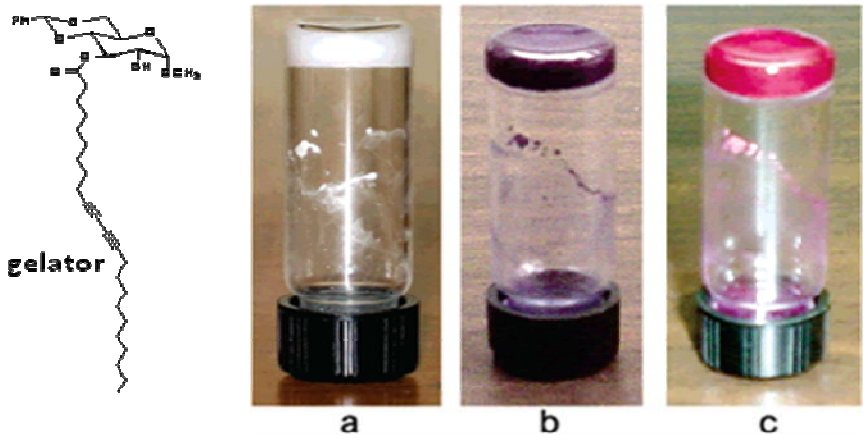

Figure 1.7 Diacetylenic organogels and the corresponding PDAs.[91] (a) The stable white gel; (b) a deep blue-purple PDA gel formed by UV treatment; and (c) the PDA gel blue→red transition after heating.

Recently, diacetylenic organogels have also drawn a lot of attention. The noncovalently organized fibrous networks formed after gellation of some lipids are found to be suitable for the diacetylene 1,4-polymerization upon UV irradiation. Thus the stable covalently linked PDA networks can be obtained.[91-98] One special example is shown in **Figure 1.7**, in which the gelator is a simple sugar modified by a diacetylene tail via an ester group. However, most of these diacetylenic gelators contain either urethane or amide functionalities that contribute to both the gel formation and topochemical

geometry control through their strong H-bonding characteristics. Masuda and coworkers determined the molecular weight of soluble PDAs made by this method and found that the products are mainly oligomers instead of real polymers (ranging from 13-mer to 64-mer).[92,93] This result indicates that although the supramolecular architecture in these organogels can provide local ordered organization of the diacetylene moieties, it is still far from ideal as achieved by diacetylenes in crystalline state.

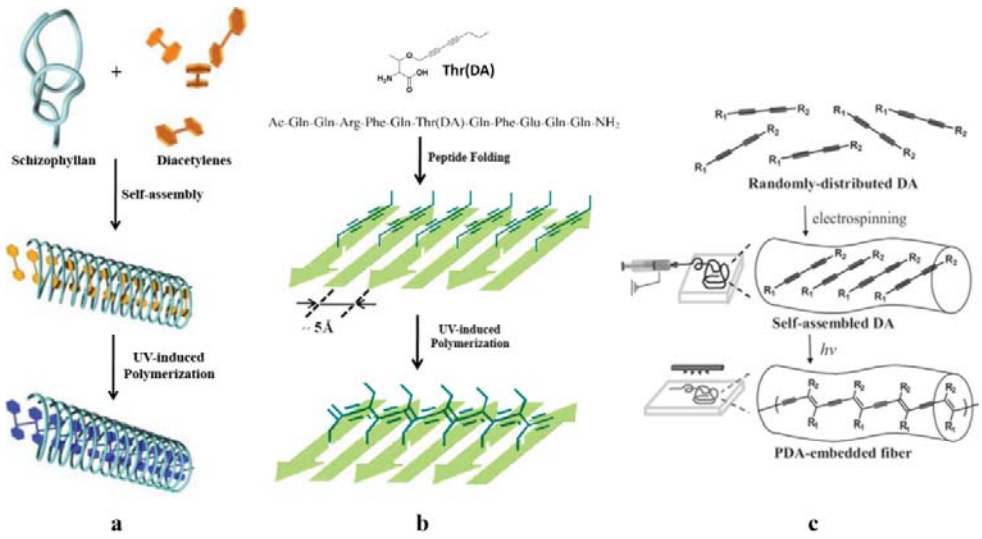

Figure 1.8 PDAs prepared in other supramolecular templates: (a) one-dimensional helical host;[99] (b) anti-parallel β-sheet;[100] (c) electron-spun microfibers.[101]

Moreover, diacetylenes have also been reported recently to undergo desired topochemical polymerization in other sophisticate supramolecular architectures, such as the one-dimensional helical host formed by polysaccharide Schizophyllan,[99] the anti-parallel β-sheet formed by peptide containing diacetylene modified amino acids[100] and the electron-spun microfibers of Poly(methyl methacrylate) (PMMA) embedded with diacetylene monomers (**Figure 1.8**).[101] All this work not only provides new methods of synthesizing PDAs, it also demonstrats the potential of producing specific PDA-base

materials in a highly efficient engineering manner for applications where the unique properties of PDAs can be utilized.

1.3. Properties and Applications of PDA Materials

The most prominent properties that are often claimed for PDA materials are the quick and large nonlinearity responses, the ultrafast photoconductivities, and the sensitive and precise chromatic behavior.

1.3.1. Nonlinear Optical Properties

Nonlinear optics is a major branch of modern optics. It has become more and more important since the introduction of laser technology in the 1960's due to the fact that laser beams possess the energy density necessary to produce nonlinear effects. The advantage of nonlinear optical materials to lasers and electrooptics became clear in the early days of lasers, since it enables expansion of their limited spectral regime. Particularly, nonlinear optical materials produce other frequencies due to the nonlinear dependence of their refraction indexes on the applied electric field. This results in either harmonic generation or frequency shifting. Today, there are a large number of nonlinear optical materials for specific wavelengths, with various damage thresholds, and with various optical characteristics. The unique nonlinear photon absorption characteristics of

each nonlinear optical material and its various applications are mutually connected. They have made a lot of useful technologies possible, including lithography, biological imaging, photodynamic therapy, optical data storage and others.

The influence of one-dimensional conjugation and electronic delocalization on the nonlinear optical properties of organic molecules, polyenes for instance,[102,103] was already well understood in the early 1970's. However, more extensive theoretical and application studies were largely restricted by the difficulties in growing good optical-quality samples of such molecular systems. Fortunately, the success in preparing large, near defect-free PDA single crystals through solid state topochemical polymerization showed the bright future along this line. The preliminary study regarding the nonlinear optics in the crystals of poly(bis-(phenyl)-urethane of 5,7-dodecadiyne-1,2-diol) or poly(TCDU), as well as in the crystals of poly(PTS) done by Sauteret *et al.*,[5] showed that the third-order susceptibilities ($\chi^{(3)}$, related to "third harmonic generation") of these materials can reach very high values comparable to those of inorganic semiconductors. Soon after, Lequime and Hermann[104] reported the large two-photon absorption coefficient observed in the crystals of poly(PTS). These two pioneering results thus stimulated the interest in using PDA materials as nonlinear optical materials.

Over the past few decades, various PDAs as well as a variety of bulk states of these materials have been evaluated for their nonlinear optical properties. The value of the refractive nonlinearity n_2 reported for single crystal poly(PTS) is still the largest nonresonant nonlinearity known for any material, although the poor processability prevents application of poly(PTS) in operating devices. Recently, Polyakov *et al.*[105] reported their improved femtosecond measurements of the dispersion in the nonlinear

refraction and multi-photon absorption (MPA) in poly(PTS) crystals, over the spectral range 1200-2200 nm. It was found that in addition to the major contribution of 2PA, 3- and 4PA mechanisms also contribute to the nonlinear absorption at most wavelengths. The authors also investigated the intensity dependence at each wavelength to identify the different contribution by each photo absorption mechanism.

In order to improve the processability of PDA materials for low cost applications in nonlinear optical devices, soluble PDAs are highly desired. The most extensively studied organosoluble PDAs are the class of poly(*n*-BCMU). For example, the remarkably large two-photon absorption coefficient β of poly(3-BCMU) has been measured in solution,[106] in gel,[107] in a wave guide,[108] and in a spin-coated film.[109] Interestingly, β shows a remarkable dependence on the excitation wavelength in all these samples. Therefore, it seems that the excellent nonlinear optical response is a fundamental property of the PDA backbone, regardless or at least less related to the physical state of this material.

1.3.2. Electroconductivity and Photoconductivity

The electroconductivity of PDA materials used to gain a great deal of attention in the early days as a result of their conjugated backbone and high oxidation stability. Similar to PAs, the conductivity of pristine PDAs falls in the level of insulators ($\sigma < 10^{-12}$ S/cm).[110] However, unlike PAs which can be easily transferred into semiconductors or even conductors upon doping,[9] it has been disappointing to find that PDAs cannot be doped very well because of the high degree of crystallinity in the polymers resulting from the

unique solid state topochemical polymerization.[110,111] The close packing of PDA polymer chains in the crystals prevents the dopant molecules efficiently diffusing into the polymer bulk and thus impedes the creation of sufficient concentration of free charge carriers (electrons and holes), as they can in the case of PAs. A careful study done by Ferrer-Angela *et al.*[112] regarding the electroconductivity of the crystals of poly(1,6-di-(*N*-carbazolyl)-2,4-hexadiyne-1,6-diol), or poly(DCHD), doped by SbF_5 clearly showed that the conductivity increase by four orders of magnitude (from the original value $\sigma \approx 5 \times 10^{-12}$ S/cm) occurred very rapidly over the course of a few minutes, and a further increase took place during the next several hours. This two-stage process indicates that the penetration of the dopant into the nearsurface layers occurs rapidly and that diffusion of the dopant into the bulk is hindered. A nonuniform distribution of the dopant in the bulk of the polymer was also observed in this work. Marikhin *et al.*[113] hypothesized that varying the size and morphology of the PDA crystals may provide a way of manipulating the doping efficiency and thereby the conductivity of PDA crystals. Experimentally, the authors did find the correlation between the particle size of the single crystals of poly(1,1,6,6- tetraphenylhexadiynediamin) (poly(TPHDDA)) and their dc conductivities in different doped states. In addition, a record value of the conductivity (3×10^{-2} S/cm) for PDA materials was also obtained from the most optimized morphology in this case.

Alternative methods have been applied in order to improve the dopant concentrations in PDAs as well. A Japanese group led by Kotaka circumvented the low permeability of various dopants in PDAs by focusing on soluble polydiacetylenes such as poly(3-BCMU) and poly(4-BCMU). The fairly loose packing of polymer chains in the solution-cast films[111,114-116] or sol-gels[117,118] of these two PDAs makes it possible to dope these

materials much more efficiently and thereby to increase the conductivity in comparison with the original value by about two orders of magnitude. Nakanishi *et al.*, however, described the growth of single crystals of monomers of poly(PTS) and several other diacetylenes from solutions already containing dopant (I_2). The subsequent solid state polymerization of such iodine-saturated monomer crystals gave these PDAs a conductivity as high as 10^{-5} S/cm. Seiferheld and Baessler[119] achieved a similar conductivity in the single crystals of poly(DCHD) by injecting dopant into the crystal lattice under an electric field from electrolytes containing Ce^{3+}/Ce^{4+} or I^{3-}/I^{-} redox pairs. An equal improvement in the conductivity of PDAs was also realized using the ion implantation technique. Sakamoto *et al.*[110] compared the enhanced conductivities of poly(PTS) and poly(DCHD) attained by ion implantation ($^{75}As^{+}$) and found that there is a 10^5 - 10^6 times of more increase in poly(DCHD) than poly(PTS). The doping of poly(DCHD) single crystals by iodine can also be promoted at very high temperatures (330 - 380 °C) as described by Ebisawa *et al.*[120] At such temperature the doping was even accompanied by alteration of the chemical structure of the side-chain substituents in the original polymer, but the conductivity increased to $\sigma \sim 10^{-3}$ S/cm as a result.

Although by using the techniques mentioned above significant increases in conductivity are obtained upon doping in comparison to the undoped state, PDA materials can only be brought up to wide-bandgap semiconductors with gaps about 2 eV,[121,122] and their electroconductivity values are still significantly below the level achieved for PAs.

Generally speaking, at normal conditions the concentrations of the charge carriers (even in doped materials) are negligible, as accounts for the poor electroconductivity of

PDAs. However, it's been know that carriers can be populated by exterior energy, for example photons of suitable energy, to obtain observable currents. Indeed, the photoconductivity of PDAs was noticed soon after the reliable synthesis via topochemical polymerization was discovered. Scherman and Wegner[123] first reported the photoconductive properties of poly(PTS) although their measurements were restricted to only a few wavelengths in the visible region. Later, Lochner *et al.*[124] measured the stationary photoconductivity of poly(PTS) single crystals. Their results show that the number of charge carrier pairs (electron-hole pairs) generated per absorbed photo is only 10^{-4} or less. The same group further studied the steady state photoconduction action spectra of poly(TCDU) single crystals, which was found comparable to that of poly(PTS).[125] Although these results suggested that crystalline PDAs were poor photoconductors, their experimental evidence clearly demonstrated that the mobility of charge carriers is higher in the direction parallel to the chain axis than in the perpendicular direction. Several other independent experiments also confirm the pronounced anisotropy of electric properties. The photoconductivities measured in the direction parallel to that of polymer chains are a few orders of magnitude lower than those measured perpendicular to the chains.[126,127] Estimations of the mobility in the chain direction range from 10^0 cm^2/Vs[128-130] to 10^5 cm^2/Vs.[131] However, no direct measurements of macroscopic carrier mobilities have been successfully performed.

Siddiqui[132] reported the photoconduction spectrum of poly(PTS) single crystals in the photo energy range 0.62 - 3.1 eV for the conduction along the polymer chain direction. For $h\nu < 2$ eV, photos are absorbed by the ionization of defects; for 2 eV $< h\nu < E_g$ (E_g = band gap energy of PTS), photon absorption mainly creates excitions which may

subsequently either recombine or dissociate into free electron-hole pairs; for $hv > E_g$, the process of direct creation of electron-hole pairs competes with that of excition.

The photoconductivity of non-crystalline PDA materials is also of great interest. As the first example in literature, Ohnuma and coworkers[133] evaluated the photoconductive properties in a chloroform-cast film of poly(3-BCMU). The photocurrent responds to illumination very slowly, with a time scale of 30 - 40 s. In the measurements at wavelength between 300 and 800 nm, the strong photocurrent was observed at $\lambda < 500$ nm, while the weak photocurrent was observed in between visible and near IR region. The spectral dependence of the photocurrent is similar to that of single crystal samples. Donovan *et al.*[134] observed a quasi 2-dimensional charge carrier motion in the plane of a PDA film (LB multilayer films of poly(10,12-penta-cosa-diynoic acid), poly(PCDA)) under the influence of an externally applied electric field. The measured charge (Q) is linear to the electric field. The variation of Q on light intensity (I) is dependent on the gap width. A lower limit of the carrier drift velocity is estimated to be 8×10^3 m/s, which is substantially higher than that found in poly(PTS) single crystals. The Tripathy group[135] synthesized and characterized poly((8-butoxycarbonyl)methylurethanyl)-1-(5-pyrimidyl)octa-1,3-diyne, or poly(BPOD). This unique PDA is featured by its organo-solubility and direct aromatic side group attachment. The steady state photocurrent density in solution-cast film of poly(BPOD) is determined to be 5×10^{-9} A/cm^2. The photoconductivity action spectrum shows a direct band to band transition above 2.4 eV and the dependence on both electric field and temperature.

Mechanistically, the processes that are crucial for the understanding of any photoelectric elements, such as photostimulated charge carrier generation and charge

carrier transport, are subject to dispute. The one-dimensional model of geminate recombination of bound electron-hole pairs by Onsager's theory[136] is generally accepted to interpret the photoconductivity of most PDA materials. Donovan and Spagnoli found that in both 100%[137] and partial[138] polymerized poly(4-BCMU) single crystals, the carriers travel distances substantially greater than the length of polymer chains, although the environment surroundings of each individual polymer chain are quite different in these two samples. The authors interpreted their result using the Onsager model as well as interchain tunnelling effect. Moller and Weiser[139] also did similar studies. They compared the photocurrent of fully polymerized single crystals of poly(DCHD) and poly(4-BCMU) with those of chains diluted in the corresponding monomer crystals. Interestingly, the dependence of light intensity on transport properties is most pronounced in the case of isolated chains where dc currents show large fluctuations after illumination. They proposed tunneling of carriers to sidegroups of the PDA chain as initial step of pair separation to explain the observation of photo-excited carrier escape from a chain to recombine on another chain.

However, Moses[129] and Blum[140] both questioned the Onsager's theory on the basis of the new photoconduction behavior found in poly(PTS) single crystals. Moses *et al.* measured the photocurrent decay and found it actually consists of a temperature-independent fast (picoseconds) initial component and a longer-time (nanosecond) component with magnitude that is strongly temperature dependent. The longer-lived carriers yield a mobility of 5 cm^2/Vs at room temperature. Blum and Bassler noted the drift velocity is weakly field dependent only at $E = 5\times 10^3$ V/cm and starts approaching a

linear relation for E = 2 × 10^4 V/cm. This effect can be attributed to field-dependent barrier crossing rates and accounts for field-dependent carrier discharge and trapping.

The measurements of PDA conductivity performance depend on the characterization methods and therefore are mostly studied by physicists and material scientists. Nonetheless, chemists can certainly modulate these properties by altering the chemical structural of PDAs, such as attaching different side groups to alter the π-electron chacteraitics,[135] or by controlling the supramolecular structures of these materials to change the effective conjugation length (ECL) in the polymer backbones.[141] It is worth pointing out that although the PDAs along with all the other CPs offer an excellent model as potential molecular wires, the importance as well as interest in the conductivities is no longer the main stream in this field. On the other hand, their unique photophysical properties are more exciting and realistic to applications.

1.3.3. Chromism

It has been noticed since the very early days that the conjugated polymer chains of PDAs in bulk polymer crystals can have different absorption spectra at certain conditions, often seen as "blue" and "red" phases, plus "purple" phases sometimes. Usually, PDA crystals are either blue or red at all temperatures *T* while in some cases a first-order reversible or irreversible transition between a lower *T* blue phase and an higher *T* red one is observed.[142-145] Furthermore, in the reversible case the crystal quality degrades after each transition, thereby the blue phase produced after a temperature cycle is less well

ordered than the original one, but still blue.[146] Similar phase transition was also found reversibly photo-induced. Koshihara *et al.*[147] reported the extremely efficient photochromism of poly(4-BCMU). It is found that the photoexcitation across the band gap with an intensity above a threshold value is necessary to cause the photoinduced blue ↔ red transition. And the threshold excitation intensity is fairly low for the poly(4-BCMU) single crystals, corresponding to only one absorbed photon per 500 repeat units of the polymer.

In the less well-ordered condensed phases, such as LB mono and multilayers, films on water surface, membranes, and vesicles, PDAs also show blue and red phases. These two phases can sometimes be reversibly interconverted into each other.[74,148] But more often, a blue phase is irreversibly converted into a red one, either as polymerization proceeds (as a function of polymer content), or by heating a completely polymerized sample.[68,149]

In solution, however, the phase transition of PDAs is much more complicated. The colors can switch between yellow ↔ blue,[150-153] yellow ↔ red,[152,153] red ↔ blue[154] or red ↔ purple[155] reversibly when the solvent/nonsolvent ratio varies or the temperature alters.[152,156] In the majority of the known cases, formation of the blue or red solutions (or suspensions) is followed by precipitation or gel formation.[152,157,158]

The origin of the color transition of PDAs has been a point of considerable debate. At the heart of the debate is the fundamental question, what kind of molecular structure exactly does each phase adopt? Although the answer is not certain yet, one perspective is generally accepted, that is, a certain color appears to indicate the existence of a corresponding phase in which ECL varies accordingly. ECL is not a precisely defined

quantity, but it is usually taken as the length of the oligomer that would absorb at the same wavelength as the polymer sample considered.

In PDA single crystals, polymer chains of the blue phase are known to be planar with the so-called "ene-yne" bond alternation, corresponding to relatively long ECL.[159] However, there is still no general agreement on the conformation of red chains, and therefore no agreement on the nature of the phase transitions either. The formation of the red phase is often claimed to be related to a decrease of order (nonplanarity) which would cause a shortening of the ECL.[97] But different opinions do exist. Schott studied isolated poly(3-BCMU) chains, either blue or red, dispersed in their single crystal monomer matrix. He concluded that "In the controversial red phase the polymer chains can be quasi-perfect quantum wires. The color transition in crystalline state is between two different chain conformations, and each may, or may not, be perfectly ordered. Disorder, when it occurs, is a consequence of the transformation, instead of the cause."[160]

Differently, the existence of blue and red colors does not require perfect order at all in LB films and other, even less ordered, solid phases. In these "soft" materials, the blue and red phases have an absorption threshold near 640 and 550 nm, respectively. In the extreme case of blue or red cast films and gels of soluble PDAs, the polymer backbone may be even more disordered, but the absorption maximum is still near 620 or 540 nm. These facts are not that surprising, considering the exciton size is very small, ~ 2 nm. Hence even though all mesoscopic coherence properties are lost in disordered samples, the exciton energy is not much affected as long as the ECL is still much larger than the exciton size provided the local geometry of the chain stays the same.

The mechanistical issue of the PDA solvatochromism is again much more complicated. In good solvents, PDAs are yellow (λ_{max} near 470 nm), and a decrease of solvent quality, either by decreasing the temperature or by adding a non solvent, produces red or blue "solutions" at low concentrations, and gels at higher ones.[156] These solutions are, in fact, suspensions of red or blue aggregates.[161] There are different opinions on whether this chromatic transition is a purely intramolecular effect or an intermolecular effect induced by aggregation of the PDA chains in poor solvation conditions. In the former case, it has been argued that the color change is a result of a backbone conformational change: either a rod-to-coil[158,162] or planar-to-nonplanar transition.[163] Advocates of the intermolecular process, such as Wegner *et al.*[164] and Hsu *et al.*[165], suggested that the solvatochromic shift is the consequence of aggregation of the wormlike coils present in the yellow solution. Kim *et al.*[155] claimed that the chromatic transitions are primarily a result of changes in the conformational ordering of the polymer backbone and that aggregation only occurs as a secondary consequence of the conformational change. The exact nature of the structure and conformation of the backbone and side groups in the yellow, blue, and red solutions and what drives the transition between them still remains unclear. However, evidence does show that the structure and packing of the side groups play an important role in inducing the chromic change. For example, most solutions of poly(*n*-BCMU) having an odd number of methylene groups adjacent to the polymer backbone undergo a change from blue to yellow, while those having an even number of methylenes undergo red to yellow transitions.[152,156,163,165-167] This odd-even effect does not include poly(1-BCMU), since it exhibits a red phase at low temperatures.[163] Poly(*n*-BCMU) with an odd number of

methylene groups can readily adopt a strain-free planar conformation with intramolecular hydrogen bonds between adjacent side groups in the blue phase. In contrast, poly(*n*-BCMU) having an even number of methylene groups can form intramolecular hydrogen bonds only in a slightly twisted, nonplanar conformation.[143,167] This results in a shorter ECL than in the planar conformation of the blue form. It is believed that the ECL is substantially smaller in the yellow solutions as a result of static and/or dynamic disorder in the polymer backbone. The average ECL of the blue PDAs, having the lowest-energy optical transition with a wavelength maximum (λ_{max}) between 600 and 700 nm, has been estimated to be larger than 30 repeat units. The red materials (500 nm < λ_{max} < 600 nm) have an ECL between 10 and 20 repeat units, while the yellow structures (400 nm < λ_{max} < 500 nm) have an ECL shorter than six repeat units.

Although the microscopic mechanism of the PDA chromism has not been completely elucidated, the transition is apparently a process in which the polymer chain conformation is firstly affected, and its electronic state alters consequently. A variety of environmental perturbations, such as solvent quality,[153,168] temperature,[143,169-172] *p*H variations,[82,172,173] mechanical stress,[174-176] chemical vapor exposure,[177] and biomolecular binding/unbinding can cause the polymer chain conformation changes and therefore the remarkable color transitions. Thus a lot of PDA systems have been investigated to seek for their analytical applications. Among them, PDA-based chemo/biosensors seem to be more promising to compete with the current available techniques.

In 1993, Charych *et al.*[178] first reported the biosensors based on PDA liposomes and films incorporating PCDA tails with sialic acid headgroups. This assay demonstrates blue → red color transition corresponding to the inhibiting event of influenza virus. After this

pioneering work, the same group and many other researchers have developed many more PDA-based detection platforms for the colorimetric analysis of metal ions,[179] small organic molecules,[180-182] enzymes,[183-187] DNAs,[188] virus[189] and bacteria.[190] **Figure 1.9** illustrates the general mechanisms of how these sensory designs work.

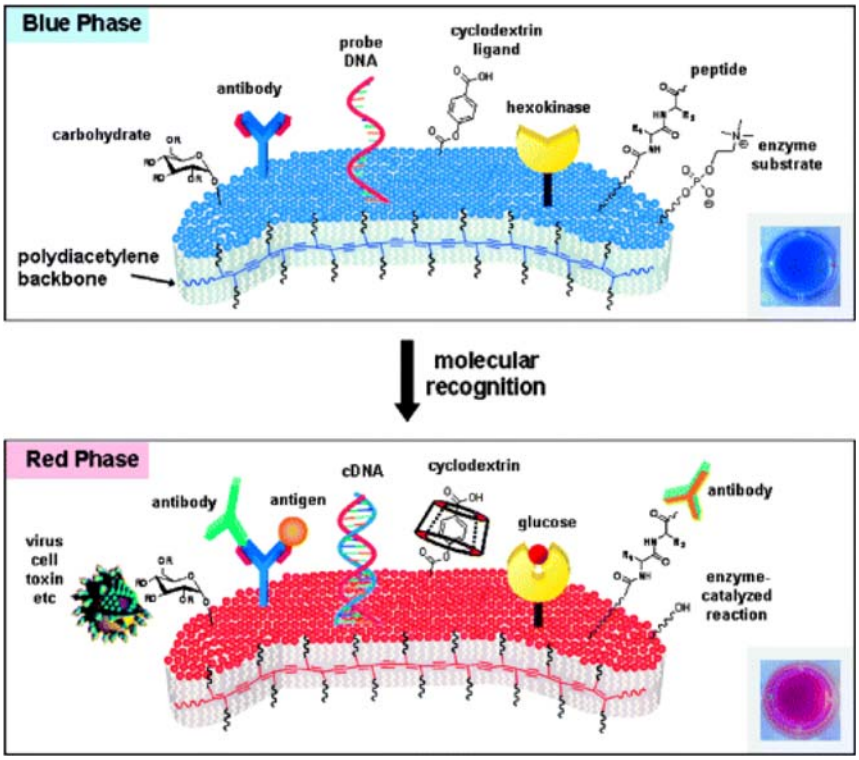

Figure 1.9 A schematic representation of surface ligands and their interactions with target molecules in colorimetric PDA sensors.[191]

Kolusheva *et al.* developed a system for selective detection of alkali metal ions embedding an ionophore (valinomycin or monensin) into a PDA liposome, as demonstrated in **Figure 1.10**.[179]

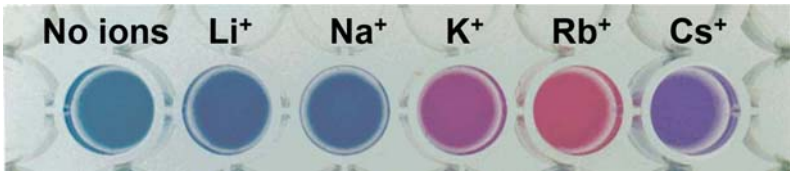

Figure 1.10. Valinomycin/PDA liposome solutions after addition of cations (con. = 10 mM).[179]

As for the detection of small organic molecules, Cheng and Stevens[180] demonstrated an elegant PDA/hexokinase conjugate for the colorimetric detection of glucose, utilizing the conformational changes of the ligand upon binding analyte. While the Ahn and Kim group reported sensitive cyclodextrin(CD)-induced color changes in both PDA vesicles[181] and LS films.[182] **Figure 1.11** shows the obvious color change in PDA vesicles solution upon the addition of CDs with different size. The authors proposed that the supramolecular interactions between CDs and PDA side groups will break the H-bonds among the carboxylic acids to different level. As a result, the conformation of PDA backbones changes and the colorimetric response is observed.

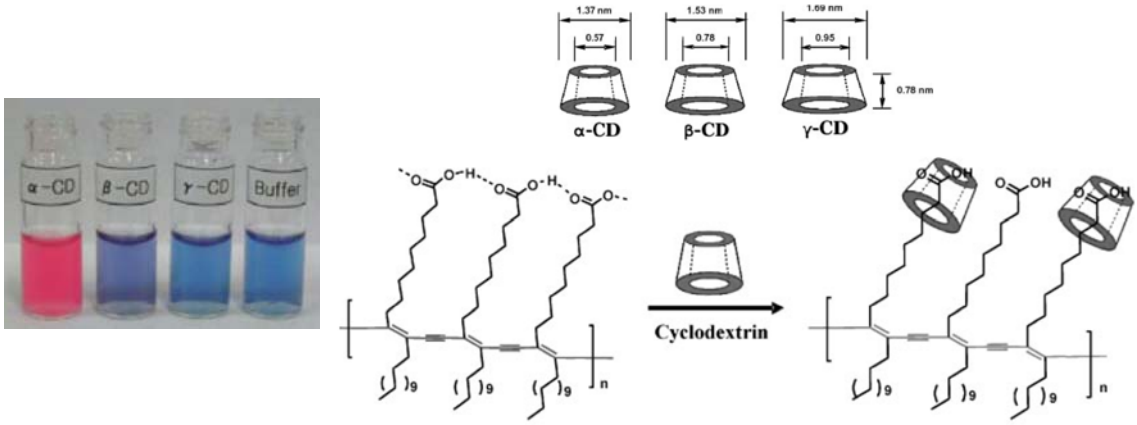

Figure 1.11. Colorimetric responses of PDA vesicle solutions treated by different CDs.[181]

In biosensing, Pan and Charych[183] extended their PDA-based sensor for influenza virus detection to enzyme detection. They created an artificial cell membranes made from

lipid PDA to mimic membrane processes of molecular recognition and signal transduction. By incorporating the ganglioside GM1 into PDA liposomes, molecular recognition of cholera toxin at the interface of the liposome resulted in a change of the membrane color. The same group also described a similar PDA vesicles composed a glycerophospholipid, dimyristoylphosphatidylcholine (DMPC).[184] This sensory system can be used for detecting Phospholipase A_2, which is known to be the enzyme catalyzing the hydrolysis of the acyl ester bond exclusively at the 2-acyl position in glycerophospholipids. Recently, colorimetric PDA sensor systems based on specific antibody–antigen interactions have been developed.[185-187]

PDA-based chemo/biosensors have shown their great potential in real applications, especially because of their relatively low cost and the label-free characteristics. However, considerable further work is still needed before reliable commercial products can challenge the current analytical assays.

Chapter Two

Single-Crystal-to-Single-Crystal (SCSC) Polymerization of Novel Diacetylenes

2.1. Introduction

As a result of the considerable dynamic research activities concerning PDA materials in the past four decades, a vast number of PDAs with various functional side chains attached to the ene-yne backbone have been synthesized. It is known that if external delocalization π-electron streams are incorporated into the highly conjugation π-system of the polymer backbone, the electronic and optical properties of PDA materials can be remarkably enhanced.[192,193] To obtain this kind of unconventional PDAs, extra conjugated systems, typically aromatic pendent groups for instance, need to be either bonded directly to the diacetylene moiety in the monomers prior polymerization or attached to the polymer backbone through a post chemical modification process. The later route seems to be extremely difficult considering that until now there is only one PDA, polyiododiacetylene, successfully obtained recently,[194] which has necessary reactive functional groups (iodide in this case) directly bonded to the polymer mainchain. Unfortunately, this single candidate suffers extreme solubility problems that have prevented modification till now. The pre-polymerization route, however, seems to be more likely. The majority of the reported polydiacetylenes are formed from the monomers without any aromatic groups in the structure at all or with aromatic groups

spaced from the diacetylene core by saturated linkers, such as esters, ethers and aliphatic alkyl chains. There are some poly(aryldiacetylenes) claimed to have been made by the γ-ray induced polymerization of randomly packed aryldiacetylenes in solid state,[193] however, the yield and quality of the as-obtained polymers are poor. Furthermore, their molecular structures are lack of well characterization caused by the solubility problems.

Therefore some kind of controllable strategy is definitely necessary for the successful synthesis of poly(aryldiacetylenes). Our host-guest cocrystal strategy has been proven to be a powerful approach to PDAs as discussed in Chapter One. It is also a better solution to such a hard problem as will be explained in detail in the following section. More importantly, this powerful method also provides a great possibility that such reactions would take place within a SCSC environment. This result has an extra advantage which allows one to map out exact reaction trajectories and prepare crystalline poly(aryldiacetylenes) with highly ordered structures.

It has been a long-standing goal to realize the SCSC polymerization of aryldiacetylenes, from the point of view of either physical organic chemistry or material chemistry. The major project of my dissertation research was therefore to conduct the study of the SCSC polymerization of aryldiacetylenes. The challenge was, no one had really succeeded before. The positive results were fairly rare and even the best ones were far from yielding the true crystals of poly(aryldiacetylenes).

In 1978, Day and Lando[195] reported the first example. They succeeded in polymerizing a cyclic bisphenyldiacetylene (**11**) to an extent of 35% as confirmed by single crystal X-ray diffraction. Nakanishi and coworkers[196] studied the solid state polymerization of another bisphenyldiacetylene (**12**) and was able to obtain up to only

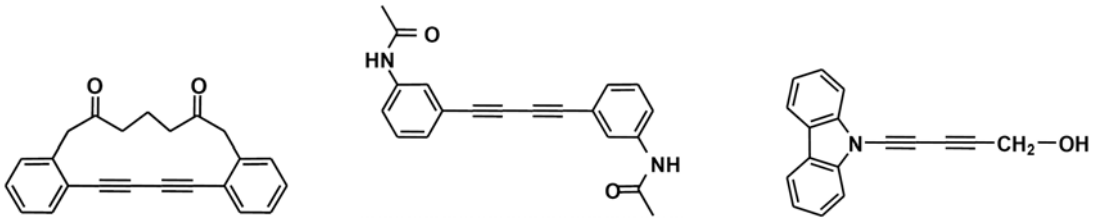

11 **12** **13**

20% extent of polymer in monomer single crystals. In both of these two studies, not only the diacetylene moieties, the phenyl groups also demonstrate an obvious motion associated with the polymerization. Such a major structural adjustment in the solid state may cause serious strains that can eventually destroy the original crystal lattice required for further polymerization. There is only one literature report[197] that claims a successful topochemical SCSC polymerization in the monomer single crystals of 1-(*N*-carbazolyl)-penta-1,3-diyn-5-ol (**13**), but no detailed crystal structure information of the resulting polymer was reported.

In our own work, there were also similar unsuccessful experiences.[51] As shown in **Figure 2.1**, the dipyridyldiacetylenes are nicely aligned in the host-guest cocrystal system but the crystals crumbled into a purple powder as the *γ*-ray-induced polymerization proceeded. However, in this case the polymers, or at least oligomers, must have been generated given that the Raman spectrum of the insoluble product shows signals corresponding to typical PDA type structure. We believe that the rigid pyridine groups are responsible for the loss of crystallinity during polymerization.

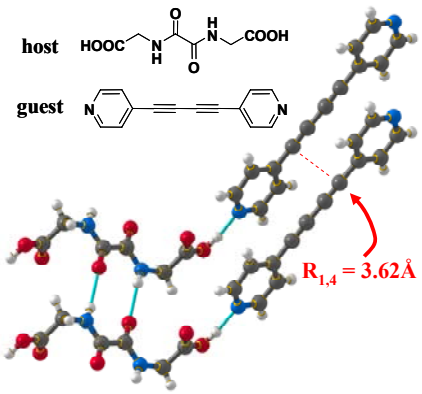

Figure 2.1 The cocrystal of dipyridyldiacetylene and oxalamide of glycine.

Again, recent similar studies found in the literature, sometimes with even better monomer packing parameters than ours, all reported failures. For example, Curtis and coworkers have found that in the single crystals of **14**, 1,4-bis-5-(4,4'-di-*n*-butyl-2,2'-bithiazole)-1,3-butadiyne, the monomers are perfectly aligned for topochemical 1,4-polymerization ($\mathbf{R_{1,4}}$ = 3.48 Å). Based on the packing parameters of the diacetylenes in the crystals of **14**, this example could be the most promising system for attaining crystalline poly(aryldiacetylene) ever since. Unfortunately, no polymerization occurred at all under a variety of conditions, not to mention the SCSC transition. The authors also attributed the lack of topochemical polymerization to the extremely high rigidity of this molecule due to the direct attachment of aromatic groups on the diacetylene moiety.

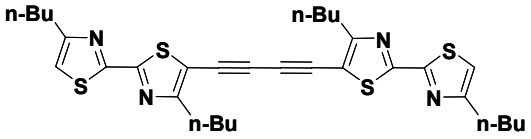

14

2.2. Molecular Design of the Novel Diacetylenes

According to the failed examples mentioned above, it is clear that a successful SCSC polymerization of aryldiacetylenes needs not only the perfect monomer alignment required by the topochemical polymerization constraints, but also enough molecular flexibility to tolerate the remarkable structural adjustments towards the polymer crystals.

In most cases where our group obtained the polydiacetylene crystals, the reaction pathway followed what we call the "turnstile" mechanism.[47,49] As illustrated in **Figure 2.2 a**, when energy is applied the monomers pivot around their centers of mass in a

conrotary manner bringing the neighboring C_1 and C_4 carbon atoms together to form a new bond. The required atom movement is just over 1 Å for each reacting atom. The "turnstile" mechanism is also frequently seen in literature examples, exclusively for symmetrical diacetylene monomers.[198-203]

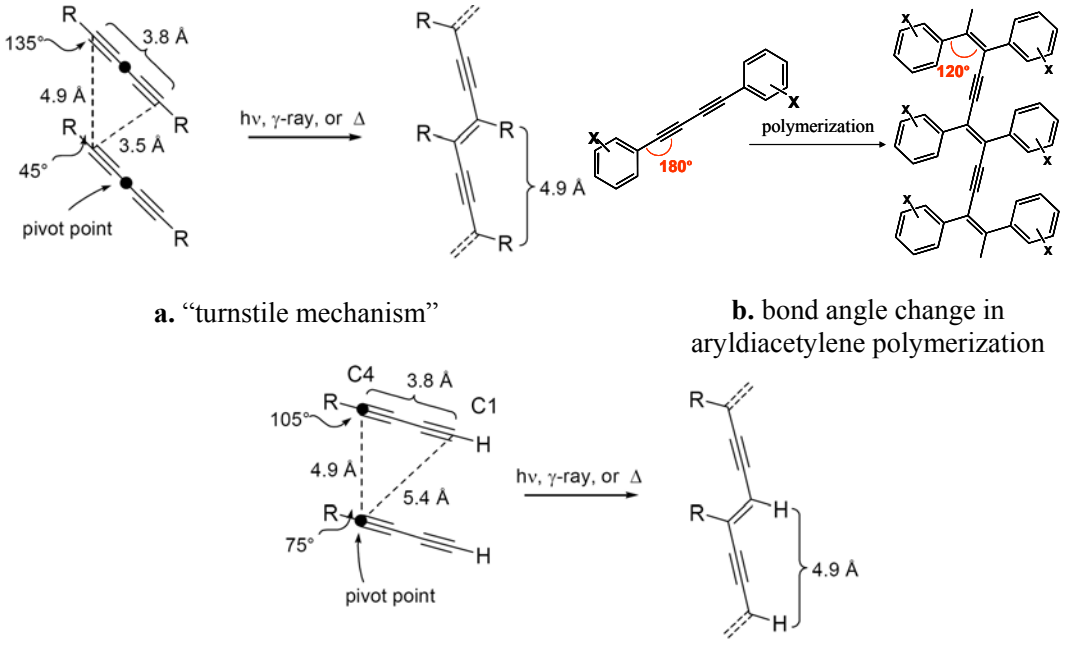

a. "turnstile mechanism"

b. bond angle change in aryldiacetylene polymerization

c. "swinging gate mechanism"

Figure 2.2 Possible mechanisms for the topochemical polymerization of diacetylenes.

In the case of an aryldiacetylene, however, the linear *sp* hybridized carbon atoms in the monomers become trigonal centers with bond angles of 120° in the polymers. The total angle change is 60° so the other half of the movement, another 30°, must involve the aromatic ring (**Figure 2.2 b**). This 30° movement of the rigid ring may just be too disruptive for the crystal lattice to remain intact. "How to live with it" is the most difficult part in this project.

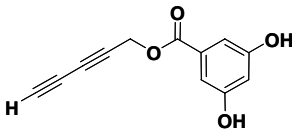

15

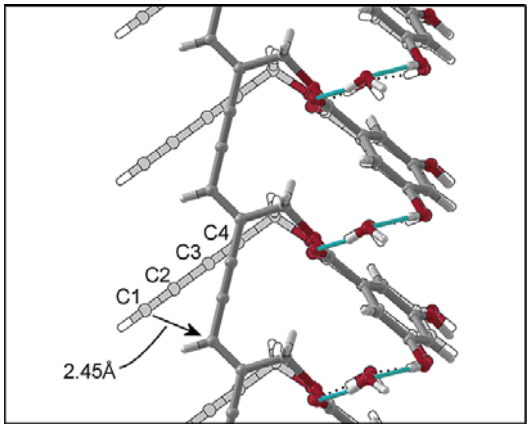

Figure 2.3 The "swinging gate" motion in the polymerization of **15•H_2O**.

A mono substituted or terminal aryl diacetylene may be the solution. One can imagine a second mechanism for the polymerization. In a previous study[49] our group found a reaction trajectory very different from the common "turnstile" mechanism, suggesting that perhaps the unsymmetrical aryldiacetylenes can provide us an alternate way of preparing poly(aryldiacetylene) crystals. The inspiration came from a single crystal of penta-2,4-diynyl 3,5-dihydroxybenzoate (**15**) monohydrate, which underwent a facile SCSC polymerization with only moderate heating (**Figure 2.3**). What surprised us was that the reaction trajectory showed a dramatic movement of 2.5 Å by the terminal C_1 carbon as the major contribution to the overall structural adjustment, while C_4 and its attached CH_2 group only moved slightly. Thereby we proposed a "swinging gate" mechanism, in which the C_4 serves as a pivot point and all movement would take place at the terminal end of the diacetylene functionality for new bond generation (**Figure 2.2 c**). The same mechanism could work just as well for a terminal aryldiacetylene.

Inspired by this result, I decided to use unsymmetrical aryldiacetylenes as new guest monomers. According to the rational analysis stated above, these novel aryldiacetylenes should have only one aryl group bonded to one side the diacetylene core while leaving the other side free or "freely substituted" (by spacers such as methylene group), as makes

our target guest molecules either terminal aryldiacetylenes or alkyl aryldiacetylenes. Another requirement determined by our host-guest strategy is that H-bond donor(s) or acceptor(s) has to be incorporated in the structure as well. Finally I designed some guest molecules as the candidates to pair with the host molecules best performing in diacetylene topochemical polymerization based on our previous experiences, as shown in **Figure 2.4**. Most of these diacetylene guests are unknown compounds from the literature to date.

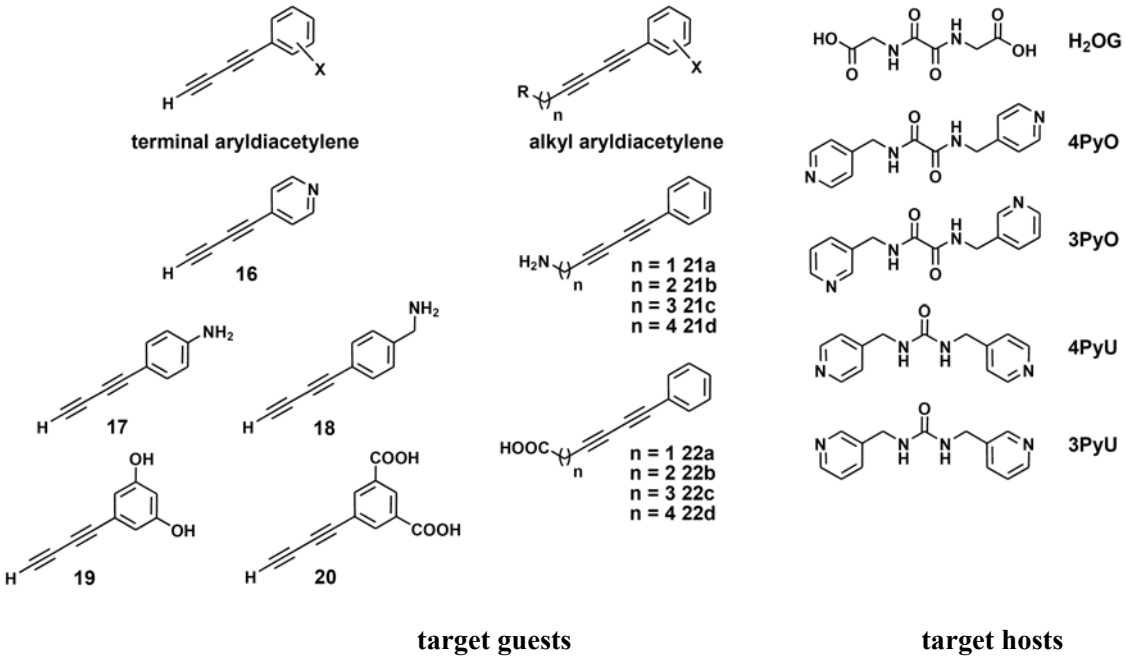

Figure 2.4 The target host and guest molecules.

Among all these target guests, the terminal ones seem to be most promising for the SCSC polymerization according to our success with the first terminal diacetylene polymerization. If the terminal aryldiacetylenes can also polymerize in the "swinging gate" fashion I would have a great chance to realize the SCSC transformation in an aryldiacetylene system.

The first guest molecule of such kind we actually studied was **16**, because it is the direct descendant of dipyridyldiacetylene that we knew in the cocrystals the monomer packing is good enough for 1,4-polymerization. This part of work was done by Mr. Ti Wang,[204] one of the previous students in our group. Unfortunately, as a good cocrystallization synthon in general concept, this terminal pyridyldiacetylene didn't show any tendency to form high quality cocrystals with **H_2OG** for the structure determination in single crystal X-ray diffraction experiment.

I started my project by focusing on molecules **17** and **18**. They are both structurally related to the pyridyl analogue except that the N atom, a necessary H-bond acceptor, is pulled out of the aromatic ring. Since the most logical host that we are going to use for these guests is still **H_2OG**, **18** seems to be a better choice than **17** considering that the stronger basicity **18** will be more favorable for the H-bonding connection between hosts and guests, which we know is very important in setting the desired repeat distance in the packing of guest molecules. In addition, the aryl analogue of the terminal alkyldiacetylene from which we found the "swinging gate" mechanism, guest **19**, as well as its carboxylic acid version **20**, are also of interest.

Other than terminal aryldiacetylenes, some of the unsymmetrical alkyl aryldiacetylenes, **21** and **22** for instance, are also considered as good guest candidates. Although they are assumed to be less free in a sense than the terminal ones, they are definitely more flexible than diaryldiacetylenes.

It is worth mentioning that the guest molecules listed in **Figure 2.3** were just from our initial plan, with the research progressing, some major modifications were found to be necessary and will be addressed later accordingly.

2.3. SCSC Polymerization of Terminal Aryldiacetylenes

The first terminal diacetylene that we focused on is *p*-diacetylenyl benzylamine **18**. This compound is unknown from the literature. What is known about terminal aryldiacetylenes is that almost all of them are unstable to isolation because of their rapid degradation or polymerization, especially in a condensed state at ambient conditions.[205] Generally speaking, a extremely pure system is a must for growing high quality single crystals and the most commonly used growth setups are at ambient conditions. Therefore, the potential chemical instability of **18** may be a serious problem during the cocrystal growth even if the compound itself can be synthesized and isolated with acceptable purity.

Another potential problem lies in the cocrystal system itself. When a carboxylic acid H-bonds to a pyridine as in our initial trial, there will be no formal charge transfer and no ion formation. A typical substituted pyridinium ion has a pK_a of about 6, less acidic than a typical carboxylic acid pK_a of about 4.5, but not by much.[206-208] In solution a carboxylic acid will protonate a pyridine, but in the solid state in the absence of stabilizing solvent molecules there usually is no proton transfer and a carboxylic acid will simply form a H-bond with pyridine. The situation with **18** is different. A substituted benzylammonium ion has a pK_a of about 9.5, considerably less acidic than a carboxylic acid. Proton transfer is expected even in the solid state and an ammonium carboxylate salt will form instead of a cocrystal. The resulting primary ammonium and carboxylate anion will form strong H-bonds (essentially ionic interactions) and will likely dominate the molecular packing of the crystal. It was not at all clear to us that the necessary one dimensional α-network based upon weaker amide-to-amide hydrogen bonds between the

hosts would form in the presence of the ionic centers (**Figure 2.5**). A recent paper by Aakeroy *et al.*[209] focuses on this problem. The authors prepared and compared 61 different cocrystals with 21 different organic salts. The series of cocrystals gave crystals with predicted stoichiometries 95% of the time, but 45% of the salts gave alternate stoichiometries or incorporated solvent.

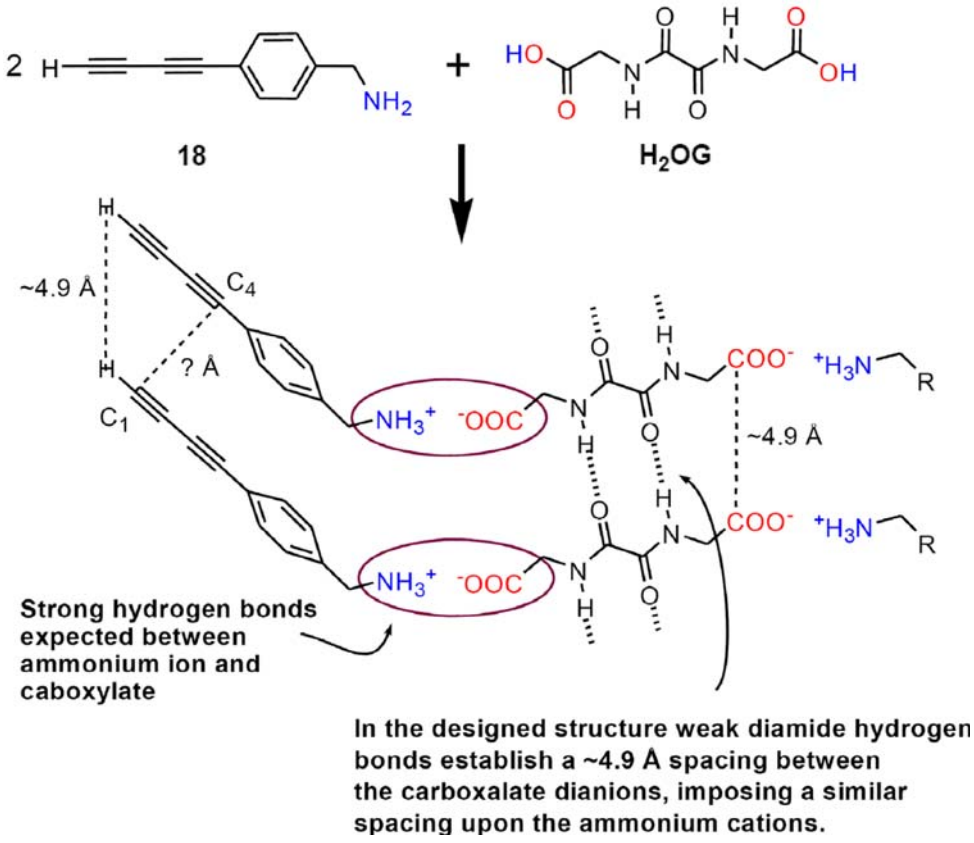

Figure 2.5 Can weak H-bond and strong H-bond coexist?

We were thus somewhat apprehensive that the structure in **Figure 2.5** might not form. In this designed layout, the critical repeat distance **d** is determined by the weaker H-bonds while the strong ones associate hosts and guests to pass the correct **d** value along to the diacetylene units. So the question we were facing was, can these two different interactions coexist in a salt system, clearly segregated?

2.3.1. Model Studies of Primary Amine/H_2OG Salts

Before proceeding with the somewhat complex synthesis toward our target compound **18**, we decided to do some model studies on similar salt systems to seek for the answer to the question raised at the end of last section. A series of ten different salts of our host dicarboxylic acid **H_2OG** were tested.

Our test series started with the ammonium ion, including the simple alkyl ammonium ions from methyl through hexyl, plus the cyclic ammonium ions, cyclohexyl, benzyl and 4-acetynylbenzyl ones. The salts were all prepared by adding two equivalents of each primary amine to small quantities of dicarboxylic acid **H_2OG** in water or water/methanol solutions. In each case crystals formed upon slow evaporation at a temperature of about 35° C. Once a first crystal structure was obtained from each of the test cases, no further investigations were made. We made no attempt to find a second polymorph or solvate of any of the model compounds. Our initial results confirmed the observations of Aakeroy, the simplest salts all failed to give predicted stoichiometries. Indeed we seemed to have undertaken a study of chaos.

2.3.1.1. Ammonium Salt

The first case illustrates the problem. One characteristic of dicarboxylic acids is that quite often their half neutralized salts will readily crystallize from solution, often giving excellent crystals. Crystals of most half-neutralized dicarboxylic acids contain a strong hydrogen bond between the remaining carboxylic acid hydrogen and the single

carboxylate. A common example is potassium hydrogen tartrate, a well known crystalline byproduct of wine making.[210] A search of the Cambridge Structural Database (CSD) yields a raw count of 195 structures containing the hydrogen tartrate ion, but only 144 structures containing the tartrate dianion. Hydrates are also common; 67 of hydrogen tartrate structures and 107 of the tartrates are hydrates.

Thus we are not surprised to find that **H_2OG** crystallizes from aqueous ammonia to give the hydrated half-neutralized salt **$NH_4HOG•2H_2O$** (**Figure 2.6**). The **HOG^{-1}** ions form a hydrogen bonded chain. One set of amide-amide H-bonds forms, but the linear α-network of amide H-bonds shown in **Figure 2.5** is not found. Instead the second amide oxygen atom forms a H-bond to an ammonium ion.

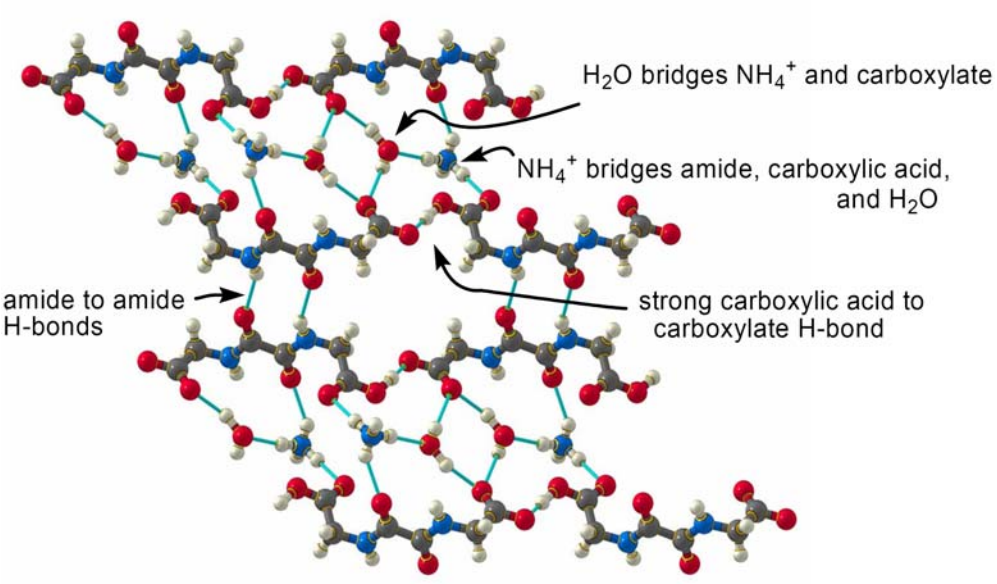

Figure 2.6 The crystal structure of **$NH_4HOG•2H_2O$**.

2.3.1.2. Methyl- and Ethylammonium Salts

Methyl and ethyl amine form similar salts with **H_2OG.** The supramolecular chemistries of the two salts are the same, but the crystallographic symmetries are different, as shown in **Figure 2.7**. In this case the dicarboxylic acid host is fully neutralized to form a dicarboxylate anion. The ammonium ions bridge a water molecule plus two carboxylates end to end. The amide hydrogen atom forms a H-bond to a carboxylate as well. The design of **Figure 2.5** is still unfulfilled.

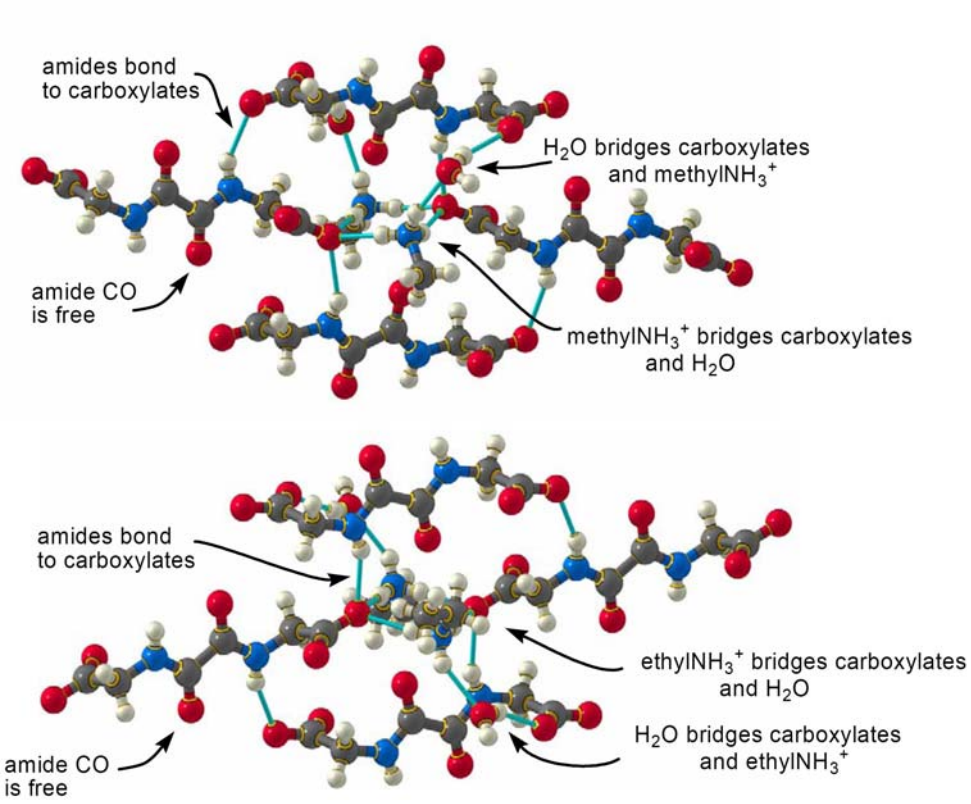

Figure 2.7 The crystal structures of **$(CH_3NH_3)_2OG•2H_2O$** and **$(CH_3CH_2NH_3)_2OG•2H_2O$**.

2.3.1.3. Propylammonium Salt

With propylamine, a fully neutralized anhydrous salt formed (**Figure 2.8**). The oxalamide α-network is seen for the first time, but with two molecules per asymmetric unit, not one. This means the crystallographic repeat unit is doubled to 10 Å instead of the necessary 5 Å. The propyl ammonium ions form a full set of H-bonds to the carboxylates, but because of the multiple molecules in the asymmetric unit the structure is once again an unsuitable model for a designed diacetylene polymerization.

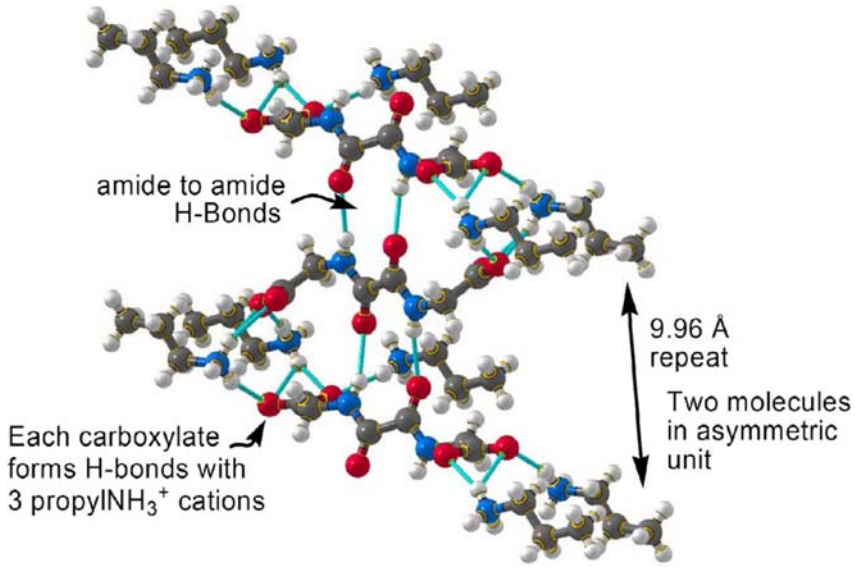

Figure 2.8 The crystal structure of **(propylNH$_3$)$_2$OG**.

2.3.1.4. Butylammonium Salt

The salt with butyl amine, **(butylNH$_3$)$_2$OG**, was not at all encouraging (**Figure 2.9)**. There are two molecules in the asymmetric unit and seemingly no pattern to the H-bonds. One pair of molecules forms a diamide dimer, but the other molecule in the asymmetric unit forms only amide to carboxylate H-bonds.

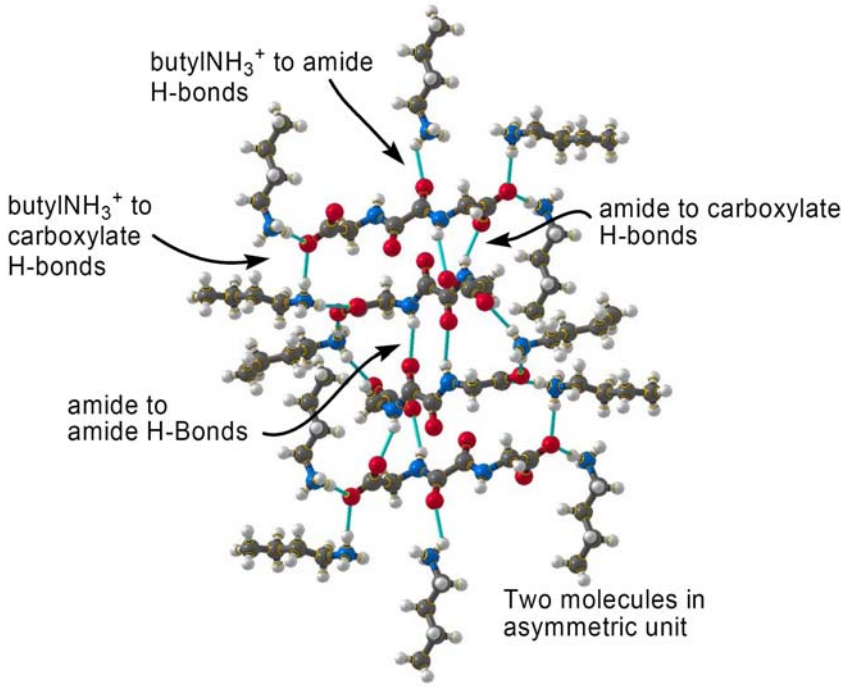

Figure 2.9 The crystal structure of **(butylNH$_3$)$_2$OG**.

2.3.1.5. Pentyl- and Hexylammonium Salts

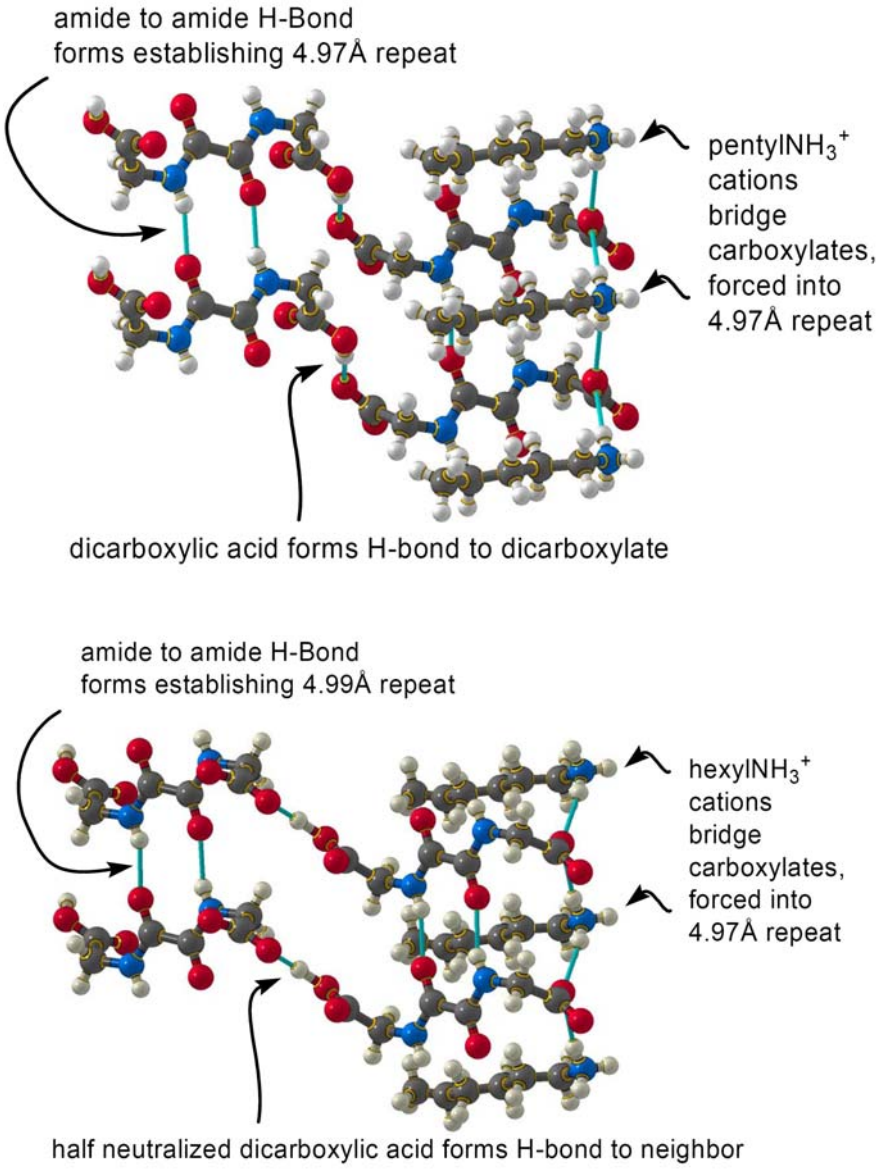

Figure 2.10 The crystal structures of **(pentylNH$_3$)$_2$OG·H$_2$OG** and **(hexylNH$_3$)$_2$HOG**.

As shown in **Figure 2.10**, the results with pentyl and hexyl ammine were much closer to the designed structure shown in **Figure 2.5**. The host molecules of both structures form a one dimensional amide-to-amide H-bonded α-network. Superficially the two structures look similar, but a closer look shows that their stoichiometries are different. The

hexylamine structure is the simplest; it is the hexylammonium salt of the half neutralized host, **HOG^{-1}**. The pentylamine structure has one fully neutralized **OG^{-2}** dianion plus one fully protonated diacid molecule, **H_2OG**. However, the important fact is that both structures exhibit the targeted 4.9 Å repeat distance established by the amide-amide H-bonds. In each structure there is a segregation of the weak amide-amide H-bonds from the stronger carboxylate-ammonium and carboxylate-carboxylic acid H-bonds.

2.3.1.6. Cyclic Primary Ammonium Salt

The next logical step in our series of model salts was to examine cyclic primary amine salts. Cyclohexyl and benzyl amine formed simple fully neutralized salts, of the form **$(RNH_3)_2$OG**. They both crystallized in the triclinic $P\bar{1}$ space group with one formula unit per unit cell. They both also formed a two dimensional β-network of $p\bar{1}$ layer group symmetry exhibiting the Supramol. Chem. projected in **Figure 2.5**. These layers are pictured in **Figure 2.11** along with sketch of the two-dimensional layer unit-cells. There are two independent H-bond α-networks along the short (~ 5 Å) unit cell direction, as shown in **Figure 2.12**. The first is the oxalamide α-network, previously shown to be a reliable functionality for establishing a 4.9 - 5.0 Å spacing. Parallel to the oxalamide α-network is a α-network of alternating pairs of primary ammonium cations and carboxylate anions.

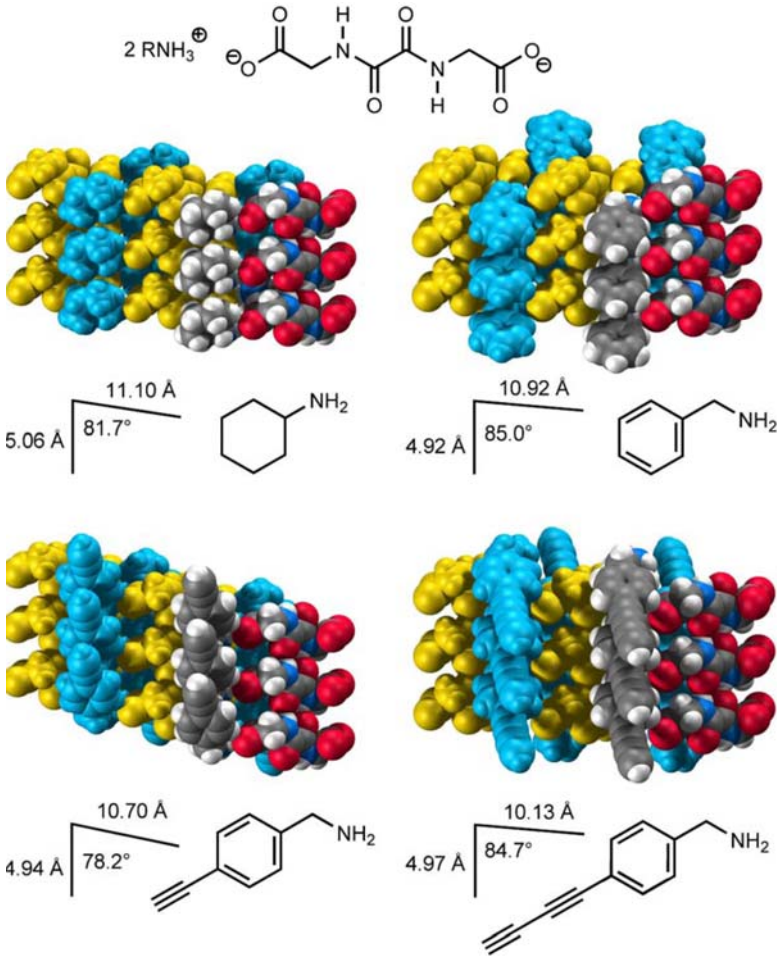

Figure 2.11 The crystal structures of four cyclic ammonium salts of the form $(\mathbf{RNH_3})_2\mathbf{OG}$. The supramolecular chemistries of the four α-networks are identical. Each layer contains the two independent α-networks bond networks shown below in **Figure 2.12**. The four layers each have $p\bar{1}$ layer group symmetry with two dimensional unit cells of similar dimensions as indicated in the drawing.

The primary ammonium carboxylate network has been seen before. Sada and co-workers[211] recently published a comprehensive CSD analysis of ammonium carboxylate structures. They identified 1070 examples of primary alkyl ammonium carboxylate salts. These salts form a wide variety of one and two dimensional hydrogen bonded networks. Only 47 less than five percent of the structures form the one dimensional α-network shown in **Figure 2.12b**. These 47 structures were not identified specifically and we have

not reproduced their extensive study ourselves, but a more casual perusal of the CSD indicates that this network is found in structures of various racemic α-amino acids. Qualitatively the crystallographic repeat distances appear to range from about 4.6 Å to 4.9 Å, generally shorter than the distance targeted and found in the salt system studied here. A typical example is racemic phenyl glycine which contains the α -network of **Figure 2.12b** with a repeat distance of 4.85 Å.[212]

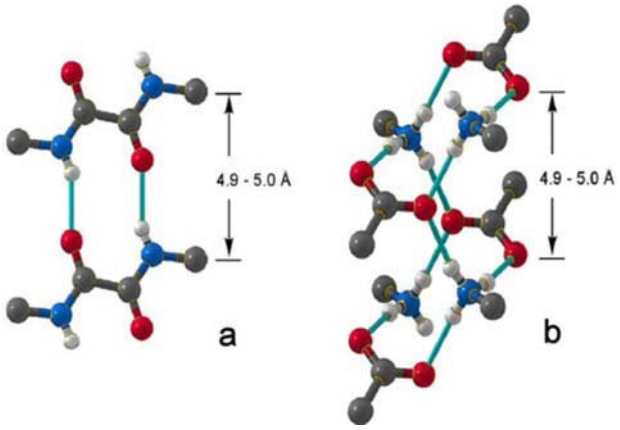

Figure 2.12 Two independent H-bond α-networks in **$(RNH_3)_2OG$** salts.
(a) host-host; (b) host-guest.

The model studies gave us a strong indication that the design of **Figure 2.5** would work, thus we proceeded with the synthesis of **18**. As described later in the following section (**Scheme 2.1**), the monoacetylene compound 4-acetynylbenzylamine (**27**) was a model compound from the synthesis. This gave us the opportunity for one more model crystallographic study. The amine **27** also forms a simple salt of the form, **$(RNH_3)_2OG$**, with a layer structure analogous to the cyclohexyl and benzylamine salts (**Figure 2.11**). The only difference in the structure is the orientation of the 4-acetynylbenzyl group, which can be seen to bend "up" opposite in direction to the benzyl group that bends "down".

The four cyclic primary ammonium salts all form isostructural layers as shown in **Figure 2.11**. In **Figure 2.13** a top view of these layers can be seen.

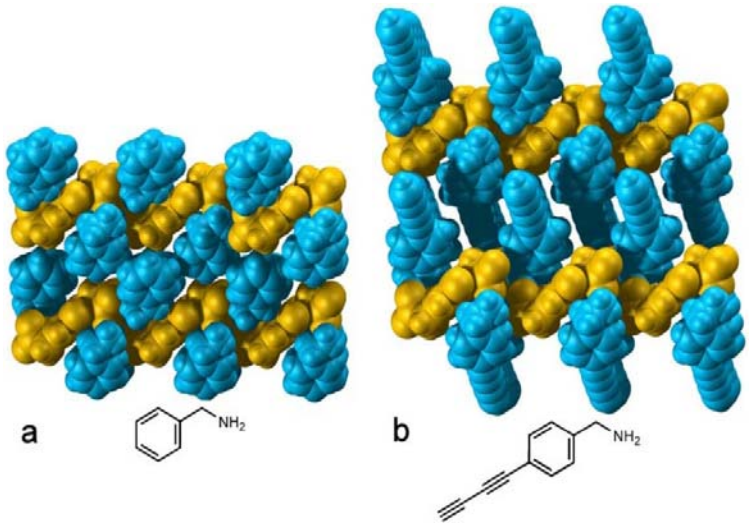

Figure 2.13 A top view of two of the layers shown in **Figure 2.11**. (a) **(benzylNH$_3$)$_2$OG**; (b) **(18H)$_2$OG**. The layers form an inverse bilayer with the hydrophobic tails (in blue) of the ammonium salts filling the space between the hydrogen bonded anions (in yellow).

The layers have taken on the form of a reverse bilayer with the charged residues in the center of the layer and the nonpolar greasy tails pointing outward on both sides of the layer. Such layered organic salts have been seen before. Good examples include Zaworotko's[213] *N,N*-dibenzylammonium carboxylate laminated clay mimics and Ward's[214] guanidinium sulfonates. A common theme to these layered salts seems to be the need for a greasy group of sufficient size to drive the bilayer formation via the hydrophobic-hydrophobic interactions. This is illustrated by the fact that the smaller alkyl ammonium cations in this study failed to form the layer structures formed by the larger and greasier ammonium cations (**Table 2.1**). In addition, our results also implies that the π-π interactions may also play active roles, as found in the cases of the benzyl-, 4-acetynylbenzyl- and the targeted 4-diacetylenylbenzyl ammonium salts.

Table 2.1. Summary of the structural characteristics in $(\mathbf{RNH_2})_x(\mathbf{H_2og})_y$ salts.

R	Stoichiometry (x:y)	Desired H-bond α-networks among hosts	Repeat Distance
H, CH_3, ethyl *n*-propyl, *n*-butyl	1:1 or 2:1 (*w* H_2O)	Not found	wrong
n-pentyl *n*-hexyl	1:1	found	4.97 Å 4.99 Å
cyclohexyl benzyl 4-acetynylbenzyl 4-diacetynylbenzyl	2:1	found	5.06 Å 4.92 Å 4.94 Å 4.93 Å

The conclusion on the basis of model studies is somewhat obvious that, with the increasing of the amine's hydrophobicity, the oxalamide *α*-networks segregate more independently from the ammonium/carboxylate ionic interactions and the **d** value tends to be translated to guest molecules more reliably.

Overall these model studies gave us a strong indication that the strategy of **Figure 2.5** would work, since the target guest molecule **18** is even more hydrophobic than benzyl- and 4-acetynylbenzylamine.

2.3.2. The Synthesis of 18

We then proceeded with the synthesis of 4-diacetylenylbenzylamine **18**. As outlined in **Scheme 2.1**, Starting with 4-bromobenzyaldehyde, with three continuous steps of Sonogashira coupling, deprotection of silyl group and reduction, alcohol **25** was obtained. The benzyl alcohol was converted to azide **26** in one step using Reddy's procedure[215] and

Scheme 2.1

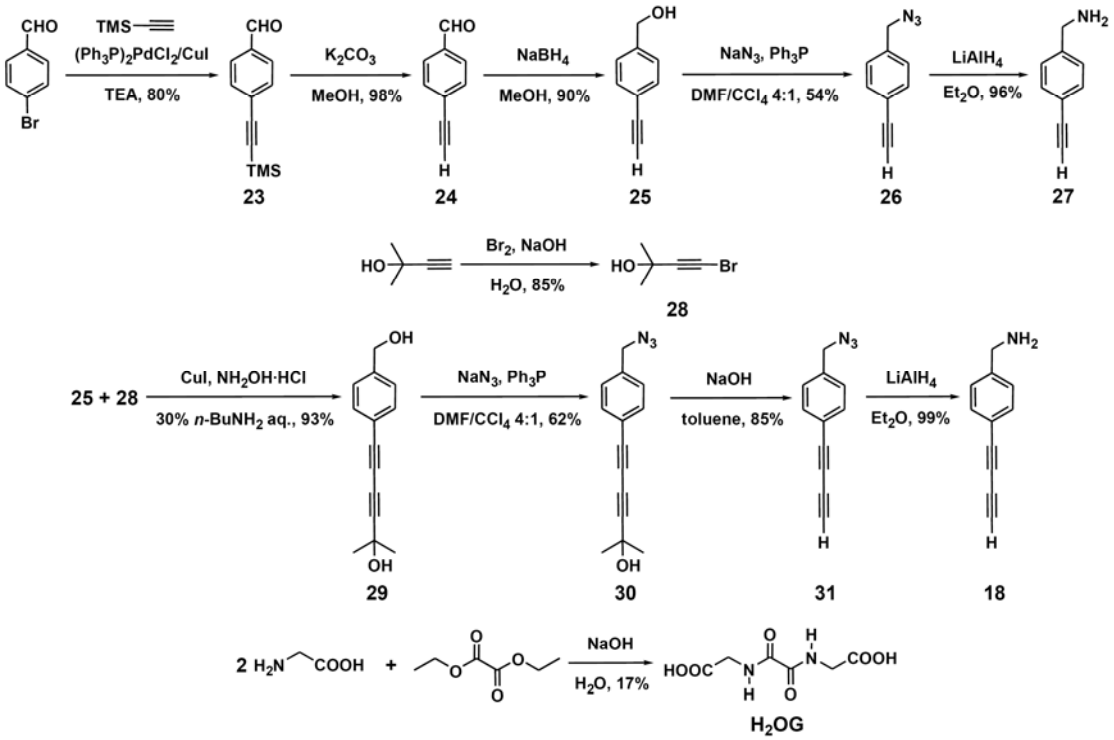

continuously reduced to 4-acetynylbenzylamine **27** to afford a third cyclic primary amine for model studies. For the terminal diacetylene synthesis, another building block, bromide **28** was first attained from 2-methyl-3-butyl-2-ol independently. Then a Cadiot-Chodkiewicz coupling of **25** and **28** afforded the protected diacetylene species **29**, which was converted to azide **30** using the same reagents as for making **26**. After the elimination of acetone protecting group followed by a reduction of the azide group, the target compound **18** was obtained neatly in an overall 35% yield. Not surprisingly, **18** was found chemically unstable as a terminal aryldiacetylene. It can be stored in solution at low temperature for months. However, once the stock solution is concentrated, this reactive amine turns quickly from white crystals into a deep-colored insoluble solid, as most of the terminal aryldiacetylenes discussed in literature.[205] Therefore extra care is absolutely necessary whenever this compound is used, either in the synthetic phase or in

the crystal growth experiments. **H_2OG** can be synthesized according to the procedure adapted from literature.[216]

2.3.3. 4-Diacetylenylbenzylammonium Salt

Primary amine **18** also formed a simple salt of the form **$(RNH_3)_2$OG** with the host, as shown in **Figure 2.14a**. The structure was a close analogue of the three cyclic primary amine salts studied as models. The all important diacetylene repeat distance was 4.97 Å and the neighboring C_1-C_4 distance $\mathbf{R_{1,4}}$ was 3.58 Å. These parameters are well within the range needed for 1,4-polymerization.

As we examined the various model salts we made no attempt to search for polymorphs of alternate solvated crystals, but with diacetylene **18** an active search for alternate crystalline forms was not necessary. The ready polymerization of the diacetylene moiety introduces color into the crystals making it very easy to choose crystal variants. We found two alternate crystalline forms without really looking for them. The desired solvent free salt discussed above came out of mixed methanol/water solutions as pink needles, but they were accompanied by red plates of a hydrated crystalline form, **$(18H)_2$OG•$2H_2O$**, as shown in **Figure 2.14b**.

The host anions in the hydrate do not align in accordance with the design of **Figure 2.5**. However, the ammonium ions do form a water bridged network along a glide plane that brings neighboring diacetylenes into approximate alignment with a repeat distance of 9.53 Å for a pair of symmetry related molecules. Neighboring molecules have a C_1-C_1

distance of 4.81 Å and a C_1-C_4 contact is 3.52 Å, even shorter than the value of 3.57 Å found in the anhydrous crystal. Thus we had in hand two possible candidate structures for our topochemical polymerization, one designed and one accidental.

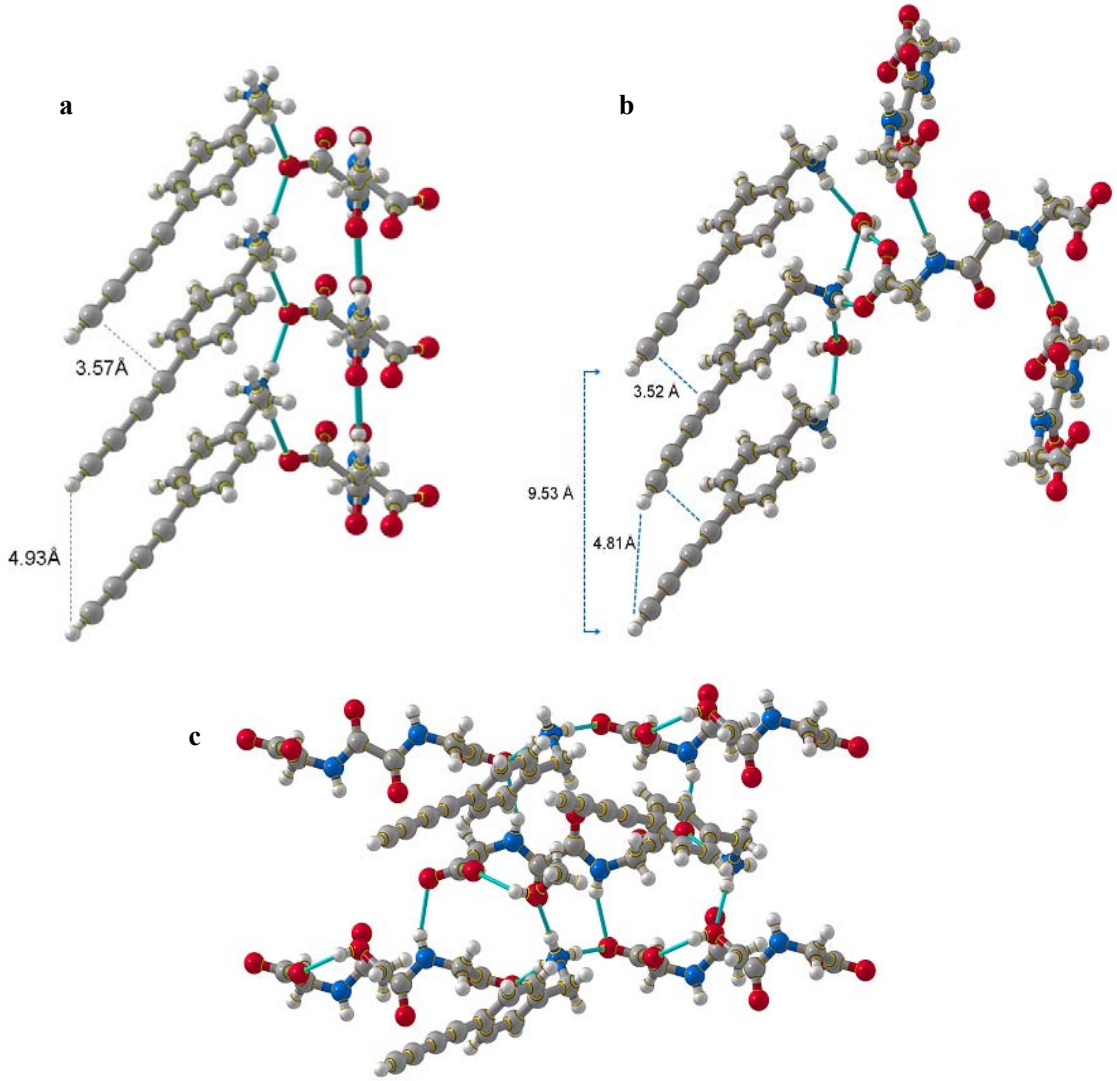

Figure 2.14 (a) Desired salt of **18** in the form **$(RNH_3)_2OG$**; (b) The salt of **18** in the form of hydrate **$(18H)_2OG•2H_2O$**; (c) The salt of **18** in the form of solvate **$(18H)_2OG•2CH_2OH$**.

We also found a third crystalline form, a methanol solvate, **$(18H)_2OG•2CH_2OH$**, as shown in **Figure 2.14c.** In this form the diacetylenes ammonium cations are well

separated and there are no amide-amide hydrogen bonds. This form seems totally unsuitable for a topochemical polymerization.

Once we realized that the **18** readily formed solvated crystals it became important to find a way of growing the solvent free form. Extensive optimization experiments finally pointed out that this could be done simply by using pure 1-propanol for the recrystallization, although the efficiency of this supramolecular synthesis is limited by the poor solubility of **H_2OG** in 1-propanol.

The high quality single crystals of **18/H_2OG** salt were difficult to grow. All three forms of **18/H_2OG** salts were finally obtained by solvent evaporation of the shoichiometric quantities of host and guest in anhydrous methanol (yielding the methanol solvate crystals readily in solution) or alcohol/H_2O mixture at room temperature. It is crucial that the evaporation rate is much faster than normal, as the conditions used for the model salts can take from overnight to a couple of days before the crystals appear. The quick evaporation approach is very important when dealing with unstable compounds like **18** and can be realized using a wide-open container like a petri dish. It usually takes less than 30 min to get high quality single crystals of **18/H_2OG** salts from about 10 mL solution. The regular slow evaporation never worked well due to the problems presumably caused by the chemical instability of **18** in a concentrated state. Other standard techniques for crystal growth, such as cooling method, vapor diffusion and solvent diffusion, have also been tested although none of them yielded good results. This is probably caused by the huge difference between the solubility of **18** and **H_2OG**.

2.3.4. The Polymerization of 18/H_2OG salts

Our crystallographic work provided two candidate crystals for the topochemical polymerization study. The designed solvent free structure, **$(18H)_2OG$,** and the unexpected hydrate, **$(18H)_2OG•2H_2O$**. Both of the hydrate and anhydrous salt crystals formed as red plates suggesting that some degree of polymerization was already taking place at room temperature, as shown in **Figure 2.15**.

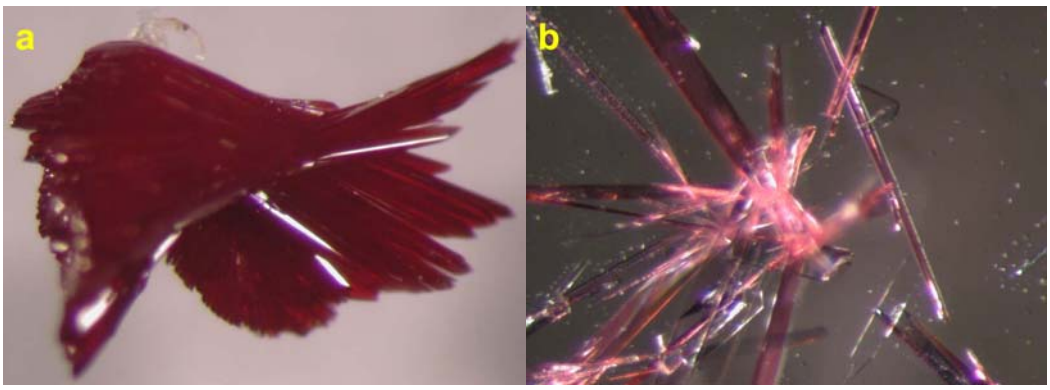

Figure 2.15 Optical images of **$(18H)_2OG$** (a) and **$(18H)_2OG•2H_2O$** (b) single crystals.

In the case of **$(18H)_2OG•2H_2O$**, the crystal structure showed that the monomers were aligned along a glide plane with good structural parameters for a polymerization (**Figure 2.14b**). Heating the crystals turned their color from the original red to a much darker essentially black color. Such color changes are usually indicative of polymerization. The single crystal used for the original structure determination was heated in a controlled manner to 80 °C for 12 hours in a vacuum. A visual examination of the crystal showed a darker color, but numerous cracks had developed and major portions of the crystal simply crumbled away. The crystal was returned to the diffractometer and reexamined. No further diffraction could be observed. Other crystals of the hydrate showed similar changes upon heating. It seems most likely that these changes are due to loss of water

from the crystals. Since the anhydrous crystals were giving us better results we abandoned our studies of the hydrate.

The **$(18H)_2OG$** salt, however, does undergo a SCSC polymerization. This transition was driven by a slow heating protocol over a period of about three months total in order to preserve the crystal integrity, as summarized in **Table 2.2**. At the end of each heating period the same single crystal was returned to the diffractometer and a new data set was obtained. The final one providing enough diffraction peaks for structural solution demonstrated that the degree of conversion from monomer to polymer was about 80% according to the percentage of the atomic occupancies in either of the two forms.

Scheme 2.2 pictures this SCSC transformation. On the left is a view of the crystal structure of the monomer salt. The right hand side shows a similar view of the polymerized structure.

Scheme 2.2

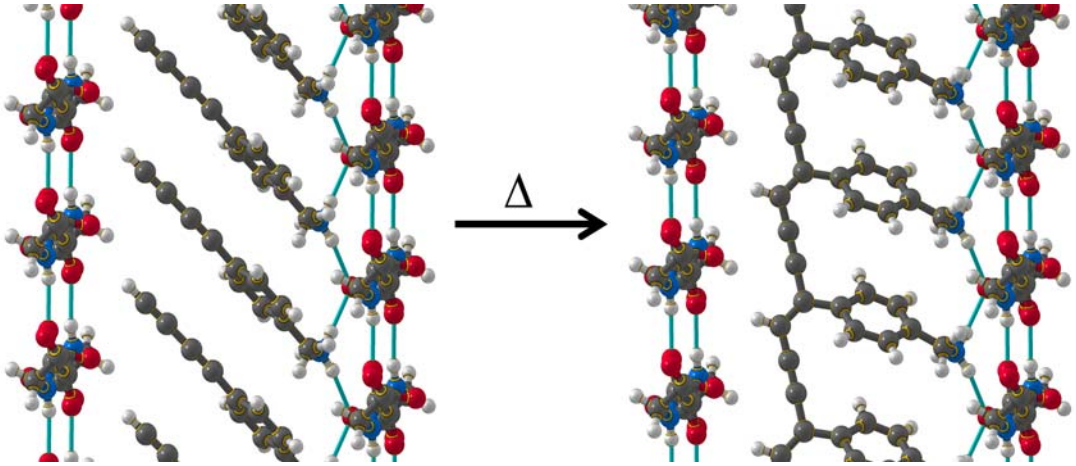

Table 2.2 Single Crystal Annealing History and Resulting Unit Cell Constants of **$(18H)_2OG$** single crystals

	Heating Temp.(°C)	Heating Interval (days)	Cum. Time (days)	a (Å)	b (Å)	c (Å)	α (°)	α (°)	γ (°)	Volume (Å^3)	Percent Polymer
1[a]	'	'	'	4.931(3)	10.017(7)	13.738(9)	85.899(14)	84.56(2)	85.141(16)	671.7(8)	0
2	100	1	1	4.913(2)	10.032(3)	13.752(4)	85.437(6)	84.967(7)	85.201(6)	671.0(4)	11
3	100	2	3	4.908(1)	10.029(3)	13.741(4)	85.123(7)	85.141(6)	85.225(5)	669.5(3)	14
4	100	3	6	4.914(1)	10.048(2)	13.754(3)	84.784(6)	85.293(4)	85.220(6)	672.1(3)	25
5	100	4	10	4.909(2)	10.046(4)	13.738(5)	84.172(7)	85.592(6)	85.255(7)	670.1(4)	30
6	100	7	17	4.912(2)	10.061(5)	13.740(6)	83.478(7)	85.857(10)	85.221(8)	671.0(5)	34
7	100	7	24	4.917(3)	10.075(7)	13.744(9)	82.745(8)	86.223(13)	85.270(10)	672.1(7)	38
8	100	7	31	4.910(2)	10.066(4)	13.723(5)	82.422(6)	86.377(8)	85.273(7)	669.1(5)	45
9	120	7	38	4.901(1)	10.071(3)	13.693(4)	81.027(5)	87.160(8)	85.367(7)	665.0(3)	50
10	130	7	45	4.899(1)	10.075(3)	13.680(4)	80.483(6)	87.538(5)	85.453(6)	663.5(3)	55
11	130	7	52	4.899(2)	10.083(3)	13.690(4)	79.831(7)	88.034(6)	85.553(7)	663.4(3)	57
12	145	14	66	4.886(2)	10.072(4)	13.670(5)	79.154(6)	88.615(9)	85.662(8)	658.8(4)	78
13[b]	160	17	83	-	-	-	-	-	-	-	

a. Experiment 1 gives the cell constants of the monomer crystal before any heat treatment.
b. Experiment 13 destroyed the crystal integrity; no unit cell could be obtained.
c. The percentage of polymerization is a qualitative estimate based upon fractional atom occupations in least squares refinement.

The polymerization is also confirmed by other characterizations. Thermoanalysis was used to evaluate the energetics of the polymerization, as shown by the differential scanning calorimetry (DSC) curve (**Figure 2.16**). The DSC scan at a heating rate at 10 °C/min shows an exothermic peak at 207 °C and an endothermic peak at 266 °C. The exothermic peak appears as expected with a range from 140 °C to 225 °C, indicating the

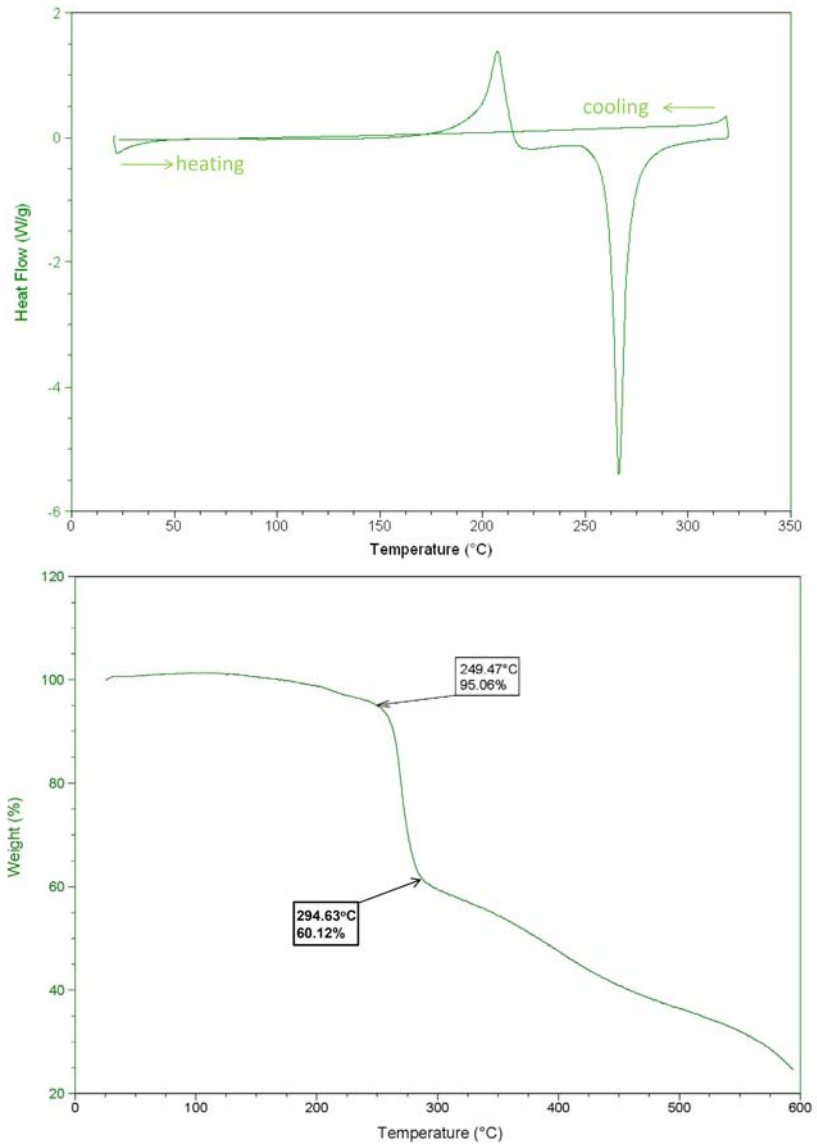

Figure 2.16 DSC (top) and TGA (bottom) scans of **$(18H)_2OG$** (heating rate at 10 °C/min).

topochemical polymerization of the monomers **18** in the salt. Considering that the heating rate of DSC experiment is much faster than the condition we used for promoting the thermally SCSC polymerization, the temperature range of this exothermic peak corresponds well with our annealing process that provided increasing degree of the polymerization according to X-ray diffraction data. The enthalpy of polymerization ΔHp is -31.4 kcal/mol, calculated from the area of the exothermic peak. This value falls in the range of -30 to -40 kcal/mol reported for typical diacetylene solid state polymerizations.[217] The cooling cycle of the polymerized material did not show any peak, indicating that the polymer single crystal is very stable and remains intact in the entire temperature range (up to 325 °C) after solid state polymerization. The absence of typical polymer thermal transition temperatures, such as T_g and T_m, indicates that the expected rigid conjugated polydiacetylene backbone has formed after thermopolymerization.

However, the second peak showing after the polymerization peak is a little ambiguous. The energy associated with this change is dramatically high, indicating a violent endothermic reaction. Since it is known that the host compound **H_2OG** used in this salt shows decomposition also starting at about 245-250 °C, which perfectly matches the starting point of this sharp peak ranging from 250 °C to 300 °C, we believe this endothermic process is presumably related to the decomposition of **H_2OG**. This conclusion is further supported by thermogravimetric Analysis (TGA) result of **(18H)$_2$OG**. There is about 40% weight loss between 250-280 °C, as matches well with the weight percentage of **H_2OG** in the salt.

The FTIR spectra of the **(18H)$_2$OG** crystals were measured before and after annealing (**Figure 2.17**). As expected, the stretching vibration bands of C≡Cs (2202 and 2054 cm^{-1})

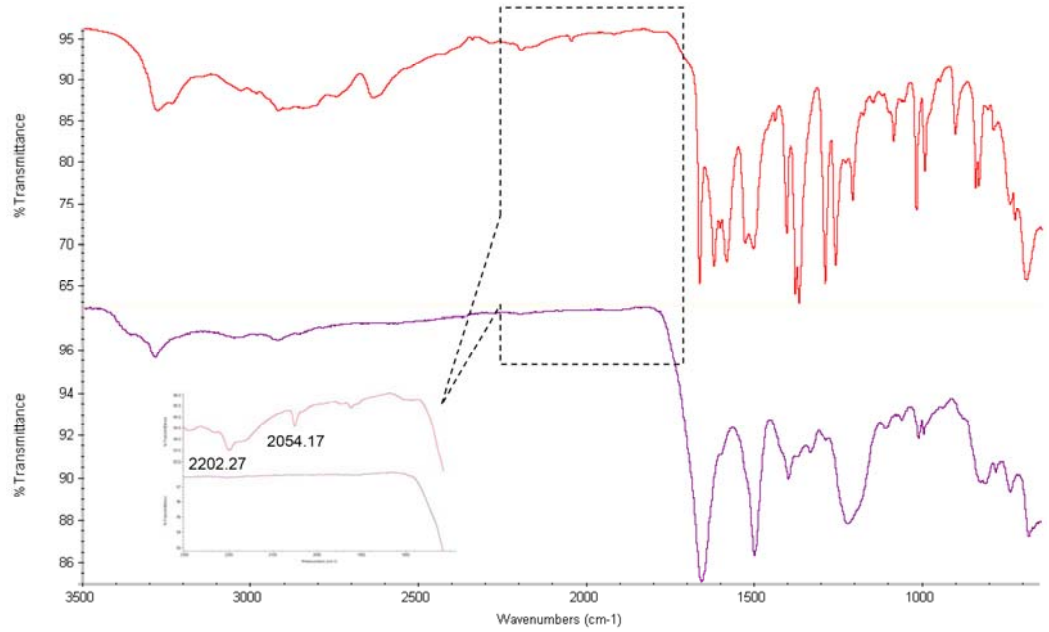

Figure 2.17 FIIR spectra of **$(18H)_2OG$** monomer crystal (top) and polymer crystals (bottom).

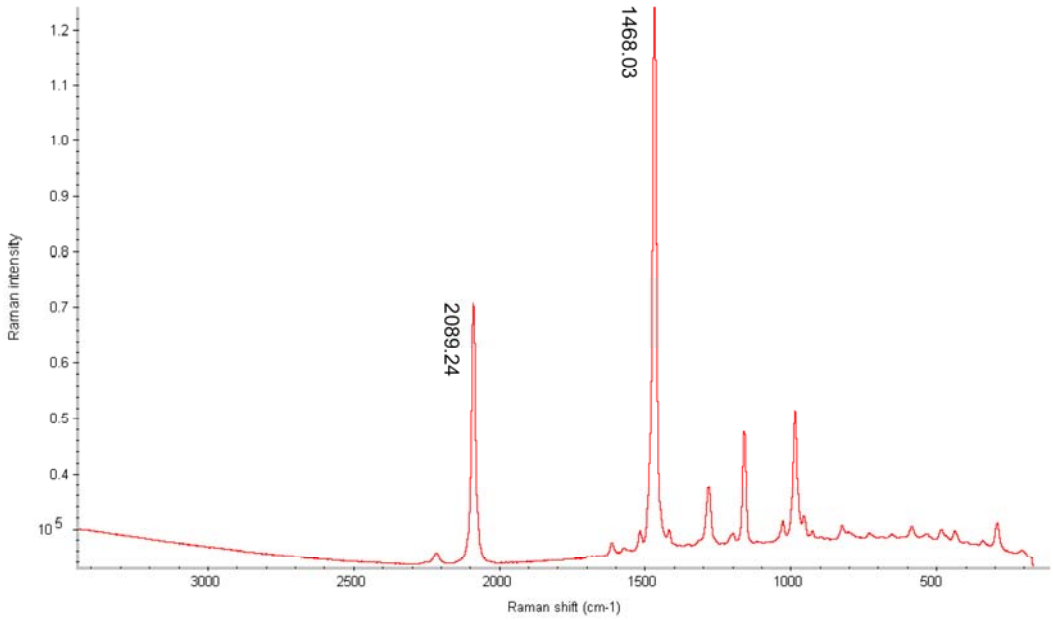

Figure 2.18 Raman spectrum of **$(18H)_2OG$** polymer crystals.

are visible in the monomer because of the asymmetry.[218-224] While after heat treatment, there is no any typical C≡C stretching observed in this region (the inset of **Figure 2.17**). The disappear of C≡C indicates 1,4-polymerization of diacetylenes because in the

resulting polymer backbone the new generated C≡C is much more symmetric than that of monomer. In addition, the band around 1600 cm^{-1} became broader and stronger due to the formation of C=C double bonds.[65] This conclusion is further supported by the Raman spectrum (**Figure 2.18**) of the resulting polymer, where the typical absorption of PDAs can be found at 1468 and 2089 cm^{-1}, respectively, referring to corresponding C=C and C≡C bonds in the backbone.

2.3.5. The Polymerization Mechanism Analysis

A detailed structural analysis of the monomeric and polymeric forms of **$(18H)_2$OG** is shown in **Figure 2.19**. The monomer atoms are colored normally; the polymer in all green. The two structures were superimposed by using closest carbonyl carbon atom of the nearest oxalamide host molecule to establish a common origin. The *z* axis of a common orthogonal coordinate system was defined by the short *a* axes of the two superimposed unit cells. The plane of the two central carbonyl groups was used to establish the *xz* coordinate plane; the *y* axis was normal to this plane. The top of the figure shows a side view of the monomers and the corresponding polymer. The bottom of the figure shows a top view of the same structure and includes the host molecule. The host molecule changes very little during the polymerization reaction, while the monomers move downward bending at the middle C_4 carbon. There is also a sideways movement as seen in the top view. C_4 moves the most by 2.97 Å. The initial monomer spacing of 4.93

Å is very close to the ideal value. The corresponding polymer value is slightly shorter at 4.89 Å. Upon polymerization the phenyl ring turns on its axis by about 50°.

As discussed in the molecular design part (**section 2.2**) we chose to study an terminal aryldiacetylene working on the assumption that the major movement during the polymerization would involve the hydrogen end of the diacetylene and the phenyl end would not need to move much or at all. An examination of **Figure 2.16** shows that the

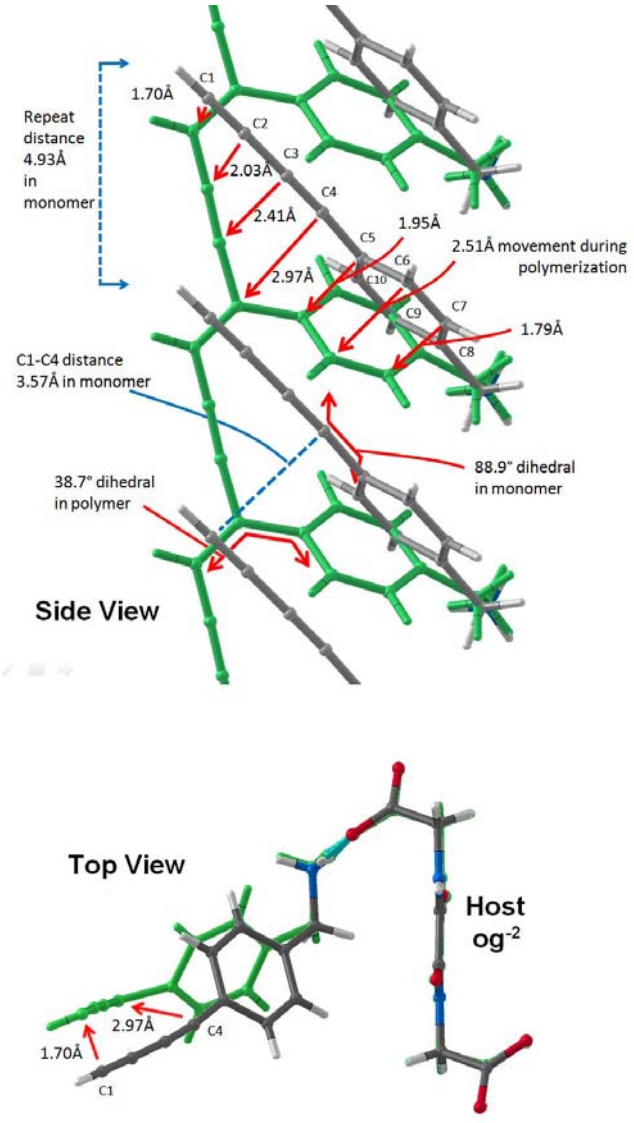

Figure 2.19 Unexpected mechanism of the topochemical polymerization in **$(18H)_2OG$**.

opposite has occurred. The terminal C_1 carbon has moved the least, 1.7 Å, while C_4 next to the phenyl ring has moved the most, 3.0 Å, a very large movement when compared to previous topochemical reactions. The entire phenyl group has pivoted on its axis roughly along the C_8-C_9 bond and moved "downward" and to the side following the C_4 atom. The same phenomena has been observed in the Nakanishi's work, where the authors reported only a 20% polymerization in the monomer crystals.[196]

As mentioned in the introduction of this chapter, the advantage of attaching aromatic pedant groups to the PDA backbone relies on the extension of the π-conjugation system and therefore largely improves the electronic properties of the polymer materials. One thing needs to be clear, however, that the effective extension of the entire π system can be obtained only if the aromatic side groups adopt a conformation co-planar to the ene-yne polymer backbone. Have we succeeded in attaining such a planar structure in the polymer crystal of **$(18H)_2$OG**?

In the monomer structure the phenyl ring has a dihedral angle of 89.9° with respect to the short crystallographic axis of 4.93 Å. In the polymer the phenyl pivot has brought this dihedral angle down to 38.7°. This is essentially as small as this dihedral angle can go since the nonbonded contacts between atoms of neighboring phenyl rings are in van der Waals contact of 3.3 Å (**Figure 2.20**). This result indicates that even in the most ideal

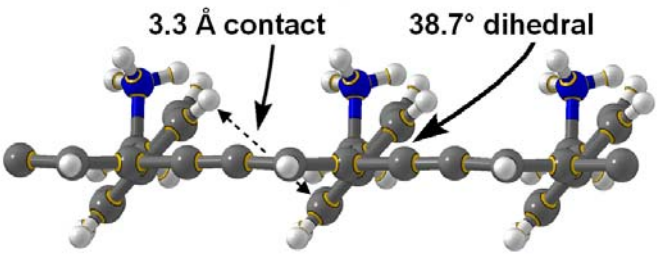

Figure 2.20. The illustration of the relative positions of neighboring phenyl rings along the backbone in the polymer crystals.

case like the one we are showing here, a perfect coplanar polymer structure incorporating the π-electrons from the aromatic side groups is still very difficult to achieve.

Table 2.3 The dihedral angle and the ph-ph contacts in the oligomers of phenyldiacetylene.

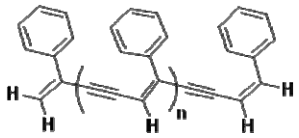	Dihedral Angle (at Minimum Energy)	ph-ph Contact (Å)
n=0, Dimer	56.5 °	4.449
n=1, Trimer	57.2 °	4.517
n=2, Tetramer	58 °	4.571
n=3, Pentamer	58.3 °	4.591
n=4, Hexamer	58.5 °	4.605
n=5, Heptamer	58.7 °	4.618
n=6, Octamer	58.8 °	4.625
n=7, Nonamer	58.9 °	4.631
n=8, Dodecamer	59 °	4.638

Molecular modeling studies on oligomers of phenyldiacetylene somehow support this conclusion. This work was done by Spartan® using density functional theory (DFT) method. As summarized in **Table 2.3**, a series of oligomers from dimer through dodecamer were explored to search for their dihedral angles (with respect to the plane containing oligomers ene-yne chain) corresponding to the molecular conformation with minimum energy. It is clear that the dihedral angle will likely reach down to 60° (starting from 90° in the monomer assemblies and expecting 0° in a planar structure) in an infinite polymer of phenyldiacetylene as the trend shows in the plot of dihedral angle *vs.* number of repeat unit (**Figure 2.21a**). In addition, the contact between neighboring phenyl rings is reaching ~ 4.64 Å (**Figure 2.21b**). The computational data don't exactly match the values observed from experimental results, probably because of three reasons. Firstly, the

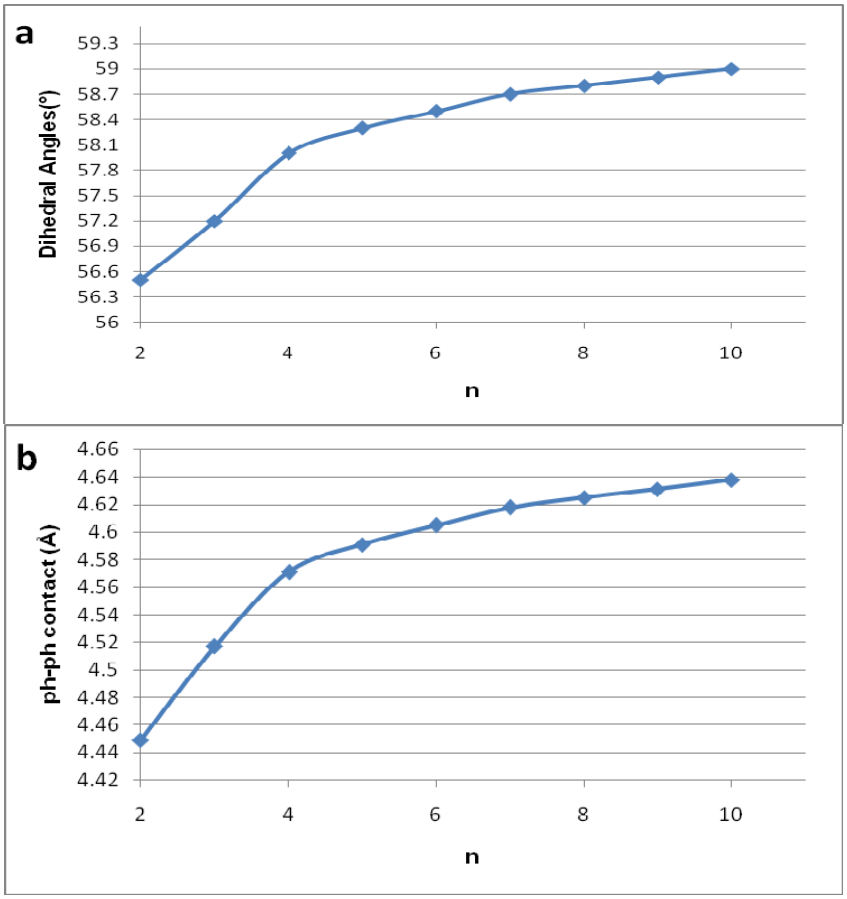

Figure 2.21. Plot of dihedral angles *vs.* n (a) and plot of ph-ph contact *vs.* n (b).

nonbonded constrains existing in the solid state is ignored in the computational models. In modeling, the molecules are completely isolated in the space. The maximum of the phenyl ring's pivot is determined by the most stable conformation where the neighboring phenyl rings start avoiding each other to minimize the energy. However, in crystals the surrounding molecules can introduce space effect to promote a further pivot with more compact orientation. Secondly, the energy contribution gained from more extended delocalization is different in these two situations. Because of the molecular size limit in computational models (only up to ten repeat units), the energy lowering caused by the *p* orbital overlapping will not show too much advantage. In polymer of **18**, the

accumulative effect due to the infinite number (relative to modeling objectives) of repeat units must be dominant and thus favor a more planar conformation to minimize the energy. Lastly, the dipoles in **$(18H)_2OG$** and computational models are also very different. The host-gust salt **$(18H)_2OG$** is an ionic system, while the models are in neutral state. This fact may cause some unexpected influence to the most stable conformation.

Hence, although molecular modeling didn't provide completely positive answer to the most favorable conformation adopted by poly**18**, it still clearly demonstrates that there is a limit for the pivoting of phenyl rings towards the planar conformation.

In order to create a new PDA materials with coplanar aromatic side groups attached to the ene-yne backbone, a less crowded poly(aryldiacetylene) such as the structures shown in **Figure 2.22** may be able to avoid the neighboring conflictions seen in our results and thus provide useful mateirals with the most optimized electronic properties. Although the steric hindrance between the phenyl ring and H atom could still increase the energy barrier in a planar conformation, it should be much less than that seem in the polymer of **18** and similar aryldiacetylenes. Unfortunately, the less crowded poly(aryldiacetylenes) proposed in **Figure 2.22** is a much greater challenge for topochemical polymerization. We haven't been able to come up any good supramolecular architectures for such copolymer-type poly(aryldiacetylenes).

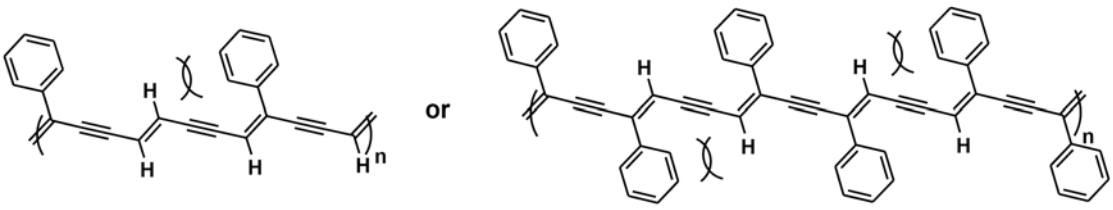

Figure 2.22 Possible poly(aryldiacetylenes) with planar structure.

2.3.6. Why Not the "Swinging Gate" Mechanism?

In our initial design, we hoped that the lately discovered polymerization mechanism found in a termianl diacetylene could also take place to facilitate the SCSC trasfermation in arydiacetylenes. Surprisingly, as we disscused in previous section, the terminal end of **18** moves the least while the phenyl-substituted end moves the most when polymerization proceeds. Such a reaction pathway is totally opposite to the "swinging gate" mechanism. Hence, we were very curious about what is making the free termianl end hard to move.

As dipcted in **Figure 2.23**, when we carefully investigated the surroundings around each terminal diacetylene molecule in the monomer crystals of **$(18H)_2OG$**, the interaction between a **18^+** and a **OG^{2-}** in the next layer caused our attention. There is actually a short H bond between the carboxylate oxygen and terminal diacetylene hydrogen (O---H—C_{sp}). We believe this strong interaction can largely change the actual flexibility of molecule **18**

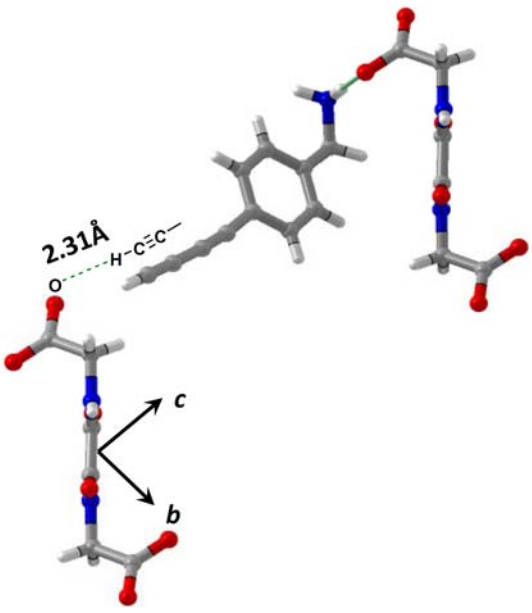

Figure 2.23 The undesired H-bond between neighboring host and guest in **$(18H)_2OG$**.

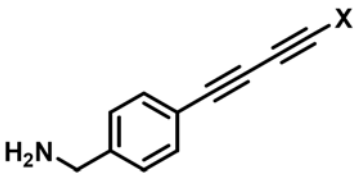

32 X = Cl
33 X = Br
34 X = I
35 X = CH_3

Figure 2.24 Proposed analogues of **18** for breaking the undesired host-guest interaction.

as a reactive species, although we first chose it as the solution to the SCSC polymerization in an aryldiacetylene because of its free terminal end. In the host-guest salt, the termianl ends are simply held by this H-bond trying to stay at where they were since the host $\mathbf{OG^{2-}}$ itself barely moves during polymerization. Therefore, back to molecualr design, we think the "swinging gate" mechamism may still be a very likely reaction pathway if we can eliminate such an undesired interaction between host and guest. The analogues of **18** by capping the terminal end with simple substituents seem to be the most straightfoward modifications at this stage, as proposed in **Figure 2.24**.

2.4. Studies of Diacetylene Analogues 32 - 35

Capping **18** with a halogen atom started from the halidation of azide **31**, which is followed by reduction to generate corresoding amine (**Scheme 2.3**). Unfortunately, these amines are extremly unstable, probably due to the reaction between primary amines and halodiacetylenes.[225]

Scheme 2.3

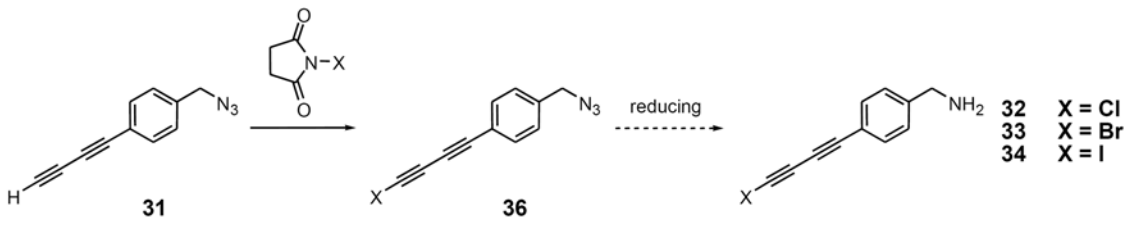

Scheme 2.4

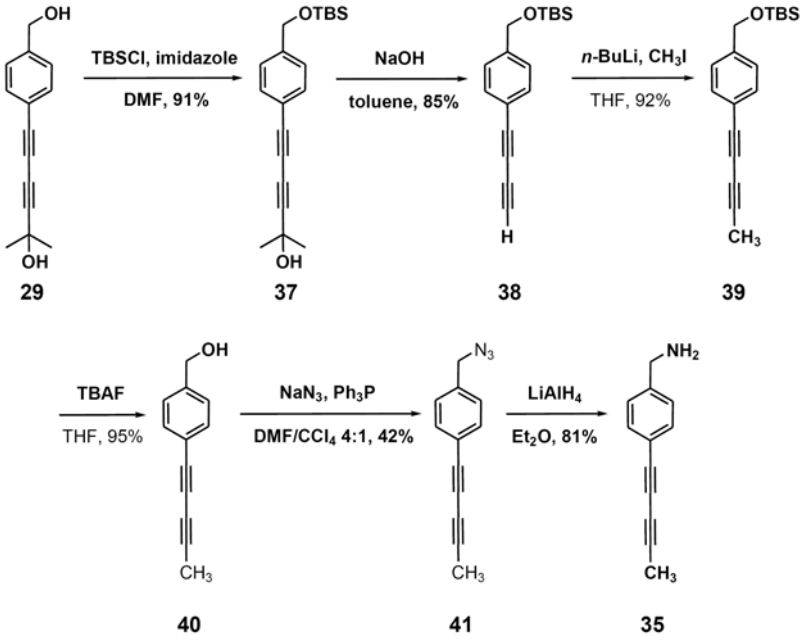

On the other hand, aryldiacetylene **35** was synthesized using the sequence shown in **Scheme 2.4**. Also starting from the intermediate **29** towards the synthesis of **18**, the hydroxyl group was first protected by TBS group. After the acetone protecting group was removed at basic condition, the terminal diacetylene **38** was capped by a methyl group. Removing the TBS group afforded alcohol **40**, which was turned into azide and then reduced to amine **35** using the same reactions applied for **18**. **35** also demonstrates reactivity by itself in condensed state, but it is much more stable than the terminal analogues.

The host-guest salt, **35/H_2OG**, also readily formed the anticipated structure as **(35H)$_2$OG** from wet methanol solution. The crystals are totally colorless, indicating to molecular packing invalid for topochemical polymerization. Indeed, as shown in **Figure 2.25**, although the repeat distance is a little bit shorter than the ideal 4.9 Å, it is still within the appropriate range. However, the declination angle is about 15 ° more than the

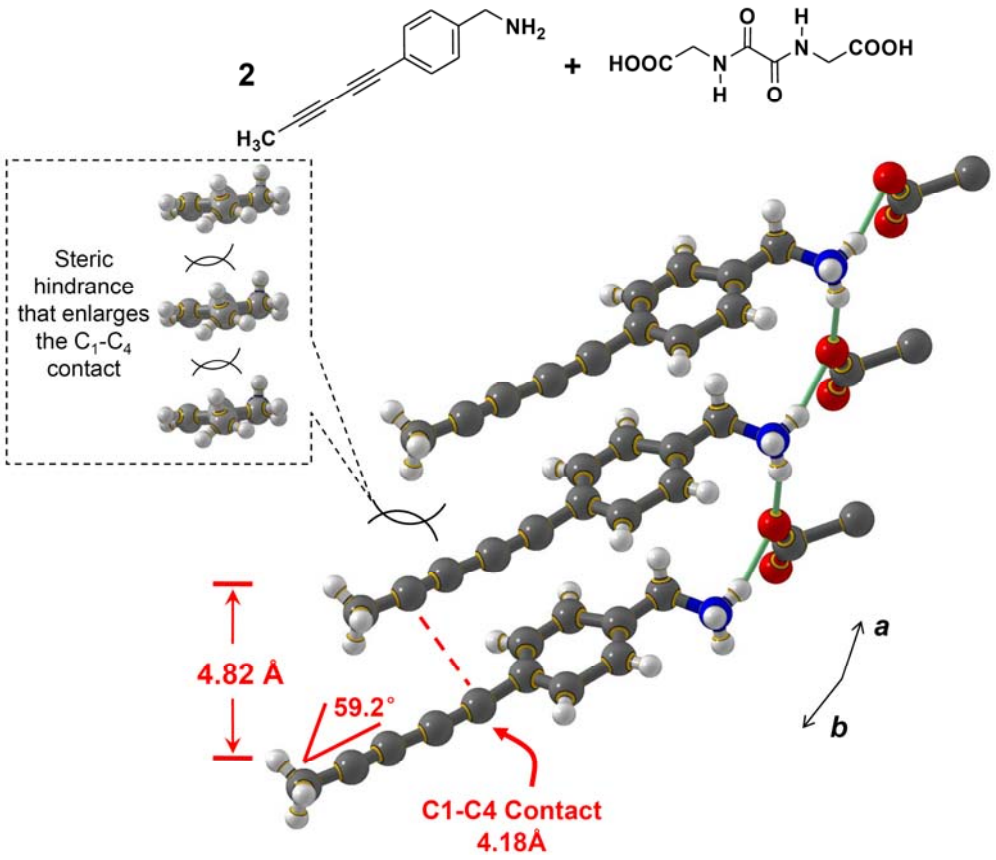

Figure 2.25 Crystal structure of **$(35H)_2OG$**.

proper one. As a result, the C_1-C_4 contact is around 4.2 Å, which is too long for the possible polymerization. Presumably, this is caused by the steric effect introducing by the methyl group.

The annealing treatment was applied on the crystals of **$(35H)_2OG$**. With the increase of heating temperature, the single crystal of **$(35H)_2OG$** turned from colorless plate into soft purplish rubber-like material. There was no melting up to 300 ºC. Due to the poor packing of diacetylenes, diffraction experiment didn't show any sign of topochemical polymerization in the heated sample, which eventually lost the crystalline feature.

In this section, modified phenyldiacetylenes were synthesized in order to explore the possibilities of polymerize aryldiacetylenes through the "swinging gate" pathway.

Although no success was made in our design yet, it is certain that the unsymmetrical aryldiacetylenes are the most promising objectives. It also shows how subtle that a minor chemical change in the diacetylene monomer can modulate its molecular packing as well as topochemical reactivity.

2.5. Studies of Diacetylenes 19 and 20

We also studied the other two terminal aryldiacetylenes on our candidate list. Compounds **19** and **20** were synthesized as shown in **Scheme 2.5** and **Scheme 2.6**.

Scheme 2.5

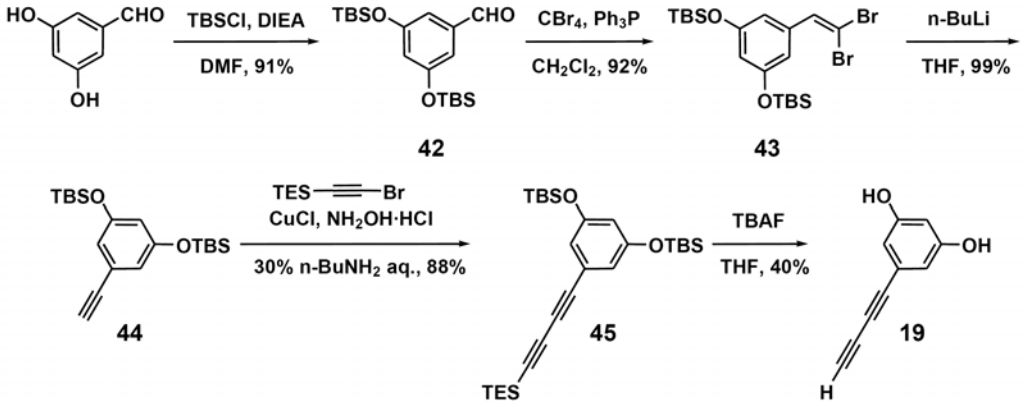

The synthesis of **19** was started from 3,5-dihydroxybenzaldehyde. After TBS protection, aldehyde **42** was treated by Corey-Fuchs reaction condition to afford the terminal acetylene **44** in decent yield. Followed by a standard Cadiot-Chodkiewicz cross coupling with (bromoethynyl)triethylsilane, **44** was transformed into protected diacetylene **45**. In the final step, all three silyl protecting groups were removed by TBAF to generate the desired terminal aryldiacetylene **19**. Unfortunately, this diacetylenic

resorcinol was turned out to be extremely unstable, even in solution. The most optimized isolation was carried on column chromatography. However, once the solution was concentrated to certain point, intractable dark precipitates started to form. Therefore, the successful preparation of **19** was only confirmed by H^1 NMR using a sample with the residue of eluting solvent (ethyl acetate) from flash chromatography.

As for **20**, the synthesis is straightforward except that the proper procedure involving a hydrolysis→esterification→hydrolysis process was used in order to avoid the trouble caused by the instability featuring terminal phenyldiacetylene, similar to that of **19**.

Scheme 2.6

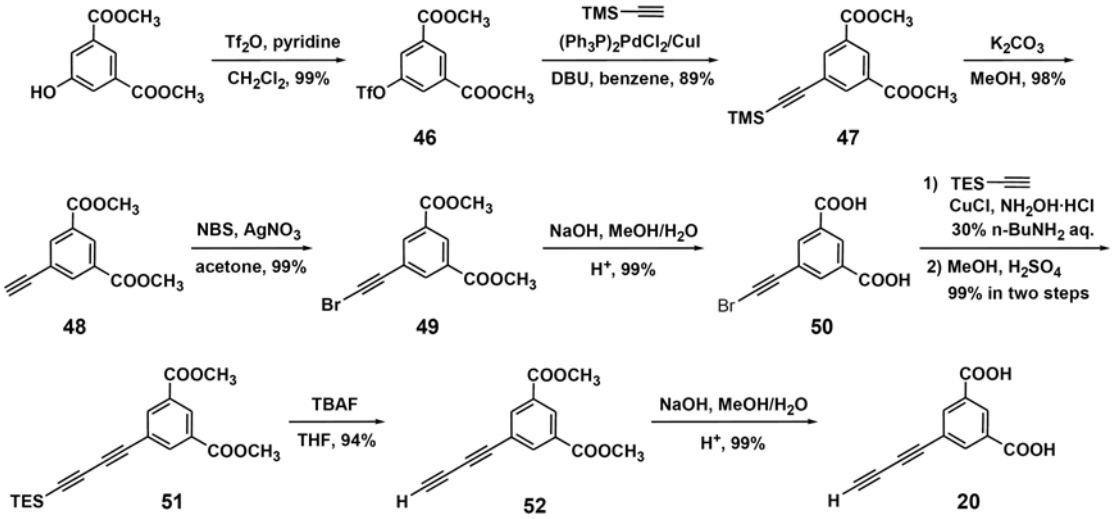

Beginning with the hydroxyl activation of dimethyl 5-hydroxyisophthalate by triflic anhydride, the triflate **46** was coupled with trimethylsilylacetylene to afford the TMS protected phenyl acetylene **47**. In the next step the weak base treatment took off the TMS group and yielded the terminal acetylene **48**, which was transformed to bromide **49** using NBS bromination. The next step should be Cadiot-Chodkiewicz coupling of **49** and triethylsilylacetylene. However, it is found that under the standard Cadiot-Chodkiewicz

coupling condition there was unexpected reaction between the ester group and one of the reagents, *n*-butylamine, yielding an amide as the major product. I had to hydrolyze dimethyl isophthalate **49** to its dicarboxylic acid form **50** prior to the Cadiot-Chodkiewicz coupling, which generated the TES protected diacetylene in it acid form as well. Although in principle a simple deprotection would give the final product, it's not a practical way of getting **20** with acceptable purity due to its instability. Therefore the dicarboxylic acid was converted to its methyl ester after the cross coupling reaction to give isolated intermediate **51** by flash column chromatography. After removing the TES group, the terminal phenyldiacetylene **52** was released in the methyl ester form, which seemed to be more stable than the target molecule **20**. For the sake of deactivation, methyl ester **52** was kept in freezer as a stock solution in ether and whenever needed the fresh **20** can be prepared quickly by a simple step of hydrolysis.

Pure fresh terminal aryldiacetylene **20** was cocrystallized with four different pyridyl hosts listed in **Figure 2.4**. As the host and guest are both bifunctional for H-bonding interactions, we were expecting to get the 1:1 cocrystals, like our first terminal diacetylene case in which the two carboxylic acid groups of each diacetylene molecule both H-bond to the pyridine N of the hosts. (**Figure 2.26a**).

However, after trying various single crystal growth methods and conditions we were only able to get the cocrystals of **20•(4PyO)$_2$** and **20•(4PyU)$_2$**, both in the 2:1 form and having similar crystal structures (except that the urea group is disordered in **20•(4PyU)$_2$**). **Figure 2.26b** shows the crystal structure of **20•(4PyO)$_2$** looking along the *a* axis that parallels the H-bond α-network of the oxalamides, the two carboxylic acid groups of each diacetylene H-bond differently, one to the pyridine in the host and the other to one

−COOH of the neighboring guest molecule, forming a carboxylic acid dimer. The spacing of the diacetylene units in this cocrystal system is deviated greatly from the valid packing for topochemical polymerization. In both of these two cases, the polymerization of the terminal aryldiacetylene was not observed.

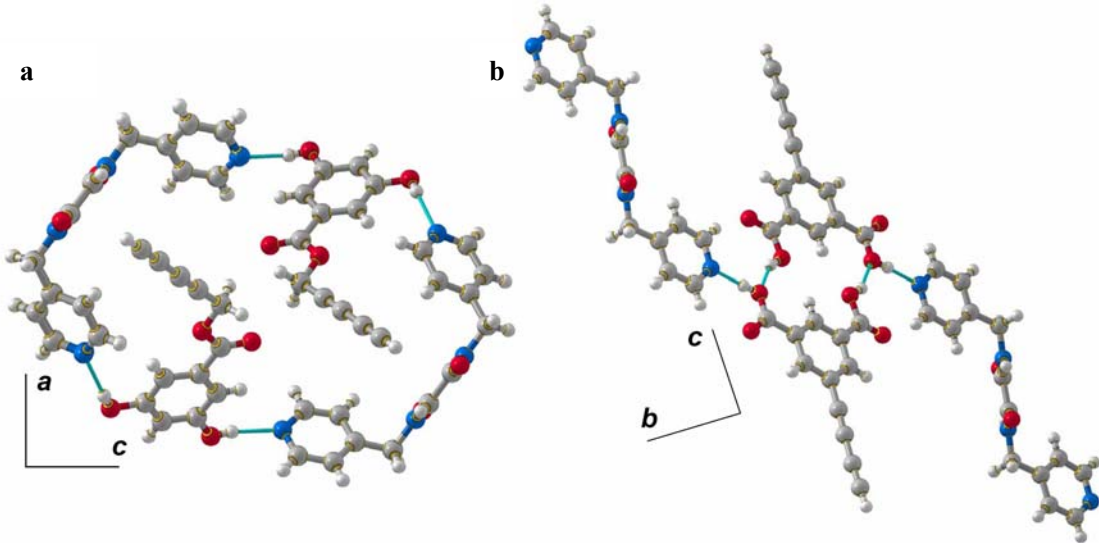

Figure 2.26 Cocrystal structures of (a) **15•4PyO** and (b) **20•(4PyO)$_2$**.

2.6. Attempt to Polymerize Alkyl Aryldiacetylenes

The successful SCSC polymerization yet totally unexpected mechanism found in the terminal aryldiacetylene case of **18** implies that our initial thoughts about using mono aryldiacetylene as the solution to such long-standing goal are essentially reasonable while the perspective about the freedom of these novel aryldiacetylene could be somehow arbitrary. At least in this particular case, the terminal end of **18** lost its flexibility in the supramolecular assemblies due to unexpected H-bonds. Thus in addition to the terminal

aryldiacetylenes discussed in previous sections, we also chose alkyl aryldiacetylenes, **21** and **22** for example, as the guest molecule in the salt or cocrystal systems. The methylene group in such molecules seems to have moderate freedom associated with the structural adjustment as the polymerization proceeds according to our own experience as well as many other literature results.

2.6.1. The Synthesis of 21 and 22

Different number of methylenes between the diacetylene moiety and the H-bonding functional group is known to be critical for providing the supramolecular architecture for readily topochemical polymerizations of many symmetrical diacetylenes and a so-called odd-even effect is generally referred to such observations. Although there is no such obvious relationship regarding to the corresponding crystal symmetry for our unsymmetrical aryldiacetylene systems, it still would be worth of exploring the supramolecular properties of a series of homologues with increasing number of methylenes.

The procedure shown in **Scheme 2.7** was followed to synthesize the **21** series. Compound **21a** (n = 1) was not obtained because in the hydroxyl activation step from **54** to **55** the homoether (**55a'**) of the substrate formed almost immediately once the tosulate was generated. As for the low yield from **54b** to **55b**, it was caused by the unavoidable α-elimination of the corresponding tosulate which yielded a side product as an ene-diyne.

Scheme 2.7

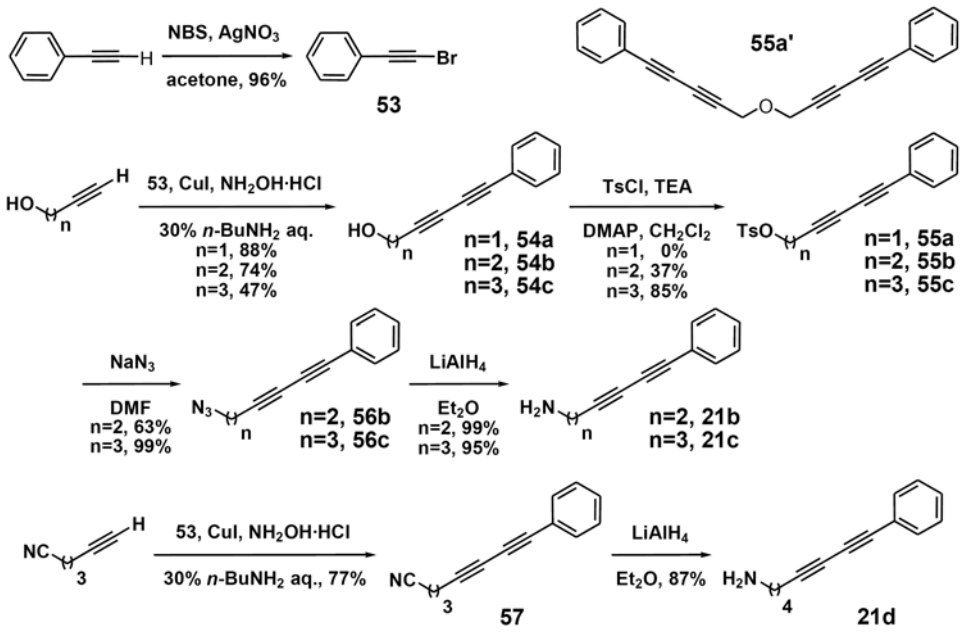

The **22** series were simply synthesized in a one-step reaction shown in **Scheme 2.8**. The Chodkiewicz-Cadiot coupling was modified to optimize the yields and **22b-d** (n = 2-4) were obtained for the crystallography experiments.

Scheme 2.8

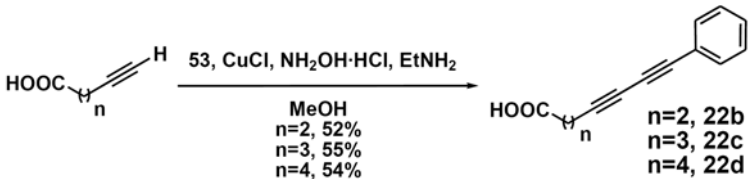

2.6.2. The Salts of 21

21b-d was used to prepared the corresponding salts with **H_2OG**, however, only the even-number guests, **21b** (n = 2) and **21b** (n = 4), were able to form salts as high quality

single crystals. Unfortunately, in both of two cases the critical H-bond α-networks among the host molecules were not found. Instead, all of the six oxygen atoms in each **H_2OG** form H-bonds individually with ammoniums of six different guest molecules, as are indicated by arrows shown in **Figure 2.27a** and **c**.

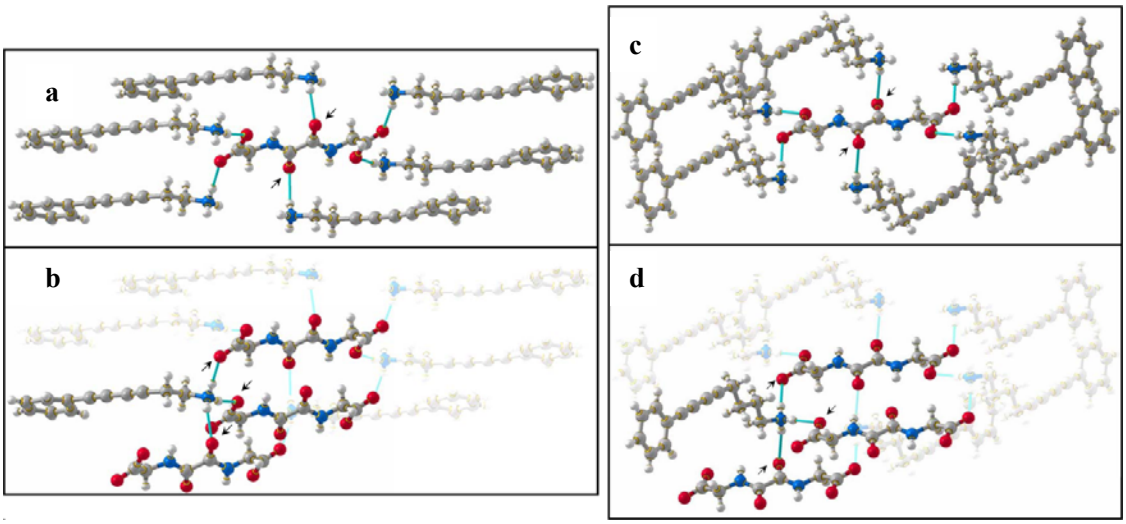

Figure 2.27 Host-guest interactions: (a) and (b) **(21bH)$_2$OG**; (c) and (d) **(21dH)$_2$OG.**

According to the model study, the salts of **H_2OG**/greasy primary amines should form salts with independent H-bond α-networks and carboxylate/ammonium interactions. But the situation in cases of **21b** and **21d** does not fit in this conclusion. The reason is probably because of a strong intramolecular H-bond between the carboxylate oxygen and the amide hydrogen in the deprotonated host of both of these two salts, as may interfere with the formation of the desired H-bond α-networks. These intramolecular H-bonds seem to be the result of a remarkable twist (a rotation of 92.3º by comparing the "good" structure with the "bad" structure, as shown in **Figure 2.28**) along the CH_2−NH bond in glycine part of the host, which brings the carboxylate oxygen close enough to the amide hydrogen to form a strong intramolecular H-bond (2.35 Å). Such abnormal structural misbehaver of the **OG^{2-}** was not observed in any of the obtained structures in the model

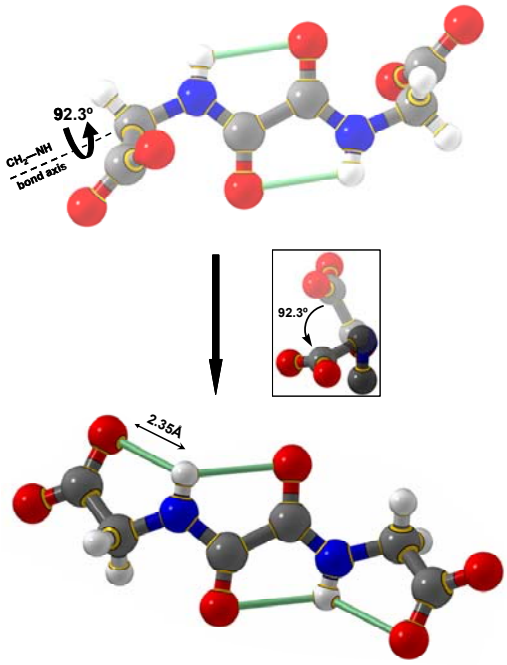

Figure 2.28 Illustration of intramolecular H-bond caused by the twist at CH_2 of the host in $(RNH_3)_2OG$ salts. Top (light colored): OG^{2-} in **(18H)$_2$OG**; Bottom (dark colored): OG^{2-} in **(21dH)$_2$OG**; Inset: overlap of the two hosts (viewing along the CH_2–NH bond axis and for clarity, only half of the molecule is shown and hydrogen atoms are omitted).

systems or the **18** salt, indicating that this may not be the most favorable structure adopted by **H_2OG** in crystals. And to the best of our knowledge, it is also rarely seem. According to CSD, there is only one similar example documented, also from our group.[46] Therefore due to the wrong connections among molecules in both **(21bH)$_2$OG** and **(21dH)$_2$OG**, it is not surprising that neither of these two salts has the desired alignments for the diacetylene units in their crystals.

Scheme 2.9

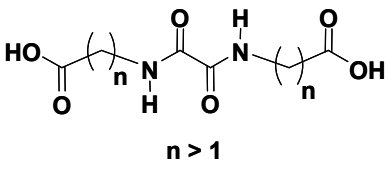

Further efforts have been made using analogues of **H_2OG** such as hosts shown in **Scheme 2.9**, with the reasoning of breaking the undesired intramolecular H-bond by elongating the distance between amide and carboxylate groups. However,

no suitable single crystals were ever obtained.

2.6.3. The Cocrystals of 22

Compounds **22b-d** were used to prepare the corresponding cocrystals with **3PyU**, **4PyU**, **3PyO** and **4PyO**. Although in all of the as-obtained cocrystals the host-guest Supramol. Chem. is found correctly, the packing parameters seem to be unsatisfactory for topochemical polymerization in all cases except **(22b)$_2$•4PyO** (highlighted in red), as summarized in **Table 2.4**. Even in cocrystal **(22b)$_2$•4PyO** the C_1-C_4 contact is 3.68 Å,

Table 2.4 The packing parameters in cocrystals of **22**.

Cocrystals	**d** (Å)	**γ** (°)	**$R_{1,4}$** (Å)
(22b)$_2$•3PyU	4.95	53.1	3.91
(22b)$_2$•4PyU	4.60	61.5	4.36
(22b)$_2$•4PyO	5.09	46.7	3.68
(22c)$_2$•4PyU	4.66	62.4	4.45
(22c)$_2$•3PyO	4.99	63.8	4.72
(22c)$_2$•4PyO	5.22	46.6	3.97
(22d)$_2$•4PyU	4.66	60.1	4.16
(22d)$_2$•4PyO	5.08	47.6	3.81

which is a close distance comparing to the ideal value of 3.5 Å but still not good enough for an aryldiacetylene SCSC polymerization. Moderate heating below its melting point was able to make the color of the original cocrystal turn from white to deep blue, indicating partial polymerization of the guest diacetylene in solid state. Unfortunately, further thermal annealing experiments on the deep blue single crystal either made it disappear by sublimation or destroyed its crystallinity. The sublimation was observed

when maintaining the moderate annealing temperature while increasing the treatment time. Instead, heating the sample in capillary tubes to avoid sublimation and treating at elevated temperature destroyed the sing crystal lattice. UV-irradiation was also applied to the crystals of **(22b)$_2$•4PyO**, but no sign of SCSC polymerization was detected in the single crystal diffraction experiments although the UV-irradiated single crystals became darker and insoluble materials were generated, indicating the formation of polymeric diacetylenes.

It is noticed that all these eight cocrystals show certain common feature in their packing, especially the intermolecular relationship between the diacetylene monomers. Using the cocrystal structure of **(22b)$_2$•4PyO** as an example as depicted in **Figure 2.29**, there is an obvious slip that prevents the face-face stacking of the phenyl diacetylene moieties. This is a commonly seen phenomenon in the π-π stacking of aromatics. However, this kind of slip should be avoided in our work because it clearly extends the

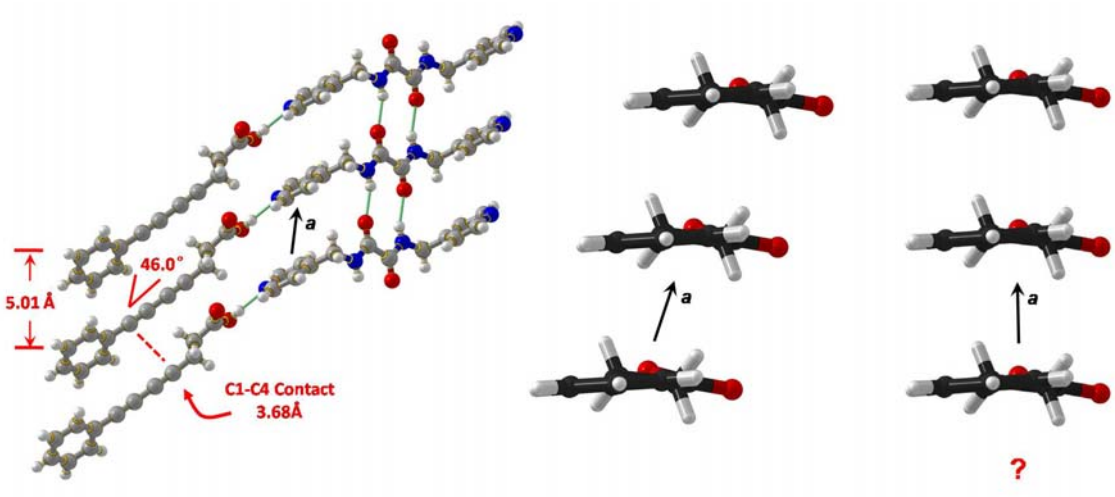

Figure 2.29 The structure of cocrystal **(22b)$_2$•4PyO** (left); the slipped stacking of **22b** looking into the diacetylene axis (middle) and the desired face-face stacking for reducing the diacetylene intermolecular contact (right). The arrow shows the unit cell *a* axis.

distance between the diacetylene units. In a face-face stacking, on the other hand, the diacetylene spacing should be shorter and more likely for aryldiacetylene SCSC polymerization. Given the reliable Supramol. Chem. shown in these cocrystals, if there is an additional way of forcing the face-face stacking, we should be able to significantly increase the possibilities of the SCSC polymerization in these cocrystals.

The phenyl-perfluorophenyl stacking interactions were considered to achieve this goal. Now the task is shifted to create a three-component cocrystal system, with an expected structure shown in **Figure 2.30**.

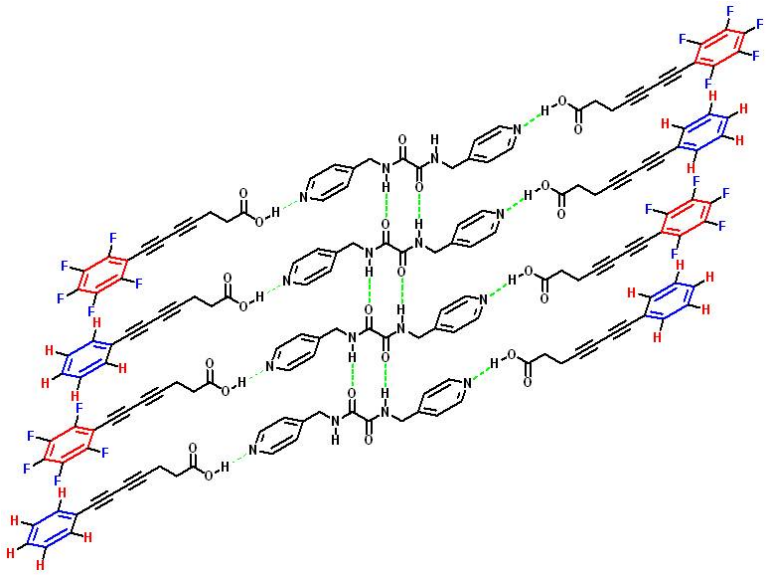

Figure 2.30 The sandwich-type structure in the three-component cocrystal system designed for the promotion of a face-face stacking of aryldiacetylenes. Blue and red colors indicate the partial negative and positive portions respectively in the phenyl moieties.

In this design, both the H-bonding and phenyl-perfluorophenyl interactions will facilitate the desired control of the aryldiacetylene stacking. In addition, in the new plan the number of methylene spacers should be the same in both two guest molecules to minimize any uncertain factors that could affect the molecular packing. Therefore, the

perfluoro counterparts of **22b-d** needs to be prepared. This was done by the sequence shown in **Scheme 2.10**.

Starting from the Sonogashira coupling between trimethylsilylacetylene and perfluorobromobenzene, acetylene **58** was obtained. Due to strong tendency of OH substitution at the *para* position and the great volatility of the product, extra care is needed in the following deprotection of silyl group in order to get a good yield for the terminal acetylene **59**. After a standard procedure of NBS bromination, bromide **60** was prepared. In the final step, Cadiot-Chodkiewicz coupling condition afforded target perfluorophenyl diacetylenes **61b-d** in moderate yields.

Scheme 2.10

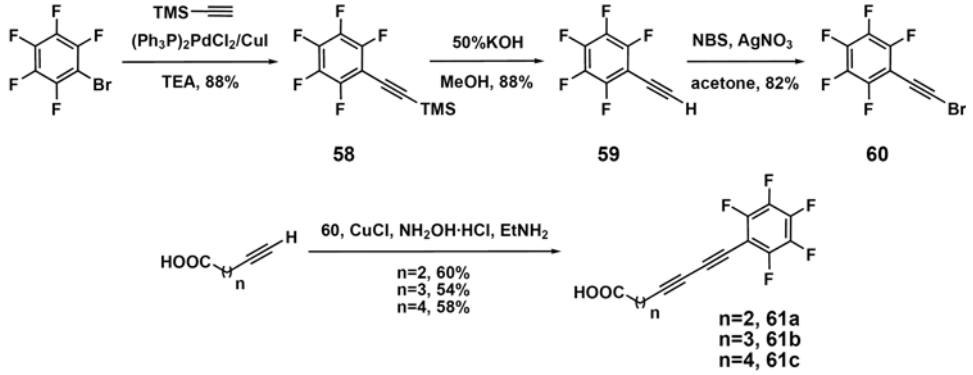

Although the building blocks of the three-component cocrystal system are not difficult to prepare, the assembly of such system is expected to be a great challenge. Compared with the well studied two-component cocrystals, the three-component ones would be far more complicated in many aspects, such as the solubility issues, the manners of supramolecular connections between each component and so on. As a result, the examples of three- or other multi-component cocrystal systems are rarely seen in literature. According to our new design, the cocrystals made of **22**, **61** and **host** with a

stoichiometry of 1:1:1 in moles are expected to have a formula of **22•61•host** and similar crystal structure shown **Figure 2.27**. The preliminary results are somewhat encouraging. For example, the cocrystals of **22b•61b•4PyO** slowly turned from white to purple at room temperature, indicating the correct monomer packing and consequent partial topochemical polymerization. In addition, the cocrystals show a melting point different from any of the three components as well as those of any possible two-component cocrystals. Unfortunately, no large single crystal was obtained from this system although the cocrystals look very crystalline under microscope. Therefore we turned to X-ray powder diffraction for revealing the molecular structure information of these cocrystals. This part of the work is in collaboration with Professor Peter Stephens and his student Kevin Stone, Department of Physics and Astronomy at Stony Brook University. This part of work is still in progress.

2.7. Conclusion remarks

In order to achieve the SCSC polymerization of aryldiacetylene, various monoaryl diacetylenes were synthesized and tested for their possibilities of topochemical polymerization. This long-standing goal was finally realized in the host-guest salt of a novel terminal phenyldiacetylene. The structural analysis of both the monomer and polymer crystals illustrated that the polymerization undergoes via an unexpected mechanism in which the movement of the whole rigid phenyl ring is involved in such a challenging monomer→polymer transition.

Chapter Three

Synthesis and Characterizations of Soluble PDAs

3.1. Introduction

As stated in Chapter One, there is little published example that has investigated the detailed structure and properties of PDAs as compared to the other well-defined polymers. Except for poly(*n*-BCMU), poly(PTS) and very few others, most of the PDAs are used directly after polymerization, without thorough isolation and characterization on the polymer itself. This situation is somewhat understandable considering the synthetic difficulty and poor processability of PDAs.

Being the most extensively studied PDAs, poly(*n*-BCMU)s are prepared from their monomer crystals. They also have excellent solubility in organic solvents, so that many fundamental studies regarding to their molecular structures, properties and interrelationship are possible. These materials have been studied in various physical states, such as extreme dilute solutions,[226] solutions,[106] gels[107,117,118] and solid states.[109] Most of the knowledge that have been gained by today to explain the general mechanism of PDAs chromism properties are based on the relative results found in the studies on poly(*n*-BCMU)s.

The same solubility problem actually extends to the entire CPs family. Polymer chemists have long sought to prepare soluble CPs in order to modulate their structures and properties. The introduction of greasy side chains onto the conjugated backbone has

been proven to be a breakthrough to improving the solubility,[227,228] even though this strategy will usually sacrifice partial ECL which is critical to the macroscopic properties of the corresponding materials. Another approach is to attach charged pedant groups onto the CPs backbones.[229] The modified polymers will possess solubility in aqueous media and/or polar organic solvents.

As a special class of CPs, the water soluble ones have received considerable interest very recently.[230] A new name, conjugated polyelectrolytes (CPEs), has been coined and widely accepted. Not surprisingly, CPEs naturally combine the ability of forming tunable complex supramolecular architectures, originating from the conventional polyelectrolytes,[231] with the distinctive optical and electronic properties, inherited from the parent CPs. More importantly, since these properties are very sensitive to the CPE supramolecular structures that respond strongly to local chemical and physical perturbations. They are more tunable compared to that of their CP counterparties. Therefore, CPEs are very good candidates for sensory materials, particularly for biological systems due to their water compatibility and the characteristics analogous to the natural biomacromolecules (proteins, DNAs and RNAs) due to a similar charge density along the polymer backbone.[232-235]

3.2. The Synthesis of Poly(octa-5,7-diyn-1-amine)

In the first project of this dissertation research, the success in control the supramolecular structure of a salt formed by aryldiacetylenic amines and carboxylic acids not only lead to the first SCSC polymerization of aryldiacetylenes, it also implied that PDA-based CPEs may be prepared in the same way. As shown in **Scheme 2.2**, after topochemical polymerization of **$(18H)_2$OG** the resulting PDA is charged because of the ammonium cations. Unfortunately, even after the host carboxylic anions were removed by aqueous base extraction, the neutral PDAs of **18** showed no solubility in either organic solvents or aqueous acids. This result indicates that the charge caused by ammonium cations attached on polymer backbone is still not strong enough for solubilizing the hydrophobic mainchain as well as the phenyl side groups. In order to improve the water solubility, a less greasy monomer analogue to **18** seems to be necessary. A group of new diacetylenic amines were designed and synthesized as shown in **Scheme 3.1**. The synthesis of **66b-c** is essentially the same as the preparation of **21b-c**.

Scheme 3.1

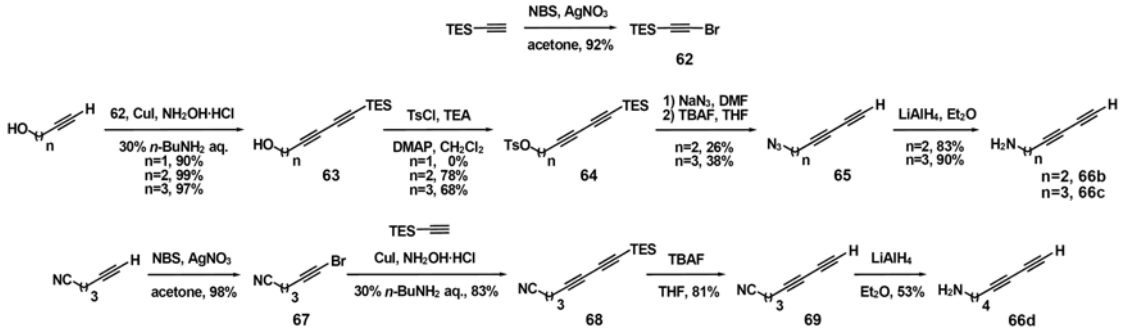

Using these new terminal diacetylenes, I was able to obtained one polymer from the salt of **$(66dH)_2$OG**, as confirmed by single crystal X-ray diffraction. The crystal structure

is turned out to be unexpected. Different from the designed manner, as shown by the model studies and the salt of **$(18H)_2$OG** discussed in Chapter Two, there is no amide-to-amide H-bonding α-network as expected (**Figure 3.1**). It seems that in this case the hydrophobic-hydrophobic interactions between the greasy tails of the amines are not strong enough to help the segregation of strong and weak H-bonds. Luckily, the guest molecules still pack with a separation of 4.8 Å. After heating treatment at a moderate temperature, 100% polymerization transition was obtained with a SCSC process. However, the polymer of **66d** didn't show an obvious improvement in its water solubility compared with poly**18**. This result is somehow reasonable considering that monomer **66d** is the most hydrophobic one in the series of **66**, probably similar to **18**. Unfortunately, the proper salts of both **66b** and **66c** could not be formed. Therefore, I still don't know if a water soluble cationic PDA can be made from these two monomers.

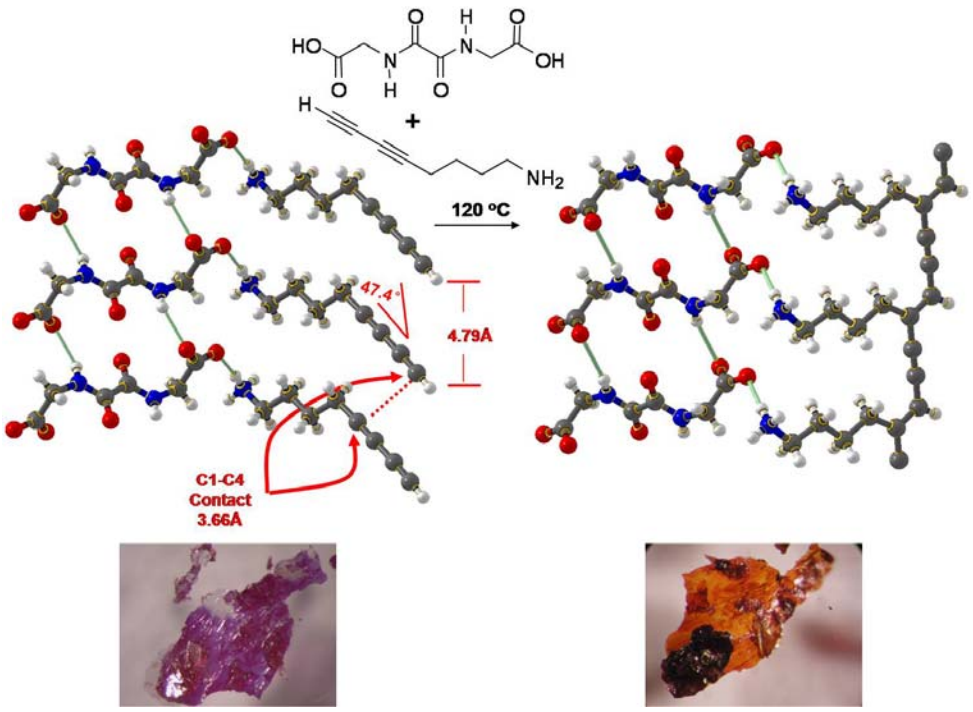

Figure 3.1 The topochemical polymerization of salt **$(66dH)_2$OG**. The partially polymerized monomer salt crystals turned from blue to yellow polymer crystals smoothly.

3.3. The Synthesis of Poly(deca-4,6-diynedioic acid)

Fortunately, there is one case in which the as-obtained PDA shows excellent solubility in weak aqueous base due to the dicarboxylic acid groups installed in the monomers initially for host-guest H-bonding. This result was actually discovered by a previous colleague in the group.[236] But no solution studies were conducted. In this section, some new results of the synthesis and characterizations of this neat soluble PDA will be discussed.

This particular water soluble PDA is made from a diacetylenic dicarboxylic acid, deca-4,6-diynedioic acid **70**. This symmetric diacetylene monomer can be easily synthesized by the homocoupling of 4-pentynoic acid under the Hay coupling conditions, as shown in **Scheme 3.2**.

Scheme 3.2

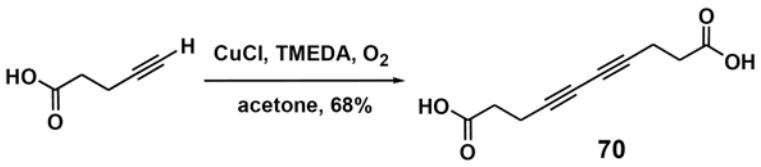

Scheme 3.3

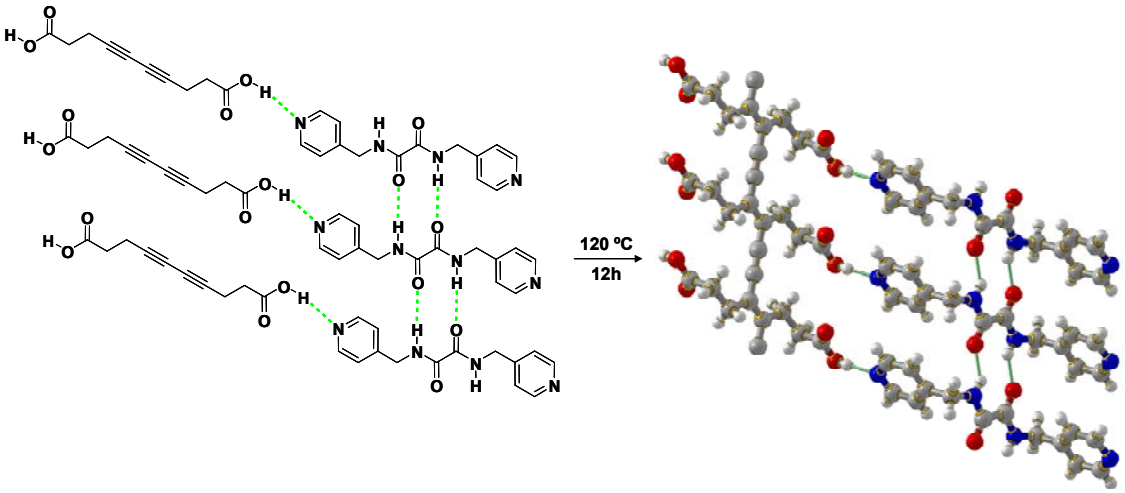

Once cocrystallized with **4PyO**, the diacetylenes are packed so perfectly that the topochemical 1,4-polymerization occurs spontaneously leading to polymer crystals. The monomer single crystals were never obtained, thus the packing parameters of **70** in its cocrystals remain unclear. **Scheme 3.3** shows the schematic cocrystal of **70•4PyO** and the crystal structure of the resulting polymer.

The freshly-prepared **70•4PyO** cocrystals are pinkish needles, which can be transferred to 100% polymer crystals with metallic luster after annealing at 120 ºC for 12h, as shown in **Figure 3.2**.

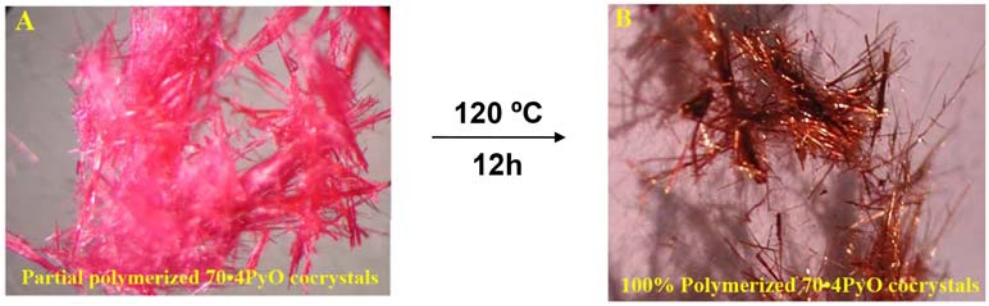

Figure 3.2 The optical images of partial polymer cocrystal (A) and 100% polymer cocrystal (B).

As mentioned before, the polymer shows great aqueous solubility in its ionic form. In fact, the polymer cocrystals are also soluble in weak aqueous base. Such a property offers an opportunity of isolating the polymer of **70**, poly**70**, as a pure polymer from the host-guest system. In principle, in each host-guest PDA systems the non-polymer components (including the host molecules, unreacted monomers and short oligomers) can be removed by extraction. Unfortunately, there is no guarantee that all of these impurities could be completely removed since the extraction process basically relies on the efficient diffusion of solvent molecules into the crystal lattice. It actually would be very difficult for the

solvent molecules to thoroughly diffuse into the highly packed crystalline or semi-crystalline PDA host-guest assemblies. However, in the case that the PDA cocrystals are soluble, the situation is totally different. By dissolving the cocrystals in weak aqueous base, the crystalline phase is totally broken up and a clear solution of the host-guest system is obtained. When the resulting solution is acidified, poly**70** starts to precipitate and can be collected and easily cleaned by filtration and rinsing. In addition, the as-obtained poly**70** can be further purified by removing the short oligomers using a dialysis protocol on its sodium salt form of $\mathbf{Na}^{+}$poly**70**$^{-}$ to narrow the molecular weight distribution.

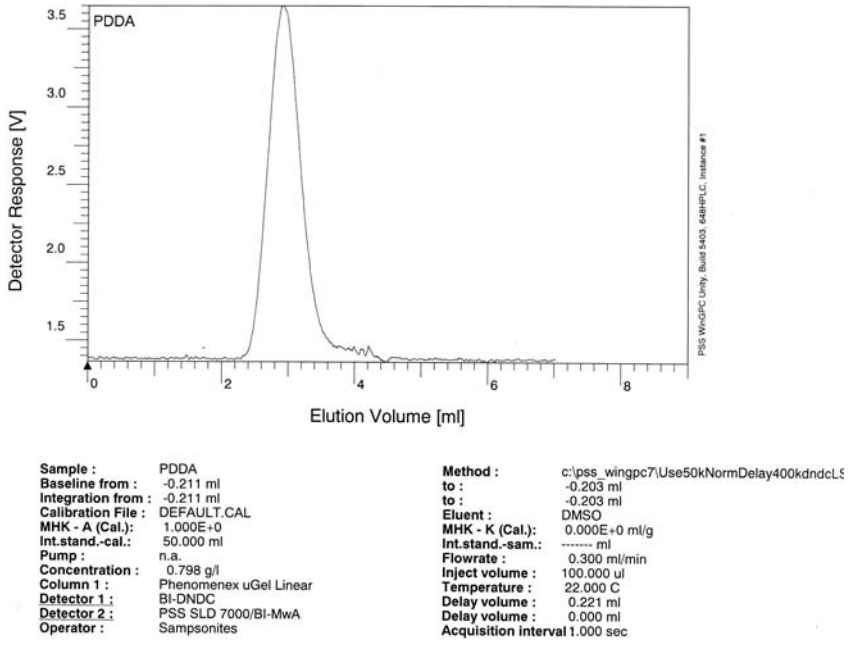

Figure 3.3 GPC Spectra of poly**70** (mobile phase: DMSO; temp.: 70 ºC).

In addition to weak aqueous base, the pure poly**70** is also found to be soluble in DMSO. Such a good solubility provided us the opportunity to determine the molecular size of poly**70** using Gel Permeation Chromatography (GPC) with DMSO being the mobile phase (**Figure 3.3**). This is the first time that we were able to estimate how large

the PDA molecules can be prepared using our host-guest strategy. It shows that PDA corresponding to around 800 monomeric units (M_w = 1.58×10^5 g/mol) is formed in this case. And the molecular weight distribution (PDI = 1.50) is much narrower than most of the PDAs reported. Plus nearly quantitative isolation yield of poly**70**, all evidence demonstrates that the host-guest strategy is a very efficient means of making high quality PDAs.

3.4. Solution Studies of Poly(deca-4,6-diynedioic acid)

The purified poly**70** has a deep red color. In aqueous solution, its ionic form shows a remarkable chromism dependence upon the pH of solution (adjusted by addition of

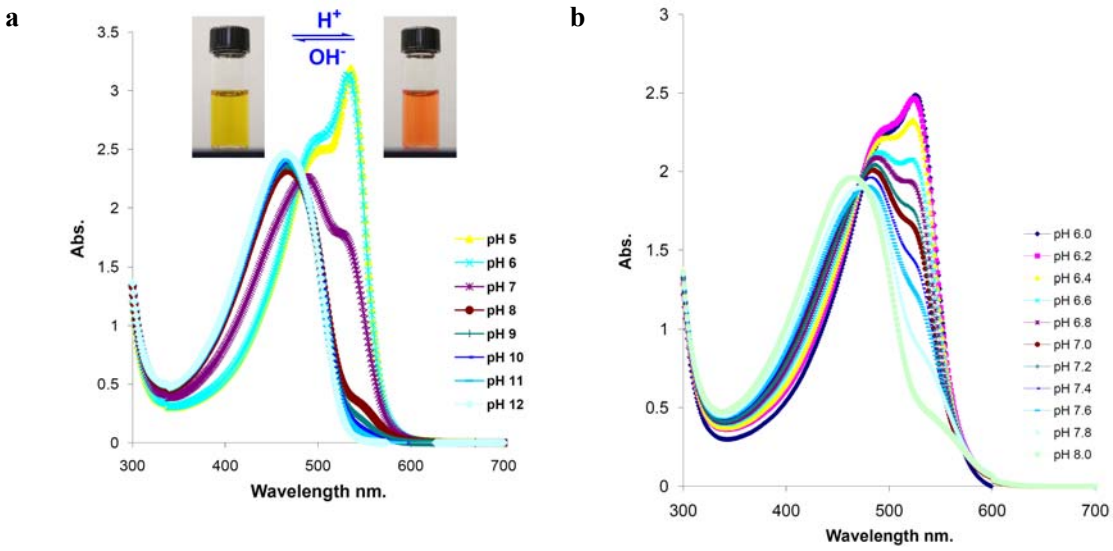

Figure 3.4 Electronic absorption of poly**70** at different pHs. (a) From 5 to 12; (b) from 6 to 8.

NaOH or HCl). As shown in **Figure 3.4a**, the red↔yellow color change of poly**70** solution is totally reversible between acidic and basic conditions. The maximum in the optical absorption spectra is seen to shift from 530 nm at pH 6 to 460 nm at pH about 8. However, when pH is above 8 or below 6, the spectra seems to remain constant in either condition. Specifically, when pH is below 6, the maximum absorption appears at 530 nm with a moderate shoulder 490 nm. And when pH is above 8, the spectrum shows as a structureless peak with the maximum absorption blue-shift to 460 nm as well as a little tail centering at around 530 nm, which seemly corresponds to the structure showing at acidic condition and eventually disappears at pH above 12. The transition between these two distinctive absorption behaviors can be seen more clearly between pH 6 and 8, as shown in **Figure 3.4b**. There is an obvious isosbestic point at about 475 nm, indicating the polymer molecules go directly from one conformation to the other.

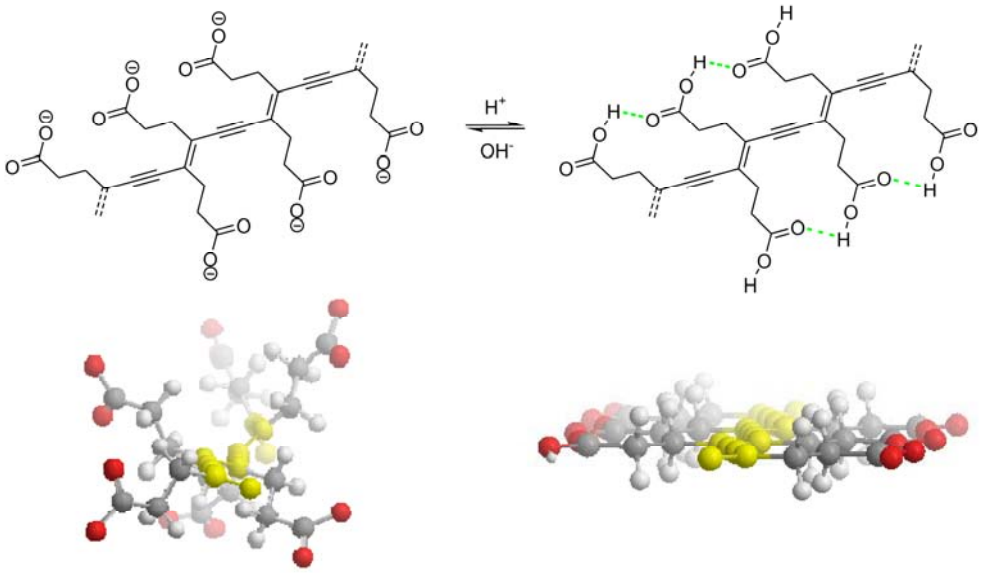

Figure 3.5 The extreme situation of pH-induced reversible planar/nonplanar conformations adopted by poly**70** in aqueous solution (in the molecular models, yellow: ene-yne backbone; grey: carbon atoms in the side chains; red: carboxylate oxygen atoms).

As illustrated in **Figure 3.5**, in the yellow (basic) solution (ε_{530} = 7280 $M^{-1}cm^{-1}$), since the side groups will be deprotonated to generate more anions, the negative/negative repulsion between the adjacent anionic side groups would force the whole polymer molecule away from the planar backbone featuring the conjugated polymers. Therefore the nonplanar conformation will cause the decrease in the ECL of poly**70** and absorb low energy. On the other hand, in the red (acidic) solution (ε_{460} = 8200 $M^{-1}cm^{-1}$), the carboxylic acids dangling around the main chain of poly**70** can form either inter- or intramolecular H-bonds which will facilitate the planarity of the polymer backbone and consequently increase the ECL of polymer molecules in the solution. With more and more HCl added to lower the pH, the polymer/solvent interactions decrease and the polymer/polymer interactions increase, as leads to the aggregation and eventually precipitating as fibrous red materials at pH < 6.

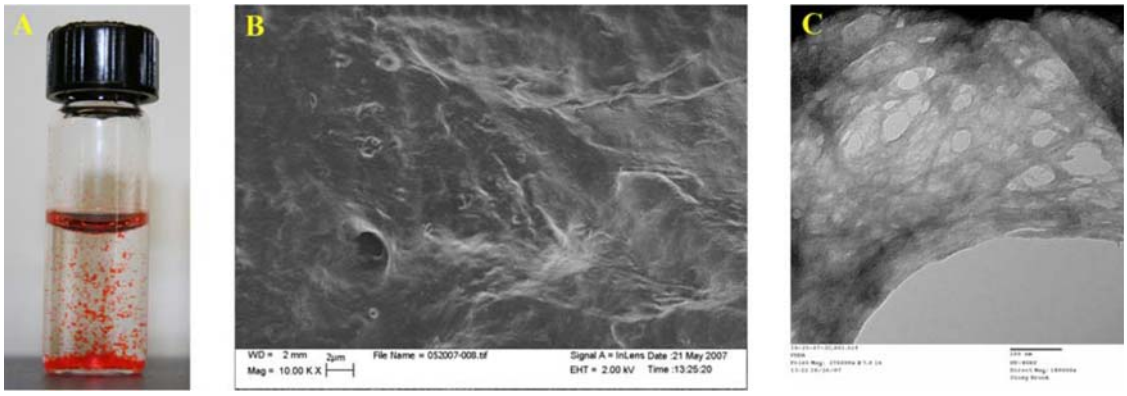

Figure 3.6 The morphologies of poly**70** in water suspension (A) and cast films (B. SEM image and C. TEM image).

These red polymer fibers seem to have certain interesting morphology in the suspension, however, the electronic microscopy doesn't show any obvious self-assembling 1-dimensional structure other than amorphous deposits. This is probably due

to the great tendency to aggregate in solvent-free state cause by the strong intermolecular H-bonding (**Figure 3.6**).

3.5. Conclusion Remarks

PDAs with charged side groups are successfully synthesized using host-guest strategy in order to prepare soluble PDA materials. Among all three PDAs, the two polymers bearing ammonium cations in each repeat unit, poly**18** and poly**66d**, both show very poor solubility. However, the negatively charged poly**70** show great solubility in aqueous media and its neutral form also shows good solubility in polar organic solvents. The solubility of poly**70** allows the molecular weight determination on PDAs made by host-guest strategy for the first time using standard characterization method. These results demonstrate that our host-guest strategy can provide PDA materials in excellent quality. The solution studies on poly**70** show that this material has remarkable chromism properties in dependence upon pH conditions.

Chapter Four

Experiment section

General Information

Materials - The chemicals were purchased from Acros Organics or Aldrich Co. and used without purification unless otherwise stated. All solvents were purified using Solvent Purification System 400-4 from Innovative Technology, Inc. All reactions were carried out under N_2 atmosphere. TLC was performed on Whatman AL SIL G/UV_{254} and flash chromatography was carried out on silica gel 60 (Merck; 230-400 mesh ASTM).

Melting Points - Melting points were measured on a Thomas Hoover Capillary melting point apparatus and are uncorrected.

NMR - ^{1}H spectra were recorded on a Varian Gemini-300 (300 MHz) or Inova-400 NMR (400 MHz) spectrometer and are reported in ppm using solvent as an internal standard. Data are reported as: [δ shift]([s= singlet, d=doublet, t=triplet, q=quartet, p=pentet or quintet, m=multiplet, b=broad], [integration], and [*J*=coupling constant in Hz]). Proton decoupled ^{13}C spectra were recorded on a Varian Gemini-300 (75 MHz) or Inova-400 NMR (100 MHz) spectrometer and are reported in ppm using solvent as internal standard.

IR – Infrared spectroscopy were performed using a Thermo Nicolet 380 FTIR spectrometer equipped with a Smart Collector accessory for diffuse reflectance. The data

were collected using pure solid samples and analyzed using the Omnic software suite (Nicolet, USA).

Raman - Raman spectroscopy was performed using a Thermo Nicolet Almega dispersive Raman spectrometer coupled with an infinity corrected, confocal design microscope. The spectrometer uses a 785 nm class I laser, and the data were collected in the reflection mode of the microscope at a slit width of 25 μm. The data were collected and analyzed using the Omnic software suite (Nicolet, USA).

UV – UV-vis spectroscopy was recorded using a Shimadzu UV-2550 UV-vis spectrometer.

GPC – GPC analysis was carried on a 5μ Linear(2) Phenogel^{TM} GPC column (Phenomenex, USA) equipped with a HPLC pump (Shimadzu LC-10AD). Three different types of detector are used sequentially: UV detector (SPD-20A, Shimadzu), static light scattering detector (BI-MwA molecular weight analyzer, Brookhaven Instruments Corporation) and refractive index detector (BI-DNDC, Brookhaven Instruments Corporation). The experiment used dimethyl sulfoxide (DMSO) containing 5g/L of LiBr as an eluent at 70 °C with a flow rate of 0.3 mL/min. The calibration was against standard dextran samples.

X-ray Diffraction - Crystals were selected and mounted on glass fibers using epoxy glue. The crystals were optically centered on a Bruker AXS SMART CCD diffractometer and diffraction data were collected using a Siemens graphite-monochromated Mo radiation tube. The unit cells were determined by a least-squares analysis using the SMART software package. The structures were solved and refined with standard SHELX procedures. The quality of the structures varied due to the quality of the available single

crystals. In the best cases, hydrogen atoms were located in difference maps and refined. In the cases with poorer data sets, the hydrogen atoms were placed in calculated positions and added as fixed contributions.

Thermal Analysis - Differential scanning calorimetry (DSC) and thermal gravimetry (TGA) were conducted on a TA instruments Q100 and Hi-Res TGA 2950. Both thermal techniques used a heating rate of 10 °C/min under nitrogen.

Salt Formations

All the salts reported in this dissertation were prepared using the general procedure as followed. The solution of 2 equivalent of primary amine in appropriate solvent and the solution of 1 equivalent of **H_2OG** in methanol (or methanol with certain amount of H_2O) were mixed. The solution mixture was allowed to sit at ambient temperature for slow

Table 4.1 The experimental details of host-guest salts.

Salts	Solvent	Morphology	Color	Melt point (ºC)
$NH_4HOG•2H_2O$	H_2O	thick plate	colorless	
$(CH_3NH_3)_2OG•2H_2O$	H_2O	needles	colorless	
$(CH_3CH_2NH_3)_2OG•2H_2O$	H_2O	needles	colorless	
$(propylNH_3)_2OG$	Methanol/H_2O	needles	colorless	
$(butylNH_3)_2OG$	Methanol/H_2O	thin plate	colorless	
$(pentylNH_3)_2OG·H_2OG$	Methanol/H_2O	needles	colorless	
$(hexylNH_3)_2HOG$	Methanol/H_2O	needles	colorless	
$(cyclohexylNH_3)_2OG$	Methanol/H_2O	needles	colorless	
$(benzylNH_3)_2OG$	Methanol/H_2O	needles	colorless	
$(18H)_2OG$	1-propanol		pink	-
$(18H)_2OG•2H_2O$	Methanol/H_2O(<1:4)		red	-
$(18H)_2OG•2CH_2OH$	absolute Methanol		colorless[a]	-

a. The color of the fresh-made cocrystal was white/colorless and slowly turned into pinkish at ambient conditions.

evaporation until qualified single crystals of the corresponding salt formed. **Table 4.1** summaries the details for each salt.

Cocrystallization

For each cocrystal system, the single crystals were grown by slow evaporation of the solution in appropriate solvent(s) of the two components with the corresponding stoichiometries determined by keeping the host-guest H-bond donor/acceptor ratio as 1:1. Typically, 0.02 mmol of **3PyU** and 0.04 mmol of **22b** were dissolved in 10 mL of methanol, and the solution was allowed to evaporate at ambient conditions yielding the single crystals qualified for diffraction test. See **Table 4.2** for details for each cocrystal.

Table 4.2 The experimental details of cocrystallization.

Cocrystals	Solvent	Morphology	Color [a]	Melt point (ºC)
(22b)$_2$•3PyU	methanol	thick plate	purplish red	136-137.5
(22b)$_2$•4PyU	1-propanol	needles	blue	142-144
(22b)$_2$•4PyO	methanol	needles	purple	164-166
(22c)$_2$•4PyU	1-propanol	needles	blue	135-137
(22c)$_2$•3PyO	1-propanol	thin plate	blue	145-146.5
(22c)$_2$•4PyO	methanol	needles	blue	125-126
(22d)$_2$•4PyU	1-propanol	needles	light green	134-136
(22d)$_2$•4PyO	methanol	needles	pink	153-154
70•4PyO	1.5:1(*vol.*) t-BuOH/H_2O	needles	pink	-

a. The color of the fresh-made cocrystal was white/colorless and slowly changed afterwards at ambient conditions. The description stated here is the stable status with no more change after storage. Exceptional for **70•4PyO**.

Thermal polymerization

(18H)$_2$OG: After collecting the data for solving the monomer structure, the same mounted single crystal used in the initial X-ray experiment was heated repeatedly for a total time of 82 days at temperature rising from 100 °C to 160 °C under vacuum to monitor the SCSC polymerization. At the end of each heating period the crystal was returned to the diffractometer and new data set was obtained.

70•4PyO: The pinkish partially-polymerized monomer cocrystals were heated at 100 °C for 12h to yield fully-polymerized polymer cocrystals with metallic luster.

Synthesis

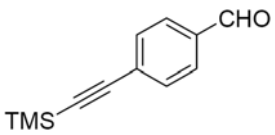

4-((Trimethylsilyl)ethynyl)benzaldehyde (23). A degassed solution of 4-bromobenzaldehyde (1.85g, 10mmol), CuI (0.19 g, 1.00 mmol) and $(Ph_3P)_2PdCl_2$ (0.35 g, 0.50 mmol) in TEA (50 mL) was heated up to 90°C. Then trimethylsilylacetylene (2.10 g, 15.00 mmol) was added dropwise over 1 h. The mixture was continuously heated at gentle reflux until (up to 2 h) all the 4-bromobenzaldehyde was transformed (by TLC). The solvent was evaporated and the residue was treated with hexanes. Filtration through silica gel and evaporation of the solvent yielded 1.94 g (80%) of analytically pure **23** as yellow crystals. Mp 67-68.5 °C (lit. 66-67 °C); **^{1}H-NMR** (400 MHz, $CDCl_3$) δ 10.00 (s, 1H), 7.82 (d, 2H, *J* = 8.4 Hz),

7.60 (d, 2H, *J* = 8.4 Hz), 0.27 (s, 9H); **^{13}C-NMR** (100 MHz, $CDCl_3$) δ 191.41, 135.59, 132.48, 129.43, 129.36, 103.83, 99.03, -0.22.

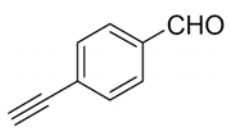

4-Ethynylbenzaldehyde (24). To the solution of **23** (1.94 g, 7.95 mmol) in 30 mL of MeOH was added anhydrous K_2CO_3 (0.12 g, 0.88 mmol) at rt. The mixture was vigorously stirred for 2 h before the solvent was removed *in vacuo*. The residue was washed with 200 mL of water and extracted with 3 × 20 mL of CH_2Cl_2. The organic layers were combined, washed with 3 × 20 mL of sat aq $NH_4^+Cl^-$, and then dried over $MgSO_4$. Evaporation *in vacuo* gave a solid that was recrystallized out of hexanes to yield 1.07 g (98%) of **24** as yellow crystals. Mp 88-89 °C (lit. 88-90 °C); **^{1}H-NMR** (400 MHz, $CDCl_3$) δ10.02 (s, 1H), 7.84 (d, 2H, *J* = 8.4 Hz), 7.64 (d, 2H, *J* = 8.4 Hz), 3.29 (s, 1H); **^{13}C-NMR** (100 MHz, $CDCl_3$) δ 191.33, 135.94, 132.68, 129.46, 128.29, 82.60, 81.02.

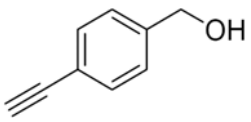

4-Ethynylbenzylalcohol (25). To a solution of **24** (0.65 g, 5.00 mmol) in MeOH (30 mL) at 0°C was added $NaBH_4$ (0.05 mg, 1.25 mmol). The reaction was stirred for 0.5 h before quenched with 100 mL of water. The resulting biphase was extracted with 3 × 30 mL of Et_2O. The combined organic layers were washed with 2 × 20 mL of brine and dried over $MgSO_4$. Concentration *in vacuo* yielded 0.59 g (90%) of alcohol **25** as yellow oil. **^{1}H-NMR** (400 MHz, $CDCl_3$) δ 7.48 (d, 2H, *J* = 8.4 Hz), 7.30 (d, 2H, *J* = 8.4 Hz), 4.67 (s, 2H), 3.07 (s, 1H); **^{13}C-NMR** (100 MHz, $CDCl_3$) δ 141.55, 132.27, 126.67, 121.26, 83.45, 77.18, 64.77.

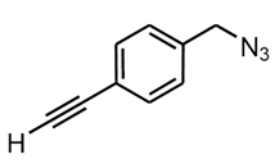

1-(Azidomethyl)-4-ethynylbenzene (26). To a solution of **25** (0.67 g, 5 mmol) in 16 mL of DMF were added Ph_3P (1.32 g, 5 mmol) and NaN_3 (0.40 g, 6 mmol), followed by addition of 4 mL CCl_4 all at once with syringe. The clear yellow solution turned into cloudy within a few minutes. The reaction was then heated at reflux under vigorous stirring for 6 h and then cooled to room temperature. The resulting brown solution was poured into 125 mL of water and extracted with 3 × 30 mL of Et_2O. The combined organic layers were washed with 2 × 20 mL brine and dried over $MgSO_4$. Concentration *in vacuo* gave yellow thick oil that was purified by flash chromatography (7:1 hexanes/EtOAc) to yield 0.43 g (54%) of azide **26** as yellow oil. **^{1}H-NMR** (400 MHz, $CDCl_3$) δ 7.51 (d, 2H, *J* = 8.4 Hz), 7.28 (d, 2H, *J* = 8.4 Hz), 4.35 (s, 2H), 3.10 (s, 1H); **^{13}C-NMR** (100 MHz, $CDCl_3$) δ 136.30, 132.79, 128.27, 122.37, 83.31, 78.03, 54.62.

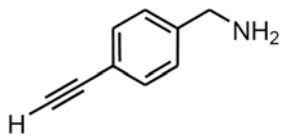

(4-Ethynylphenyl)methanamine (27). To a solution of **26** (0.43 g, 2.7 mmol) in 10 mL of anhydrous Et_2O at 0°C was added $LiAlH_4$ (5.4 mmol, 5.4 mL, 1.0M in Et_2O) dropwise. The reaction was quenched by the slow addition of 5 mL 15% wt aqueous NaOH and the slurry was vigorously stirred for 0.5 h at 0 °C. The resulting slurry was filtered and the filtrate was washed with 100 mL water and extracted with 3 × 30 mL of Et_2O. The combined organic layers were washed with 2 × 20 mL of brine and dried over $MgSO_4$. Concentration *in vacuo* yielded 0.34 g (96%) of amine **27** as colorless crystals. Mp 66-67 °C; **^{1}H-NMR** (400 MHz, $CDCl_3$) δ 7.46 (d, 2H, *J* = 8.0 Hz), 7.27 (d, 2H, *J* = 8.0 Hz),

3.87 (s, 2H), 3.05 (s, 1H); **^{13}C-NMR** (100 MHz, $CDCl_3$) δ 144.26, 132.50, 127.20, 120.67, 83.80, 77.09, 46.40.

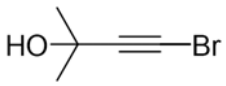

1-Bromo-3-hydroxy-3,3-dimethylpropyne (28). To a solution of KOH (32.26 g, 576 mmol) in 130 mL water was added Br_2 (11.59 g, 72.5 mmol) dropwise at -15 °C with vigorous stirring. The dark red color discharged and the mixture was stirred for an additional 10min. To the resulting solution 3-hydroxy-3,3-dimethylpropyne (8.4 g, 100 mmol) in 20 mL of hexanes was added through an additional funnel. The mixture was stirred for another 10min after the addition was finished. The biphase was extracted with 3 × 50 mL of CH_2Cl_2. The combined organic layers were washed with 3 × 30 mL of brine and dried over $MgSO_4$, followed by concentration *in vacuo* to give tan oil that was distill *in vacuo* to yield 12.50 g (85%) of the bromide **28** as colorless oil. **^{1}H-NMR** (400 MHz, $CDCl_3$) δ 1.51 (s, 6H); **^{13}C-NMR** (100 MHz, $CDCl_3$) δ 84.52, 66.23, 42.76, 31.16.

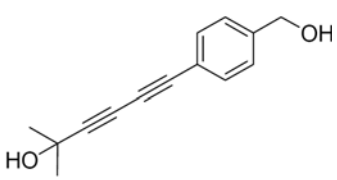

6-(4-Hydroxymethyl-phenyl)-2-methyl-hexa-3,5-diyn-2-ol (29). To a solution of **25** (0.66 g, 5.00 mmol) in 50 mL of 30% aq n-butylamine at 0°C were added CuCl (0.011 g, 0.11 mmol) and NH_2OH•HCl (0.032 g, 0.46 mmol). A bright yellow suspension was formed immediately. Then **28** (0.98 g, 6.01 mmol) was syringed into the resulting slurry that turned from bright yellow into green with the addition. A small amount of NH_2OH•HCl was added to bring the mixture back into yellow. This was repeated a few times during the following 6h. When the reaction finished it was a clear yellow solution

that was adjusted to PH = 2 with 1.0M HCl and extracted with 3 × 20 mL of Et_2O. The combined organic layers were washed with 3 × 20 mL of sat aq $NH_4^+Cl^-$, 3×20 mL of brine and dried over $MgSO_4$. Concentration *in vacuo* yielded yellow crystals that were recrystallized out of EtOH to give 1.00 g (93%) of diacetylene **29** as colorless crystals. Mp 108-109.5 °C; **^{1}H-NMR** (400 MHz, $CDCl_3$) δ 7.48 (d, 2H, *J* = 8.4 Hz), 7.32 (d, 2H, *J* = 8.4 Hz), 4.71 (s, 2H), 1.58 (s, 6H) **^{13}C-NMR** (100 MHz, $CDCl_3$) δ 142.35, 132.93, 127.00, 120.94, 86.94, 78.88, 73.38, 67.27, 65.98, 65.03, 31.34.

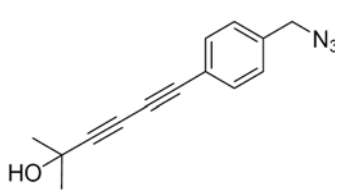

6-(4-Azidomethyl-phenyl)-2-methyl-hexa-3,5-diyn-2-ol (30). To a solution of **29** (1.00 g, 4.67 mmol) in 16 mL of DMF at rt were added Ph_3P (1.22 g, 4.67 mmol) and NaN_3 (0.36 g, 5.54 mmol), followed by addition of 4 mL of CCl_4 all at once with syringe. The clear yellow solution turned into cloudy within a few minutes. The reaction was heated at reflux under vigorous stirring for 6h and then cooled to rt. The resulting brown solution was poured into water (125 mL) and extracted with 3 × 30 mL of Et_2O. The combined organic layers were washed with 2 × 20 mL of brine and dried over $MgSO_4$. Concentration *in vacuo* gave yellow thick oil that was purified by flash chromatography (5:1 hexanes/EtOAc) to yield 0.69 g (62%) of azide **30** as yellow oil. **^{1}H-NMR** (300 MHz, $CDCl_3$) δ 7.50 (d, 2H, *J* = 8.4 Hz), 7.27 (d, 2H, *J* = 8.4 Hz), 4.35 (s, 2H), 1.58 (s, 6H) **^{13}C-NMR** (100 MHz, $CDCl_3$) δ 136.85, 133.16, 128.34, 121.81, 87.26, 78.41, 73.97, 67.17, 65.98, 54.61, 31.32.

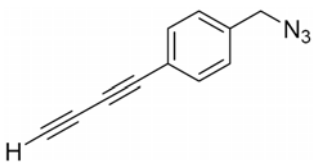

1-Azidomethyl-4-buta-1,3-diynyl-benzene (31). To a solution of **30** (0.17 g, 0.8 mmol) in 10 mL of toluene was added powder NaOH (0.13 g, 3.1 mmol). The mixture was heated to 60 °C under vigorous stirring for 2 h and then cooled to room temperature. The solid was removed by filtration and the filtrate was concentrated *in vacuo*. The residue was then purified by flash chromatography (5:1 hexanes/EtOAc) to yield 0.10 g (82%) deprotected azide **31** as yellow oil, which was unstable in condensed state and turned dark quickly. **^{1}H-NMR** (400 MHz, $CDCl_3$) δ 7.53 (d, 2H, *J* = 8.4 Hz), 7.29 (d, 2H, *J* = 8.4 Hz), 4.36 (s, 2H), 2.50 (s, 1H); **^{13}C-NMR** (100 MHz, $CDCl_3$) δ 136.94, 133.19, 128.10, 121.01, 74.72, 74.06, 71.60, 67.98, 54.35.

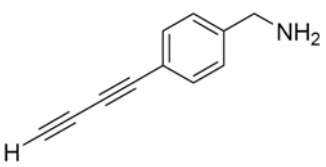

4-Buta-1,3-diynyl-benzylamine (18). To a solution of **31** (0.10 g, 0.6 mmol) in 10 mL of anhydrous Et_2O at 0 °C was added $LiAlH_4$ (1.2 mmol, 1.2 mL, 1.0M in Et_2O) dropwise. The reaction was quenched by the addition of 5 mL of 15% wt aq NaOH and the slurry was vigorously stirred for 0.5 h at 0 °C. The resulting slurry was filtered and the filtrate was washed with 50 mL water and extracted with 3 × 15 mL of Et_2O. The combined organic layers were washed with 2 × 20 mL of brine and dried over $MgSO_4$. Concentration *in vacuo* yielded 83 mg (99%) of amine **18** as colorless crystals, which were only stable in solution otherwise would change color very quickly from pink to red, and finally to black. **^{1}H-NMR** (400 MHz, $CDCl_3$) δ 7.48 (d, 2H, *J* = 8.0 Hz), 7.28 (d, 2H, *J* = 8.0 Hz), 3.88 (s, 2H), 2.47 (s, 1H); **^{13}C-NMR** (400 MHz, $CDCl_3$) δ 144.94, 132.96, 127.12, 119.30, 75.35, 73.23, 71.13, 68.16, 46.18.

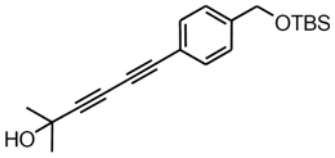

6-(4-((Tert-butyldimethylsilyloxy)methyl)phenyl)-2-methylhexa-3,5-diyn-2-ol (37). A homogenous solution of *t*-butyldimethylsilyl chloride (0.90 g, 6.00 mmol), and imidazole (0.85 g, 12.50 mmol) in 0.5 mL of DMF was stirred until a light yellow color forms. **29** (1.07 g, 5.00 mmol) was added and the reaction was allowed to proceed at rt for 24 h. The yellow reaction mixture was poured into 50 mL of H_2O and extracted with 3 × 20 mL of Et_2O. The combined organic layers were washed with 3 × 20 mL of brine and dried over $MgSO_4$. Concentration *in vacuo* yielded a yellow oil that was purified by flash chromatography (5:1 hexanes:EtOAc) to give 1.49 g (91%) of TBS protected product **37** as colorless crystals. Mp 51.5-53 °C; **^{1}H-NMR** (400 MHz, $CDCl_3$) δ 7.44 (d, 2H, *J* = 8 Hz), 7.27 (d, 2H, *J* = 8 Hz), 4.73 (s, 2H), 1.58 (s, 6H), 0.94 (s, 9H), 0.09 (s, 6H) **^{13}C-NMR** (100 MHz, $CDCl_3$) δ 142.94, 132.63, 125.89, 119.86, 86.47, 78.89, 72.71, 67.14, 65.72, 64.52, 31.12, 25.89, 18.36, -5.32.

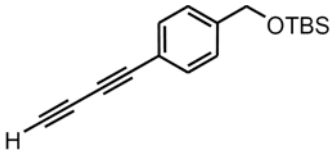

(4-(Buta-1,3-diynyl)benzyloxy)(tert-butyl)dimethylsilane (38). To the solution of **37** (0.059 g, 0.17 mmol) in 15 mL of toluene was added powder NaOH (0.014 g, 0.34 mmol). The mixture was heated to 70 °C under vigorous stirring for 5 h and then cooled to room temperature. The solid was removed by filtration and the filtrate was concentrated *in vacuo*. The residue was then purified by flash chromatography (10:1 hexanes/EtOAc) to yield 0.038 g (75%) terminal diacetylene **38** as light yellow oil. **^{1}H-NMR** (400 MHz, $CDCl_3$) δ 7.48 (d, 2H, *J* = 8.4 Hz), 7.29 (d, 2H, *J* = 8.4 Hz), 4.74 (s, 2H), 2.47 (s, 1H),

0.94 (s, 9H), 0.10 (s, 6H); **^{13}C-NMR** (100 MHz, $CDCl_3$) δ 143.29, 132.71, 125.92, 119.32, 75.52, 73.09, 71.07, 71.04, 68.22, 64.51, 25.90, 18.38, -5.31.

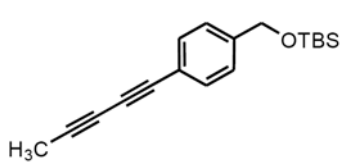

Tert-butyldimethyl(4-(penta-1,3-diynyl)benzyloxy)silane (39). To the solution of **38** (0.031 g, 0.11 mmol) in 1 mL of anhydrous THF was added *n*-BuLi (0.09 mL, 0.22 mmol, 2.5 M in hexanes) at -78 °C. The mixture was stirred for 10 minutes followed by addition of iodomethane (0.036 mg, 0.25 mmol). It was allowed to proceed for another 1h before 10 mL of 10% HCl was poured into to quench the reaction. After extracted with 3 × 10 mL of EtO_2, the organic layers was washed with 3 × 10 mL of H_2O and dried over with $MgSO_4$. Concentration *in vacuo* yielded a yellow oil that was further purified by flash chromatography (20:1 hexanes/EtOAc) to yield 0.030 g (92%) methyl acpped diacetylene **39** as colorless oil. **^{1}H-NMR** (400 MHz, $CDCl_3$) δ 7.44 (d, 2H, *J* = 8 Hz), 7.26 (d, 2H, *J* = 8 Hz), 4.72 (s, 2H), 2.02 (s, 3H), 0.94 (s, 9H), 0.09 (s, 6H); **^{13}C-NMR** (100 MHz, $CDCl_3$) δ 142.46, 132.42, 125.85, 120.40, 80.05, 74.30, 73.97, 64.56, 64.39, 25.90, 18.37, 4.60, -5.31.

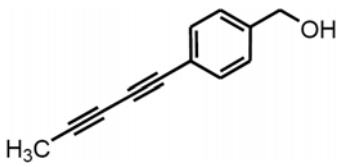

(4-(Penta-1,3-diynyl)phenyl)methanol (40). To a solution of **39** (0.35 g, 1.19 mmol) in 10.5 mL of THF/MeOH (20:1) at 0 °C was added 1.8 mL of 1.0M TBAF dropwise. After the addition was finished, the reaction mixture was stirred at rt for about 8 h to let the reaction complete. The light yellow solution was quenched by pouring in 30 mL of sat aq $NH_4^+Cl^-$, followed by extraction with 3 × 10 mL of ether. The combined organic extracts

were washed with 3 × 10 mL of brine, dried over $MgSO_4$ and concentrated *in vacuo*. Purification of the residue by flash chromatography (5:1 Hexanes/EtOAc) yielded 0.19 g (95%) of alcohol **40** as white crystals, which turns into pinkish quickly in ambient light. Mp 110-111 °C; **^{1}H-NMR** (400 MHz, $CDCl_3$) δ 7.45 (d, 2H, *J* = 8.4 Hz), 7.28 (d, 2H, *J* = 8.4 Hz), 4.66 (d, 2H, *J* = 5.6 Hz), 2.01 (s, 3H); **^{13}C-NMR** (100 MHz, $CDCl_3$) δ 141.62, 132.64, 126.70, 121.16, 80.38, 74.41, 73.93, 64.74, 64.27, 4.56

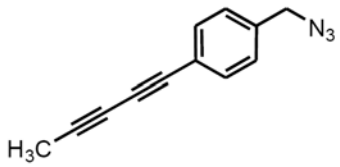

1-(Azidomethyl)-4-(penta-1,3-diynyl)benzene (41). To the solution of **40** (0.19 g, 1.13 mmol) in 4 mL of DMF at rt was added Ph_3P (0.30 g, 1.13 mmol) and NaN_3 (0.088 g, 1.36 mmol), followed by addition of 1 mL of CCl_4 all at once with syringe. The clear solution turned into cloudy within a few minutes. The reaction was then heated at reflux under vigorous stirring for 6h and then cooled to rt. The resulting yellow solution was poured into 30 mL of H_2O and extracted with 3 × 10 mL of Et_2O. The combined organic layers were washed with 2 × 10 mL of brine and dried over $MgSO_4$. Concentration *in vacuo* gave yellow thick oil that was purified by flash chromatography (10:1 hexanes/EtOAc) to yield 0.094 g (62%) of azide **41** as colorless oil. **^{1}H-NMR** (400 MHz, $CDCl_3$) δ 7.48 (d, 2H, *J* = 8.4 Hz), 7.26 (d, 2H, *J* = 8.4 Hz), 4.34 (s, 2H), 2.02 (s, 3H) **^{13}C-NMR** (100 MHz, $CDCl_3$) δ 136.10, 132.90, 128.04, 122.08, 80.72, 75.02, 73.51, 64.21, 54.39, 4.60.

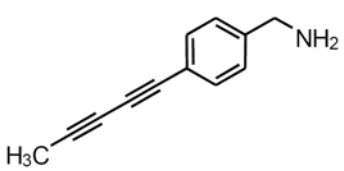

(4-(Penta-1,3-diynyl)phenyl)methanamine (35). To the solution of **41** (0.050 g, 0.26 mmol) in 5 mL of anhydrous

Et_2O at 0°C was added $LiAlH_4$ (0.5 mL, 1.0 M in Et_2O, 0.50 mmol) dropwise. The reaction was quenched in 10 min by 0.5 mL of 15% wt aq NaOH followed by adding some $MgSO_4$. The slurry was vigorously stirred for 0.5 h and filtered to remov the solid. The filtrate was concentrated *in vacuo* to yield 0.035 g (81%) of amine **35** as yellow crystals. **^{1}H-NMR** (400 MHz, $CDCl_3$) δ 7.43 (d, 2H, *J* = 8.0 Hz), 7.24 (d, 2H, *J* = 8.0 Hz), 3.86 (sb, 2H), 2.01 (s, 3H); **^{13}C-NMR** (100 MHz, $CDCl_3$) δ 144.11, 132.66, 127.01, 120.35, 80.15, 74.12, 74.08, 64.30, 46.13, 4.55.

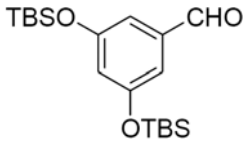

3,5-Bis(tert-butyldimethylsilyloxy)benzaldehyde (42). DIEA (2.27 g, 17.52 mmol) was added to a solution of 3,5-dihydroxybenzaldehyde (1.10 g, 7.96 mmol) in 10 mL of DMF, and the solution was stirred for 15 min. The silyl chloride (2.76 g, 18.32 mmol) was added and the light brown solution stirred for 16 h at rt. The mixture was poured into 100 mL of water, extracted with 3 × 30 mL of CH_2Cl_2 and dried over $MgSO_4$. Removal of the solvent *in vacuo* yielded a brown oil that was purified by flash column chromatography (9:1 hexanes/ethyl acetate) to yield 2.65 g (91%) of the disilyl ether **42** as a tan oil. **^{1}H NMR** (400 MHz, $CDCl_3$) δ 9.86 (s, 1H), 6.95 (d, 2H, *J* = 2.4 Hz), 6.59 (t, 1H, *J* = 2.4 Hz), 0.99 (s, 18H), 0.22 (s, 12H); **^{13}C NMR** (100 MHz, $CDCl_3$) δ 191.84, 157.26, 138.34, 118.41, 114.37, 25.60, 18.19, -4.43.

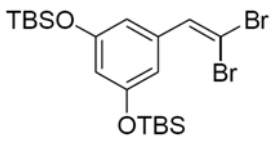

(5-(2,2-Dibromovinyl)-1,3-phenylene)bis(oxy)bis(tert-butyldimethylsilane) (43). To the solution of CBr_4 (3.55 g, 10.70 mmol) in 10 mL of CH_2Cl_2 at 0 °C was added Ph_3P

(5.61 g, 21.39 mmol) in two portions. The resulting orange-red solution was stirred for 10 minutes before adding the solution of **42** (2.62 g, 7.13 mmol) dropwise. After the addition was finished, the reaction was stirred at rt in darkness. After 3 h, the mixture was poured into 100 mL of H_2O, extracted with 3 × 30 mL of CH_2Cl_2 and dried over $MgSO_4$. After emoval of the solvent *in vacuo*, the residue was purified by flash column chromatography (12:1 hexanes/ethyl acetate) to yield 3.40g (92%) of the dibromoethene **43** as a yellow oil. **^{1}H NMR** (300 MHz, $CDCl_3$) δ 7.37 (s, 1H), 6.67 (dd, 2H, *J* = 0.6, 2.1 Hz), 6.35 (t, 1H, *J* = 2.1 Hz), 0.99 (s, 18H), 0.22 (s, 12H); **^{13}C NMR** (75 MHz, $CDCl_3$) δ 156.47, 136.70, 136.61, 113.43, 112.67, 89.45, 25.68, 18.21, -4.38.

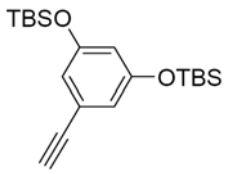

(5-Ethynyl-1,3-phenylene)bis(oxy)bis(tert-butyldimethylsilane) (44). To the solution of **43** (3.40 g, 6.54 mmol) in 15 mL of anhydrous THF at -78 °C was added 30 mL *n*-BuLi (1.6 M in hexanes) dropwise. The resulting dark brown mixture was stirred for 3 h before quenched by the 10 mL of 10% HCl followed by pouring in 50 mL of H_2O. The mixture was then extracted with 3 × 30 mL of CH_2Cl_2 and dried over $MgSO_4$. After emoval of the solvent *in vacuo*, the residue was purified by flash column chromatography (12:1 hexanes/ethyl acetate) to yield 2.35 g (100%) of the acetylene **44** as a yellow oil. **^{1}H NMR** (400 MHz, $CDCl_3$) δ 6.60 (d, 2H, *J* = 2.4 Hz), 6.34 (t, 1H, *J* = 2.4 Hz), 3.01 (s, 1H), 0.97 (s, 18H), 0.19 (s, 12H).

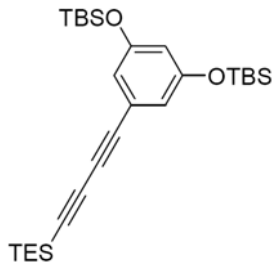

(5-((Triethylsilyl)buta-1,3-diynyl)-1,3-phenylene)bis(oxy)bis(tert-butyldimethylsilane) (45). To a solution of CuCl (0.002 g, 0.02 mmol) and NH_2OH•HCl (0.006 g, 0.09 mmol) in 10 mL of 30% aq. *n*-butylamine at 0 °C were added **44** (0.36 g, 1 mmol). Bright yellow slurry was formed immediately. Then (bromoethynyl)triethylsilane (0.26 g, 1.2 mmol) was syringed into the slurry that turned from bright yellow into green with the addition of the bromide. A small amount of NH_2OH•HCl was added to bring the mixture back into yellow. This was repeated a few times during the next 15 min. When the reaction completed it became a clear orange solution that was adjusted to PH = 2 with 1.0 M HCl and extracted with 3 × 20 mL of Et_2O. The combined organic layers were washed with 3 × 20 mL of sat aq $NH_4^+Cl^-$, 3 × 20 mL of brine and dried over $MgSO_4$. Concentration *in vacuo* yielded yellow oil that was purified by flash chromatography (5:1 Hexanes/EtOAc) to give 2.94 g (88%) of diacetylene **45** as tan oil.

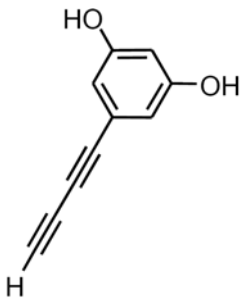

5-(Buta-1,3-diynyl)benzene-1,3-diol (19). To a solution of **45** (0.25 g, 0.5 mmol) in 5 mL of THF/MeOH (20:1) at 0 °C was added 0.75 mL of 1.0 M TBAF dropwise. After the addition was finished, the reaction mixture was stirred at rt for about 2 h to let the reaction complete. The light yellow solution was quenched by pouring in 30 mL of sat aq $NH_4^+Cl^-$, followed by extraction with 3 × 10 mL of ether. The combined organic extracts were washed with 3 × 10 mL of brine, dried over $MgSO_4$ and concentrated *in vacuo* to yielded 0.032 g (40% according to

the NMR data) diacetylene **19** a light liquid, which is very unstable in condensed state; **^{1}H-NMR** (400 MHz, $CDCl_3$) δ 6.80, (b, 2H), 6.57 (d, 2H, J = 2.4 Hz), 6.42 (t, 1H, J = 2.4 Hz), 2.46 (s, 1H); **^{13}C-NMR** (100 MHz, $CDCl_3$) δ 157.16, 122.69, 112.39, 105.47, 75.20, 73.27, 71.61, 67.56.

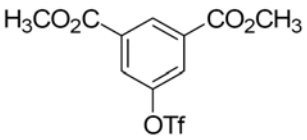

Dimethyl 5-(trifluoromethylsulfonyloxy)isophthalate (46). At 0 °C, the dimethyl 5-hydroxyisophthalate (8.4 g, 40.00 mmol) and pyridine (4.7 mL, 58.00 mmol) were dissolved in 200 mL of CH_2Cl_2. To the above solution was syringed in trifluoromethanesulfonic anhydride (11.62 g, 6.83 mL, 41.20 mmol). The mixture was stirred for 20 min and then quenched with 50 mL of 5% HCl. The organic layer was washed with 3 × 50 mL of 1 M HCl, 3 × 50 mL of sat aq $NaHCO_3$, 3 × 50 mL of brine and dried over $MgSO_4$. Concentration *in vacuo* yielded crude product that was passed through a ca. 10 cm plug of silica gel (CH_2Cl_2) to afford 13.57 g (99%) of the triflate **46** as a cuticolor liquid. **^{1}H NMR** (400 MHz, $CDCl_3$) δ8.71 (s, 1H), 8.11 (d, 2H, J = 0.8), 3.98 (s, 6H); **^{13}C NMR** (100 MHz, $CDCl_3$) δ164.6, 149.5, 133.3, 130.6, 126.8, 117.3.6, 53.2.

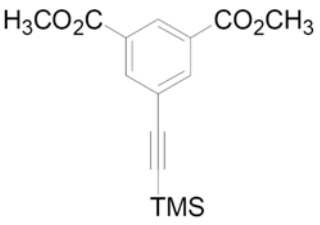

Dimethyl 5-((trimethylsilyl)ethynyl)isophthalate (47). To the solution of (trimethylsilyl)acetylene (1.90 g, 2.43 mL, 13.59 mmol), **46** (4.23 g, 12.37 mmol) and DBU (2.27 g, 2.23 mL, 14.95 mmol) in 50 mL of benzene was added $Pd(Ph_3P)_2Cl_2$ (95 mg, 0.14 mmol) and CuI (52 mg,0.27 mmol). The reaction was stirred

at room temperature for 24 h. Then the mixture was washed with 3 × 20 mL of 1 M HCl, 3 × 20 mL of brine and dried over $MgSO_4$. Concentration *in vacuo* yielded crude product that was passed through a ca. 10 cm plug of silica gel (CH_2Cl_2) to afford 3.74g (89%) of the acetylene **47** as white crystals. **^{1}H NMR** (300 MHz, $CDCl_3$) δ8.60 (t, 1H, *J* = 1.5), 8.29 (d, 2H, *J* = 1.5), 3.95 (s, 6H), 0.27 (s, 9H).

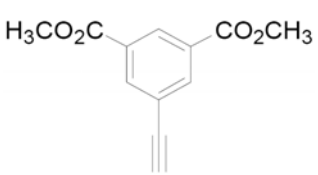

Dimethyl 5-ethynylisophthalate (48). To the solution of **47** (3.74 g, 11.2 mmol) in 40 mL of MeOH was added anhydrous K_2CO_3 (0.17 g, 1.2 mmol). The mixture was vigorously stirred for 2 h before the solvent was removed *in vacuo*. The residue was washed with 200 mL of water and extracted with 3 × 30 mL of ether. The organic layers were combined, washed with 3 × 30 mL of sat aq $NH_4^+Cl^-$ and dried over $MgSO_4$. Evaporation *in vacuo* gave a solid that was filtered through silica gel to yield 4.37 g (98%) of the terminal acetylene **48** as white crystals. **^{1}H NMR** (400 MHz, $CDCl_3$) δ8.62 (t, 1H, *J* = 1.6), 8.30 (d, 2H, *J* = 1.6), 3.94 (s, 6H), 3.17 (s, 1H); **^{13}C NMR** (100 MHz, $CDCl_3$) δ165.6, 137.3, 131.2, 130.9, 123.4, 81.8, 79.4, 52.8.

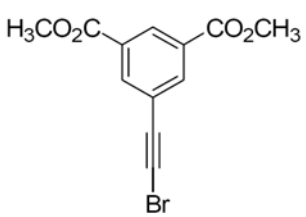

Dimethyl 5-(bromoethynyl)isophthalate (49). To the solution of NBS (0.88 g, 4.9 mmol) in 30mL of acetone, **48** (1.0 g, 4.6 mmol) was added. At the end $AgNO_3$ (0.22 g, 1.28 mmol) was added all at once to the mixture solution, which turned cloudy in 5 min. The reaction was stirred overnight. To work up, acetone was removed *in vacuo* before ice water was added. After extracted with 3 × 20 mL of

ether, the organic phase was washed with 3 × 20 mL of brine and dried over $MgSO_4$. Removal of the solvent afforded 1.31 g (99%) of the bromide **49** as white crystals. **^{1}H NMR** (400 MHz, $CDCl_3$) δ8.61 (t, 1H, *J* = 1.6), 8.26 (d, 2H, *J* = 1.6), 3.94 (s, 6H). **^{13}C NMR** (100 MHz, $CDCl_3$) δ165.60, 137.12, 131.22, 130.71, 123.96, 78.41, 52.77.

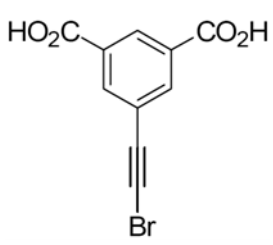

5-(Bromoethynyl)isophthalic acid (50). To the solution of **49** (1.31 g, 4.4 mmol) in 20 mL of MeOH, an aq solution of NaOH (0.71 g, 17 mmol) was added. After vigorously stirred for 10 min, the mixture was adjusted to PH = 2 with 5% HCl. The precipitates were collected by filtration to give 1.17 g (99%) of the diacid **50** as white crystals. **^{1}H NMR** (400 MHz, DMSO) δ8.41 (t, 1H, *J* = 1.6), 8.13 (d, 2H, *J* = 1.6). **^{13}C NMR** (100 MHz, DMSO) δ165.65, 135.94, 132.01, 129.97, 122.88, 77.88, 55.44.

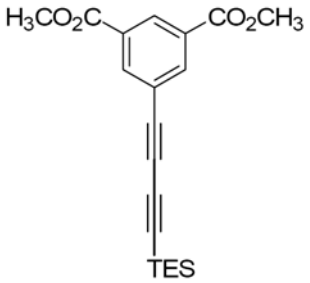

Dimethyl 5-((triethylsilyl)buta-1,3-diynyl)isophthalate (51). To a solution of (triethylsilanyl)acetylene (0.57 mL, 3.2 mmol) in 10 mL of 30% aq n-butylamine at 0°C were added CuCl (5 mg, 0.05 mmol) and NH_2OH•HCl (7.9 mg, 0.24 mmol). A bright yellow suspension was formed immediately. Then the solution of **50** (0.71 g, 2.6 mmol) in 30 mL 30% aq n-butylamine was added into the resulting slurry that turned from bright yellow into green with the addition of the bromide. A small amount of NH_2OH•HCl was added to bring the mixture back into yellow. The bromide was totally consumed after 30 min (by TLC) when the

reaction turned into rusty color. The reaction was quenched with 1.0 M HCl until PH = 2 and extracted with 3 × 30 mL of Et_2O. The combined organic layers were washed with 3 × 20 mL of sat. aq. $NH_4^+Cl^-$, 3 × 20 mL of brine and dried over $MgSO_4$. Concentration *in vacuo* yielded crude diacetylene as brown oil that was then treated with acidic MeOH at refluxing temperature for 6h. The reaction was quenched with 100 mL of water, extracted with 3 × 20 mL of ether and dried over $MgSO_4$. Concentration *in vacuo* yielded the crude product that was purified by flash chromatography (5:1 Hexanes:Ethyl Acetate) to afford 0.46 g (99%) of diacetylene **51** as yellow crystals. **^{1}H NMR** (300 MHz, CD_3Cl) δ8.63 (t, 1H, *J* = 1.5), 8.31 (d, 2H, *J* = 1.5), 3.94 (s, 6H), 1.03 (t, 9H, *J* = 7.8), 0.67 (q, 6H, *J* = 7.8); **^{13}C NMR** (75 MHz, $CDCl_3$) δ165.25, 137.41, 131.10, 130.91, 90.39, 88.19, 76.14, 73.63, 52.57, 7.34, 4.13.

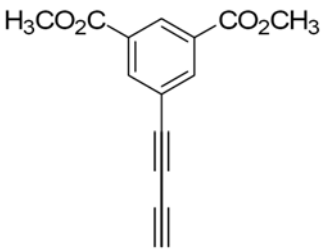

Dimethyl 5-(buta-1,3-diynyl)isophthalate (52). To a solution of **51** (0.57 mL, 3.2 mmol) in 30 mL of the mixture solvents of THF/MeOH (20:1) was added TBAF (6.2 mL, 1.0 M in THF, 6.2 mmol) at rt. The reaction was complete in 10 min (by TLC) and the solvent was removed *in vacuo*. The residue was taken up in 50 mL of ether, which was washed with 3 × 10 mL of sat aq $NH_4^+Cl^-$, 3 × 10 mL of brineand dried over $MgSO_4$. Concentration *in vacuo* followed by flash chromatography (5:1 Hexanes:Ethyl Acetate) yielded 0.100 g (94%) of the terminal diacetylene **52** as yellow crystals. **^{1}H NMR** (300 MHz, CD_3Cl) δ8.66 (t, 1H, *J* = 1.5), 8.34 (d, 2H, *J* = 1.5), 3.96 (s, 6H), 2.53 (s, 1H).

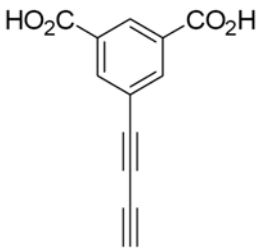

5-(Buta-1,3-diynyl)isophthalic acid (20). To the solution of **52** (1.31 g, 4.4 mmol) in 20 mL of MeOH, an aq solution of NaOH (0.71 g, 17 mmol) was added. After vigorously stirred for 10 min, the mixture was adjusted to PH = 2 with 5% HCl. The precipitates were collected by filtration give 1.17 g (99%) of the diacid **20** as white crystals. **^{1}H NMR** (300 MHz, DMSO) δ8.46 (t, 1H, *J* = 1.5), 8.24 (d, 2H, *J* = 1.5), 4.14 (s, 1H); **^{13}C NMR** (125 MHz, DMSO) δ168.67, 139.86, 135.34, 134.00, 124.25, 80.26, 77.89, 75.93, 70.36.

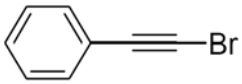

Phenylacetylene bromide (53). To the solution of phenylacetylene (1.80 g, 17.65 mmol) in acetone, NBS (3.36 g, 18.88 mmol, recrystallized out of H_2O before use) was added. At the end $AgNO_3$ (0.15 g, 0.88 mmol) was added all at once to the mixture solution, which turned cloudy in 5 min. The reaction was stirred overnight. To work up, acetone was removed *in vacuo* before ice water was added. After extracted with 3 × 30 mL of ether, the organic phase was washed with 3 × 20 mL of brine and dried over $MgSO_4$. Removal of the solvent afforded 3.05 g (96%) of the analytically pure **53** as yellow oil. **^{1}H-NMR** (300 MHz, $CDCl_3$) δ 7.47-7.28 (m, 5H); **^{13}C-NMR** (75 MHz, $CDCl_3$) δ 131.98 128.66, 128.32, 122.69, 80.03, 49.70.

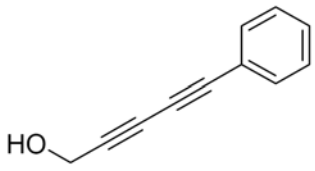

5-Phenylpenta-2,4-diyn-1-ol (54a). To a solution of CuCl (0.005 g, 0.05 mmol) and NH_2OH•HCl (0.015 g, 0.22 mmol) in 4 mL of 30% aq n-butylamine at 0 °C were

added propargyl alcohol (0.13 g, 2.41 mmol). Bright yellow slurry was formed immediately. Then **53** (0.46 g, 2.53 mmol) was syringed into the slurry that turned from bright yellow into blue with the addition of the bromide. A small amount of NH_2OH•HCl was added to bring the mixture back into yellow. This was repeated a few times during the next 15 min. When the reaction completed it became a clear brown solution that was adjusted to PH = 2 with 1.0 M HCl and extracted with 3 × 20 mL of Et_2O. The combined organic layers were washed with 3 × 20 mL of sat aq $NH_4^+Cl^-$, 3 × 20 mL of brine and dried over $MgSO_4$. Concentration *in vacuo* yielded brown oil that was purified by flash chromatography (5:1 Hexanes/EtOAc) to give 0.28 g (88%) of diacetylene **54a** as yellow oil. **^{1}H-NMR** (400 MHz, $CDCl_3$) δ 7.51-7.31 (m, 5H), 4.42 (s, 2H) **^{13}C-NMR** (100 MHz, $CDCl_3$) δ 132.59, 129.35, 128.41, 121.37, 80.39, 78.60, 73.13, 70.47, 51.68.

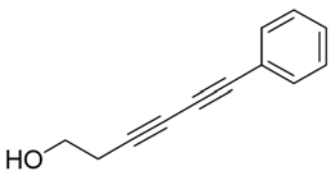

6-Phenylhexa-3,5-diyn-1-ol (54b). To a solution of CuCl (0.020 g, 0.20 mmol) and NH_2OH•HCl (0.063 g, 0.90 mmol) in 20 mL of 30% aq n-butylamine at 0 °C were added 3-butyn-1-ol (0.70 g, 10.00 mmol). Bright yellow slurry was formed immediately. Then **53** (1.90 g, 10.50 mmol) was syringed into the slurry that turned from bright yellow into blue with the addition of the bromide. A small amount of NH_2OH•HCl was added to bring the mixture back into yellow. This was repeated a few times during the next 20 minutes. When the reaction completed it became a clear yellow solution that was adjusted to PH = 2 with 1.0 M HCl and extracted with 3 × 30 mL of Et_2O. The combined organic layers were washed with 3 × 20 mL of sat aq $NH_4^+Cl^-$, 3 × 20 mL of brine and dried over $MgSO_4$. Concentration *in vacuo* yielded yellow oil that was purified by flash

chromatography (5:1 Hexanes/EtOAc) to give 1.25 g (74%) of diacetylene **54b** as tan oil. **^{1}H-NMR** (400 MHz, $CDCl_3$) δ 7.49-7.28 (m, 5H), 3.80 (t, 2H, *J* = 6.4 Hz), 2.65 (t, 2H, *J* = 6.4 Hz); **^{13}C-NMR** (100 MHz, $CDCl_3$) δ 132.53, 129.03, 128.36, 121.73, 80.94, 75.38, 73.91, 66.85, 60.77, 32.99.

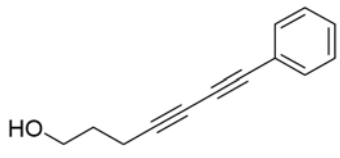

7-Phenylhepta-4,6-diyn-1-ol (54c). To a solution of CuCl (0.020 g, 0.20 mmol) and NH_2OH•HCl (0.063 g, 0.90 mmol) in 20 mL of 30% aq n-butylamine at 0°C was added 4-pentyn-1-ol (0.84 g, 10.00 mmol). Bright yellow slurry was formed immediately. Then **53** (1.82 g, 10.05 mmol) was syringed into the slurry that turned from bright yellow into blue with the addition of the bromide. A small amount of NH_2OH•HCl was added to bring the mixture back into yellow. This was repeated a few times during the next 30 minutes. When the reaction completed it became a clear yellow solution that was adjusted to PH = 2 with 1.0M HCl and extracted with 3 × 20 mL of Et_2O. The combined organic layers were washed with 3 × 20 mL of sat aq $NH_4^+Cl^-$, 3 × 20 mL of brine and dried over $MgSO_4$. Concentration *in vacuo* yielded brown oil that was purified by flash chromatography (5:1 Hexanes/EtOAc) to give 0.87 g (47%) of diacetylene **54c** as yellow oil. **^{1}H-NMR** (400 MHz, $CDCl_3$) δ 7.49-7.28 (m, 5H), 3.79 (t, 2H, *J* = 6.8 Hz), 2.51 (t, 2H, *J* = 6.8 Hz), 1.84 (p, 2H, *J* = 6.8 Hz), 1.50 (s, 1H); **^{13}C-NMR** (100 MHz, $CDCl_3$) δ 132.49, 128.88, 128.34, 121.95, 83.74, 74.97, 74.15, 65.55, 61.39, 30.90, 16.12.

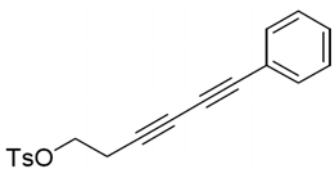

6-Phenylhexa-3,5-diynyl 4-methylbenzenesulfonate (55b). To a solution of **54b** (0.25 g, 1.46 mmol), TEA (0.16 g, 1.60 mmol) and DMAP (0.18 g, 1.46 mmol) in 1.5 mL of CH_2Cl_2 at 0 °C was added TsCl (0.28 g, 1.46 mmol). After 3 h, the reaction was quenched with 30 mL of H_2O, extracted with 3 × 15 mL of CH_2Cl_2, and the combined organic extracts were dried over $MgSO_4$ and concentrated *in vacuo*. Purification of the residue by flash chromatography (5:1 Hexanes/EtOAc) yielded 0.18 g (37%) of tosulate **55b** as colorless oil**.** **^{1}H-NMR** (400 MHz, $CDCl_3$) δ 7.83 (d, 2H, *J* = 8 Hz), 7.47 (d, 2H, *J* = 8 Hz), 7.38-7.30 (m, 5H), 4.14 (t, 2H, *J* = 6.8 Hz), 2.73 (t, 9H, *J* = 6.8 Hz), 2.44 (s, 3H); **^{13}C-NMR** (100 MHz, $CDCl_3$) δ 145.06, 132.63, 132.51, 129.91, 129.17, 128.38, 127.96, 121.46, 77.93, 75.85, 73.63, 67.31, 66.93, 21.62, 20.57.

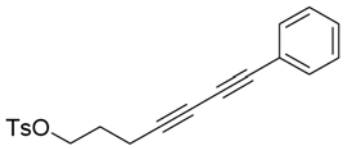

7-Phenylhepta-4,6-diynyl 4-methylbenzenesulfonate (55c). To a solution of **54c** (0.60 g, 3.27 mmol), TEA (0.36 g, 3.60 mmol) and DMAP (0.40 g, 3.27 mmol) in 3 mL of CH_2Cl_2 at 0°C was added TsCl (0.62 g, 3.27 mmol). After 3 h, the reaction was quenched with 50 mL of H_2O, extracted with 3 × 20 mL of CH_2Cl_2, and the combined organic extracts were dried over $MgSO_4$ and concentrated *in vacuo*. Purification of the residue by flash chromatography (3:1 Hexanes/EtOAc) yielded 0.94 g (85%) of tosulate **55c** as white crystals. Mp 81-82.5 °C; **^{1}H-NMR** (400 MHz, $CDCl_3$) δ 7.80 (d, 2H, *J* = 8 Hz), 7.46 (d, 2H, *J* = 8 Hz), 7.37-7.29 (m, 5H), 4.15 (t, 2H, *J* = 6.8 Hz), 2.43 (t, 2H, *J* = 6.8 Hz), 2.42 (s, 3H), 1.90 (p, 2H, *J* = 6.8 Hz); **^{13}C-NMR** (100 MHz, $CDCl_3$) δ 144.89,

132.68, 132.42, 129.88, 128.99, 128.35, 127.87, 121.70, 81.86, 75.18, 73.93, 68.48, 66.13, 27.50, 21.60, 15.82.

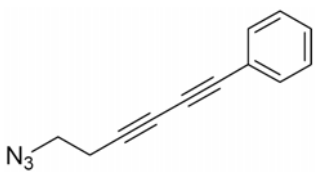

(6-Azidohexa-1,3-diynyl)benzene (56b). To a solution of **55b** (0.17 g, 0.54 mmol) in 5 mL of DMF at rt was added NaN_3 (0.038 g, 0.59 mmol). The reaction mixture was then refluxed at 70 °C for 6 h. After cooled to rt, 30 mL of H_2O was added to the mixture and the aqueous phase was extracted with 3 × 15 mL of EtOAc. The combined organic extracts were washed with 3 × 10 mL of brine, dried over $MgSO_4$ and concentrated *in vacuo*. Purification of the residue by flash chromatography (5:1 Hexanes/EtOAc) yielded 0.41 g (46%) of azide **56b** as colorless oil**.** **^{1}H-NMR** (400 MHz, $CDCl_3$) δ 7.50-7.27 (m, 5H), 3.47 (t, 2H, *J* = 6.8 Hz), 2.66 (t, 2H, *J* = 6.8 Hz); **^{13}C-NMR** (100 MHz, $CDCl_3$) δ 132.58, 129.11, 128.37, 121.63, 79.82, 75.85, 73.34, 67.16, 49.45, 20.62.

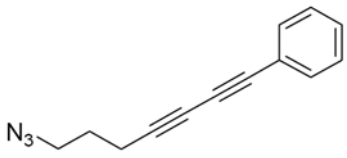

(7-Azidohepta-1,3-diynyl)benzene (56c). To a solution of **55c** (0.40 g, 1.19 mmol) in 10 mL of DMF at rt was added NaN_3 (0.085 g, 1.31 mmol). The reaction mixture was then refluxed at 70 °C for 6 h. After cooled to rt, 30 mL of H_2O was added to the mixture and the aqueous phase was extracted with 3 × 15 mL of EtOAc. The combined organic extracts were washed with 3 × 10 mL of brine, dried over $MgSO_4$ and concentrated *in vacuo*. Purification of the residue by flash chromatography (3:1 Hexanes/EtOAc) yielded 0.25 g (100%) of azide **56c** as colorless oil**.** **^{1}H-NMR** (400 MHz, $CDCl_3$) δ 7.50-7.29 (m,

5H), 3.46 (t, 2H, *J* = 6.8 Hz), 2.49 (t, 2H, *J* = 6.8 Hz), 2.49 (p, 2H, *J* = 6.8 Hz); **^{13}C-NMR** (100 MHz, $CDCl_3$) δ 132.48, 128.95, 128.33, 121.77, 82.48, 75.24, 73.99, 66.10, 50.02, 27.51, 16.87..

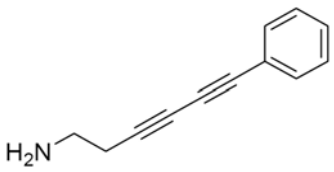

6-Phenylhexa-3,5-diyn-1-amine (21b). To a solution of **56b** (0.066 g, 0.34 mmol) in 2.5 mL of anhydrous ether at 0 °C was added 0.7mL 1.0M LAH dropwise. The reaction was quenched by adding 1 mL of 6.5 N NaOH after 10 min. The resulting slurry was dried over $MgSO_4$ and the organic phase was collected by filtration. The filtrate was concentration *in vacuo* to yield 0.057 g (100%) of amine **21b** as yellow oil**. ^{1}H-NMR** (400 MHz, $CDCl_3$) δ 7.49-7.28 (m, 5H), 2.91 (t, 2H, *J* = 6.4 Hz), 2.51 (t, 2H, *J* = 6.4 Hz), 1.54 (b, 2H); **^{13}C-NMR** (100 MHz, $CDCl_3$) δ 132.50, 128.93, 128.34, 121.86, 82.40, 75.10, 74.09, 66.44, 40.85, 24.72.

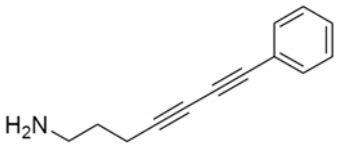

7-Phenylhepta-4,6-diyn-1-amine (21c). To a solution of **56c** (0.58 g, 4.36 mmol) in 20 mL of anhydrous ether at 0 °C was added 8.7 mL 1.0 M LAH dropwise. The reaction was quenched by adding 5 mL of 6.5 N NaOH after 10 min. The resulting slurry was dried over $MgSO_4$ and the organic phase was collected by filtration. The filtrate was concentration *in vacuo* to yield 1.15 g (95%) of amine **21c** as yellow oil**. ^{1}H-NMR** (400 MHz, $CDCl_3$) δ 2.64 (t, 2H, *J* = 6.8 Hz), 2.22 (dt, 2H, *J* = 1.2, 6.8 Hz), 1.93 (t, 1H, *J* = 1.2 Hz), 1.50 (m, 4H), 1.40 (b, 2H); **^{13}C-NMR** (100 MHz, $CDCl_3$) δ 77.93, 68.23, 64.79, 654.57, 41.39, 32.58, 25.20, 18.74.

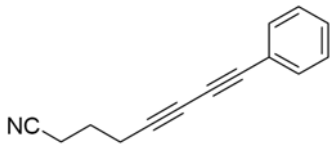

8-Phenylocta-5,7-diynenitrile (57). To a solution of CuCl (0.021 g, 0.22 mmol) and NH_2OH•HCl (0.067 g, 0.97 mmol) in 20 mL of 30% aq n-butylamine at 0°C was added 5-hexynenitrile (1.00 g, 10.75 mmol). Bright yellow slurry was formed immediately. Then **53** (2.14 g, 11.83 mmol) was syringed into the slurry that turned from bright yellow into blue with the addition of the bromide. A small amount of NH_2OH•HCl was added to bring the mixture back into yellow. This was repeated a few times during the next 30 min. When the reaction completed it became a clear yellow solution that was adjusted to PH = 2 with 1.0 M HCl and extracted with 3 × 20 mL of Et_2O. The combined organic layers were washed with 3 × 20 mL of sat aq $NH_4^+Cl^-$, 3 × 20 mL of brine and dried over $MgSO_4$. Concentration *in vacuo* yielded brown oil that was purified by flash chromatography (5:1 Hexanes/EtOAc) to give 1.60 g (77%) of diacetylene **57** as tan oil. **^{1}H-NMR** (400 MHz, $CDCl_3$) δ 7.49-7.29 (m, 5H), 2.57-2.50 (m, 4H), 2.51 (p, 2H, *J* = 6.8 Hz); **^{13}C-NMR** (100 MHz, $CDCl_3$) δ 132.45, 129.06, 128.34, 121.50, 118.74, 81.10, 75.64, 73.68, 66.89, 24.17, 18.61, 16.11.

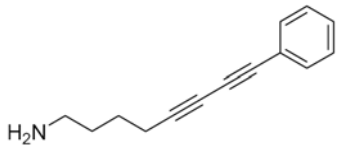

8-Phenylocta-5,7-diyn-1-amine (21d). To a solution of **57** (1.30 g, 6.75 mmol) in 30 mL of anhydrous ether at -78 °C was added 27 mL 1.0 M LAH dropwise. The reaction was stirred at -78 °C for 24 h before quenched by adding 10 mL of 6.5 N NaOH. The resulting slurry was dried over $MgSO_4$ and the organic phase was collected by filtration. The filtrate was concentration *in vacuo* to yield 1.16 g (87%) of amine **21d** as yellow oil**.**

^{1}H-NMR (400 MHz, $CDCl_3$) δ 7.48-7.27 (m, 5H), 2.73 (b, 2H), 2.39 (t, 2H, *J* = 6.4Hz), 1.60 (b, 4H), 1.30 (b, 2H); **^{13}C-NMR** (100 MHz, $CDCl_3$) δ 132.46, 128.80, 128.31, 122.02, 84.34, 74.83, 74.26, 65.34, 41.62, 32.85, 25.57, 19.45.

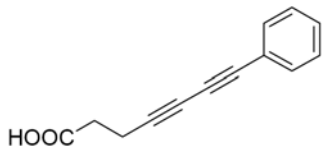

7-Phenylhepta-4,6-diynoic acid (22b). CuCl (0.023 g, 0.24 mmol) and 0.7 mL of $EtNH_2$ (70% aq solution) was dissolved in 10 mL of MeOH to give a dark blue solution, to which was added NH_2OH•HCl (0.049 g, 0.71 mmol) to discharge the blue color. Then 4-pentynoic acid (0.23 g, 2.37 mmol) was added into the mixture at 0 °C to give bright yellow slurry. At the end, **53** (0.45 g, 2.49 mmol) was syringed into the slurry that turned from bright yellow into blue with the addition of the bromide. A small amount of NH_2OH•HCl was added to bring the mixture back into yellow. This was repeated a few times if necessary during the following 30 min. The final yellow reaction mixture was quenched with 1.0 M HCl and was adjusted to PH = 2 followed by extraction with 3 × 25 mL of Et_2O. The organic phase was washed with 3 × 15 mL of sat aq $NH_4^+Cl^-$, 3 × 15 mL of brine and dried over $MgSO_4$. The yellow residue was recrystallized out of EtOAc/Hexanes to give 0.24 g (52%) of the phenyl diacetylene **22b** as white crystals. Mp 132-134 °C; **^{1}H-NMR** (400 MHz, $CDCl_3$) δ 7.49-7.30 (b, 5H,), 2.69 (m, 4H); **^{13}C-NMR** (100 MHz, $CDCl_3$) δ 176.93, 132.54, 129.01, 128.35, 121.76, 81.66, 75.54, 73.92, 32.65, 15.22.

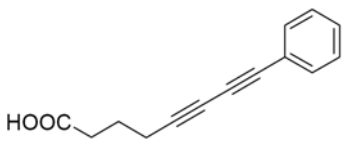

8-Phenylocta-5,7-diynoic acid (22c). CuCl (0.079 g, 0.80 mmol) and 3.2 mL of $EtNH_2$ (70% aq solution) was

dissolved in 40 mL of to give a dark blue solution, to which was added NH_2OH•HCl (0.17 g, 2.40 mmol) to discharge the blue color. Then 5-hexynoic acid (0.90 g, 8.00 mmol) was added into the mixture at 0 °C to give bright yellow slurry. At the end, **53** (1.52 g, 8.40 mmol) was syringed into the slurry that turned from bright yellow into blue with the addition of the bromide. A small amount of NH_2OH•HCl was added to bring the mixture back into yellow. This was repeated a few times if necessary during the following 30 min. The final yellow reaction mixture was quenched with 1.0 M HCl and was adjusted to PH = 2 followed by extraction with 3 × 50 mL of Et_2O. The organic phase was washed with 3 × 30 mL of sat aq $NH_4^+Cl^-$, 3 × 30 mL of brine and dried over $MgSO_4$. The yellow residue was recrystallized out of Hexanes to give 0.93 g (55%) of the phenyl diacetylene **22c** as white crystals. Mp 81-81.5 °C; **^{1}H-NMR** (400 MHz, $CDCl_3$) δ 7.49-7.28 (b, 5H,), 2.55 (t, 2H, *J* = 7.2 Hz), 2.49 (t, 2H, *J* = 7.2 Hz), 1.91 (p, 2H, *J* = 7.2 Hz); **^{13}C-NMR** (100 MHz, $CDCl_3$) δ 177.60, 132.53, 128.94, 128.35, 121.90, 82.90, 75.20, 74.06, 66.15, 32.36, 32.16, 18.94.

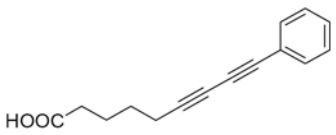

9-Phenylnona-6,8-diynoic acid (22d). CuCl (0.053 g, 0.53 mmol) and 2.2 mL of $EtNH_2$ (70% aq solution) was dissolved in 25 mL of to give a dark blue solution, to which was added NH_2OH•HCl (0.11 g, 1.60 mmol) to discharge the blue color. Then 6-heptnoic acid (0.67 g, 5.35 mmol) was added into the mixture at 0 °C to give bright yellow slurry. At the end, **53** (1.02 g, 5.62 mmol) was syringed into the slurry that turned from bright yellow into blue with the addition of the bromide. A small amount of NH_2OH•HCl was added to bring the mixture back into yellow. This was repeated a few times if necessary

during the following 30 minutes. The final yellow reaction mixture was quenched with 1.0 M HCl and was adjusted to PH = 2 followed by extraction with 3 × 30 mL of Et_2O. The organic phase was washed with 3 × 20 mL of sat aq $NH_4^+Cl^-$, 3 × 20 mL of brine and dried over $MgSO_4$. The yellow residue was recrystallized out of Hexanes to give 0.68 g (54%) of the phenyl diacetylene **22d** as white crystals. Mp 103-105 °C; **^{1}H-NMR** (400 MHz, $CDCl_3$) δ 7.49-7.28 (b, 5H,), 2.41 (dt, 4H, *J* = 2, 7.2 Hz), 1.80 (m, 2H), 1.66 (m, 2H); **^{13}C-NMR** (100 MHz, $CDCl_3$) δ 179.51, 132.49, 128.85, 128.32, 121.89, 83.74, 74.98, 74.21, 65.60, 33.40, 27.51, 23.77, 19.31.

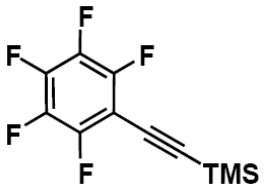

Trimethyl((pentafluorophenyl)ethynyl)silane (58). A degassed solution of bromopentafluorobenzene (9.72 g, 39.36 mmol), CuI (0.75 g, 3.94 mmol) and $(Ph_3P)_2PdCl_2$ (1.38 g, 1.97 mmol) in 50 mL of TEA was heated up to 90 °C. Then trimethylsilylacetylene (8.27 g, 59.04 mmol) was added dropwise over 1 h. The mixture was continuously heated at gentle reflux until (up to 2 h) all the 4-bromobenzaldehyde was transformed (by TLC). The solvent was evaporated and the residue was treated with hexanes. Filtration through silica gel and evaporation of the solvent yielded 10.45 g (88%) of **58** as yellow oil. **^{1}H-NMR** (400 MHz, $CDCl_3$) δ 0.28 (s, 1H).

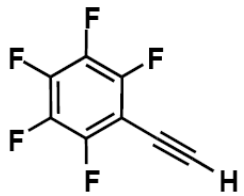

1-Ethynyl-2,3,4,5,6-pentafluorobenzene (59). To the solution of **58** (10.45 g, 34.15 mmol) in 50mL of MeOH was added 0.05 mL of 50% KOH at rt. The exothermic reaction was vigorously stirred for 10 minutes before

quenching with 50 mL of H_2O and acidifying with 3 mL of 10% HCl. The mixture was extracted with 3 × 30 mL of diethyl ether. The combined organic phase was washed with 3 × 20 mL of sat aq NH_4+Cl-, and then dried over $MgSO_4$. After removal of most of the solvent, the residue was distilled at reduced pressure (1 torr) to afford 5.77 g (88%) of **59** as colorless liquid. **^{1}H-NMR** (400 MHz, $CDCl_3$) δ3.61 (s, 1H); **^{13}C-NMR** (100 MHz, $CDCl_3$) δ 89.79, 67.57, 60.38.

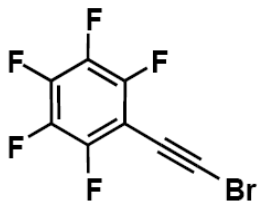

1-(Bromoethynyl)-2,3,4,5,6-pentafluorobenzene (60). To the solution of **59** (0.433 g, 2.25 mmol) in acetone, NBS (0.430 g, 2.41 mmol, recrystallized out of H_2O before use) was added. At the end $AgNO_3$ (0.019 g, 0.11 mmol) was added all at once to the mixture solution, which turned cloudy in 5 min. The reaction was stirred overnight. To work up, acetone was removed *in vacuo* before ice water was added. After extracted with 3 × 30 mL of ether, the organic phase was washed with 3 × 20 mL of brine and dried over $MgSO_4$. Removal of the solvent afforded 0.500 g (81%) of **60** as colorless oil. **^{13}C-NMR** (100 MHz, $CDCl_3$) δ 64.48 63.41.

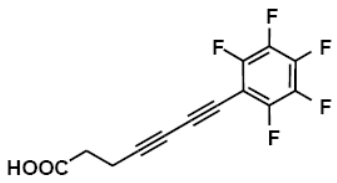

7-(pentafluorophenyl)hepta-4,6-diynoic acid (61b). CuCl (0.012 g, 0.12 mmol) and 0.5 mL of $EtNH_2$ (70% aq solution) was dissolved in 5 mL of MeOH to give a dark blue solution, to which was added NH_2OH•HCl (0.026 g, 0.37 mmol) to discharge the blue color. Then 4-pentynoic acid (0.12 g, 1.24 mmol) was added into the mixture at 0 °C to give bright yellow slurry. At the end, **60** (0.35 g, 1.31

mmol) was syringed into the slurry that turned from bright yellow into blue with the addition of the bromide. A small amount of NH_2OH•HCl was added to bring the mixture back into yellow. This was repeated a few times if necessary during the following 30 minutes. The final yellow reaction mixture was quenched with 1.0 M HCl and was adjusted to PH = 2 followed by extraction with 3 × 20 mL of Et_2O. The organic phase was washed with 3 × 15 mL of sat aq $NH_4^+Cl^-$, 3 × 15 mL of brine and dried over $MgSO_4$. The yellow residue was recrystallized out of EtOAc/Hexanes to give 0.21 g (60%) of **61b** as white crystals. Mp 115-117 °C; **^{1}H-NMR** (400 MHz, CD_3OD) δ 2.71 (t, 2H, *J* = 6.8 Hz), 2.60 (t, 2H, *J* = 6.8 Hz); **^{13}C-NMR** (100 MHz, CD_3OD) δ 174.99, 88.61, 86.61, 65.06, 59.20, 33.49, 16.28.

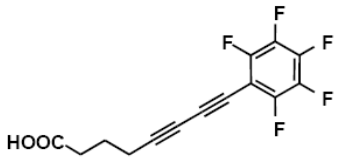

8-(Pentafluorophenyl)octa-5,7-diynoic acid (61c). CuCl (0.007 g, 0.07 mmol) and 0.5 mL of $EtNH_2$ (70% aq solution) was dissolved in 5 mL of MeOH to give a dark blue solution, to which was added NH_2OH•HCl (0.015 g, 0.22 mmol) to discharge the blue color. Then 4-pentynoic acid (0.08 g, 0.74 mmol) was added into the mixture at 0 °C to give bright yellow slurry. At the end, **60** (0.21 g, 0.77 mmol) was syringed into the slurry that turned from bright yellow into blue with the addition of the bromide. A small amount of NH_2OH•HCl was added to bring the mixture back into yellow. This was repeated a few times if necessary during the following 30 minutes. The final yellow reaction mixture was quenched with 1.0 M HCl and was adjusted to PH = 2 followed by extraction with 3 × 20 mL of Et_2O. The organic phase was washed with 3 × 15 mL of sat aq $NH_4^+Cl^-$, 3 × 15 mL of brine and dried over

$MgSO_4$. The yellow residue was recrystallized out of EtOAc/Hexanes to give 0.12 g (54%) of **61c** as white crystals. Mp 93-94 °C; **^{1}H-NMR** (400 MHz, CD_3OD) δ 2.55 (t, 2H, *J* = 6.8 Hz), 2.52 (t, 2H, *J* = 6.8 Hz), 1.94 (p, 2H, *J* = 6.8 Hz); **^{13}C-NMR** (100 MHz, CD_3OD) δ 178.51, 87.11, 85.70, 65.30, 58.55, 32.46, 22.82, 18.95.

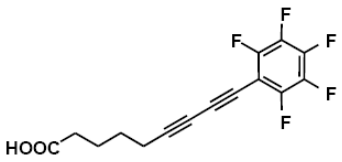

9-(Pentafluorophenyl)nona-6,8-diynoic acid (61d). CuCl (0.007 g, 0.07 mmol) and 0.5 mL of $EtNH_2$ (70% aq solution) was dissolved in 5 mL of MeOH to give a dark blue solution, to which was added NH_2OH•HCl (0.015 g, 0.21 mmol) to discharge the blue color. Then 4-pentynoic acid (0.087 g, 0.71 mmol) was added into the mixture at 0 °C to give bright yellow slurry. At the end, **59** (0.20 g, 0.75 mmol) was syringed into the slurry that turned from bright yellow into blue with the addition of the bromide. A small amount of NH_2OH•HCl was added to bring the mixture back into yellow. This was repeated a few times if necessary during the following 30 minutes. The final yellow reaction mixture was quenched with 1.0 M HCl and was adjusted to PH = 2 followed by extraction with 3 × 20 mL of Et_2O. The organic phase was washed with 3 × 15 mL of sat aq $NH_4^+Cl^-$, 3 × 15 mL of brine and dried over $MgSO_4$. The yellow residue was recrystallized out of EtOAc/Hexanes to give 0.13 g (58%) of **61d** as white crystals. Mp 103-105 °C; **^{1}H-NMR** (400 MHz, CD_3OD) δ 2.44 (t, 2H, *J* = 6.8 Hz), 2.42 (t, 2H, *J* = 6.8 Hz), 1.79 (m, 2H), 1.68 (m, 2H); **^{13}C-NMR** (100 MHz, CD_3OD) δ 179.18, 87.96, 85.89, 64.82, 58.30, 33.31, 27.20, 23.77, 19.39.

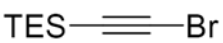

(Bromoethynyl)triethylsilane (62). To the solution of

triethylsilylacetylene (3.60 g, 25.66 mmol) in acetone, NBS (4.89 g, 27.47 mmol, recrystallized out of H_2O before use) was added. At the end $AgNO_3$ (0.22 g, 1.28 mmol) was added all at once to the mixture solution, which turned cloudy in 5 min. The reaction was stirred overnight. To work up, acetone was removed *in vacuo* before ice water was added. After extracted with 3 × 30 mL of ether, the organic phase was washed with 3 × 20 mL of brine and dried over $MgSO_4$. Removal of the solvent afforded 5.08 g (90%) of **62** as tan oil. **^{1}H-NMR** (300 MHz, $CDCl_3$) δ 0.99 (t, 3H *J* = 7.8 Hz), 0.61 (q, 2H, *J* = 7.8 Hz); **^{13}C-NMR** (75 MHz, $CDCl_3$) δ 84.58, 61.61, 7.28, 4.27.

General procedure for the hydroxyl alkyl diacetylene synthesis: 0.02 Equiv of CuCl was dissolved in 30% aq n-butylamine to give a dark blue solution, to which was added 0.09 equiv of NH_2OH•HCl to discharge the blue color. Then 1 equiv of the terminal acetylene was added into the mixture at 0 °C to give bright yellow slurry. At the end, 1.05 equiv of the (bromoethynyl)triethylsilane was syringed into the slurry that turned from bright yellow into green or blue with the addition of the bromide. A small amount of NH_2OH•HCl was added to bring the mixture back into yellow. This was repeated a few times if necessary during the following 15-30 min. When the reaction completed it became a clear solution with yellow, or rusty, or red color depending on the substrate. The reaction was quenched with 1.0 M HCl and was adjusted to PH = 2 followed by extraction with Et_2O. The organic phase was washed with sat aq $NH_4^+Cl^-$, brine and dried over $MgSO_4$. Concentration *in vacuo* followed by flash chromatography yielded the analytically pure product as light colored oil.

5-(Triethylsilyl)penta-2,4-diyn-1-ol (63a). 2.94 g (90% yield). Tan oil. **^{1}H-NMR** (300 MHz, $CDCl_3$) δ 4.34 (s, 2H), 1.00 (t, 9H, *J* = 7.8 Hz), 0.63 (q, 6H, *J* = 7.8 Hz).

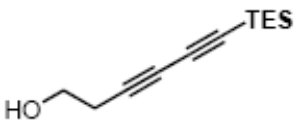

6-(Triethylsilyl)hexa-3,5-diyn-1-ol (63b). 2.30 g (99% yield). Tan oil. **^{1}H-NMR** (300 MHz, $CDCl_3$) δ 3.76 (t, 2H, *J* = 6 Hz), 2.55 (t, 2H, *J* = 6 Hz), 1.00 (t, 9H, *J* = 7.8 Hz), 0.62 (q, 6H, *J* = 7.8 Hz).

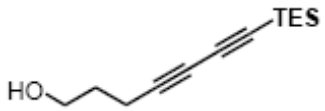

7-(Triethylsilyl)hepta-4,6-diyn-1-ol (63c). 4.32 g (97% yield). Yellow oil. **^{1}H-NMR** (400 MHz, $CDCl_3$) δ 3.74 (t, 2H, *J* = 6.4 Hz), 2.41 (t, 2H, *J* = 6.4 Hz), 1.78 (p, 2H, *J* = 6.4 Hz), 0.99 (t, 9H, *J* = 8 Hz), 0.61 (q, 6H, *J* = 8 Hz); **^{13}C-NMR** (100 MHz, $CDCl_3$) δ 89.17, 81.34, 78.34, 66.11, 61.32, 30.75, 15.75, 7.32, 4.20.

General procedure for the tosulate synthesis: 1 equiv of *p*-toluenesulfonyl chloride was added to a solution of 1 equiv of alcohol, 1.1 of equiv triethylamine and 1 equiv of 4-dimethylaminopyridine in CH_2Cl_2 at 0 °C. After 3 h, the reaction was quenched with H_2O, extracted with CH_2Cl_2, and the combined organic extracts were dried over $MgSO_4$ and concentrated *in vacuo*. Purification of the residue by flash chromatography yielded the analytically pure product as colorless oil.

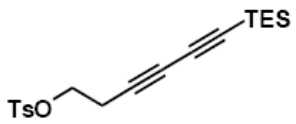

6-(Triethylsilyl)hexa-3,5-diynyl 4-methylbenzenesulfonate (64b). 0.25 g (78% yield). Colorless oil**.** **^{1}H-NMR** (400 MHz, $CDCl_3$) δ 7.80 (d, 2H, *J* = 8 Hz), 7.35 (d, 2H, *J* = 8 Hz), 4.08 (t, 2H, *J* = 8 Hz), 2.64 (t, 2H, *J* = 8 Hz), 2.46 (s, 3H), 0.99 (t, 9H, *J* = 8 Hz), 0.61 (q, 6H, *J* = 8 Hz); **^{13}C-NMR** (100 MHz, $CDCl_3$) δ 145.05, 132.64, 129.92, 128.02, 88.59, 82.81, 72.54, 67.89, 66.79, 21.66, 20.26, 7.32, 4.14.

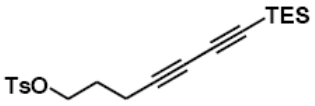

7-(Triethylsilyl)hepta-4,6-diynyl 4-methylbenzenesulfonate (64c). 2.31 g (68% yield). Colorless oil**.** **^{1}H-NMR** (400 MHz, $CDCl_3$) δ 7.79 (d, 2H, *J* = 8 Hz), 7.35 (d, 2H, *J* = 8 Hz), 4.12 (t, 2H, *J* = 6 Hz), 2.45 (s, 3H), 2.34 (t, 2H, *J* = 6 Hz), 1.86 (p, 2H, *J* = 6 Hz), 0.99 (t, 9H, *J* = 8 Hz), 0.62 (q, 6H, *J* = 8 Hz); **^{13}C-NMR** (100 MHz, $CDCl_3$) δ 144.86, 132.81, 129.90, 127.90, 88.92, 81.82, 76.55, 68.54, 66.66, 27.51, 21.65, 15.55, 7.33, 4.18.

General procedure for the azide synthesis: 1.1 equiv of NaN_3 was added to a solution of 1 equiv of tosulate in DMF at rt. The reaction mixture was then refluxed at 70 °C for 6 h. After cooled to rt, H_2O was added to the mixture and the aqueous phase was extracted with EtOAc. The combined organic extracts were washed with brine, dried over $MgSO_4$ and concentrated *in vacuo*. Purification of the residue by flash chromatography yielded the analytically pure product as colorless oil.

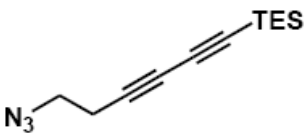

(6-Azidohexa-1,3-diynyl)triethylsilane. 0.41 g (46% yield). Colorless oil**.** **^{1}H-NMR** (400 MHz, $CDCl_3$) δ 3.43 (t, 2H, *J* = 6.8 Hz), 2.56 (t, 2H, *J* = 6.8 Hz), 0.99 (t, 9H, *J* = 8 Hz), 0.62 (q, 6H, *J* = 8 Hz); **^{13}C-NMR** (100 MHz, $CDCl_3$) δ 88.68, 82.68, 74.43, 67.64, 66.79, 49.33, 20.25, 7.30, 4.14.

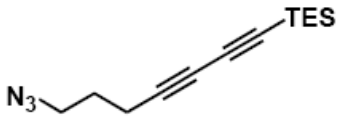

(7-Azidohepta-1,3-diynyl)triethylsilane. 0.83 g (55% yield). Colorless oil**.** **^{1}H-NMR** (400 MHz, $CDCl_3$) δ 3.42 (t, 2H, *J*=6.8 Hz), 2.40 (t, 2H, *J* = 6.8 Hz), 1.80 (p, 2H, *J* = 6.8 Hz), 0.99 (t, 9H, *J* = 8 Hz), 0.62 (q, 6H, *J* = 8 Hz); **^{13}C-NMR** (100 MHz, $CDCl_3$) δ 88.98, 81.85, 77.11, 66.66, 50.02, 27.43, 16.57, 7.33, 4.19.

General procedure for the silyl deprotection: 1.5 equiv of tetrabutylammonium fluoride trihydrate (1.0M in THF w 5% H_2O) was added dropwise to the solution of 1 equiv TES protected diacetylene in THF/MeOH (20:1) at 0 °C. After the addition was finished, the reaction mixture was stirred at rt for about 1 h. To work up, the light yellow solution was poured into sat aq $NH4^{+}Cl^{-}$, followed by extraction with ether. The combined organic extracts were washed with brine, dried over $MgSO_4$ and concentrated *in vacuo*. Purification of the residue by flash chromatography yielded the analytically pure terminal diacetylene as tan oil.

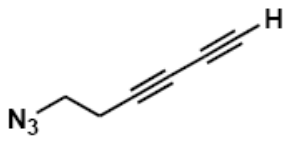

6-Azidohexa-1,3-diyne (65b). 0.12 g (56% yield). Tan oil**.** **^{1}H-NMR** (400 MHz, $CDCl_3$) δ 3.43 (t, 2H, *J* = 6.8 Hz), 2.55 (dt, 2H, *J* = 1.2, 6.8 Hz), 2.02 (t, 1H, *J* = 1.2 Hz); **^{13}C-**

NMR (100 MHz, $CDCl_3$) δ 73.79, 67.83, 65.70, 49.20, 20.10.

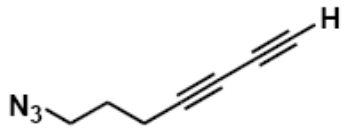

7-Azidohepta-1,3-diyne (65c). 0.32 g (70% yield). Tan oil**.** **^{1}H-NMR** (400 MHz, $CDCl_3$) δ 3.42 (t, 2H, *J* = 6.8 Hz), 2.39 (dt, 2H, *J* = 1.2, 6.8 Hz), 1.99 (t, 1H, *J* = 1.2 Hz), 1.80 (p, 2H, *J* = 6.8 Hz); **^{13}C-NMR** (100 MHz, $CDCl_3$) δ 76.34, 68.08, 65.66, 65.09, 49.96, 27.29, 16.33.

General procedure for the azide reduction: 2 equiv of lithium aluminum hydride (1.0M in ether) was added dropwise to the solution of 1 equiv azide in anhydrous ether at 0 °C. The reaction was quenched by adding 6.5N NaOH after 10 minutes. The resulting slurry was dried over $MgSO_4$ and the organic phase was collected by filtration. The filtrate was concentration *in vacuo* to yield the analytically pure primary amine as colorless oil.

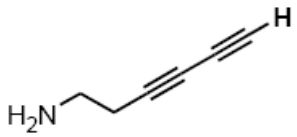

Hexa-3,5-diyn-1-amine (66b). 0.076 g (83% yield). Colorless oil**.** **^{1}H-NMR** (400 MHz, $CDCl_3$) δ 2.84 (t, 2H, *J* = 6. 4 Hz), 2.37 (dt, 2H, *J* = 1.2, 6.4 Hz), 1.97 (t, 1H, *J* = 1.2 Hz), 1.34 (b, 2H); **^{13}C-NMR** (100 MHz, $CDCl_3$) δ 76.25, 68.13, 65.91, 64.88, 40.56, 24.09.

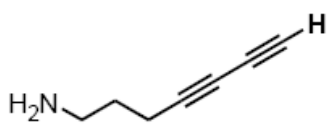

Hepta-4,6-diyn-1-amine (66c). 0.42 g (91% yield). Colorless oil**.** **^{1}H-NMR** (400 MHz, $CDCl_3$) δ 2.64 (t, 2H, *J*

= 6.8 Hz), 2.22 (dt, 2H, *J* = 1.2, 6.8 Hz), 1.93 (t, 1H, *J* = 1.2 Hz), 1.50 (m, 4H), 1.40 (b, 2H); **^{13}C-NMR** (100 MHz, $CDCl_3$) δ 77.93, 68.23, 64.79, 654.57, 41.39, 32.58, 25.20, 18.74.

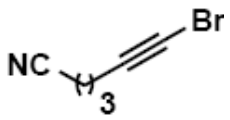

6-Bromohex-5-ynenitrile (67). To the solution of triethylsilylacetylene (0.65 g, 6.95 mmol) in acetone, NBS (1.32 g, 7.43 mmol, recrystallized out of H_2O before use) was added. At the end $AgNO_3$ (0.059 g, 0.35 mmol) was added all at once to the mixture solution, which turned cloudy in 5 min. The reaction was stirred overnight. To work up, acetone was removed *in vacuo* before ice water was added. After extracted with 3 × 20 mL of ether, the organic phase was washed with 3 × 20 mL of brine and dried over $MgSO_4$. Removal of the solvent afforded 1.17 g (98%) of **67** as colorless oil. **^{1}H-NMR** (300 MHz, $CDCl_3$) δ 2.48 (t, 2H *J* = 6.9 Hz), 2.39 (t, 2H, *J* = 6.9 Hz), 1.86 (p, 2H, *J* = 6.9 Hz); **^{13}C-NMR** (75 MHz, $CDCl_3$) δ 118.84, 77.42, 40.26, 24.14, 18.70, 16.04.

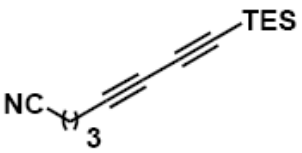

8-(Triethylsilyl)octa-5,7-diynenitrile (68). To a solution of CuCl (0.013 g, 0.14 mmol) and NH_2OH•HCl (0.042 g, 0.61 mmol) in 10 mL of 30% aq n-butylamine at 0°C were added triethylsilylacetylene (1.14 g, 8.14 mmol). Bright yellow slurry was formed immediately. Then **67** (1.17 g, 6.78 mmol) was syringed into the slurry that turned from bright yellow into blue with the addition of the bromide. A small amount of NH_2OH•HCl was added to bring the mixture back into yellow. This was repeated a few times during the next 15 minutes. When the reaction completed it became a red solution that was

adjusted to PH = 2 with 1.0M HCl and extracted with 3 × 20 mL of Et_2O. The combined organic layers were washed with 3 × 20 mL of sat aq $NH_4^+Cl^-$, 3 × 20 mL of brine and dried over $MgSO_4$. Concentration *in vacuo* yielded yellow oil that was purified by flash chromatography (3:1 Hexanes/EtOAc) to give 1.32 g (83%) of **68** as tan oil. **^{1}H-NMR** (300 MHz, $CDCl_3$) δ 2.51 (t, 2H, *J* = 6.9 Hz), 2.48 (t, 2H, *J* = 6.9 Hz), 1.90 (q, 2H, *J* = 6.9 Hz), 0.99 (t, 9H, *J* = 8.4 Hz), 0.62(q, 6H, *J* = 8.4 Hz) **^{13}C-NMR** (75 MHz, $CDCl_3$) δ 118.74, 88.65, 82.54, 75.72, 67.50, 24.16, 18.36, 16.20, 7.32, 4.15.

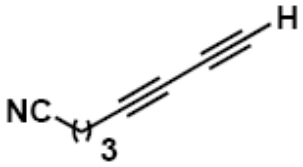

Octa-5,7-diynenitrile (69). To a solution of **68** (0.65 g, 2.81 mmol) in 3 mL of THF/MeOH (20:1) at 0 °C was added 5.6 mL 1.0 M TBAF dropwise. After the addition was finished, the reaction mixture was stirred at rt for about 1 h. To work up, the yellow solution was poured into 20 mL of sat aq $NH_4^+Cl^-$, followed by extraction with 3 × 15 mL of ether. The combined organic extracts were washed with 3 × 15 mL of brine, dried over $MgSO_4$ and concentrated *in vacuo*. Purification of the residue by flash chromatography (5:1 Hexanes/EtOAc) yielded 0.27 g (81%) of **69** as tan oil**. ^{1}H-NMR** (400 MHz, $CDCl_3$) δ 2.52-2.45 (m, 4H), 2.55 (t, 1H, *J* = 1.2Hz), 1.91 (p, 2H, *J* = 7.2 Hz).

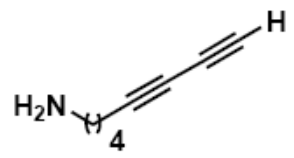

Octa-5,7-diyn-1-amine (66d). To a solution of **69** (0.27 g, 2.33 mmol) in 10 mL of anhydrous ether at -78 °C was added 9.3 mL 1.0 M LAH dropwise. The reaction was stirred at -78 °C for 24 h before quenched by adding 5 mL of 6.5 N NaOH. The resulting

slurry was dried over $MgSO_4$ and the organic phase was collected by filtration. The filtrate was concentration *in vacuo* to yield 0.15 g (53%) of **66d** as yellow oil**.** **^{1}H-NMR** (400 MHz, $CDCl_3$) δ 2.64 (t, 2H, *J* = 6.8Hz), 2.22 (dt, 2H, *J* = 1.2, 6.8Hz), 1.93 (t, 1H, *J* = 1.2 Hz), 1.54-1.44 (m, 4H), 1.40 (b, 2H); **^{13}C-NMR** (100 MHz, $CDCl_3$) δ 77.93, 68.23, 64.79, 64.57, 41.39, 32.58, 25.20, 18.74.

Bibliography

(1) Shirakawa.H; Ikeda, S. Infrared Spectra of Poly(Acetylene). *Polym.J.* **1971**, *2*, 231-244.

(2) Sperry, J. K.; Foulger, S. H.; Han, M. G.; Ingram, S. T.; (Clemson University, USA). Application: WO. Patent Number: 2007-US7237, 2007111996, 2007.

(3) Burroughes, J. H.; Jones, C. A.; Friend, R. H. New Semiconductor-Device Physics in Polymer Diodes and Transistors. *Nature* **1988**, *335*, 137-141.

(4) Sirringhaus, H.; Tessler, N.; Friend, R. H. Integrated optoelectronic devices based on conjugated polymers. *Science* **1998**, *280*, 1741-1744.

(5) Sauteret, C.; Hermann, J. P.; Frey, R.; Pradere, F.; Ducuing, J.; Baughman, R. H.; Chance, R. R. Optical Nonlinearities in One-Dimensional-Conjugated Polymer Crystals. *Phys. Rev. Lett.* **1976**, *36*, 956-959.

(6) Burroughes, J. H.; Bradley, D. D. C.; Brown, A. R.; Marks, R. N.; Mackay, K.; Friend, R. H.; Burns, P. L.; Holmes, A. B. Light-Emitting-Diodes Based on Conjugated Polymers. *Nature* **1990**, *347*, 539-541.

(7) Friend, R. H.; Gymer, R. W.; Holmes, A. B.; Burroughes, J. H.; Marks, R. N.; Taliani, C.; Bradley, D. D. C.; Dos Santos, D. A.; Bredas, J. L.; Logdlund, M.; Salaneck, W. R. Electroluminescence in conjugated polymers. *Nature* **1999**, *397*, 121-128.

(8) Wang, C. S.; Lee, C. Y. C.; Amold, F. E. Mechanical and electrical properties of heat-treated ladder polymer fiber. *Mater. Res. Soc. Symp. Proc.* **1992**, *247*, 747-752.

(9) Chiang, C. K.; Fincher, C. R.; Park, Y. W.; Heeger, A. J.; Shirakawa, H.; Louis, E. J.; Gau, S. C.; Macdiarmid, A. G. Electrical-Conductivity in Doped Polyacetylene. *Phys. Rev. Lett.* **1977**, *39*, 1098-1101.

(10) Tour, J. M. Conjugated macromolecules of precise length and constitution. Organic synthesis for the construction of nanoarchitectures. *Chem. Rev.* **1996**, *96*, 537-553.

(11) Feast, W. J.; Tsibouklis, J.; Pouwer, K. L.; Groenendaal, L.; Meijer, E. W. Synthesis, processing and material properties of conjugated polymers. *Polymer* **1996**, *37*, 5017-5047.

(12) Masuda, T.; Karim, S. M. A.; Nomura, R. Synthesis of acetylene-based widely conjugated polymers by metathesis polymerization and polymer properties. *J. Mol. Catal. A: Chem.* **2000**, *160*, 125-131.

(13) Yamamoto, T. pi-Conjugated polymers with electronic and optical functionalities: Preparation by organometallic polycondensation, properties, and applications. *Macromol. Rapid Commun.* **2002**, *23*, 583-606.

(14) Pron, A.; Rannou, P. Processible conjugated polymers: from organic semiconductors to organic metals and superconductors. *Prog. Polym. Sci.* **2002**, *27*, 135-190.

(15) Morin, J. F.; Leclerc, M.; Ades, D.; Siove, A. Polycarbazoles: 25 years of progress. *Macromol. Rapid Commun.* **2005**, *26*, 761-778.

(16) Skotheim, T. A.; Reynolds, J.; Ed. Conjugated Polymers: Theory, Synthesis, Properties, and Characterization (Handbook of Conducting Polymers).

Conjugated Polymers: Theory, Synthesis, Properties, and Characterization (Handbook of Conducting Polymers) **CRC; 3 edition (December 26, 2006)**.
(17) Ito, T.; Shirakaw.H; Ikeda, S. Simultaneous Polymerization and Formation of Polyacetylene Film on Surface of Concentrated Soluble Ziegler-Type Catalyst Solution. *J. Polym. Sci., Part A: Polym. Chem.* **1974**, *12*, 11-20.
(18) Masuda, T.; Higashimura, T. Synthesis of High Polymers from Substituted Acetylenes - Exploitation of Molybdenum-Based and Tungsten-Based Catalysts. *Acc. Chem. Res.* **1984**, *17*, 51-56.
(19) Lam, J. W. Y.; Tang, B. Z. Functional polyacetylenes. *Acc. Chem. Res.* **2005**, *38*, 745-754.
(20) Kovacic, P.; Jones, M. B. Dehydro Coupling of Aromatic Nuclei by Catalyst Oxidant Systems - Poly(Para-Phenylene). *Chem. Rev.* **1987**, *87*, 357-379.
(21) Miyakoshi, R.; Shimono, K.; Yokoyama, A.; Yokozawa, T. Catalyst-transfer polycondensation for the synthesis of poly(p-phenylene) with controlled molecular weight and low polydispersity. *J. Am. Chem. Soc.* **2006**, *128*, 16012-16013.
(22) Bao, Z. N.; Chen, Y. M.; Cai, R. B.; Yu, L. P. Conjugated Liquid-Crystalline Polymers - Soluble and Fusible Poly(Phenylenevinylene) by the Heck Coupling Reaction. *Macromolecules* **1993**, *26*, 5281-5286.
(23) Zhou, Q.; Swager, T. M. Fluorescent chemosensors based on energy migration in conjugated polymers: The molecular wire approach to increased sensitivity. *J. Am. Chem. Soc.* **1995**, *117*, 12593-12602.
(24) Kloppenburg, L.; Jones, D.; Bunz, U. H. F. High molecular weight poly(p-phenyleneethynylene)s by alkyne metathesis utilizing "instant" catalysts: A synthetic study. *Macromolecules* **1999**, *32*, 4194-4203.
(25) Glaser, C. contribution to the chemistry of phenylacetylenes. *Ber.* **1869**, *2*, 422-424.
(26) Hay, A. S. Oxidative Coupling of Acetylenes. *J. Org. Chem.* **1960**, *25*, 1275-1276.
(27) Hay, A. S. Oxidative Coupling of Acetylenes .2. *J. Org. Chem.* **1962**, *27*, 3320-3321.
(28) Chodkiewicz, W. Synthesis of Acetylenic Compounds. *Ann. Chim.* **1957**, 819-869.
(29) Wityak, J.; Chan, J. B. Synthesis of 1,3-Diynes Using Palladium-Copper Catalysis. *Synth. Commun.* **1991**, *21*, 977-979.
(30) *IUPAC Compendium of Chemical Terminology, 2nd Ed.(1997)*.
(31) Wegner, G. Topochemical Reactions of Monomers with Conjugated Triple Bonds .I. Polymerization of 2.4-Hexadiyn-1.6-Diols Deivatives in Crystalline State. *Z. Naturforsch., B: Chem. Sci.* **1969**, *B 24*, 824-832.
(32) Baughman, R. H. Solid-State Synthesis of Large Polymer Single-Crystals. *J. Polym. Sci., Part B: Polym. Phys.* **1974**, *12*, 1511-1535.
(33) McGhie, A. R.; Kalyanaraman, P. S.; Garito, A. F. Kinetics of Thermal Polymerization in Solid-State - 2,4-Hexadiyne-1,6 Diol Bis (Para-Toluenesulfonate). *J. Polym. Sci., Part C: Polym. Lett.* **1978**, *16*, 335-338.
(34) Bloor, D.; Koski, L.; Stevens, G. C.; Preston, F. H.; Ando, D. J. Solid-State Polymerization of Bis-(Para-Toluene Sulfonate) of 2,4-Hexadiyne-1,6-Diol .1. X-

Ray-Diffraction and Spectroscopic Observations. *J. Mater. Sci.* **1975**, *10*, 1678-1688.
(35) Baughman, R. H. Solid-State Reaction-Kinetics in Single-Phase Polymerizations. *J. Chem. Phys.* **1978**, *68*, 3110-3121.
(36) Chance, R. R.; Eckhardt, H.; Swerdloff, M.; Federici, R. R.; Szobota, J. S.; Turi, E. A.; Boudreaux, D. S.; Schott, M. Urethane-Substituted Polydiacetylenes - Solid-State Polymerization, Crystal Optics, and Conformational Transitions. *ACS Symp. Ser.* **1987**, *337*, 140-151.
(37) Spagnoli, S.; Berrehar, J.; LapersonneMeyer, C.; Schott, M.; Rameau, A.; Rawiso, M. gamma-ray polymerization of urethane-substituted diacetylenes: Reactivity and chain lengths. *Macromolecules* **1996**, *29*, 5615-5620.
(38) Zhao, X. Q.; Chang, Y. L.; Fowler, F. W.; Lauher, J. W. An Approach to the Design of Molecular-Solids - the Ureylenedicarboxylic Acids. *J. Am. Chem. Soc.* **1990**, *112*, 6627-6634.
(39) Chang, Y. L.; West, M. A.; Fowler, F. W.; Lauher, J. W. An Approach to the Design of Molecular-Solids - Strategies for Controlling the Assembly of Molecules into 2-Dimensional Layered Structures. *J. Am. Chem. Soc.* **1993**, *115*, 5991-6000.
(40) Toledo, L. M.; Lauher, J. W.; Fowler, F. W. Design of Molecular-Solids - Application of 2-Amini-4(1h)-Pyridones to the Preparation of Hydrogen-Bonded Alpha-Networks and Beta-Networks. *Chem. Mater.* **1994**, *6*, 1222-1226.
(41) Toledo, L. M.; Musa, K. M.; Lauher, J. W.; Fowler, F. W. Development of Strategies for the Preparation of Designed Solids - an Investigation of the 2-Amino-4(1h)-Pyrimidone Ring-System for the Molecular Self-Assembly of Hydrogen-Bonded Alpha-Networks and Beta-Networks. *Chem. Mater.* **1995**, *7*, 1639-1647.
(42) Liao, R. F.; Lauher, J. W.; Fowler, F. W. The application of the 2-amino-4-pyrimidones to supramolecular synthesis. *Tetrahedron* **1996**, *52*, 3153-3162.
(43) Coe, S.; Kane, J. J.; Nguyen, T. L.; Toledo, L. M.; Wininger, E.; Fowler, F. W.; Lauher, J. W. Molecular symmetry and the design of molecular solids: The oxalamide functionality as a persistent hydrogen bonding unit. *J. Am. Chem. Soc.* **1997**, *119*, 86-93.
(44) Nguyen, T. L.; Scott, A.; Dinkelmeyer, B.; Fowler, F. W.; Lauher, J. W. Design of molecular solids: utility of the hydroxyl functionality as a predictable design element. *New J. Chem.* **1998**, *22*, 129-135.
(45) Kane, J. J.; Nguyen, T.; Xiao, J.; Fowler, F. W.; Lauher, J. W. The host guest co-crystal approach to supramolecular structure. *Mol. Cryst. Liq. Cryst.* **2001**, *356*, 449-458.
(46) Nguyen, T. L.; Fowler, F. W.; Lauher, J. W. Commensurate and incommensurate hydrogen bonds. An exercise in crystal engineering. *J. Am. Chem. Soc.* **2001**, *123*, 11057-11064.
(47) Kane, J. J.; Liao, R. F.; Lauher, J. W.; Fowler, F. W. Preparation of Layered Diacetylenes as a Demonstration of Strategies for Supramolecular Synthesis. *J. Am. Chem. Soc.* **1995**, *117*, 12003-12004.
(48) Fowler, F. W.; Lauher, J. W. A rational design of molecular materials. *J. Phys. Org. Chem.* **2000**, *13*, 850-857.

(49) Xi, O. Y.; Fowler, F. W.; Lauher, J. W. Single-crystal-to-single-crystal topochemical polymerizations of a terminal diacetylene: Two remarkable transformations give the same conjugated polymer. *J. Am. Chem. Soc.* **2003**, *125*, 12400-12401.
(50) Curtis, S. M.; Le, N.; Nguyen, T.; Xi, O. Y.; Tran, T.; Fowler, F. W.; Lauher, J. W. What have we learned about topochemical diacetylene polymerizations? *Supramol. Chem.* **2005**, *17*, 31-36.
(51) Curtis, S. M.; Le, N.; Fowler, F. W.; Lauher, J. W. A rational approach to the preparation of polydipyridyldiacetylenes: An exercise in crystal design. *Cryst. Growth Des.* **2005**, *5*, 2313-2321.
(52) Okuno, T.; Izuoka, A.; Ito, T.; Kubo, S.; Sugawara, T.; Sato, N.; Sugawara, Y. Reactivity of mesogenic diacetylenes coupled with phase transitions between crystal and liquid crystal phases. *J. Chem. Soc., Perkin Trans. 2* **1998**, 889-895.
(53) Xiao, J.; Yang, M.; Lauher, J. W.; Fowler, F. W. A supramolecular solution to a long-standing problem: The 1,6-polymerization of a triacetylene. *Angew. Chem. Int. Ed.* **2000**, *39*, 2132-2135.
(54) Hoang, T.; Lauher, J. W.; Fowler, F. W. The topochemical 1,16-polymerization of a triene. *J. Am. Chem. Soc.* **2002**, *124*, 10656-10657.
(55) Ouyang, X.; Fowler, F. W.; Lauher, J. W. Single-crystal-to-single-crystal topochemical polymerizations of a terminal diacetylene: Two remarkable transformations give the same conjugated polymer. *J. Am. Chem. Soc.* **2003**, *125*, 12400-12401.
(56) Grant, B.; Clecak, N. J.; Cox, R. J. Novel Liquid-Crystalline Materials - Synthesis and Preliminary Characterization of New 4,4'-Disubstituted Diphenyldiacetylene, Tolane and Stilbene Derivatives. *Mol. Cryst. Liq. Cryst.* **1979**, *51*, 209-214.
(57) Garito, A. F.; Teng, C. C.; Wong, K. Y.; Khamiri, O. Z. Molecular Optics - Nonlinear Optical Processes in Organic and Polymer Crystals. *Mol. Cryst. Liq. Cryst.* **1984**, *106*, 219-258.
(58) Tsibouklis, J.; Werninck, A. R.; Shand, A. J.; Milburn, G. H. W. The Synthesis, Polymerization and 2nd Order Non-Linear Optical-Properties of Novel, Conjugated, Unsymmetrical Diacetylenes Showing Liquid-Crystal Behavior. *Liq. Cryst.* **1988**, *3*, 1393-1400.
(59) Plachetta, C.; Rau, N. O.; Schulz, R. C. Some Soluble Polydiacetylenes Derived from 10,12-Docosadiyn-1,22-Diol. *Mol. Cryst. Liq. Cryst.* **1983**, *96*, 141-151.
(60) Milburn, G. H. W.; Werninck, A.; Tsibouklis, J.; Bolton, E.; Thomson, G.; Shand, A. J. Synthesis and Properties of Some Novel Unsymmetrically Substituted Diacetylenes. *Polymer* **1989**, *30*, 1004-1007.
(61) Izuoka, A.; Okuno, T.; Ito, T.; Sugawara, T.; Sato, N.; Kamei, S.; Tohyama, K. Kinetic Feature of Nematic Phase Polymerization of Diacetylenes. *Mol. Cryst. Liq. Cryst.* **1993**, *226*, 201-205.
(62) Hammond, P. T.; Rubner, M. F. Synthesis and Characterization of New Mesogenic Diacetylene Monomers and Their Polymers. *Macromolecules* **1995**, *28*, 795-805.
(63) Chang, J. Y.; Baik, J. H.; Lee, C. B.; Han, M. J.; Hong, S. K. Liq. Cryst. obtained from disclike mesogenic diacetylenes and their polymerization. *J. Am. Chem. Soc.* **1997**, *119*, 3197-3198.

(64) Lee, C. J.; Lee, S. J.; Chang, J. Y. Synthesis of a polymerizable discotic liquid crystalline compound with a 1,3,5-triazine core. *Tetrahedron Lett.* **2002**, *43*, 3863-3866.
(65) Cho, H. J.; Seo, K.; Lee, C. J.; Yun, H.; Chang, J. Y. Rodlike mesogenic molecules consisting of two diacetylenic groups: mesomorphic behavior and photoimaging. *J. Mater. Chem.* **2003**, *13*, 986-990.
(66) Huo, Q.; Russell, K. C.; Leblanc, R. M. Chromatic studies of a polymerizable diacetylene hydrogen bonding self-assembly: A "self-folding" process to explain the chromatic changes of polydiacetylenes. *Langmuir* **1999**, *15*, 3972-3980.
(67) Lee, S. B.; Koepsel, R.; Stolz, D. B.; Warriner, H. E.; Russell, A. J. Self-assembly of biocidal nanotubes from a single-chain diacetylene amine salt. *J. Am. Chem. Soc.* **2004**, *126*, 13400-13405.
(68) Okada, S.; Peng, S.; Spevak, W.; Charych, D. Color and chromism of polydiacetylene vesicles. *Acc. Chem. Res.* **1998**, *31*, 229-239.
(69) Huo, Q.; Russev, S.; Hasegawa, T.; Nishijo, J.; Umemura, J.; Puccetti, G.; Russell, K. C.; Leblanc, R. M. A Langmuir monolayer with a nontraditional molecular architecture. *J. Am. Chem. Soc.* **2000**, *122*, 7890-7897.
(70) Sui, G.; Micic, M.; Huo, Q.; Leblanc, R. M. Studies of a novel polymerizable amphiphilic dendrimer. *Colloids Surf., A* **2000**, *171*, 185-197.
(71) Tachibana, H.; Yamanaka, Y.; Sakai, H.; Abe, M.; Matsumoto, M. Effect of position of butadiyne moiety in amphiphilic diacetylenes on the polymerization in the Langmuir-Blodgett films. *Macromolecules* **1999**, *32*, 8306-8309.
(72) Mueller, A.; O'Brien, D. F. Supramolecular materials via polymerization of mesophases of hydrated amphiphiles. *Chem. Rev.* **2002**, *102*, 727-757.
(73) Hub, H. H.; Hupfer, B.; Koch, H.; Ringsdorf, H. Polyreactions in Ordered Systems .20. Polymerizable Phospholipid Analogs - New Stable Biomembrane and Cell Models. *Angew. Chem. Int. Ed.* **1980**, *19*, 938-940.
(74) Jonas, U.; Shah, K.; Norvez, S.; Charych, D. H. Reversible color switching and unusual solution polymerization of hydrazide-modified diacetylene lipids. *J. Am. Chem. Soc.* **1999**, *121*, 4580-4588.
(75) Kunitake, T.; Okahata, Y.; Shimomura, M.; Yasunami, S. I.; Takarabe, K. Formation of Stable Bilayer Assemblies in Water from Single-Chain Amphiphiles - Relationship between the Amphiphile Structure and the Aggregate Morphology. *J. Am. Chem. Soc.* **1981**, *103*, 5401-5413.
(76) Shimizu, T.; Masuda, M.; Minamikawa, H. Supramolecular nanotube architectures based on amphiphilic molecules. *Chem. Rev.* **2005**, *105*, 1401-1443.
(77) Yager, P.; Schoen, P. E. Formation of Tubules by a Polymerizable Surfactant. *Mol. Cryst. Liq. Cryst.* **1984**, *106*, 371-381.
(78) Schoen, P. E.; Yager, P. Spectroscopic Studies of Polymerized Surfactants - 1,2-Bis(10,12-Tricosadiynoyl) -Sn-Glycero-3-Phosphocholine. *J. Polym. Sci., Part B: Polym. Phys.* **1985**, *23*, 2203-2216.
(79) Yager, P.; Schoen, P. E.; Davies, C.; Price, R.; Singh, A. Structure of Lipid Tubules Formed from a Polymerizable Lecithin. *Biophys. J.* **1985**, *48*, 899-906.
(80) Thomas, B. N.; Corcoran, R. C.; Cotant, C. L.; Lindemann, C. M.; Kirsch, J. E.; Persichini, P. J. Phosphonate lipid tubules. 1. *J. Am. Chem. Soc.* **1998**, *120*, 12178-12186.

(81) Cheng, Q.; Yamamoto, M.; Stevens, R. C. Amino acid terminated polydiacetylene lipid microstructures: Morphology and chromatic transition. *Langmuir* **2000**, *16*, 5333-5342.
(82) Song, J.; Cheng, Q.; Kopta, S.; Stevens, R. C. Modulating artificial membrane morphology: pH-induced chromatic transition and nanostructural transformation of a bolaamphiphilic conjugated polymer from blue helical ribbons to red nanofibers. *J. Am. Chem. Soc.* **2001**, *123*, 3205-3213.
(83) Thomas, B. N.; Lindemann, C. M.; Corcoran, R. C.; Cotant, C. L.; Kirsch, J. E.; Persichini, P. J. Phosphonate lipid tubules II. *J. Am. Chem. Soc.* **2002**, *124*, 1227-1233.
(84) Mishra, B. K.; Garrett, C. C.; Thomas, B. N. Phospholipid tubelets. *J. Am. Chem. Soc.* **2005**, *127*, 4254-4259.
(85) Zhou, W. D.; Li, Y. L.; Zhu, D. B. Progress in polydiacetylene nanowires by self-assembly and self-polymerization. *Chem. Asian J.* **2007**, *2*, 222-229.
(86) Shirakawa, M.; Fujita, N.; Shinkai, S. A stable single piece of unimolecularly pi-stacked porphyrin aggregate in a thixotropic low molecular weight gel: A one-dimensional molecular template for polydiacetylene wiring up to several tens of micrometers in length. *J. Am. Chem. Soc.* **2005**, *127*, 4164-4165.
(87) Lu, Y. F.; Yang, Y.; Sellinger, A.; Lu, M. C.; Huang, J. M.; Fan, H. Y.; Haddad, R.; Lopez, G.; Burns, A. R.; Sasaki, D. Y.; Shelnutt, J.; Brinker, C. J. Self-assembly of mesoscopically ordered chromatic polydiacetylene/silica nanocomposites. *Nature* **2001**, *410*, 913-917.
(88) Yang, Y.; Lu, Y. F.; Lu, M. C.; Huang, J. M.; Haddad, R.; Xomeritakis, G.; Liu, N. G.; Malanoski, A. P.; Sturmayr, D.; Fan, H. Y.; Sasaki, D. Y.; Assink, R. A.; Shelnutt, J. A.; van Swol, F.; Lopez, G. P.; Burns, A. R.; Brinker, C. J. Functional nanocomposites prepared by self-assembly and polymerization of diacetylene surfactants and silicic acid. *J. Am. Chem. Soc.* **2003**, *125*, 1269-1277.
(89) Peng, H. S.; Tang, J.; Pang, J. B.; Chen, D. Y.; Yang, L.; Ashbaugh, H. S.; Brinker, C. J.; Yang, Z. Z.; Lu, Y. F. Polydiacetylene/silica nanocomposites with tunable mesostructure and thermochromatism from diacetylenic assembling molecules. *J. Am. Chem. Soc.* **2005**, *127*, 12782-12783.
(90) Peng, H. S.; Tang, J.; Yang, L.; Pang, J. B.; Ashbaugh, H. S.; Brinker, C. J.; Yang, Z. Z.; Lu, Y. F. Responsive periodic mesoporous polydiacetylene/silica nanocomposites. *J. Am. Chem. Soc.* **2006**, *128*, 5304-5305.
(91) Nie, X. P.; Wang, G. J. Synthesis and self-assembling properties of diacetylene-containing glycolipids. *J. Org. Chem.* **2006**, *71*, 4734-4741.
(92) Masuda, M.; Hanada, T.; Okada, Y.; Yase, K.; Shimizu, T. Polymerization in nanometer-sized fibers: Molecular packing order and polymerizability. *Macromolecules* **2000**, *33*, 9233-9238.
(93) Masuda, M.; Hanada, T.; Yase, K.; Shimizu, T. Polymerization of bolaform butadiyne 1-glucosamide in self-assembled nanoscale-fiber morphology. *Macromolecules* **1998**, *31*, 9403-9405.
(94) Tamaoki, N.; Shimada, S.; Okada, Y.; Belaissaoui, A.; Kruk, G.; Yase, K.; Matsuda, H. Polymerization of a diacetylene dicholesteryl ester having two urethanes in organic gel states. *Langmuir* **2000**, *16*, 7545-7547.

(95) George, M.; Weiss, R. G. Low molecular-mass gelators with diyne functional groups and their unpolymerized and polymerized gel assemblies. *Chem. Mater.* **2003**, *15*, 2879-2888.
(96) Aoki, K.; Kudo, M.; Tamaoki, N. Novel odd/even effect of alkylene chain length on the photopolymerizability of organogelators. *Org. Lett.* **2004**, *6*, 4009-4012.
(97) Nagasawa, J.; Kudo, M.; Hayashi, S.; Tamaoki, N. Organogelation of diacetylene cholesteryl esters having two urethane linkages and their photopolymerization in the gel state. *Langmuir* **2004**, *20*, 7907-7916.
(98) Dautel, O. J.; Robitzer, M.; Lere-Porte, J. P.; Serein-Spirau, F.; Moreau, J. J. E. Self-organized ureido substituted diacetylenic organogel. Photopolymerization of one-dimensional supramolecular assemblies to give conjugated nanofibers. *J. Am. Chem. Soc.* **2006**, *128*, 16213-16223.
(99) Hasegawa, T.; Haraguchi, S.; Numata, M.; Li, C.; Bae, A. H.; Fujisawa, T.; Kaneko, K.; Sakurai, K.; Shinkai, S. Poly(diacetylene)-nanofibers can be fabricated through photo-irradiation using natural polysaccharide schizophyllan as a one-dimensional mold. *Org. Biomol. Chem.* **2005**, *3*, 4321-4328.
(100) Mori, T.; Fukawa, Y.; Shimoyama, K.; Minagawa, K. Polymerization of diacetylene using beta-sheet as a template. *Int. J. Mod. Phys. B* **2006**, *20*, 3872-3877.
(101) Chae, S. K.; Park, H.; Yoon, J.; Lee, C. H.; Ahn, D. J.; Kim, J. M. Polydiacetylene supramolecules in electrospun microfibers: Fabrication, micropatterning, and sensor applications. *Adv. Mater.* **2007**, *19*, 521-524.
(102) Hermann, J. P.; Ricard, D.; Ducuing, J. Optical Nonlinearities in Conjugated Systems - Beta-Carotene. *Appl. Phys. Lett.* **1973**, *23*, 178-180.
(103) Hermann, J. P.; Ducuing, J. Third-Order Polarizabilities of Long-Chain Molecules. *J. Appl. Phys.* **1974**, *45*, 5100-5102.
(104) Lequime, M.; Hermann, J. P. Reversible Creation of Defects by Light in One Dimensional Conjugated Polymers. *Chem. Phys.* **1977**, *26*, 431-437.
(105) Polyakov, S.; Yoshino, F.; Liu, M.; Stegeman, G. Nonlinear refraction and multiphoton absorption in polydiacetylenes from 1200 to 2200 nm. *Phys. Rev. B: Condens. Matter* **2004**, *69*.
(106) Chance, R. R.; Shand, M. L.; Hogg, C.; Silbey, R. 3-Wave Mixing in Conjugated Polymer-Solutions - 2-Photon Absorption in Polydiacetylenes. *Phys. Rev. B: Condens. Matter* **1980**, *22*, 3540-3550.
(107) Nunzi, J. M.; Grec, D. Picosecond Phase Conjugation in Polydiacetylene Gels. *J. Appl. Phys.* **1987**, *62*, 2198-2202.
(108) Pender, W. A.; Boyle, A. J.; Lambkin, P.; Blau, W. J.; Mazaheri, K.; Westland, D. J.; Skarda, V.; Sparpaglione, M. Nonlinear Absorption in Polydiacetylene Wave-Guides. *Appl. Phys. Lett.* **1995**, *66*, 786-788.
(109) Banfi, G.; Fortusini, D.; Dainesi, P.; Grando, D.; Sottini, S. Two-photon absorption spectrum of 3-butoxycarbonylmethylurethane polydiacetylene thin films. *J. Chem. Phys.* **1998**, *108*, 4319-4323.
(110) Sakamoto, M.; Wasserman, B.; Dresselhaus, M. S.; Wnek, G. E.; Elman, B. S.; Sandman, D. J. Enhanced Electrical-Conductivity of Polydiacetylene Crystals by Chemical Doping and Ion-Implantation. *J. Appl. Phys.* **1986**, *60*, 2788-2796.

(111) Ohnuma, H.; Inoue, K.; Se, K.; Kotaka, T. Urethane-Substituted Poly(Diacetylene) - Electrical-Conductivity of Poly[5,7-Dodecadiyne-1,12-Diol Bis([(Normal-Butoxycarbonyl)Methyl]Urethane)] in Amorphous and Single-Crystalline Forms. *Macromolecules* **1984**, *17*, 1285-1287.
(112) Ferreranglada, N.; Bloor, D.; Chalmers, I. F.; Hunt, I. G.; Hercliffe, R. D. Antimony Pentafluoride Doping of a Polydiacetylene. *J. Mater. Sci. Letters* **1985**, *4*, 83-86.
(113) Marikhin, V. A.; Guk, E. G.; Myasnikova, L. P. New approach to achieving the potentially high conductivity of polydiacetylene. *Phys. Solid State* **1997**, *39*, 686-689.
(114) Se, K.; Ohnuma, H.; Kotaka, T. Urethane-Substituted Poly(Diacetylenes) - Structure and Electrical-Properties of Poly[4,6-Decadiyne-1,10-Diol Bis([(N-Butoxycarbonyl)Methyl]Urethane)]. *Macromolecules* **1983**, *16*, 1581-1587.
(115) Se, K.; Ohnuma, H.; Kotaka, T. Electrical-Conductivity of Urethane-Substituted Poly(Diacetylenes) - Effect of Substituent Side Groups and Molecular-Weights. *Macromolecules* **1984**, *17*, 2126-2131.
(116) Ohnuma, H.; Hasegawa, K.; Se, K.; Kotaka, T. Anisotropic Electrical-Conductivity of Oriented Poly(Diacetylene) Films. *Macromolecules* **1985**, *18*, 2339-2341.
(117) Chen, P. F.; Adachi, K.; Kotaka, T. Electrical-Conductivity of Polydiacetylene, Poly[5,7-Dodecadiyn-1,12-Diol-Bis(N-Butoxy Carbonylmethyl Urethane)] Gel - Sol-Gel Transition and Conduction Mechanism. *Polymer* **1992**, *33*, 1363-1369.
(118) Chen, P. F.; Adachi, K.; Kotaka, T. Electrical-Conductivity of Polydiacetylene P(4bcmu) Gel .2. A Percolation Model for Elasticity and Conductivity. *Polymer* **1992**, *33*, 1813-1815.
(119) Seiferheld, U.; Baessler, H. Field-driven reversible doping of a polydiacetylene crystal (DCH). *Solid State Commun.* **1983**, *47*, 391-393.
(120) Ebisawa, F.; Kurihara, T.; Tabei, H. Electrical-Properties of I-2-Doped Polydiacetylene. *Synth. Met.* **1987**, *18*, 431-436.
(121) Sebastian, L.; Weiser, G. Electroreflectance Studies on the Excitons in Pts and Dchd Single-Crystals. *Chem. Phys.* **1981**, *62*, 447-457.
(122) Sebastian, L.; Weiser, G. One-Dimensional Wide Energy-Bands in a Polydiacetylene Revealed by Electroreflectance. *Phys. Rev. Lett.* **1981**, *46*, 1156-1159.
(123) Scherman.W; Wegner, G. Topochemical Reactions of Monomers with Conjugated Triple Bonds .10. Electrical-Conductivity of Single-Crystals from Polydiacetylenes. *Makromolekulare Chemie-Macromol. Chem. Phys.s* **1974**, *175*, 667-674.
(124) Lochner, K.; Reimer, B.; Bassler, H. Photocarrier Generation in a One-Dimensional Solid - Polydiacetylene-Bis(Toluenesulfonate). *Phys. Status Solidi B* **1976**, *76*, 533-540.
(125) Lochner, K.; Bassler, H.; Tieke, B.; Wegner, G. Photoconduction in Polydiacetylene Multilayer Structures and Single-Crystals - Evidence for Band-to-Band Excitation. *Phys. Status Solidi B* **1978**, *88*, 653-661.

(126) Orczyk, M.; Sworakowski, J.; Schott, M.; Bertault, M. Evolution of Photoelectric Signal in Pts Diacetylene Single-Crystals during Solid-State Polymerization. *Chem. Phys.* **1988**, *121*, 245-254.
(127) Orczyk, M. Photoconductivity Action Spectra in Single-Crystals of Polydiacetylenes. *Synth. Met.* **1990**, *37*, 321-325.
(128) Reimer, B.; Bassler, H. Transient Photoconduction in a Polydiacetylene Single-Crystal - Determination of Transit-Time, Free Lifetime, and Recombination Time of Charge-Carriers. *Phys. Status Solidi B* **1978**, *85*, 145-153.
(129) Moses, D.; Sinclair, M.; Heeger, A. J. Carrier Photogeneration and Mobility in Polydiacetylene - Fast Transient Photoconductivity. *Phys. Rev. Lett.* **1987**, *58*, 2710-2713.
(130) Siddiqui, A. S. Electron-Mobility in Single-Crystal Polydiacetylene Toluene Sulfonate (Pda-Ts). *J. Phys. C: Solid State Phys.* **1980**, *13*, 1079-1084.
(131) Donovan, K. J.; Wilson, E. G. Demonstration of High-Mobility One-Dimensional Semiconducting Polymers. *J. Phys. C: Solid State Phys.* **1979**, *12*, 4857-4869.
(132) Siddiqui, A. S. Photoconductivity in Single-Crystal Polydiacetylene-Toluene Sulfonate. *J. Phys. C: Solid State Phys.* **1980**, *13*, 2147-2159.
(133) Ohnuma, H.; Hasegawa, K.; Kotaka, T. Photoconductivity of a Urethane-Substituted Poly(Diacetylene) Film. *Nippon Kagaku Kaishi* **1986**, 412-415.
(134) Donovan, K. J.; Sudiwala, R. V.; Wilson, E. G. Fast Photoconduction in Langmuir-Blodgett Multilayers of Polydiacetylenes. *Thin Solid Films* **1992**, *210*, 271-273.
(135) Ravindran, T.; Kim, W. H.; Jain, A. K.; Kumar, J.; Tripathy, S. K. Photoconduction in a Polydiacetylene Film. *J. Phys.: Condens. Matter* **1995**, *7*, 1315-1325.
(136) Onsager, L. Initial recombination of ions. *Phys. Rev.* **1938**, *54*, 554-557.
(137) Donovan, K. J.; Spagnoli, S. Carrier range on conjugated polymers as molecular wires. Example: polydiacetylene, 4BCMU. *Chem. Phys.* **1999**, *247*, 293-298.
(138) Spagnoli, S.; Donovan, K. J.; Scott, K.; Somerton, M.; Wilson, E. G. Carrier range on finite, isolated molecular wires in a monomer crystalline matrix - Example: polydiacetylene, 4BCMU. *Chem. Phys.* **1999**, *250*, 71-79.
(139) Moller, S.; Weiser, G. Photoconductivity of polydiacetylene chains in polymer and monomer single crystals. *Chem. Phys.* **1999**, *246*, 483-494.
(140) Blum, T.; Bassler, H. Reinvestigation of Generation and Transport of Charge-Carriers in Crystalline Polydiacetylenes (Pdas). *Chem. Phys.* **1988**, *123*, 431-441.
(141) Hoofman, R.; Gelinck, G. H.; Siebbeles, L. D. A.; de Haas, M. P.; Warman, J. M.; Bloor, D. Influence of backbone conformation on the photoconductivity of polydiacetylene chains. *Macromolecules* **2000**, *33*, 9289-9297.
(142) Chance, R. R.; Baughman, R. H.; Muller, H.; Eckhardt, C. J. Thermochromism in a Polydiacetylene Crystal. *J. Chem. Phys.* **1977**, *67*, 3616-3618.
(143) Chance, R. R.; Patel, G. N.; Witt, J. D. Thermal Effects on the Optical-Properties of Single-Crystals and Solution-Cast Films of Urethane Substituted Polydiacetylenes. *J. Chem. Phys.* **1979**, *71*, 206-211.
(144) Eckhardt, H.; Eckhardt, C. J.; Yee, K. C. Thermal Effects on the Optical-Spectra of a Polydiacetylene - Poly(1,2-Bis[4-(Isopropylcarbamoyloxy)-Normal-Butyl]-1-Buten-3-Ynylene). *J. Chem. Phys.* **1979**, *70*, 5498-5502.

(145) Koshihara, S.; Tokura, Y.; Takeda, K.; Koda, T.; Kobayashi, A. Reversible and Irreversible Thermochromic Phase-Transitions in Single-Crystals of Polydiacetylenes Substituted with Alkyl-Urethanes. *J. Chem. Phys.* **1990**, *92*, 7581-7588.
(146) Hankin, S. H. W.; Downey, M. J.; Sandman, D. J. On the Structural Origins of Solid-State Urethane Polydiacetylene Thermochromism - Thermal and Structural-Properties of Ipudo Monomer and Polymer. *Polymer* **1992**, *33*, 5098-5101.
(147) Koshihara, S.; Tokura, Y.; Takeda, K.; Koda, T. Reversible Photoinduced Phase-Transitions in Single-Crystals of Polydiacetylenes. *Phys. Rev. Lett.* **1992**, *68*, 1148-1151.
(148) Itoh, T.; Shichi, T.; Yui, T.; Takahashi, H.; Inui, Y.; Takagi, K. Reversible color changes in lamella hybrids of poly(diacetylenecarboxylates) incorporated in layered double hydroxide nanosheets. *J. Phys. Chem. B* **2005**, *109*, 3199-3206.
(149) Tieke, B. Polymerization of Butadiene and Butadiyne (Diacetylene) Derivatives in Layer Structures. *Adv. Polym. Sci.* **1985**, *71*, 79-151.
(150) Patel, G. N.; Chance, R. R.; Witt, J. D. Visual Conformational Transition in a Polymer-Solution. *J. Polym. Sci., Part C: Polym. Lett.* **1978**, *16*, 607-614.
(151) Patel, G. N.; Walsh, E. K. Polydiacetylenes - Solution Conformation Characteristics. *J. Polym. Sci., Part C: Polym. Lett.* **1979**, *17*, 203-208.
(152) Patel, G. N.; Chance, R. R.; Witt, J. D. Planar-Nonplanar Conformational Transition in Conjugated Polymer-Solutions. *J. Chem. Phys.* **1979**, *70*, 4387-4392.
(153) Chance, R. R. Chromism in Polydiacetylene Solutions and Crystals. *Macromolecules* **1980**, *13*, 396-398.
(154) Wenz, G.; Muller, M. A.; Schmidt, M.; Wegner, G. Structure of Poly(Diacetylenes) in Solution. *Macromolecules* **1984**, *17*, 837-850.
(155) Kim, W. H.; Kodali, N. B.; Kumar, J.; Tripathy, S. K. A Novel, Soluble Poly(Diacetylene) Containing an Aromatic Substituent. *Macromolecules* **1994**, *27*, 1819-1824.
(156) Patel, G. N.; Witt, J. D.; Khanna, Y. P. Thermochromism in Polydiacetylene Solutions. *J. Polym. Sci., Part B: Polym. Phys.* **1980**, *18*, 1383-1391.
(157) Lim, K. C.; Kapitulnik, A.; Zacher, R.; Heeger, A. J. Conformation of Polydiacetylene Macromolecules in Solution - Field-Induced Birefringence and Rotational Diffusion Constant. *J. Chem. Phys.* **1985**, *82*, 516-521.
(158) Lim, K. C.; Heeger, A. J. Spectroscopic and Light-Scattering Studies of the Conformational (Rod-to-Coil) Transition of Poly(Diacetylene) in Solution. *J. Chem. Phys.* **1985**, *82*, 522-530.
(159) Enkelmann, V. Structural Aspects of the Topochemical Polymerization of Diacetylenes. *Adv. Polym. Sci.* **1984**, *63*, 91-136.
(160) Schott, M. The colors of polydiacetylenes: a commentary. *J. Phys. Chem. B* **2006**, *110*, 15864-15868.
(161) Li, Y. J.; Chu, B. Structure of Aggregates of P4bcmu in Dilute Thf/Toluene Solutions. *Macromolecules* **1991**, *24*, 4115-4122.
(162) Lim, K. C.; Fincher, C. R.; Heeger, A. J. Rod-to-Coil Transition of a Conjugated Polymer in Solution. *Phys. Rev. Lett.* **1983**, *50*, 1934-1937.

(163) Patel, G. N.; Miller, G. G. Structure-Property Relationships of Diacetylenes and Their Polymers. *J. Macromol. Sci., Phys.* **1981**, *B20*, 111-131.
(164) Rawiso, M.; Aime, J. P.; Fave, J. L.; Schott, M.; Muller, M. A.; Schmidt, M.; Baumgartl, H.; Wegner, G. Solutions of Polydiacetylenes in Good and Poor Solvents - a Light and Neutron-Scattering Study. *J. Phys.* **1988**, *49*, 861-880.
(165) Coyne, L. D.; Chang, C.; Hsu, S. L. Spectroscopic Characterization of the Chromic Transition Observed for Polydiacetylenes. *Makromolekulare Chemie-Macromol. Chem. Phys.* **1987**, *188*, 2311-2316.
(166) Peiffer, D. G.; Chung, T. C.; Schulz, D. N.; Agarwal, P. K.; Garner, R. T.; Kim, M. W. Rod to Coil Transition and Aggregation in Soluble Polydiacetylenes - Semidilute Regime. *J. Chem. Phys.* **1986**, *85*, 4712-4718.
(167) Brown, A. J.; Rumbles, G.; Phillips, D.; Bloor, D. Sidegroup Dependence of Chromism in Polydiacetylenes. *Chem. Phys. Letters* **1988**, *151*, 247-252.
(168) Bloor, D. Dissolution and spectroscopic properties of the polydiacetylene poly(10,12-docosadiyne-1,12-diol-bisethylurethane). *Macromol. Chem. Phys.* **2001**, *202*, 1410-1423.
(169) Singh, A.; Thompson, R. B.; Schnur, J. M. Reversible Thermochromism in Photopolymerized Phosphatidylcholine Vesicles. *J. Am. Chem. Soc.* **1986**, *108*, 2785-2787.
(170) Beckham, H. W.; Rubner, M. F. On the Origin of Thermochromism in Cross-Polymerized Diacetylene-Functionalized Polyamides. *Macromolecules* **1993**, *26*, 5198-5201.
(171) Yuan, Z. Z.; Lee, C. W.; Lee, S. H. Reversible thermochromism in hydrogen-bonded polymers containing polydiacetylenes. *Angew. Chem. Int. Ed.* **2004**, *43*, 4197-4200.
(172) Ahn, D. J.; Chae, E. H.; Lee, G. S.; Shim, H. Y.; Chang, T. E.; Ahn, K. D.; Kim, J. M. Colorimetric reversibility of polydiacetylene supramolecules having enhanced hydrogen-bonding under thermal and pH stimuli. *J. Am. Chem. Soc.* **2003**, *125*, 8976-8977.
(173) Kew, S. J.; Hall, E. A. H. pH response of carboxy-terminated colorimetric polydiacetylene vesicles. *Anal. Chem.* **2006**, *78*, 2231-2238.
(174) Carpick, R. W.; Sasaki, D. Y.; Marcus, M. S.; Eriksson, M. A.; Burns, A. R. Polydiacetylene films: a review of recent investigations into chromogenic transitions and nanomechanical properties. *J. Phys.: Condens. Matter* **2004**, *16*, R679-R697.
(175) Nallicheri, R. A.; Rubner, M. F. Investigations of the Mechanochromic Behavior of Poly(Urethane Diacetylene) Segmented Copolymers. *Macromolecules* **1991**, *24*, 517-525.
(176) Carpick, R. W.; Mayer, T. M.; Sasaki, D. Y.; Burns, A. R. Spectroscopic ellipsometry and fluorescence study of thermochromism in an ultrathin poly(diacetylene) film: Reversibility and transition kinetics. *Langmuir* **2000**, *16*, 4639-4647.
(177) Yoon, J.; Chae, S. K.; Kim, J. M. Colorimetric sensors for volatile organic compounds (VOCs) based on conjugated polymer-embedded electrospun fibers. *J. Am. Chem. Soc.* **2007**, *129*, 3038-3039.

(178) Charych, D. H.; Nagy, J. O.; Spevak, W.; Bednarski, M. D. Direct Colorimetric Detection of a Receptor-Ligand Interaction by a Polymerized Bilayer Assembly. *Science* **1993**, *261*, 585-588.
(179) Kolusheva, S.; Shahal, T.; Jelinek, R. Cation-selective color sensors composed of ionophore-phospholipid-polydiacetylene mixed vesicles. *J. Am. Chem. Soc.* **2000**, *122*, 776-780.
(180) Cheng, Q.; Stevens, R. C. Coupling of an induced fit enzyme to polydiacetylene thin films: Colorimetric detection of glucose. *Adv. Mater.* **1997**, *9*, 481-&.
(181) Kim, J. M.; Lee, J. S.; Woo, S. Y.; Ahn, D. J. Unique effects of cyclodextrins on the formation and colorimetric transition of polydiacetylene vesicles. *Macromol. Chem. Phys.* **2005**, *206*, 2299-2306.
(182) Cho, J. T.; Woo, S. M.; Ahn, D. J.; Ahn, K. D.; Lee, H.; Kim, J. M. Cyclodextrin-induced color changes in polymerized diacetylene Langmuir-Schaefer films. *Chemistry Letters* **2003**, *32*, 282-283.
(183) Pan, J. J.; Charych, D. Molecular recognition and colorimetric detection of cholera toxin by poly(diacetylene) liposomes incorporating G(m1) ganglioside. *Langmuir* **1997**, *13*, 1365-1367.
(184) Okada, S. Y.; Jelinek, R.; Charych, D. Induced color change of conjugated polymeric vesicles by interfacial catalysis of phospholipase A(2). *Angew. Chem. Int. Ed.* **1999**, *38*, 655-659.
(185) Gill, I.; Ballesteros, A. Immunoglobulin-polydiacetylene sol-gel nanocomposites as solid-state chromatic biosensors. *Angew. Chem. Int. Ed.* **2003**, *42*, 3264-3267.
(186) Kolusheva, S.; Kafri, R.; Katz, M.; Jelinek, R. Rapid colorimetric detection of antibody-epitope recognition at a biomimetic membrane interface. *J. Am. Chem. Soc.* **2001**, *123*, 417-422.
(187) Lee, S. W.; Kang, C. D.; Yang, D. H.; Lee, J. S.; Kim, J. M.; Ahn, D. J.; Sim, S. J. The development of a generic bioanalytical matrix using polydiacetylenes. *Adv. Funct. Mater.* **2007**, *17*, 2038-2044.
(188) Wang, C. G.; Ma, Z. F. Colorimetric detection of oligonucleotides using a polydiacetylene vesicle sensor. *Anal. BioAnal. Chem.* **2005**, *382*, 1708-1710.
(189) Reichert, A.; Nagy, J. O.; Spevak, W.; Charych, D. Polydiacetylene Liposomes Functionalized with Sialic-Acid Bind and Colorimetrically Detect Influenza-Virus. *J. Am. Chem. Soc.* **1995**, *117*, 829-830.
(190) Ma, Z. F.; Li, J. R.; Liu, M. H.; Cao, J.; Zou, Z. Y.; Tu, J.; Jiang, L. Colorimetric detection of Escherichia coli by polydiacetylene vesicles functionalized with glycolipid. *J. Am. Chem. Soc.* **1998**, *120*, 12678-12679.
(191) Ahn, D. J.; Kim, J. M. Fluorogenic Polydiacetylene Supramolecules: Immobilization, Micropatterning, and Application to Label-Free Chemosensors. *J. Am. Chem. Soc.* **2008**, ASAP, Web Release Date: March 19, 2008
(192) Paley, M. S.; Frazier, D. O.; Abeledeyem, H.; McManus, S. P.; Zutaut, S. E. Synthesis, Vapor Growth, Polymerization, and Characterization of Thin-Films of Novel Diacetylene Derivatives of Pyrrole - the Use of Computer Modeling to Predict Chemical and Optical-Properties of These Diacetylenes and Poly(Diacetylenes). *J. Am. Chem. Soc.* **1992**, *114*, 3247-3251.

(193) Sarkar, A.; Okada, S.; Matsuzawa, H.; Matsuda, H.; Nakanishi, H. Novel polydiacetylenes for optical materials: beyond the conventional polydiacetylenes. *J. Mater. Chem.* **2000**, *10*, 819-828.
(194) Sun, A. W.; Lauher, J. W.; Goroff, N. S. Preparation of poly(diiododiacetylene), an ordered conjugated polymer of carbon and iodine. *Science* **2006**, *312*, 1030-1034.
(195) Day, D.; Lando, J. B. Structural Relationships in Solid-State Synthesis of Poly(Bis-Phenyl Glutarate Diacetylene). *J. Polym. Sci., Part B: Polym. Phys.* **1978**, *16*, 1009-1022.
(196) Nakanishi, H.; Matsuda, H.; Kato, M.; Theocharis, C. R.; Jones, W. Single-Crystal Study of the Solid-State Polymerization of Butadiynylenebis-(Meta-Acetamidobenzene). *J. Chem. Soc., Perkin Trans. 2* **1986**, 1965-1967.
(197) Matsuda, H.; Nakanishi, H.; Hosomi, T.; Kato, M. Synthesis and Solid-State Polymerization of a New Diacetylene - 1-(N-Carbazolyl)Penta-1,3-Diyn-5-Ol. *Macromolecules* **1988**, *21*, 1238-1240.
(198) Wilson, R. B.; Duesler, E. N.; Curtin, D. Y.; Paul, I. C.; Baughman, R. H.; Preziosi, A. F. Diacetylene Monomers and Polymers with Chiral Substituents - Structure, Solid-State Polymerization, and Properties. *J. Am. Chem. Soc.* **1982**, *104*, 509-516.
(199) Brouty, C.; Spinat, P.; Whuler, A. Structural Study of the Solid Monomer-Polymer Solution of Bis[(Para-Chlorophenyl)Carbamate] of 2,4-Hexadiyne-1,6-Diyl, C20h14cl2n2o4. *Acta Crystallogr., Sect. C: Cryst. Struct. Commun.* **1984**, *40*, 1619-1624.
(200) Aime, J. P.; Schott, M.; Bertault, M.; Toupet, L. Study of Reactive Diacetylenes - Structure of Monomer and Polymer Pfbs Crystals. *Acta Crystallogr., Sect. B: Struct. Sci.* **1988**, *44*, 617-624.
(201) Foley, J. L.; Li, L.; Sandman, D. J.; Vela, M. J.; Foxman, B. M.; Albro, R.; Eckhardt, C. J. Side group interactions in a polydiacetylene single crystal. *J. Am. Chem. Soc.* **1999**, *121*, 7262-7263.
(202) Irngartinger, H.; Skipinski, M. Synthesis, X-ray structure analysis and topochemical photopolymerization of 2,5-dimethoxyphenyl- and quinone-substituted octa-3,5-diynes. *Tetrahedron* **2000**, *56*, 6781-6794.
(203) Xu, R.; Gramlich, V.; Frauenrath, H. Alternating diacetylene copolymer utilizing perfluorophenyl-phenyl interactions. *J. Am. Chem. Soc.* **2006**, *128*, 5541-5547.
(204) Wang, T. The Topochemical Polymerization of Diacetylenes using Supramolecular Host-Guest Chemistry. *Master Thesis, Stony Brook University,* **2005**.
(205) West, K.; Wang, C. S.; Batsanov, A. S.; Bryce, M. R. Are terminal aryl butadiynes stable? Synthesis and X-ray crystal structures of a series of aryl- and heteroaryl-butadiynes (Ar-C C-C C-H). *J. Org. Chem.* **2006**, *71*, 8541-8544.
(206) Lee, I.; Kim, C. K.; Han, I. S.; Lee, H. W.; Kim, W. K.; Kim, Y. B. Theoretical studies of solvent effect on the basicity of substituted pyridines. *J. Phys. Chem. B* **1999**, *103*, 7302-7307.
(207) Chen, I. J.; MacKerell, A. D. Computation of the influence of chemical substitution on the pK(a) of pyridine using semiempirical and ab initio methods. *Theor. Chem. Acc.* **2000**, *103*, 483-494.

(208) Adam, K. R. New density functional and atoms in molecules method of computing relative pK(a) values in solution. *J. Phys. Chem. A* **2002**, *106*, 11963-11972.
(209) Aakeroy, C. B.; Fasulo, M. E.; Desper, J. Cocrystal or salt: Does it really matter? *Mol. Pharm.* **2007**, *4*, 317-322.
(210) Kroon, J.; Kanters, J. A. Hydrogen-Bonding Potassium Hydrogen Meso-Tartrate - Low-Temperature X-Ray Study. *Acta Crystallogr., Sec. B: Struct. Crystallogr.y Cryst. Chem.* **1972**, *B 28*, 714-722.
(211) Sada, K.; Tani, T.; Shinkai, S. Organic ammonium carboxylates as supramolecular building blocks: The role of ionic hydrogen bonding. *Synlett* **2006**, 2364-2374.
(212) Dalhus, B.; Görbitz, C. H. DL-Aminophenylacetic acid. *Acta Cryst. C* **1999**, *55*.
(213) Biradha, K.; Dennis, D.; MacKinnon, V. A.; Sharma, C. V. K.; Zaworotko, M. J. Supramolecular synthesis of organic laminates with affinity for aromatic guests: A new class of clay mimics. *J. Am. Chem. Soc.* **1998**, *120*, 11894-11903.
(214) Horner, M. J.; Holman, K. T.; Ward, M. D. Lamellae-nanotube isomerism in hydrogen-bonded host frameworks. *Angew. Chem. Int. Ed.* **2001**, *40*, 4045-4048.
(215) Reddy, G. V. S.; Rao, G. V.; Subramanyam, R. V. K.; Iyengar, D. S. A new novel and practical one pot methodology for conversion of alcohols to amines. *Synth. Commun.* **2000**, *30*, 2233-2237.
(216) Hearn, W. R.; Hendry, R. A. Stereoisomerism of N,N'-Oxalylbis-(Alanine) Derivatives. *J. Am. Chem. Soc.* **1957**, *79*, 5213-5217.
(217) Patel, G. N.; Chance, R. R.; Turi, E. A.; Khanna, Y. P. Energetics and Mechanism of Solid-State Polymerization of Diacetylenes. *J. Am. Chem. Soc.* **1978**, *100*, 6644-6649.
(218) Mochizuki, E.; Shibamoto, Y.; Yano, K.; Kanehisa, N.; Kai, Y.; Tagawa, S.; Yamamoto, Y. Crystal structures and solid-state reactivities of 1,4-and 1,2-bis(5-hydroxypenta-1,3-diynyl)benzenes and 1-(5-hydroxypenta-1,3-diynyl)-4-ethynylbenzene. *J. Chem. Soc., Perkin Trans. 2* **2000**, 155-159.
(219) Ziessel, R.; Suffert, J.; Youinou, M. T. General method for the preparation of alkyne-functionalized oligopyridine building blocks. *J. Org. Chem.* **1996**, *61*, 6535-6546.
(220) Leznoff, C. C.; Suchozak, B. Octaarylethynyl and octaarylbutadiynyl phthalocyanines. *Can. J. Chem.* **2001**, *79*, 878-887.
(221) Wan, W. B.; Haley, M. M. Carbon networks based on dehydrobenzoannulenes. 4. Synthesis of "star" and "trefoil" graphdiyne substructures via sixfold cross-coupling of hexaiodobenzene. *J. Org. Chem.* **2001**, *66*, 3893-3901.
(222) Inoue, K.; Koga, N.; Iwamura, H. An Approach to Organic Ferromagnets - Synthesis and Characterization of 1-Phenyl-1,3-Butadiyne Polymers Having a Persistent Nitroxide Group on the Phenyl Ring. *J. Am. Chem. Soc.* **1991**, *113*, 9803-9810.
(223) Klinger, C.; Vostirowsky, O.; Hirsch, A. Synthesis of alkylene-bridged diphenyl-oligoynes. *Eur. J. Org. Chem.* **2006**, 1508-1524.
(224) Gibtner, T.; Hampel, F.; Gisselbrecht, J. P.; Hirsch, A. End-cap stabilized oligoynes: Model compounds for the linear sp carbon allotrope carbyne. *Chem. Eur. J.* **2002**, *8*, 408-432.

(225) Huh, D. H.; Jeong, J. S.; Lee, H. B.; Ryu, H.; Kim, Y. G. An efficient method for one-carbon elongation of aryl aldehydes via their dibromoalkene derivatives. *Tetrahedron* **2002**, *58*, 9925-9932.
(226) Chu, B.; Xu, R. L. Chromatic Transition of Polydiacetylene in Solution. *Acc. Chem. Res.* **1991**, *24*, 384-389.
(227) Sato, M.; Tanaka, S.; Kaeriyama, K. Soluble Conducting Polythiophenes. *J. Chem. Soc., Chem. Commun.* **1986**, 873-874.
(228) Hotta, S.; Rughooputh, D. D. V.; Heeger, A. J.; Wudl, F. Spectroscopic Studies of Soluble Poly(3-Alkylthienylenes). *Macromolecules* **1987**, *20*, 212-215.
(229) Patil, A. O.; Ikenoue, Y.; Wudl, F.; Heeger, A. J. Water-Soluble Conducting Polymers. *J. Am. Chem. Soc.* **1987**, *109*, 1858-1859.
(230) Pinto, M. R.; Schanze, K. S. Conjugated polyelectrolytes: Synthesis and applications. *Synthesis-Stuttgart* **2002**, 1293-1309.
(231) Kotz, J.; Kosmella, S.; Beitz, T. Self-assembled polyelectrolyte systems. *Prog. Polym. Sci.* **2001**, *26*, 1199-1232.
(232) Thomas, S. W.; Joly, G. D.; Swager, T. M. Chemical sensors based on amplifying fluorescent conjugated polymers. *Chem. Rev.* **2007**, *107*, 1339-1386.
(233) Liu, B.; Bazan, G. C. Homogeneous fluorescence-based DNA detection with water-soluble conjugated polymers. *Chem. Mater.* **2004**, *16*, 4467-4476.
(234) Achyuthan, K. E.; Bergstedt, T. S.; Chen, L.; Jones, R. M.; Kumaraswamy, S.; Kushon, S. A.; Ley, K. D.; Lu, L.; McBranch, D.; Mukundan, H.; Rininsland, F.; Shi, X.; Xia, W.; Whitten, D. G. Fluorescence superquenching of conjugated polyelectrolytes: applications for biosensing and drug discovery. *J. Mater. Chem.* **2005**, *15*, 2648-2656.
(235) Ambade, A. V.; Sandanaraj, B. S.; Klaikherd, A.; Thayumanavan, S. Fluorescent polyelectrolytes as protein sensors. *Polym. Int.* **2007**, *56*, 474-481.
(236) Tran, T. The Preparation of Polydiacetylenes Using Supramol. Chem.. *Master Thesis, Stony Brook University,* **2001**.

Appendix

Crystallography Data (CIF files in text form)

$NH_4HOG•2H_2O$

```
data_jlht

_audit_creation_method            SHELXL-97
_chemical_name_systematic
;
 ?
;
_chemical_name_common             ?
_chemical_melting_point           ?
_chemical_formula_moiety          ?
_chemical_formula_sum
 'C6 H13 N3 O7'
_chemical_formula_weight          239.19

loop_
 _atom_type_symbol
 _atom_type_description
 _atom_type_scat_dispersion_real
 _atom_type_scat_dispersion_imag
 _atom_type_scat_source
'C'  'C'   0.0033   0.0016
'International Tables Vol C Tables 4.2.6.8 and 6.1.1.4'
'H'  'H'   0.0000   0.0000
'International Tables Vol C Tables 4.2.6.8 and 6.1.1.4'
'N'  'N'   0.0061   0.0033
'International Tables Vol C Tables 4.2.6.8 and 6.1.1.4'
'O'  'O'   0.0106   0.0060
'International Tables Vol C Tables 4.2.6.8 and 6.1.1.4'

_symmetry_cell_setting            Triclinic
_symmetry_space_group_name_H-M    P-1

loop_
 _symmetry_equiv_pos_as_xyz
 'x, y, z'
 '-x, -y, -z'

_cell_length_a                    4.4968(7)
```

```
_cell_length_b                  10.4078(16)
_cell_length_c                  11.8210(18)
_cell_angle_alpha                70.645(2)
_cell_angle_beta                 85.722(3)
_cell_angle_gamma                84.971(3)
_cell_volume                    519.36(14)
_cell_formula_units_Z            2
_cell_measurement_temperature    273(2)
_cell_measurement_reflns_used    ?
_cell_measurement_theta_min      ?
_cell_measurement_theta_max      ?

_exptl_crystal_description       ?
_exptl_crystal_colour            ?
_exptl_crystal_size_max          .6
_exptl_crystal_size_mid          .5
_exptl_crystal_size_min          .4
_exptl_crystal_density_meas      ?
_exptl_crystal_density_diffrn    1.530
_exptl_crystal_density_method    'not measured'
_exptl_crystal_F_000             252
_exptl_absorpt_coefficient_mu    0.140
_exptl_absorpt_correction_type   none
_exptl_absorpt_correction_T_min  ?
_exptl_absorpt_correction_T_max  ?
_exptl_absorpt_process_details   ?

_exptl_special_details
;
 ?
;

_diffrn_ambient_temperature      273(2)
_diffrn_radiation_wavelength     0.71073
_diffrn_radiation_type           MoK\a
_diffrn_radiation_source         'fine-focus sealed tube'
_diffrn_radiation_monochromator  graphite
_diffrn_measurement_device_type  'CCD area detector'
_diffrn_measurement_method       'phi and omega scans'
_diffrn_detector_area_resol_mean  ?
_diffrn_standards_number         ?
_diffrn_standards_interval_count  ?
_diffrn_standards_interval_time  ?
_diffrn_standards_decay_%        ?
_diffrn_reflns_number            3118
_diffrn_reflns_av_R_equivalents  0.0228
```

```
_diffrn_reflns_av_sigmaI/netI    0.0335
_diffrn_reflns_limit_h_min       -5
_diffrn_reflns_limit_h_max       3
_diffrn_reflns_limit_k_min       -13
_diffrn_reflns_limit_k_max       12
_diffrn_reflns_limit_l_min       -14
_diffrn_reflns_limit_l_max       14
_diffrn_reflns_theta_min         1.83
_diffrn_reflns_theta_max         28.60
_reflns_number_total             2450
_reflns_number_gt                1545
_reflns_threshold_expression     >2sigma(I)

_computing_data_collection       'Bruker SMART'
_computing_cell_refinement       'Bruker SMART'
_computing_data_reduction        'Bruker SAINT'
_computing_structure_solution    'SHELXS-97 (Sheldrick, 1990)'
_computing_structure_refinement  'SHELXL-97 (Sheldrick, 1997)'
_computing_molecular_graphics    'Bruker SHELXTL'
_computing_publication_material  'Bruker SHELXTL'

_refine_special_details
;
 Refinement of F^2^ against ALL reflections.  The weighted R-factor wR and
 goodness of fit S are based on F^2^, conventional R-factors R are based
 on F, with F set to zero for negative F^2^. The threshold expression of
 F^2^ > 2sigma(F^2^) is used only for calculating R-factors(gt) etc. and is
 not relevant to the choice of reflections for refinement.  R-factors based
 on F^2^ are statistically about twice as large as those based on F, and R-
 factors based on ALL data will be even larger.
;

_refine_ls_structure_factor_coef  Fsqd
_refine_ls_matrix_type           full
_refine_ls_weighting_scheme      calc
_refine_ls_weighting_details
 'calc w=1/[\s^2^(Fo^2^)+(0.1247P)^2^+0.0072P] where P=(Fo^2^+2Fc^2^)/3'
_atom_sites_solution_primary     direct
_atom_sites_solution_secondary   difmap
_atom_sites_solution_hydrogens   geom
_refine_ls_hydrogen_treatment    mixed
_refine_ls_extinction_method     ?
_refine_ls_extinction_coef       ?
_refine_ls_extinction_expression
 'Fc^*^=kFc[1+0.001xFc^2^\l^3^/sin(2\q)]^-1/4^'
_refine_ls_number_reflns         2450
```

```
_refine_ls_number_parameters      169
_refine_ls_number_restraints      0
_refine_ls_R_factor_all           0.0822
_refine_ls_R_factor_gt            0.0626
_refine_ls_wR_factor_ref          0.1985
_refine_ls_wR_factor_gt           0.1757
_refine_ls_goodness_of_fit_ref    1.070
_refine_ls_restrained_S_all       1.070
_refine_ls_shift/su_max           0.000
_refine_ls_shift/su_mean          0.000

loop_
 _atom_site_label
 _atom_site_type_symbol
 _atom_site_fract_x
 _atom_site_fract_y
 _atom_site_fract_z
 _atom_site_U_iso_or_equiv
 _atom_site_adp_type
 _atom_site_occupancy
 _atom_site_symmetry_multiplicity
 _atom_site_calc_flag
 _atom_site_refinement_flags
 _atom_site_disorder_assembly
 _atom_site_disorder_group
O3 O 0.4222(4) 0.82621(17) 0.05081(15) 0.0497(5) Uani 1 1 d . . .
N1 N 0.0810(4) 0.68326(18) 0.16275(17) 0.0439(5) Uani 1 1 d . . .
H1 H -0.0788 0.6765 0.2085 0.053 Uiso 1 1 calc R . .
O6 O -0.0890(4) 1.22188(18) 0.33021(15) 0.0537(5) Uani 1 1 d . . .
O2 O 0.5502(4) 0.37627(17) 0.19174(16) 0.0550(5) Uani 1 1 d . . .
O4 O -0.1869(4) 0.88578(18) 0.23386(16) 0.0544(5) Uani 1 1 d . . .
O5 O 0.2461(5) 1.0499(2) 0.35272(17) 0.0658(6) Uani 1 1 d . . .
N2 N 0.1568(4) 1.03150(18) 0.12816(17) 0.0418(5) Uani 1 1 d . . .
H2 H 0.3151 1.0415 0.0814 0.050 Uiso 1 1 calc R . .
C3 C 0.2023(5) 0.8017(2) 0.12102(19) 0.0378(5) Uani 1 1 d . . .
C4 C 0.0389(5) 0.9121(2) 0.16718(18) 0.0388(5) Uani 1 1 d . . .
C1 C 0.4369(5) 0.4782(2) 0.2206(2) 0.0420(5) Uani 1 1 d . . .
O1 O 0.5055(5) 0.50900(19) 0.30670(16) 0.0658(6) Uani 1 1 d . . .
C5 C 0.0264(6) 1.1458(2) 0.1621(2) 0.0447(6) Uani 1 1 d . . .
H5A H -0.1861 1.1556 0.1494 0.054 Uiso 1 1 calc R . .
H5B H 0.1131 1.2282 0.1097 0.054 Uiso 1 1 calc R . .
C2 C 0.2068(6) 0.5643(2) 0.1344(2) 0.0450(6) Uani 1 1 d . . .
H2A H 0.2994 0.5938 0.0540 0.054 Uiso 1 1 calc R . .
H2B H 0.0460 0.5080 0.1344 0.054 Uiso 1 1 calc R . .
C6 C 0.0697(5) 1.1340(2) 0.2906(2) 0.0420(6) Uani 1 1 d . . .
N3 N 0.6509(6) 0.8195(3) 0.4736(2) 0.0522(6) Uani 1 1 d . . .
```

H31 H 0.481(13) 0.775(5) 0.495(4) 0.121(16) Uiso 1 1 d . . .
H32 H 0.652(9) 0.867(4) 0.532(4) 0.103(12) Uiso 1 1 d . . .
O7 O 0.1915(5) 0.6351(3) 0.4689(2) 0.0695(7) Uiso 1 1 d . . .
H34 H 0.813(9) 0.755(3) 0.478(3) 0.074(9) Uiso 1 1 d . . .
H33 H 0.678(12) 0.876(4) 0.403(5) 0.126(17) Uiso 1 1 d . . .
H72 H 0.164(7) 0.588(3) 0.573(3) 0.050(8) Uiso 1 1 d . . .
H71 H 0.263(18) 0.601(7) 0.394(8) 0.23(3) Uiso 1 1 d . . .
H61 H -0.250(10) 1.296(4) 0.266(4) 0.121(15) Uiso 1 1 d . . .

loop_
 _atom_site_aniso_label
 _atom_site_aniso_U_11
 _atom_site_aniso_U_22
 _atom_site_aniso_U_33
 _atom_site_aniso_U_23
 _atom_site_aniso_U_13
 _atom_site_aniso_U_12
O3 0.0480(10) 0.0517(10) 0.0563(10) -0.0298(8) 0.0041(8) 0.0028(8)
N1 0.0438(10) 0.0394(10) 0.0488(11) -0.0179(8) -0.0017(9) 0.0090(8)
O6 0.0631(11) 0.0588(11) 0.0463(9) -0.0315(8) -0.0095(8) 0.0205(9)
O2 0.0608(11) 0.0475(10) 0.0621(11) -0.0288(8) -0.0127(9) 0.0189(8)
O4 0.0535(10) 0.0591(11) 0.0522(10) -0.0255(8) 0.0102(8) 0.0056(8)
O5 0.0795(14) 0.0679(11) 0.0566(11) -0.0336(9) -0.0314(10) 0.0365(10)
N2 0.0439(10) 0.0428(10) 0.0441(10) -0.0240(8) -0.0026(8) 0.0073(8)
C3 0.0377(11) 0.0437(12) 0.0354(10) -0.0194(9) -0.0086(9) 0.0107(9)
C4 0.0421(12) 0.0456(12) 0.0327(10) -0.0206(9) -0.0084(9) 0.0127(10)
C1 0.0436(12) 0.0398(11) 0.0441(12) -0.0171(9) -0.0025(10) 0.0036(9)
O1 0.0787(14) 0.0671(12) 0.0622(12) -0.0396(10) -0.0257(10) 0.0315(10)
C5 0.0548(14) 0.0431(12) 0.0409(12) -0.0227(10) -0.0110(10) 0.0152(10)
C2 0.0476(13) 0.0379(11) 0.0528(13) -0.0207(10) -0.0058(11) 0.0061(10)
C6 0.0449(12) 0.0438(12) 0.0408(11) -0.0202(9) -0.0070(10) 0.0081(10)
N3 0.0524(13) 0.0622(14) 0.0445(13) -0.0222(12) -0.0081(10) 0.0068(12)

_geom_special_details
;
 All esds (except the esd in the dihedral angle between two l.s. planes)
 are estimated using the full covariance matrix. The cell esds are taken
 into account individually in the estimation of esds in distances, angles
 and torsion angles; correlations between esds in cell parameters are only
 used when they are defined by crystal symmetry. An approximate (isotropic)
 treatment of cell esds is used for estimating esds involving l.s. planes.
;

loop_
 _geom_bond_atom_site_label_1
 _geom_bond_atom_site_label_2

```
 _geom_bond_distance
 _geom_bond_site_symmetry_2
 _geom_bond_publ_flag
O3 C3 1.230(3) . ?
N1 C3 1.318(3) . ?
N1 C2 1.445(3) . ?
O6 C6 1.299(3) . ?
O2 C1 1.273(3) . ?
O4 C4 1.230(3) . ?
O5 C6 1.214(3) . ?
N2 C4 1.318(3) . ?
N2 C5 1.442(3) . ?
C3 C4 1.538(3) . ?
C1 O1 1.230(3) . ?
C1 C2 1.517(3) . ?
C5 C6 1.508(3) . ?

loop_
 _geom_angle_atom_site_label_1
 _geom_angle_atom_site_label_2
 _geom_angle_atom_site_label_3
 _geom_angle
 _geom_angle_site_symmetry_1
 _geom_angle_site_symmetry_3
 _geom_angle_publ_flag
C3 N1 C2 122.40(19) . . ?
C4 N2 C5 121.50(19) . . ?
O3 C3 N1 125.0(2) . . ?
O3 C3 C4 121.5(2) . . ?
N1 C3 C4 113.47(19) . . ?
O4 C4 N2 125.2(2) . . ?
O4 C4 C3 119.9(2) . . ?
N2 C4 C3 114.97(19) . . ?
O1 C1 O2 125.4(2) . . ?
O1 C1 C2 121.7(2) . . ?
O2 C1 C2 112.9(2) . . ?
N2 C5 C6 114.36(18) . . ?
N1 C2 C1 114.1(2) . . ?
O5 C6 O6 121.7(2) . . ?
O5 C6 C5 122.6(2) . . ?
O6 C6 C5 115.73(19) . . ?

_diffrn_measured_fraction_theta_max    0.925
_diffrn_reflns_theta_full              28.60
_diffrn_measured_fraction_theta_full   0.925
_refine_diff_density_max    0.333
```

```
_refine_diff_density_min   -0.421
_refine_diff_density_rms    0.067
```

$(CH_3NH_3)_2OG•2H_2O$

data_jgt

_audit_creation_method SHELXL-97
_chemical_name_systematic
;
?
;
_chemical_name_common ?
_chemical_melting_point ?
_chemical_formula_moiety ?
_chemical_formula_sum
'C8 H22 N4 O8'
_chemical_formula_weight 302.30

loop_
_atom_type_symbol
_atom_type_description
_atom_type_scat_dispersion_real
_atom_type_scat_dispersion_imag
_atom_type_scat_source
'C' 'C' 0.0033 0.0016
'International Tables Vol C Tables 4.2.6.8 and 6.1.1.4'
'H' 'H' 0.0000 0.0000
'International Tables Vol C Tables 4.2.6.8 and 6.1.1.4'
'N' 'N' 0.0061 0.0033
'International Tables Vol C Tables 4.2.6.8 and 6.1.1.4'
'O' 'O' 0.0106 0.0060
'International Tables Vol C Tables 4.2.6.8 and 6.1.1.4'

_symmetry_cell_setting Monoclinic
_symmetry_space_group_name_H-M P21/c

loop_
_symmetry_equiv_pos_as_xyz
'x, y, z'
'-x, y+1/2, -z+1/2'
'-x, -y, -z'
'x, -y-1/2, z-1/2'

_cell_length_a 13.9089(16)
_cell_length_b 7.6850(9)
_cell_length_c 14.2279(16)
_cell_angle_alpha 90.00
_cell_angle_beta 97.758(2)

```
_cell_angle_gamma                90.00
_cell_volume                     1506.9(3)
_cell_formula_units_Z            4
_cell_measurement_temperature    273(2)
_cell_measurement_reflns_used    ?
_cell_measurement_theta_min      ?
_cell_measurement_theta_max      ?

_exptl_crystal_description       ?
_exptl_crystal_colour            ?
_exptl_crystal_size_max          .6
_exptl_crystal_size_mid          .4
_exptl_crystal_size_min          .1
_exptl_crystal_density_meas      ?
_exptl_crystal_density_diffrn    1.332
_exptl_crystal_density_method    'not measured'
_exptl_crystal_F_000             648
_exptl_absorpt_coefficient_mu    0.118
_exptl_absorpt_correction_type   none
_exptl_absorpt_correction_T_min  ?
_exptl_absorpt_correction_T_max  ?
_exptl_absorpt_process_details   ?

_exptl_special_details
;
 ?
;

_diffrn_ambient_temperature      273(2)
_diffrn_radiation_wavelength     0.71073
_diffrn_radiation_type           MoK\a
_diffrn_radiation_source         'fine-focus sealed tube'
_diffrn_radiation_monochromator  graphite
_diffrn_measurement_device_type  'CCD area detector'
_diffrn_measurement_method       'phi and omega scans'
_diffrn_detector_area_resol_mean ?
_diffrn_standards_number         ?
_diffrn_standards_interval_count ?
_diffrn_standards_interval_time  ?
_diffrn_standards_decay_%        ?
_diffrn_reflns_number            6436
_diffrn_reflns_av_R_equivalents  0.0360
_diffrn_reflns_av_sigmaI/netI    0.0288
_diffrn_reflns_limit_h_min       -15
_diffrn_reflns_limit_h_max       15
_diffrn_reflns_limit_k_min       -8
```

```
_diffrn_reflns_limit_k_max       6
_diffrn_reflns_limit_l_min      -12
_diffrn_reflns_limit_l_max       15
_diffrn_reflns_theta_min         1.48
_diffrn_reflns_theta_max         23.28
_reflns_number_total            2171
_reflns_number_gt               1628
_reflns_threshold_expression     >2sigma(I)

_computing_data_collection       'Bruker SMART'
_computing_cell_refinement       'Bruker SMART'
_computing_data_reduction        'Bruker SAINT'
_computing_structure_solution    'SHELXS-97 (Sheldrick, 1990)'
_computing_structure_refinement   'SHELXL-97 (Sheldrick, 1997)'
_computing_molecular_graphics    'Bruker SHELXTL'
_computing_publication_material   'Bruker SHELXTL'

_refine_special_details
;
 Refinement of F^2^ against ALL reflections.  The weighted R-factor wR and
 goodness of fit S are based on F^2^, conventional R-factors R are based
 on F, with F set to zero for negative F^2^. The threshold expression of
 F^2^ > 2sigma(F^2^) is used only for calculating R-factors(gt) etc. and is
 not relevant to the choice of reflections for refinement.  R-factors based
 on F^2^ are statistically about twice as large as those based on F, and R-
 factors based on ALL data will be even larger.
;

_refine_ls_structure_factor_coef  Fsqd
_refine_ls_matrix_type           full
_refine_ls_weighting_scheme      calc
_refine_ls_weighting_details
 'calc w=1/[\s^2^(Fo^2^)+(0.1226P)^2^+0.0000P] where P=(Fo^2^+2Fc^2^)/3'
_atom_sites_solution_primary     direct
_atom_sites_solution_secondary    difmap
_atom_sites_solution_hydrogens    geom
_refine_ls_hydrogen_treatment    mixed
_refine_ls_extinction_method     ?
_refine_ls_extinction_coef       ?
_refine_ls_extinction_expression
 'Fc^*^=kFc[1+0.001xFc^2^\l^3^/sin(2\q)]^-1/4^'
_refine_ls_number_reflns         2171
_refine_ls_number_parameters     212
_refine_ls_number_restraints     0
_refine_ls_R_factor_all          0.0723
_refine_ls_R_factor_gt           0.0594
```

```
_refine_ls_wR_factor_ref         0.1692
_refine_ls_wR_factor_gt          0.1553
_refine_ls_goodness_of_fit_ref   1.028
_refine_ls_restrained_S_all      1.028
_refine_ls_shift/su_max          0.001
_refine_ls_shift/su_mean         0.000

loop_
 _atom_site_label
 _atom_site_type_symbol
 _atom_site_fract_x
 _atom_site_fract_y
 _atom_site_fract_z
 _atom_site_U_iso_or_equiv
 _atom_site_adp_type
 _atom_site_occupancy
 _atom_site_symmetry_multiplicity
 _atom_site_calc_flag
 _atom_site_refinement_flags
 _atom_site_disorder_assembly
 _atom_site_disorder_group
O3 O 0.61470(10) 0.15270(19) 0.28130(11) 0.0470(5) Uani 1 1 d . . .
N2 N 0.13687(12) 0.1435(2) 0.29015(13) 0.0428(5) Uani 1 1 d . . .
H2 H 0.1514 0.2513 0.3005 0.051 Uiso 1 1 calc R . .
O6 O -0.11091(10) 0.01331(19) 0.21248(11) 0.0459(5) Uani 1 1 d . . .
N1 N 0.36422(12) 0.0214(2) 0.22388(13) 0.0433(5) Uani 1 1 d . . .
H1 H 0.3511 -0.0878 0.2186 0.052 Uiso 1 1 calc R . .
O1 O 0.30457(12) 0.2873(2) 0.25221(14) 0.0636(6) Uani 1 1 d . . .
O2 O 0.19549(11) -0.1218(2) 0.25906(12) 0.0541(5) Uani 1 1 d . . .
C4 C 0.20366(15) 0.0365(3) 0.26607(15) 0.0392(6) Uani 1 1 d . . .
N3 N 0.80164(15) 1.0766(3) 0.37803(17) 0.0505(6) Uani 1 1 d . . .
O5 O 0.00382(12) 0.1135(2) 0.13174(12) 0.0589(6) Uani 1 1 d . . .
C3 C 0.29708(15) 0.1284(3) 0.24712(16) 0.0418(6) Uani 1 1 d . . .
C6 C -0.02667(16) 0.0706(3) 0.20619(17) 0.0399(6) Uani 1 1 d . . .
C5 C 0.04028(15) 0.0845(3) 0.29958(16) 0.0423(6) Uani 1 1 d . . .
H5A H 0.0117 0.1641 0.3409 0.051 Uiso 1 1 calc R . .
H5B H 0.0447 -0.0288 0.3299 0.051 Uiso 1 1 calc R . .
C2 C 0.45873(15) 0.0807(3) 0.20707(17) 0.0455(6) Uani 1 1 d . . .
H2A H 0.4513 0.1917 0.1744 0.055 Uiso 1 1 calc R . .
H2B H 0.4845 -0.0014 0.1651 0.055 Uiso 1 1 calc R . .
O4 O 0.50687(15) 0.0733(4) 0.37304(13) 0.0948(8) Uani 1 1 d . . .
C1 C 0.53167(16) 0.1021(3) 0.29504(17) 0.0450(6) Uani 1 1 d . . .
C7 C 0.8284(2) 0.9384(5) 0.4462(2) 0.0839(10) Uani 1 1 d . . .
H7A H 0.8970 0.9426 0.4667 0.126 Uiso 1 1 calc R . .
H7B H 0.8117 0.8279 0.4170 0.126 Uiso 1 1 calc R . .
H7C H 0.7942 0.9535 0.4999 0.126 Uiso 1 1 calc R . .
```

O7 O 0.36535(17) 0.9191(3) 0.46350(18) 0.0814(7) Uani 1 1 d . . .
N4 N 0.70466(13) 0.0982(3) 0.11384(14) 0.0526(6) Uani 1 1 d . . .
H4A H 0.6728 0.0878 0.1638 0.079 Uiso 1 1 calc R . .
H4B H 0.6966 0.2053 0.0903 0.079 Uiso 1 1 calc R . .
H4C H 0.7675 0.0785 0.1316 0.079 Uiso 1 1 calc R . .
C8 C 0.6669(2) -0.0280(5) 0.0414(2) 0.0874(10) Uani 1 1 d . . .
H8A H 0.7044 -0.0228 -0.0104 0.131 Uiso 1 1 calc R . .
H8B H 0.6004 -0.0014 0.0188 0.131 Uiso 1 1 calc R . .
H8C H 0.6711 -0.1428 0.0682 0.131 Uiso 1 1 calc R . .
H5N H 0.8168(18) 1.175(4) 0.3990(18) 0.053(8) Uiso 1 1 d . . .
H4N H 0.729(2) 1.092(4) 0.355(2) 0.080(8) Uiso 1 1 d . . .
H6N H 0.8270(18) 1.058(3) 0.3262(19) 0.057(8) Uiso 1 1 d . . .
O8 O 0.87733(19) 0.3857(4) 0.46691(19) 0.0857(8) Uani 1 1 d . . .
H1O8 H 0.895(3) 0.461(5) 0.422(3) 0.131(15) Uiso 1 1 d . . .
H2O8 H 0.920(3) 0.385(5) 0.521(3) 0.110(13) Uiso 1 1 d . . .
H2O7 H 0.416(4) 0.903(6) 0.523(4) 0.156(18) Uiso 1 1 d . . .
H1O7 H 0.398(2) 0.971(4) 0.425(2) 0.087(11) Uiso 1 1 d . . .

loop_
 _atom_site_aniso_label
 _atom_site_aniso_U_11
 _atom_site_aniso_U_22
 _atom_site_aniso_U_33
 _atom_site_aniso_U_23
 _atom_site_aniso_U_13
 _atom_site_aniso_U_12
O3 0.0288(9) 0.0484(10) 0.0646(11) 0.0006(7) 0.0087(7) -0.0045(7)
N2 0.0282(11) 0.0390(11) 0.0614(13) -0.0037(8) 0.0069(9) -0.0038(8)
O6 0.0298(9) 0.0469(10) 0.0609(11) -0.0006(7) 0.0058(7) -0.0031(6)
N1 0.0287(11) 0.0418(11) 0.0596(12) -0.0030(9) 0.0065(9) -0.0023(8)
O1 0.0449(11) 0.0417(11) 0.1076(15) -0.0007(9) 0.0223(10) -0.0043(7)
O2 0.0419(10) 0.0370(10) 0.0849(13) -0.0015(8) 0.0145(8) -0.0029(7)
C4 0.0273(12) 0.0434(14) 0.0462(13) -0.0012(10) 0.0020(9) -0.0028(10)
N3 0.0380(13) 0.0668(17) 0.0464(14) -0.0025(11) 0.0046(11) -0.0005(10)
O5 0.0458(11) 0.0858(13) 0.0466(11) 0.0049(8) 0.0114(8) -0.0037(8)
C3 0.0305(13) 0.0409(14) 0.0535(15) 0.0011(10) 0.0042(10) -0.0018(10)
C6 0.0308(13) 0.0366(12) 0.0536(15) -0.0027(10) 0.0109(11) 0.0035(9)
C5 0.0290(12) 0.0495(14) 0.0491(15) -0.0015(10) 0.0080(10) -0.0032(9)
C2 0.0286(13) 0.0537(14) 0.0556(15) 0.0010(10) 0.0111(11) -0.0045(10)
O4 0.0584(13) 0.179(2) 0.0462(13) 0.0080(12) 0.0054(10) -0.0502(14)
C1 0.0324(13) 0.0507(14) 0.0528(16) 0.0012(11) 0.0087(11) -0.0060(10)
C7 0.082(2) 0.105(3) 0.0663(19) 0.0176(18) 0.0135(17) 0.0131(18)
O7 0.0604(13) 0.1206(19) 0.0634(14) -0.0075(12) 0.0090(11) -0.0369(12)
N4 0.0359(12) 0.0737(15) 0.0481(13) 0.0004(9) 0.0055(9) 0.0007(9)
C8 0.084(2) 0.112(3) 0.066(2) -0.0209(18) 0.0050(17) -0.0187(18)
O8 0.0818(16) 0.1147(19) 0.0577(14) -0.0064(12) -0.0009(12) -0.0384(13)

```
_geom_special_details
;
 All esds (except the esd in the dihedral angle between two l.s. planes)
 are estimated using the full covariance matrix.  The cell esds are taken
 into account individually in the estimation of esds in distances, angles
 and torsion angles; correlations between esds in cell parameters are only
 used when they are defined by crystal symmetry.  An approximate (isotropic)
 treatment of cell esds is used for estimating esds involving l.s. planes.
;

loop_
 _geom_bond_atom_site_label_1
 _geom_bond_atom_site_label_2
 _geom_bond_distance
 _geom_bond_site_symmetry_2
 _geom_bond_publ_flag
O3 C1 1.259(3) . ?
N2 C4 1.320(3) . ?
N2 C5 1.441(3) . ?
O6 C6 1.266(3) . ?
N1 C3 1.320(3) . ?
N1 C2 1.441(3) . ?
O1 C3 1.227(3) . ?
O2 C4 1.224(3) . ?
C4 C3 1.535(3) . ?
N3 C7 1.452(4) . ?
O5 C6 1.238(3) . ?
C6 C5 1.520(3) . ?
C2 C1 1.510(3) . ?
O4 C1 1.226(3) . ?
N4 C8 1.461(4) . ?

loop_
 _geom_angle_atom_site_label_1
 _geom_angle_atom_site_label_2
 _geom_angle_atom_site_label_3
 _geom_angle
 _geom_angle_site_symmetry_1
 _geom_angle_site_symmetry_3
 _geom_angle_publ_flag
C4 N2 C5 121.68(19) . . ?
C3 N1 C2 122.46(19) . . ?
O2 C4 N2 125.41(19) . . ?
O2 C4 C3 120.96(19) . . ?
N2 C4 C3 113.6(2) . . ?
```

O1 C3 N1 125.3(2) . . ?
O1 C3 C4 121.0(2) . . ?
N1 C3 C4 113.7(2) . . ?
O5 C6 O6 125.5(2) . . ?
O5 C6 C5 119.29(19) . . ?
O6 C6 C5 115.23(19) . . ?
N2 C5 C6 114.17(18) . . ?
N1 C2 C1 115.00(19) . . ?
O4 C1 O3 124.9(2) . . ?
O4 C1 C2 119.4(2) . . ?
O3 C1 C2 115.6(2) . . ?

_diffrn_measured_fraction_theta_max 0.998
_diffrn_reflns_theta_full 23.28
_diffrn_measured_fraction_theta_full 0.998
_refine_diff_density_max 0.379
_refine_diff_density_min -0.313
_refine_diff_density_rms 0.064

$(CH_3CH_2NH_3)_2OG•2H_2O$

```
data_jlc1t

_audit_creation_method            SHELXL-97
_chemical_name_systematic
;
 ?
;
_chemical_name_common              ?
_chemical_melting_point           ?
_chemical_formula_moiety          ?
_chemical_formula_sum
 'C10 H26 N4 O8'
_chemical_formula_weight          330.35

loop_
 _atom_type_symbol
 _atom_type_description
 _atom_type_scat_dispersion_real
 _atom_type_scat_dispersion_imag
 _atom_type_scat_source
 'C'  'C'   0.0033   0.0016
 'International Tables Vol C Tables 4.2.6.8 and 6.1.1.4'
 'H'  'H'   0.0000   0.0000
 'International Tables Vol C Tables 4.2.6.8 and 6.1.1.4'
 'N'  'N'   0.0061   0.0033
 'International Tables Vol C Tables 4.2.6.8 and 6.1.1.4'
 'O'  'O'   0.0106   0.0060
 'International Tables Vol C Tables 4.2.6.8 and 6.1.1.4'

_symmetry_cell_setting            Monoclinic
_symmetry_space_group_name_H-M    P21/n

loop_
 _symmetry_equiv_pos_as_xyz
 'x, y, z'
 '-x+1/2, y+1/2, -z+1/2'
 '-x, -y, -z'
 'x-1/2, -y-1/2, z-1/2'

_cell_length_a                    8.969(2)
_cell_length_b                    7.779(2)
_cell_length_c                    11.803(3)
_cell_angle_alpha                 90.00
_cell_angle_beta                  95.522(4)
```

```
_cell_angle_gamma                90.00
_cell_volume                     819.7(4)
_cell_formula_units_Z            2
_cell_measurement_temperature    273(2)
_cell_measurement_reflns_used    ?
_cell_measurement_theta_min      ?
_cell_measurement_theta_max      ?

_exptl_crystal_description       ?
_exptl_crystal_colour            ?
_exptl_crystal_size_max          .5
_exptl_crystal_size_mid          .1
_exptl_crystal_size_min          .1
_exptl_crystal_density_meas      ?
_exptl_crystal_density_diffrn    1.338
_exptl_crystal_density_method    'not measured'
_exptl_crystal_F_000             356
_exptl_absorpt_coefficient_mu    0.115
_exptl_absorpt_correction_type   none
_exptl_absorpt_correction_T_min  ?
_exptl_absorpt_correction_T_max  ?
_exptl_absorpt_process_details   ?

_exptl_special_details
;
 ?
;

_diffrn_ambient_temperature      273(2)
_diffrn_radiation_wavelength     0.71073
_diffrn_radiation_type           MoK\a
_diffrn_radiation_source         'fine-focus sealed tube'
_diffrn_radiation_monochromator  graphite
_diffrn_measurement_device_type  'CCD area detector'
_diffrn_measurement_method       'phi and omega scans'
_diffrn_detector_area_resol_mean ?
_diffrn_standards_number         ?
_diffrn_standards_interval_count ?
_diffrn_standards_interval_time  ?
_diffrn_standards_decay_%        ?
_diffrn_reflns_number            2234
_diffrn_reflns_av_R_equivalents  0.1275
_diffrn_reflns_av_sigmaI/netI    0.1400
_diffrn_reflns_limit_h_min       -8
_diffrn_reflns_limit_h_max       9
_diffrn_reflns_limit_k_min       -1
```

```
_diffrn_reflns_limit_k_max       10
_diffrn_reflns_limit_l_min       -15
_diffrn_reflns_limit_l_max       14
_diffrn_reflns_theta_min         2.73
_diffrn_reflns_theta_max         28.35
_reflns_number_total             1824
_reflns_number_gt                734
_reflns_threshold_expression     >2sigma(I)

_computing_data_collection       'Bruker SMART'
_computing_cell_refinement       'Bruker SMART'
_computing_data_reduction        'Bruker SAINT'
_computing_structure_solution    'SHELXS-97 (Sheldrick, 1990)'
_computing_structure_refinement   'SHELXL-97 (Sheldrick, 1997)'
_computing_molecular_graphics    'Bruker SHELXTL'
_computing_publication_material   'Bruker SHELXTL'

_refine_special_details
;
 Refinement of F^2^ against ALL reflections.  The weighted R-factor wR and
 goodness of fit S are based on F^2^, conventional R-factors R are based
 on F, with F set to zero for negative F^2^. The threshold expression of
 F^2^ > 2sigma(F^2^) is used only for calculating R-factors(gt) etc. and is
 not relevant to the choice of reflections for refinement.  R-factors based
 on F^2^ are statistically about twice as large as those based on F, and R-
 factors based on ALL data will be even larger.
;

_refine_ls_structure_factor_coef  Fsqd
_refine_ls_matrix_type           full
_refine_ls_weighting_scheme      calc
_refine_ls_weighting_details
 'calc w=1/[\s^2^(Fo^2^)+(0.1666P)^2^+0.0000P] where P=(Fo^2^+2Fc^2^)/3'
_atom_sites_solution_primary     direct
_atom_sites_solution_secondary    difmap
_atom_sites_solution_hydrogens    geom
_refine_ls_hydrogen_treatment    mixed
_refine_ls_extinction_method     ?
_refine_ls_extinction_coef       ?
_refine_ls_extinction_expression
 'Fc^*^=kFc[1+0.001xFc^2^\l^3^/sin(2\q)]^-1/4^'
_refine_ls_number_reflns         1824
_refine_ls_number_parameters     110
_refine_ls_number_restraints     0
_refine_ls_R_factor_all          0.1240
_refine_ls_R_factor_gt           0.0899
```

```
_refine_ls_wR_factor_ref         0.1905
_refine_ls_wR_factor_gt          0.2419
_refine_ls_goodness_of_fit_ref   0.973
_refine_ls_restrained_S_all      0.973
_refine_ls_shift/su_max          0.006
_refine_ls_shift/su_mean         0.002

loop_
 _atom_site_label
 _atom_site_type_symbol
 _atom_site_fract_x
 _atom_site_fract_y
 _atom_site_fract_z
 _atom_site_U_iso_or_equiv
 _atom_site_adp_type
 _atom_site_occupancy
 _atom_site_symmetry_multiplicity
 _atom_site_calc_flag
 _atom_site_refinement_flags
 _atom_site_disorder_assembly
 _atom_site_disorder_group
O3 O 0.0979(4) 0.0749(3) 0.6649(2) 0.0387(10) Uani 1 1 d . . .
O1 O 0.4597(3) 0.2042(3) 0.9418(2) 0.0427(10) Uani 1 1 d . . .
N1 N 0.4055(5) -0.0600(4) 0.8663(2) 0.0358(11) Uani 1 1 d . . .
H1 H 0.4139 -0.1689 0.8776 0.043 Uiso 1 1 calc R . .
C3 C 0.1641(6) 0.0285(4) 0.7602(3) 0.0315(13) Uani 1 1 d . . .
C1 C 0.4625(5) 0.0465(4) 0.9471(3) 0.0283(12) Uani 1 1 d . . .
O2 O 0.1011(4) 0.0097(5) 0.8483(2) 0.0598(13) Uani 1 1 d . . .
C2 C 0.3295(6) 0.0009(5) 0.7600(3) 0.0359(14) Uani 1 1 d . . .
H2A H 0.3461 -0.0815 0.7008 0.043 Uiso 1 1 calc R . .
H2B H 0.3750 0.1085 0.7403 0.043 Uiso 1 1 calc R . .
N2 N 0.1857(5) 1.0218(4) 0.4408(3) 0.0419(12) Uani 1 1 d . . .
H2C H 0.2197 1.1207 0.4155 0.063 Uiso 1 1 calc R . .
H2D H 0.1678 1.0335 0.5133 0.063 Uiso 1 1 calc R . .
H2E H 0.1014 0.9929 0.3992 0.063 Uiso 1 1 calc R . .
C4 C 0.2988(8) 0.8862(7) 0.4317(5) 0.0689(17) Uani 1 1 d . . .
H4A H 0.3965 0.9316 0.4587 0.083 Uiso 1 1 calc R . .
H4B H 0.2773 0.7915 0.4810 0.083 Uiso 1 1 calc R . .
C5 C 0.3045(8) 0.8227(12) 0.3200(5) 0.112(3) Uani 1 1 d . . .
H5A H 0.2054 0.7927 0.2883 0.168 Uiso 1 1 calc R . .
H5B H 0.3674 0.7227 0.3221 0.168 Uiso 1 1 calc R . .
H5C H 0.3447 0.9096 0.2738 0.168 Uiso 1 1 calc R . .
O4 O 0.1416(5) 0.8296(6) 0.0541(4) 0.0811(17) Uani 1 1 d . . .
H11 H 0.077(7) 0.884(6) 0.092(4) 0.062(16) Uiso 1 1 d . . .
H10 H 0.141(9) 0.855(10) -0.006(6) 0.12(3) Uiso 1 1 d . . .
```

```
loop_
 _atom_site_aniso_label
 _atom_site_aniso_U_11
 _atom_site_aniso_U_22
 _atom_site_aniso_U_33
 _atom_site_aniso_U_23
 _atom_site_aniso_U_13
 _atom_site_aniso_U_12
O3 0.026(3) 0.0473(14) 0.0396(14) 0.0038(10) -0.0141(13) 0.0033(13)
O1 0.036(3) 0.0402(14) 0.0489(15) 0.0021(10) -0.0122(14) 0.0008(13)
N1 0.028(3) 0.0406(15) 0.0366(16) 0.0006(11) -0.0093(15) 0.0071(14)
C3 0.014(4) 0.0414(17) 0.0370(19) 0.0029(13) -0.0061(18) 0.0014(17)
C1 0.015(4) 0.0430(18) 0.0398(19) 0.0025(13) -0.0093(18) -0.0032(15)
O2 0.028(3) 0.105(3) 0.0473(16) 0.0208(15) 0.0091(16) 0.0198(18)
C2 0.018(5) 0.056(2) 0.0315(17) 0.0026(14) -0.0092(18) -0.0028(19)
N2 0.015(4) 0.0605(19) 0.0498(19) -0.0032(13) 0.0008(16) -0.0009(16)
C4 0.029(5) 0.082(4) 0.093(4) -0.008(3) -0.005(3) -0.001(3)
C5 0.068(7) 0.167(7) 0.101(5) -0.040(5) 0.004(4) 0.044(6)
O4 0.073(4) 0.107(3) 0.067(2) 0.031(2) 0.022(2) 0.054(3)

_geom_special_details
;
 All esds (except the esd in the dihedral angle between two l.s. planes)
 are estimated using the full covariance matrix.  The cell esds are taken
 into account individually in the estimation of esds in distances, angles
 and torsion angles; correlations between esds in cell parameters are only
 used when they are defined by crystal symmetry.  An approximate (isotropic)
 treatment of cell esds is used for estimating esds involving l.s. planes.
;

loop_
 _geom_bond_atom_site_label_1
 _geom_bond_atom_site_label_2
 _geom_bond_distance
 _geom_bond_site_symmetry_2
 _geom_bond_publ_flag
O3 C3 1.273(4) . ?
O1 C1 1.228(4) . ?
N1 C1 1.327(4) . ?
N1 C2 1.449(5) . ?
C3 O2 1.239(5) . ?
C3 C2 1.499(7) . ?
C1 C1 1.542(6) 3_657 ?
N2 C4 1.474(8) . ?
C4 C5 1.413(8) . ?
```

```
loop_
 _geom_angle_atom_site_label_1
 _geom_angle_atom_site_label_2
 _geom_angle_atom_site_label_3
 _geom_angle
 _geom_angle_site_symmetry_1
 _geom_angle_site_symmetry_3
 _geom_angle_publ_flag
C1 N1 C2 122.3(3) . . ?
O2 C3 O3 124.3(5) . . ?
O2 C3 C2 121.1(4) . . ?
O3 C3 C2 114.6(3) . . ?
O1 C1 N1 125.6(3) . . ?
O1 C1 C1 121.0(4) . 3_657 ?
N1 C1 C1 113.4(4) . 3_657 ?
N1 C2 C3 115.4(3) . . ?
C5 C4 N2 113.9(5) . . ?

_diffrn_measured_fraction_theta_max    0.897
_diffrn_reflns_theta_full              28.35
_diffrn_measured_fraction_theta_full   0.897
_refine_diff_density_max    0.389
_refine_diff_density_min   -0.370
_refine_diff_density_rms    0.089
```

$(propylNH_3)_2OG$

```
data_jlj

_audit_creation_method           SHELXL-97
_chemical_name_systematic
;
 ?
;
_chemical_name_common            ?
_chemical_melting_point          ?
_chemical_formula_moiety         ?
_chemical_formula_sum
 'C12 H26 N4 O6'
_chemical_formula_weight         322.37

loop_
 _atom_type_symbol
 _atom_type_description
 _atom_type_scat_dispersion_real
 _atom_type_scat_dispersion_imag
 _atom_type_scat_source
'C'  'C'   0.0033   0.0016
'International Tables Vol C Tables 4.2.6.8 and 6.1.1.4'
'H'  'H'   0.0000   0.0000
'International Tables Vol C Tables 4.2.6.8 and 6.1.1.4'
'N'  'N'   0.0061   0.0033
'International Tables Vol C Tables 4.2.6.8 and 6.1.1.4'
'O'  'O'   0.0106   0.0060
'International Tables Vol C Tables 4.2.6.8 and 6.1.1.4'

_symmetry_cell_setting           Triclinic
_symmetry_space_group_name_H-M    P-1

loop_
 _symmetry_equiv_pos_as_xyz
'x, y, z'
'-x, -y, -z'

_cell_length_a                 9.962(2)
_cell_length_b                 9.965(2)
_cell_length_c                 10.064(2)
_cell_angle_alpha               70.093(4)
_cell_angle_beta                69.558(4)
_cell_angle_gamma                66.216(3)
_cell_volume                   833.1(3)
```

```
_cell_formula_units_Z            2
_cell_measurement_temperature    273(2)
_cell_measurement_reflns_used    ?
_cell_measurement_theta_min      ?
_cell_measurement_theta_max      ?

_exptl_crystal_description       ?
_exptl_crystal_colour            ?
_exptl_crystal_size_max          .7
_exptl_crystal_size_mid          .4
_exptl_crystal_size_min          .3
_exptl_crystal_density_meas      ?
_exptl_crystal_density_diffrn    1.285
_exptl_crystal_density_method    'not measured'
_exptl_crystal_F_000             348
_exptl_absorpt_coefficient_mu    0.103
_exptl_absorpt_correction_type   none
_exptl_absorpt_correction_T_min  ?
_exptl_absorpt_correction_T_max  ?
_exptl_absorpt_process_details   ?

_exptl_special_details
;
 ?
;

_diffrn_ambient_temperature      273(2)
_diffrn_radiation_wavelength     0.71073
_diffrn_radiation_type           MoK\a
_diffrn_radiation_source         'fine-focus sealed tube'
_diffrn_radiation_monochromator  graphite
_diffrn_measurement_device_type  'CCD area detector'
_diffrn_measurement_method       'phi and omega scans'
_diffrn_detector_area_resol_mean  ?
_diffrn_standards_number         ?
_diffrn_standards_interval_count  ?
_diffrn_standards_interval_time  ?
_diffrn_standards_decay_%        ?
_diffrn_reflns_number            4907
_diffrn_reflns_av_R_equivalents  0.0180
_diffrn_reflns_av_sigmaI/netI    0.0565
_diffrn_reflns_limit_h_min       -13
_diffrn_reflns_limit_h_max       12
_diffrn_reflns_limit_k_min       -13
_diffrn_reflns_limit_k_max       12
_diffrn_reflns_limit_l_min       -12
```

```
_diffrn_reflns_limit_l_max       13
_diffrn_reflns_theta_min         2.22
_diffrn_reflns_theta_max         28.36
_reflns_number_total             4012
_reflns_number_gt                1828
_reflns_threshold_expression     >2sigma(I)

_computing_data_collection       'Bruker SMART'
_computing_cell_refinement       'Bruker SMART'
_computing_data_reduction        'Bruker SAINT'
_computing_structure_solution    'SHELXS-97 (Sheldrick, 1990)'
_computing_structure_refinement  'SHELXL-97 (Sheldrick, 1997)'
_computing_molecular_graphics    'Bruker SHELXTL'
_computing_publication_material  'Bruker SHELXTL'

_refine_special_details
;
Refinement of F^2^ against ALL reflections.  The weighted R-factor wR and
goodness of fit S are based on F^2^, conventional R-factors R are based
on F, with F set to zero for negative F^2^. The threshold expression of
F^2^ > 2sigma(F^2^) is used only for calculating R-factors(gt) etc. and is
not relevant to the choice of reflections for refinement.  R-factors based
on F^2^ are statistically about twice as large as those based on F, and R-
factors based on ALL data will be even larger.
;

_refine_ls_structure_factor_coef  Fsqd
_refine_ls_matrix_type           full
_refine_ls_weighting_scheme      calc
_refine_ls_weighting_details
'calc w=1/[\s^2^(Fo^2^)+(0.1374P)^2^+0.0000P] where P=(Fo^2^+2Fc^2^)/3'
_atom_sites_solution_primary     direct
_atom_sites_solution_secondary   difmap
_atom_sites_solution_hydrogens   geom
_refine_ls_hydrogen_treatment    mixed
_refine_ls_extinction_method     ?
_refine_ls_extinction_coef       ?
_refine_ls_extinction_expression
'Fc^*^=kFc[1+0.001xFc^2^\l^3^/sin(2\q)]^-1/4^'
_refine_ls_number_reflns         4012
_refine_ls_number_parameters     203
_refine_ls_number_restraints     0
_refine_ls_R_factor_all          0.1251
_refine_ls_R_factor_gt           0.0734
_refine_ls_wR_factor_ref         0.2305
_refine_ls_wR_factor_gt          0.2021
```

```
_refine_ls_goodness_of_fit_ref    0.959
_refine_ls_restrained_S_all       0.959
_refine_ls_shift/su_max           0.032
_refine_ls_shift/su_mean          0.010

loop_
 _atom_site_label
 _atom_site_type_symbol
 _atom_site_fract_x
 _atom_site_fract_y
 _atom_site_fract_z
 _atom_site_U_iso_or_equiv
 _atom_site_adp_type
 _atom_site_occupancy
 _atom_site_symmetry_multiplicity
 _atom_site_calc_flag
 _atom_site_refinement_flags
 _atom_site_disorder_assembly
 _atom_site_disorder_group
O3 O 0.4352(2) 0.3761(2) 0.4711(2) 0.0531(6) Uani 1 1 d . . .
O6 O -0.0735(2) 0.4603(2) 0.3895(2) 0.0531(6) Uani 1 1 d . . .
O4 O 0.3841(3) 0.1285(2) 0.1733(2) 0.0595(7) Uani 1 1 d . . .
N1 N 0.6706(3) 0.3893(3) 0.4030(3) 0.0426(6) Uani 1 1 d . . .
H1 H 0.7269 0.4354 0.4039 0.051 Uiso 1 1 calc R . .
N2 N 0.1690(3) 0.4109(3) 0.3839(2) 0.0428(6) Uani 1 1 d . . .
H2 H 0.2282 0.4150 0.4264 0.051 Uiso 1 1 calc R . .
O1 O 0.7212(3) 0.1840(3) 0.1499(2) 0.0677(7) Uani 1 1 d . . .
O5 O 0.3243(3) 0.1058(2) 0.4110(2) 0.0647(7) Uani 1 1 d . . .
C3 C 0.5250(3) 0.4336(3) 0.4662(3) 0.0387(7) Uani 1 1 d . . .
C6 C 0.0216(3) 0.4636(3) 0.4367(3) 0.0383(7) Uani 1 1 d . . .
C2 C 0.7372(3) 0.2666(3) 0.3327(3) 0.0441(7) Uani 1 1 d . . .
H2A H 0.7100 0.1801 0.4005 0.053 Uiso 1 1 calc R . .
H2B H 0.8465 0.2397 0.3097 0.053 Uiso 1 1 calc R . .
N3 N 0.4483(3) 0.7173(3) 0.0588(3) 0.0534(7) Uani 1 1 d . . .
H3A H 0.4965 0.6254 0.1043 0.080 Uiso 1 1 calc R . .
H3B H 0.5155 0.7620 -0.0025 0.080 Uiso 1 1 calc R . .
H3C H 0.3939 0.7102 0.0092 0.080 Uiso 1 1 calc R . .
C5 C 0.2351(4) 0.3465(3) 0.2576(3) 0.0502(8) Uani 1 1 d . . .
H5A H 0.3039 0.3989 0.1873 0.060 Uiso 1 1 calc R . .
H5B H 0.1548 0.3659 0.2134 0.060 Uiso 1 1 calc R . .
C4 C 0.3197(3) 0.1805(3) 0.2851(3) 0.0459(8) Uani 1 1 d . . .
O2 O 0.6330(3) 0.4270(3) 0.1324(3) 0.0759(8) Uani 1 1 d . . .
C1 C 0.6906(4) 0.2985(4) 0.1941(3) 0.0479(8) Uani 1 1 d . . .
C8 C 0.2087(6) 0.7969(8) 0.2334(6) 0.119(2) Uani 1 1 d . . .
H8A H 0.2203 0.6952 0.2930 0.143 Uiso 1 1 calc R . .
H8B H 0.1618 0.8089 0.1584 0.143 Uiso 1 1 calc R . .
```

C7 C 0.3471(5) 0.8072(6) 0.1671(5) 0.0967(15) Uani 1 1 d . . .
H7A H 0.3990 0.7810 0.2425 0.116 Uiso 1 1 calc R . .
H7B H 0.3354 0.9124 0.1191 0.116 Uiso 1 1 calc R . .
C9 C 0.0998(5) 0.9032(5) 0.3277(5) 0.0853(13) Uani 1 1 d . . .
H9A H 0.1497 0.9080 0.3913 0.128 Uiso 1 1 calc R . .
H9B H 0.0154 0.8681 0.3849 0.128 Uiso 1 1 calc R . .
H9C H 0.0643 1.0018 0.2674 0.128 Uiso 1 1 calc R . .
N4 N 0.3564(3) 0.0702(3) 0.6846(3) 0.0569(7) Uani 1 1 d . . .
H4A H 0.3253 -0.0099 0.7275 0.085 Uiso 1 1 calc R . .
H4B H 0.4571 0.0404 0.6606 0.085 Uiso 1 1 calc R . .
H4C H 0.3224 0.1201 0.6047 0.085 Uiso 1 1 calc R . .
C10 C 0.2973(4) 0.1704(4) 0.7863(4) 0.0621(10) Uani 1 1 d . . .
H10A H 0.3505 0.1235 0.8634 0.074 Uiso 1 1 calc R . .
H10B H 0.3172 0.2648 0.7343 0.074 Uiso 1 1 calc R . .
C11 C 0.1342(4) 0.2017(4) 0.8514(4) 0.0707(11) Uani 1 1 d . . .
H11A H 0.1137 0.1075 0.9031 0.085 Uiso 1 1 calc R . .
H11B H 0.0805 0.2500 0.7747 0.085 Uiso 1 1 calc R . .
C12 C 0.0768(5) 0.3035(5) 0.9566(5) 0.0864(13) Uani 1 1 d . . .
H12A H 0.1223 0.2516 1.0378 0.130 Uiso 1 1 calc R . .
H12B H -0.0312 0.3292 0.9910 0.130 Uiso 1 1 calc R . .
H12C H 0.1033 0.3938 0.9073 0.130 Uiso 1 1 calc R . .

loop_
 _atom_site_aniso_label
 _atom_site_aniso_U_11
 _atom_site_aniso_U_22
 _atom_site_aniso_U_33
 _atom_site_aniso_U_23
 _atom_site_aniso_U_13
 _atom_site_aniso_U_12
O3 0.0450(12) 0.0578(14) 0.0686(15) -0.0330(11) -0.0083(11) -0.0182(11)
O6 0.0427(12) 0.0704(15) 0.0569(13) -0.0326(11) -0.0119(11) -0.0145(11)
O4 0.0678(15) 0.0496(13) 0.0544(13) -0.0278(11) -0.0014(12) -0.0111(11)
N1 0.0350(13) 0.0517(15) 0.0502(14) -0.0282(12) -0.0081(12) -0.0115(11)
N2 0.0359(13) 0.0474(14) 0.0456(14) -0.0244(11) -0.0072(11) -0.0053(11)
O1 0.102(2) 0.0642(16) 0.0523(13) -0.0262(11) -0.0190(14) -0.0310(14)
O5 0.0870(18) 0.0493(14) 0.0467(14) -0.0107(11) -0.0149(13) -0.0129(12)
C3 0.0392(16) 0.0435(16) 0.0382(15) -0.0147(12) -0.0121(13) -0.0116(13)
C6 0.0398(16) 0.0347(15) 0.0386(15) -0.0104(12) -0.0067(14) -0.0113(13)
C2 0.0384(16) 0.0450(17) 0.0511(17) -0.0229(14) -0.0146(14) -0.0028(13)
N3 0.0631(17) 0.0524(16) 0.0418(14) -0.0142(12) -0.0087(13) -0.0168(13)
C5 0.0529(19) 0.0465(18) 0.0437(17) -0.0199(14) -0.0036(15) -0.0079(15)
C4 0.0422(17) 0.0450(17) 0.0501(19) -0.0191(15) -0.0059(15) -0.0118(14)
O2 0.096(2) 0.0575(16) 0.0622(15) -0.0040(12) -0.0367(15) -0.0068(14)
C1 0.0519(19) 0.0501(19) 0.0412(17) -0.0132(15) -0.0091(15) -0.0159(15)
C8 0.080(3) 0.198(6) 0.107(4) -0.094(4) 0.001(3) -0.045(4)

C7 0.070(3) 0.138(4) 0.099(3) -0.079(3) 0.001(3) -0.027(3)
C9 0.078(3) 0.091(3) 0.068(3) -0.034(2) -0.003(2) -0.009(2)
N4 0.0623(18) 0.0511(16) 0.0455(15) -0.0169(12) -0.0071(14) -0.0073(13)
C10 0.075(2) 0.048(2) 0.058(2) -0.0192(16) -0.0056(19) -0.0179(17)
C11 0.066(2) 0.068(2) 0.071(2) -0.0247(19) -0.003(2) -0.0194(19)
C12 0.082(3) 0.089(3) 0.070(3) -0.042(2) 0.001(2) -0.008(2)

_geom_special_details
;
All esds (except the esd in the dihedral angle between two l.s. planes)
are estimated using the full covariance matrix. The cell esds are taken
into account individually in the estimation of esds in distances, angles
and torsion angles; correlations between esds in cell parameters are only
used when they are defined by crystal symmetry. An approximate (isotropic)
treatment of cell esds is used for estimating esds involving l.s. planes.
;

loop_
_geom_bond_atom_site_label_1
_geom_bond_atom_site_label_2
_geom_bond_distance
_geom_bond_site_symmetry_2
_geom_bond_publ_flag
O3 C3 1.223(3) . ?
O6 C6 1.214(3) . ?
O4 C4 1.253(4) . ?
N1 C3 1.316(4) . ?
N1 C2 1.430(3) . ?
N2 C6 1.318(4) . ?
N2 C5 1.446(3) . ?
O1 C1 1.250(4) . ?
O5 C4 1.237(4) . ?
C3 C3 1.519(5) 2_666 ?
C6 C6 1.526(5) 2_566 ?
C2 C1 1.515(4) . ?
N3 C7 1.476(5) . ?
C5 C4 1.500(4) . ?
O2 C1 1.212(4) . ?
C8 C7 1.335(6) . ?
C8 C9 1.496(6) . ?
N4 C10 1.480(4) . ?
C10 C11 1.468(5) . ?
C11 C12 1.522(5) . ?

loop_
_geom_angle_atom_site_label_1

```
 _geom_angle_atom_site_label_2
 _geom_angle_atom_site_label_3
 _geom_angle
 _geom_angle_site_symmetry_1
 _geom_angle_site_symmetry_3
 _geom_angle_publ_flag
C3 N1 C2 121.6(2) . . ?
C6 N2 C5 122.7(3) . . ?
O3 C3 N1 124.5(3) . . ?
O3 C3 C3 121.6(3) . 2_666 ?
N1 C3 C3 113.9(3) . 2_666 ?
O6 C6 N2 125.0(3) . . ?
O6 C6 C6 121.8(3) . 2_566 ?
N2 C6 C6 113.2(3) . 2_566 ?
N1 C2 C1 114.5(3) . . ?
N2 C5 C4 116.0(2) . . ?
O5 C4 O4 124.8(3) . . ?
O5 C4 C5 120.1(3) . . ?
O4 C4 C5 115.1(3) . . ?
O2 C1 O1 124.9(3) . . ?
O2 C1 C2 120.5(3) . . ?
O1 C1 C2 114.5(3) . . ?
C7 C8 C9 119.2(5) . . ?
C8 C7 N3 119.6(4) . . ?
C11 C10 N4 112.4(3) . . ?
C10 C11 C12 111.2(3) . . ?

_diffrn_measured_fraction_theta_max    0.960
_diffrn_reflns_theta_full              28.36
_diffrn_measured_fraction_theta_full   0.960
_refine_diff_density_max    0.523
_refine_diff_density_min   -0.365
_refine_diff_density_rms    0.063
```

$(butylNH_3)_2OG$

```
data_jlgt

_audit_creation_method            SHELXL-97
_chemical_name_systematic
;
 ?
;
_chemical_name_common             ?
_chemical_melting_point           ?
_chemical_formula_moiety          ?
_chemical_formula_sum
 'C14 H30 N4 O6'
_chemical_formula_weight          350.42

loop_
 _atom_type_symbol
 _atom_type_description
 _atom_type_scat_dispersion_real
 _atom_type_scat_dispersion_imag
 _atom_type_scat_source
 'C'  'C'   0.0033   0.0016
 'International Tables Vol C Tables 4.2.6.8 and 6.1.1.4'
 'H'  'H'   0.0000   0.0000
 'International Tables Vol C Tables 4.2.6.8 and 6.1.1.4'
 'N'  'N'   0.0061   0.0033
 'International Tables Vol C Tables 4.2.6.8 and 6.1.1.4'
 'O'  'O'   0.0106   0.0060
 'International Tables Vol C Tables 4.2.6.8 and 6.1.1.4'

_symmetry_cell_setting            Triclinic
_symmetry_space_group_name_H-M    P-1

loop_
 _symmetry_equiv_pos_as_xyz
 'x, y, z'
 '-x, -y, -z'

_cell_length_a                    9.3650(11)
_cell_length_b                    12.6982(14)
_cell_length_c                    12.7582(14)
_cell_angle_alpha                 75.762(2)
_cell_angle_beta                  75.679(2)
_cell_angle_gamma                 82.023(2)
_cell_volume                      1420.0(3)
```

```
_cell_formula_units_Z            3
_cell_measurement_temperature    273(2)
_cell_measurement_reflns_used    ?
_cell_measurement_theta_min      ?
_cell_measurement_theta_max      ?

_exptl_crystal_description       ?
_exptl_crystal_colour            ?
_exptl_crystal_size_max          .6
_exptl_crystal_size_mid          .4
_exptl_crystal_size_min          .25
_exptl_crystal_density_meas      ?
_exptl_crystal_density_diffrn    1.229
_exptl_crystal_density_method    'not measured'
_exptl_crystal_F_000             570
_exptl_absorpt_coefficient_mu    0.096
_exptl_absorpt_correction_type   none
_exptl_absorpt_correction_T_min  ?
_exptl_absorpt_correction_T_max  ?
_exptl_absorpt_process_details   ?

_exptl_special_details
;
 ?
;

_diffrn_ambient_temperature      273(2)
_diffrn_radiation_wavelength     0.71073
_diffrn_radiation_type           MoK\a
_diffrn_radiation_source         'fine-focus sealed tube'
_diffrn_radiation_monochromator  graphite
_diffrn_measurement_device_type  'CCD area detector'
_diffrn_measurement_method       'phi and omega scans'
_diffrn_detector_area_resol_mean ?
_diffrn_standards_number         ?
_diffrn_standards_interval_count ?
_diffrn_standards_interval_time  ?
_diffrn_standards_decay_%        ?
_diffrn_reflns_number            8840
_diffrn_reflns_av_R_equivalents  0.0283
_diffrn_reflns_av_sigmaI/netI    0.0807
_diffrn_reflns_limit_h_min       -12
_diffrn_reflns_limit_h_max       7
_diffrn_reflns_limit_k_min       -16
_diffrn_reflns_limit_k_max       12
_diffrn_reflns_limit_l_min       -17
```

```
_diffrn_reflns_limit_l_max       16
_diffrn_reflns_theta_min         1.66
_diffrn_reflns_theta_max         28.33
_reflns_number_total             6098
_reflns_number_gt                2453
_reflns_threshold_expression     >2sigma(I)

_computing_data_collection       'Bruker SMART'
_computing_cell_refinement       'Bruker SMART'
_computing_data_reduction        'Bruker SAINT'
_computing_structure_solution    'SHELXS-97 (Sheldrick, 1990)'
_computing_structure_refinement  'SHELXL-97 (Sheldrick, 1997)'
_computing_molecular_graphics    'Bruker SHELXTL'
_computing_publication_material  'Bruker SHELXTL'

_refine_special_details
;
Refinement of F^2^ against ALL reflections.  The weighted R-factor wR and
goodness of fit S are based on F^2^, conventional R-factors R are based
on F, with F set to zero for negative F^2^. The threshold expression of
F^2^ > 2sigma(F^2^) is used only for calculating R-factors(gt) etc. and is
not relevant to the choice of reflections for refinement.  R-factors based
on F^2^ are statistically about twice as large as those based on F, and R-
factors based on ALL data will be even larger.
;

_refine_ls_structure_factor_coef  Fsqd
_refine_ls_matrix_type           full
_refine_ls_weighting_scheme      calc
_refine_ls_weighting_details
'calc w=1/[\s^2^(Fo^2^)+(0.1494P)^2^+0.0000P] where P=(Fo^2^+2Fc^2^)/3'
_atom_sites_solution_primary     direct
_atom_sites_solution_secondary   difmap
_atom_sites_solution_hydrogens   geom
_refine_ls_hydrogen_treatment    mixed
_refine_ls_extinction_method     SHELXL
_refine_ls_extinction_coef       0.003(3)
_refine_ls_extinction_expression
'Fc^*^=kFc[1+0.001xFc^2^\l^3^/sin(2\q)]^-1/4^'
_refine_ls_number_reflns         6098
_refine_ls_number_parameters     332
_refine_ls_number_restraints     0
_refine_ls_R_factor_all          0.1538
_refine_ls_R_factor_gt           0.0785
_refine_ls_wR_factor_ref         0.2612
_refine_ls_wR_factor_gt          0.2144
```

```
_refine_ls_goodness_of_fit_ref    0.885
_refine_ls_restrained_S_all       0.885
_refine_ls_shift/su_max           0.000
_refine_ls_shift/su_mean          0.000

loop_
 _atom_site_label
 _atom_site_type_symbol
 _atom_site_fract_x
 _atom_site_fract_y
 _atom_site_fract_z
 _atom_site_U_iso_or_equiv
 _atom_site_adp_type
 _atom_site_occupancy
 _atom_site_symmetry_multiplicity
 _atom_site_calc_flag
 _atom_site_refinement_flags
 _atom_site_disorder_assembly
 _atom_site_disorder_group
O6 O 0.4346(3) 0.91304(19) 0.9459(2) 0.0662(7) Uani 1 1 d . . .
N2 N 0.3092(3) 0.8985(2) 0.8221(2) 0.0524(7) Uani 1 1 d . . .
H2 H 0.2691 0.9317 0.7678 0.063 Uiso 1 1 calc R . .
N3 N 0.4844(3) 1.1189(2) 0.8443(2) 0.0582(8) Uani 1 1 d . . .
H3 H 0.5059 1.0845 0.9062 0.070 Uiso 1 1 calc R . .
O7 O 0.3585(3) 1.1092(2) 0.7159(2) 0.0701(8) Uani 1 1 d . . .
O8 O 0.7733(3) 1.1412(2) 0.7357(2) 0.0673(7) Uani 1 1 d . . .
O9 O 0.7538(3) 1.3141(2) 0.7489(2) 0.0727(8) Uani 1 1 d . . .
O4 O 0.4334(3) 0.6170(2) 0.8982(2) 0.0772(8) Uani 1 1 d . . .
C7 C 0.4075(4) 1.0692(3) 0.7991(3) 0.0508(8) Uani 1 1 d . . .
C6 C 0.3838(4) 0.9523(3) 0.8627(3) 0.0491(8) Uani 1 1 d . . .
O5 O 0.5326(3) 0.7470(2) 0.7571(2) 0.0744(8) Uani 1 1 d . . .
C9 C 0.7007(4) 1.2264(3) 0.7576(3) 0.0544(9) Uani 1 1 d . . .
C4 C 0.4337(4) 0.7119(3) 0.8365(3) 0.0554(9) Uani 1 1 d . . .
C5 C 0.2937(4) 0.7839(3) 0.8678(3) 0.0559(9) Uani 1 1 d . . .
H5A H 0.2151 0.7623 0.8422 0.067 Uiso 1 1 calc R . .
H5B H 0.2647 0.7719 0.9480 0.067 Uiso 1 1 calc R . .
C8 C 0.5344(4) 1.2260(3) 0.7974(3) 0.0637(10) Uani 1 1 d . . .
H8A H 0.5014 1.2699 0.8526 0.076 Uiso 1 1 calc R . .
H8B H 0.4888 1.2598 0.7354 0.076 Uiso 1 1 calc R . .
O1 O 0.3529(3) 1.0313(2) 0.4332(2) 0.0719(8) Uani 1 1 d . . .
N1 N 0.4069(3) 0.8789(2) 0.5554(2) 0.0531(7) Uani 1 1 d . . .
H1 H 0.4659 0.8453 0.5971 0.064 Uiso 1 1 calc R . .
O3 O 0.1292(3) 0.9397(2) 0.6693(2) 0.0637(7) Uani 1 1 d . . .
O2 O 0.0205(3) 0.8410(2) 0.5950(2) 0.0802(9) Uani 1 1 d . . .
C3 C 0.4318(4) 0.9772(3) 0.4946(3) 0.0532(9) Uani 1 1 d . . .
C1 C 0.1328(4) 0.8744(3) 0.6097(3) 0.0538(9) Uani 1 1 d . . .
```

C2 C 0.2806(4) 0.8276(3) 0.5522(3) 0.0606(10) Uani 1 1 d . . .
H2A H 0.2930 0.7507 0.5862 0.073 Uiso 1 1 calc R . .
H2B H 0.2789 0.8335 0.4753 0.073 Uiso 1 1 calc R . .
N6 N 0.2275(3) 0.0868(2) 0.2538(2) 0.0631(9) Uani 1 1 d . . .
H6A H 0.1439 0.0924 0.3044 0.095 Uiso 1 1 calc R . .
H6B H 0.3016 0.1054 0.2760 0.095 Uiso 1 1 calc R . .
H6C H 0.2464 0.0183 0.2455 0.095 Uiso 1 1 calc R . .
N5 N 0.0552(3) 0.1674(2) 0.6011(2) 0.0645(8) Uani 1 1 d . . .
H5C H 0.0411 0.1578 0.5378 0.097 Uiso 1 1 calc R . .
H5D H -0.0294 0.1617 0.6520 0.097 Uiso 1 1 calc R . .
H5E H 0.1232 0.1169 0.6245 0.097 Uiso 1 1 calc R . .
C13 C 0.2124(4) 0.1595(3) 0.1478(3) 0.0652(10) Uani 1 1 d . . .
H13A H 0.3100 0.1762 0.1034 0.078 Uiso 1 1 calc R . .
H13B H 0.1584 0.2274 0.1619 0.078 Uiso 1 1 calc R . .
C14 C 0.1345(4) 0.1127(3) 0.0834(3) 0.0588(9) Uani 1 1 d . . .
H14A H 0.0422 0.0873 0.1309 0.071 Uiso 1 1 calc R . .
H14B H 0.1949 0.0503 0.0606 0.071 Uiso 1 1 calc R . .
C11 C 0.1058(6) 0.2762(4) 0.5832(5) 0.1025(16) Uani 1 1 d . . .
H11A H 0.0256 0.3299 0.5664 0.123 Uiso 1 1 calc R . .
H11B H 0.1246 0.2838 0.6523 0.123 Uiso 1 1 calc R . .
C15 C 0.1023(4) 0.1938(3) -0.0180(3) 0.0684(11) Uani 1 1 d . . .
H15A H 0.0427 0.2564 0.0053 0.082 Uiso 1 1 calc R . .
H15B H 0.1949 0.2191 -0.0651 0.082 Uiso 1 1 calc R . .
C16 C 0.0230(5) 0.1496(4) -0.0851(3) 0.0817(13) Uani 1 1 d . . .
H16A H 0.0840 0.0908 -0.1130 0.123 Uiso 1 1 calc R . .
H16B H 0.0028 0.2065 -0.1462 0.123 Uiso 1 1 calc R . .
H16C H -0.0683 0.1234 -0.0391 0.123 Uiso 1 1 calc R . .
C17 C 0.2307(7) 0.3016(5) 0.5005(5) 0.1141(18) Uani 1 1 d . . .
H17A H 0.2191 0.2871 0.4320 0.137 Uiso 1 1 calc R . .
H17B H 0.3163 0.2568 0.5212 0.137 Uiso 1 1 calc R . .
C18 C 0.2553(11) 0.4323(8) 0.4821(7) 0.186(5) Uani 1 1 d . . .
H18A H 0.1876 0.4784 0.4402 0.224 Uiso 1 1 calc R . .
H18B H 0.2414 0.4527 0.5526 0.224 Uiso 1 1 calc R . .
N4 N 0.6717(3) 0.4673(2) 0.8777(3) 0.0667(9) Uani 1 1 d . . .
H4A H 0.6890 0.4212 0.8328 0.100 Uiso 1 1 calc R . .
H4B H 0.5904 0.5108 0.8687 0.100 Uiso 1 1 calc R . .
H4C H 0.6591 0.4300 0.9478 0.100 Uiso 1 1 calc R . .
C21 C 0.7973(6) 0.5331(5) 0.8514(5) 0.1147(19) Uani 1 1 d . . .
H21A H 0.7879 0.5904 0.7867 0.138 Uiso 1 1 calc R . .
H21B H 0.7877 0.5683 0.9125 0.138 Uiso 1 1 calc R . .
C24 C 1.0672(6) 0.5519(5) 0.7991(6) 0.126(2) Uani 1 1 d . . .
H24A H 1.0681 0.5998 0.7269 0.151 Uiso 1 1 calc R . .
H24B H 1.0568 0.5971 0.8522 0.151 Uiso 1 1 calc R . .
C23 C 1.2059(8) 0.4850(6) 0.7952(6) 0.139(2) Uani 1 1 d . . .
H23A H 1.2052 0.4373 0.8665 0.209 Uiso 1 1 calc R . .
H23B H 1.2859 0.5309 0.7761 0.209 Uiso 1 1 calc R . .

H23C H 1.2185 0.4424 0.7404 0.209 Uiso 1 1 calc R . .
C19 C 0.3946(12) 0.4397(8) 0.4253(10) 0.216(5) Uani 1 1 d . . .
H19A H 0.4587 0.3893 0.4658 0.324 Uiso 1 1 calc R . .
H19B H 0.4212 0.5126 0.4146 0.324 Uiso 1 1 calc R . .
H19C H 0.4045 0.4227 0.3545 0.324 Uiso 1 1 calc R . .
C22 C 0.9362(7) 0.4842(6) 0.8314(6) 0.143(3) Uani 1 1 d . . .
H22A H 0.9439 0.4459 0.7729 0.172 Uiso 1 1 calc R . .
H22B H 0.9468 0.4292 0.8976 0.172 Uiso 1 1 calc R . .

loop_
 _atom_site_aniso_label
 _atom_site_aniso_U_11
 _atom_site_aniso_U_22
 _atom_site_aniso_U_33
 _atom_site_aniso_U_23
 _atom_site_aniso_U_13
 _atom_site_aniso_U_12
O6 0.0797(19) 0.0550(15) 0.0689(17) -0.0059(13) -0.0310(14) -0.0098(13)
N2 0.0574(18) 0.0467(16) 0.0546(17) -0.0099(13) -0.0177(14) -0.0013(13)
N3 0.068(2) 0.0465(17) 0.0600(18) -0.0034(14) -0.0166(15) -0.0153(14)
O7 0.090(2) 0.0595(16) 0.0624(16) -0.0059(13) -0.0253(15) -0.0098(13)
O8 0.0689(18) 0.0536(15) 0.0780(18) -0.0250(13) -0.0071(13) 0.0021(12)
O9 0.0716(18) 0.0524(16) 0.093(2) -0.0247(14) -0.0022(14) -0.0165(13)
O4 0.094(2) 0.0519(16) 0.0698(17) -0.0029(14) -0.0068(15) 0.0092(13)
C7 0.053(2) 0.0437(19) 0.052(2) -0.0094(16) -0.0069(17) -0.0004(16)
C6 0.045(2) 0.0451(19) 0.056(2) -0.0131(17) -0.0094(16) -0.0010(15)
O5 0.0666(18) 0.0745(18) 0.0641(17) -0.0054(14) 0.0023(14) 0.0065(14)
C9 0.066(2) 0.047(2) 0.051(2) -0.0122(17) -0.0131(17) -0.0069(18)
C4 0.062(2) 0.049(2) 0.056(2) -0.0134(18) -0.0148(19) -0.0015(17)
C5 0.058(2) 0.045(2) 0.064(2) -0.0096(17) -0.0145(17) -0.0040(16)
C8 0.059(2) 0.046(2) 0.084(3) -0.0112(19) -0.013(2) -0.0071(17)
O1 0.0602(17) 0.0871(18) 0.0706(17) 0.0035(14) -0.0341(14) -0.0150(14)
N1 0.0428(16) 0.0610(19) 0.0550(17) -0.0065(15) -0.0147(13) -0.0075(13)
O3 0.0566(16) 0.0679(16) 0.0692(16) -0.0206(14) -0.0154(12) -0.0015(12)
O2 0.0547(17) 0.114(2) 0.0814(19) -0.0235(17) -0.0193(14) -0.0282(15)
C3 0.045(2) 0.069(2) 0.0453(19) -0.0055(18) -0.0143(16) -0.0073(17)
C1 0.050(2) 0.057(2) 0.053(2) -0.0015(18) -0.0179(17) -0.0070(17)
C2 0.058(2) 0.062(2) 0.064(2) -0.0173(19) -0.0118(18) -0.0111(18)
N6 0.069(2) 0.0670(19) 0.0588(19) -0.0217(16) -0.0275(15) 0.0156(15)
N5 0.073(2) 0.0558(18) 0.0606(19) -0.0072(15) -0.0112(16) -0.0080(15)
C13 0.064(2) 0.052(2) 0.081(3) -0.013(2) -0.023(2) -0.0023(18)
C14 0.061(2) 0.062(2) 0.057(2) -0.0148(18) -0.0155(18) -0.0046(18)
C11 0.093(4) 0.110(4) 0.112(4) -0.037(3) -0.007(3) -0.040(3)
C15 0.063(3) 0.069(3) 0.066(2) -0.005(2) -0.015(2) 0.0015(19)
C16 0.076(3) 0.107(3) 0.063(3) -0.026(2) -0.020(2) 0.010(2)
C17 0.116(5) 0.120(4) 0.095(4) -0.009(3) -0.008(3) -0.028(4)

C18 0.202(9) 0.239(10) 0.120(6) -0.005(6) -0.001(6) -0.153(9)
N4 0.063(2) 0.0563(18) 0.076(2) -0.0190(16) -0.0014(16) -0.0061(15)
C21 0.097(4) 0.109(4) 0.156(5) -0.075(4) -0.006(4) -0.027(3)
C24 0.087(4) 0.124(5) 0.192(7) -0.071(5) -0.034(4) -0.019(4)
C23 0.115(5) 0.150(6) 0.166(6) -0.052(5) -0.025(4) -0.039(4)
C19 0.270(14) 0.171(8) 0.264(13) -0.090(9) -0.138(11) 0.008(9)
C22 0.093(5) 0.159(6) 0.217(8) -0.123(6) -0.020(4) -0.021(4)

_geom_special_details
;
All esds (except the esd in the dihedral angle between two l.s. planes)
are estimated using the full covariance matrix. The cell esds are taken
into account individually in the estimation of esds in distances, angles
and torsion angles; correlations between esds in cell parameters are only
used when they are defined by crystal symmetry. An approximate (isotropic)
treatment of cell esds is used for estimating esds involving l.s. planes.
;

loop_
_geom_bond_atom_site_label_1
_geom_bond_atom_site_label_2
_geom_bond_distance
_geom_bond_site_symmetry_2
_geom_bond_publ_flag
O6 C6 1.235(4) . ?
N2 C6 1.308(4) . ?
N2 C5 1.442(4) . ?
N3 C7 1.327(4) . ?
N3 C8 1.437(4) . ?
O7 C7 1.227(4) . ?
O8 C9 1.249(4) . ?
O9 C9 1.252(4) . ?
O4 C4 1.267(4) . ?
C7 C6 1.523(5) . ?
O5 C4 1.230(4) . ?
C9 C8 1.514(5) . ?
C4 C5 1.517(5) . ?
O1 C3 1.230(4) . ?
N1 C3 1.314(4) . ?
N1 C2 1.441(4) . ?
O3 C1 1.247(4) . ?
O2 C1 1.258(4) . ?
C3 C3 1.523(7) 2_676 ?
C1 C2 1.513(5) . ?
N6 C13 1.466(4) . ?
N5 C11 1.469(5) . ?

C13 C14 1.489(5) . ?
C14 C15 1.509(5) . ?
C11 C17 1.382(7) . ?
C15 C16 1.506(5) . ?
C17 C18 1.658(10) . ?
C18 C19 1.330(12) . ?
N4 C21 1.461(6) . ?
C21 C22 1.354(7) . ?
C24 C23 1.447(8) . ?
C24 C22 1.511(7) . ?

loop_
 _geom_angle_atom_site_label_1
 _geom_angle_atom_site_label_2
 _geom_angle_atom_site_label_3
 _geom_angle
 _geom_angle_site_symmetry_1
 _geom_angle_site_symmetry_3
 _geom_angle_publ_flag
C6 N2 C5 120.4(3) . . ?
C7 N3 C8 124.7(3) . . ?
O7 C7 N3 126.1(3) . . ?
O7 C7 C6 121.6(3) . . ?
N3 C7 C6 112.3(3) . . ?
O6 C6 N2 123.8(3) . . ?
O6 C6 C7 120.9(3) . . ?
N2 C6 C7 115.4(3) . . ?
O8 C9 O9 125.4(4) . . ?
O8 C9 C8 118.5(3) . . ?
O9 C9 C8 116.1(3) . . ?
O5 C4 O4 126.4(3) . . ?
O5 C4 C5 120.2(3) . . ?
O4 C4 C5 113.3(3) . . ?
N2 C5 C4 113.6(3) . . ?
N3 C8 C9 113.7(3) . . ?
C3 N1 C2 120.0(3) . . ?
O1 C3 N1 124.3(3) . . ?
O1 C3 C3 120.6(4) . 2_676 ?
N1 C3 C3 115.1(4) . 2_676 ?
O3 C1 O2 124.7(3) . . ?
O3 C1 C2 119.5(3) . . ?
O2 C1 C2 115.8(3) . . ?
N1 C2 C1 115.1(3) . . ?
N6 C13 C14 113.5(3) . . ?
C13 C14 C15 112.7(3) . . ?
C17 C11 N5 116.9(5) . . ?

C16 C15 C14 114.3(3) . . ?
C11 C17 C18 109.2(5) . . ?
C19 C18 C17 103.5(10) . . ?
C22 C21 N4 119.1(5) . . ?
C23 C24 C22 112.0(6) . . ?
C21 C22 C24 119.7(6) . . ?

_diffrn_measured_fraction_theta_max 0.860
_diffrn_reflns_theta_full 28.33
_diffrn_measured_fraction_theta_full 0.860
_refine_diff_density_max 0.600
_refine_diff_density_min -0.340
_refine_diff_density_rms 0.059

(pentylNH$_3$)$_2$OG·H$_2$OG

```
data_jat

_audit_creation_method           SHELXL-97
_chemical_name_systematic
;
 ?
;
_chemical_name_common            ?
_chemical_melting_point          ?
_chemical_formula_moiety         ?
_chemical_formula_sum
 'C11 H21 N3 O6'
_chemical_formula_weight         291.31

loop_
 _atom_type_symbol
 _atom_type_description
 _atom_type_scat_dispersion_real
 _atom_type_scat_dispersion_imag
 _atom_type_scat_source
 'C'  'C'   0.0033   0.0016
 'International Tables Vol C Tables 4.2.6.8 and 6.1.1.4'
 'H'  'H'   0.0000   0.0000
 'International Tables Vol C Tables 4.2.6.8 and 6.1.1.4'
 'N'  'N'   0.0061   0.0033
 'International Tables Vol C Tables 4.2.6.8 and 6.1.1.4'
 'O'  'O'   0.0106   0.0060
 'International Tables Vol C Tables 4.2.6.8 and 6.1.1.4'

_symmetry_cell_setting           Triclinic
_symmetry_space_group_name_H-M    P-1

loop_
 _symmetry_equiv_pos_as_xyz
 'x, y, z'
 '-x, -y, -z'

_cell_length_a                   5.0096(10)
_cell_length_b                   11.818(2)
_cell_length_c                   14.202(3)
_cell_angle_alpha                 74.787(4)
_cell_angle_beta                 81.591(4)
_cell_angle_gamma                    77.922(4)
_cell_volume                     789.6(3)
```

```
_cell_formula_units_Z            2
_cell_measurement_temperature    273(2)
_cell_measurement_reflns_used    ?
_cell_measurement_theta_min      ?
_cell_measurement_theta_max      ?

_exptl_crystal_description       ?
_exptl_crystal_colour            ?
_exptl_crystal_size_max          .4
_exptl_crystal_size_mid          .35
_exptl_crystal_size_min          .2
_exptl_crystal_density_meas      ?
_exptl_crystal_density_diffrn    1.225
_exptl_crystal_density_method    'not measured'
_exptl_crystal_F_000             312
_exptl_absorpt_coefficient_mu    0.100
_exptl_absorpt_correction_type   none
_exptl_absorpt_correction_T_min  ?
_exptl_absorpt_correction_T_max  ?
_exptl_absorpt_process_details   ?

_exptl_special_details
;
 ?
;

_diffrn_ambient_temperature      273(2)
_diffrn_radiation_wavelength     0.71073
_diffrn_radiation_type           MoK\a
_diffrn_radiation_source         'fine-focus sealed tube'
_diffrn_radiation_monochromator  graphite
_diffrn_measurement_device_type  'CCD area detector'
_diffrn_measurement_method       'phi and omega scans'
_diffrn_detector_area_resol_mean ?
_diffrn_standards_number         ?
_diffrn_standards_interval_count ?
_diffrn_standards_interval_time  ?
_diffrn_standards_decay_%        ?
_diffrn_reflns_number            4705
_diffrn_reflns_av_R_equivalents  0.0296
_diffrn_reflns_av_sigmaI/netI    0.0479
_diffrn_reflns_limit_h_min       -5
_diffrn_reflns_limit_h_max       6
_diffrn_reflns_limit_k_min       -15
_diffrn_reflns_limit_k_max       13
_diffrn_reflns_limit_l_min       -18
```

```
_diffrn_reflns_limit_l_max       18
_diffrn_reflns_theta_min         1.49
_diffrn_reflns_theta_max         28.05
_reflns_number_total             3558
_reflns_number_gt                1694
_reflns_threshold_expression     >2sigma(I)

_computing_data_collection       'Bruker SMART'
_computing_cell_refinement       'Bruker SMART'
_computing_data_reduction        'Bruker SAINT'
_computing_structure_solution    'SHELXS-97 (Sheldrick, 1990)'
_computing_structure_refinement  'SHELXL-97 (Sheldrick, 1997)'
_computing_molecular_graphics    'Bruker SHELXTL'
_computing_publication_material  'Bruker SHELXTL'

_refine_special_details
;
Refinement of F^2^ against ALL reflections.  The weighted R-factor wR and
goodness of fit S are based on F^2^, conventional R-factors R are based
on F, with F set to zero for negative F^2^. The threshold expression of
F^2^ > 2sigma(F^2^) is used only for calculating R-factors(gt) etc. and is
not relevant to the choice of reflections for refinement.  R-factors based
on F^2^ are statistically about twice as large as those based on F, and R-
factors based on ALL data will be even larger.
;

_refine_ls_structure_factor_coef  Fsqd
_refine_ls_matrix_type           full
_refine_ls_weighting_scheme      calc
_refine_ls_weighting_details
'calc w=1/[\s^2^(Fo^2^)+(0.1701P)^2^+0.0000P] where P=(Fo^2^+2Fc^2^)/3'
_atom_sites_solution_primary     direct
_atom_sites_solution_secondary   difmap
_atom_sites_solution_hydrogens   geom
_refine_ls_hydrogen_treatment    mixed
_refine_ls_extinction_method     SHELXL
_refine_ls_extinction_coef       0.030(11)
_refine_ls_extinction_expression
'Fc^*^=kFc[1+0.001xFc^2^\l^3^/sin(2\q)]^-1/4^'
_refine_ls_number_reflns         3558
_refine_ls_number_parameters     188
_refine_ls_number_restraints     0
_refine_ls_R_factor_all          0.1204
_refine_ls_R_factor_gt           0.0687
_refine_ls_wR_factor_ref         0.1976
_refine_ls_wR_factor_gt          0.1712
```

```
_refine_ls_goodness_of_fit_ref    0.934
_refine_ls_restrained_S_all       0.934
_refine_ls_shift/su_max           0.000
_refine_ls_shift/su_mean          0.000

loop_
 _atom_site_label
 _atom_site_type_symbol
 _atom_site_fract_x
 _atom_site_fract_y
 _atom_site_fract_z
 _atom_site_U_iso_or_equiv
 _atom_site_adp_type
 _atom_site_occupancy
 _atom_site_symmetry_multiplicity
 _atom_site_calc_flag
 _atom_site_refinement_flags
 _atom_site_disorder_assembly
 _atom_site_disorder_group
O1 O 0.1801(3) 0.06813(18) 0.04847(16) 0.0673(6) Uani 1 1 d . . .
N1 N 0.6070(4) 0.08182(19) 0.07259(16) 0.0524(6) Uani 1 1 d . . .
H1 H 0.7806 0.0586 0.0614 0.063 Uiso 1 1 calc R . .
O2 O 0.4379(4) 0.32389(19) -0.00917(16) 0.0728(7) Uani 1 1 d . . .
O3 O 0.1687(5) 0.34192(19) 0.12561(18) 0.0875(8) Uani 1 1 d . . .
C1 C 0.4324(5) 0.0414(2) 0.03347(18) 0.0466(6) Uani 1 1 d . . .
C2 C 0.5060(6) 0.1651(2) 0.1344(2) 0.0570(7) Uani 1 1 d . . .
H2A H 0.6586 0.1769 0.1634 0.068 Uiso 1 1 calc R . .
H2B H 0.3785 0.1312 0.1872 0.068 Uiso 1 1 calc R . .
C3 C 0.3623(5) 0.2859(2) 0.0777(2) 0.0565(7) Uani 1 1 d . . .
O6 O 0.1134(4) 0.74061(19) 0.71711(17) 0.0721(7) Uani 1 1 d . . .
O4 O 0.1789(4) 0.5786(2) 0.53722(18) 0.0800(7) Uani 1 1 d . . .
N2 N 0.6023(4) 0.6024(2) 0.55471(17) 0.0607(7) Uani 1 1 d . . .
H2 H 0.7765 0.5804 0.5440 0.073 Uiso 1 1 calc R . .
C6 C 0.3185(6) 0.6573(3) 0.6981(2) 0.0619(8) Uani 1 1 d . . .
C5 C 0.4957(6) 0.6971(3) 0.6050(2) 0.0654(8) Uani 1 1 d . . .
H5A H 0.3892 0.7629 0.5616 0.078 Uiso 1 1 calc R . .
H5B H 0.6480 0.7258 0.6204 0.078 Uiso 1 1 calc R . .
C4 C 0.4308(5) 0.5498(3) 0.5252(2) 0.0578(7) Uani 1 1 d . . .
O5 O 0.3629(6) 0.5587(3) 0.7511(2) 0.1082(10) Uani 1 1 d . . .
N3 N 1.0690(5) 0.5930(2) 0.10749(19) 0.0704(7) Uani 1 1 d . . .
H3A H 0.9080 0.6176 0.0826 0.106 Uiso 1 1 calc R . .
H3B H 1.1145 0.5142 0.1174 0.106 Uiso 1 1 calc R . .
H3C H 1.1967 0.6270 0.0658 0.106 Uiso 1 1 calc R . .
C8 C 0.9983(14) 0.7466(4) 0.1985(4) 0.1385(19) Uani 1 1 d . . .
H8A H 0.8260 0.7814 0.1702 0.166 Uiso 1 1 calc R . .
H8B H 1.1405 0.7822 0.1537 0.166 Uiso 1 1 calc R . .
```

C7 C 1.0494(10) 0.6265(4) 0.2007(3) 0.1050(13) Uani 1 1 d . . .
H7A H 0.9049 0.5908 0.2440 0.126 Uiso 1 1 calc R . .
H7B H 1.2199 0.5910 0.2300 0.126 Uiso 1 1 calc R . .
C9 C 0.9827(15) 0.7841(6) 0.2939(4) 0.147(2) Uani 1 1 d . . .
H9A H 0.8306 0.7523 0.3353 0.176 Uiso 1 1 calc R . .
H9B H 1.1472 0.7405 0.3243 0.176 Uiso 1 1 calc R . .
C11 C 0.936(2) 0.9287(5) 0.3931(4) 0.205(4) Uani 1 1 d . . .
H11A H 0.9125 0.8623 0.4476 0.307 Uiso 1 1 calc R . .
H11B H 0.7806 0.9918 0.3949 0.307 Uiso 1 1 calc R . .
H11C H 1.0997 0.9566 0.3969 0.307 Uiso 1 1 calc R . .
C10 C 0.957(3) 0.8918(7) 0.3027(5) 0.237(5) Uani 1 1 d . . .
H10A H 0.7955 0.9358 0.2706 0.285 Uiso 1 1 calc R . .
H10B H 1.1121 0.9227 0.2626 0.285 Uiso 1 1 calc R . .
H3 H 0.005(9) 0.705(4) 0.787(3) 0.121(14) Uiso 1 1 d . . .

loop_
 _atom_site_aniso_label
 _atom_site_aniso_U_11
 _atom_site_aniso_U_22
 _atom_site_aniso_U_33
 _atom_site_aniso_U_23
 _atom_site_aniso_U_13
 _atom_site_aniso_U_12
O1 0.0281(10) 0.0923(15) 0.0971(15) -0.0582(12) 0.0043(9) -0.0071(9)
N1 0.0287(11) 0.0664(14) 0.0719(14) -0.0402(11) -0.0022(9) -0.0020(9)
O2 0.0632(14) 0.0789(14) 0.0720(14) -0.0205(11) 0.0125(11) -0.0131(11)
O3 0.0836(16) 0.0628(13) 0.1060(18) -0.0362(12) 0.0367(13) -0.0019(11)
C1 0.0301(12) 0.0548(15) 0.0597(15) -0.0270(12) 0.0003(10) -0.0048(11)
C2 0.0447(15) 0.0708(18) 0.0648(16) -0.0377(14) -0.0038(12) -0.0048(13)
C3 0.0431(15) 0.0596(17) 0.0737(19) -0.0327(14) 0.0107(13) -0.0142(13)
O6 0.0603(13) 0.0703(13) 0.0843(15) -0.0357(11) 0.0113(11) 0.0007(11)
O4 0.0294(11) 0.1113(18) 0.1200(18) -0.0722(15) 0.0047(10) -0.0100(11)
N2 0.0325(11) 0.0881(17) 0.0747(15) -0.0462(13) 0.0061(10) -0.0137(11)
C6 0.0532(18) 0.070(2) 0.0708(19) -0.0373(16) -0.0015(14) -0.0067(15)
C5 0.0446(16) 0.080(2) 0.082(2) -0.0398(16) 0.0032(14) -0.0153(14)
C4 0.0304(13) 0.082(2) 0.0678(17) -0.0346(15) 0.0043(11) -0.0102(13)
O5 0.104(2) 0.0924(19) 0.0956(18) -0.0141(15) 0.0240(15) 0.0204(15)
N3 0.0636(16) 0.0630(15) 0.0804(17) -0.0190(13) 0.0045(13) -0.0080(12)
C8 0.189(6) 0.098(4) 0.124(4) -0.039(3) 0.031(4) -0.034(4)
C7 0.102(3) 0.111(3) 0.100(3) -0.032(2) 0.008(2) -0.020(3)
C9 0.217(6) 0.138(5) 0.100(3) -0.055(3) 0.004(4) -0.045(4)
C11 0.388(12) 0.129(5) 0.116(4) -0.049(4) -0.034(6) -0.056(6)
C10 0.453(16) 0.148(6) 0.124(5) -0.064(4) -0.008(7) -0.055(8)

_geom_special_details
;

```
 All esds (except the esd in the dihedral angle between two l.s. planes)
 are estimated using the full covariance matrix.  The cell esds are taken
 into account individually in the estimation of esds in distances, angles
 and torsion angles; correlations between esds in cell parameters are only
 used when they are defined by crystal symmetry.  An approximate (isotropic)
 treatment of cell esds is used for estimating esds involving l.s. planes.
;

loop_
 _geom_bond_atom_site_label_1
 _geom_bond_atom_site_label_2
 _geom_bond_distance
 _geom_bond_site_symmetry_2
 _geom_bond_publ_flag
O1 C1 1.238(3) . ?
N1 C1 1.326(3) . ?
N1 C2 1.453(3) . ?
O2 C3 1.229(3) . ?
O3 C3 1.271(3) . ?
C1 C1 1.531(4) 2_655 ?
C2 C3 1.530(4) . ?
O6 C6 1.317(3) . ?
O4 C4 1.235(3) . ?
N2 C4 1.330(3) . ?
N2 C5 1.451(3) . ?
C6 O5 1.205(4) . ?
C6 C5 1.504(4) . ?
C4 C4 1.527(5) 2_666 ?
N3 C7 1.462(5) . ?
C8 C7 1.381(6) . ?
C8 C9 1.520(7) . ?
C9 C10 1.289(8) . ?
C11 C10 1.444(8) . ?

loop_
 _geom_angle_atom_site_label_1
 _geom_angle_atom_site_label_2
 _geom_angle_atom_site_label_3
 _geom_angle
 _geom_angle_site_symmetry_1
 _geom_angle_site_symmetry_3
 _geom_angle_publ_flag
C1 N1 C2 120.2(2) . . ?
O1 C1 N1 123.6(2) . . ?
O1 C1 C1 121.9(3) . 2_655 ?
N1 C1 C1 114.5(2) . 2_655 ?
```

N1 C2 C3 112.5(2) . . ?
O2 C3 O3 123.8(3) . . ?
O2 C3 C2 119.8(2) . . ?
O3 C3 C2 116.4(3) . . ?
C4 N2 C5 120.0(2) . . ?
O5 C6 O6 123.2(3) . . ?
O5 C6 C5 123.0(3) . . ?
O6 C6 C5 113.8(3) . . ?
N2 C5 C6 112.7(3) . . ?
O4 C4 N2 123.0(2) . . ?
O4 C4 C4 122.3(3) . 2_666 ?
N2 C4 C4 114.8(3) . 2_666 ?
C7 C8 C9 118.8(5) . . ?
C8 C7 N3 117.5(4) . . ?
C10 C9 C8 126.0(6) . . ?
C9 C10 C11 126.5(7) . . ?

_diffrn_measured_fraction_theta_max 0.925
_diffrn_reflns_theta_full 28.05
_diffrn_measured_fraction_theta_full 0.925
_refine_diff_density_max 0.337
_refine_diff_density_min -0.275
_refine_diff_density_rms 0.066

$(hexylNH_3)_2HOG$

```
data_jlk

_audit_creation_method           SHELXL-97
_chemical_name_systematic
;
 ?
;
_chemical_name_common            ?
_chemical_melting_point          ?
_chemical_formula_moiety         ?
_chemical_formula_sum
 'C12 H23 N3 O6'
_chemical_formula_weight         305.3

loop_
 _atom_type_symbol
 _atom_type_description
 _atom_type_scat_dispersion_real
 _atom_type_scat_dispersion_imag
 _atom_type_scat_source
 'C'  'C'   0.0033   0.0016
 'International Tables Vol C Tables 4.2.6.8 and 6.1.1.4'
 'H'  'H'   0.0000   0.0000
 'International Tables Vol C Tables 4.2.6.8 and 6.1.1.4'
 'N'  'N'   0.0061   0.0033
 'International Tables Vol C Tables 4.2.6.8 and 6.1.1.4'
 'O'  'O'   0.0106   0.0060
 'International Tables Vol C Tables 4.2.6.8 and 6.1.1.4'

_symmetry_cell_setting           Monoclinic
_symmetry_space_group_name_H-M    P21/n

loop_
 _symmetry_equiv_pos_as_xyz
 'x, y, z'
 '-x+1/2, y+1/2, -z+1/2'
 '-x, -y, -z'
 'x-1/2, -y-1/2, z-1/2'

_cell_length_a                   4.994(3)
_cell_length_b                   16.209(11)
_cell_length_c                   20.341(14)
_cell_angle_alpha                 90.00
_cell_angle_beta                  90.221(13)
```

```
_cell_angle_gamma                90.00
_cell_volume                     1646.7(19)
_cell_formula_units_Z            4
_cell_measurement_temperature    273(2)
_cell_measurement_reflns_used    ?
_cell_measurement_theta_min      ?
_cell_measurement_theta_max      ?

_exptl_crystal_description       ?
_exptl_crystal_colour            ?
_exptl_crystal_size_max          .6
_exptl_crystal_size_mid          .1
_exptl_crystal_size_min          .1
_exptl_crystal_density_meas      ?
_exptl_crystal_density_diffrn    1.232
_exptl_crystal_density_method    'not measured'
_exptl_crystal_F_000             656
_exptl_absorpt_coefficient_mu    0.099
_exptl_absorpt_correction_type   none
_exptl_absorpt_correction_T_min  ?
_exptl_absorpt_correction_T_max  ?
_exptl_absorpt_process_details   ?

_exptl_special_details
;
 ?
;

_diffrn_ambient_temperature      273(2)
_diffrn_radiation_wavelength     0.71073
_diffrn_radiation_type           MoK\a
_diffrn_radiation_source         'fine-focus sealed tube'
_diffrn_radiation_monochromator  graphite
_diffrn_measurement_device_type  'CCD area detector'
_diffrn_measurement_method       'phi and omega scans'
_diffrn_detector_area_resol_mean ?
_diffrn_standards_number         ?
_diffrn_standards_interval_count ?
_diffrn_standards_interval_time  ?
_diffrn_standards_decay_%        ?
_diffrn_reflns_number            10185
_diffrn_reflns_av_R_equivalents  0.1120
_diffrn_reflns_av_sigmaI/netI    0.2784
_diffrn_reflns_limit_h_min       -6
_diffrn_reflns_limit_h_max       6
_diffrn_reflns_limit_k_min       -20
```

```
_diffrn_reflns_limit_k_max       11
_diffrn_reflns_limit_l_min       -26
_diffrn_reflns_limit_l_max       26
_diffrn_reflns_theta_min         1.61
_diffrn_reflns_theta_max         28.48
_reflns_number_total             3752
_reflns_number_gt                1281
_reflns_threshold_expression     >2sigma(I)

_computing_data_collection       'Bruker SMART'
_computing_cell_refinement       'Bruker SMART'
_computing_data_reduction        'Bruker SAINT'
_computing_structure_solution    'SHELXS-97 (Sheldrick, 1990)'
_computing_structure_refinement  'SHELXL-97 (Sheldrick, 1997)'
_computing_molecular_graphics    'Bruker SHELXTL'
_computing_publication_material  'Bruker SHELXTL'

_refine_special_details
;
 Refinement of F^2^ against ALL reflections.  The weighted R-factor wR and
 goodness of fit S are based on F^2^, conventional R-factors R are based
 on F, with F set to zero for negative F^2^. The threshold expression of
 F^2^ > 2sigma(F^2^) is used only for calculating R-factors(gt) etc. and is
 not relevant to the choice of reflections for refinement.  R-factors based
 on F^2^ are statistically about twice as large as those based on F, and R-
 factors based on ALL data will be even larger.
;

_refine_ls_structure_factor_coef  Fsqd
_refine_ls_matrix_type           full
_refine_ls_weighting_scheme      calc
_refine_ls_weighting_details
 'calc w=1/[\s^2^(Fo^2^)+(0.0740P)^2^+0.0000P] where P=(Fo^2^+2Fc^2^)/3'
_atom_sites_solution_primary     direct
_atom_sites_solution_secondary   difmap
_atom_sites_solution_hydrogens   geom
_refine_ls_hydrogen_treatment    mixed
_refine_ls_extinction_method     SHELXL
_refine_ls_extinction_coef       0.0075(17)
_refine_ls_extinction_expression
 'Fc^*^=kFc[1+0.001xFc^2^\l^3^/sin(2\q)]^-1/4^'
_refine_ls_number_reflns         3752
_refine_ls_number_parameters     197
_refine_ls_number_restraints     0
_refine_ls_R_factor_all          0.3593
_refine_ls_R_factor_gt           0.0642
```

```
_refine_ls_wR_factor_ref         0.2207
_refine_ls_wR_factor_gt          0.1367
_refine_ls_goodness_of_fit_ref   0.957
_refine_ls_restrained_S_all      0.657
_refine_ls_shift/su_max          0.000
_refine_ls_shift/su_mean         0.000

loop_
 _atom_site_label
 _atom_site_type_symbol
 _atom_site_fract_x
 _atom_site_fract_y
 _atom_site_fract_z
 _atom_site_U_iso_or_equiv
 _atom_site_adp_type
 _atom_site_occupancy
 _atom_site_symmetry_multiplicity
 _atom_site_calc_flag
 _atom_site_refinement_flags
 _atom_site_disorder_assembly
 _atom_site_disorder_group
O2 O 1.0193(7) 0.7958(3) 0.17913(16) 0.0841(14) Uani 1 1 d . . .
O4 O 0.6051(9) 0.7654(3) 0.4630(2) 0.0908(15) Uani 1 1 d . . .
N2 N 0.5775(9) 0.7908(3) 0.1600(2) 0.0619(14) Uani 1 1 d . . .
H2 H 0.4190 0.7903 0.1765 0.074 Uiso 1 1 calc R . .
O1 O 0.4897(7) 0.8069(3) 0.29212(16) 0.0867(14) Uani 1 1 d . . .
C7 C 0.7208(12) 0.8026(4) 0.2722(3) 0.0651(18) Uani 1 1 d . . .
C10 C 0.7884(12) 0.7959(3) 0.1987(3) 0.0591(16) Uani 1 1 d . . .
C8 C 0.8898(11) 0.8158(4) 0.3819(2) 0.0740(19) Uani 1 1 d . . .
H8A H 0.7867 0.8656 0.3897 0.089 Uiso 1 1 calc R . .
H8B H 1.0628 0.8228 0.4029 0.089 Uiso 1 1 calc R . .
C11 C 0.6149(11) 0.7857(4) 0.0889(2) 0.0719(18) Uani 1 1 d . . .
H11A H 0.4461 0.7710 0.0685 0.086 Uiso 1 1 calc R . .
H11B H 0.7427 0.7424 0.0792 0.086 Uiso 1 1 calc R . .
O5 O 0.8586(9) 0.8593(3) 0.0093(2) 0.1055(17) Uani 1 1 d . . .
N1 N 0.9305(9) 0.8064(3) 0.3110(2) 0.0711(15) Uani 1 1 d . . .
H1 H 1.0896 0.8034 0.2950 0.085 Uiso 1 1 calc R . .
O6 O 0.6572(8) 0.9328(3) 0.0850(2) 0.0914(16) Uani 1 1 d . . .
N3 N 0.3336(9) 0.5224(3) 0.4073(2) 0.0957(18) Uani 1 1 d . . .
H3A H 0.1908 0.4923 0.4178 0.144 Uiso 1 1 calc R . .
H3B H 0.3569 0.5618 0.4373 0.144 Uiso 1 1 calc R . .
H3C H 0.4778 0.4902 0.4062 0.144 Uiso 1 1 calc R . .
C9 C 0.7500(14) 0.7452(5) 0.4134(3) 0.079(2) Uani 1 1 d . . .
O3 O 0.7650(11) 0.6761(3) 0.3928(2) 0.126(2) Uani 1 1 d . . .
C12 C 0.7143(13) 0.8662(5) 0.0597(3) 0.074(2) Uani 1 1 d . . .
C5 C 0.288(2) 0.5173(8) 0.2890(5) 0.212(6) Uani 1 1 d . . .
```

H14A H 0.1504 0.4755 0.2942 0.255 Uiso 1 1 calc R . .
H14B H 0.4581 0.4888 0.2855 0.255 Uiso 1 1 calc R . .
C6 C 0.2922(19) 0.5611(6) 0.3413(5) 0.167(4) Uani 1 1 d . . .
H13A H 0.1239 0.5909 0.3432 0.201 Uiso 1 1 calc R . .
H13B H 0.4321 0.6020 0.3357 0.201 Uiso 1 1 calc R . .
C4 C 0.236(3) 0.5628(8) 0.2230(6) 0.215(6) Uani 1 1 d . . .
H15A H 0.0778 0.5963 0.2297 0.258 Uiso 1 1 calc R . .
H15B H 0.3843 0.6009 0.2173 0.258 Uiso 1 1 calc R . .
C3 C 0.206(4) 0.5284(10) 0.1703(7) 0.318(10) Uani 1 1 d . . .
H16A H 0.0459 0.4950 0.1744 0.382 Uiso 1 1 calc R . .
H16B H 0.3546 0.4902 0.1659 0.382 Uiso 1 1 calc R . .
C2 C 0.185(5) 0.5703(12) 0.1090(6) 0.317(11) Uani 1 1 d . . .
H17A H 0.0060 0.5935 0.1081 0.381 Uiso 1 1 calc R . .
H17B H 0.3067 0.6168 0.1119 0.381 Uiso 1 1 calc R . .
C1 C 0.216(5) 0.5448(14) 0.0619(7) 0.382(13) Uani 1 1 d . . .
H18A H 0.1421 0.4902 0.0604 0.572 Uiso 1 1 calc R . .
H18B H 0.4045 0.5424 0.0529 0.572 Uiso 1 1 calc R . .
H18C H 0.1295 0.5786 0.0295 0.572 Uiso 1 1 calc R . .
H4 H 0.481(13) 0.714(4) 0.488(3) 0.13(2) Uiso 1 1 d . . .

loop_
 _atom_site_aniso_label
 _atom_site_aniso_U_11
 _atom_site_aniso_U_22
 _atom_site_aniso_U_33
 _atom_site_aniso_U_23
 _atom_site_aniso_U_13
 _atom_site_aniso_U_12
O2 0.040(3) 0.151(4) 0.061(3) -0.004(2) 0.009(2) -0.002(3)
O4 0.098(4) 0.108(4) 0.065(3) -0.005(3) 0.035(3) -0.014(3)
N2 0.045(3) 0.095(4) 0.046(3) 0.001(3) 0.003(2) -0.010(3)
O1 0.039(3) 0.159(4) 0.063(3) -0.005(3) 0.007(2) -0.006(3)
C7 0.040(4) 0.096(5) 0.059(5) 0.004(4) 0.001(3) -0.004(4)
C10 0.045(4) 0.081(5) 0.052(4) 0.008(3) 0.001(3) -0.004(4)
C8 0.063(4) 0.105(6) 0.053(4) -0.002(4) -0.003(3) -0.016(4)
C11 0.066(4) 0.102(6) 0.048(4) -0.007(4) 0.001(3) 0.000(4)
O5 0.133(4) 0.108(4) 0.075(3) 0.015(3) 0.050(3) 0.036(3)
N1 0.043(3) 0.115(4) 0.055(3) -0.001(3) 0.005(3) -0.002(3)
O6 0.100(4) 0.076(4) 0.098(4) -0.003(3) 0.020(3) 0.016(3)
N3 0.099(4) 0.104(5) 0.083(4) -0.015(3) 0.019(3) -0.017(3)
C9 0.081(5) 0.095(7) 0.062(5) 0.004(5) 0.009(4) -0.018(5)
O3 0.164(5) 0.101(5) 0.113(4) -0.004(4) 0.049(3) -0.004(4)
C12 0.079(5) 0.081(6) 0.063(5) 0.006(5) 0.000(4) 0.002(5)
C5 0.301(14) 0.232(14) 0.104(9) -0.051(9) 0.032(9) -0.091(11)
C6 0.182(9) 0.195(12) 0.125(9) 0.030(8) 0.018(8) -0.066(8)
C4 0.313(15) 0.228(15) 0.105(10) 0.048(10) 0.002(11) -0.013(11)

C3 0.55(3) 0.27(2) 0.130(13) 0.027(13) -0.064(17) -0.072(16)
C2 0.60(3) 0.263(18) 0.093(11) 0.040(13) -0.095(18) -0.028(17)
C1 0.56(3) 0.40(3) 0.185(18) 0.07(2) -0.11(3) 0.02(2)

_geom_special_details
;
All esds (except the esd in the dihedral angle between two l.s. planes)
are estimated using the full covariance matrix. The cell esds are taken
into account individually in the estimation of esds in distances, angles
and torsion angles; correlations between esds in cell parameters are only
used when they are defined by crystal symmetry. An approximate (isotropic)
treatment of cell esds is used for estimating esds involving l.s. planes.
;

loop_
_geom_bond_atom_site_label_1
_geom_bond_atom_site_label_2
_geom_bond_distance
_geom_bond_site_symmetry_2
_geom_bond_publ_flag
O2 C10 1.220(5) . ?
O4 C9 1.284(7) . ?
N2 C10 1.317(6) . ?
N2 C11 1.460(5) . ?
O1 C7 1.225(5) . ?
C7 N1 1.312(6) . ?
C7 C10 1.538(6) . ?
C8 N1 1.465(5) . ?
C8 C9 1.484(8) . ?
C11 C12 1.517(8) . ?
O5 C12 1.258(6) . ?
O6 C12 1.230(7) . ?
N3 C6 1.497(9) . ?
C9 O3 1.199(7) . ?
C5 C6 1.280(10) . ?
C5 C4 1.552(13) . ?
C4 C3 1.218(13) . ?
C3 C2 1.425(18) . ?
C2 C1 1.05(2) . ?

loop_
_geom_angle_atom_site_label_1
_geom_angle_atom_site_label_2
_geom_angle_atom_site_label_3
_geom_angle
_geom_angle_site_symmetry_1

```
 _geom_angle_site_symmetry_3
 _geom_angle_publ_flag
C10 N2 C11 119.5(4) . . ?
O1 C7 N1 123.5(5) . . ?
O1 C7 C10 122.1(5) . . ?
N1 C7 C10 114.3(5) . . ?
O2 C10 N2 124.1(5) . . ?
O2 C10 C7 121.7(5) . . ?
N2 C10 C7 114.2(5) . . ?
N1 C8 C9 114.2(5) . . ?
N2 C11 C12 112.5(5) . . ?
C7 N1 C8 119.0(5) . . ?
O3 C9 O4 123.2(7) . . ?
O3 C9 C8 122.7(7) . . ?
O4 C9 C8 114.1(7) . . ?
O6 C12 O5 123.5(7) . . ?
O6 C12 C11 121.0(6) . . ?
O5 C12 C11 115.5(7) . . ?
C6 C5 C4 117.2(13) . . ?
C5 C6 N3 121.1(11) . . ?
C3 C4 C5 124.3(14) . . ?
C4 C3 C2 124.2(17) . . ?
C1 C2 C3 127(3) . . ?

_diffrn_measured_fraction_theta_max    0.899
_diffrn_reflns_theta_full              28.48
_diffrn_measured_fraction_theta_full   0.899
_refine_diff_density_max    0.227
_refine_diff_density_min   -0.214
_refine_diff_density_rms    0.060
```

(cyclohexylNH$_3$)$_2$OG

```
data_jla

_audit_creation_method           SHELXL-97
_chemical_name_systematic
;
 ?
;
_chemical_name_common            ?
_chemical_melting_point          ?
_chemical_formula_moiety         ?
_chemical_formula_sum
 'C18 H34 N4 O6'
_chemical_formula_weight         402.49

loop_
 _atom_type_symbol
 _atom_type_description
 _atom_type_scat_dispersion_real
 _atom_type_scat_dispersion_imag
 _atom_type_scat_source
'C'  'C'   0.0033   0.0016
'International Tables Vol C Tables 4.2.6.8 and 6.1.1.4'
'H'  'H'   0.0000   0.0000
'International Tables Vol C Tables 4.2.6.8 and 6.1.1.4'
'N'  'N'   0.0061   0.0033
'International Tables Vol C Tables 4.2.6.8 and 6.1.1.4'
'O'  'O'   0.0106   0.0060
'International Tables Vol C Tables 4.2.6.8 and 6.1.1.4'

_symmetry_cell_setting           Triclinic
_symmetry_space_group_name_H-M    P-1

loop_
 _symmetry_equiv_pos_as_xyz
 'x, y, z'
 '-x, -y, -z'

_cell_length_a                   5.0552(15)
_cell_length_b                   9.651(3)
_cell_length_c                   11.101(3)
_cell_angle_alpha                 81.894(6)
_cell_angle_beta                 81.684(6)
_cell_angle_gamma                    83.687(5)
_cell_volume                     528.3(3)
```

```
_cell_formula_units_Z            1
_cell_measurement_temperature    273(2)
_cell_measurement_reflns_used    ?
_cell_measurement_theta_min      ?
_cell_measurement_theta_max      ?

_exptl_crystal_description       ?
_exptl_crystal_colour            ?
_exptl_crystal_size_max          .6
_exptl_crystal_size_mid          .3
_exptl_crystal_size_min          .2
_exptl_crystal_density_meas      ?
_exptl_crystal_density_diffrn    1.265
_exptl_crystal_density_method    'not measured'
_exptl_crystal_F_000             218
_exptl_absorpt_coefficient_mu    0.095
_exptl_absorpt_correction_type   none
_exptl_absorpt_correction_T_min  ?
_exptl_absorpt_correction_T_max  ?
_exptl_absorpt_process_details   ?

_exptl_special_details
;
 ?
;

_diffrn_ambient_temperature      273(2)
_diffrn_radiation_wavelength     0.71073
_diffrn_radiation_type           MoK\a
_diffrn_radiation_source         'fine-focus sealed tube'
_diffrn_radiation_monochromator  graphite
_diffrn_measurement_device_type  'CCD area detector'
_diffrn_measurement_method       'phi and omega scans'
_diffrn_detector_area_resol_mean  ?
_diffrn_standards_number         ?
_diffrn_standards_interval_count  ?
_diffrn_standards_interval_time  ?
_diffrn_standards_decay_%        ?
_diffrn_reflns_number            2818
_diffrn_reflns_av_R_equivalents  0.0192
_diffrn_reflns_av_sigmaI/netI    0.0306
_diffrn_reflns_limit_h_min       -6
_diffrn_reflns_limit_h_max       5
_diffrn_reflns_limit_k_min       -12
_diffrn_reflns_limit_k_max       11
_diffrn_reflns_limit_l_min       -14
```

```
_diffrn_reflns_limit_l_max       9
_diffrn_reflns_theta_min         1.87
_diffrn_reflns_theta_max         28.11
_reflns_number_total             2362
_reflns_number_gt                1641
_reflns_threshold_expression     >2sigma(I)

_computing_data_collection       'Bruker SMART'
_computing_cell_refinement       'Bruker SMART'
_computing_data_reduction        'Bruker SAINT'
_computing_structure_solution    'SHELXS-97 (Sheldrick, 1990)'
_computing_structure_refinement  'SHELXL-97 (Sheldrick, 1997)'
_computing_molecular_graphics    'Bruker SHELXTL'
_computing_publication_material  'Bruker SHELXTL'

_refine_special_details
;
Refinement of F^2^ against ALL reflections.  The weighted R-factor wR and
goodness of fit S are based on F^2^, conventional R-factors R are based
on F, with F set to zero for negative F^2^. The threshold expression of
F^2^ > 2sigma(F^2^) is used only for calculating R-factors(gt) etc. and is
not relevant to the choice of reflections for refinement.  R-factors based
on F^2^ are statistically about twice as large as those based on F, and R-
factors based on ALL data will be even larger.
;

_refine_ls_structure_factor_coef  Fsqd
_refine_ls_matrix_type           full
_refine_ls_weighting_scheme      calc
_refine_ls_weighting_details
'calc w=1/[\s^2^(Fo^2^)+(0.1308P)^2^+0.0061P] where P=(Fo^2^+2Fc^2^)/3'
_atom_sites_solution_primary     direct
_atom_sites_solution_secondary   difmap
_atom_sites_solution_hydrogens   geom
_refine_ls_hydrogen_treatment    mixed
_refine_ls_extinction_method     SHELXL
_refine_ls_extinction_coef       0.10(2)
_refine_ls_extinction_expression
'Fc^*^=kFc[1+0.001xFc^2^\l^3^/sin(2\q)]^-1/4^'
_refine_ls_number_reflns         2162
_refine_ls_number_parameters     132
_refine_ls_number_restraints     0
_refine_ls_R_factor_all          0.0745
_refine_ls_R_factor_gt           0.0631
_refine_ls_wR_factor_ref         0.1990
_refine_ls_wR_factor_gt          0.1841
```

```
_refine_ls_goodness_of_fit_ref    1.097
_refine_ls_restrained_S_all       1.097
_refine_ls_shift/su_max           0.067
_refine_ls_shift/su_mean          0.035

loop_
 _atom_site_label
 _atom_site_type_symbol
 _atom_site_fract_x
 _atom_site_fract_y
 _atom_site_fract_z
 _atom_site_U_iso_or_equiv
 _atom_site_adp_type
 _atom_site_occupancy
 _atom_site_symmetry_multiplicity
 _atom_site_calc_flag
 _atom_site_refinement_flags
 _atom_site_disorder_assembly
 _atom_site_disorder_group
O1 O 0.2977(3) 0.41258(15) 0.93399(13) 0.0490(4) Uani 1 1 d . . .
O2 O 0.0888(3) 0.50335(14) 0.66442(13) 0.0479(4) Uani 1 1 d . . .
N1 N -0.1295(3) 0.40141(17) 0.90131(14) 0.0408(5) Uani 1 1 d . . .
H1 H -0.2965 0.4266 0.9221 0.049 Uiso 1 1 calc R . .
N2 N 0.5781(3) 0.63640(18) 0.60327(15) 0.0460(5) Uani 1 1 d . . .
H2A H 0.6118 0.6520 0.5218 0.069 Uiso 1 1 calc R . .
H2B H 0.4374 0.5861 0.6247 0.069 Uiso 1 1 calc R . .
H2C H 0.7208 0.5893 0.6332 0.069 Uiso 1 1 calc R . .
O3 O 0.2905(4) 0.29130(17) 0.64139(15) 0.0720(6) Uani 1 1 d . . .
C1 C 0.0549(3) 0.44835(18) 0.95467(16) 0.0372(5) Uani 1 1 d . . .
C3 C 0.1252(4) 0.3733(2) 0.69571(17) 0.0429(5) Uani 1 1 d . . .
C4 C 0.5179(4) 0.7740(2) 0.65398(17) 0.0397(5) Uani 1 1 d . . .
H4 H 0.375(4) 0.829(2) 0.612(2) 0.048 Uiso 1 1 calc . . .
C2 C -0.0528(4) 0.3082(2) 0.80843(17) 0.0439(5) Uani 1 1 d . . .
H2D H -0.2138 0.2823 0.7825 0.053 Uiso 1 1 calc R . .
H2E H 0.0425 0.2231 0.8441 0.053 Uiso 1 1 calc R . .
C9 C 0.4189(4) 0.7504(2) 0.78979(18) 0.0487(6) Uani 1 1 d . . .
H9A H 0.5526 0.6901 0.8319 0.058 Uiso 1 1 calc R . .
H9B H 0.2553 0.7033 0.8028 0.058 Uiso 1 1 calc R . .
C5 C 0.7654(4) 0.8551(2) 0.6277(2) 0.0499(6) Uani 1 1 d . . .
H5A H 0.8167 0.8736 0.5397 0.060 Uiso 1 1 calc R . .
H5B H 0.9134 0.7991 0.6629 0.060 Uiso 1 1 calc R . .
C8 C 0.3649(5) 0.8890(3) 0.8430(2) 0.0587(6) Uani 1 1 d . . .
H8A H 0.2169 0.9448 0.8075 0.070 Uiso 1 1 calc R . .
H8B H 0.3128 0.8708 0.9309 0.070 Uiso 1 1 calc R . .
C6 C 0.7095(5) 0.9933(2) 0.6817(2) 0.0600(6) Uani 1 1 d . . .
H6A H 0.8727 1.0407 0.6685 0.072 Uiso 1 1 calc R . .
```

H6B H 0.5758 1.0532 0.6394 0.072 Uiso 1 1 calc R . .
C7 C 0.6104(5) 0.9715(3) 0.8175(2) 0.0638(7) Uani 1 1 d . . .
H7A H 0.5655 1.0620 0.8473 0.077 Uiso 1 1 calc R . .
H7B H 0.7519 0.9210 0.8612 0.077 Uiso 1 1 calc R . .

loop_
 _atom_site_aniso_label
 _atom_site_aniso_U_11
 _atom_site_aniso_U_22
 _atom_site_aniso_U_33
 _atom_site_aniso_U_23
 _atom_site_aniso_U_13
 _atom_site_aniso_U_12
O1 0.0365(8) 0.0590(9) 0.0531(9) -0.0219(7) 0.0017(6) -0.0020(6)
O2 0.0519(9) 0.0400(9) 0.0492(9) -0.0047(6) 0.0021(6) -0.0053(6)
N1 0.0345(8) 0.0491(10) 0.0395(9) -0.0167(7) 0.0064(6) -0.0071(7)
N2 0.0479(10) 0.0433(10) 0.0445(9) -0.0090(7) 0.0058(7) -0.0059(7)
O3 0.0886(13) 0.0601(11) 0.0528(10) -0.0108(8) 0.0226(9) 0.0191(9)
C1 0.0363(10) 0.0387(11) 0.0345(9) -0.0051(8) 0.0041(7) -0.0053(8)
C3 0.0446(10) 0.0457(12) 0.0376(10) -0.0101(8) -0.0003(8) -0.0016(8)
C4 0.0402(10) 0.0365(10) 0.0396(10) -0.0053(8) 0.0032(7) -0.0021(8)
C2 0.0484(11) 0.0404(11) 0.0436(11) -0.0145(8) 0.0043(8) -0.0085(8)
C9 0.0540(12) 0.0499(12) 0.0409(11) -0.0066(9) 0.0055(8) -0.0135(9)
C5 0.0454(12) 0.0505(13) 0.0516(12) -0.0079(9) 0.0072(8) -0.0107(9)
C8 0.0587(14) 0.0642(15) 0.0537(13) -0.0217(11) 0.0097(10) -0.0126(11)
C6 0.0656(15) 0.0469(13) 0.0672(15) -0.0102(11) 0.0066(11) -0.0195(11)
C7 0.0640(15) 0.0613(15) 0.0707(16) -0.0248(12) 0.0019(11) -0.0190(12)

_geom_special_details
;
 All esds (except the esd in the dihedral angle between two l.s. planes)
 are estimated using the full covariance matrix. The cell esds are taken
 into account individually in the estimation of esds in distances, angles
 and torsion angles; correlations between esds in cell parameters are only
 used when they are defined by crystal symmetry. An approximate (isotropic)
 treatment of cell esds is used for estimating esds involving l.s. planes.
;

loop_
 _geom_bond_atom_site_label_1
 _geom_bond_atom_site_label_2
 _geom_bond_distance
 _geom_bond_site_symmetry_2
 _geom_bond_publ_flag
O1 C1 1.235(2) . ?
O2 C3 1.255(2) . ?

```
N1 C1 1.324(2) . ?
N1 C2 1.446(2) . ?
N2 C4 1.499(2) . ?
O3 C3 1.238(2) . ?
C1 C1 1.521(3) 2_567 ?
C3 C2 1.532(3) . ?
C4 C9 1.512(3) . ?
C4 C5 1.519(3) . ?
C9 C8 1.520(3) . ?
C5 C6 1.521(3) . ?
C8 C7 1.519(3) . ?
C6 C7 1.512(3) . ?

loop_
 _geom_angle_atom_site_label_1
 _geom_angle_atom_site_label_2
 _geom_angle_atom_site_label_3
 _geom_angle
 _geom_angle_site_symmetry_1
 _geom_angle_site_symmetry_3
 _geom_angle_publ_flag
C1 N1 C2 120.65(16) . . ?
O1 C1 N1 123.73(17) . . ?
O1 C1 C1 121.6(2) . 2_567 ?
N1 C1 C1 114.66(19) . 2_567 ?
O3 C3 O2 125.44(19) . . ?
O3 C3 C2 116.46(18) . . ?
O2 C3 C2 118.08(17) . . ?
N2 C4 C9 110.39(16) . . ?
N2 C4 C5 109.83(16) . . ?
C9 C4 C5 111.71(17) . . ?
N1 C2 C3 113.26(16) . . ?
C4 C9 C8 110.85(18) . . ?
C4 C5 C6 110.41(17) . . ?
C7 C8 C9 111.54(19) . . ?
C7 C6 C5 111.94(19) . . ?
C6 C7 C8 110.91(19) . . ?

_diffrn_measured_fraction_theta_max    0.916
_diffrn_reflns_theta_full              28.11
_diffrn_measured_fraction_theta_full   0.916
_refine_diff_density_max    0.319
_refine_diff_density_min   -0.360
_refine_diff_density_rms    0.063
```

(benzylNH$_3$)$_2$OG

```
data_ja

_audit_creation_method            SHELXL-97
_chemical_name_systematic
;
 ?
;
_chemical_name_common             ?
_chemical_melting_point           ?
_chemical_formula_moiety          ?
_chemical_formula_sum
 'C20 H26 N4 O6'
_chemical_formula_weight          418.4

loop_
 _atom_type_symbol
 _atom_type_description
 _atom_type_scat_dispersion_real
 _atom_type_scat_dispersion_imag
 _atom_type_scat_source
'C'  'C'   0.0033   0.0016
 'International Tables Vol C Tables 4.2.6.8 and 6.1.1.4'
 'H'  'H'   0.0000   0.0000
 'International Tables Vol C Tables 4.2.6.8 and 6.1.1.4'
 'N'  'N'   0.0061   0.0033
 'International Tables Vol C Tables 4.2.6.8 and 6.1.1.4'
 'O'  'O'   0.0106   0.0060
 'International Tables Vol C Tables 4.2.6.8 and 6.1.1.4'

_symmetry_cell_setting            Triclinic
_symmetry_space_group_name_H-M    P-1

loop_
 _symmetry_equiv_pos_as_xyz
 'x, y, z'
 '-x, -y, -z'

_cell_length_a                    4.9193(9)
_cell_length_b                    10.2941(19)
_cell_length_c                    10.765(2)
_cell_angle_alpha                 88.508(5)
_cell_angle_beta                  76.911(4)
_cell_angle_gamma                 85.008(4)
_cell_volume                      528.94(18)
```

```
_cell_formula_units_Z            1
_cell_measurement_temperature    273(2)
_cell_measurement_reflns_used    ?
_cell_measurement_theta_min      ?
_cell_measurement_theta_max      ?

_exptl_crystal_description       ?
_exptl_crystal_colour            ?
_exptl_crystal_size_max          .5
_exptl_crystal_size_mid          .2
_exptl_crystal_size_min          .2
_exptl_crystal_density_meas      ?
_exptl_crystal_density_diffrn    1.314
_exptl_crystal_density_method    'not measured'
_exptl_crystal_F_000             222
_exptl_absorpt_coefficient_mu    0.098
_exptl_absorpt_correction_type   none
_exptl_absorpt_correction_T_min  ?
_exptl_absorpt_correction_T_max  ?
_exptl_absorpt_process_details   ?

_exptl_special_details
;
 ?
;

_diffrn_ambient_temperature      273(2)
_diffrn_radiation_wavelength     0.71073
_diffrn_radiation_type           MoK\a
_diffrn_radiation_source         'fine-focus sealed tube'
_diffrn_radiation_monochromator  graphite
_diffrn_measurement_device_type  'CCD area detector'
_diffrn_measurement_method       'phi and omega scans'
_diffrn_detector_area_resol_mean ?
_diffrn_standards_number         ?
_diffrn_standards_interval_count ?
_diffrn_standards_interval_time  ?
_diffrn_standards_decay_%        ?
_diffrn_reflns_number            3258
_diffrn_reflns_av_R_equivalents  0.0352
_diffrn_reflns_av_sigmaI/netI    0.0333
_diffrn_reflns_limit_h_min       -6
_diffrn_reflns_limit_h_max       5
_diffrn_reflns_limit_k_min       -13
_diffrn_reflns_limit_k_max       11
_diffrn_reflns_limit_l_min       -14
```

```
_diffrn_reflns_limit_l_max       14
_diffrn_reflns_theta_min         1.94
_diffrn_reflns_theta_max         28.31
_reflns_number_total             2264
_reflns_number_gt                1758
_reflns_threshold_expression     >2sigma(I)

_computing_data_collection       'Bruker SMART'
_computing_cell_refinement       'Bruker SMART'
_computing_data_reduction        'Bruker SAINT'
_computing_structure_solution    'SHELXS-97 (Sheldrick, 1990)'
_computing_structure_refinement  'SHELXL-97 (Sheldrick, 1997)'
_computing_molecular_graphics    'Bruker SHELXTL'
_computing_publication_material  'Bruker SHELXTL'

_refine_special_details
;
Refinement of F^2^ against ALL reflections.  The weighted R-factor wR and
goodness of fit S are based on F^2^, conventional R-factors R are based
on F, with F set to zero for negative F^2^. The threshold expression of
F^2^ > 2sigma(F^2^) is used only for calculating R-factors(gt) etc. and is
not relevant to the choice of reflections for refinement.  R-factors based
on F^2^ are statistically about twice as large as those based on F, and R-
factors based on ALL data will be even larger.
;

_refine_ls_structure_factor_coef  Fsqd
_refine_ls_matrix_type           full
_refine_ls_weighting_scheme      calc
_refine_ls_weighting_details
'calc w=1/[\s^2^(Fo^2^)+(0.1742P)^2^+0.2125P] where P=(Fo^2^+2Fc^2^)/3'
_atom_sites_solution_primary     direct
_atom_sites_solution_secondary   difmap
_atom_sites_solution_hydrogens   geom
_refine_ls_hydrogen_treatment    mixed
_refine_ls_extinction_method     SHELXL
_refine_ls_extinction_coef       0.15(4)
_refine_ls_extinction_expression
'Fc^*^=kFc[1+0.001xFc^2^\l^3^/sin(2\q)]^-1/4^'
_refine_ls_number_reflns         2264
_refine_ls_number_parameters     138
_refine_ls_number_restraints     0
_refine_ls_R_factor_all          0.0956
_refine_ls_R_factor_gt           0.0847
_refine_ls_wR_factor_ref         0.2383
_refine_ls_wR_factor_gt          0.2172
```

```
_refine_ls_goodness_of_fit_ref    1.149
_refine_ls_restrained_S_all       1.149
_refine_ls_shift/su_max           0.000
_refine_ls_shift/su_mean          0.000

loop_
 _atom_site_label
 _atom_site_type_symbol
 _atom_site_fract_x
 _atom_site_fract_y
 _atom_site_fract_z
 _atom_site_U_iso_or_equiv
 _atom_site_adp_type
 _atom_site_occupancy
 _atom_site_symmetry_multiplicity
 _atom_site_calc_flag
 _atom_site_refinement_flags
 _atom_site_disorder_assembly
 _atom_site_disorder_group
O3 O 0.4143(4) 0.8525(2) 0.97440(19) 0.0474(6) Uani 1 1 d . . .
N1 N 0.6984(4) 0.6139(2) 0.8972(2) 0.0410(6) Uani 1 1 d . . .
H1 H 0.8550 0.5946 0.9188 0.049 Uiso 1 1 calc R . .
O1 O 0.2492(4) 0.5700(2) 0.9194(3) 0.0601(7) Uani 1 1 d . . .
O2 O 0.3424(6) 0.8904(2) 0.7797(2) 0.0631(8) Uani 1 1 d . . .
C1 C 0.4759(5) 0.5503(3) 0.9495(3) 0.0421(7) Uani 1 1 d . . .
N2 N -0.1534(5) 0.8687(2) 0.1062(2) 0.0449(7) Uani 1 1 d . . .
H2A H -0.2049 0.9408 0.1525 0.067 Uiso 1 1 calc R . .
H2B H -0.2687 0.8621 0.0543 0.067 Uiso 1 1 calc R . .
H2C H 0.0207 0.8725 0.0604 0.067 Uiso 1 1 calc R . .
C3 C 0.4586(6) 0.8280(3) 0.8575(3) 0.0408(7) Uani 1 1 d . . .
C2 C 0.6759(6) 0.7161(3) 0.8034(3) 0.0439(7) Uani 1 1 d . . .
H2D H 0.6245 0.6791 0.7308 0.053 Uiso 1 1 calc R . .
H2E H 0.8571 0.7504 0.7735 0.053 Uiso 1 1 calc R . .
C4 C -0.1655(7) 0.7540(3) 0.1917(3) 0.0494(8) Uani 1 1 d . . .
H4A H -0.1004 0.6765 0.1406 0.059 Uiso 1 1 calc R . .
H4B H -0.3590 0.7458 0.2349 0.059 Uiso 1 1 calc R . .
C5 C 0.0072(6) 0.7599(3) 0.2907(3) 0.0464(7) Uani 1 1 d . . .
C6 C 0.0785(8) 0.6437(4) 0.3481(4) 0.0668(10) Uani 1 1 d . . .
H6 H 0.0302 0.5652 0.3218 0.080 Uiso 1 1 calc R . .
C8 C 0.2967(10) 0.7593(7) 0.4854(4) 0.0892(16) Uani 1 1 d . . .
H8 H 0.3887 0.7597 0.5519 0.107 Uiso 1 1 calc R . .
C7 C 0.2236(10) 0.6453(6) 0.4457(5) 0.0892(16) Uani 1 1 d . . .
H7 H 0.2709 0.5673 0.4842 0.107 Uiso 1 1 calc R . .
C10 C 0.0887(9) 0.8748(4) 0.3287(4) 0.0716(11) Uani 1 1 d . . .
H10 H 0.0470 0.9530 0.2892 0.086 Uiso 1 1 calc R . .
C9 C 0.2325(10) 0.8736(5) 0.4256(5) 0.0877(15) Uani 1 1 d . . .
```

H9 H 0.2863 0.9515 0.4506 0.105 Uiso 1 1 calc R . .

loop_
 _atom_site_aniso_label
 _atom_site_aniso_U_11
 _atom_site_aniso_U_22
 _atom_site_aniso_U_33
 _atom_site_aniso_U_23
 _atom_site_aniso_U_13
 _atom_site_aniso_U_12
O3 0.0459(12) 0.0529(12) 0.0449(12) 0.0007(9) -0.0144(9) -0.0009(9)
N1 0.0295(11) 0.0419(12) 0.0532(14) 0.0099(10) -0.0139(9) -0.0035(8)
O1 0.0369(11) 0.0642(14) 0.0852(17) 0.0274(12) -0.0278(11) -0.0092(9)
O2 0.0809(17) 0.0559(13) 0.0579(14) 0.0014(10) -0.0352(13) 0.0149(12)
C1 0.0314(13) 0.0413(14) 0.0555(16) 0.0064(12) -0.0145(11) -0.0032(10)
N2 0.0466(13) 0.0496(13) 0.0409(12) 0.0036(10) -0.0168(10) -0.0006(10)
C3 0.0407(14) 0.0404(14) 0.0442(14) 0.0037(11) -0.0153(11) -0.0055(10)
C2 0.0401(14) 0.0474(15) 0.0440(14) 0.0073(12) -0.0100(11) -0.0030(11)
C4 0.0539(17) 0.0490(16) 0.0494(16) 0.0039(12) -0.0183(13) -0.0103(12)
C5 0.0445(15) 0.0547(16) 0.0392(14) 0.0058(12) -0.0112(11) 0.0026(12)
C6 0.061(2) 0.069(2) 0.070(2) 0.0277(18) -0.0167(17) -0.0045(16)
C8 0.068(3) 0.152(5) 0.048(2) 0.007(3) -0.0240(18) 0.011(3)
C7 0.074(3) 0.117(4) 0.076(3) 0.051(3) -0.025(2) 0.000(3)
C10 0.084(3) 0.061(2) 0.082(3) -0.0121(19) -0.050(2) 0.0122(18)
C9 0.082(3) 0.107(3) 0.085(3) -0.034(3) -0.048(2) 0.021(3)

_geom_special_details
;
 All esds (except the esd in the dihedral angle between two l.s. planes)
 are estimated using the full covariance matrix. The cell esds are taken
 into account individually in the estimation of esds in distances, angles
 and torsion angles; correlations between esds in cell parameters are only
 used when they are defined by crystal symmetry. An approximate (isotropic)
 treatment of cell esds is used for estimating esds involving l.s. planes.
;

loop_
 _geom_bond_atom_site_label_1
 _geom_bond_atom_site_label_2
 _geom_bond_distance
 _geom_bond_site_symmetry_2
 _geom_bond_publ_flag
O3 C3 1.256(3) . ?
N1 C1 1.330(4) . ?
N1 C2 1.454(4) . ?
O1 C1 1.229(3) . ?

```
O2 C3 1.251(3) . ?
C1 C1 1.526(5) 2_667 ?
N2 C4 1.475(4) . ?
C3 C2 1.532(4) . ?
C4 C5 1.511(4) . ?
C5 C10 1.381(5) . ?
C5 C6 1.387(5) . ?
C6 C7 1.399(7) . ?
C8 C7 1.364(8) . ?
C8 C9 1.373(8) . ?
C10 C9 1.386(6) . ?

loop_
 _geom_angle_atom_site_label_1
 _geom_angle_atom_site_label_2
 _geom_angle_atom_site_label_3
 _geom_angle
 _geom_angle_site_symmetry_1
 _geom_angle_site_symmetry_3
 _geom_angle_publ_flag
C1 N1 C2 119.8(2) . . ?
O1 C1 N1 123.3(3) . . ?
O1 C1 C1 122.2(3) . 2_667 ?
N1 C1 C1 114.5(3) . 2_667 ?
O2 C3 O3 124.8(3) . . ?
O2 C3 C2 116.6(3) . . ?
O3 C3 C2 118.5(2) . . ?
N1 C2 C3 112.4(2) . . ?
N2 C4 C5 113.9(3) . . ?
C10 C5 C6 119.1(3) . . ?
C10 C5 C4 123.3(3) . . ?
C6 C5 C4 117.5(3) . . ?
C5 C6 C7 119.6(4) . . ?
C7 C8 C9 119.0(4) . . ?
C8 C7 C6 121.1(4) . . ?
C5 C10 C9 120.1(4) . . ?
C8 C9 C10 121.0(5) . . ?

_diffrn_measured_fraction_theta_max    0.856
_diffrn_reflns_theta_full              28.31
_diffrn_measured_fraction_theta_full   0.856
_refine_diff_density_max    0.439
_refine_diff_density_min   -0.349
_refine_diff_density_rms    0.089
```

(4-ethynylbenzylNH$_3$)$_2$OG

data_d:\zhong\zl7\work\zl7t

```
_audit_creation_method            SHELXL-97
_chemical_name_systematic
;
 ?
;
_chemical_name_common             ?
_chemical_melting_point           ?
_chemical_formula_moiety          ?
_chemical_formula_sum
 'C24 H26 N4 O6'
_chemical_formula_weight          466.49

loop_
 _atom_type_symbol
 _atom_type_description
 _atom_type_scat_dispersion_real
 _atom_type_scat_dispersion_imag
 _atom_type_scat_source
 'C'  'C'   0.0033   0.0016
 'International Tables Vol C Tables 4.2.6.8 and 6.1.1.4'
 'H'  'H'   0.0000   0.0000
 'International Tables Vol C Tables 4.2.6.8 and 6.1.1.4'
 'N'  'N'   0.0061   0.0033
 'International Tables Vol C Tables 4.2.6.8 and 6.1.1.4'
 'O'  'O'   0.0106   0.0060
 'International Tables Vol C Tables 4.2.6.8 and 6.1.1.4'

_symmetry_cell_setting            Monoclinic
_symmetry_space_group_name_H-M    P21/n

loop_
 _symmetry_equiv_pos_as_xyz
 'x, y, z'
 '-x+1/2, y+1/2, -z+1/2'
 '-x, -y, -z'
 'x-1/2, -y-1/2, z-1/2'

_cell_length_a                    4.943(2)
_cell_length_b                    23.463(9)
_cell_length_c                    10.699(4)
_cell_angle_alpha                 90.00
_cell_angle_beta                  101.774(7)
```

```
_cell_angle_gamma                90.00
_cell_volume                     1214.8(8)
_cell_formula_units_Z            2
_cell_measurement_temperature    273(2)
_cell_measurement_reflns_used    ?
_cell_measurement_theta_min      ?
_cell_measurement_theta_max      ?

_exptl_crystal_description       ?
_exptl_crystal_colour            ?
_exptl_crystal_size_max          ?
_exptl_crystal_size_mid          ?
_exptl_crystal_size_min          ?
_exptl_crystal_density_meas      0
_exptl_crystal_density_diffrn    1.275
_exptl_crystal_density_method    'not measured'
_exptl_crystal_F_000             492
_exptl_absorpt_coefficient_mu    0.093
_exptl_absorpt_correction_type   none
_exptl_absorpt_correction_T_min  ?
_exptl_absorpt_correction_T_max  ?
_exptl_absorpt_process_details   ?

_exptl_special_details
;
 ?
;

_diffrn_ambient_temperature      273(2)
_diffrn_radiation_wavelength     0.71073
_diffrn_radiation_type           MoK\a
_diffrn_radiation_source         'fine-focus sealed tube'
_diffrn_radiation_monochromator  graphite
_diffrn_measurement_device_type  'CCD area detector'
_diffrn_measurement_method       'phi and omega scans'
_diffrn_detector_area_resol_mean  ?
_diffrn_standards_number         ?
_diffrn_standards_interval_count  ?
_diffrn_standards_interval_time  ?
_diffrn_standards_decay_%        ?
_diffrn_reflns_number            7557
_diffrn_reflns_av_R_equivalents  0.1563
_diffrn_reflns_av_sigmaI/netI    0.2992
_diffrn_reflns_limit_h_min       -6
_diffrn_reflns_limit_h_max       6
_diffrn_reflns_limit_k_min       -29
```

```
_diffrn_reflns_limit_k_max       27
_diffrn_reflns_limit_l_min       -14
_diffrn_reflns_limit_l_max       11
_diffrn_reflns_theta_min         1.74
_diffrn_reflns_theta_max         28.77
_reflns_number_total             2816
_reflns_number_gt                655
_reflns_threshold_expression     >2sigma(I)

_computing_data_collection       'Bruker SMART'
_computing_cell_refinement       'Bruker SMART'
_computing_data_reduction        'Bruker SAINT'
_computing_structure_solution    'SHELXS-97 (Sheldrick, 1990)'
_computing_structure_refinement   'SHELXL-97 (Sheldrick, 1997)'
_computing_molecular_graphics    'Bruker SHELXTL'
_computing_publication_material   'Bruker SHELXTL'

_refine_special_details
;
 Refinement of F^2^ against ALL reflections.  The weighted R-factor wR and
 goodness of fit S are based on F^2^, conventional R-factors R are based
 on F, with F set to zero for negative F^2^. The threshold expression of
 F^2^ > 2sigma(F^2^) is used only for calculating R-factors(gt) etc. and is
 not relevant to the choice of reflections for refinement.  R-factors based
 on F^2^ are statistically about twice as large as those based on F, and R-
 factors based on ALL data will be even larger.
;

_refine_ls_structure_factor_coef  Fsqd
_refine_ls_matrix_type           full
_refine_ls_weighting_scheme      calc
_refine_ls_weighting_details
 'calc w=1/[\s^2^(Fo^2^)+(0.1152P)^2^+0.0000P] where P=(Fo^2^+2Fc^2^)/3'
_atom_sites_solution_primary     direct
_atom_sites_solution_secondary    difmap
_atom_sites_solution_hydrogens    geom
_refine_ls_hydrogen_treatment    mixed
_refine_ls_extinction_method     none
_refine_ls_extinction_coef       ?
_refine_ls_number_reflns         2816
_refine_ls_number_parameters     155
_refine_ls_number_restraints     0
_refine_ls_R_factor_all          0.2736
_refine_ls_R_factor_gt           0.0792
_refine_ls_wR_factor_ref         0.2584
_refine_ls_wR_factor_gt          0.1758
```

```
_refine_ls_goodness_of_fit_ref    0.720
_refine_ls_restrained_S_all       0.720
_refine_ls_shift/su_max           0.000
_refine_ls_shift/su_mean          0.000

loop_
 _atom_site_label
 _atom_site_type_symbol
 _atom_site_fract_x
 _atom_site_fract_y
 _atom_site_fract_z
 _atom_site_U_iso_or_equiv
 _atom_site_adp_type
 _atom_site_occupancy
 _atom_site_symmetry_multiplicity
 _atom_site_calc_flag
 _atom_site_refinement_flags
 _atom_site_disorder_assembly
 _atom_site_disorder_group
O3 O 0.7344(7) 0.00989(16) 0.8407(3) 0.0587(11) Uani 1 1 d . . .
O1 O 0.2723(7) 0.03159(15) 0.5840(3) 0.0620(11) Uani 1 1 d . . .
N1 N 0.2571(8) 0.45156(16) 0.6406(4) 0.0551(12) Uani 1 1 d . . .
H1A H 0.4193 0.4694 0.6566 0.083 Uiso 1 1 calc R . .
H1B H 0.1222 0.4767 0.6402 0.083 Uiso 1 1 calc R . .
H1C H 0.2333 0.4346 0.5648 0.083 Uiso 1 1 calc R . .
O2 O 0.6487(8) 0.09652(16) 0.9037(4) 0.0713(12) Uani 1 1 d . . .
N2 N 0.7252(8) 0.04796(18) 0.5981(4) 0.0548(12) Uani 1 1 d . . .
H2 H 0.8696 0.0403 0.5680 0.066 Uiso 1 1 calc R . .
C11 C 0.7445(11) 0.0886(2) 0.7006(5) 0.0558(15) Uani 1 1 d . . .
H11A H 0.6061 0.1180 0.6754 0.067 Uiso 1 1 calc R . .
H11B H 0.9246 0.1067 0.7149 0.067 Uiso 1 1 calc R . .
C12 C 0.7036(10) 0.0619(3) 0.8243(5) 0.0524(14) Uani 1 1 d . . .
C10 C 0.4909(11) 0.0226(2) 0.5501(5) 0.0481(13) Uani 1 1 d . . .
C2 C 0.4795(11) 0.3654(2) 0.7558(6) 0.0559(16) Uani 1 1 d . . .
C4 C 0.7387(12) 0.2939(2) 0.6740(6) 0.0675(17) Uani 1 1 d . . .
H4 H 0.7793 0.2743 0.6044 0.081 Uiso 1 1 calc R . .
C5 C 0.8793(12) 0.2808(2) 0.7939(6) 0.0596(16) Uani 1 1 d . . .
C8 C 1.0834(14) 0.2365(3) 0.8128(6) 0.0675(17) Uani 1 1 d . . .
C3 C 0.5362(13) 0.3358(3) 0.6536(6) 0.0696(17) Uani 1 1 d . . .
H3 H 0.4398 0.3438 0.5713 0.083 Uiso 1 1 calc R . .
C6 C 0.8200(13) 0.3093(3) 0.8961(6) 0.0725(18) Uani 1 1 d . . .
H6 H 0.9135 0.3004 0.9783 0.087 Uiso 1 1 calc R . .
C7 C 0.6212(13) 0.3513(2) 0.8772(6) 0.0699(17) Uani 1 1 d . . .
H7 H 0.5815 0.3706 0.9473 0.084 Uiso 1 1 calc R . .
C1 C 0.2515(11) 0.4085(2) 0.7402(5) 0.0642(17) Uani 1 1 d . . .
H1D H 0.0760 0.3886 0.7202 0.077 Uiso 1 1 calc R . .
```

H1E H 0.2611 0.4279 0.8211 0.077 Uiso 1 1 calc R . .
C9 C 1.2542(14) 0.2019(3) 0.8327(6) 0.085(2) Uani 1 1 d . . .
H9 H 1.3911 0.1741 0.8487 0.102 Uiso 1 1 calc R . .

loop_
 _atom_site_aniso_label
 _atom_site_aniso_U_11
 _atom_site_aniso_U_22
 _atom_site_aniso_U_33
 _atom_site_aniso_U_23
 _atom_site_aniso_U_13
 _atom_site_aniso_U_12
O3 0.047(2) 0.052(3) 0.072(3) 0.003(2) 0.0018(19) 0.0035(18)
O1 0.034(2) 0.081(3) 0.070(3) -0.014(2) 0.009(2) -0.0043(19)
N1 0.047(3) 0.049(3) 0.064(3) 0.004(2) -0.002(2) 0.002(2)
O2 0.092(3) 0.065(3) 0.054(3) -0.004(2) 0.009(2) 0.016(2)
N2 0.037(3) 0.067(3) 0.059(3) -0.011(3) 0.007(2) -0.010(2)
C11 0.051(4) 0.045(3) 0.066(4) -0.011(3) -0.001(3) -0.009(3)
C12 0.036(3) 0.060(4) 0.056(4) -0.002(3) -0.004(3) -0.001(3)
C10 0.035(3) 0.053(4) 0.051(3) 0.007(2) 0.000(3) -0.004(3)
C2 0.051(4) 0.051(4) 0.063(4) 0.005(3) 0.008(3) 0.005(3)
C4 0.070(4) 0.060(4) 0.068(5) -0.004(3) 0.003(4) 0.007(3)
C5 0.058(4) 0.047(4) 0.069(4) 0.002(3) 0.000(4) 0.003(3)
C8 0.068(5) 0.053(4) 0.074(5) -0.001(3) -0.003(4) 0.006(3)
C3 0.076(5) 0.070(4) 0.058(4) 0.003(3) 0.003(3) 0.019(3)
C6 0.083(5) 0.064(4) 0.062(5) 0.004(3) -0.004(4) 0.013(4)
C7 0.082(5) 0.059(4) 0.068(5) -0.001(3) 0.013(4) 0.007(3)
C1 0.064(4) 0.057(4) 0.074(4) 0.010(3) 0.019(3) 0.016(3)
C9 0.080(5) 0.077(5) 0.090(5) 0.003(4) 0.002(4) 0.014(4)

_geom_special_details
;
 All esds (except the esd in the dihedral angle between two l.s. planes)
 are estimated using the full covariance matrix. The cell esds are taken
 into account individually in the estimation of esds in distances, angles
 and torsion angles; correlations between esds in cell parameters are only
 used when they are defined by crystal symmetry. An approximate (isotropic)
 treatment of cell esds is used for estimating esds involving l.s. planes.
;

loop_
 _geom_bond_atom_site_label_1
 _geom_bond_atom_site_label_2
 _geom_bond_distance
 _geom_bond_site_symmetry_2
 _geom_bond_publ_flag

```
O3 C12 1.237(6) . ?
O1 C10 1.227(5) . ?
N1 C1 1.473(6) . ?
O2 C12 1.245(6) . ?
N2 C10 1.310(6) . ?
N2 C11 1.442(6) . ?
C11 C12 1.515(7) . ?
C10 C10 1.523(10) 3_656 ?
C2 C3 1.371(7) . ?
C2 C7 1.384(7) . ?
C2 C1 1.498(7) . ?
C4 C5 1.363(7) . ?
C4 C3 1.389(7) . ?
C5 C6 1.365(7) . ?
C5 C8 1.432(8) . ?
C8 C9 1.160(8) . ?
C6 C7 1.377(7) . ?

loop_
 _geom_angle_atom_site_label_1
 _geom_angle_atom_site_label_2
 _geom_angle_atom_site_label_3
 _geom_angle
 _geom_angle_site_symmetry_1
 _geom_angle_site_symmetry_3
 _geom_angle_publ_flag
C10 N2 C11 121.0(4) . . ?
N2 C11 C12 113.0(4) . . ?
O3 C12 O2 125.8(5) . . ?
O3 C12 C11 119.8(5) . . ?
O2 C12 C11 114.4(5) . . ?
O1 C10 N2 124.5(5) . . ?
O1 C10 C10 120.7(6) . 3_656 ?
N2 C10 C10 114.7(6) . 3_656 ?
C3 C2 C7 118.8(5) . . ?
C3 C2 C1 121.6(6) . . ?
C7 C2 C1 119.4(5) . . ?
C5 C4 C3 121.4(6) . . ?
C4 C5 C6 119.5(6) . . ?
C4 C5 C8 120.4(6) . . ?
C6 C5 C8 120.2(6) . . ?
C9 C8 C5 177.1(7) . . ?
C2 C3 C4 119.4(6) . . ?
C5 C6 C7 119.8(6) . . ?
C6 C7 C2 121.2(6) . . ?
N1 C1 C2 114.8(4) . . ?
```

_diffrn_measured_fraction_theta_max 0.889
_diffrn_reflns_theta_full 28.77
_diffrn_measured_fraction_theta_full 0.889
_refine_diff_density_max 0.366
_refine_diff_density_min -0.337
_refine_diff_density_rms 0.111

18/H_2OG hydrate

```
data_zl44m

_audit_creation_method            SHELXL-97
_chemical_name_systematic
;
 ?
;
_chemical_name_common              ?
_chemical_melting_point           ?
_chemical_formula_moiety          ?
_chemical_formula_sum
 'C34 H38 N6 O14'
_chemical_formula_weight          754.70

loop_
 _atom_type_symbol
 _atom_type_description
 _atom_type_scat_dispersion_real
 _atom_type_scat_dispersion_imag
 _atom_type_scat_source
 'C'  'C'   0.0033   0.0016
 'International Tables Vol C Tables 4.2.6.8 and 6.1.1.4'
 'H'  'H'   0.0000   0.0000
 'International Tables Vol C Tables 4.2.6.8 and 6.1.1.4'
 'N'  'N'   0.0061   0.0033
 'International Tables Vol C Tables 4.2.6.8 and 6.1.1.4'
 'O'  'O'   0.0106   0.0060
 'International Tables Vol C Tables 4.2.6.8 and 6.1.1.4'

_symmetry_cell_setting            monoclinic
_symmetry_space_group_name_H-M    P21/c

loop_
 _symmetry_equiv_pos_as_xyz
 'x, y, z'
 '-x, y+1/2, -z+1/2'
 '-x, -y, -z'
 'x, -y-1/2, z-1/2'

_cell_length_a                    15.822(15)
_cell_length_b                    9.289(8)
_cell_length_c                    9.526(9)
_cell_angle_alpha                 90.00
_cell_angle_beta                  100.914(12)
```

```
_cell_angle_gamma                90.00
_cell_volume                     1375(2)
_cell_formula_units_Z            2
_cell_measurement_temperature    273(2)
_cell_measurement_reflns_used    ?
_cell_measurement_theta_min      ?
_cell_measurement_theta_max      ?

_exptl_crystal_description       ?
_exptl_crystal_colour            ?
_exptl_crystal_size_max          ?
_exptl_crystal_size_mid          ?
_exptl_crystal_size_min          ?
_exptl_crystal_density_meas      ?
_exptl_crystal_density_diffrn    1.823
_exptl_crystal_density_method    'not measured'
_exptl_crystal_F_000             792
_exptl_absorpt_coefficient_mu    0.144
_exptl_absorpt_correction_type   ?
_exptl_absorpt_correction_T_min  ?
_exptl_absorpt_correction_T_max  ?
_exptl_absorpt_process_details   ?

_exptl_special_details
;
 ?
;

_diffrn_ambient_temperature      273(2)
_diffrn_radiation_wavelength     0.71073
_diffrn_radiation_type           MoK\a
_diffrn_radiation_source         'fine-focus sealed tube'
_diffrn_radiation_monochromator  graphite
_diffrn_measurement_device_type  ?
_diffrn_measurement_method       ?
_diffrn_detector_area_resol_mean ?
_diffrn_standards_number         ?
_diffrn_standards_interval_count ?
_diffrn_standards_interval_time  ?
_diffrn_standards_decay_%        ?
_diffrn_reflns_number            7907
_diffrn_reflns_av_R_equivalents  0.3862
_diffrn_reflns_av_sigmaI/netI    0.7183
_diffrn_reflns_limit_h_min       -20
_diffrn_reflns_limit_h_max       19
_diffrn_reflns_limit_k_min       -8
```

```
_diffrn_reflns_limit_k_max       11
_diffrn_reflns_limit_l_min       -11
_diffrn_reflns_limit_l_max       12
_diffrn_reflns_theta_min         1.31
_diffrn_reflns_theta_max         28.39
_reflns_number_total             3083
_reflns_number_gt                515
_reflns_threshold_expression     >2sigma(I)

_computing_data_collection       ?
_computing_cell_refinement       ?
_computing_data_reduction        ?
_computing_structure_solution    'SHELXS-97 (Sheldrick, 1990)'
_computing_structure_refinement   'SHELXL-97 (Sheldrick, 1997)'
_computing_molecular_graphics    ?
_computing_publication_material   ?

_refine_special_details
;
 Refinement of F^2^ against ALL reflections.  The weighted R-factor wR and
 goodness of fit S are based on F^2^, conventional R-factors R are based
 on F, with F set to zero for negative F^2^. The threshold expression of
 F^2^ > 2sigma(F^2^) is used only for calculating R-factors(gt) etc. and is
 not relevant to the choice of reflections for refinement.  R-factors based
 on F^2^ are statistically about twice as large as those based on F, and R-
 factors based on ALL data will be even larger.
;

_refine_ls_structure_factor_coef  Fsqd
_refine_ls_matrix_type           full
_refine_ls_weighting_scheme      calc
_refine_ls_weighting_details
 'calc w=1/[\s^2^(Fo^2^)+(0.1229P)^2^+0.0000P] where P=(Fo^2^+2Fc^2^)/3'
_atom_sites_solution_primary     direct
_atom_sites_solution_secondary    difmap
_atom_sites_solution_hydrogens    geom
_refine_ls_hydrogen_treatment    mixed
_refine_ls_extinction_method     none
_refine_ls_extinction_coef       ?
_refine_ls_number_reflns         3083
_refine_ls_number_parameters     186
_refine_ls_number_restraints     0
_refine_ls_R_factor_all          0.4409
_refine_ls_R_factor_gt           0.0791
_refine_ls_wR_factor_ref         0.3348
_refine_ls_wR_factor_gt          0.1806
```

```
_refine_ls_goodness_of_fit_ref    0.767
_refine_ls_restrained_S_all       0.767
_refine_ls_shift/su_max           1.131
_refine_ls_shift/su_mean          0.006

loop_
 _atom_site_label
 _atom_site_type_symbol
 _atom_site_fract_x
 _atom_site_fract_y
 _atom_site_fract_z
 _atom_site_U_iso_or_equiv
 _atom_site_adp_type
 _atom_site_occupancy
 _atom_site_symmetry_multiplicity
 _atom_site_calc_flag
 _atom_site_refinement_flags
 _atom_site_disorder_assembly
 _atom_site_disorder_group
C26 C 0.6659(6) 0.3626(11) 0.7397(10) 0.056(3) Uani 1 1 d . . .
H26 H 0.6858 0.4478 0.7062 0.068 Uiso 1 1 calc R . .
C27 C 0.6710(6) 0.1068(12) 0.7642(11) 0.066(3) Uani 1 1 d . . .
H27 H 0.6954 0.0185 0.7486 0.079 Uiso 1 1 calc R . .
C28 C 0.7737(6) 0.2295(10) 0.6280(10) 0.055(3) Uani 1 1 d . . .
H28A H 0.7884 0.1304 0.6115 0.066 Uiso 1 1 calc R . .
H28B H 0.7530 0.2740 0.5357 0.066 Uiso 1 1 calc R . .
C1 C 0.4979(6) 0.2473(11) 0.9396(10) 0.053(3) Uani 1 1 d . . .
C2 C 0.5998(6) 0.3659(11) 0.8133(10) 0.060(3) Uani 1 1 d . . .
H2 H 0.5760 0.4540 0.8313 0.072 Uiso 1 1 calc R . .
C3 C 0.3768(7) 0.2640(11) 1.0778(11) 0.063(3) Uani 1 1 d . . .
N3 N 0.9052(5) 0.8984(8) 0.5141(7) 0.043(2) Uani 1 1 d . . .
H3 H 0.8869 0.8886 0.4236 0.051 Uiso 1 1 calc R . .
C6 C 0.6054(7) 0.1117(12) 0.8340(11) 0.067(3) Uani 1 1 d . . .
H6 H 0.5842 0.0263 0.8649 0.081 Uiso 1 1 calc R . .
O5 O 0.8877(4) 0.6090(6) 0.5009(6) 0.0479(19) Uani 1 1 d . . .
O1 O 0.9281(5) 0.3383(7) 0.4568(8) 0.053(2) Uani 1 1 d . . .
O4 O 0.8159(4) 0.6008(7) 0.6818(7) 0.054(2) Uani 1 1 d . . .
C12 C 0.4399(6) 0.2552(11) 1.0008(10) 0.059(3) Uani 1 1 d . . .
N4 N 0.8520(5) 0.3065(8) 0.7012(8) 0.055(2) Uani 1 1 d . . .
H4A H 0.8399 0.3993 0.7098 0.082 Uiso 1 1 calc R . .
H4B H 0.8934 0.2977 0.6502 0.082 Uiso 1 1 calc R . .
H4C H 0.8698 0.2687 0.7876 0.082 Uiso 1 1 calc R . .
C13 C 0.9744(6) 0.9778(11) 0.5575(11) 0.043(3) Uani 1 1 d . . .
C16 C 0.8535(6) 0.6643(10) 0.5939(11) 0.039(2) Uani 1 1 d . . .
C17 C 0.7033(6) 0.2325(12) 0.7145(9) 0.047(3) Uani 1 1 d . . .
C18 C 0.8586(5) 0.8273(10) 0.6101(10) 0.044(3) Uani 1 1 d . . .
```

H18A H 0.8005 0.8656 0.5947 0.053 Uiso 1 1 calc R . .
H18B H 0.8859 0.8501 0.7075 0.053 Uiso 1 1 calc R . .
O3 O 1.0008(5) 1.0142(8) 0.6821(8) 0.082(3) Uani 1 1 d . . .
C23 C 0.3240(7) 0.2759(11) 1.1480(11) 0.070(3) Uani 1 1 d . . .
H23 H 0.2820 0.2854 1.2038 0.084 Uiso 1 1 calc R . .
C25 C 0.5680(6) 0.2417(12) 0.8613(10) 0.046(3) Uani 1 1 d . . .
H30 H 0.973(4) 0.321(8) 0.483(7) 0.00(2) Uiso 1 1 d . . .

loop_
 _atom_site_aniso_label
 _atom_site_aniso_U_11
 _atom_site_aniso_U_22
 _atom_site_aniso_U_33
 _atom_site_aniso_U_23
 _atom_site_aniso_U_13
 _atom_site_aniso_U_12
C26 0.058(7) 0.049(8) 0.076(8) 0.004(6) 0.048(6) -0.004(6)
C27 0.069(8) 0.049(8) 0.092(9) -0.002(7) 0.045(7) 0.002(7)
C28 0.053(7) 0.065(8) 0.048(6) -0.019(6) 0.011(5) -0.002(6)
C1 0.039(6) 0.073(8) 0.050(6) 0.005(6) 0.019(5) 0.001(6)
C2 0.069(8) 0.044(8) 0.071(8) 0.003(6) 0.023(7) 0.017(6)
C3 0.078(8) 0.060(9) 0.063(8) -0.009(6) 0.038(7) -0.004(7)
N3 0.048(5) 0.052(6) 0.032(5) -0.005(4) 0.013(4) -0.022(5)
C6 0.085(8) 0.050(8) 0.082(8) 0.002(6) 0.055(7) -0.011(7)
O5 0.058(4) 0.041(4) 0.053(5) -0.002(4) 0.031(4) 0.010(4)
O1 0.040(5) 0.052(5) 0.070(5) -0.009(4) 0.022(4) 0.001(4)
O4 0.058(4) 0.034(4) 0.080(5) 0.016(4) 0.038(4) 0.003(3)
C12 0.051(7) 0.070(8) 0.067(7) -0.012(6) 0.038(6) 0.007(6)
N4 0.068(6) 0.053(6) 0.053(5) 0.004(4) 0.038(5) 0.009(5)
C13 0.048(7) 0.044(7) 0.039(7) -0.001(6) 0.017(5) 0.005(6)
C16 0.042(6) 0.023(7) 0.049(7) 0.004(6) -0.002(5) 0.006(5)
C17 0.049(6) 0.056(8) 0.037(6) -0.014(6) 0.016(5) 0.002(6)
C18 0.032(6) 0.049(7) 0.060(7) 0.002(6) 0.029(5) -0.014(5)
O3 0.087(6) 0.114(7) 0.050(5) -0.010(5) 0.026(4) -0.050(5)
C23 0.086(9) 0.071(9) 0.054(7) 0.000(6) 0.018(7) 0.007(7)
C25 0.050(6) 0.042(7) 0.050(6) 0.000(6) 0.017(5) -0.002(6)

_geom_special_details
;
 All esds (except the esd in the dihedral angle between two l.s. planes)
 are estimated using the full covariance matrix. The cell esds are taken
 into account individually in the estimation of esds in distances, angles
 and torsion angles; correlations between esds in cell parameters are only
 used when they are defined by crystal symmetry. An approximate (isotropic)
 treatment of cell esds is used for estimating esds involving l.s. planes.
;

```
loop_
 _geom_bond_atom_site_label_1
 _geom_bond_atom_site_label_2
 _geom_bond_distance
 _geom_bond_site_symmetry_2
 _geom_bond_publ_flag
C26 C2 1.365(11) . ?
C26 C17 1.386(12) . ?
C27 C6 1.335(11) . ?
C27 C17 1.394(12) . ?
C28 N4 1.485(10) . ?
C28 C17 1.506(11) . ?
C1 C12 1.179(11) . ?
C1 C25 1.450(12) . ?
C2 C25 1.371(12) . ?
C3 C23 1.170(12) . ?
C3 C12 1.348(13) . ?
N3 C13 1.321(10) . ?
N3 C18 1.439(9) . ?
C6 C25 1.391(12) . ?
O5 C16 1.235(10) . ?
O4 C16 1.261(10) . ?
C13 O3 1.229(10) . ?
C13 C13 1.537(17) 3_776 ?
C16 C18 1.522(11) . ?

loop_
 _geom_angle_atom_site_label_1
 _geom_angle_atom_site_label_2
 _geom_angle_atom_site_label_3
 _geom_angle
 _geom_angle_site_symmetry_1
 _geom_angle_site_symmetry_3
 _geom_angle_publ_flag
C2 C26 C17 120.1(9) . . ?
C6 C27 C17 120.7(10) . . ?
N4 C28 C17 111.8(7) . . ?
C12 C1 C25 178.1(11) . . ?
C26 C2 C25 121.2(9) . . ?
C23 C3 C12 177.3(12) . . ?
C13 N3 C18 123.5(7) . . ?
C27 C6 C25 121.4(10) . . ?
C1 C12 C3 176.8(11) . . ?
O3 C13 N3 124.5(8) . . ?
O3 C13 C13 119.1(13) . 3_776 ?
```

N3 C13 C13 116.4(12) . 3_776 ?
O5 C16 O4 127.4(9) . . ?
O5 C16 C18 117.7(9) . . ?
O4 C16 C18 114.9(9) . . ?
C26 C17 C27 118.4(8) . . ?
C26 C17 C28 119.7(10) . . ?
C27 C17 C28 121.8(10) . . ?
N3 C18 C16 114.6(8) . . ?
C2 C25 C6 118.2(9) . . ?
C2 C25 C1 120.4(10) . . ?
C6 C25 C1 121.4(10) . . ?

_diffrn_measured_fraction_theta_max 0.893
_diffrn_reflns_theta_full 28.39
_diffrn_measured_fraction_theta_full 0.893
_refine_diff_density_max 0.358
_refine_diff_density_min -0.299
_refine_diff_density_rms 0.079

18/H_2OG methanol solvate

```
data_zl39m

_audit_creation_method            SHELXL-97
_chemical_name_systematic
;
 ?
;
_chemical_name_common              ?
_chemical_melting_point           ?
_chemical_formula_moiety          ?
_chemical_formula_sum
 'C30 H34 N4 O8'
_chemical_formula_weight          578.61

loop_
 _atom_type_symbol
 _atom_type_description
 _atom_type_scat_dispersion_real
 _atom_type_scat_dispersion_imag
 _atom_type_scat_source
'C'  'C'   0.0033   0.0016
 'International Tables Vol C Tables 4.2.6.8 and 6.1.1.4'
 'H'  'H'   0.0000   0.0000
 'International Tables Vol C Tables 4.2.6.8 and 6.1.1.4'
 'N'  'N'   0.0061   0.0033
 'International Tables Vol C Tables 4.2.6.8 and 6.1.1.4'
 'O'  'O'   0.0106   0.0060
 'International Tables Vol C Tables 4.2.6.8 and 6.1.1.4'

_symmetry_cell_setting            Monoclinic
_symmetry_space_group_name_H-M    P21/c

loop_
 _symmetry_equiv_pos_as_xyz
 'x, y, z'
 '-x, y+1/2, -z+1/2'
 '-x, -y, -z'
 'x, -y-1/2, z-1/2'

_cell_length_a                    13.594(5)
_cell_length_b                    8.266(3)
_cell_length_c                    13.865(5)
_cell_angle_alpha                  90.00
_cell_angle_beta                   100.435(6)
```

```
_cell_angle_gamma                90.00
_cell_volume                     1532.3(10)
_cell_formula_units_Z            2
_cell_measurement_temperature    273(2)
_cell_measurement_reflns_used    214
_cell_measurement_theta_min      3.05
_cell_measurement_theta_max      11.85

_exptl_crystal_description       ?
_exptl_crystal_colour            ?
_exptl_crystal_size_max          ?
_exptl_crystal_size_mid          ?
_exptl_crystal_size_min          ?
_exptl_crystal_density_meas      0
_exptl_crystal_density_diffrn    1.254
_exptl_crystal_density_method    'not measured'
_exptl_crystal_F_000             612
_exptl_absorpt_coefficient_mu    0.092
_exptl_absorpt_correction_type   none
_exptl_absorpt_correction_T_min  ?
_exptl_absorpt_correction_T_max  ?
_exptl_absorpt_process_details   ?

_exptl_special_details
;
 ?
;

_diffrn_ambient_temperature      273(2)
_diffrn_radiation_wavelength     0.71073
_diffrn_radiation_type           MoK\a
_diffrn_radiation_source         'fine-focus sealed tube'
_diffrn_radiation_monochromator  graphite
_diffrn_measurement_device_type  'CCD area detector'
_diffrn_measurement_method       'phi and omega scans'
_diffrn_detector_area_resol_mean  ?
_diffrn_standards_number         ?
_diffrn_standards_interval_count  ?
_diffrn_standards_interval_time  ?
_diffrn_standards_decay_%        ?
_diffrn_reflns_number            9328
_diffrn_reflns_av_R_equivalents  0.5040
_diffrn_reflns_av_sigmaI/netI    0.9525
_diffrn_reflns_limit_h_min       -17
_diffrn_reflns_limit_h_max       17
_diffrn_reflns_limit_k_min       -8
```

```
_diffrn_reflns_limit_k_max       10
_diffrn_reflns_limit_l_min       -18
_diffrn_reflns_limit_l_max       12
_diffrn_reflns_theta_min         1.52
_diffrn_reflns_theta_max         28.64
_reflns_number_total             3522
_reflns_number_gt                544
_reflns_threshold_expression     >2sigma(I)

_computing_data_collection       'Bruker SMART'
_computing_cell_refinement       'Bruker SMART'
_computing_data_reduction        'Bruker SAINT'
_computing_structure_solution    'SHELXS-97 (Sheldrick, 1990)'
_computing_structure_refinement   'SHELXL-97 (Sheldrick, 1997)'
_computing_molecular_graphics    'Bruker SHELXTL'
_computing_publication_material   'Bruker SHELXTL'

_refine_special_details
;
 Refinement of F^2^ against ALL reflections.  The weighted R-factor wR and
 goodness of fit S are based on F^2^, conventional R-factors R are based
 on F, with F set to zero for negative F^2^. The threshold expression of
 F^2^ > 2sigma(F^2^) is used only for calculating R-factors(gt) etc. and is
 not relevant to the choice of reflections for refinement.  R-factors based
 on F^2^ are statistically about twice as large as those based on F, and R-
 factors based on ALL data will be even larger.
;

_refine_ls_structure_factor_coef  Fsqd
_refine_ls_matrix_type           full
_refine_ls_weighting_scheme      calc
_refine_ls_weighting_details
 'calc w=1/[\s^2^(Fo^2^)+(0.0003P)^2^+0.0000P] where P=(Fo^2^+2Fc^2^)/3'
_atom_sites_solution_primary     direct
_atom_sites_solution_secondary    difmap
_atom_sites_solution_hydrogens    geom
_refine_ls_hydrogen_treatment    mixed
_refine_ls_extinction_method     none
_refine_ls_extinction_coef       ?
_refine_ls_number_reflns         3522
_refine_ls_number_parameters     193
_refine_ls_number_restraints     0
_refine_ls_R_factor_all          0.4736
_refine_ls_R_factor_gt           0.0974
_refine_ls_wR_factor_ref         0.3831
_refine_ls_wR_factor_gt          0.2081
```

```
_refine_ls_goodness_of_fit_ref    0.833
_refine_ls_restrained_S_all       0.833
_refine_ls_shift/su_max           0.001
_refine_ls_shift/su_mean          0.000

loop_
 _atom_site_label
 _atom_site_type_symbol
 _atom_site_fract_x
 _atom_site_fract_y
 _atom_site_fract_z
 _atom_site_U_iso_or_equiv
 _atom_site_adp_type
 _atom_site_occupancy
 _atom_site_symmetry_multiplicity
 _atom_site_calc_flag
 _atom_site_refinement_flags
 _atom_site_disorder_assembly
 _atom_site_disorder_group
C9 C 0.4950(8) 0.2470(14) 0.5078(9) 0.076(4) Uani 1 1 d . . .
C6 C 0.7028(9) 0.2374(12) 0.7073(8) 0.067(3) Uani 1 1 d . . .
H6 H 0.7289 0.3083 0.6664 0.081 Uiso 1 1 calc R . .
N1 N 0.0219(5) 1.0680(9) 0.3850(5) 0.048(2) Uani 1 1 d . . .
H1 H 0.0101 1.1681 0.3956 0.058 Uiso 1 1 calc R . .
C13 C 0.0494(7) 1.0206(11) 0.2916(6) 0.052(3) Uani 1 1 d . . .
H13A H 0.0990 0.9352 0.3038 0.062 Uiso 1 1 calc R . .
H13B H 0.0801 1.1125 0.2652 0.062 Uiso 1 1 calc R . .
O1 O 0.0320(5) 0.8153(9) 0.4509(5) 0.063(2) Uani 1 1 d . . .
O3 O -0.0097(5) 0.9218(7) 0.1347(5) 0.053(2) Uani 1 1 d . . .
C10 C 0.4254(9) 0.2838(13) 0.4250(10) 0.076(4) Uani 1 1 d . . .
C5 C 0.6120(9) 0.1737(14) 0.6753(9) 0.063(3) Uani 1 1 d . . .
C2 C 0.7224(8) 0.0947(13) 0.8583(8) 0.054(3) Uani 1 1 d . . .
N2 N 0.8637(5) -0.0566(8) 0.9565(5) 0.054(2) Uani 1 1 d . . .
H2A H 0.8400 -0.1520 0.9332 0.081 Uiso 1 1 calc R . .
H2B H 0.8996 -0.0696 1.0164 0.081 Uiso 1 1 calc R . .
H2C H 0.9023 -0.0153 0.9172 0.081 Uiso 1 1 calc R . .
C3 C 0.6283(9) 0.0260(14) 0.8251(9) 0.081(4) Uani 1 1 d . . .
H3 H 0.6034 -0.0478 0.8653 0.098 Uiso 1 1 calc R . .
C12 C 0.0150(7) 0.9573(13) 0.4543(7) 0.046(3) Uani 1 1 d . . .
C1 C 0.7781(8) 0.0564(11) 0.9610(7) 0.061(3) Uani 1 1 d . . .
H1A H 0.8033 0.1557 0.9937 0.073 Uiso 1 1 calc R . .
H1B H 0.7325 0.0069 0.9987 0.073 Uiso 1 1 calc R . .
C8 C 0.5514(8) 0.2122(13) 0.5817(9) 0.068(3) Uani 1 1 d . . .
C7 C 0.7597(8) 0.2026(12) 0.7987(9) 0.061(3) Uani 1 1 d . . .
H7 H 0.8216 0.2513 0.8191 0.073 Uiso 1 1 calc R . .
O4 O 0.2157(7) 0.1461(10) 0.6227(7) 0.099(3) Uani 1 1 d . . .
```

H3A H 0.2097 0.1026 0.6745 0.148 Uiso 1 1 calc R . .
C15 C 0.2726(10) 0.0497(16) 0.5736(11) 0.115(5) Uani 1 1 d . . .
H15A H 0.2748 0.0959 0.5106 0.172 Uiso 1 1 calc R . .
H15B H 0.2435 -0.0564 0.5652 0.172 Uiso 1 1 calc R . .
H15C H 0.3392 0.0420 0.6108 0.172 Uiso 1 1 calc R . .
O2 O -0.1236(6) 0.9611(9) 0.2304(5) 0.073(3) Uani 1 1 d . . .
C11 C 0.3624(11) 0.3103(16) 0.3581(10) 0.113(5) Uani 1 1 d . . .
H11 H 0.3121 0.3314 0.3046 0.136 Uiso 1 1 calc R . .
C4 C 0.5719(8) 0.0625(15) 0.7368(9) 0.078(4) Uani 1 1 d . . .
H4 H 0.5090 0.0166 0.7169 0.093 Uiso 1 1 calc R . .
C14 C -0.0388(9) 0.9617(12) 0.2146(8) 0.051(3) Uani 1 1 d . . .

loop_
 _atom_site_aniso_label
 _atom_site_aniso_U_11
 _atom_site_aniso_U_22
 _atom_site_aniso_U_33
 _atom_site_aniso_U_23
 _atom_site_aniso_U_13
 _atom_site_aniso_U_12
C9 0.075(9) 0.111(11) 0.040(8) -0.001(8) 0.006(7) 0.008(8)
C6 0.075(9) 0.075(9) 0.054(9) 0.019(7) 0.014(7) 0.024(8)
N1 0.079(6) 0.047(6) 0.020(5) -0.001(4) 0.011(4) 0.003(5)
C13 0.074(7) 0.061(7) 0.028(6) -0.006(5) 0.028(6) -0.017(6)
O1 0.101(6) 0.052(5) 0.039(5) -0.003(4) 0.023(4) 0.011(5)
O3 0.080(5) 0.052(5) 0.030(4) -0.004(3) 0.019(4) -0.001(4)
C10 0.096(10) 0.075(9) 0.053(10) -0.004(7) 0.008(8) 0.000(8)
C5 0.052(8) 0.071(9) 0.065(9) 0.001(7) 0.009(8) 0.015(7)
C2 0.053(7) 0.060(8) 0.047(7) -0.008(6) 0.008(6) -0.004(6)
N2 0.065(6) 0.070(6) 0.029(5) 0.006(4) 0.016(4) -0.005(5)
C3 0.070(8) 0.099(10) 0.070(9) 0.027(8) -0.001(7) -0.007(8)
C12 0.055(7) 0.048(8) 0.034(7) 0.009(6) 0.006(5) 0.001(6)
C1 0.072(8) 0.067(8) 0.046(7) 0.000(6) 0.013(6) 0.018(7)
C8 0.075(9) 0.075(9) 0.056(9) -0.010(7) 0.018(7) 0.010(7)
C7 0.052(7) 0.063(9) 0.069(9) 0.002(7) 0.015(7) -0.014(6)
O4 0.108(7) 0.094(7) 0.106(8) 0.031(6) 0.051(6) 0.010(6)
C15 0.123(12) 0.106(12) 0.134(14) 0.041(10) 0.072(11) 0.003(10)
O2 0.062(5) 0.111(7) 0.049(5) -0.004(4) 0.018(4) 0.016(5)
C11 0.130(13) 0.147(14) 0.053(10) -0.005(9) -0.008(9) 0.000(10)
C4 0.060(8) 0.105(11) 0.062(9) 0.011(8) -0.004(7) -0.006(8)
C14 0.083(9) 0.033(6) 0.032(7) -0.004(5) -0.001(7) 0.015(7)

_geom_special_details
;
 All esds (except the esd in the dihedral angle between two l.s. planes)
 are estimated using the full covariance matrix. The cell esds are taken

```
 into account individually in the estimation of esds in distances, angles
 and torsion angles; correlations between esds in cell parameters are only
 used when they are defined by crystal symmetry.  An approximate (isotropic)
 treatment of cell esds is used for estimating esds involving l.s. planes.
;

loop_
 _geom_bond_atom_site_label_1
 _geom_bond_atom_site_label_2
 _geom_bond_distance
 _geom_bond_site_symmetry_2
 _geom_bond_publ_flag
C9 C8 1.198(13) . ?
C9 C10 1.383(14) . ?
C6 C5 1.342(13) . ?
C6 C7 1.390(12) . ?
N1 C12 1.343(11) . ?
N1 C13 1.465(11) . ?
C13 C14 1.534(12) . ?
O1 C12 1.199(9) . ?
O3 C14 1.285(12) . ?
C10 C11 1.163(13) . ?
C5 C4 1.427(14) . ?
C5 C8 1.441(15) . ?
C2 C7 1.373(13) . ?
C2 C3 1.400(13) . ?
C2 C1 1.520(12) . ?
N2 C1 1.503(10) . ?
C3 C4 1.356(13) . ?
C12 C12 1.566(19) 3_576 ?
O4 C15 1.373(13) . ?
O2 C14 1.212(12) . ?

loop_
 _geom_angle_atom_site_label_1
 _geom_angle_atom_site_label_2
 _geom_angle_atom_site_label_3
 _geom_angle
 _geom_angle_site_symmetry_1
 _geom_angle_site_symmetry_3
 _geom_angle_publ_flag
C8 C9 C10 176.7(13) . . ?
C5 C6 C7 123.2(11) . . ?
C12 N1 C13 120.8(8) . . ?
N1 C13 C14 114.1(8) . . ?
C11 C10 C9 175.8(14) . . ?
```

C6 C5 C4 118.9(11) . . ?
C6 C5 C8 123.5(12) . . ?
C4 C5 C8 117.6(11) . . ?
C7 C2 C3 118.7(10) . . ?
C7 C2 C1 121.6(10) . . ?
C3 C2 C1 119.6(11) . . ?
C4 C3 C2 122.7(12) . . ?
O1 C12 N1 126.8(10) . . ?
O1 C12 C12 123.6(12) . 3_576 ?
N1 C12 C12 109.5(11) . 3_576 ?
N2 C1 C2 110.4(8) . . ?
C9 C8 C5 174.7(12) . . ?
C2 C7 C6 118.6(10) . . ?
C3 C4 C5 117.9(11) . . ?
O2 C14 O3 127.4(10) . . ?
O2 C14 C13 121.6(10) . . ?
O3 C14 C13 110.9(10) . . ?

_diffrn_measured_fraction_theta_max 0.896
_diffrn_reflns_theta_full 28.64
_diffrn_measured_fraction_theta_full 0.896
_refine_diff_density_max 0.251
_refine_diff_density_min -0.262
_refine_diff_density_rms 0.070

$(18H)_2$OG monomer

```
data_zl23t

_audit_creation_method            SHELXL-97
_chemical_name_systematic
;
 ?
;
_chemical_name_common             ?
_chemical_melting_point           ?
_chemical_formula_moiety          ?
_chemical_formula_sum
 'C28 H26 N4 O6'
_chemical_formula_weight          514.53

loop_
 _atom_type_symbol
 _atom_type_description
 _atom_type_scat_dispersion_real
 _atom_type_scat_dispersion_imag
 _atom_type_scat_source
 'C'  'C'   0.0033   0.0016
 'International Tables Vol C Tables 4.2.6.8 and 6.1.1.4'
 'H'  'H'   0.0000   0.0000
 'International Tables Vol C Tables 4.2.6.8 and 6.1.1.4'
 'N'  'N'   0.0061   0.0033
 'International Tables Vol C Tables 4.2.6.8 and 6.1.1.4'
 'O'  'O'   0.0106   0.0060
 'International Tables Vol C Tables 4.2.6.8 and 6.1.1.4'

_symmetry_cell_setting            Triclinic
_symmetry_space_group_name_H-M    P-1

loop_
 _symmetry_equiv_pos_as_xyz
 'x, y, z'
 '-x, -y, -z'

_cell_length_a                    4.931(3)
_cell_length_b                    10.017(7)
_cell_length_c                    13.738(9)
_cell_angle_alpha                 85.899(14)
_cell_angle_beta                  84.56(2)
_cell_angle_gamma                 85.141(16)
_cell_volume                      671.7(8)
```

```
_cell_formula_units_Z            1
_cell_measurement_temperature    273(2)
_cell_measurement_reflns_used    ?
_cell_measurement_theta_min      ?
_cell_measurement_theta_max      ?

_exptl_crystal_description       ?
_exptl_crystal_colour            ?
_exptl_crystal_size_max          ?
_exptl_crystal_size_mid          ?
_exptl_crystal_size_min          ?
_exptl_crystal_density_meas      0
_exptl_crystal_density_diffrn    1.272
_exptl_crystal_density_method    'not measured'
_exptl_crystal_F_000             270
_exptl_absorpt_coefficient_mu    0.091
_exptl_absorpt_correction_type   none
_exptl_absorpt_correction_T_min  ?
_exptl_absorpt_correction_T_max  ?
_exptl_absorpt_process_details   ?

_exptl_special_details
;
 ?
;

_diffrn_ambient_temperature      273(2)
_diffrn_radiation_wavelength     0.71073
_diffrn_radiation_type           MoK\a
_diffrn_radiation_source         'fine-focus sealed tube'
_diffrn_radiation_monochromator  graphite
_diffrn_measurement_device_type  'CCD area detector'
_diffrn_measurement_method       'phi and omega scans'
_diffrn_detector_area_resol_mean ?
_diffrn_standards_number         ?
_diffrn_standards_interval_count ?
_diffrn_standards_interval_time  ?
_diffrn_standards_decay_%        ?
_diffrn_reflns_number            4339
_diffrn_reflns_av_R_equivalents  0.1403
_diffrn_reflns_av_sigmaI/netI    0.7053
_diffrn_reflns_limit_h_min       -5
_diffrn_reflns_limit_h_max       6
_diffrn_reflns_limit_k_min       -13
_diffrn_reflns_limit_k_max       13
_diffrn_reflns_limit_l_min       -18
```

```
_diffrn_reflns_limit_l_max       12
_diffrn_reflns_theta_min         1.49
_diffrn_reflns_theta_max         28.61
_reflns_number_total             2971
_reflns_number_gt                426
_reflns_threshold_expression     >2sigma(I)

_computing_data_collection       'Bruker SMART'
_computing_cell_refinement       'Bruker SMART'
_computing_data_reduction        'Bruker SAINT'
_computing_structure_solution    'SHELXS-97 (Sheldrick, 1990)'
_computing_structure_refinement  'SHELXL-97 (Sheldrick, 1997)'
_computing_molecular_graphics    'Bruker SHELXTL'
_computing_publication_material  'Bruker SHELXTL'

_refine_special_details
;
Refinement of F^2^ against ALL reflections.  The weighted R-factor wR and
goodness of fit S are based on F^2^, conventional R-factors R are based
on F, with F set to zero for negative F^2^. The threshold expression of
F^2^ > 2sigma(F^2^) is used only for calculating R-factors(gt) etc. and is
not relevant to the choice of reflections for refinement.  R-factors based
on F^2^ are statistically about twice as large as those based on F, and R-
factors based on ALL data will be even larger.
;

_refine_ls_structure_factor_coef  Fsqd
_refine_ls_matrix_type           full
_refine_ls_weighting_scheme      calc
_refine_ls_weighting_details
'calc w=1/[\s^2^(Fo^2^)+(0.0852P)^2^+0.0000P] where P=(Fo^2^+2Fc^2^)/3'
_atom_sites_solution_primary     direct
_atom_sites_solution_secondary   difmap
_atom_sites_solution_hydrogens   geom
_refine_ls_hydrogen_treatment    mixed
_refine_ls_extinction_method     none
_refine_ls_extinction_coef       ?
_refine_ls_number_reflns         2971
_refine_ls_number_parameters     173
_refine_ls_number_restraints     0
_refine_ls_R_factor_all          0.3917
_refine_ls_R_factor_gt           0.0781
_refine_ls_wR_factor_ref         0.2551
_refine_ls_wR_factor_gt          0.1611
_refine_ls_goodness_of_fit_ref   0.623
_refine_ls_restrained_S_all      0.623
```

```
_refine_ls_shift/su_max          0.016
_refine_ls_shift/su_mean         0.004

loop_
 _atom_site_label
 _atom_site_type_symbol
 _atom_site_fract_x
 _atom_site_fract_y
 _atom_site_fract_z
 _atom_site_U_iso_or_equiv
 _atom_site_adp_type
 _atom_site_occupancy
 _atom_site_symmetry_multiplicity
 _atom_site_calc_flag
 _atom_site_refinement_flags
 _atom_site_disorder_assembly
 _atom_site_disorder_group
O2 O 1.0967(9) 0.1456(5) 0.0162(4) 0.0577(16) Uani 1 1 d . . .
O1 O 1.2717(9) 0.4200(5) 0.0599(4) 0.0635(17) Uani 1 1 d . . .
O3 O 1.2175(10) 0.0901(5) 0.1682(4) 0.072(2) Uani 1 1 d . . .
N2 N 0.8316(11) 0.3798(6) 0.0785(4) 0.0526(19) Uani 1 1 d . . .
H2 H 0.6683 0.4037 0.0634 0.063 Uiso 1 1 calc R . .
N1 N 0.6237(10) 0.1483(6) 0.9149(4) 0.058(2) Uani 1 1 d . . .
H1A H 0.4646 0.1472 0.9513 0.087 Uiso 1 1 calc R . .
H1B H 0.7576 0.1527 0.9534 0.087 Uiso 1 1 calc R . .
H1C H 0.6530 0.0738 0.8826 0.087 Uiso 1 1 calc R . .
C1 C 0.6171(14) 0.2667(8) 0.8441(5) 0.060(2) Uani 1 1 d . . .
H1D H 0.7986 0.2737 0.8110 0.072 Uiso 1 1 calc R . .
H1E H 0.5704 0.3468 0.8798 0.072 Uiso 1 1 calc R . .
C2 C 0.4190(14) 0.2628(9) 0.7686(6) 0.048(2) Uani 1 1 d . . .
C3 C 0.0708(16) 0.2617(10) 0.6198(6) 0.064(3) Uani 1 1 d . . .
C4 C 0.1629(15) 0.1454(9) 0.6664(6) 0.070(3) Uani 1 1 d . . .
H4 H 0.1075 0.0648 0.6485 0.084 Uiso 1 1 calc R . .
C5 C 0.8785(14) 0.2675(8) 0.1489(5) 0.053(2) Uani 1 1 d . . .
H5A H 0.7067 0.2287 0.1688 0.064 Uiso 1 1 calc R . .
H5B H 0.9441 0.2998 0.2066 0.064 Uiso 1 1 calc R . .
C6 C -0.2686(18) 0.2465(10) 0.4842(7) 0.084(3) Uani 1 1 d . . .
C7 C 0.1485(15) 0.3811(9) 0.6487(6) 0.068(3) Uani 1 1 d . . .
H7 H 0.0832 0.4623 0.6189 0.082 Uiso 1 1 calc R . .
C8 C 1.0390(17) 0.4462(7) 0.0370(6) 0.052(2) Uani 1 1 d . . .
C9 C 0.3229(15) 0.3799(9) 0.7218(6) 0.067(3) Uani 1 1 d . . .
H9 H 0.3763 0.4609 0.7396 0.080 Uiso 1 1 calc R . .
C10 C -0.1218(17) 0.2600(9) 0.5455(6) 0.071(3) Uani 1 1 d . . .
C11 C 0.3355(15) 0.1428(10) 0.7394(6) 0.078(3) Uani 1 1 d . . .
H11 H 0.3971 0.0612 0.7695 0.093 Uiso 1 1 calc R . .
C12 C -0.4412(18) 0.2227(10) 0.4156(7) 0.086(3) Uani 1 1 d . . .
```

```
C13 C 1.0862(16) 0.1585(9) 0.1079(7) 0.053(2) Uani 1 1 d . . .
C14 C -0.5816(17) 0.1997(11) 0.3573(6) 0.108(4) Uani 1 1 d . . .
H14 H -0.6947 0.1812 0.3103 0.130 Uiso 1 1 calc R . .

loop_
 _atom_site_aniso_label
 _atom_site_aniso_U_11
 _atom_site_aniso_U_22
 _atom_site_aniso_U_33
 _atom_site_aniso_U_23
 _atom_site_aniso_U_13
 _atom_site_aniso_U_12
O2 0.055(3) 0.060(4) 0.059(4) -0.005(3) -0.012(3) -0.001(3)
O1 0.034(3) 0.064(4) 0.093(5) 0.017(3) -0.025(3) -0.004(3)
O3 0.075(4) 0.075(4) 0.068(5) -0.015(4) -0.031(3) 0.020(3)
N2 0.031(4) 0.063(5) 0.061(5) 0.001(4) -0.002(4) -0.002(4)
N1 0.057(4) 0.065(5) 0.055(5) -0.008(4) -0.013(4) -0.002(4)
C1 0.062(5) 0.066(6) 0.053(6) -0.005(5) -0.015(5) -0.007(5)
C2 0.039(5) 0.069(6) 0.037(5) -0.005(5) -0.003(4) 0.002(5)
C3 0.062(6) 0.079(8) 0.050(6) -0.001(6) -0.020(5) 0.008(6)
C4 0.065(6) 0.081(7) 0.068(7) -0.019(6) -0.024(5) -0.007(5)
C5 0.041(5) 0.065(6) 0.050(6) -0.002(5) 0.006(4) -0.002(4)
C6 0.074(7) 0.120(9) 0.056(7) -0.002(7) -0.009(6) 0.004(6)
C7 0.064(6) 0.072(7) 0.066(7) 0.002(6) -0.015(5) 0.013(5)
C8 0.038(5) 0.054(6) 0.066(7) -0.006(5) -0.017(5) 0.006(5)
C9 0.063(6) 0.082(7) 0.056(7) -0.012(6) -0.003(5) 0.001(5)
C10 0.074(7) 0.103(8) 0.036(6) 0.004(6) -0.007(5) -0.008(6)
C11 0.074(6) 0.093(8) 0.072(7) -0.005(6) -0.043(6) -0.001(5)
C12 0.057(6) 0.148(10) 0.052(7) -0.009(7) -0.005(5) 0.000(6)
C13 0.042(6) 0.065(7) 0.056(7) -0.015(6) -0.005(5) -0.011(5)
C14 0.068(7) 0.216(13) 0.041(7) -0.010(8) -0.009(5) -0.006(7)

_geom_special_details
;
 All esds (except the esd in the dihedral angle between two l.s. planes)
 are estimated using the full covariance matrix.  The cell esds are taken
 into account individually in the estimation of esds in distances, angles
 and torsion angles; correlations between esds in cell parameters are only
 used when they are defined by crystal symmetry.  An approximate (isotropic)
 treatment of cell esds is used for estimating esds involving l.s. planes.
;

loop_
 _geom_bond_atom_site_label_1
 _geom_bond_atom_site_label_2
 _geom_bond_distance
```

```
 _geom_bond_site_symmetry_2
 _geom_bond_publ_flag
O2 C13 1.271(8) . ?
O1 C8 1.220(7) . ?
O3 C13 1.233(8) . ?
N2 C8 1.328(8) . ?
N2 C5 1.448(8) . ?
N1 C1 1.480(8) . ?
C1 C2 1.495(8) . ?
C2 C9 1.368(9) . ?
C2 C11 1.400(9) . ?
C3 C4 1.354(10) . ?
C3 C7 1.382(10) . ?
C3 C10 1.460(10) . ?
C4 C11 1.373(8) . ?
C5 C13 1.533(9) . ?
C6 C10 1.183(10) . ?
C6 C12 1.375(10) . ?
C7 C9 1.381(9) . ?
C8 C8 1.481(14) 2_765 ?
C12 C14 1.154(10) . ?

loop_
 _geom_angle_atom_site_label_1
 _geom_angle_atom_site_label_2
 _geom_angle_atom_site_label_3
 _geom_angle
 _geom_angle_site_symmetry_1
 _geom_angle_site_symmetry_3
 _geom_angle_publ_flag
C8 N2 C5 120.4(6) . . ?
N1 C1 C2 114.1(7) . . ?
C9 C2 C11 117.5(7) . . ?
C9 C2 C1 119.6(8) . . ?
C11 C2 C1 122.8(8) . . ?
C4 C3 C7 118.6(8) . . ?
C4 C3 C10 120.0(9) . . ?
C7 C3 C10 121.2(9) . . ?
C3 C4 C11 122.0(9) . . ?
N2 C5 C13 112.6(6) . . ?
C10 C6 C12 176.3(12) . . ?
C9 C7 C3 120.0(8) . . ?
O1 C8 N2 121.9(7) . . ?
O1 C8 C8 123.9(11) . 2_765 ?
N2 C8 C8 114.1(9) . 2_765 ?
C2 C9 C7 121.7(8) . . ?
```

C6 C10 C3 173.8(10) . . ?
C4 C11 C2 120.1(8) . . ?
C14 C12 C6 178.2(11) . . ?
O3 C13 O2 127.3(8) . . ?
O3 C13 C5 116.2(8) . . ?
O2 C13 C5 116.4(7) . . ?

_diffrn_measured_fraction_theta_max 0.860
_diffrn_reflns_theta_full 28.61
_diffrn_measured_fraction_theta_full 0.860
_refine_diff_density_max 0.247
_refine_diff_density_min -0.266
_refine_diff_density_rms 0.063

$(18H)_2OG$ polymer

```
data_zl23kt

_audit_creation_method            SHELXL-97
_chemical_name_systematic
;
 ?
;
_chemical_name_common             ?
_chemical_melting_point           ?
_chemical_formula_moiety          ?
_chemical_formula_sum
 'C28 H26 N4 O6'
_chemical_formula_weight          514.53

loop_
 _atom_type_symbol
 _atom_type_description
 _atom_type_scat_dispersion_real
 _atom_type_scat_dispersion_imag
 _atom_type_scat_source
 'C'  'C'   0.0033   0.0016
 'International Tables Vol C Tables 4.2.6.8 and 6.1.1.4'
 'H'  'H'   0.0000   0.0000
 'International Tables Vol C Tables 4.2.6.8 and 6.1.1.4'
 'N'  'N'   0.0061   0.0033
 'International Tables Vol C Tables 4.2.6.8 and 6.1.1.4'
 'O'  'O'   0.0106   0.0060
 'International Tables Vol C Tables 4.2.6.8 and 6.1.1.4'

_symmetry_cell_setting            Triclinic
_symmetry_space_group_name_H-M    P-1

loop_
 _symmetry_equiv_pos_as_xyz
 'x, y, z'
 '-x, -y, -z'

_cell_length_a                    4.8862(19)
_cell_length_b                    10.072(4)
_cell_length_c                    13.670(5)
_cell_angle_alpha                 79.154(6)
_cell_angle_beta                  88.615(9)
_cell_angle_gamma                 85.662(8)
_cell_volume                      658.8(4)
```

```
_cell_formula_units_Z            1
_cell_measurement_temperature    273(2)
_cell_measurement_reflns_used    ?
_cell_measurement_theta_min      ?
_cell_measurement_theta_max      ?

_exptl_crystal_description       ?
_exptl_crystal_colour            ?
_exptl_crystal_size_max          ?
_exptl_crystal_size_mid          ?
_exptl_crystal_size_min          ?
_exptl_crystal_density_meas      0
_exptl_crystal_density_diffrn    1.297
_exptl_crystal_density_method    'not measured'
_exptl_crystal_F_000             270
_exptl_absorpt_coefficient_mu    0.093
_exptl_absorpt_correction_type   none
_exptl_absorpt_correction_T_min  ?
_exptl_absorpt_correction_T_max  ?
_exptl_absorpt_process_details   ?

_exptl_special_details
;
 ?
;

_diffrn_ambient_temperature      273(2)
_diffrn_radiation_wavelength     0.71073
_diffrn_radiation_type           MoK\a
_diffrn_radiation_source         'fine-focus sealed tube'
_diffrn_radiation_monochromator  graphite
_diffrn_measurement_device_type  'CCD area detector'
_diffrn_measurement_method       'phi and omega scans'
_diffrn_detector_area_resol_mean  ?
_diffrn_standards_number         ?
_diffrn_standards_interval_count  ?
_diffrn_standards_interval_time  ?
_diffrn_standards_decay_%        ?
_diffrn_reflns_number            4233
_diffrn_reflns_av_R_equivalents  0.1199
_diffrn_reflns_av_sigmaI/netI    0.7420
_diffrn_reflns_limit_h_min       -6
_diffrn_reflns_limit_h_max       6
_diffrn_reflns_limit_k_min       -13
_diffrn_reflns_limit_k_max       13
_diffrn_reflns_limit_l_min       -17
```

```
_diffrn_reflns_limit_l_max       8
_diffrn_reflns_theta_min         1.52
_diffrn_reflns_theta_max         28.50
_reflns_number_total             2916
_reflns_number_gt                339
_reflns_threshold_expression     >2sigma(I)

_computing_data_collection       'Bruker SMART'
_computing_cell_refinement       'Bruker SMART'
_computing_data_reduction        'Bruker SAINT'
_computing_structure_solution    'SHELXS-97 (Sheldrick, 1990)'
_computing_structure_refinement  'SHELXL-97 (Sheldrick, 1997)'
_computing_molecular_graphics    'Bruker SHELXTL'
_computing_publication_material  'Bruker SHELXTL'

_refine_special_details
;
Refinement of F^2^ against ALL reflections.  The weighted R-factor wR and
goodness of fit S are based on F^2^, conventional R-factors R are based
on F, with F set to zero for negative F^2^. The threshold expression of
F^2^ > 2sigma(F^2^) is used only for calculating R-factors(gt) etc. and is
not relevant to the choice of reflections for refinement.  R-factors based
on F^2^ are statistically about twice as large as those based on F, and R-
factors based on ALL data will be even larger.
;

_refine_ls_structure_factor_coef  Fsqd
_refine_ls_matrix_type           full
_refine_ls_weighting_scheme      calc
_refine_ls_weighting_details
'calc w=1/[\s^2^(Fo^2^)+(0.0319P)^2^+0.0000P] where P=(Fo^2^+2Fc^2^)/3'
_atom_sites_solution_primary     direct
_atom_sites_solution_secondary   difmap
_atom_sites_solution_hydrogens   geom
_refine_ls_hydrogen_treatment    mixed
_refine_ls_extinction_method     none
_refine_ls_extinction_coef       ?
_refine_ls_number_reflns         2916
_refine_ls_number_parameters     193
_refine_ls_number_restraints     0
_refine_ls_R_factor_all          0.4372
_refine_ls_R_factor_gt           0.0624
_refine_ls_wR_factor_ref         0.1577
_refine_ls_wR_factor_gt          0.0944
_refine_ls_goodness_of_fit_ref   0.649
_refine_ls_restrained_S_all      0.649
```

```
_refine_ls_shift/su_max          0.000
_refine_ls_shift/su_mean         0.000

loop_
 _atom_site_label
 _atom_site_type_symbol
 _atom_site_fract_x
 _atom_site_fract_y
 _atom_site_fract_z
 _atom_site_U_iso_or_equiv
 _atom_site_adp_type
 _atom_site_occupancy
 _atom_site_symmetry_multiplicity
 _atom_site_calc_flag
 _atom_site_refinement_flags
 _atom_site_disorder_assembly
 _atom_site_disorder_group
O2 O 0.0913(13) 0.1444(6) 0.0163(5) 0.105(2) Uani 1 1 d . . .
O3 O 0.2502(11) 0.0635(5) 0.1663(4) 0.106(2) Uani 1 1 d . . .
N2 N 0.4031(10) 0.8389(5) 0.0862(4) 0.102(2) Uani 1 1 d . . .
H2C H 0.3714 0.9083 0.1177 0.153 Uiso 1 1 calc R . .
H2B H 0.2604 0.8342 0.0480 0.153 Uiso 1 1 calc R . .
H2A H 0.5533 0.8508 0.0483 0.153 Uiso 1 1 calc R . .
C11 C 0.4440(16) 0.7091(7) 0.1616(6) 0.098(3) Uani 1 1 d . . .
H11A H 0.2675 0.6722 0.1782 0.118 Uiso 1 1 calc R . .
H11B H 0.5583 0.6435 0.1323 0.118 Uiso 1 1 calc R . .
C10 C 0.574(2) 0.7298(11) 0.2540(8) 0.092(3) Uani 1 1 d . . .
C6 C 0.8329(19) 0.8402(10) 0.3541(10) 0.124(4) Uani 1 1 d . . .
H6 H 0.9708 0.8981 0.3570 0.149 Uiso 1 1 calc R . .
C7 C 0.744(2) 0.8246(9) 0.2643(8) 0.106(3) Uani 1 1 d . . .
H7 H 0.8025 0.8819 0.2075 0.127 Uiso 1 1 calc R . .
C4 C 0.759(3) 0.8157(11) 0.5405(11) 0.090(4) Uani 0.78 1 d P . .
C1 C 0.557(2) 0.8389(10) 0.6078(8) 0.126(4) Uani 1 1 d . . .
H1 H 0.5971 0.8600 0.6690 0.152 Uiso 1 1 calc R . .
C9 C 0.471(2) 0.6572(11) 0.3433(11) 0.090(4) Uani 0.78 1 d P . .
H9 H 0.3484 0.5920 0.3398 0.108 Uiso 0.80 1 calc PR . .
C8 C 0.542(3) 0.6779(12) 0.4360(10) 0.110(5) Uani 0.78 1 d P . .
H8 H 0.4666 0.6276 0.4930 0.132 Uiso 0.80 1 calc PR . .
C3 C 1.047(3) 0.8265(11) 0.5692(8) 0.153(4) Uani 1 1 d . . .
C5 C 0.719(2) 0.7694(15) 0.4445(11) 0.099(4) Uani 0.78 1 d P . .
C2 C 0.295(3) 0.8295(14) 0.5805(11) 0.130(6) Uani 0.78 1 d P . .
O1 O 0.2886(11) 0.4145(5) 0.0619(5) 0.115(2) Uani 1 1 d . . .
N1 N -0.1519(13) 0.3670(7) 0.0815(5) 0.090(2) Uani 1 1 d . . .
H1A H -0.3204 0.3936 0.0679 0.108 Uiso 1 1 calc R . .
C12 C 0.044(2) 0.4376(8) 0.0384(7) 0.090(3) Uani 1 1 d . . .
C13 C -0.0866(14) 0.2442(8) 0.1520(6) 0.087(3) Uani 1 1 d . . .
```

H13B H -0.2543 0.2020 0.1750 0.105 Uiso 1 1 calc R . .
H13A H 0.0027 0.2654 0.2092 0.105 Uiso 1 1 calc R . .
C14 C 0.100(2) 0.1471(10) 0.1050(9) 0.093(4) Uani 1 1 d . . .
C9B C 0.702(6) 0.592(3) 0.288(2) 0.061(9) Uiso 0.22 1 d P . .
H9B H 0.6707 0.5183 0.2591 0.074 Uiso 0.20 1 calc PR . .
C8B C 0.887(6) 0.582(3) 0.375(2) 0.077(10) Uiso 0.22 1 d P . .
H8B H 0.9299 0.4980 0.4147 0.093 Uiso 0.20 1 calc PR . .
C5B C 0.994(8) 0.693(4) 0.398(3) 0.101(12) Uiso 0.22 1 d P . .
C2B C 0.526(17) 0.708(7) 0.596(6) 0.29(4) Uiso 0.22 1 d P . .
C3B C 0.230(9) 0.719(3) 0.487(3) 0.113(13) Uiso 0.22 1 d P . .

loop_
 _atom_site_aniso_label
 _atom_site_aniso_U_11
 _atom_site_aniso_U_22
 _atom_site_aniso_U_33
 _atom_site_aniso_U_23
 _atom_site_aniso_U_13
 _atom_site_aniso_U_12
O2 0.111(5) 0.112(5) 0.097(5) -0.029(5) -0.010(5) -0.012(3)
O3 0.130(5) 0.089(5) 0.100(5) -0.027(4) -0.012(4) 0.002(4)
N2 0.116(5) 0.095(5) 0.098(6) -0.022(5) -0.008(5) -0.018(4)
C11 0.145(8) 0.066(6) 0.080(7) -0.001(6) -0.003(6) -0.016(6)
C10 0.103(8) 0.093(9) 0.076(9) 0.004(7) -0.028(7) -0.021(6)
C6 0.103(8) 0.145(10) 0.121(10) 0.012(9) -0.064(9) -0.053(7)
C7 0.115(9) 0.088(8) 0.118(11) -0.018(7) -0.006(7) -0.025(6)
C4 0.053(10) 0.116(11) 0.109(12) -0.031(9) -0.009(10) -0.019(8)
C1 0.075(8) 0.169(11) 0.145(10) -0.053(8) 0.041(9) -0.022(7)
C9 0.095(10) 0.099(10) 0.076(9) -0.012(9) -0.012(9) -0.021(7)
C8 0.120(12) 0.101(10) 0.101(13) 0.023(9) -0.041(10) -0.051(8)
C3 0.142(12) 0.202(11) 0.123(9) -0.049(8) 0.016(11) -0.028(11)
C5 0.083(10) 0.133(13) 0.078(11) -0.001(11) 0.009(9) -0.040(8)
C2 0.079(11) 0.182(15) 0.129(12) -0.013(10) 0.003(12) -0.054(13)
O1 0.090(4) 0.106(5) 0.145(6) -0.005(4) -0.012(4) -0.020(4)
N1 0.095(6) 0.077(6) 0.094(6) -0.006(5) 0.016(5) -0.015(5)
C12 0.099(8) 0.085(8) 0.084(9) -0.004(6) 0.008(8) -0.028(8)
C13 0.077(6) 0.087(7) 0.097(8) -0.016(7) 0.009(6) -0.011(5)
C14 0.090(9) 0.068(8) 0.123(12) -0.020(9) -0.013(9) -0.019(6)

_geom_special_details
;
 All esds (except the esd in the dihedral angle between two l.s. planes)
 are estimated using the full covariance matrix. The cell esds are taken
 into account individually in the estimation of esds in distances, angles
 and torsion angles; correlations between esds in cell parameters are only
 used when they are defined by crystal symmetry. An approximate (isotropic)

treatment of cell esds is used for estimating esds involving l.s. planes.
;

loop_
 _geom_bond_atom_site_label_1
 _geom_bond_atom_site_label_2
 _geom_bond_distance
 _geom_bond_site_symmetry_2
 _geom_bond_publ_flag
O2 C14 1.220(9) . ?
O3 C14 1.272(10) . ?
N2 C11 1.508(6) . ?
C11 C10 1.484(9) . ?
C10 C7 1.340(9) . ?
C10 C9 1.403(11) . ?
C10 C9B 1.48(3) . ?
C6 C7 1.353(9) . ?
C6 C5 1.429(11) . ?
C4 C1 1.371(13) . ?
C4 C3 1.489(12) . ?
C4 C5 1.496(13) . ?
C1 C2 1.358(13) . ?
C9 C8 1.380(11) . ?
C8 C5 1.331(12) . ?
C3 C2 1.225(12) 1_655 ?
C3 C3B 1.87(4) 1_655 ?
C2 C3 1.225(12) 1_455 ?
C2 C2B 1.59(7) . ?
C2 C3B 1.90(4) . ?
O1 C12 1.241(9) . ?
N1 C12 1.297(9) . ?
N1 C13 1.438(7) . ?
C12 C12 1.519(16) 2_565 ?
C13 C14 1.508(10) . ?
C9B C8B 1.49(3) . ?
C8B C5B 1.36(4) . ?
C5B C3B 1.76(4) 1_655 ?
C2B C3B 2.09(9) . ?
C3B C3 1.87(4) 1_455 ?
C3B C5B 1.76(4) 1_455 ?

loop_
 _geom_angle_atom_site_label_1
 _geom_angle_atom_site_label_2
 _geom_angle_atom_site_label_3
 _geom_angle

```
 _geom_angle_site_symmetry_1
 _geom_angle_site_symmetry_3
 _geom_angle_publ_flag
C10 C11 N2 112.3(7) . . ?
C7 C10 C9 115.3(10) . . ?
C7 C10 C11 128.0(11) . . ?
C9 C10 C11 115.7(11) . . ?
C7 C10 C9B 111.5(13) . . ?
C9 C10 C9B 63.6(12) . . ?
C11 C10 C9B 99.5(14) . . ?
C7 C6 C5 121.1(11) . . ?
C10 C7 C6 122.6(10) . . ?
C1 C4 C3 117.2(13) . . ?
C1 C4 C5 125.9(11) . . ?
C3 C4 C5 116.7(12) . . ?
C2 C1 C4 116.6(11) . . ?
C8 C9 C10 123.2(11) . . ?
C5 C8 C9 120.4(13) . . ?
C2 C3 C4 171.0(14) 1_655 . ?
C2 C3 C3B 72.1(15) 1_655 1_655 ?
C4 C3 C3B 99.4(16) . 1_655 ?
C8 C5 C6 116.8(13) . . ?
C8 C5 C4 122.2(14) . . ?
C6 C5 C4 120.0(14) . . ?
C3 C2 C1 170.4(16) 1_455 . ?
C3 C2 C2B 129(4) 1_455 . ?
C1 C2 C2B 55(3) . . ?
C3 C2 C3B 70.0(15) 1_455 . ?
C1 C2 C3B 118.8(18) . . ?
C2B C2 C3B 73(3) . . ?
C12 N1 C13 120.0(7) . . ?
O1 C12 N1 123.8(9) . . ?
O1 C12 C12 119.6(12) . 2_565 ?
N1 C12 C12 116.4(11) . 2_565 ?
N1 C13 C14 110.5(7) . . ?
O2 C14 O3 123.6(12) . . ?
O2 C14 C13 121.7(11) . . ?
O3 C14 C13 114.5(10) . . ?
C10 C9B C8B 113(2) . . ?
C5B C8B C9B 122(3) . . ?
C8B C5B C3B 135(4) . 1_655 ?
C2 C2B C3B 60(3) . . ?
C2B C3B C2 47(2) . . ?
C2B C3B C3 80(3) . 1_455 ?
C2 C3B C3 37.9(9) . 1_455 ?
C2B C3B C5B 169(3) . 1_455 ?
```

C2 C3B C5B 143(3) . 1_455 ?
C3 C3B C5B 108(3) 1_455 1_455 ?

_diffrn_measured_fraction_theta_max 0.867
_diffrn_reflns_theta_full 28.50
_diffrn_measured_fraction_theta_full 0.867
_refine_diff_density_max 0.134
_refine_diff_density_min -0.127
_refine_diff_density_rms 0.036

$(35H)_2OG$

```
data_zl81m

_audit_creation_method            SHELXL-97
_chemical_name_systematic
;
 ?
;
_chemical_name_common             ?
_chemical_melting_point           ?
_chemical_formula_moiety          ?
_chemical_formula_sum
 'C29 H30 N4 O6'
_chemical_formula_weight          530.57

loop_
 _atom_type_symbol
 _atom_type_description
 _atom_type_scat_dispersion_real
 _atom_type_scat_dispersion_imag
 _atom_type_scat_source
 'C'  'C'   0.0033   0.0016
 'International Tables Vol C Tables 4.2.6.8 and 6.1.1.4'
 'H'  'H'   0.0000   0.0000
 'International Tables Vol C Tables 4.2.6.8 and 6.1.1.4'
 'N'  'N'   0.0061   0.0033
 'International Tables Vol C Tables 4.2.6.8 and 6.1.1.4'
 'O'  'O'   0.0106   0.0060
 'International Tables Vol C Tables 4.2.6.8 and 6.1.1.4'

_symmetry_cell_setting            Triclinic
_symmetry_space_group_name_H-M    P-1

loop_
 _symmetry_equiv_pos_as_xyz
 'x, y, z'
 '-x, -y, -z'

_cell_length_a                    4.823(8)
_cell_length_b                    5.745(9)
_cell_length_c                    24.72(4)
_cell_angle_alpha                 87.73(3)
_cell_angle_beta                  87.84(3)
_cell_angle_gamma                 82.93(3)
_cell_volume                      678.7(19)
```

```
_cell_formula_units_Z            1
_cell_measurement_temperature    273(2)
_cell_measurement_reflns_used    ?
_cell_measurement_theta_min      ?
_cell_measurement_theta_max      ?

_exptl_crystal_description       ?
_exptl_crystal_colour            ?
_exptl_crystal_size_max          ?
_exptl_crystal_size_mid          ?
_exptl_crystal_size_min          ?
_exptl_crystal_density_meas      0
_exptl_crystal_density_diffrn    1.298
_exptl_crystal_density_method    'not measured'
_exptl_crystal_F_000             280
_exptl_absorpt_coefficient_mu    0.092
_exptl_absorpt_correction_type   none
_exptl_absorpt_correction_T_min  ?
_exptl_absorpt_correction_T_max  ?
_exptl_absorpt_process_details   ?

_exptl_special_details
;
 ?
;

_diffrn_ambient_temperature      273(2)
_diffrn_radiation_wavelength     0.71073
_diffrn_radiation_type           MoK\a
_diffrn_radiation_source         'fine-focus sealed tube'
_diffrn_radiation_monochromator  graphite
_diffrn_measurement_device_type  'CCD area detector'
_diffrn_measurement_method       'phi and omega scans'
_diffrn_detector_area_resol_mean  ?
_diffrn_standards_number         ?
_diffrn_standards_interval_count  ?
_diffrn_standards_interval_time  ?
_diffrn_standards_decay_%        ?
_diffrn_reflns_number            4254
_diffrn_reflns_av_R_equivalents  0.2447
_diffrn_reflns_av_sigmaI/netI    0.9706
_diffrn_reflns_limit_h_min       -6
_diffrn_reflns_limit_h_max       6
_diffrn_reflns_limit_k_min       -7
_diffrn_reflns_limit_k_max       7
_diffrn_reflns_limit_l_min       -31
```

```
_diffrn_reflns_limit_l_max       21
_diffrn_reflns_theta_min         1.65
_diffrn_reflns_theta_max         28.60
_reflns_number_total             2958
_reflns_number_gt                386
_reflns_threshold_expression     >2sigma(I)

_computing_data_collection       'Bruker SMART'
_computing_cell_refinement       'Bruker SMART'
_computing_data_reduction        'Bruker SAINT'
_computing_structure_solution    'SHELXS-97 (Sheldrick, 1990)'
_computing_structure_refinement  'SHELXL-97 (Sheldrick, 1997)'
_computing_molecular_graphics    'Bruker SHELXTL'
_computing_publication_material  'Bruker SHELXTL'

_refine_special_details
;
Refinement of F^2^ against ALL reflections.  The weighted R-factor wR and
goodness of fit S are based on F^2^, conventional R-factors R are based
on F, with F set to zero for negative F^2^. The threshold expression of
F^2^ > 2sigma(F^2^) is used only for calculating R-factors(gt) etc. and is
not relevant to the choice of reflections for refinement.  R-factors based
on F^2^ are statistically about twice as large as those based on F, and R-
factors based on ALL data will be even larger.
;

_refine_ls_structure_factor_coef  Fsqd
_refine_ls_matrix_type           full
_refine_ls_weighting_scheme      calc
_refine_ls_weighting_details
'calc w=1/[\s^2^(Fo^2^)+(0.2000P)^2^+0.0000P] where P=(Fo^2^+2Fc^2^)/3'
_atom_sites_solution_primary     direct
_atom_sites_solution_secondary   difmap
_atom_sites_solution_hydrogens   geom
_refine_ls_hydrogen_treatment    mixed
_refine_ls_extinction_method     none
_refine_ls_extinction_coef       ?
_refine_ls_number_reflns         2958
_refine_ls_number_parameters     201
_refine_ls_number_restraints     0
_refine_ls_R_factor_all          0.5337
_refine_ls_R_factor_gt           0.2045
_refine_ls_wR_factor_ref         0.5583
_refine_ls_wR_factor_gt          0.4675
_refine_ls_goodness_of_fit_ref   0.891
_refine_ls_restrained_S_all      0.891
```

```
_refine_ls_shift/su_max          1.763
_refine_ls_shift/su_mean         0.106

loop_
 _atom_site_label
 _atom_site_type_symbol
 _atom_site_fract_x
 _atom_site_fract_y
 _atom_site_fract_z
 _atom_site_U_iso_or_equiv
 _atom_site_adp_type
 _atom_site_occupancy
 _atom_site_symmetry_multiplicity
 _atom_site_calc_flag
 _atom_site_refinement_flags
 _atom_site_disorder_assembly
 _atom_site_disorder_group
C10 C 0.418(4) 0.619(4) 0.2299(7) 0.079(6) Uani 1 1 d . . .
H10 H 0.3816 0.6740 0.1946 0.095 Uiso 1 1 calc R . .
C9 C 0.310(4) 0.430(3) 0.2475(7) 0.056(5) Uani 1 1 d . . .
C2 C 1.190(4) 1.130(4) 0.4361(8) 0.100(7) Uani 1 1 d . . .
O2 O 0.980(3) 0.822(2) 0.1340(5) 0.095(5) Uani 1 1 d . . .
C6 C 0.658(4) 0.658(4) 0.3130(7) 0.074(6) Uani 1 1 d . . .
C1 C 1.321(4) 1.287(3) 0.4744(7) 0.106(8) Uani 1 1 d . . .
H1A H 1.2781 1.4486 0.4627 0.159 Uiso 1 1 calc R . .
H1B H 1.5199 1.2458 0.4738 0.159 Uiso 1 1 calc R . .
H1C H 1.2465 1.2655 0.5105 0.159 Uiso 1 1 calc R . .
C3 C 1.092(4) 1.004(4) 0.4089(8) 0.102(8) Uani 1 1 d . . .
N2 N 0.119(3) 0.335(3) 0.1580(6) 0.092(6) Uani 1 1 d . . .
H2A H 0.0612 0.4856 0.1505 0.138 Uiso 1 1 calc R . .
H2B H 0.0064 0.2460 0.1430 0.138 Uiso 1 1 calc R . .
H2C H 0.2926 0.2997 0.1447 0.138 Uiso 1 1 calc R . .
C14 C 0.592(4) 0.857(4) 0.0721(7) 0.084(7) Uani 1 1 d . . .
C12 C 0.113(3) 0.291(3) 0.2174(8) 0.076(6) Uani 1 1 d . . .
H12A H 0.1648 0.1251 0.2250 0.092 Uiso 1 1 calc R . .
H12B H -0.0761 0.3323 0.2314 0.092 Uiso 1 1 calc R . .
O3 O 0.635(3) 1.134(3) 0.1342(5) 0.105(5) Uani 1 1 d . . .
C5 C 0.824(4) 0.769(3) 0.3481(7) 0.068(5) Uani 1 1 d . . .
C4 C 0.951(4) 0.870(4) 0.3767(7) 0.088(7) Uani 1 1 d . . .
C8 C 0.379(4) 0.324(4) 0.3010(9) 0.121(9) Uani 1 1 d . . .
H8 H 0.3086 0.1887 0.3144 0.145 Uiso 1 1 calc R . .
C11 C 0.584(3) 0.743(3) 0.2609(8) 0.070(6) Uani 1 1 d . . .
H11 H 0.6454 0.8810 0.2469 0.084 Uiso 1 1 calc R . .
C7 C 0.567(4) 0.445(4) 0.3317(8) 0.083(7) Uani 1 1 d . . .
H7 H 0.6281 0.3798 0.3648 0.099 Uiso 1 1 calc R . .
C13 C 0.765(5) 0.939(4) 0.1179(8) 0.076(6) Uani 1 1 d . . .
```

O1A O 0.761(6) 0.359(6) 0.0460(12) 0.104(11) Uani 0.50 1 d P . .
O1B O 0.971(7) 0.798(6) -0.0101(12) 0.098(11) Uani 0.50 1 d P . .
C21 C 0.886(6) 0.598(8) 0.0189(12) 0.139(18) Uani 1 1 d . . .
N1B N 0.80(2) 0.768(12) 0.036(4) 0.55(9) Uani 0.50 1 d P . .
N1A N 0.759(8) 0.595(11) 0.0503(16) 0.088(16) Uani 0.50 1 d P . .

loop_
 _atom_site_aniso_label
 _atom_site_aniso_U_11
 _atom_site_aniso_U_22
 _atom_site_aniso_U_33
 _atom_site_aniso_U_23
 _atom_site_aniso_U_13
 _atom_site_aniso_U_12
C10 0.104(16) 0.109(18) 0.032(11) 0.007(12) -0.012(11) -0.045(15)
C9 0.067(13) 0.056(12) 0.042(12) -0.018(11) -0.023(10) 0.014(10)
C2 0.077(15) 0.140(19) 0.080(16) -0.024(16) -0.035(13) 0.018(14)
O2 0.133(13) 0.100(11) 0.058(9) -0.020(8) -0.058(9) -0.013(9)
C6 0.106(16) 0.093(17) 0.024(11) -0.001(12) -0.001(11) -0.022(14)
C1 0.128(19) 0.145(19) 0.063(14) -0.004(14) -0.007(13) -0.090(16)
C3 0.084(15) 0.131(18) 0.098(16) -0.069(15) -0.066(13) 0.002(13)
N2 0.113(14) 0.128(14) 0.050(10) -0.017(10) 0.009(9) -0.071(11)
C14 0.073(14) 0.138(18) 0.047(12) -0.071(12) 0.020(10) -0.015(12)
C12 0.066(13) 0.085(14) 0.085(15) -0.021(13) -0.029(11) -0.023(11)
O3 0.065(9) 0.150(13) 0.106(11) -0.086(10) 0.024(8) -0.022(8)
C5 0.073(13) 0.069(13) 0.062(13) -0.009(11) -0.017(11) 0.002(11)
C4 0.058(13) 0.143(19) 0.064(13) -0.063(14) -0.018(11) 0.009(12)
C8 0.102(18) 0.18(2) 0.095(18) -0.077(19) -0.003(15) -0.036(17)
C11 0.059(12) 0.068(13) 0.081(15) -0.015(13) -0.022(11) 0.015(10)
C7 0.069(14) 0.096(16) 0.082(16) -0.032(15) -0.039(12) 0.014(13)
C13 0.071(16) 0.098(17) 0.058(14) -0.015(13) 0.013(12) 0.004(13)
O1A 0.13(3) 0.10(2) 0.08(2) -0.009(19) 0.062(19) -0.04(2)
O1B 0.12(3) 0.13(3) 0.047(18) 0.01(2) -0.052(18) -0.01(2)
C21 0.10(3) 0.31(6) 0.023(18) 0.02(3) -0.039(16) -0.09(3)
N1B 1.1(2) 0.32(7) 0.32(12) -0.20(8) 0.15(11) -0.57(12)
N1A 0.06(3) 0.18(5) 0.03(2) -0.03(3) -0.04(2) 0.00(3)

_geom_special_details
;
 All esds (except the esd in the dihedral angle between two l.s. planes)
 are estimated using the full covariance matrix. The cell esds are taken
 into account individually in the estimation of esds in distances, angles
 and torsion angles; correlations between esds in cell parameters are only
 used when they are defined by crystal symmetry. An approximate (isotropic)
 treatment of cell esds is used for estimating esds involving l.s. planes.
;

```
loop_
 _geom_bond_atom_site_label_1
 _geom_bond_atom_site_label_2
 _geom_bond_distance
 _geom_bond_site_symmetry_2
 _geom_bond_publ_flag
C10 C9 1.31(2) . ?
C10 C11 1.40(2) . ?
C9 C8 1.47(2) . ?
C9 C12 1.54(2) . ?
C2 C3 1.16(2) . ?
C2 C1 1.54(3) . ?
O2 C13 1.23(2) . ?
C6 C7 1.40(2) . ?
C6 C11 1.40(2) . ?
C6 C5 1.42(2) . ?
C3 C4 1.38(2) . ?
N2 C12 1.48(2) . ?
C14 N1B 1.39(12) . ?
C14 C13 1.55(2) . ?
C14 N1A 1.71(6) . ?
O3 C13 1.29(2) . ?
C5 C4 1.17(2) . ?
C8 C7 1.46(2) . ?
O1A C21 1.67(5) . ?
O1A O1B 1.72(4) 2_765 ?
O1B C21 1.43(5) . ?
O1B O1A 1.72(4) 2_765 ?
C21 N1A 0.97(4) . ?
C21 N1B 1.11(9) . ?
C21 C21 1.75(8) 2_765 ?

loop_
 _geom_angle_atom_site_label_1
 _geom_angle_atom_site_label_2
 _geom_angle_atom_site_label_3
 _geom_angle
 _geom_angle_site_symmetry_1
 _geom_angle_site_symmetry_3
 _geom_angle_publ_flag
C9 C10 C11 124.0(18) . . ?
C10 C9 C8 120.4(18) . . ?
C10 C9 C12 127.3(18) . . ?
C8 C9 C12 112.3(19) . . ?
C3 C2 C1 177(2) . . ?
```

C7 C6 C11 117.9(19) . . ?
C7 C6 C5 117.3(17) . . ?
C11 C6 C5 125(2) . . ?
C2 C3 C4 174(2) . . ?
N1B C14 C13 101(4) . . ?
N1B C14 N1A 39(4) . . ?
C13 C14 N1A 107.9(18) . . ?
N2 C12 C9 114.0(16) . . ?
C4 C5 C6 177(2) . . ?
C5 C4 C3 176(2) . . ?
C7 C8 C9 115(2) . . ?
C10 C11 C6 119.9(19) . . ?
C6 C7 C8 122(2) . . ?
O2 C13 O3 131(2) . . ?
O2 C13 C14 122.5(19) . . ?
O3 C13 C14 106.9(19) . . ?
C21 O1A O1B 86(2) . 2_765 ?
C21 O1B O1A 95(3) . 2_765 ?
N1A C21 N1B 62(8) . . ?
N1A C21 O1B 128(7) . . ?
N1B C21 O1B 65(7) . . ?
N1A C21 O1A 55(5) . . ?
N1B C21 O1A 117(8) . . ?
O1B C21 O1A 173(2) . . ?
N1A C21 C21 139(7) . 2_765 ?
N1B C21 C21 157(9) . 2_765 ?
O1B C21 C21 93(3) . 2_765 ?
O1A C21 C21 86(4) . 2_765 ?
C21 N1B C14 139(10) . . ?
C21 N1A C14 118(7) . . ?

_diffrn_measured_fraction_theta_max 0.846
_diffrn_reflns_theta_full 28.60
_diffrn_measured_fraction_theta_full 0.846
_refine_diff_density_max 0.509
_refine_diff_density_min -0.365
_refine_diff_density_rms 0.116

20 hydrate

```
data_zl48m1

_audit_creation_method           SHELXL-97
_chemical_name_systematic
;
 ?
;
_chemical_name_common            ?
_chemical_melting_point          ?
_chemical_formula_moiety         ?
_chemical_formula_sum
 'C8.33 H6.67 O4.17'
_chemical_formula_weight         173.47

loop_
 _atom_type_symbol
 _atom_type_description
 _atom_type_scat_dispersion_real
 _atom_type_scat_dispersion_imag
 _atom_type_scat_source
 'C'  'C'   0.0033   0.0016
 'International Tables Vol C Tables 4.2.6.8 and 6.1.1.4'
 'H'  'H'   0.0000   0.0000
 'International Tables Vol C Tables 4.2.6.8 and 6.1.1.4'
 'O'  'O'   0.0106   0.0060
 'International Tables Vol C Tables 4.2.6.8 and 6.1.1.4'

_symmetry_cell_setting           triclinic
_symmetry_space_group_name_H-M    P-1

loop_
 _symmetry_equiv_pos_as_xyz
 'x, y, z'
 '-x, y+1/2, -z+1/2'
 '-x, -y, -z'
 'x, -y-1/2, z-1/2'

_cell_length_a                   11.257(17)
_cell_length_b                   16.53(3)
_cell_length_c                   7.273(11)
_cell_angle_alpha                 90.00
_cell_angle_beta                  97.04(3)
_cell_angle_gamma                   90.00
_cell_volume                     1343(4)
```

```
_cell_formula_units_Z            6
_cell_measurement_temperature    273(2)
_cell_measurement_reflns_used    ?
_cell_measurement_theta_min      ?
_cell_measurement_theta_max      ?

_exptl_crystal_description       ?
_exptl_crystal_colour            ?
_exptl_crystal_size_max          ?
_exptl_crystal_size_mid          ?
_exptl_crystal_size_min          ?
_exptl_crystal_density_meas      ?
_exptl_crystal_density_diffrn    1.287
_exptl_crystal_density_method    'not measured'
_exptl_crystal_F_000             540
_exptl_absorpt_coefficient_mu    0.105
_exptl_absorpt_correction_type   ?
_exptl_absorpt_correction_T_min  ?
_exptl_absorpt_correction_T_max  ?
_exptl_absorpt_process_details   ?

_exptl_special_details
;
 ?
;

_diffrn_ambient_temperature      273(2)
_diffrn_radiation_wavelength     0.71073
_diffrn_radiation_type           MoK\a
_diffrn_radiation_source         'fine-focus sealed tube'
_diffrn_radiation_monochromator  graphite
_diffrn_measurement_device_type  ?
_diffrn_measurement_method       ?
_diffrn_detector_area_resol_mean ?
_diffrn_standards_number         ?
_diffrn_standards_interval_count ?
_diffrn_standards_interval_time  ?
_diffrn_standards_decay_%        ?
_diffrn_reflns_number            6925
_diffrn_reflns_av_R_equivalents  0.3205
_diffrn_reflns_av_sigmaI/netI    0.5607
_diffrn_reflns_limit_h_min       -13
_diffrn_reflns_limit_h_max       14
_diffrn_reflns_limit_k_min       -21
_diffrn_reflns_limit_k_max       21
_diffrn_reflns_limit_l_min       -8
```

```
_diffrn_reflns_limit_l_max       9
_diffrn_reflns_theta_min         1.82
_diffrn_reflns_theta_max         28.29
_reflns_number_total             2925
_reflns_number_gt                419
_reflns_threshold_expression     >2sigma(I)

_computing_data_collection       ?
_computing_cell_refinement       ?
_computing_data_reduction        ?
_computing_structure_solution    'SHELXS-97 (Sheldrick, 1990)'
_computing_structure_refinement  'SHELXL-97 (Sheldrick, 1997)'
_computing_molecular_graphics    ?
_computing_publication_material  ?

_refine_special_details
;
 Refinement of F^2^ against ALL reflections.  The weighted R-factor wR and
 goodness of fit S are based on F^2^, conventional R-factors R are based
 on F, with F set to zero for negative F^2^. The threshold expression of
 F^2^ > 2sigma(F^2^) is used only for calculating R-factors(gt) etc. and is
 not relevant to the choice of reflections for refinement.  R-factors based
 on F^2^ are statistically about twice as large as those based on F, and R-
 factors based on ALL data will be even larger.
;

_refine_ls_structure_factor_coef  Fsqd
_refine_ls_matrix_type           full
_refine_ls_weighting_scheme      calc
_refine_ls_weighting_details
 'calc w=1/[\s^2^(Fo^2^)+(0.2000P)^2^+0.0000P] where P=(Fo^2^+2Fc^2^)/3'
_atom_sites_solution_primary     direct
_atom_sites_solution_secondary   difmap
_atom_sites_solution_hydrogens   geom
_refine_ls_hydrogen_treatment    mixed
_refine_ls_extinction_method     none
_refine_ls_extinction_coef       ?
_refine_ls_number_reflns         2925
_refine_ls_number_parameters     162
_refine_ls_number_restraints     0
_refine_ls_R_factor_all          0.5040
_refine_ls_R_factor_gt           0.1764
_refine_ls_wR_factor_ref         0.5301
_refine_ls_wR_factor_gt          0.4197
_refine_ls_goodness_of_fit_ref   0.941
_refine_ls_restrained_S_all      0.941
```

```
_refine_ls_shift/su_max          0.569
_refine_ls_shift/su_mean         0.047

loop_
 _atom_site_label
 _atom_site_type_symbol
 _atom_site_fract_x
 _atom_site_fract_y
 _atom_site_fract_z
 _atom_site_U_iso_or_equiv
 _atom_site_adp_type
 _atom_site_occupancy
 _atom_site_symmetry_multiplicity
 _atom_site_calc_flag
 _atom_site_refinement_flags
 _atom_site_disorder_assembly
 _atom_site_disorder_group
O3 O 0.5254(9) 0.1251(5) 0.7403(15) 0.083(4) Uani 1 1 d . . .
O1 O 0.5280(10) 0.4243(5) 0.7345(17) 0.097(4) Uani 1 1 d . . .
C1 C 0.3604(14) 0.3494(8) 0.8124(19) 0.062(4) Uani 1 1 d . . .
C2 C 0.2510(15) 0.2051(7) 0.867(2) 0.077(5) Uani 1 1 d . . .
H2 H 0.2146 0.1564 0.8907 0.092 Uiso 1 1 calc R . .
C3 C 0.2496(12) 0.3488(8) 0.865(2) 0.064(4) Uani 1 1 d . . .
H3 H 0.2147 0.3978 0.8910 0.077 Uiso 1 1 calc R . .
C4 C 0.3613(13) 0.2049(7) 0.819(2) 0.056(4) Uani 1 1 d . . .
C5 C 0.0681(13) 0.2817(9) 0.9305(19) 0.064(4) Uani 1 1 d . . .
C6 C 0.4187(14) 0.1276(9) 0.782(2) 0.074(5) Uani 1 1 d . . .
O4 O 0.3648(8) 0.0607(5) 0.8188(15) 0.087(4) Uani 1 1 d . . .
H4 H 0.4058 0.0219 0.7956 0.130 Uiso 1 1 calc R . .
C7 C 0.4227(11) 0.2739(8) 0.7924(17) 0.058(4) Uani 1 1 d . . .
H7 H 0.5007 0.2727 0.7626 0.069 Uiso 1 1 calc R . .
C8 C 0.1871(12) 0.2796(8) 0.882(2) 0.069(4) Uani 1 1 d . . .
O2 O 0.3750(9) 0.4894(5) 0.8267(16) 0.098(4) Uani 1 1 d . . .
H2A H 0.4159 0.5289 0.8080 0.147 Uiso 1 1 calc R . .
C9 C 0.4287(15) 0.4248(8) 0.784(2) 0.078(6) Uani 1 1 d . . .
C10 C -0.0282(14) 0.2884(9) 0.977(2) 0.078(5) Uani 1 1 d . . .
C11 C -0.1402(16) 0.2941(9) 1.026(3) 0.121(8) Uani 1 1 d . . .
C14 C -0.2412(17) 0.3040(13) 1.056(3) 0.154(10) Uani 1 1 d . . .
H14 H -0.3198 0.3118 1.0793 0.185 Uiso 1 1 calc R . .
H102 H -0.066(10) 0.966(8) 0.622(18) 0.12(5) Uiso 1 1 d . . .
H101 H 0.157(6) 0.923(4) 0.966(10) 0.000(19) Uiso 1 1 d . . .
O5 O 0.041(5) 0.961(2) 0.918(6) 0.64(5) Uani 1 1 d . . .

loop_
 _atom_site_aniso_label
 _atom_site_aniso_U_11
```

```
 _atom_site_aniso_U_22
 _atom_site_aniso_U_33
 _atom_site_aniso_U_23
 _atom_site_aniso_U_13
 _atom_site_aniso_U_12
O3 0.084(7) 0.043(6) 0.133(10) 0.007(6) 0.060(7) -0.003(5)
O1 0.117(9) 0.039(6) 0.146(12) 0.002(6) 0.064(8) 0.006(7)
C1 0.088(11) 0.040(9) 0.060(12) -0.008(8) 0.017(9) -0.011(9)
C2 0.124(14) 0.013(8) 0.103(14) 0.004(7) 0.048(11) 0.000(7)
C3 0.055(9) 0.056(10) 0.087(13) -0.002(9) 0.029(9) 0.005(8)
C4 0.055(9) 0.034(9) 0.084(12) 0.004(8) 0.024(9) 0.007(7)
C5 0.052(9) 0.080(11) 0.060(10) -0.005(9) 0.010(8) 0.005(9)
C6 0.093(13) 0.041(10) 0.095(15) 0.010(10) 0.039(11) 0.004(9)
O4 0.087(7) 0.031(5) 0.148(11) -0.011(7) 0.036(7) 0.002(6)
C7 0.066(9) 0.039(8) 0.073(11) -0.001(9) 0.034(8) -0.010(9)
C8 0.077(9) 0.029(8) 0.109(13) 0.001(9) 0.045(9) -0.010(8)
O2 0.114(9) 0.041(6) 0.150(11) 0.000(7) 0.059(8) 0.007(6)
C9 0.090(13) 0.028(9) 0.124(17) 0.004(10) 0.052(12) 0.009(9)
C10 0.066(10) 0.075(13) 0.093(13) -0.016(9) 0.010(10) -0.005(9)
C11 0.074(12) 0.083(15) 0.22(2) -0.004(12) 0.074(15) 0.000(10)
C14 0.084(13) 0.26(3) 0.121(18) 0.001(17) 0.026(13) 0.033(16)
O5 1.02(10) 0.31(5) 0.46(7) 0.00(4) -0.48(7) -0.21(6)

_geom_special_details
;
 All esds (except the esd in the dihedral angle between two l.s. planes)
 are estimated using the full covariance matrix.  The cell esds are taken
 into account individually in the estimation of esds in distances, angles
 and torsion angles; correlations between esds in cell parameters are only
 used when they are defined by crystal symmetry.  An approximate (isotropic)
 treatment of cell esds is used for estimating esds involving l.s. planes.
;

loop_
 _geom_bond_atom_site_label_1
 _geom_bond_atom_site_label_2
 _geom_bond_distance
 _geom_bond_site_symmetry_2
 _geom_bond_publ_flag
O3 C6 1.274(14) . ?
O1 C9 1.217(14) . ?
C1 C3 1.349(16) . ?
C1 C7 1.447(16) . ?
C1 C9 1.492(17) . ?
C2 C4 1.328(17) . ?
C2 C8 1.436(16) . ?
```

```
C3 C8 1.357(16) . ?
C4 C7 1.361(15) . ?
C4 C6 1.474(16) . ?
C5 C10 1.180(17) . ?
C5 C8 1.427(18) . ?
C6 O4 1.304(14) . ?
O2 C9 1.282(14) . ?
C10 C11 1.35(2) . ?
C11 C14 1.196(19) . ?

loop_
 _geom_angle_atom_site_label_1
 _geom_angle_atom_site_label_2
 _geom_angle_atom_site_label_3
 _geom_angle
 _geom_angle_site_symmetry_1
 _geom_angle_site_symmetry_3
 _geom_angle_publ_flag
C3 C1 C7 119.9(12) . . ?
C3 C1 C9 123.7(14) . . ?
C7 C1 C9 116.3(14) . . ?
C4 C2 C8 121.0(11) . . ?
C1 C3 C8 122.6(13) . . ?
C2 C4 C7 122.9(12) . . ?
C2 C4 C6 119.7(13) . . ?
C7 C4 C6 117.3(13) . . ?
C10 C5 C8 175.3(17) . . ?
O3 C6 O4 119.8(13) . . ?
O3 C6 C4 121.3(14) . . ?
O4 C6 C4 118.1(13) . . ?
C4 C7 C1 116.5(11) . . ?
C3 C8 C2 116.5(12) . . ?
C3 C8 C5 121.0(13) . . ?
C2 C8 C5 122.2(13) . . ?
O1 C9 O2 123.7(14) . . ?
O1 C9 C1 122.8(14) . . ?
O2 C9 C1 113.4(14) . . ?
C5 C10 C11 177.8(19) . . ?
C14 C11 C10 174(2) . . ?

_diffrn_measured_fraction_theta_max    0.879
_diffrn_reflns_theta_full              28.29
_diffrn_measured_fraction_theta_full   0.879
_refine_diff_density_max    0.582
_refine_diff_density_min   -0.452
_refine_diff_density_rms    0.135
```

20•(4PyO)$_2$

```
data_zl17t

_audit_creation_method           SHELXL-97
_chemical_name_systematic
;
 ?
;
_chemical_name_common            ?
_chemical_melting_point          ?
_chemical_formula_moiety         ?
_chemical_formula_sum
 'C38 H26 N4 O10'
_chemical_formula_weight         698.63

loop_
 _atom_type_symbol
 _atom_type_description
 _atom_type_scat_dispersion_real
 _atom_type_scat_dispersion_imag
 _atom_type_scat_source
'C'  'C'   0.0033   0.0016
 'International Tables Vol C Tables 4.2.6.8 and 6.1.1.4'
 'H'  'H'   0.0000   0.0000
 'International Tables Vol C Tables 4.2.6.8 and 6.1.1.4'
 'N'  'N'   0.0061   0.0033
 'International Tables Vol C Tables 4.2.6.8 and 6.1.1.4'
 'O'  'O'   0.0106   0.0060
 'International Tables Vol C Tables 4.2.6.8 and 6.1.1.4'

_symmetry_cell_setting           Triclinic
_symmetry_space_group_name_H-M    P-1

loop_
 _symmetry_equiv_pos_as_xyz
 'x, y, z'
 '-x, -y, -z'

_cell_length_a                  5.0431(16)
_cell_length_b                  10.771(3)
_cell_length_c                  15.611(5)
_cell_angle_alpha                86.266(6)
_cell_angle_beta                 87.933(5)
_cell_angle_gamma                    84.726(6)
_cell_volume                    842.2(5)
```

```
_cell_formula_units_Z            1
_cell_measurement_temperature    273(2)
_cell_measurement_reflns_used    ?
_cell_measurement_theta_min      ?
_cell_measurement_theta_max      ?

_exptl_crystal_description       ?
_exptl_crystal_colour            ?
_exptl_crystal_size_max          ?
_exptl_crystal_size_mid          ?
_exptl_crystal_size_min          ?
_exptl_crystal_density_meas      0
_exptl_crystal_density_diffrn    1.377
_exptl_crystal_density_method    'not measured'
_exptl_crystal_F_000             362
_exptl_absorpt_coefficient_mu    0.102
_exptl_absorpt_correction_type   none
_exptl_absorpt_correction_T_min  ?
_exptl_absorpt_correction_T_max  ?
_exptl_absorpt_process_details   ?

_exptl_special_details
;
 ?
;

_diffrn_ambient_temperature      273(2)
_diffrn_radiation_wavelength     0.71073
_diffrn_radiation_type           MoK\a
_diffrn_radiation_source         'fine-focus sealed tube'
_diffrn_radiation_monochromator  graphite
_diffrn_measurement_device_type  'CCD area detector'
_diffrn_measurement_method       'phi and omega scans'
_diffrn_detector_area_resol_mean  ?
_diffrn_standards_number         ?
_diffrn_standards_interval_count  ?
_diffrn_standards_interval_time  ?
_diffrn_standards_decay_%        ?
_diffrn_reflns_number            5081
_diffrn_reflns_av_R_equivalents  0.0605
_diffrn_reflns_av_sigmaI/netI    0.3086
_diffrn_reflns_limit_h_min       -6
_diffrn_reflns_limit_h_max       6
_diffrn_reflns_limit_k_min       -11
_diffrn_reflns_limit_k_max       14
_diffrn_reflns_limit_l_min       -17
```

```
_diffrn_reflns_limit_l_max       20
_diffrn_reflns_theta_min         1.31
_diffrn_reflns_theta_max         28.54
_reflns_number_total             3633
_reflns_number_gt                747
_reflns_threshold_expression     >2sigma(I)

_computing_data_collection       'Bruker SMART'
_computing_cell_refinement       'Bruker SMART'
_computing_data_reduction        'Bruker SAINT'
_computing_structure_solution    'SHELXS-97 (Sheldrick, 1990)'
_computing_structure_refinement  'SHELXL-97 (Sheldrick, 1997)'
_computing_molecular_graphics    'Bruker SHELXTL'
_computing_publication_material  'Bruker SHELXTL'

_refine_special_details
;
Refinement of F^2^ against ALL reflections.  The weighted R-factor wR and
goodness of fit S are based on F^2^, conventional R-factors R are based
on F, with F set to zero for negative F^2^. The threshold expression of
F^2^ > 2sigma(F^2^) is used only for calculating R-factors(gt) etc. and is
not relevant to the choice of reflections for refinement.  R-factors based
on F^2^ are statistically about twice as large as those based on F, and R-
factors based on ALL data will be even larger.
;

_refine_ls_structure_factor_coef  Fsqd
_refine_ls_matrix_type           full
_refine_ls_weighting_scheme      calc
_refine_ls_weighting_details
'calc w=1/[\s^2^(Fo^2^)+(0.2000P)^2^+0.0000P] where P=(Fo^2^+2Fc^2^)/3'
_atom_sites_solution_primary     direct
_atom_sites_solution_secondary   difmap
_atom_sites_solution_hydrogens   geom
_refine_ls_hydrogen_treatment    mixed
_refine_ls_extinction_method     none
_refine_ls_extinction_coef       ?
_refine_ls_number_reflns         3633
_refine_ls_number_parameters     235
_refine_ls_number_restraints     0
_refine_ls_R_factor_all          0.2866
_refine_ls_R_factor_gt           0.0811
_refine_ls_wR_factor_ref         0.3342
_refine_ls_wR_factor_gt          0.1957
_refine_ls_goodness_of_fit_ref   0.661
_refine_ls_restrained_S_all      0.661
```

```
_refine_ls_shift/su_max          0.040
_refine_ls_shift/su_mean         0.006

loop_
 _atom_site_label
 _atom_site_type_symbol
 _atom_site_fract_x
 _atom_site_fract_y
 _atom_site_fract_z
 _atom_site_U_iso_or_equiv
 _atom_site_adp_type
 _atom_site_occupancy
 _atom_site_symmetry_multiplicity
 _atom_site_calc_flag
 _atom_site_refinement_flags
 _atom_site_disorder_assembly
 _atom_site_disorder_group
C25 C 0.2754(14) 0.9934(6) 0.6775(4) 0.0568(19) Uani 1 1 d . . .
C2 C 0.0195(14) 0.3453(7) 0.7093(4) 0.065(2) Uani 1 1 d . . .
H2 H -0.1012 0.2865 0.7237 0.078 Uiso 1 1 calc R . .
O7 O 0.0769(10) 0.7711(5) 0.4820(3) 0.0786(17) Uani 1 1 d . . .
H7 H 0.0216 0.7253 0.4481 0.118 Uiso 1 1 calc R . .
C4 C 0.2820(13) 0.5050(6) 0.7507(4) 0.0502(18) Uani 1 1 d . . .
C6 C -0.0298(15) 0.8896(7) 0.7720(4) 0.061(2) Uani 1 1 d . . .
N3 N 0.3410(11) 0.5492(5) 0.9036(3) 0.0568(16) Uani 1 1 d . . .
H3 H 0.1815 0.5465 0.9246 0.068 Uiso 1 1 calc R . .
C10 C 0.3778(13) 0.5889(6) 0.8150(4) 0.0554(19) Uani 1 1 d . . .
H10A H 0.5661 0.5964 0.8035 0.066 Uiso 1 1 calc R . .
H10B H 0.2857 0.6715 0.8054 0.066 Uiso 1 1 calc R . .
O9 O 0.7728(10) 0.5186(5) 0.9313(3) 0.0678(16) Uani 1 1 d . . .
C13 C -0.2543(19) 0.8524(7) 0.9249(5) 0.088(3) Uani 1 1 d . . .
C15 C -0.460(3) 0.8240(9) 1.0727(6) 0.132(5) Uani 1 1 d . . .
H15 H -0.5380 0.8156 1.1274 0.158 Uiso 1 1 calc R . .
N2 N 0.1011(12) 0.3636(6) 0.6283(3) 0.0635(18) Uani 1 1 d . . .
C20 C -0.1528(16) 0.8706(7) 0.8556(5) 0.071(2) Uani 1 1 d . . .
O10 O 0.5480(10) 1.1483(5) 0.7153(3) 0.0749(16) Uani 1 1 d . . .
O8 O -0.2136(12) 0.6821(5) 0.5685(3) 0.0881(19) Uani 1 1 d . . .
C22 C -0.0469(16) 0.7575(7) 0.5542(4) 0.062(2) Uani 1 1 d . . .
C24 C 0.1566(14) 0.9764(7) 0.7584(4) 0.061(2) Uani 1 1 d . . .
H24 H 0.2015 1.0227 0.8031 0.073 Uiso 1 1 calc R . .
C27 C 0.5413(15) 0.5169(7) 0.9537(4) 0.0504(19) Uani 1 1 d . . .
C26 C 0.2679(17) 0.4487(8) 0.6064(4) 0.079(3) Uani 1 1 d . . .
H26 H 0.3247 0.4587 0.5492 0.095 Uiso 1 1 calc R . .
O11 O 0.5555(11) 1.0939(5) 0.5809(3) 0.0893(19) Uani 1 1 d . . .
H11 H 0.6636 1.1464 0.5748 0.134 Uiso 1 1 calc R . .
C30 C 0.3599(15) 0.5224(7) 0.6645(4) 0.070(2) Uani 1 1 d . . .
```

H30 H 0.4729 0.5833 0.6469 0.084 Uiso 1 1 calc R . .
C29 C 0.1111(14) 0.4122(7) 0.7726(4) 0.060(2) Uani 1 1 d . . .
H29 H 0.0593 0.3957 0.8296 0.072 Uiso 1 1 calc R . .
C32 C 0.0285(14) 0.8350(6) 0.6237(4) 0.0519(18) Uani 1 1 d . . .
C33 C 0.2081(14) 0.9229(6) 0.6115(4) 0.056(2) Uani 1 1 d . . .
H33 H 0.2876 0.9357 0.5573 0.068 Uiso 1 1 calc R . .
C35 C -0.0949(15) 0.8213(6) 0.7046(4) 0.059(2) Uani 1 1 d . . .
H35 H -0.2239 0.7650 0.7137 0.070 Uiso 1 1 calc R . .
C37 C 0.4687(15) 1.0861(7) 0.6614(4) 0.060(2) Uani 1 1 d . . .
C38 C -0.366(2) 0.8342(8) 1.0058(5) 0.104(4) Uani 1 1 d . . .

loop_
 _atom_site_aniso_label
 _atom_site_aniso_U_11
 _atom_site_aniso_U_22
 _atom_site_aniso_U_33
 _atom_site_aniso_U_23
 _atom_site_aniso_U_13
 _atom_site_aniso_U_12
C25 0.072(5) 0.051(5) 0.051(4) -0.010(4) 0.002(4) -0.024(4)
C2 0.074(5) 0.069(5) 0.059(5) -0.024(4) 0.008(4) -0.041(4)
O7 0.108(4) 0.098(4) 0.042(3) -0.027(3) 0.010(3) -0.067(4)
C4 0.057(5) 0.057(5) 0.041(4) -0.012(3) -0.002(3) -0.020(4)
C6 0.087(6) 0.053(5) 0.046(4) -0.010(4) 0.013(4) -0.028(4)
N3 0.052(4) 0.090(5) 0.033(3) -0.018(3) 0.003(3) -0.026(3)
C10 0.056(5) 0.065(5) 0.051(4) -0.002(4) -0.015(3) -0.029(4)
O9 0.044(3) 0.115(5) 0.048(3) -0.010(3) 0.001(2) -0.025(3)
C13 0.146(8) 0.074(6) 0.052(5) -0.014(4) 0.026(5) -0.055(6)
C15 0.231(13) 0.104(8) 0.070(6) -0.032(6) 0.058(7) -0.065(8)
N2 0.076(5) 0.068(4) 0.051(4) -0.013(3) 0.003(3) -0.029(4)
C20 0.102(7) 0.061(5) 0.054(5) -0.015(4) 0.021(4) -0.033(5)
O10 0.098(4) 0.078(4) 0.056(3) -0.023(3) 0.008(3) -0.037(3)
O8 0.123(5) 0.100(4) 0.054(3) -0.014(3) 0.006(3) -0.076(4)
C22 0.085(6) 0.068(5) 0.038(4) -0.011(4) 0.005(4) -0.025(5)
C24 0.076(5) 0.060(5) 0.047(4) -0.009(4) 0.007(4) -0.012(4)
C27 0.042(4) 0.072(5) 0.043(4) -0.027(4) -0.003(4) -0.024(4)
C26 0.108(7) 0.096(7) 0.042(4) -0.020(4) 0.002(4) -0.049(6)
O11 0.121(5) 0.107(4) 0.053(3) -0.029(3) 0.024(3) -0.076(4)
C30 0.088(6) 0.079(6) 0.049(4) -0.011(4) 0.006(4) -0.040(5)
C29 0.068(5) 0.066(5) 0.054(4) -0.015(4) 0.009(4) -0.037(4)
C32 0.070(5) 0.050(4) 0.040(4) -0.006(3) 0.001(3) -0.025(4)
C33 0.076(5) 0.058(5) 0.039(4) -0.013(3) 0.004(3) -0.024(4)
C35 0.079(5) 0.057(5) 0.044(4) -0.005(4) 0.006(4) -0.031(4)
C37 0.077(6) 0.059(5) 0.049(5) -0.017(4) 0.010(4) -0.023(4)
C38 0.183(10) 0.085(7) 0.049(5) -0.021(5) 0.051(6) -0.049(7)

```
_geom_special_details
;
 All esds (except the esd in the dihedral angle between two l.s. planes)
 are estimated using the full covariance matrix.  The cell esds are taken
 into account individually in the estimation of esds in distances, angles
 and torsion angles; correlations between esds in cell parameters are only
 used when they are defined by crystal symmetry.  An approximate (isotropic)
 treatment of cell esds is used for estimating esds involving l.s. planes.
;

loop_
 _geom_bond_atom_site_label_1
 _geom_bond_atom_site_label_2
 _geom_bond_distance
 _geom_bond_site_symmetry_2
 _geom_bond_publ_flag
C25 C33 1.390(9) . ?
C25 C24 1.387(8) . ?
C25 C37 1.463(9) . ?
C2 N2 1.324(8) . ?
C2 C29 1.376(9) . ?
O7 C22 1.275(7) . ?
C4 C30 1.394(8) . ?
C4 C29 1.397(8) . ?
C4 C10 1.513(8) . ?
C6 C24 1.387(9) . ?
C6 C35 1.388(9) . ?
C6 C20 1.436(9) . ?
N3 C27 1.307(8) . ?
N3 C10 1.433(7) . ?
O9 C27 1.208(7) . ?
C13 C20 1.193(9) . ?
C13 C38 1.373(10) . ?
C15 C38 1.135(10) . ?
N2 C26 1.320(9) . ?
O10 C37 1.210(8) . ?
O8 C22 1.226(8) . ?
C22 C32 1.492(9) . ?
C27 C27 1.520(12) 2_667 ?
C26 C30 1.364(9) . ?
O11 C37 1.316(7) . ?
C32 C33 1.369(9) . ?
C32 C35 1.394(8) . ?

loop_
 _geom_angle_atom_site_label_1
```

```
 _geom_angle_atom_site_label_2
 _geom_angle_atom_site_label_3
 _geom_angle
 _geom_angle_site_symmetry_1
 _geom_angle_site_symmetry_3
 _geom_angle_publ_flag
C33 C25 C24 119.8(7) . . ?
C33 C25 C37 120.0(6) . . ?
C24 C25 C37 120.2(6) . . ?
N2 C2 C29 120.8(6) . . ?
C30 C4 C29 117.4(6) . . ?
C30 C4 C10 119.1(6) . . ?
C29 C4 C10 123.4(6) . . ?
C24 C6 C35 119.7(6) . . ?
C24 C6 C20 119.8(6) . . ?
C35 C6 C20 120.5(7) . . ?
C27 N3 C10 122.4(6) . . ?
N3 C10 C4 116.0(5) . . ?
C20 C13 C38 178.1(9) . . ?
C2 N2 C26 120.4(6) . . ?
C13 C20 C6 178.7(8) . . ?
O8 C22 O7 123.0(6) . . ?
O8 C22 C32 120.3(6) . . ?
O7 C22 C32 116.6(6) . . ?
C25 C24 C6 119.3(6) . . ?
O9 C27 N3 124.4(6) . . ?
O9 C27 C27 121.6(8) . 2_667 ?
N3 C27 C27 113.9(8) . 2_667 ?
N2 C26 C30 122.4(7) . . ?
C26 C30 C4 119.0(7) . . ?
C2 C29 C4 119.8(6) . . ?
C33 C32 C35 117.7(6) . . ?
C33 C32 C22 123.2(6) . . ?
C35 C32 C22 119.0(6) . . ?
C32 C33 C25 122.0(6) . . ?
C6 C35 C32 121.5(7) . . ?
O10 C37 O11 122.4(7) . . ?
O10 C37 C25 124.9(6) . . ?
O11 C37 C25 112.7(6) . . ?
C15 C38 C13 177.4(10) . . ?

_diffrn_measured_fraction_theta_max    0.846
_diffrn_reflns_theta_full              28.54
_diffrn_measured_fraction_theta_full   0.846
_refine_diff_density_max    0.400
_refine_diff_density_min   -0.407
```

_refine_diff_density_rms 0.126

20•(4PyU)$_2$

```
data_zl54am

_audit_creation_method            SHELXL-97
_chemical_name_systematic
;
 ?
;
_chemical_name_common             ?
_chemical_melting_point           ?
_chemical_formula_moiety          ?
_chemical_formula_sum
 'C34 H26 N4 O9'
_chemical_formula_weight          634.59

loop_
 _atom_type_symbol
 _atom_type_description
 _atom_type_scat_dispersion_real
 _atom_type_scat_dispersion_imag
 _atom_type_scat_source
 'C'  'C'   0.0033   0.0016
 'International Tables Vol C Tables 4.2.6.8 and 6.1.1.4'
 'H'  'H'   0.0000   0.0000
 'International Tables Vol C Tables 4.2.6.8 and 6.1.1.4'
 'N'  'N'   0.0061   0.0033
 'International Tables Vol C Tables 4.2.6.8 and 6.1.1.4'
 'O'  'O'   0.0106   0.0060
 'International Tables Vol C Tables 4.2.6.8 and 6.1.1.4'

_symmetry_cell_setting            Triclinic
_symmetry_space_group_name_H-M    P-1

loop_
 _symmetry_equiv_pos_as_xyz
 'x, y, z'
 '-x, -y, -z'

_cell_length_a                    4.688(2)
_cell_length_b                    11.406(5)
_cell_length_c                    15.073(6)
_cell_angle_alpha                 93.945(9)
_cell_angle_beta                  95.451(9)
_cell_angle_gamma                 93.792(9)
_cell_volume                      798.3(6)
```

```
_cell_formula_units_Z            1
_cell_measurement_temperature    273(2)
_cell_measurement_reflns_used    209
_cell_measurement_theta_min      2.17
_cell_measurement_theta_max      21.86

_exptl_crystal_description       ?
_exptl_crystal_colour            ?
_exptl_crystal_size_max          ?
_exptl_crystal_size_mid          ?
_exptl_crystal_size_min          ?
_exptl_crystal_density_meas      0
_exptl_crystal_density_diffrn    1.320
_exptl_crystal_density_method    'not measured'
_exptl_crystal_F_000             330
_exptl_absorpt_coefficient_mu    0.097
_exptl_absorpt_correction_type   none
_exptl_absorpt_correction_T_min  ?
_exptl_absorpt_correction_T_max  ?
_exptl_absorpt_process_details   ?

_exptl_special_details
;
 ?
;

_diffrn_ambient_temperature      273(2)
_diffrn_radiation_wavelength     0.71073
_diffrn_radiation_type           MoK\a
_diffrn_radiation_source         'fine-focus sealed tube'
_diffrn_radiation_monochromator  graphite
_diffrn_measurement_device_type  'CCD area detector'
_diffrn_measurement_method       'phi and omega scans'
_diffrn_detector_area_resol_mean  ?
_diffrn_standards_number         ?
_diffrn_standards_interval_count  ?
_diffrn_standards_interval_time  ?
_diffrn_standards_decay_%        ?
_diffrn_reflns_number            5065
_diffrn_reflns_av_R_equivalents  0.1664
_diffrn_reflns_av_sigmaI/netI    0.5897
_diffrn_reflns_limit_h_min       -4
_diffrn_reflns_limit_h_max       6
_diffrn_reflns_limit_k_min       -15
_diffrn_reflns_limit_k_max       14
_diffrn_reflns_limit_l_min       -19
```

```
_diffrn_reflns_limit_l_max       20
_diffrn_reflns_theta_min         1.79
_diffrn_reflns_theta_max         28.48
_reflns_number_total             3484
_reflns_number_gt                633
_reflns_threshold_expression     >2sigma(I)

_computing_data_collection       'Bruker SMART'
_computing_cell_refinement       'Bruker SMART'
_computing_data_reduction        'Bruker SAINT'
_computing_structure_solution    'SHELXS-97 (Sheldrick, 1990)'
_computing_structure_refinement  'SHELXL-97 (Sheldrick, 1997)'
_computing_molecular_graphics    'Bruker SHELXTL'
_computing_publication_material  'Bruker SHELXTL'

_refine_special_details
;
Refinement of F^2^ against ALL reflections.  The weighted R-factor wR and
goodness of fit S are based on F^2^, conventional R-factors R are based
on F, with F set to zero for negative F^2^. The threshold expression of
F^2^ > 2sigma(F^2^) is used only for calculating R-factors(gt) etc. and is
not relevant to the choice of reflections for refinement.  R-factors based
on F^2^ are statistically about twice as large as those based on F, and R-
factors based on ALL data will be even larger.
;

_refine_ls_structure_factor_coef  Fsqd
_refine_ls_matrix_type           full
_refine_ls_weighting_scheme      calc
_refine_ls_weighting_details
'calc w=1/[\s^2^(Fo^2^)+(0.0000P)^2^+0.0000P] where P=(Fo^2^+2Fc^2^)/3'
_atom_sites_solution_primary     direct
_atom_sites_solution_secondary   difmap
_atom_sites_solution_hydrogens   geom
_refine_ls_hydrogen_treatment    mixed
_refine_ls_extinction_method     none
_refine_ls_extinction_coef       ?
_refine_ls_number_reflns         3484
_refine_ls_number_parameters     261
_refine_ls_number_restraints     0
_refine_ls_R_factor_all          0.3991
_refine_ls_R_factor_gt           0.0955
_refine_ls_wR_factor_ref         0.3580
_refine_ls_wR_factor_gt          0.2059
_refine_ls_goodness_of_fit_ref   0.827
_refine_ls_restrained_S_all      0.827
```

```
_refine_ls_shift/su_max          0.365
_refine_ls_shift/su_mean         0.019

loop_
 _atom_site_label
 _atom_site_type_symbol
 _atom_site_fract_x
 _atom_site_fract_y
 _atom_site_fract_z
 _atom_site_U_iso_or_equiv
 _atom_site_adp_type
 _atom_site_occupancy
 _atom_site_symmetry_multiplicity
 _atom_site_calc_flag
 _atom_site_refinement_flags
 _atom_site_disorder_assembly
 _atom_site_disorder_group
C18A C 0.411(10) -0.084(4) 0.357(2) 0.036(10) Uani 0.50 1 d P . .
C18B C 0.459(13) -0.091(6) 0.332(3) 0.083(18) Uani 0.50 1 d P . .
O5 O 0.812(4) 0.0033(12) 0.4950(10) 0.064(4) Uani 0.50 1 d P . .
C2 C 0.034(2) 0.6732(8) 0.1188(6) 0.054(3) Uani 1 1 d . . .
O3 O 0.5555(15) 0.4046(6) 0.0821(4) 0.085(3) Uani 1 1 d . . .
H3 H 0.6643 0.3516 0.0771 0.128 Uiso 1 1 calc R . .
O2 O 0.0756(14) 0.7377(6) -0.0251(4) 0.075(2) Uani 1 1 d . . .
H2 H 0.0202 0.7861 -0.0594 0.113 Uiso 1 1 calc R . .
O4 O 0.5509(15) 0.3465(6) 0.2202(4) 0.077(2) Uani 1 1 d . . .
O1 O -0.2089(16) 0.8292(6) 0.0613(4) 0.084(2) Uani 1 1 d . . .
C7 C 0.2788(19) 0.5090(8) 0.1759(6) 0.048(2) Uani 1 1 d . . .
C6 C 0.175(2) 0.5269(8) 0.2581(6) 0.059(3) Uani 1 1 d . . .
H6 H 0.2244 0.4797 0.3042 0.071 Uiso 1 1 calc R . .
C1 C 0.2132(19) 0.5800(8) 0.1060(5) 0.055(3) Uani 1 1 d . . .
H1 H 0.2870 0.5660 0.0514 0.066 Uiso 1 1 calc R . .
C9 C -0.129(2) 0.6376(9) 0.3556(7) 0.070(3) Uani 1 1 d . . .
C4 C -0.068(2) 0.6895(8) 0.2019(6) 0.061(3) Uani 1 1 d . . .
H4 H -0.1830 0.7518 0.2116 0.073 Uiso 1 1 calc R . .
C8 C 0.480(2) 0.4127(9) 0.1627(7) 0.062(3) Uani 1 1 d . . .
C5 C -0.010(2) 0.6189(9) 0.2705(6) 0.057(3) Uani 1 1 d . . .
C3 C -0.042(2) 0.7525(9) 0.0492(6) 0.061(3) Uani 1 1 d . . .
C11 C -0.351(3) 0.6648(11) 0.5036(7) 0.101(5) Uani 1 1 d . . .
C10 C -0.233(3) 0.6498(10) 0.4255(6) 0.082(4) Uani 1 1 d . . .
C12 C -0.468(3) 0.6756(11) 0.5683(8) 0.115(5) Uani 1 1 d . . .
H12 H -0.5608 0.6842 0.6198 0.138 Uiso 1 1 calc R . .
C15 C 0.315(2) -0.0113(8) 0.2741(6) 0.051(3) Uani 1 1 d . . .
C16 C 0.383(2) -0.0314(9) 0.1877(6) 0.073(3) Uani 1 1 d . . .
H16 H 0.4951 -0.0929 0.1731 0.087 Uiso 1 1 calc R . .
N1 N 0.1127(16) 0.1250(7) 0.1407(5) 0.062(2) Uani 1 1 d . . .
```

C14 C 0.144(2) 0.0803(9) 0.2917(6) 0.061(3) Uani 1 1 d . . .
H14 H 0.0972 0.0978 0.3495 0.073 Uiso 1 1 calc R . .
C13 C 0.044(2) 0.1449(9) 0.2234(7) 0.068(3) Uani 1 1 d . . .
H13 H -0.0749 0.2047 0.2356 0.081 Uiso 1 1 calc R . .
C17 C 0.285(2) 0.0391(9) 0.1235(6) 0.069(3) Uani 1 1 d . . .
H17 H 0.3404 0.0271 0.0660 0.083 Uiso 1 1 calc R . .
N2B N 0.359(7) -0.058(3) 0.429(3) 0.089(10) Uani 0.50 1 d P . .
N2A N 0.574(7) -0.026(2) 0.4258(18) 0.083(8) Uani 0.50 1 d P . .
C19 C 0.50(2) 0.024(3) 0.504(6) 0.057(12) Uani 0.50 1 d P . .
H2B H 0.15(7) -0.09(3) 0.45(2) 0.5(2) Uiso 1 1 d . . .
H18C H 0.35(2) -0.147(8) 0.343(7) 0.05(4) Uiso 1 1 d . . .

loop_
 _atom_site_aniso_label
 _atom_site_aniso_U_11
 _atom_site_aniso_U_22
 _atom_site_aniso_U_33
 _atom_site_aniso_U_23
 _atom_site_aniso_U_13
 _atom_site_aniso_U_12
C18A 0.064(19) 0.05(2) 0.000(18) 0.020(16) 0.028(17) 0.041(17)
C18B 0.14(4) 0.11(3) 0.000(16) -0.006(16) 0.042(17) -0.01(3)
O5 0.046(9) 0.084(11) 0.060(10) 0.007(8) -0.015(8) 0.020(8)
C2 0.055(7) 0.051(7) 0.056(6) 0.010(5) 0.002(5) 0.009(5)
O3 0.111(6) 0.106(6) 0.054(4) 0.027(4) 0.033(4) 0.058(5)
O2 0.106(6) 0.088(6) 0.043(4) 0.030(4) 0.025(4) 0.044(5)
O4 0.104(6) 0.078(6) 0.056(4) 0.026(4) 0.016(4) 0.037(5)
O1 0.116(6) 0.082(5) 0.062(4) 0.021(4) 0.018(4) 0.048(5)
C7 0.054(6) 0.048(6) 0.042(5) 0.010(5) 0.006(5) 0.003(5)
C6 0.077(8) 0.053(7) 0.051(6) 0.017(5) 0.009(6) 0.013(6)
C1 0.075(7) 0.057(7) 0.038(5) 0.013(5) 0.013(5) 0.022(6)
C9 0.088(8) 0.063(8) 0.061(7) 0.015(6) 0.003(7) 0.018(7)
C4 0.076(8) 0.054(7) 0.055(6) 0.004(6) 0.007(6) 0.016(6)
C8 0.059(7) 0.055(8) 0.071(8) -0.002(6) 0.003(6) 0.006(6)
C5 0.071(7) 0.063(7) 0.040(6) 0.021(5) 0.010(5) 0.011(6)
C3 0.069(8) 0.066(8) 0.048(6) 0.009(6) -0.008(6) 0.021(6)
C11 0.162(13) 0.094(10) 0.054(7) 0.009(7) 0.033(9) 0.033(9)
C10 0.116(10) 0.098(10) 0.039(6) 0.017(6) 0.015(7) 0.030(8)
C12 0.157(13) 0.117(12) 0.076(9) 0.004(9) 0.030(9) 0.029(10)
C15 0.061(7) 0.050(7) 0.044(6) 0.013(5) 0.002(5) 0.013(5)
C16 0.099(9) 0.079(9) 0.043(6) 0.011(6) 0.003(6) 0.029(7)
N1 0.066(6) 0.077(7) 0.046(5) 0.019(5) 0.006(4) 0.013(5)
C14 0.080(7) 0.065(7) 0.041(6) 0.007(5) 0.012(5) 0.025(6)
C13 0.076(8) 0.068(8) 0.064(7) 0.020(6) 0.011(6) 0.024(6)
C17 0.083(8) 0.072(8) 0.052(6) 0.003(6) -0.002(6) 0.024(7)
N2B 0.09(2) 0.10(2) 0.08(3) 0.04(2) -0.01(2) 0.03(2)

N2A 0.13(3) 0.098(19) 0.015(14) 0.010(11) -0.030(17) 0.04(2)
C19 0.11(3) 0.01(3) 0.05(2) 0.03(3) 0.00(2) 0.01(4)

_geom_special_details
;
All esds (except the esd in the dihedral angle between two l.s. planes)
are estimated using the full covariance matrix. The cell esds are taken
into account individually in the estimation of esds in distances, angles
and torsion angles; correlations between esds in cell parameters are only
used when they are defined by crystal symmetry. An approximate (isotropic)
treatment of cell esds is used for estimating esds involving l.s. planes.
;

loop_
_geom_bond_atom_site_label_1
_geom_bond_atom_site_label_2
_geom_bond_distance
_geom_bond_site_symmetry_2
_geom_bond_publ_flag
C18A N2B 1.16(5) . ?
C18A C15 1.59(3) . ?
C18B C15 1.46(5) . ?
C18B N2A 1.58(6) . ?
O5 C19 1.48(11) 2_656 ?
O5 C19 1.50(11) . ?
O5 N2B 1.58(4) 2_656 ?
O5 O5 1.77(3) 2_756 ?
C2 C4 1.388(11) . ?
C2 C1 1.413(11) . ?
C2 C3 1.465(12) . ?
O3 C8 1.296(10) . ?
O2 C3 1.300(10) . ?
O4 C8 1.224(10) . ?
O1 C3 1.227(9) . ?
C7 C6 1.382(10) . ?
C7 C1 1.395(10) . ?
C7 C8 1.511(12) . ?
C6 C5 1.416(11) . ?
C9 C10 1.206(12) . ?
C9 C5 1.456(12) . ?
C4 C5 1.373(11) . ?
C11 C12 1.165(13) . ?
C11 C10 1.353(14) . ?
C15 C16 1.377(10) . ?
C15 C14 1.386(10) . ?
C16 C17 1.366(11) . ?

N1 C13 1.325(10) . ?
N1 C17 1.339(10) . ?
C14 C13 1.371(11) . ?
N2B C19 1.18(10) 2_656 ?
N2B C19 1.49(10) . ?
N2B O5 1.58(4) 2_656 ?
N2A C19 1.15(10) 2_656 ?
N2A C19 1.35(9) . ?
C19 C19 0.54(7) 2_656 ?
C19 N2A 1.15(10) 2_656 ?
C19 N2B 1.18(10) 2_656 ?
C19 O5 1.48(11) 2_656 ?

loop_
 _geom_angle_atom_site_label_1
 _geom_angle_atom_site_label_2
 _geom_angle_atom_site_label_3
 _geom_angle
 _geom_angle_site_symmetry_1
 _geom_angle_site_symmetry_3
 _geom_angle_publ_flag
N2B C18A C15 123(2) . . ?
C15 C18B N2A 111(4) . . ?
C19 O5 C19 21(3) 2_656 . ?
C19 O5 N2B 58(4) 2_656 2_656 ?
C19 O5 N2B 45(4) . 2_656 ?
C19 O5 O5 164(2) 2_656 2_756 ?
C19 O5 O5 169(4) . 2_756 ?
N2B O5 O5 124(2) 2_656 2_756 ?
C4 C2 C1 117.3(8) . . ?
C4 C2 C3 119.8(9) . . ?
C1 C2 C3 122.8(9) . . ?
C6 C7 C1 122.2(9) . . ?
C6 C7 C8 118.7(9) . . ?
C1 C7 C8 119.0(9) . . ?
C7 C6 C5 118.4(8) . . ?
C7 C1 C2 119.5(8) . . ?
C10 C9 C5 178.0(12) . . ?
C5 C4 C2 123.6(9) . . ?
O4 C8 O3 124.4(9) . . ?
O4 C8 C7 123.6(10) . . ?
O3 C8 C7 111.9(9) . . ?
C4 C5 C6 118.9(8) . . ?
C4 C5 C9 121.5(9) . . ?
C6 C5 C9 119.6(8) . . ?
O1 C3 O2 122.1(9) . . ?

O1 C3 C2 120.9(9) . . ?
O2 C3 C2 117.0(9) . . ?
C12 C11 C10 176.0(15) . . ?
C9 C10 C11 179.3(12) . . ?
C16 C15 C14 117.6(9) . . ?
C16 C15 C18B 110.5(16) . . ?
C14 C15 C18B 131.8(16) . . ?
C16 C15 C18A 126.6(13) . . ?
C14 C15 C18A 115.8(12) . . ?
C18B C15 C18A 16.5(18) . . ?
C17 C16 C15 119.9(9) . . ?
C13 N1 C17 118.8(8) . . ?
C13 C14 C15 119.6(8) . . ?
N1 C13 C14 122.2(9) . . ?
N1 C17 C16 121.9(9) . . ?
C19 N2B C18A 135(6) 2_656 . ?
C19 N2B C19 19(4) 2_656 . ?
C18A N2B C19 134(6) . . ?
C19 N2B O5 64(5) 2_656 2_656 ?
C18A N2B O5 157(3) . 2_656 ?
C19 N2B O5 58(4) . 2_656 ?
C19 N2A C19 23(3) 2_656 . ?
C19 N2A C18B 134(6) 2_656 . ?
C19 N2A C18B 146(6) . . ?
C19 C19 N2A 100(10) 2_656 2_656 ?
C19 C19 N2B 115(10) 2_656 2_656 ?
N2A C19 N2B 54(4) 2_656 2_656 ?
C19 C19 N2A 57(10) 2_656 . ?
N2A C19 N2A 157(3) 2_656 . ?
N2B C19 N2A 132(9) 2_656 . ?
C19 C19 N2B 46(10) 2_656 . ?
N2A C19 N2B 122(7) 2_656 . ?
N2B C19 N2B 161(4) 2_656 . ?
N2A C19 N2B 43(3) . . ?
C19 C19 O5 81(10) 2_656 2_656 ?
N2A C19 O5 66(5) 2_656 2_656 ?
N2B C19 O5 119(8) 2_656 2_656 ?
N2A C19 O5 107(6) . 2_656 ?
N2B C19 O5 64(4) . 2_656 ?
C19 C19 O5 78(10) 2_656 . ?
N2A C19 O5 118(7) 2_656 . ?
N2B C19 O5 71(6) 2_656 . ?
N2A C19 O5 61(4) . . ?
N2B C19 O5 100(5) . . ?
O5 C19 O5 159(3) 2_656 . ?

```
_diffrn_measured_fraction_theta_max    0.861
_diffrn_reflns_theta_full              28.48
_diffrn_measured_fraction_theta_full   0.861
_refine_diff_density_max    0.223
_refine_diff_density_min   -0.248
_refine_diff_density_rms    0.059
```

$(21bH)_2OG$

```
data_zl43m

_audit_creation_method            SHELXL-97
_chemical_name_systematic
;
 ?
;
_chemical_name_common              ?
_chemical_melting_point           ?
_chemical_formula_moiety          ?
_chemical_formula_sum
 'C30 H30 N4 O6'
_chemical_formula_weight          542.58

loop_
 _atom_type_symbol
 _atom_type_description
 _atom_type_scat_dispersion_real
 _atom_type_scat_dispersion_imag
 _atom_type_scat_source
'C'  'C'   0.0033   0.0016
 'International Tables Vol C Tables 4.2.6.8 and 6.1.1.4'
 'H'  'H'   0.0000   0.0000
 'International Tables Vol C Tables 4.2.6.8 and 6.1.1.4'
 'N'  'N'   0.0061   0.0033
 'International Tables Vol C Tables 4.2.6.8 and 6.1.1.4'
 'O'  'O'   0.0106   0.0060
 'International Tables Vol C Tables 4.2.6.8 and 6.1.1.4'

_symmetry_cell_setting            Triclinic
_symmetry_space_group_name_H-M    P1

loop_
 _symmetry_equiv_pos_as_xyz
 'x, y, z'

_cell_length_a                    5.839(14)
_cell_length_b                    7.704(19)
_cell_length_c                    16.04(4)
_cell_angle_alpha                  89.47(4)
_cell_angle_beta                  82.03(4)
_cell_angle_gamma                     86.13(5)
_cell_volume                      713(3)
_cell_formula_units_Z             1
```

```
_cell_measurement_temperature    273(2)
_cell_measurement_reflns_used    275
_cell_measurement_theta_min      2.56
_cell_measurement_theta_max      18.31

_exptl_crystal_description       ?
_exptl_crystal_colour            ?
_exptl_crystal_size_max          ?
_exptl_crystal_size_mid          ?
_exptl_crystal_size_min          ?
_exptl_crystal_density_meas      0
_exptl_crystal_density_diffrn    1.263
_exptl_crystal_density_method    'not measured'
_exptl_crystal_F_000             286
_exptl_absorpt_coefficient_mu    0.089
_exptl_absorpt_correction_type   none
_exptl_absorpt_correction_T_min  ?
_exptl_absorpt_correction_T_max  ?
_exptl_absorpt_process_details   ?

_exptl_special_details
;
 ?
;

_diffrn_ambient_temperature      273(2)
_diffrn_radiation_wavelength     0.71073
_diffrn_radiation_type           MoK\a
_diffrn_radiation_source         'fine-focus sealed tube'
_diffrn_radiation_monochromator  graphite
_diffrn_measurement_device_type  'CCD area detector'
_diffrn_measurement_method       'phi and omega scans'
_diffrn_detector_area_resol_mean  ?
_diffrn_standards_number         ?
_diffrn_standards_interval_count  ?
_diffrn_standards_interval_time  ?
_diffrn_standards_decay_%        ?
_diffrn_reflns_number            4143
_diffrn_reflns_av_R_equivalents  2.6804
_diffrn_reflns_av_sigmaI/netI    0.9263
_diffrn_reflns_limit_h_min       -7
_diffrn_reflns_limit_h_max       7
_diffrn_reflns_limit_k_min       -9
_diffrn_reflns_limit_k_max       7
_diffrn_reflns_limit_l_min       -20
_diffrn_reflns_limit_l_max       18
```

```
_diffrn_reflns_theta_min         1.28
_diffrn_reflns_theta_max         28.62
_reflns_number_total             3488
_reflns_number_gt                731
_reflns_threshold_expression     >2sigma(I)

_computing_data_collection       'Bruker SMART'
_computing_cell_refinement       'Bruker SMART'
_computing_data_reduction        'Bruker SAINT'
_computing_structure_solution    'SHELXS-97 (Sheldrick, 1990)'
_computing_structure_refinement  'SHELXL-97 (Sheldrick, 1997)'
_computing_molecular_graphics    'Bruker SHELXTL'
_computing_publication_material  'Bruker SHELXTL'

_refine_special_details
;
 Refinement of F^2^ against ALL reflections.  The weighted R-factor wR and
 goodness of fit S are based on F^2^, conventional R-factors R are based
 on F, with F set to zero for negative F^2^. The threshold expression of
 F^2^ > 2sigma(F^2^) is used only for calculating R-factors(gt) etc. and is
 not relevant to the choice of reflections for refinement.  R-factors based
 on F^2^ are statistically about twice as large as those based on F, and R-
 factors based on ALL data will be even larger.
;

_refine_ls_structure_factor_coef  Fsqd
_refine_ls_matrix_type           full
_refine_ls_weighting_scheme      calc
_refine_ls_weighting_details
 'calc w=1/[\s^2^(Fo^2^)+(0.0916P)^2^+0.0000P] where P=(Fo^2^+2Fc^2^)/3'
_atom_sites_solution_primary     direct
_atom_sites_solution_secondary   difmap
_atom_sites_solution_hydrogens   geom
_refine_ls_hydrogen_treatment    mixed
_refine_ls_extinction_method     none
_refine_ls_extinction_coef       ?
_refine_ls_abs_structure_details
 'Flack H D (1983), Acta Cryst. A39, 876-881'
_refine_ls_abs_structure_Flack   10(8)
_refine_ls_number_reflns         3488
_refine_ls_number_parameters     363
_refine_ls_number_restraints     3
_refine_ls_R_factor_all          0.3857
_refine_ls_R_factor_gt           0.0667
_refine_ls_wR_factor_ref         0.2338
_refine_ls_wR_factor_gt          0.1305
```

```
_refine_ls_goodness_of_fit_ref    0.732
_refine_ls_restrained_S_all       0.732
_refine_ls_shift/su_max           1.493
_refine_ls_shift/su_mean          0.274

loop_
 _atom_site_label
 _atom_site_type_symbol
 _atom_site_fract_x
 _atom_site_fract_y
 _atom_site_fract_z
 _atom_site_U_iso_or_equiv
 _atom_site_adp_type
 _atom_site_occupancy
 _atom_site_symmetry_multiplicity
 _atom_site_calc_flag
 _atom_site_refinement_flags
 _atom_site_disorder_assembly
 _atom_site_disorder_group
O5 O 0.268(3) -0.118(2) 0.9415(11) 0.084(5) Uani 1 1 d . . .
N3 N 0.524(3) 0.144(2) 0.9255(11) 0.059(5) Uani 1 1 d . . .
H3 H 0.3764 0.1660 0.9319 0.070 Uiso 1 1 calc R . .
O2 O 0.312(2) 0.3911(18) 0.8403(10) 0.072(5) Uani 1 1 d . . .
C1 C 0.534(4) 0.394(3) 0.8349(13) 0.051(6) Uani 1 1 d . . .
O3 O 0.930(2) 0.765(2) 0.7735(11) 0.074(5) Uani 1 1 d . . .
O4 O 0.644(2) 0.953(2) 0.7412(10) 0.069(5) Uani 1 1 d . . .
O1 O 0.873(2) 0.2502(19) 0.8792(9) 0.061(4) Uani 1 1 d . . .
O6 O 0.550(3) -0.309(2) 0.9728(10) 0.065(4) Uani 1 1 d . . .
N2 N 0.013(3) 0.601(2) -0.0331(11) 0.068(6) Uani 1 1 d . . .
H2A H 0.0596 0.5314 -0.0772 0.102 Uiso 1 1 calc R . .
H2B H 0.0804 0.7009 -0.0410 0.102 Uiso 1 1 calc R . .
H2C H -0.1399 0.6206 -0.0274 0.102 Uiso 1 1 calc R . .
C2 C 0.325(6) -0.118(4) 0.4453(17) 0.090(8) Uani 1 1 d . . .
H2 H 0.1885 -0.1655 0.4360 0.108 Uiso 1 1 calc R . .
N1 N 1.176(3) 0.061(2) 0.7500(10) 0.066(6) Uani 1 1 d . . .
H1A H 1.3232 0.0202 0.7444 0.099 Uiso 1 1 calc R . .
H1B H 1.0843 -0.0233 0.7675 0.099 Uiso 1 1 calc R . .
H1C H 1.1535 0.1474 0.7875 0.099 Uiso 1 1 calc R . .
C3 C 0.781(5) 0.620(3) 0.3135(16) 0.079(8) Uani 1 1 d . . .
N4 N 0.654(3) 0.503(2) 0.7918(12) 0.061(5) Uani 1 1 d . . .
H4 H 0.8015 0.4838 0.7881 0.073 Uiso 1 1 calc R . .
C4 C -0.035(4) 0.347(3) 0.0740(18) 0.098(9) Uani 1 1 d . . .
H4A H -0.2014 0.3717 0.0857 0.117 Uiso 1 1 calc R . .
H4B H -0.0042 0.2612 0.0294 0.117 Uiso 1 1 calc R . .
C5 C 0.461(5) -0.182(4) 0.5035(17) 0.075(8) Uani 1 1 d . . .
H5 H 0.4211 -0.2879 0.5277 0.090 Uiso 1 1 calc R . .
```

C6 C 0.118(6) 0.212(4) 0.208(2) 0.101(9) Uani 1 1 d . . .
C7 C 0.627(3) -0.014(3) 0.9593(14) 0.064(6) Uani 1 1 d . . .
H7A H 0.6523 0.0065 1.0168 0.076 Uiso 1 1 calc R . .
H7B H 0.7762 -0.0446 0.9263 0.076 Uiso 1 1 calc R . .
C8 C 0.628(5) -0.119(3) 0.5284(13) 0.073(8) Uani 1 1 d . . .
H8 H 0.6941 -0.1716 0.5727 0.088 Uiso 1 1 calc R . .
C9 C 0.890(5) 0.546(3) 0.380(2) 0.085(8) Uani 1 1 d . . .
C10 C 0.672(5) 0.257(3) 0.8829(13) 0.059(7) Uani 1 1 d . . .
C11 C 1.118(4) 0.130(3) 0.6654(15) 0.082(9) Uani 1 1 d . . .
H11A H 1.1637 0.0426 0.6221 0.099 Uiso 1 1 calc R . .
H11B H 0.9527 0.1584 0.6685 0.099 Uiso 1 1 calc R . .
C12 C 0.605(5) 0.104(4) 0.4282(17) 0.091(8) Uani 1 1 d . . .
H12 H 0.6523 0.2072 0.4031 0.109 Uiso 1 1 calc R . .
C13 C 0.468(4) -0.167(4) 0.9575(14) 0.057(7) Uani 1 1 d . . .
C14 C 1.152(5) 0.376(4) 0.567(2) 0.083(10) Uani 1 1 d . . .
C15 C 0.580(5) 0.547(3) 0.2992(19) 0.095(10) Uani 1 1 d . . .
H15 H 0.5226 0.4585 0.3340 0.114 Uiso 1 1 calc R . .
C16 C 0.415(4) 0.027(3) 0.4013(15) 0.069(7) Uani 1 1 d . . .
C17 C 0.975(5) 0.496(4) 0.443(2) 0.083(9) Uani 1 1 d . . .
C18 C 0.048(4) 0.279(3) 0.1469(17) 0.086(8) Uani 1 1 d . . .
C19 C 0.210(5) 0.152(4) 0.276(2) 0.095(9) Uani 1 1 d . . .
C20 C 0.080(3) 0.515(3) 0.0440(13) 0.061(7) Uani 1 1 d . . .
H20A H 0.0475 0.5990 0.0895 0.073 Uiso 1 1 calc R . .
H20B H 0.2464 0.4889 0.0349 0.073 Uiso 1 1 calc R . .
C21 C 0.300(4) 0.095(4) 0.3282(19) 0.083(9) Uani 1 1 d . . .
C22 C 0.727(4) 0.799(3) 0.7545(14) 0.062(6) Uani 1 1 d . . .
C23 C 0.721(4) 0.032(3) 0.4900(14) 0.071(7) Uani 1 1 d . . .
H23 H 0.8517 0.0787 0.5057 0.085 Uiso 1 1 calc R . .
C24 C 0.573(4) 0.655(3) 0.7478(16) 0.078(9) Uani 1 1 d . . .
H24A H 0.4155 0.6910 0.7721 0.093 Uiso 1 1 calc R . .
H24B H 0.5721 0.6265 0.6891 0.093 Uiso 1 1 calc R . .
C25 C 0.839(5) 0.766(3) 0.2743(16) 0.079(7) Uani 1 1 d . . .
H25 H 0.9560 0.8255 0.2930 0.095 Uiso 1 1 calc R . .
C26 C 1.243(4) 0.283(3) 0.6457(15) 0.072(7) Uani 1 1 d . . .
H26A H 1.4078 0.2516 0.6330 0.087 Uiso 1 1 calc R . .
H26B H 1.2188 0.3619 0.6935 0.087 Uiso 1 1 calc R . .
C27 C 1.071(5) 0.425(3) 0.5130(18) 0.091(10) Uani 1 1 d . . .
C28 C 0.534(4) 0.739(4) 0.1911(17) 0.101(10) Uani 1 1 d . . .
H28 H 0.4516 0.7769 0.1478 0.121 Uiso 1 1 calc R . .
C29 C 0.738(6) 0.837(4) 0.2074(18) 0.125(11) Uani 1 1 d . . .
H29 H 0.7900 0.9331 0.1764 0.150 Uiso 1 1 calc R . .
C30 C 0.467(6) 0.605(4) 0.235(2) 0.158(16) Uani 1 1 d . . .
H30 H 0.3414 0.5473 0.2222 0.189 Uiso 1 1 calc R . .

loop_
 _atom_site_aniso_label

_atom_site_aniso_U_11
_atom_site_aniso_U_22
_atom_site_aniso_U_33
_atom_site_aniso_U_23
_atom_site_aniso_U_13
_atom_site_aniso_U_12
O5 0.068(12) 0.065(12) 0.125(14) 0.024(9) -0.019(11) -0.036(10)
N3 0.059(12) 0.045(12) 0.073(13) 0.021(10) -0.008(10) -0.014(9)
O2 0.050(9) 0.041(9) 0.129(13) 0.010(8) -0.022(9) -0.014(7)
C1 0.034(13) 0.051(14) 0.073(15) 0.010(11) -0.022(12) -0.018(11)
O3 0.029(9) 0.064(11) 0.132(14) 0.036(10) -0.027(9) -0.012(8)
O4 0.035(9) 0.061(12) 0.114(13) 0.020(9) -0.014(8) -0.014(8)
O1 0.030(8) 0.076(11) 0.077(11) 0.020(8) -0.006(8) -0.020(8)
O6 0.059(11) 0.052(11) 0.082(12) 0.018(9) -0.001(8) -0.011(9)
N2 0.049(12) 0.045(11) 0.114(15) 0.019(10) -0.028(11) -0.010(9)
C2 0.114(19) 0.09(2) 0.064(17) -0.011(14) 0.012(15) -0.039(16)
N1 0.065(12) 0.071(13) 0.066(13) 0.011(10) -0.005(10) -0.036(10)
C3 0.10(2) 0.069(19) 0.070(17) -0.025(14) -0.017(15) -0.025(15)
N4 0.029(10) 0.058(14) 0.100(15) 0.006(11) -0.019(10) -0.007(10)
C4 0.083(18) 0.10(2) 0.12(2) -0.013(18) -0.006(17) -0.064(15)
C5 0.09(2) 0.075(19) 0.057(18) -0.010(14) 0.008(16) -0.014(17)
C6 0.11(2) 0.09(2) 0.10(2) 0.000(16) 0.012(18) -0.020(17)
C7 0.045(13) 0.074(16) 0.074(15) 0.007(11) -0.005(11) -0.027(12)
C8 0.10(2) 0.070(16) 0.045(13) 0.024(11) -0.009(14) -0.013(15)
C9 0.11(2) 0.056(18) 0.088(19) -0.012(14) -0.004(18) -0.024(15)
C10 0.070(18) 0.050(15) 0.054(15) 0.007(11) 0.018(15) -0.039(15)
C11 0.103(19) 0.057(16) 0.11(2) 0.016(14) -0.063(15) -0.042(14)
C12 0.11(2) 0.09(2) 0.075(17) 0.007(14) -0.007(16) -0.016(18)
C13 0.039(15) 0.09(2) 0.043(13) 0.004(13) 0.004(12) -0.026(16)
C14 0.06(2) 0.07(2) 0.13(3) 0.015(19) -0.030(19) -0.028(16)
C15 0.10(2) 0.066(18) 0.13(2) 0.035(15) -0.049(19) -0.029(16)
C16 0.072(17) 0.062(16) 0.068(18) 0.027(13) -0.006(14) 0.014(13)
C17 0.08(2) 0.08(2) 0.10(2) 0.014(17) -0.037(18) -0.041(15)
C18 0.12(2) 0.065(18) 0.09(2) 0.032(14) -0.034(16) -0.037(14)
C19 0.11(2) 0.07(2) 0.11(2) 0.013(17) -0.03(2) 0.000(16)
C20 0.035(12) 0.082(17) 0.062(14) 0.018(12) 0.008(10) -0.017(11)
C21 0.068(16) 0.10(2) 0.09(2) 0.024(16) -0.032(16) -0.024(15)
C22 0.055(16) 0.054(16) 0.080(16) 0.022(12) -0.015(12) -0.013(13)
C23 0.088(16) 0.053(15) 0.069(15) 0.000(11) 0.001(14) 0.000(12)
C24 0.067(15) 0.069(18) 0.109(19) 0.048(15) -0.052(14) -0.018(14)
C25 0.085(15) 0.055(15) 0.10(2) 0.022(14) -0.028(14) -0.023(13)
C26 0.084(17) 0.059(15) 0.084(16) 0.044(12) -0.041(14) -0.022(12)
C27 0.10(2) 0.056(15) 0.14(2) 0.055(15) -0.080(18) -0.035(14)
C28 0.072(15) 0.15(3) 0.08(2) -0.014(18) -0.018(15) -0.013(18)
C29 0.18(3) 0.09(2) 0.10(2) 0.044(16) -0.02(2) -0.03(2)
C30 0.18(3) 0.16(3) 0.15(3) 0.06(2) -0.09(3) -0.10(2)

```
_geom_special_details
;
 All esds (except the esd in the dihedral angle between two l.s. planes)
 are estimated using the full covariance matrix.  The cell esds are taken
 into account individually in the estimation of esds in distances, angles
 and torsion angles; correlations between esds in cell parameters are only
 used when they are defined by crystal symmetry.  An approximate (isotropic)
 treatment of cell esds is used for estimating esds involving l.s. planes.
;

loop_
 _geom_bond_atom_site_label_1
 _geom_bond_atom_site_label_2
 _geom_bond_distance
 _geom_bond_site_symmetry_2
 _geom_bond_publ_flag
O5 C13 1.26(3) . ?
N3 C10 1.38(3) . ?
N3 C7 1.45(2) . ?
O2 C1 1.29(2) . ?
C1 N4 1.27(3) . ?
C1 C10 1.548(14) . ?
O3 C22 1.27(2) . ?
O4 C22 1.28(3) . ?
O1 C10 1.17(3) . ?
O6 C13 1.21(3) . ?
N2 C20 1.48(2) . ?
C2 C5 1.37(4) . ?
C2 C16 1.41(3) . ?
N1 C11 1.53(2) . ?
C3 C25 1.33(3) . ?
C3 C9 1.41(4) . ?
C3 C15 1.38(3) . ?
N4 C24 1.45(2) . ?
C4 C18 1.41(3) . ?
C4 C20 1.54(3) . ?
C5 C8 1.23(3) . ?
C6 C18 1.22(4) . ?
C6 C19 1.33(4) . ?
C7 C13 1.55(3) . ?
C8 C23 1.42(3) . ?
C9 C17 1.24(4) . ?
C11 C26 1.44(3) . ?
C12 C23 1.37(3) . ?
C12 C16 1.41(3) . ?
```

C14 C27 1.09(3) . ?
C14 C26 1.58(3) . ?
C15 C30 1.35(4) . ?
C16 C21 1.50(4) . ?
C17 C27 1.41(4) . ?
C19 C21 1.13(3) . ?
C22 C24 1.49(3) . ?
C25 C29 1.39(3) . ?
C28 C30 1.30(4) . ?
C28 C29 1.51(4) . ?

loop_
 _geom_angle_atom_site_label_1
 _geom_angle_atom_site_label_2
 _geom_angle_atom_site_label_3
 _geom_angle
 _geom_angle_site_symmetry_1
 _geom_angle_site_symmetry_3
 _geom_angle_publ_flag
C10 N3 C7 117.6(19) . . ?
O2 C1 N4 124(2) . . ?
O2 C1 C10 119.9(14) . . ?
N4 C1 C10 115.6(13) . . ?
C5 C2 C16 113(3) . . ?
C25 C3 C9 124(2) . . ?
C25 C3 C15 119(3) . . ?
C9 C3 C15 116(3) . . ?
C1 N4 C24 128.2(18) . . ?
C18 C4 C20 112(2) . . ?
C8 C5 C2 129(3) . . ?
C18 C6 C19 174(3) . . ?
N3 C7 C13 111.0(17) . . ?
C5 C8 C23 121(2) . . ?
C17 C9 C3 174(3) . . ?
O1 C10 N3 126(2) . . ?
O1 C10 C1 123.4(14) . . ?
N3 C10 C1 110.1(17) . . ?
C26 C11 N1 107.7(16) . . ?
C23 C12 C16 122(2) . . ?
O6 C13 O5 130(2) . . ?
O6 C13 C7 116(2) . . ?
O5 C13 C7 113(3) . . ?
C27 C14 C26 172(3) . . ?
C30 C15 C3 120(3) . . ?
C12 C16 C2 119(2) . . ?
C12 C16 C21 123(2) . . ?

C2 C16 C21 118(3) . . ?
C9 C17 C27 176(3) . . ?
C6 C18 C4 177(3) . . ?
C21 C19 C6 174(4) . . ?
N2 C20 C4 118.1(19) . . ?
C19 C21 C16 177(3) . . ?
O4 C22 O3 124(2) . . ?
O4 C22 C24 117(2) . . ?
O3 C22 C24 120(2) . . ?
C12 C23 C8 115(3) . . ?
N4 C24 C22 110.0(16) . . ?
C3 C25 C29 125(3) . . ?
C11 C26 C14 108.4(19) . . ?
C14 C27 C17 177(3) . . ?
C30 C28 C29 123(3) . . ?
C25 C29 C28 111(3) . . ?
C28 C30 C15 120(3) . . ?

_diffrn_measured_fraction_theta_max 0.827
_diffrn_reflns_theta_full 28.62
_diffrn_measured_fraction_theta_full 0.827
_refine_diff_density_max 0.201
_refine_diff_density_min -0.225
_refine_diff_density_rms 0.067

$(21dH)_2OG$

```
data_zl49t

_audit_creation_method            SHELXL-97
_chemical_name_systematic
;
 ?
;
_chemical_name_common             ?
_chemical_melting_point           ?
_chemical_formula_moiety          ?
_chemical_formula_sum
 'C34 H38 N4 O6'
_chemical_formula_weight          598.68

loop_
 _atom_type_symbol
 _atom_type_description
 _atom_type_scat_dispersion_real
 _atom_type_scat_dispersion_imag
 _atom_type_scat_source
 'C'  'C'   0.0033   0.0016
 'International Tables Vol C Tables 4.2.6.8 and 6.1.1.4'
 'H'  'H'   0.0000   0.0000
 'International Tables Vol C Tables 4.2.6.8 and 6.1.1.4'
 'N'  'N'   0.0061   0.0033
 'International Tables Vol C Tables 4.2.6.8 and 6.1.1.4'
 'O'  'O'   0.0106   0.0060
 'International Tables Vol C Tables 4.2.6.8 and 6.1.1.4'

_symmetry_cell_setting            Triclinic
_symmetry_space_group_name_H-M    P-1

loop_
 _symmetry_equiv_pos_as_xyz
 'x, y, z'
 '-x, -y, -z'

_cell_length_a                    5.610(2)
_cell_length_b                    8.254(3)
_cell_length_c                    17.284(6)
_cell_angle_alpha                 83.265(6)
_cell_angle_beta                  89.803(6)
_cell_angle_gamma                 80.592(7)
_cell_volume                      784.0(5)
```

```
_cell_formula_units_Z            1
_cell_measurement_temperature    273(2)
_cell_measurement_reflns_used    ?
_cell_measurement_theta_min      ?
_cell_measurement_theta_max      ?

_exptl_crystal_description       ?
_exptl_crystal_colour            ?
_exptl_crystal_size_max          ?
_exptl_crystal_size_mid          ?
_exptl_crystal_size_min          ?
_exptl_crystal_density_meas      0
_exptl_crystal_density_diffrn    1.268
_exptl_crystal_density_method    'not measured'
_exptl_crystal_F_000             318
_exptl_absorpt_coefficient_mu    0.088
_exptl_absorpt_correction_type   none
_exptl_absorpt_correction_T_min  ?
_exptl_absorpt_correction_T_max  ?
_exptl_absorpt_process_details   ?

_exptl_special_details
;
 ?
;

_diffrn_ambient_temperature      273(2)
_diffrn_radiation_wavelength     0.71073
_diffrn_radiation_type           MoK\a
_diffrn_radiation_source         'fine-focus sealed tube'
_diffrn_radiation_monochromator  graphite
_diffrn_measurement_device_type  'CCD area detector'
_diffrn_measurement_method       'phi and omega scans'
_diffrn_detector_area_resol_mean ?
_diffrn_standards_number         ?
_diffrn_standards_interval_count ?
_diffrn_standards_interval_time  ?
_diffrn_standards_decay_%        ?
_diffrn_reflns_number            4643
_diffrn_reflns_av_R_equivalents  0.0348
_diffrn_reflns_av_sigmaI/netI    0.1035
_diffrn_reflns_limit_h_min       -7
_diffrn_reflns_limit_h_max       5
_diffrn_reflns_limit_k_min       -10
_diffrn_reflns_limit_k_max       9
_diffrn_reflns_limit_l_min       -21
```

```
_diffrn_reflns_limit_l_max       22
_diffrn_reflns_theta_min         1.19
_diffrn_reflns_theta_max         28.28
_reflns_number_total             3350
_reflns_number_gt                1358
_reflns_threshold_expression     >2sigma(I)

_computing_data_collection       'Bruker SMART'
_computing_cell_refinement       'Bruker SMART'
_computing_data_reduction        'Bruker SAINT'
_computing_structure_solution    'SHELXS-97 (Sheldrick, 1990)'
_computing_structure_refinement  'SHELXL-97 (Sheldrick, 1997)'
_computing_molecular_graphics    'Bruker SHELXTL'
_computing_publication_material  'Bruker SHELXTL'

_refine_special_details
;
 Refinement of F^2^ against ALL reflections.  The weighted R-factor wR and
 goodness of fit S are based on F^2^, conventional R-factors R are based
 on F, with F set to zero for negative F^2^. The threshold expression of
 F^2^ > 2sigma(F^2^) is used only for calculating R-factors(gt) etc. and is
 not relevant to the choice of reflections for refinement.  R-factors based
 on F^2^ are statistically about twice as large as those based on F, and R-
 factors based on ALL data will be even larger.
;

_refine_ls_structure_factor_coef  Fsqd
_refine_ls_matrix_type           full
_refine_ls_weighting_scheme      calc
_refine_ls_weighting_details
 'calc w=1/[\s^2^(Fo^2^)+(0.0801P)^2^+0.0000P] where P=(Fo^2^+2Fc^2^)/3'
_atom_sites_solution_primary     direct
_atom_sites_solution_secondary   difmap
_atom_sites_solution_hydrogens   geom
_refine_ls_hydrogen_treatment    mixed
_refine_ls_extinction_method     none
_refine_ls_extinction_coef       ?
_refine_ls_number_reflns         3350
_refine_ls_number_parameters     200
_refine_ls_number_restraints     0
_refine_ls_R_factor_all          0.1346
_refine_ls_R_factor_gt           0.0560
_refine_ls_wR_factor_ref         0.1479
_refine_ls_wR_factor_gt          0.1246
_refine_ls_goodness_of_fit_ref   0.743
_refine_ls_restrained_S_all      0.743
```

```
_refine_ls_shift/su_max          0.000
_refine_ls_shift/su_mean         0.000

loop_
 _atom_site_label
 _atom_site_type_symbol
 _atom_site_fract_x
 _atom_site_fract_y
 _atom_site_fract_z
 _atom_site_U_iso_or_equiv
 _atom_site_adp_type
 _atom_site_occupancy
 _atom_site_symmetry_multiplicity
 _atom_site_calc_flag
 _atom_site_refinement_flags
 _atom_site_disorder_assembly
 _atom_site_disorder_group
O2 O 0.8162(3) 0.3975(2) 0.06593(9) 0.0522(5) Uani 1 1 d . . .
O3 O 0.5118(3) 0.5647(2) 0.10981(11) 0.0592(5) Uani 1 1 d . . .
O1 O 0.2088(3) 0.0698(2) 0.02973(11) 0.0624(5) Uani 1 1 d . . .
N1 N 0.5552(4) 0.1597(2) 0.05308(11) 0.0474(5) Uani 1 1 d . . .
H1 H 0.7102 0.1385 0.0507 0.057 Uiso 1 1 calc R . .
C1 C 0.4284(5) 0.0629(3) 0.02253(13) 0.0433(6) Uani 1 1 d . . .
C2 C 0.4481(5) 0.2996(3) 0.09038(15) 0.0509(7) Uani 1 1 d . . .
H2A H 0.4167 0.2627 0.1443 0.061 Uiso 1 1 calc R . .
H2B H 0.2944 0.3467 0.0650 0.061 Uiso 1 1 calc R . .
C3 C 0.6049(5) 0.4312(3) 0.08813(13) 0.0427(6) Uani 1 1 d . . .
N2 N 1.0291(3) 0.6725(2) 0.09120(11) 0.0474(5) Uani 1 1 d . . .
H2C H 1.1880 0.6414 0.0979 0.071 Uiso 1 1 calc R . .
H2D H 0.9998 0.7457 0.0489 0.071 Uiso 1 1 calc R . .
H2E H 0.9607 0.5846 0.0854 0.071 Uiso 1 1 calc R . .
C4 C 0.9289(5) 0.7478(3) 0.15918(14) 0.0503(7) Uani 1 1 d . . .
H4A H 0.7539 0.7667 0.1551 0.060 Uiso 1 1 calc R . .
H4B H 0.9805 0.8543 0.1597 0.060 Uiso 1 1 calc R . .
C13 C 0.1603(5) 0.8003(3) 0.71645(15) 0.0610(8) Uani 1 1 d . . .
H13 H 0.3024 0.7330 0.7354 0.073 Uiso 1 1 calc R . .
C12 C 0.1255(5) 0.8440(3) 0.63704(15) 0.0583(7) Uani 1 1 d . . .
C6 C 0.8520(5) 0.6967(3) 0.30066(15) 0.0615(8) Uani 1 1 d . . .
H6A H 0.6889 0.6769 0.2922 0.074 Uiso 1 1 calc R . .
H6B H 0.8450 0.8149 0.3010 0.074 Uiso 1 1 calc R . .
C11 C 0.3059(6) 0.7878(4) 0.58428(17) 0.0666(8) Uani 1 1 d . . .
C5 C 1.0065(5) 0.6419(3) 0.23403(14) 0.0553(7) Uani 1 1 d . . .
H5A H 1.1739 0.6476 0.2454 0.066 Uiso 1 1 calc R . .
H5B H 0.9951 0.5277 0.2285 0.066 Uiso 1 1 calc R . .
C15 C -0.2201(6) 0.9526(3) 0.74002(16) 0.0628(8) Uani 1 1 d . . .
H15 H -0.3366 0.9907 0.7749 0.075 Uiso 1 1 calc R . .
```

C10 C 0.4560(6) 0.7433(4) 0.53920(17) 0.0699(9) Uani 1 1 d . . .
C9 C 0.6297(6) 0.6942(4) 0.48702(16) 0.0696(8) Uani 1 1 d . . .
C8 C 0.7759(6) 0.6547(4) 0.44069(17) 0.0692(8) Uani 1 1 d . . .
C16 C -0.2603(6) 0.9954(4) 0.66200(17) 0.0723(9) Uani 1 1 d . . .
H16 H -0.4040 1.0615 0.6438 0.087 Uiso 1 1 calc R . .
C17 C -0.0885(6) 0.9408(4) 0.61076(17) 0.0705(9) Uani 1 1 d . . .
H17 H -0.1164 0.9694 0.5575 0.085 Uiso 1 1 calc R . .
C14 C -0.0130(5) 0.8554(3) 0.76715(16) 0.0595(8) Uani 1 1 d . . .
H14 H 0.0116 0.8260 0.8205 0.071 Uiso 1 1 calc R . .
C7 C 0.9439(5) 0.6090(4) 0.37960(16) 0.0725(9) Uani 1 1 d . . .
H7A H 0.9652 0.4903 0.3783 0.087 Uiso 1 1 calc R . .
H7B H 1.0998 0.6378 0.3910 0.087 Uiso 1 1 calc R . .

loop_
 _atom_site_aniso_label
 _atom_site_aniso_U_11
 _atom_site_aniso_U_22
 _atom_site_aniso_U_33
 _atom_site_aniso_U_23
 _atom_site_aniso_U_13
 _atom_site_aniso_U_12
O2 0.0363(10) 0.0604(11) 0.0634(11) -0.0165(9) 0.0144(9) -0.0120(9)
O3 0.0391(10) 0.0594(12) 0.0849(13) -0.0296(10) 0.0108(9) -0.0101(9)
O1 0.0384(11) 0.0650(12) 0.0881(14) -0.0196(10) 0.0078(10) -0.0135(9)
N1 0.0385(12) 0.0458(12) 0.0593(13) -0.0079(10) 0.0040(10) -0.0094(10)
C1 0.0462(17) 0.0365(14) 0.0462(15) 0.0029(11) -0.0007(12) -0.0091(13)
C2 0.0486(16) 0.0498(15) 0.0574(16) -0.0108(13) 0.0110(13) -0.0145(13)
C3 0.0400(16) 0.0518(16) 0.0376(13) -0.0062(12) 0.0043(12) -0.0107(13)
N2 0.0365(12) 0.0560(13) 0.0518(12) -0.0123(10) 0.0106(10) -0.0096(10)
C4 0.0433(15) 0.0562(16) 0.0542(16) -0.0194(14) 0.0129(12) -0.0074(13)
C13 0.0624(19) 0.0664(18) 0.0539(18) -0.0052(15) 0.0062(15) -0.0111(15)
C12 0.0597(19) 0.0695(19) 0.0494(17) -0.0106(14) 0.0132(15) -0.0193(16)
C6 0.0586(19) 0.0690(18) 0.0576(17) -0.0142(15) 0.0128(14) -0.0081(15)
C11 0.068(2) 0.076(2) 0.0577(18) -0.0090(16) 0.0080(16) -0.0152(17)
C5 0.0562(18) 0.0573(17) 0.0521(16) -0.0120(13) 0.0162(13) -0.0051(14)
C15 0.064(2) 0.068(2) 0.0592(19) -0.0063(15) 0.0221(16) -0.0217(17)
C10 0.072(2) 0.083(2) 0.0545(18) -0.0081(16) 0.0134(17) -0.0116(18)
C9 0.079(2) 0.081(2) 0.0488(17) -0.0067(16) 0.0168(17) -0.0136(18)
C8 0.079(2) 0.072(2) 0.0548(18) -0.0045(15) 0.0152(17) -0.0093(17)
C16 0.057(2) 0.092(2) 0.064(2) 0.0012(17) 0.0096(16) -0.0100(17)
C17 0.067(2) 0.094(2) 0.0496(17) 0.0016(16) 0.0036(16) -0.0185(19)
C14 0.063(2) 0.0687(19) 0.0473(16) -0.0006(14) 0.0088(15) -0.0174(16)
C7 0.079(2) 0.077(2) 0.0577(18) -0.0045(16) 0.0204(16) -0.0058(18)

_geom_special_details
;

```
 All esds (except the esd in the dihedral angle between two l.s. planes)
 are estimated using the full covariance matrix.  The cell esds are taken
 into account individually in the estimation of esds in distances, angles
 and torsion angles; correlations between esds in cell parameters are only
 used when they are defined by crystal symmetry.  An approximate (isotropic)
 treatment of cell esds is used for estimating esds involving l.s. planes.
;

loop_
 _geom_bond_atom_site_label_1
 _geom_bond_atom_site_label_2
 _geom_bond_distance
 _geom_bond_site_symmetry_2
 _geom_bond_publ_flag
O2 C3 1.242(3) . ?
O3 C3 1.239(3) . ?
O1 C1 1.231(3) . ?
N1 C1 1.308(3) . ?
N1 C2 1.433(3) . ?
C1 C1 1.498(5) 2_655 ?
C2 C3 1.503(3) . ?
N2 C4 1.461(3) . ?
C4 C5 1.497(3) . ?
C13 C14 1.365(4) . ?
C13 C12 1.384(4) . ?
C12 C17 1.375(4) . ?
C12 C11 1.418(4) . ?
C6 C5 1.507(3) . ?
C6 C7 1.517(4) . ?
C11 C10 1.189(4) . ?
C15 C14 1.351(4) . ?
C15 C16 1.363(4) . ?
C10 C9 1.370(4) . ?
C9 C8 1.179(4) . ?
C8 C7 1.454(4) . ?
C16 C17 1.364(4) . ?

loop_
 _geom_angle_atom_site_label_1
 _geom_angle_atom_site_label_2
 _geom_angle_atom_site_label_3
 _geom_angle
 _geom_angle_site_symmetry_1
 _geom_angle_site_symmetry_3
 _geom_angle_publ_flag
C1 N1 C2 123.1(2) . . ?
```

O1 C1 N1 124.3(2) . . ?
O1 C1 C1 120.9(3) . 2_655 ?
N1 C1 C1 114.9(3) . 2_655 ?
N1 C2 C3 112.9(2) . . ?
O3 C3 O2 125.4(2) . . ?
O3 C3 C2 116.6(2) . . ?
O2 C3 C2 118.0(2) . . ?
N2 C4 C5 112.27(19) . . ?
C14 C13 C12 120.3(3) . . ?
C17 C12 C13 118.5(3) . . ?
C17 C12 C11 121.1(3) . . ?
C13 C12 C11 120.4(3) . . ?
C5 C6 C7 113.4(2) . . ?
C10 C11 C12 178.8(3) . . ?
C4 C5 C6 111.3(2) . . ?
C14 C15 C16 120.7(3) . . ?
C11 C10 C9 179.2(3) . . ?
C8 C9 C10 178.3(4) . . ?
C9 C8 C7 176.2(3) . . ?
C15 C16 C17 119.7(3) . . ?
C16 C17 C12 120.7(3) . . ?
C15 C14 C13 120.1(3) . . ?
C8 C7 C6 111.1(2) . . ?

_diffrn_measured_fraction_theta_max 0.861
_diffrn_reflns_theta_full 28.28
_diffrn_measured_fraction_theta_full 0.861
_refine_diff_density_max 0.190
_refine_diff_density_min -0.199
_refine_diff_density_rms 0.046

22b

```
data_zl58m

_audit_creation_method           SHELXL-97
_chemical_name_systematic
;
 ?
;
_chemical_name_common            ?
_chemical_melting_point          ?
_chemical_formula_moiety         ?
_chemical_formula_sum
 'C13 H10 O2'
_chemical_formula_weight         198.21

loop_
 _atom_type_symbol
 _atom_type_description
 _atom_type_scat_dispersion_real
 _atom_type_scat_dispersion_imag
 _atom_type_scat_source
'C'  'C'   0.0033   0.0016
 'International Tables Vol C Tables 4.2.6.8 and 6.1.1.4'
 'H'  'H'   0.0000   0.0000
 'International Tables Vol C Tables 4.2.6.8 and 6.1.1.4'
 'O'  'O'   0.0106   0.0060
 'International Tables Vol C Tables 4.2.6.8 and 6.1.1.4'

_symmetry_cell_setting           Triclinic
_symmetry_space_group_name_H-M    P-1

loop_
 _symmetry_equiv_pos_as_xyz
 'x, y, z'
 '-x, -y, -z'

_cell_length_a                   5.748(4)
_cell_length_b                   7.687(6)
_cell_length_c                   12.853(10)
_cell_angle_alpha                 96.068(15)
_cell_angle_beta                 97.184(15)
_cell_angle_gamma                106.743(16)
_cell_volume                     533.5(7)
_cell_formula_units_Z            2
_cell_measurement_temperature    273(2)
```

```
_cell_measurement_reflns_used    379
_cell_measurement_theta_min      2.80
_cell_measurement_theta_max      19.00

_exptl_crystal_description       ?
_exptl_crystal_colour            ?
_exptl_crystal_size_max          ?
_exptl_crystal_size_mid          ?
_exptl_crystal_size_min          ?
_exptl_crystal_density_meas      0
_exptl_crystal_density_diffrn    1.234
_exptl_crystal_density_method    'not measured'
_exptl_crystal_F_000             208
_exptl_absorpt_coefficient_mu    0.083
_exptl_absorpt_correction_type   none
_exptl_absorpt_correction_T_min  ?
_exptl_absorpt_correction_T_max  ?
_exptl_absorpt_process_details   ?

_exptl_special_details
;
 ?
;

_diffrn_ambient_temperature      273(2)
_diffrn_radiation_wavelength     0.71073
_diffrn_radiation_type           MoK\a
_diffrn_radiation_source         'fine-focus sealed tube'
_diffrn_radiation_monochromator  graphite
_diffrn_measurement_device_type  'CCD area detector'
_diffrn_measurement_method       'phi and omega scans'
_diffrn_detector_area_resol_mean  ?
_diffrn_standards_number         ?
_diffrn_standards_interval_count  ?
_diffrn_standards_interval_time  ?
_diffrn_standards_decay_%        ?
_diffrn_reflns_number            3373
_diffrn_reflns_av_R_equivalents  0.0391
_diffrn_reflns_av_sigmaI/netI    0.1275
_diffrn_reflns_limit_h_min       -7
_diffrn_reflns_limit_h_max       6
_diffrn_reflns_limit_k_min       -10
_diffrn_reflns_limit_k_max       8
_diffrn_reflns_limit_l_min       -16
_diffrn_reflns_limit_l_max       16
_diffrn_reflns_theta_min         1.62
```

```
_diffrn_reflns_theta_max         28.48
_reflns_number_total             2326
_reflns_number_gt                690
_reflns_threshold_expression     >2sigma(I)

_computing_data_collection       'Bruker SMART'
_computing_cell_refinement       'Bruker SMART'
_computing_data_reduction        'Bruker SAINT'
_computing_structure_solution    'SHELXS-97 (Sheldrick, 1990)'
_computing_structure_refinement  'SHELXL-97 (Sheldrick, 1997)'
_computing_molecular_graphics    'Bruker SHELXTL'
_computing_publication_material  'Bruker SHELXTL'

_refine_special_details
;
 Refinement of F^2^ against ALL reflections.  The weighted R-factor wR and
 goodness of fit S are based on F^2^, conventional R-factors R are based
 on F, with F set to zero for negative F^2^. The threshold expression of
 F^2^ > 2sigma(F^2^) is used only for calculating R-factors(gt) etc. and is
 not relevant to the choice of reflections for refinement.  R-factors based
 on F^2^ are statistically about twice as large as those based on F, and R-
 factors based on ALL data will be even larger.
;

_refine_ls_structure_factor_coef  Fsqd
_refine_ls_matrix_type           full
_refine_ls_weighting_scheme      calc
_refine_ls_weighting_details
 'calc w=1/[\s^2^(Fo^2^)+(0.0711P)^2^+0.0000P] where P=(Fo^2^+2Fc^2^)/3'
_atom_sites_solution_primary     direct
_atom_sites_solution_secondary   difmap
_atom_sites_solution_hydrogens   geom
_refine_ls_hydrogen_treatment    mixed
_refine_ls_extinction_method     none
_refine_ls_extinction_coef       ?
_refine_ls_number_reflns         2326
_refine_ls_number_parameters     136
_refine_ls_number_restraints     0
_refine_ls_R_factor_all          0.2031
_refine_ls_R_factor_gt           0.0482
_refine_ls_wR_factor_ref         0.1683
_refine_ls_wR_factor_gt          0.1092
_refine_ls_goodness_of_fit_ref   0.777
_refine_ls_restrained_S_all      0.777
_refine_ls_shift/su_max          0.000
_refine_ls_shift/su_mean         0.000
```

```
loop_
 _atom_site_label
 _atom_site_type_symbol
 _atom_site_fract_x
 _atom_site_fract_y
 _atom_site_fract_z
 _atom_site_U_iso_or_equiv
 _atom_site_adp_type
 _atom_site_occupancy
 _atom_site_symmetry_multiplicity
 _atom_site_calc_flag
 _atom_site_refinement_flags
 _atom_site_disorder_assembly
 _atom_site_disorder_group
C8 C 0.4093(6) 0.8637(4) 0.6771(2) 0.0596(8) Uani 1 1 d . . .
C6 C 0.0181(7) 0.7426(4) 0.5309(3) 0.0683(9) Uani 1 1 d . . .
O1 O -0.6801(4) 0.6223(3) 0.02957(17) 0.0932(8) Uani 1 1 d . . .
H1 H -0.8027 0.5870 -0.0165 0.140 Uiso 1 1 calc R . .
C7 C 0.1965(6) 0.7971(4) 0.5971(3) 0.0680(9) Uani 1 1 d . . .
C2 C -0.5274(5) 0.6246(4) 0.2064(2) 0.0661(9) Uani 1 1 d . . .
H2A H -0.4588 0.7573 0.2162 0.079 Uiso 1 1 calc R . .
H2B H -0.4009 0.5729 0.1869 0.079 Uiso 1 1 calc R . .
C5 C -0.1946(6) 0.6799(4) 0.4561(3) 0.0721(10) Uani 1 1 d . . .
O2 O -0.9455(4) 0.4798(3) 0.12587(17) 0.0917(8) Uani 1 1 d . . .
C9 C 0.6355(6) 0.9591(4) 0.6542(3) 0.0697(9) Uani 1 1 d . . .
H9 H 0.6501 0.9809 0.5852 0.084 Uiso 1 1 calc R . .
C4 C -0.3775(6) 0.6277(4) 0.3927(3) 0.0704(9) Uani 1 1 d . . .
C13 C 0.3933(6) 0.8351(4) 0.7812(3) 0.0726(9) Uani 1 1 d . . .
H13 H 0.2428 0.7719 0.7987 0.087 Uiso 1 1 calc R . .
C3 C -0.5938(5) 0.5663(4) 0.3106(2) 0.0710(9) Uani 1 1 d . . .
H3A H -0.7188 0.6185 0.3314 0.085 Uiso 1 1 calc R . .
H3B H -0.6608 0.4335 0.3019 0.085 Uiso 1 1 calc R . .
C10 C 0.8379(6) 1.0216(4) 0.7316(3) 0.0811(10) Uani 1 1 d . . .
H10 H 0.9894 1.0841 0.7147 0.097 Uiso 1 1 calc R . .
C12 C 0.5973(7) 0.8992(5) 0.8581(3) 0.0848(11) Uani 1 1 d . . .
H12 H 0.5846 0.8787 0.9275 0.102 Uiso 1 1 calc R . .
C1 C -0.7378(7) 0.5672(4) 0.1187(3) 0.0709(10) Uani 1 1 d . . .
C11 C 0.8194(7) 0.9929(5) 0.8339(3) 0.0840(11) Uani 1 1 d . . .
H11 H 0.9572 1.0371 0.8867 0.101 Uiso 1 1 calc R . .

loop_
 _atom_site_aniso_label
 _atom_site_aniso_U_11
 _atom_site_aniso_U_22
 _atom_site_aniso_U_33
```

```
 _atom_site_aniso_U_23
 _atom_site_aniso_U_13
 _atom_site_aniso_U_12
C8 0.057(2) 0.0574(19) 0.062(2) 0.0090(16) 0.0066(18) 0.0155(16)
C6 0.066(2) 0.065(2) 0.074(2) 0.0160(17) 0.013(2) 0.0166(17)
O1 0.0699(16) 0.1204(18) 0.0722(16) 0.0251(14) 0.0097(13) -0.0004(13)
C7 0.066(2) 0.065(2) 0.073(2) 0.0119(17) 0.015(2) 0.0170(18)
C2 0.057(2) 0.064(2) 0.069(2) 0.0121(17) 0.0075(18) 0.0072(16)
C5 0.065(2) 0.074(2) 0.073(2) 0.0201(18) 0.012(2) 0.0105(18)
O2 0.0650(16) 0.1079(18) 0.0775(16) 0.0276(13) 0.0001(13) -0.0122(13)
C9 0.061(2) 0.079(2) 0.071(2) 0.0208(18) 0.0156(19) 0.0188(18)
C4 0.066(2) 0.067(2) 0.076(2) 0.0204(17) 0.011(2) 0.0134(18)
C13 0.065(2) 0.077(2) 0.076(2) 0.0241(18) 0.022(2) 0.0126(18)
C3 0.071(2) 0.069(2) 0.068(2) 0.0112(17) 0.0050(19) 0.0158(17)
C10 0.054(2) 0.086(2) 0.100(3) 0.018(2) 0.019(2) 0.0107(18)
C12 0.092(3) 0.095(3) 0.067(2) 0.020(2) 0.008(2) 0.026(2)
C1 0.070(2) 0.070(2) 0.065(2) 0.0111(18) 0.006(2) 0.0114(19)
C11 0.076(3) 0.093(3) 0.076(3) 0.012(2) -0.005(2) 0.022(2)

_geom_special_details
;
 All esds (except the esd in the dihedral angle between two l.s. planes)
 are estimated using the full covariance matrix.  The cell esds are taken
 into account individually in the estimation of esds in distances, angles
 and torsion angles; correlations between esds in cell parameters are only
 used when they are defined by crystal symmetry.  An approximate (isotropic)
 treatment of cell esds is used for estimating esds involving l.s. planes.
;

loop_
 _geom_bond_atom_site_label_1
 _geom_bond_atom_site_label_2
 _geom_bond_distance
 _geom_bond_site_symmetry_2
 _geom_bond_publ_flag
C8 C9 1.381(4) . ?
C8 C13 1.389(4) . ?
C8 C7 1.424(4) . ?
C6 C7 1.187(4) . ?
C6 C5 1.386(5) . ?
O1 C1 1.311(4) . ?
C2 C1 1.474(4) . ?
C2 C3 1.514(4) . ?
C5 C4 1.184(4) . ?
O2 C1 1.210(3) . ?
C9 C10 1.364(4) . ?
```

```
C4 C3 1.453(4) . ?
C13 C12 1.367(4) . ?
C10 C11 1.369(5) . ?
C12 C11 1.364(4) . ?

loop_
 _geom_angle_atom_site_label_1
 _geom_angle_atom_site_label_2
 _geom_angle_atom_site_label_3
 _geom_angle
 _geom_angle_site_symmetry_1
 _geom_angle_site_symmetry_3
 _geom_angle_publ_flag
C9 C8 C13 118.1(3) . . ?
C9 C8 C7 121.5(3) . . ?
C13 C8 C7 120.4(3) . . ?
C7 C6 C5 178.2(4) . . ?
C6 C7 C8 179.4(4) . . ?
C1 C2 C3 113.7(3) . . ?
C4 C5 C6 179.2(4) . . ?
C10 C9 C8 120.9(3) . . ?
C5 C4 C3 176.9(3) . . ?
C12 C13 C8 120.4(3) . . ?
C4 C3 C2 110.4(3) . . ?
C9 C10 C11 120.4(3) . . ?
C11 C12 C13 120.6(3) . . ?
O2 C1 O1 121.8(3) . . ?
O2 C1 C2 124.9(3) . . ?
O1 C1 C2 113.3(3) . . ?
C12 C11 C10 119.6(3) . . ?

_diffrn_measured_fraction_theta_max    0.864
_diffrn_reflns_theta_full              28.48
_diffrn_measured_fraction_theta_full   0.864
_refine_diff_density_max    0.149
_refine_diff_density_min   -0.155
_refine_diff_density_rms    0.035
```

22c

```
data_zl57m

_audit_creation_method           SHELXL-97
_chemical_name_systematic
;
 ?
;
_chemical_name_common            ?
_chemical_melting_point          ?
_chemical_formula_moiety         ?
_chemical_formula_sum
 'C14 H12 O2'
_chemical_formula_weight         212.24

loop_
 _atom_type_symbol
 _atom_type_description
 _atom_type_scat_dispersion_real
 _atom_type_scat_dispersion_imag
 _atom_type_scat_source
'C'  'C'   0.0033   0.0016
'International Tables Vol C Tables 4.2.6.8 and 6.1.1.4'
'H'  'H'   0.0000   0.0000
'International Tables Vol C Tables 4.2.6.8 and 6.1.1.4'
'O'  'O'   0.0106   0.0060
'International Tables Vol C Tables 4.2.6.8 and 6.1.1.4'

_symmetry_cell_setting           Triclinic
_symmetry_space_group_name_H-M    P-1

loop_
 _symmetry_equiv_pos_as_xyz
 'x, y, z'
 '-x, -y, -z'

_cell_length_a                 6.360(6)
_cell_length_b                 8.151(7)
_cell_length_c                 11.523(11)
_cell_angle_alpha               76.87(2)
_cell_angle_beta               85.153(18)
_cell_angle_gamma                84.16(2)
_cell_volume                   577.6(9)
_cell_formula_units_Z            2
_cell_measurement_temperature    273(2)
```

```
_cell_measurement_reflns_used     242
_cell_measurement_theta_min       2.81
_cell_measurement_theta_max       18.61

_exptl_crystal_description        ?
_exptl_crystal_colour             ?
_exptl_crystal_size_max           ?
_exptl_crystal_size_mid           ?
_exptl_crystal_size_min           ?
_exptl_crystal_density_meas       0
_exptl_crystal_density_diffrn     1.220
_exptl_crystal_density_method     'not measured'
_exptl_crystal_F_000              224
_exptl_absorpt_coefficient_mu     0.081
_exptl_absorpt_correction_type    none
_exptl_absorpt_correction_T_min   ?
_exptl_absorpt_correction_T_max   ?
_exptl_absorpt_process_details    ?

_exptl_special_details
;
 ?
;

_diffrn_ambient_temperature       273(2)
_diffrn_radiation_wavelength      0.71073
_diffrn_radiation_type            MoK\a
_diffrn_radiation_source          'fine-focus sealed tube'
_diffrn_radiation_monochromator   graphite
_diffrn_measurement_device_type   'CCD area detector'
_diffrn_measurement_method        'phi and omega scans'
_diffrn_detector_area_resol_mean  ?
_diffrn_standards_number          ?
_diffrn_standards_interval_count  ?
_diffrn_standards_interval_time   ?
_diffrn_standards_decay_%         ?
_diffrn_reflns_number             2495
_diffrn_reflns_av_R_equivalents   0.0222
_diffrn_reflns_av_sigmaI/netI     0.2329
_diffrn_reflns_limit_h_min        -4
_diffrn_reflns_limit_h_max        8
_diffrn_reflns_limit_k_min        -8
_diffrn_reflns_limit_k_max        10
_diffrn_reflns_limit_l_min        -14
_diffrn_reflns_limit_l_max        13
_diffrn_reflns_theta_min          1.82
```

```
_diffrn_reflns_theta_max         28.73
_reflns_number_total             2220
_reflns_number_gt                545
_reflns_threshold_expression     >2sigma(I)

_computing_data_collection       'Bruker SMART'
_computing_cell_refinement       'Bruker SMART'
_computing_data_reduction        'Bruker SAINT'
_computing_structure_solution    'SHELXS-97 (Sheldrick, 1990)'
_computing_structure_refinement  'SHELXL-97 (Sheldrick, 1997)'
_computing_molecular_graphics    'Bruker SHELXTL'
_computing_publication_material  'Bruker SHELXTL'

_refine_special_details
;
 Refinement of F^2^ against ALL reflections.  The weighted R-factor wR and
 goodness of fit S are based on F^2^, conventional R-factors R are based
 on F, with F set to zero for negative F^2^. The threshold expression of
 F^2^ > 2sigma(F^2^) is used only for calculating R-factors(gt) etc. and is
 not relevant to the choice of reflections for refinement.  R-factors based
 on F^2^ are statistically about twice as large as those based on F, and R-
 factors based on ALL data will be even larger.
;

_refine_ls_structure_factor_coef  Fsqd
_refine_ls_matrix_type           full
_refine_ls_weighting_scheme      calc
_refine_ls_weighting_details
 'calc w=1/[\s^2^(Fo^2^)+(0.0822P)^2^+0.0000P] where P=(Fo^2^+2Fc^2^)/3'
_atom_sites_solution_primary     direct
_atom_sites_solution_secondary   difmap
_atom_sites_solution_hydrogens   geom
_refine_ls_hydrogen_treatment    mixed
_refine_ls_extinction_method     none
_refine_ls_extinction_coef       ?
_refine_ls_number_reflns         2220
_refine_ls_number_parameters     145
_refine_ls_number_restraints     0
_refine_ls_R_factor_all          0.2660
_refine_ls_R_factor_gt           0.0692
_refine_ls_wR_factor_ref         0.2165
_refine_ls_wR_factor_gt          0.1533
_refine_ls_goodness_of_fit_ref   0.787
_refine_ls_restrained_S_all      0.787
_refine_ls_shift/su_max          0.000
_refine_ls_shift/su_mean         0.000
```

```
loop_
 _atom_site_label
 _atom_site_type_symbol
 _atom_site_fract_x
 _atom_site_fract_y
 _atom_site_fract_z
 _atom_site_U_iso_or_equiv
 _atom_site_adp_type
 _atom_site_occupancy
 _atom_site_symmetry_multiplicity
 _atom_site_calc_flag
 _atom_site_refinement_flags
 _atom_site_disorder_assembly
 _atom_site_disorder_group
O1 O 0.0740(6) 0.2893(4) -0.0238(3) 0.0797(13) Uani 1 1 d . . .
H1 H -0.0157 0.3697 -0.0378 0.120 Uiso 1 1 calc R . .
C5 C 0.8642(8) 0.1110(7) 0.2549(5) 0.0626(17) Uani 1 1 d . . .
C6 C 0.9738(8) 0.1509(7) 0.3179(5) 0.0634(17) Uani 1 1 d . . .
C1 C 0.2184(9) 0.3243(8) 0.0396(5) 0.0608(16) Uani 1 1 d . . .
C8 C 1.2103(9) 0.2307(6) 0.4655(5) 0.0626(18) Uani 1 1 d . . .
C7 C 1.1018(8) 0.1948(7) 0.3968(5) 0.0632(17) Uani 1 1 d . . .
O2 O 0.2165(6) 0.4550(5) 0.0708(4) 0.0812(14) Uani 1 1 d . . .
C3 C 0.5420(8) 0.2172(6) 0.1492(5) 0.0636(16) Uani 1 1 d . . .
H3A H 0.4680 0.2317 0.2238 0.076 Uiso 1 1 calc R . .
H3B H 0.6038 0.3220 0.1122 0.076 Uiso 1 1 calc R . .
C2 C 0.3858(8) 0.1843(7) 0.0690(5) 0.0663(16) Uani 1 1 d . . .
H2A H 0.4605 0.1656 -0.0044 0.080 Uiso 1 1 calc R . .
H2B H 0.3200 0.0818 0.1074 0.080 Uiso 1 1 calc R . .
C9 C 1.3373(10) 0.2770(7) 0.5483(5) 0.0619(16) Uani 1 1 d . . .
C4 C 0.7187(8) 0.0764(6) 0.1759(5) 0.0667(17) Uani 1 1 d . . .
H4A H 0.6577 -0.0290 0.2122 0.080 Uiso 1 1 calc R . .
H4B H 0.7953 0.0630 0.1017 0.080 Uiso 1 1 calc R . .
C10 C 1.2532(9) 0.3833(8) 0.6183(6) 0.0770(19) Uani 1 1 d . . .
H10 H 1.1132 0.4281 0.6114 0.092 Uiso 1 1 calc R . .
C11 C 1.3730(12) 0.4254(7) 0.6992(6) 0.088(2) Uani 1 1 d . . .
H11 H 1.3141 0.4991 0.7464 0.106 Uiso 1 1 calc R . .
C13 C 1.6623(10) 0.2490(8) 0.6423(6) 0.085(2) Uani 1 1 d . . .
H13 H 1.8006 0.2010 0.6517 0.102 Uiso 1 1 calc R . .
C14 C 1.5439(9) 0.2095(7) 0.5605(5) 0.0752(18) Uani 1 1 d . . .
H14 H 1.6032 0.1367 0.5127 0.090 Uiso 1 1 calc R . .
C12 C 1.5764(13) 0.3600(9) 0.7105(6) 0.086(2) Uani 1 1 d . . .
H12 H 1.6579 0.3902 0.7645 0.103 Uiso 1 1 calc R . .

loop_
 _atom_site_aniso_label
```

```
 _atom_site_aniso_U_11
 _atom_site_aniso_U_22
 _atom_site_aniso_U_33
 _atom_site_aniso_U_23
 _atom_site_aniso_U_13
 _atom_site_aniso_U_12
O1 0.077(3) 0.080(3) 0.087(3) -0.025(2) -0.025(2) 0.000(2)
C5 0.052(4) 0.072(4) 0.063(4) -0.012(3) -0.014(3) 0.000(3)
C6 0.051(4) 0.062(4) 0.076(5) -0.016(3) -0.008(3) 0.006(3)
C1 0.056(4) 0.071(5) 0.056(4) -0.016(4) -0.012(3) 0.006(4)
C8 0.065(4) 0.058(4) 0.064(4) -0.011(3) -0.018(3) 0.005(3)
C7 0.054(4) 0.061(4) 0.066(4) -0.004(3) 0.003(3) 0.006(3)
O2 0.086(3) 0.068(3) 0.093(3) -0.024(3) -0.032(2) 0.008(2)
C3 0.060(3) 0.064(4) 0.068(4) -0.018(3) -0.006(3) 0.002(3)
C2 0.070(4) 0.056(4) 0.073(4) -0.013(3) -0.009(3) 0.001(3)
C9 0.065(4) 0.061(4) 0.056(4) -0.005(3) -0.002(3) -0.008(3)
C4 0.064(4) 0.054(4) 0.083(5) -0.015(3) -0.014(3) -0.004(3)
C10 0.073(4) 0.073(5) 0.085(5) -0.020(4) -0.005(4) 0.003(4)
C11 0.108(6) 0.070(5) 0.088(5) -0.020(4) -0.014(5) -0.005(5)
C13 0.076(5) 0.075(5) 0.105(6) -0.014(4) -0.025(5) -0.011(4)
C14 0.058(4) 0.078(5) 0.086(5) -0.015(4) -0.002(4) 0.001(4)
C12 0.106(6) 0.068(5) 0.089(6) -0.009(4) -0.034(5) -0.032(4)

_geom_special_details
;
 All esds (except the esd in the dihedral angle between two l.s. planes)
 are estimated using the full covariance matrix.  The cell esds are taken
 into account individually in the estimation of esds in distances, angles
 and torsion angles; correlations between esds in cell parameters are only
 used when they are defined by crystal symmetry.  An approximate (isotropic)
 treatment of cell esds is used for estimating esds involving l.s. planes.
;

loop_
 _geom_bond_atom_site_label_1
 _geom_bond_atom_site_label_2
 _geom_bond_distance
 _geom_bond_site_symmetry_2
 _geom_bond_publ_flag
O1 C1 1.311(6) . ?
C5 C6 1.165(7) . ?
C5 C4 1.441(6) . ?
C6 C7 1.397(7) . ?
C1 O2 1.199(6) . ?
C1 C2 1.479(7) . ?
C8 C7 1.194(7) . ?
```

```
C8 C9 1.436(7) . ?
C3 C2 1.496(6) . ?
C3 C4 1.521(6) . ?
C9 C10 1.355(7) . ?
C9 C14 1.378(7) . ?
C10 C11 1.374(7) . ?
C11 C12 1.353(8) . ?
C13 C14 1.366(7) . ?
C13 C12 1.373(8) . ?

loop_
 _geom_angle_atom_site_label_1
 _geom_angle_atom_site_label_2
 _geom_angle_atom_site_label_3
 _geom_angle
 _geom_angle_site_symmetry_1
 _geom_angle_site_symmetry_3
 _geom_angle_publ_flag
C6 C5 C4 174.9(6) . . ?
C5 C6 C7 177.9(6) . . ?
O2 C1 O1 124.2(6) . . ?
O2 C1 C2 123.1(5) . . ?
O1 C1 C2 112.7(6) . . ?
C7 C8 C9 178.7(6) . . ?
C8 C7 C6 179.1(6) . . ?
C2 C3 C4 113.3(5) . . ?
C1 C2 C3 113.2(5) . . ?
C10 C9 C14 119.2(6) . . ?
C10 C9 C8 120.4(6) . . ?
C14 C9 C8 120.4(6) . . ?
C5 C4 C3 111.8(5) . . ?
C9 C10 C11 120.5(6) . . ?
C12 C11 C10 120.2(7) . . ?
C14 C13 C12 119.7(7) . . ?
C13 C14 C9 120.4(6) . . ?
C11 C12 C13 119.9(6) . . ?

_diffrn_measured_fraction_theta_max    0.742
_diffrn_reflns_theta_full              28.73
_diffrn_measured_fraction_theta_full   0.742
_refine_diff_density_max    0.149
_refine_diff_density_min   -0.153
_refine_diff_density_rms    0.043
```

$(22b)_2$•3PyU

```
data_zl62t

_audit_creation_method            SHELXL-97
_chemical_name_systematic
;
 ?
;
_chemical_name_common              ?
_chemical_melting_point           ?
_chemical_formula_moiety          ?
_chemical_formula_sum
 'C39 H34 N4 O5'
_chemical_formula_weight          638.70

loop_
 _atom_type_symbol
 _atom_type_description
 _atom_type_scat_dispersion_real
 _atom_type_scat_dispersion_imag
 _atom_type_scat_source
 'C'  'C'   0.0033   0.0016
 'International Tables Vol C Tables 4.2.6.8 and 6.1.1.4'
 'H'  'H'   0.0000   0.0000
 'International Tables Vol C Tables 4.2.6.8 and 6.1.1.4'
 'N'  'N'   0.0061   0.0033
 'International Tables Vol C Tables 4.2.6.8 and 6.1.1.4'
 'O'  'O'   0.0106   0.0060
 'International Tables Vol C Tables 4.2.6.8 and 6.1.1.4'

_symmetry_cell_setting            Monoclinic
_symmetry_space_group_name_H-M    C2/c

loop_
 _symmetry_equiv_pos_as_xyz
 'x, y, z'
 '-x, y, -z+1/2'
 'x+1/2, y+1/2, z'
 '-x+1/2, y+1/2, -z+1/2'
 '-x, -y, -z'
 'x, -y, z-1/2'
 '-x+1/2, -y+1/2, -z'
 'x+1/2, -y+1/2, z-1/2'

_cell_length_a                    27.959(7)
```

```
_cell_length_b                  4.9517(12)
_cell_length_c                  26.208(6)
_cell_angle_alpha               90.00
_cell_angle_beta                112.726(5)
_cell_angle_gamma               90.00
_cell_volume                    3346.7(14)
_cell_formula_units_Z           4
_cell_measurement_temperature   273(2)
_cell_measurement_reflns_used   536
_cell_measurement_theta_min     2.95
_cell_measurement_theta_max     18.25

_exptl_crystal_description      ?
_exptl_crystal_colour           ?
_exptl_crystal_size_max         ?
_exptl_crystal_size_mid         ?
_exptl_crystal_size_min         ?
_exptl_crystal_density_meas     0
_exptl_crystal_density_diffrn   1.268
_exptl_crystal_density_method   'not measured'
_exptl_crystal_F_000            1344
_exptl_absorpt_coefficient_mu   0.085
_exptl_absorpt_correction_type  none
_exptl_absorpt_correction_T_min ?
_exptl_absorpt_correction_T_max ?
_exptl_absorpt_process_details  ?

_exptl_special_details
;
 ?
;

_diffrn_ambient_temperature     273(2)
_diffrn_radiation_wavelength    0.71073
_diffrn_radiation_type          MoK\a
_diffrn_radiation_source        'fine-focus sealed tube'
_diffrn_radiation_monochromator graphite
_diffrn_measurement_device_type 'CCD area detector'
_diffrn_measurement_method      'phi and omega scans'
_diffrn_detector_area_resol_mean ?
_diffrn_standards_number        ?
_diffrn_standards_interval_count ?
_diffrn_standards_interval_time ?
_diffrn_standards_decay_%       ?
_diffrn_reflns_number           9751
_diffrn_reflns_av_R_equivalents 0.1578
```

```
_diffrn_reflns_av_sigmaI/netI    0.3251
_diffrn_reflns_limit_h_min       -35
_diffrn_reflns_limit_h_max       34
_diffrn_reflns_limit_k_min       -5
_diffrn_reflns_limit_k_max       6
_diffrn_reflns_limit_l_min       -34
_diffrn_reflns_limit_l_max       34
_diffrn_reflns_theta_min         1.58
_diffrn_reflns_theta_max         28.59
_reflns_number_total             3795
_reflns_number_gt                929
_reflns_threshold_expression     >2sigma(I)

_computing_data_collection       'Bruker SMART'
_computing_cell_refinement       'Bruker SMART'
_computing_data_reduction        'Bruker SAINT'
_computing_structure_solution    'SHELXS-97 (Sheldrick, 1990)'
_computing_structure_refinement  'SHELXL-97 (Sheldrick, 1997)'
_computing_molecular_graphics    'Bruker SHELXTL'
_computing_publication_material  'Bruker SHELXTL'

_refine_special_details
;
 Refinement of F^2^ against ALL reflections.  The weighted R-factor wR and
 goodness of fit S are based on F^2^, conventional R-factors R are based
 on F, with F set to zero for negative F^2^. The threshold expression of
 F^2^ > 2sigma(F^2^) is used only for calculating R-factors(gt) etc. and is
 not relevant to the choice of reflections for refinement.  R-factors based
 on F^2^ are statistically about twice as large as those based on F, and R-
 factors based on ALL data will be even larger.
;

_refine_ls_structure_factor_coef  Fsqd
_refine_ls_matrix_type           full
_refine_ls_weighting_scheme      calc
_refine_ls_weighting_details
 'calc w=1/[\s^2^(Fo^2^)+(0.1037P)^2^+0.0000P] where P=(Fo^2^+2Fc^2^)/3'
_atom_sites_solution_primary     direct
_atom_sites_solution_secondary   difmap
_atom_sites_solution_hydrogens   geom
_refine_ls_hydrogen_treatment    mixed
_refine_ls_extinction_method     SHELXL
_refine_ls_extinction_coef       0.0016(8)
_refine_ls_extinction_expression
 'Fc^*^=kFc[1+0.001xFc^2^\l^3^/sin(2\q)]^-1/4^'
_refine_ls_number_reflns         3795
```

```
_refine_ls_number_parameters      219
_refine_ls_number_restraints      0
_refine_ls_R_factor_all           0.3144
_refine_ls_R_factor_gt            0.0820
_refine_ls_wR_factor_ref          0.3195
_refine_ls_wR_factor_gt           0.2002
_refine_ls_goodness_of_fit_ref    0.861
_refine_ls_restrained_S_all       0.861
_refine_ls_shift/su_max           0.000
_refine_ls_shift/su_mean          0.000

loop_
 _atom_site_label
 _atom_site_type_symbol
 _atom_site_fract_x
 _atom_site_fract_y
 _atom_site_fract_z
 _atom_site_U_iso_or_equiv
 _atom_site_adp_type
 _atom_site_occupancy
 _atom_site_symmetry_multiplicity
 _atom_site_calc_flag
 _atom_site_refinement_flags
 _atom_site_disorder_assembly
 _atom_site_disorder_group
O1 O 0.21885(15) 1.3846(9) 0.40589(15) 0.0686(13) Uani 1 1 d . . .
O2 O 0.26286(14) 1.4328(9) 0.35142(16) 0.0749(14) Uani 1 1 d . . .
H2 H 0.2405 1.5464 0.3365 0.112 Uiso 1 1 calc R . .
N1 N 0.04171(17) 0.3301(10) 0.2801(2) 0.0658(15) Uani 1 1 d . . .
H1 H 0.0401 0.5030 0.2768 0.079 Uiso 1 1 calc R . .
C5 C 0.1934(2) -0.0927(14) 0.2506(3) 0.0665(18) Uani 1 1 d . . .
H5 H 0.2172 -0.1553 0.2366 0.080 Uiso 1 1 calc R . .
C8 C 0.2545(2) 1.3222(12) 0.3933(2) 0.0526(15) Uani 1 1 d . . .
N2 N 0.19354(18) -0.2004(10) 0.2968(2) 0.0607(14) Uani 1 1 d . . .
C3 C 0.1241(2) 0.1016(12) 0.2913(2) 0.0516(15) Uani 1 1 d . . .
O3 O 0.0000 -0.0704(13) 0.2500 0.0724(18) Uani 1 2 d S . .
C4 C 0.1598(2) -0.1040(12) 0.3169(2) 0.0553(16) Uani 1 1 d . . .
H4 H 0.1599 -0.1770 0.3497 0.066 Uiso 1 1 calc R . .
C9 C 0.2945(2) 1.1135(12) 0.4220(2) 0.0547(16) Uani 1 1 d . . .
H9A H 0.3286 1.1960 0.4342 0.066 Uiso 1 1 calc R . .
H9B H 0.2931 0.9723 0.3958 0.066 Uiso 1 1 calc R . .
C1 C 0.0000 0.178(2) 0.2500 0.055(2) Uani 1 2 d S . .
C6 C 0.1598(2) 0.1060(14) 0.2226(2) 0.0653(18) Uani 1 1 d . . .
H6 H 0.1604 0.1750 0.1899 0.078 Uiso 1 1 calc R . .
C12 C 0.3630(2) 0.6305(14) 0.5169(3) 0.0633(18) Uani 1 1 d . . .
C10 C 0.2878(2) 0.9877(12) 0.4713(2) 0.0673(18) Uani 1 1 d . . .
```

H10A H 0.2894 1.1272 0.4979 0.081 Uiso 1 1 calc R . .
H10B H 0.2541 0.9020 0.4594 0.081 Uiso 1 1 calc R . .
C7 C 0.1251(2) 0.2027(12) 0.2433(2) 0.0617(17) Uani 1 1 d . . .
H7 H 0.1020 0.3385 0.2245 0.074 Uiso 1 1 calc R . .
C14 C 0.4414(3) 0.3109(13) 0.5540(3) 0.0669(19) Uani 1 1 d . . .
C2 C 0.0890(2) 0.2049(13) 0.3180(2) 0.0669(18) Uani 1 1 d . . .
H2A H 0.0799 0.0557 0.3364 0.080 Uiso 1 1 calc R . .
H2B H 0.1079 0.3357 0.3461 0.080 Uiso 1 1 calc R . .
C11 C 0.3281(2) 0.7882(13) 0.4973(3) 0.0631(18) Uani 1 1 d . . .
C15 C 0.4885(2) 0.1511(13) 0.5750(2) 0.0598(17) Uani 1 1 d . . .
C13 C 0.4043(3) 0.4564(14) 0.5365(3) 0.0663(18) Uani 1 1 d . . .
C18 C 0.5792(3) -0.1388(15) 0.6155(3) 0.082(2) Uani 1 1 d . . .
H18 H 0.6097 -0.2387 0.6290 0.098 Uiso 1 1 calc R . .
C16 C 0.5288(3) 0.2074(14) 0.5585(3) 0.081(2) Uani 1 1 d . . .
H16 H 0.5253 0.3473 0.5336 0.097 Uiso 1 1 calc R . .
C20 C 0.4952(3) -0.0509(14) 0.6121(3) 0.0735(19) Uani 1 1 d . . .
H20 H 0.4683 -0.0929 0.6234 0.088 Uiso 1 1 calc R . .
C17 C 0.5739(3) 0.0606(16) 0.5781(3) 0.085(2) Uani 1 1 d . . .
H17 H 0.6005 0.0972 0.5661 0.102 Uiso 1 1 calc R . .
C19 C 0.5409(3) -0.1953(14) 0.6334(3) 0.083(2) Uani 1 1 d . . .
H19 H 0.5453 -0.3293 0.6597 0.099 Uiso 1 1 calc R . .

loop_
 _atom_site_aniso_label
 _atom_site_aniso_U_11
 _atom_site_aniso_U_22
 _atom_site_aniso_U_33
 _atom_site_aniso_U_23
 _atom_site_aniso_U_13
 _atom_site_aniso_U_12
O1 0.064(3) 0.075(3) 0.075(3) 0.013(2) 0.036(2) 0.019(2)
O2 0.080(3) 0.077(3) 0.079(3) 0.025(3) 0.042(2) 0.024(2)
N1 0.053(3) 0.058(4) 0.080(3) -0.004(3) 0.018(3) 0.002(3)
C5 0.062(4) 0.069(5) 0.073(4) -0.003(4) 0.031(4) 0.002(4)
C8 0.057(4) 0.047(4) 0.052(4) 0.003(3) 0.019(3) 0.000(3)
N2 0.067(4) 0.054(4) 0.067(3) 0.006(3) 0.032(3) 0.005(3)
C3 0.048(3) 0.056(4) 0.046(3) -0.002(3) 0.012(3) -0.003(3)
O3 0.070(4) 0.044(4) 0.104(5) 0.000 0.033(4) 0.000
C4 0.057(4) 0.054(4) 0.051(3) 0.003(3) 0.017(3) -0.005(3)
C9 0.054(4) 0.052(4) 0.062(4) 0.002(3) 0.026(3) 0.011(3)
C1 0.046(6) 0.058(7) 0.061(5) 0.000 0.023(5) 0.000
C6 0.068(4) 0.070(5) 0.054(4) 0.007(4) 0.019(4) -0.001(4)
C12 0.053(4) 0.060(5) 0.079(4) 0.001(4) 0.028(4) 0.005(4)
C10 0.068(4) 0.053(5) 0.085(4) 0.011(4) 0.034(4) 0.017(3)
C7 0.064(4) 0.057(4) 0.067(4) 0.006(3) 0.029(3) 0.010(3)
C14 0.071(5) 0.051(5) 0.077(4) 0.004(4) 0.027(4) 0.003(4)

```
C2 0.061(4) 0.071(5) 0.065(4) -0.002(4) 0.019(3) -0.002(3)
C11 0.060(4) 0.055(5) 0.083(4) 0.001(4) 0.038(4) 0.001(4)
C15 0.063(4) 0.048(4) 0.063(4) 0.005(3) 0.019(3) 0.011(3)
C13 0.069(5) 0.053(5) 0.079(5) 0.000(4) 0.031(4) 0.001(4)
C18 0.082(5) 0.079(6) 0.078(5) 0.008(5) 0.024(4) 0.029(4)
C16 0.077(5) 0.073(5) 0.096(5) 0.025(4) 0.037(4) 0.020(4)
C20 0.077(5) 0.065(5) 0.079(5) -0.008(4) 0.030(4) -0.002(4)
C17 0.074(5) 0.089(6) 0.097(5) 0.014(5) 0.038(4) 0.024(5)
C19 0.096(6) 0.067(5) 0.076(5) 0.009(4) 0.024(5) 0.007(5)

_geom_special_details
;
 All esds (except the esd in the dihedral angle between two l.s. planes)
 are estimated using the full covariance matrix.  The cell esds are taken
 into account individually in the estimation of esds in distances, angles
 and torsion angles; correlations between esds in cell parameters are only
 used when they are defined by crystal symmetry.  An approximate (isotropic)
 treatment of cell esds is used for estimating esds involving l.s. planes.
;

loop_
 _geom_bond_atom_site_label_1
 _geom_bond_atom_site_label_2
 _geom_bond_distance
 _geom_bond_site_symmetry_2
 _geom_bond_publ_flag
O1 C8 1.205(6) . ?
O2 C8 1.326(6) . ?
N1 C1 1.355(7) . ?
N1 C2 1.450(7) . ?
C5 N2 1.321(7) . ?
C5 C6 1.363(8) . ?
C8 C9 1.495(7) . ?
N2 C4 1.336(7) . ?
C3 C7 1.364(7) . ?
C3 C4 1.402(7) . ?
C3 C2 1.498(7) . ?
O3 C1 1.231(9) . ?
C9 C10 1.508(7) . ?
C1 N1 1.355(7) 2 ?
C6 C7 1.368(7) . ?
C12 C11 1.200(8) . ?
C12 C13 1.371(9) . ?
C10 C11 1.454(8) . ?
C14 C13 1.200(8) . ?
C14 C15 1.450(8) . ?
```

```
C15 C20 1.357(8) . ?
C15 C16 1.382(8) . ?
C18 C19 1.355(9) . ?
C18 C17 1.358(9) . ?
C16 C17 1.373(8) . ?
C20 C19 1.380(8) . ?

loop_
 _geom_angle_atom_site_label_1
 _geom_angle_atom_site_label_2
 _geom_angle_atom_site_label_3
 _geom_angle
 _geom_angle_site_symmetry_1
 _geom_angle_site_symmetry_3
 _geom_angle_publ_flag
C1 N1 C2 120.9(6) . . ?
N2 C5 C6 122.8(6) . . ?
O1 C8 O2 123.4(6) . . ?
O1 C8 C9 125.2(5) . . ?
O2 C8 C9 111.4(5) . . ?
C5 N2 C4 117.8(5) . . ?
C7 C3 C4 116.4(5) . . ?
C7 C3 C2 123.8(6) . . ?
C4 C3 C2 119.8(5) . . ?
N2 C4 C3 123.4(5) . . ?
C8 C9 C10 113.6(5) . . ?
O3 C1 N1 123.7(4) . . ?
O3 C1 N1 123.7(4) . 2 ?
N1 C1 N1 112.6(8) . 2 ?
C5 C6 C7 119.1(6) . . ?
C11 C12 C13 175.8(7) . . ?
C11 C10 C9 110.6(5) . . ?
C3 C7 C6 120.5(6) . . ?
C13 C14 C15 176.0(7) . . ?
N1 C2 C3 114.5(5) . . ?
C12 C11 C10 175.9(7) . . ?
C20 C15 C16 118.1(6) . . ?
C20 C15 C14 121.8(6) . . ?
C16 C15 C14 120.1(6) . . ?
C14 C13 C12 177.9(7) . . ?
C19 C18 C17 121.4(7) . . ?
C17 C16 C15 121.2(7) . . ?
C15 C20 C19 121.4(7) . . ?
C18 C17 C16 118.9(7) . . ?
C18 C19 C20 119.0(7) . . ?
```

_diffrn_measured_fraction_theta_max 0.886
_diffrn_reflns_theta_full 28.59
_diffrn_measured_fraction_theta_full 0.886
_refine_diff_density_max 0.250
_refine_diff_density_min -0.257
_refine_diff_density_rms 0.057

$(22b)_2$•4PyU

```
data_zl64t

_audit_creation_method            SHELXL-97
_chemical_name_systematic
;
 ?
;
_chemical_name_common             ?
_chemical_melting_point           ?
_chemical_formula_moiety          ?
_chemical_formula_sum
 'C39 H34 N4 O5'
_chemical_formula_weight          638.70

loop_
 _atom_type_symbol
 _atom_type_description
 _atom_type_scat_dispersion_real
 _atom_type_scat_dispersion_imag
 _atom_type_scat_source
 'C'  'C'   0.0033   0.0016
 'International Tables Vol C Tables 4.2.6.8 and 6.1.1.4'
 'H'  'H'   0.0000   0.0000
 'International Tables Vol C Tables 4.2.6.8 and 6.1.1.4'
 'N'  'N'   0.0061   0.0033
 'International Tables Vol C Tables 4.2.6.8 and 6.1.1.4'
 'O'  'O'   0.0106   0.0060
 'International Tables Vol C Tables 4.2.6.8 and 6.1.1.4'

_symmetry_cell_setting            Monoclinic
_symmetry_space_group_name_H-M    C2

loop_
 _symmetry_equiv_pos_as_xyz
 'x, y, z'
 '-x, y, -z'
 'x+1/2, y+1/2, z'
 '-x+1/2, y+1/2, -z'

_cell_length_a                    32.563(16)
_cell_length_b                    4.597(2)
_cell_length_c                    11.503(6)
_cell_angle_alpha                 90.00
_cell_angle_beta                  90.610(9)
```

```
_cell_angle_gamma                90.00
_cell_volume                     1721.7(15)
_cell_formula_units_Z            2
_cell_measurement_temperature    273(2)
_cell_measurement_reflns_used    466
_cell_measurement_theta_min      3.05
_cell_measurement_theta_max      21.74

_exptl_crystal_description       ?
_exptl_crystal_colour            ?
_exptl_crystal_size_max          ?
_exptl_crystal_size_mid          ?
_exptl_crystal_size_min          ?
_exptl_crystal_density_meas      0
_exptl_crystal_density_diffrn    1.232
_exptl_crystal_density_method    'not measured'
_exptl_crystal_F_000             672
_exptl_absorpt_coefficient_mu    0.083
_exptl_absorpt_correction_type   none
_exptl_absorpt_correction_T_min  ?
_exptl_absorpt_correction_T_max  ?
_exptl_absorpt_process_details   ?

_exptl_special_details
;
 ?
;

_diffrn_ambient_temperature      273(2)
_diffrn_radiation_wavelength     0.71073
_diffrn_radiation_type           MoK\a
_diffrn_radiation_source         'fine-focus sealed tube'
_diffrn_radiation_monochromator  graphite
_diffrn_measurement_device_type  'CCD area detector'
_diffrn_measurement_method       'phi and omega scans'
_diffrn_detector_area_resol_mean  ?
_diffrn_standards_number         ?
_diffrn_standards_interval_count  ?
_diffrn_standards_interval_time  ?
_diffrn_standards_decay_%        ?
_diffrn_reflns_number            5343
_diffrn_reflns_av_R_equivalents  0.0697
_diffrn_reflns_av_sigmaI/netI    0.2891
_diffrn_reflns_limit_h_min       -41
_diffrn_reflns_limit_h_max       42
_diffrn_reflns_limit_k_min       -6
```

```
_diffrn_reflns_limit_k_max       5
_diffrn_reflns_limit_l_min       -14
_diffrn_reflns_limit_l_max       10
_diffrn_reflns_theta_min         1.25
_diffrn_reflns_theta_max         28.51
_reflns_number_total             3601
_reflns_number_gt                1286
_reflns_threshold_expression     >2sigma(I)

_computing_data_collection       'Bruker SMART'
_computing_cell_refinement       'Bruker SMART'
_computing_data_reduction        'Bruker SAINT'
_computing_structure_solution    'SHELXS-97 (Sheldrick, 1990)'
_computing_structure_refinement   'SHELXL-97 (Sheldrick, 1997)'
_computing_molecular_graphics    'Bruker SHELXTL'
_computing_publication_material   'Bruker SHELXTL'

_refine_special_details
;
 Refinement of F^2^ against ALL reflections.  The weighted R-factor wR and
 goodness of fit S are based on F^2^, conventional R-factors R are based
 on F, with F set to zero for negative F^2^. The threshold expression of
 F^2^ > 2sigma(F^2^) is used only for calculating R-factors(gt) etc. and is
 not relevant to the choice of reflections for refinement.  R-factors based
 on F^2^ are statistically about twice as large as those based on F, and R-
 factors based on ALL data will be even larger.
;

_refine_ls_structure_factor_coef  Fsqd
_refine_ls_matrix_type           full
_refine_ls_weighting_scheme      calc
_refine_ls_weighting_details
 'calc w=1/[\s^2^(Fo^2^)+(0.0816P)^2^+0.0000P] where P=(Fo^2^+2Fc^2^)/3'
_atom_sites_solution_primary     direct
_atom_sites_solution_secondary    difmap
_atom_sites_solution_hydrogens    geom
_refine_ls_hydrogen_treatment    mixed
_refine_ls_extinction_method     none
_refine_ls_extinction_coef       ?
_refine_ls_abs_structure_details
 'Flack H D (1983), Acta Cryst. A39, 876-881'
_refine_ls_abs_structure_Flack    -2(5)
_refine_ls_number_reflns         3601
_refine_ls_number_parameters     222
_refine_ls_number_restraints     1
_refine_ls_R_factor_all          0.2344
```

```
_refine_ls_R_factor_gt           0.0897
_refine_ls_wR_factor_ref         0.3616
_refine_ls_wR_factor_gt          0.2270
_refine_ls_goodness_of_fit_ref   0.922
_refine_ls_restrained_S_all      0.922
_refine_ls_shift/su_max          0.000
_refine_ls_shift/su_mean         0.000

loop_
 _atom_site_label
 _atom_site_type_symbol
 _atom_site_fract_x
 _atom_site_fract_y
 _atom_site_fract_z
 _atom_site_U_iso_or_equiv
 _atom_site_adp_type
 _atom_site_occupancy
 _atom_site_symmetry_multiplicity
 _atom_site_calc_flag
 _atom_site_refinement_flags
 _atom_site_disorder_assembly
 _atom_site_disorder_group
N1 N 0.48173(18) 0.4630(14) 0.0844(4) 0.0558(16) Uani 1 1 d . . .
H1 H 0.4802 0.2766 0.0795 0.067 Uiso 1 1 calc R . .
O2 O 0.43754(17) 1.6204(16) -0.3481(5) 0.084(2) Uani 1 1 d . . .
N2 N 0.40923(19) -0.0032(14) 0.4153(5) 0.0565(17) Uani 1 1 d . . .
C1 C 0.5000 0.617(2) 0.0000 0.047(2) Uani 1 2 d S . .
O1 O 0.5000 0.8845(19) 0.0000 0.077(2) Uani 1 2 d S . .
O3 O 0.37660(16) 1.6260(17) -0.4360(5) 0.0765(19) Uani 1 1 d . . .
C3 C 0.3884(2) 0.103(2) 0.3250(7) 0.064(2) Uani 1 1 d . . .
H3 H 0.3615 0.0412 0.3132 0.077 Uiso 1 1 calc R . .
C7 C 0.4474(2) 0.085(2) 0.4298(6) 0.063(2) Uani 1 1 d . . .
H7 H 0.4624 0.0113 0.4924 0.076 Uiso 1 1 calc R . .
C9 C 0.3824(2) 1.351(2) -0.2669(6) 0.072(3) Uani 1 1 d . . .
H9A H 0.3724 1.1774 -0.3058 0.087 Uiso 1 1 calc R . .
H9B H 0.3588 1.4518 -0.2358 0.087 Uiso 1 1 calc R . .
C5 C 0.4446(2) 0.3939(18) 0.2647(6) 0.055(2) Uani 1 1 d . . .
C13 C 0.3387(3) 0.832(2) 0.0609(7) 0.074(3) Uani 1 1 d . . .
C2 C 0.4644(3) 0.614(2) 0.1842(6) 0.071(2) Uani 1 1 d . . .
H2A H 0.4441 0.7543 0.1580 0.085 Uiso 1 1 calc R . .
H2B H 0.4860 0.7184 0.2257 0.085 Uiso 1 1 calc R . .
C8 C 0.4016(3) 1.540(2) -0.3542(7) 0.063(2) Uani 1 1 d . . .
C4 C 0.4047(2) 0.2971(19) 0.2487(6) 0.064(2) Uani 1 1 d . . .
H4 H 0.3891 0.3644 0.1861 0.077 Uiso 1 1 calc R . .
C6 C 0.4662(2) 0.279(2) 0.3584(6) 0.064(2) Uani 1 1 d . . .
H6 H 0.4933 0.3336 0.3724 0.077 Uiso 1 1 calc R . .
```

C12 C 0.3654(3) 0.965(2) -0.0133(7) 0.077(3) Uani 1 1 d . . .
C10 C 0.4098(3) 1.259(3) -0.1664(7) 0.080(3) Uani 1 1 d . . .
H10A H 0.4321 1.1409 -0.1955 0.096 Uiso 1 1 calc R . .
H10B H 0.4216 1.4302 -0.1299 0.096 Uiso 1 1 calc R . .
C11 C 0.3872(3) 1.094(2) -0.0807(7) 0.076(3) Uani 1 1 d . . .
C15 C 0.2859(3) 0.566(2) 0.1946(7) 0.072(2) Uani 1 1 d . . .
C17 C 0.2659(3) 0.363(3) 0.3773(8) 0.087(3) Uani 1 1 d . . .
H17 H 0.2720 0.3193 0.4544 0.105 Uiso 1 1 calc R . .
C16 C 0.2940(3) 0.506(2) 0.3115(7) 0.077(3) Uani 1 1 d . . .
H16 H 0.3189 0.5628 0.3447 0.093 Uiso 1 1 calc R . .
C14 C 0.3152(3) 0.709(2) 0.1219(7) 0.075(3) Uani 1 1 d . . .
C18 C 0.2291(3) 0.286(3) 0.3307(10) 0.107(4) Uani 1 1 d . . .
H18 H 0.2094 0.1945 0.3759 0.128 Uiso 1 1 calc R . .
C20 C 0.2490(3) 0.477(3) 0.1480(8) 0.102(4) Uani 1 1 d . . .
H20 H 0.2432 0.5075 0.0696 0.122 Uiso 1 1 calc R . .
C19 C 0.2214(3) 0.345(4) 0.2156(11) 0.128(5) Uani 1 1 d . . .
H19 H 0.1962 0.2923 0.1835 0.154 Uiso 1 1 calc R . .
H3B H 0.383(2) 1.77(2) -0.492(6) 0.06(2) Uiso 1 1 d . . .

loop_
 _atom_site_aniso_label
 _atom_site_aniso_U_11
 _atom_site_aniso_U_22
 _atom_site_aniso_U_33
 _atom_site_aniso_U_23
 _atom_site_aniso_U_13
 _atom_site_aniso_U_12
N1 0.082(4) 0.034(4) 0.052(3) 0.000(3) 0.018(3) 0.001(3)
O2 0.071(4) 0.107(6) 0.075(4) 0.017(4) -0.004(3) -0.007(4)
N2 0.066(4) 0.051(4) 0.052(3) 0.004(3) 0.004(3) -0.004(4)
C1 0.057(6) 0.037(7) 0.048(6) 0.000 0.008(5) 0.000
O1 0.123(7) 0.035(5) 0.075(5) 0.000 0.036(4) 0.000
O3 0.069(3) 0.091(5) 0.069(4) 0.023(4) -0.004(3) -0.011(4)
C3 0.065(5) 0.060(6) 0.067(5) 0.006(5) -0.008(4) -0.005(5)
C7 0.070(5) 0.069(6) 0.051(4) 0.006(4) -0.001(4) 0.003(5)
C9 0.076(5) 0.080(7) 0.061(5) 0.003(5) 0.006(4) -0.002(5)
C5 0.077(5) 0.037(4) 0.052(4) -0.004(4) 0.014(4) 0.000(4)
C13 0.069(5) 0.094(8) 0.059(5) 0.019(5) -0.009(4) -0.007(5)
C2 0.108(6) 0.047(5) 0.058(4) -0.008(4) 0.031(4) -0.001(5)
C8 0.060(5) 0.068(6) 0.062(5) -0.006(4) 0.010(4) -0.005(5)
C4 0.080(6) 0.058(6) 0.055(4) 0.007(4) -0.016(4) -0.002(5)
C6 0.054(4) 0.077(7) 0.062(5) 0.006(5) 0.000(4) -0.003(4)
C12 0.081(6) 0.092(8) 0.057(5) 0.013(5) -0.014(4) -0.003(6)
C10 0.085(6) 0.089(7) 0.066(5) 0.010(5) -0.004(4) -0.009(6)
C11 0.080(5) 0.090(8) 0.059(5) 0.011(5) -0.004(4) -0.001(6)
C15 0.081(5) 0.073(7) 0.060(5) -0.004(5) 0.000(4) -0.002(5)

```
C17 0.094(7) 0.102(9) 0.065(5) 0.001(5) 0.005(5) -0.006(6)
C16 0.077(5) 0.083(7) 0.072(5) 0.006(5) 0.007(4) -0.009(5)
C14 0.072(6) 0.090(7) 0.064(5) 0.006(5) -0.006(4) -0.010(5)
C18 0.072(6) 0.133(12) 0.117(9) 0.023(8) 0.007(6) -0.013(7)
C20 0.095(7) 0.127(11) 0.083(6) 0.030(7) -0.018(6) -0.048(7)
C19 0.080(7) 0.171(15) 0.134(10) 0.050(10) -0.040(7) -0.037(9)

_geom_special_details
;
 All esds (except the esd in the dihedral angle between two l.s. planes)
 are estimated using the full covariance matrix.  The cell esds are taken
 into account individually in the estimation of esds in distances, angles
 and torsion angles; correlations between esds in cell parameters are only
 used when they are defined by crystal symmetry.  An approximate (isotropic)
 treatment of cell esds is used for estimating esds involving l.s. planes.
;

loop_
 _geom_bond_atom_site_label_1
 _geom_bond_atom_site_label_2
 _geom_bond_distance
 _geom_bond_site_symmetry_2
 _geom_bond_publ_flag
N1 C1 1.344(8) . ?
N1 C2 1.461(9) . ?
O2 C8 1.229(8) . ?
N2 C7 1.318(9) . ?
N2 C3 1.327(10) . ?
C1 O1 1.231(13) . ?
C1 N1 1.344(8) 2_655 ?
O3 C8 1.299(10) . ?
C3 C4 1.365(11) . ?
C7 C6 1.360(11) . ?
C9 C8 1.471(12) . ?
C9 C10 1.512(12) . ?
C5 C6 1.385(10) . ?
C5 C4 1.385(10) . ?
C5 C2 1.520(11) . ?
C13 C14 1.187(11) . ?
C13 C12 1.369(13) . ?
C12 C11 1.213(11) . ?
C10 C11 1.448(12) . ?
C15 C20 1.372(12) . ?
C15 C16 1.396(11) . ?
C15 C14 1.434(12) . ?
C17 C18 1.356(13) . ?
```

```
C17 C16 1.360(13) . ?
C18 C19 1.372(14) . ?
C20 C19 1.338(14) . ?

loop_
 _geom_angle_atom_site_label_1
 _geom_angle_atom_site_label_2
 _geom_angle_atom_site_label_3
 _geom_angle
 _geom_angle_site_symmetry_1
 _geom_angle_site_symmetry_3
 _geom_angle_publ_flag
C1 N1 C2 119.7(7) . . ?
C7 N2 C3 117.4(7) . . ?
O1 C1 N1 121.7(5) . . ?
O1 C1 N1 121.7(5) . 2_655 ?
N1 C1 N1 116.6(9) . 2_655 ?
N2 C3 C4 123.0(7) . . ?
N2 C7 C6 123.7(7) . . ?
C8 C9 C10 116.0(7) . . ?
C6 C5 C4 116.6(7) . . ?
C6 C5 C2 120.9(8) . . ?
C4 C5 C2 122.5(7) . . ?
C14 C13 C12 177.4(11) . . ?
N1 C2 C5 109.4(7) . . ?
O2 C8 O3 122.6(8) . . ?
O2 C8 C9 123.3(8) . . ?
O3 C8 C9 114.1(7) . . ?
C3 C4 C5 119.7(7) . . ?
C7 C6 C5 119.5(7) . . ?
C11 C12 C13 176.3(10) . . ?
C11 C10 C9 111.7(7) . . ?
C12 C11 C10 174.4(9) . . ?
C20 C15 C16 118.2(8) . . ?
C20 C15 C14 119.6(7) . . ?
C16 C15 C14 122.2(7) . . ?
C18 C17 C16 120.2(9) . . ?
C17 C16 C15 120.7(8) . . ?
C13 C14 C15 178.3(10) . . ?
C17 C18 C19 118.6(9) . . ?
C19 C20 C15 119.8(9) . . ?
C20 C19 C18 122.3(9) . . ?

_diffrn_measured_fraction_theta_max    0.892
_diffrn_reflns_theta_full              28.51
_diffrn_measured_fraction_theta_full   0.892
```

```
_refine_diff_density_max    0.227
_refine_diff_density_min   -0.235
_refine_diff_density_rms    0.059
```

$(22b)_2$•4PyO

```
data_zl61t

_audit_creation_method           SHELXL-97
_chemical_name_systematic
;
 ?
;
_chemical_name_common            ?
_chemical_melting_point          ?
_chemical_formula_moiety         ?
_chemical_formula_sum
 'C40 H34 N4 O6'
_chemical_formula_weight         666.71

loop_
 _atom_type_symbol
 _atom_type_description
 _atom_type_scat_dispersion_real
 _atom_type_scat_dispersion_imag
 _atom_type_scat_source
'C'  'C'   0.0033   0.0016
 'International Tables Vol C Tables 4.2.6.8 and 6.1.1.4'
 'H'  'H'   0.0000   0.0000
 'International Tables Vol C Tables 4.2.6.8 and 6.1.1.4'
 'N'  'N'   0.0061   0.0033
 'International Tables Vol C Tables 4.2.6.8 and 6.1.1.4'
 'O'  'O'   0.0106   0.0060
 'International Tables Vol C Tables 4.2.6.8 and 6.1.1.4'

_symmetry_cell_setting           Triclinic
_symmetry_space_group_name_H-M    P-1

loop_
 _symmetry_equiv_pos_as_xyz
 'x, y, z'
 '-x, -y, -z'

_cell_length_a                  5.0890(16)
_cell_length_b                  13.163(4)
_cell_length_c                  13.197(4)
_cell_angle_alpha                85.119(7)
_cell_angle_beta                 86.399(8)
_cell_angle_gamma                84.406(7)
_cell_volume                    875.3(5)
```

```
_cell_formula_units_Z            1
_cell_measurement_temperature    273(2)
_cell_measurement_reflns_used    330
_cell_measurement_theta_min      3.10
_cell_measurement_theta_max      15.06

_exptl_crystal_description       ?
_exptl_crystal_colour            ?
_exptl_crystal_size_max          ?
_exptl_crystal_size_mid          ?
_exptl_crystal_size_min          ?
_exptl_crystal_density_meas      0
_exptl_crystal_density_diffrn    1.265
_exptl_crystal_density_method    'not measured'
_exptl_crystal_F_000             350
_exptl_absorpt_coefficient_mu    0.086
_exptl_absorpt_correction_type   none
_exptl_absorpt_correction_T_min  ?
_exptl_absorpt_correction_T_max  ?
_exptl_absorpt_process_details   ?

_exptl_special_details
;
 ?
;

_diffrn_ambient_temperature      273(2)
_diffrn_radiation_wavelength     0.71073
_diffrn_radiation_type           MoK\a
_diffrn_radiation_source         'fine-focus sealed tube'
_diffrn_radiation_monochromator  graphite
_diffrn_measurement_device_type  'CCD area detector'
_diffrn_measurement_method       'phi and omega scans'
_diffrn_detector_area_resol_mean  ?
_diffrn_standards_number         ?
_diffrn_standards_interval_count  ?
_diffrn_standards_interval_time  ?
_diffrn_standards_decay_%        ?
_diffrn_reflns_number            5427
_diffrn_reflns_av_R_equivalents  0.1061
_diffrn_reflns_av_sigmaI/netI    0.4454
_diffrn_reflns_limit_h_min       -6
_diffrn_reflns_limit_h_max       6
_diffrn_reflns_limit_k_min       -17
_diffrn_reflns_limit_k_max       13
_diffrn_reflns_limit_l_min       -16
```

```
_diffrn_reflns_limit_l_max       17
_diffrn_reflns_theta_min         1.55
_diffrn_reflns_theta_max         28.35
_reflns_number_total             3753
_reflns_number_gt                744
_reflns_threshold_expression     >2sigma(I)

_computing_data_collection       'Bruker SMART'
_computing_cell_refinement       'Bruker SMART'
_computing_data_reduction        'Bruker SAINT'
_computing_structure_solution    'SHELXS-97 (Sheldrick, 1990)'
_computing_structure_refinement  'SHELXL-97 (Sheldrick, 1997)'
_computing_molecular_graphics    'Bruker SHELXTL'
_computing_publication_material  'Bruker SHELXTL'

_refine_special_details
;
Refinement of F^2^ against ALL reflections.  The weighted R-factor wR and
goodness of fit S are based on F^2^, conventional R-factors R are based
on F, with F set to zero for negative F^2^. The threshold expression of
F^2^ > 2sigma(F^2^) is used only for calculating R-factors(gt) etc. and is
not relevant to the choice of reflections for refinement.  R-factors based
on F^2^ are statistically about twice as large as those based on F, and R-
factors based on ALL data will be even larger.
;

_refine_ls_structure_factor_coef  Fsqd
_refine_ls_matrix_type           full
_refine_ls_weighting_scheme      calc
_refine_ls_weighting_details
'calc w=1/[\s^2^(Fo^2^)+(0.0464P)^2^+0.0000P] where P=(Fo^2^+2Fc^2^)/3'
_atom_sites_solution_primary     direct
_atom_sites_solution_secondary   difmap
_atom_sites_solution_hydrogens   geom
_refine_ls_hydrogen_treatment    mixed
_refine_ls_extinction_method     none
_refine_ls_extinction_coef       ?
_refine_ls_number_reflns         3753
_refine_ls_number_parameters     230
_refine_ls_number_restraints     0
_refine_ls_R_factor_all          0.3829
_refine_ls_R_factor_gt           0.0955
_refine_ls_wR_factor_ref         0.3377
_refine_ls_wR_factor_gt          0.1969
_refine_ls_goodness_of_fit_ref   0.846
_refine_ls_restrained_S_all      0.846
```

```
_refine_ls_shift/su_max          0.000
_refine_ls_shift/su_mean         0.000

loop_
 _atom_site_label
 _atom_site_type_symbol
 _atom_site_fract_x
 _atom_site_fract_y
 _atom_site_fract_z
 _atom_site_U_iso_or_equiv
 _atom_site_adp_type
 _atom_site_occupancy
 _atom_site_symmetry_multiplicity
 _atom_site_calc_flag
 _atom_site_refinement_flags
 _atom_site_disorder_assembly
 _atom_site_disorder_group
H2C H -0.168(15) 0.271(6) 0.515(6) 0.08(3) Uiso 1 1 d . . .
O1 O -0.2406(11) -0.0186(4) 0.9150(3) 0.0701(16) Uani 1 1 d . . .
O2 O -0.0811(15) 0.3168(5) 0.4934(5) 0.095(2) Uani 1 1 d . . .
N2 N 0.2044(12) -0.0210(4) 0.8894(4) 0.0586(17) Uani 1 1 d . . .
H2 H 0.3488 -0.0136 0.9174 0.070 Uiso 1 1 calc R . .
C2 C 0.2174(14) -0.0446(5) 0.7825(5) 0.067(2) Uani 1 1 d . . .
H2A H 0.0395 -0.0486 0.7616 0.080 Uiso 1 1 calc R . .
H2B H 0.3147 -0.1111 0.7762 0.080 Uiso 1 1 calc R . .
C9 C 0.2370(16) 0.3371(6) 0.3584(6) 0.080(3) Uani 1 1 d . . .
H9A H 0.1795 0.3568 0.2903 0.096 Uiso 1 1 calc R . .
H9B H 0.3994 0.2925 0.3514 0.096 Uiso 1 1 calc R . .
C1 C -0.0208(18) -0.0108(5) 0.9440(5) 0.054(2) Uani 1 1 d . . .
N1 N 0.5934(17) 0.1842(6) 0.5901(6) 0.092(2) Uani 1 1 d . . .
C12 C 0.6668(17) 0.5198(6) 0.2822(6) 0.073(2) Uani 1 1 d . . .
C11 C 0.5045(16) 0.4825(6) 0.3385(5) 0.072(2) Uani 1 1 d . . .
C15 C 1.1993(17) 0.6438(7) 0.0845(7) 0.077(2) Uani 1 1 d . . .
C10 C 0.3034(15) 0.4328(6) 0.4033(5) 0.075(2) Uani 1 1 d . . .
H10A H 0.1451 0.4797 0.4098 0.090 Uiso 1 1 calc R . .
H10B H 0.3679 0.4150 0.4708 0.090 Uiso 1 1 calc R . .
C13 C 0.8579(17) 0.5631(7) 0.2152(6) 0.076(3) Uani 1 1 d . . .
C3 C 0.3475(14) 0.0336(7) 0.7131(5) 0.058(2) Uani 1 1 d . . .
O3 O -0.0228(15) 0.1959(6) 0.3865(5) 0.129(3) Uani 1 1 d . . .
C14 C 1.0156(17) 0.5988(6) 0.1585(6) 0.075(2) Uani 1 1 d . . .
C20 C 1.3370(17) 0.7231(7) 0.1062(6) 0.084(3) Uani 1 1 d . . .
H20 H 1.3104 0.7483 0.1702 0.101 Uiso 1 1 calc R . .
C7 C 0.5502(17) 0.0072(7) 0.6451(6) 0.086(3) Uani 1 1 d . . .
H7 H 0.6112 -0.0611 0.6393 0.103 Uiso 1 1 calc R . .
C19 C 1.5148(19) 0.7667(7) 0.0355(8) 0.095(3) Uani 1 1 d . . .
H19 H 1.6034 0.8211 0.0519 0.114 Uiso 1 1 calc R . .
```

C6 C 0.6670(18) 0.0870(9) 0.5830(6) 0.090(3) Uani 1 1 d . . .
H6 H 0.8020 0.0690 0.5352 0.108 Uiso 1 1 calc R . .
C5 C 0.395(2) 0.2057(7) 0.6534(7) 0.101(3) Uani 1 1 d . . .
H5 H 0.3347 0.2745 0.6563 0.121 Uiso 1 1 calc R . .
C18 C 1.559(2) 0.7305(8) -0.0569(8) 0.109(3) Uani 1 1 d . . .
H18 H 1.6809 0.7584 -0.1042 0.131 Uiso 1 1 calc R . .
C8 C 0.0341(18) 0.2755(9) 0.4131(8) 0.085(3) Uani 1 1 d . . .
C4 C 0.2688(18) 0.1375(7) 0.7154(6) 0.090(3) Uani 1 1 d . . .
H4 H 0.1295 0.1597 0.7595 0.108 Uiso 1 1 calc R . .
C17 C 1.426(3) 0.6541(10) -0.0795(8) 0.174(6) Uani 1 1 d . . .
H17 H 1.4521 0.6298 -0.1439 0.209 Uiso 1 1 calc R . .
C16 C 1.249(2) 0.6098(9) -0.0088(8) 0.150(5) Uani 1 1 d . . .
H16 H 1.1621 0.5554 -0.0264 0.179 Uiso 1 1 calc R . .

loop_
 _atom_site_aniso_label
 _atom_site_aniso_U_11
 _atom_site_aniso_U_22
 _atom_site_aniso_U_33
 _atom_site_aniso_U_23
 _atom_site_aniso_U_13
 _atom_site_aniso_U_12
O1 0.052(4) 0.101(4) 0.060(3) -0.005(3) -0.012(3) -0.017(3)
O2 0.105(6) 0.091(5) 0.086(5) 0.013(4) 0.015(4) -0.023(4)
N2 0.064(5) 0.077(4) 0.037(3) -0.002(3) -0.007(3) -0.013(3)
C2 0.069(6) 0.077(6) 0.058(5) -0.003(4) 0.001(4) -0.022(5)
C9 0.081(7) 0.071(6) 0.086(5) 0.003(5) 0.010(5) -0.013(5)
C1 0.061(6) 0.058(5) 0.042(4) 0.012(4) -0.007(5) -0.009(4)
N1 0.097(7) 0.094(7) 0.084(5) -0.004(5) 0.001(5) -0.012(5)
C12 0.078(7) 0.082(6) 0.060(5) -0.008(4) 0.009(5) -0.011(5)
C11 0.071(6) 0.085(6) 0.060(5) -0.007(5) 0.005(5) -0.005(5)
C15 0.073(6) 0.078(6) 0.081(6) -0.006(5) 0.007(5) -0.020(5)
C10 0.074(6) 0.084(6) 0.068(5) -0.002(5) 0.004(5) -0.018(5)
C13 0.065(6) 0.091(7) 0.073(5) -0.011(5) 0.000(5) -0.009(5)
C3 0.046(5) 0.088(7) 0.039(4) -0.003(4) 0.001(4) -0.006(5)
O3 0.149(7) 0.104(6) 0.142(6) -0.032(5) 0.027(5) -0.056(5)
C14 0.067(6) 0.088(6) 0.067(5) 0.002(5) 0.009(5) -0.011(5)
C20 0.089(7) 0.084(7) 0.080(6) -0.005(5) -0.004(5) -0.010(6)
C7 0.093(8) 0.083(6) 0.076(5) -0.004(5) 0.021(5) 0.001(5)
C19 0.100(8) 0.085(7) 0.103(7) 0.012(6) -0.003(6) -0.037(6)
C6 0.085(8) 0.118(8) 0.062(5) -0.014(6) 0.024(5) 0.004(7)
C5 0.117(9) 0.094(8) 0.087(6) -0.003(6) 0.012(6) -0.009(7)
C18 0.114(9) 0.120(9) 0.093(7) 0.015(7) 0.013(7) -0.045(7)
C8 0.074(7) 0.092(8) 0.083(7) 0.014(6) 0.016(6) -0.004(6)
C4 0.110(8) 0.087(7) 0.067(5) 0.003(5) 0.024(5) -0.009(6)
C17 0.231(15) 0.204(14) 0.116(9) -0.071(9) 0.059(9) -0.153(12)

C16 0.181(12) 0.165(11) 0.122(8) -0.057(8) 0.058(9) -0.116(10)

_geom_special_details
;
All esds (except the esd in the dihedral angle between two l.s. planes)
are estimated using the full covariance matrix. The cell esds are taken
into account individually in the estimation of esds in distances, angles
and torsion angles; correlations between esds in cell parameters are only
used when they are defined by crystal symmetry. An approximate (isotropic)
treatment of cell esds is used for estimating esds involving l.s. planes.
;

loop_
_geom_bond_atom_site_label_1
_geom_bond_atom_site_label_2
_geom_bond_distance
_geom_bond_site_symmetry_2
_geom_bond_publ_flag
O1 C1 1.221(8) . ?
O2 C8 1.311(11) . ?
N2 C1 1.317(8) . ?
N2 C2 1.467(7) . ?
C2 C3 1.496(8) . ?
C9 C8 1.488(10) . ?
C9 C10 1.512(9) . ?
C1 C1 1.559(13) 2_557 ?
N1 C5 1.293(10) . ?
N1 C6 1.307(10) . ?
C12 C11 1.189(9) . ?
C12 C13 1.403(11) . ?
C11 C10 1.461(9) . ?
C15 C16 1.346(10) . ?
C15 C20 1.372(10) . ?
C15 C14 1.440(10) . ?
C13 C14 1.168(9) . ?
C3 C7 1.362(9) . ?
C3 C4 1.389(10) . ?
O3 C8 1.199(10) . ?
C20 C19 1.388(10) . ?
C7 C6 1.429(10) . ?
C19 C18 1.344(11) . ?
C5 C4 1.346(10) . ?
C18 C17 1.330(12) . ?
C17 C16 1.388(11) . ?

loop_

```
 _geom_angle_atom_site_label_1
 _geom_angle_atom_site_label_2
 _geom_angle_atom_site_label_3
 _geom_angle
 _geom_angle_site_symmetry_1
 _geom_angle_site_symmetry_3
 _geom_angle_publ_flag
C1 N2 C2 122.2(6) . . ?
N2 C2 C3 112.6(6) . . ?
C8 C9 C10 118.8(7) . . ?
O1 C1 N2 126.5(6) . . ?
O1 C1 C1 121.6(9) . 2_557 ?
N2 C1 C1 112.0(9) . 2_557 ?
C5 N1 C6 116.4(9) . . ?
C11 C12 C13 179.5(9) . . ?
C12 C11 C10 176.8(8) . . ?
C16 C15 C20 116.3(8) . . ?
C16 C15 C14 122.3(9) . . ?
C20 C15 C14 121.4(8) . . ?
C11 C10 C9 110.5(6) . . ?
C14 C13 C12 179.2(9) . . ?
C7 C3 C4 116.6(7) . . ?
C7 C3 C2 122.0(8) . . ?
C4 C3 C2 121.4(7) . . ?
C13 C14 C15 176.8(9) . . ?
C15 C20 C19 121.8(8) . . ?
C3 C7 C6 118.4(8) . . ?
C18 C19 C20 120.1(9) . . ?
N1 C6 C7 123.2(8) . . ?
N1 C5 C4 125.8(10) . . ?
C17 C18 C19 118.9(9) . . ?
O3 C8 O2 122.4(9) . . ?
O3 C8 C9 123.8(10) . . ?
O2 C8 C9 113.8(10) . . ?
C5 C4 C3 119.6(8) . . ?
C18 C17 C16 121.2(9) . . ?
C15 C16 C17 121.7(9) . . ?

_diffrn_measured_fraction_theta_max    0.858
_diffrn_reflns_theta_full              28.35
_diffrn_measured_fraction_theta_full   0.858
_refine_diff_density_max    0.378
_refine_diff_density_min   -0.204
_refine_diff_density_rms    0.066
```

$(22c)_2$•4PyU

```
data_zl63t

_audit_creation_method            SHELXL-97
_chemical_name_systematic
;
 ?
;
_chemical_name_common              ?
_chemical_melting_point           ?
_chemical_formula_moiety          ?
_chemical_formula_sum
 'C41 H38 N4 O5'
_chemical_formula_weight          666.75

loop_
 _atom_type_symbol
 _atom_type_description
 _atom_type_scat_dispersion_real
 _atom_type_scat_dispersion_imag
 _atom_type_scat_source
 'C'  'C'   0.0033   0.0016
 'International Tables Vol C Tables 4.2.6.8 and 6.1.1.4'
 'H'  'H'   0.0000   0.0000
 'International Tables Vol C Tables 4.2.6.8 and 6.1.1.4'
 'N'  'N'   0.0061   0.0033
 'International Tables Vol C Tables 4.2.6.8 and 6.1.1.4'
 'O'  'O'   0.0106   0.0060
 'International Tables Vol C Tables 4.2.6.8 and 6.1.1.4'

_symmetry_cell_setting            Monoclinic
_symmetry_space_group_name_H-M    C2/c

loop_
 _symmetry_equiv_pos_as_xyz
 'x, y, z'
 '-x, y, -z+1/2'
 'x+1/2, y+1/2, z'
 '-x+1/2, y+1/2, -z+1/2'
 '-x, -y, -z'
 'x, -y, z-1/2'
 '-x+1/2, -y+1/2, -z'
 'x+1/2, -y+1/2, z-1/2'

_cell_length_a                    39.154(11)
```

```
_cell_length_b                  4.6572(14)
_cell_length_c                  23.855(7)
_cell_angle_alpha                90.00
_cell_angle_beta                 124.036(5)
_cell_angle_gamma                90.00
_cell_volume                    3604.6(18)
_cell_formula_units_Z            4
_cell_measurement_temperature    273(2)
_cell_measurement_reflns_used    812
_cell_measurement_theta_min      2.95
_cell_measurement_theta_max      19.68

_exptl_crystal_description       ?
_exptl_crystal_colour            ?
_exptl_crystal_size_max          ?
_exptl_crystal_size_mid          ?
_exptl_crystal_size_min          ?
_exptl_crystal_density_meas      0
_exptl_crystal_density_diffrn    1.229
_exptl_crystal_density_method    'not measured'
_exptl_crystal_F_000             1408
_exptl_absorpt_coefficient_mu    0.082
_exptl_absorpt_correction_type   none
_exptl_absorpt_correction_T_min  ?
_exptl_absorpt_correction_T_max  ?
_exptl_absorpt_process_details   ?

_exptl_special_details
;
 ?
;

_diffrn_ambient_temperature      273(2)
_diffrn_radiation_wavelength     0.71073
_diffrn_radiation_type           MoK\a
_diffrn_radiation_source         'fine-focus sealed tube'
_diffrn_radiation_monochromator  graphite
_diffrn_measurement_device_type  'CCD area detector'
_diffrn_measurement_method       'phi and omega scans'
_diffrn_detector_area_resol_mean  ?
_diffrn_standards_number         ?
_diffrn_standards_interval_count  ?
_diffrn_standards_interval_time  ?
_diffrn_standards_decay_%        ?
_diffrn_reflns_number            10101
_diffrn_reflns_av_R_equivalents  0.1231
```

```
_diffrn_reflns_av_sigmaI/netI    0.2787
_diffrn_reflns_limit_h_min       -48
_diffrn_reflns_limit_h_max       51
_diffrn_reflns_limit_k_min       -2
_diffrn_reflns_limit_k_max       6
_diffrn_reflns_limit_l_min       -29
_diffrn_reflns_limit_l_max       31
_diffrn_reflns_theta_min         1.26
_diffrn_reflns_theta_max         28.38
_reflns_number_total             3997
_reflns_number_gt                1093
_reflns_threshold_expression     >2sigma(I)

_computing_data_collection       'Bruker SMART'
_computing_cell_refinement       'Bruker SMART'
_computing_data_reduction        'Bruker SAINT'
_computing_structure_solution    'SHELXS-97 (Sheldrick, 1990)'
_computing_structure_refinement  'SHELXL-97 (Sheldrick, 1997)'
_computing_molecular_graphics    'Bruker SHELXTL'
_computing_publication_material  'Bruker SHELXTL'

_refine_special_details
;
 Refinement of F^2^ against ALL reflections.  The weighted R-factor wR and
 goodness of fit S are based on F^2^, conventional R-factors R are based
 on F, with F set to zero for negative F^2^. The threshold expression of
 F^2^ > 2sigma(F^2^) is used only for calculating R-factors(gt) etc. and is
 not relevant to the choice of reflections for refinement.  R-factors based
 on F^2^ are statistically about twice as large as those based on F, and R-
 factors based on ALL data will be even larger.
;

_refine_ls_structure_factor_coef  Fsqd
_refine_ls_matrix_type           full
_refine_ls_weighting_scheme      calc
_refine_ls_weighting_details
 'calc w=1/[\s^2^(Fo^2^)+(0.1207P)^2^+0.0000P] where P=(Fo^2^+2Fc^2^)/3'
_atom_sites_solution_primary     direct
_atom_sites_solution_secondary   difmap
_atom_sites_solution_hydrogens   geom
_refine_ls_hydrogen_treatment    mixed
_refine_ls_extinction_method     SHELXL
_refine_ls_extinction_coef       0.026(3)
_refine_ls_extinction_expression
 'Fc^*^=kFc[1+0.001xFc^2^\l^3^/sin(2\q)]^-1/4^'
_refine_ls_number_reflns         3997
```

```
_refine_ls_number_parameters      228
_refine_ls_number_restraints      0
_refine_ls_R_factor_all           0.2852
_refine_ls_R_factor_gt            0.1028
_refine_ls_wR_factor_ref          0.3357
_refine_ls_wR_factor_gt           0.2142
_refine_ls_goodness_of_fit_ref    0.881
_refine_ls_restrained_S_all       0.881
_refine_ls_shift/su_max           0.034
_refine_ls_shift/su_mean          0.001

loop_
 _atom_site_label
 _atom_site_type_symbol
 _atom_site_fract_x
 _atom_site_fract_y
 _atom_site_fract_z
 _atom_site_U_iso_or_equiv
 _atom_site_adp_type
 _atom_site_occupancy
 _atom_site_symmetry_multiplicity
 _atom_site_calc_flag
 _atom_site_refinement_flags
 _atom_site_disorder_assembly
 _atom_site_disorder_group
N1 N 0.01772(12) 0.1311(9) 0.30789(18) 0.0531(12) Uani 1 1 d . . .
H1 H 0.0166 0.3155 0.3060 0.064 Uiso 1 1 calc R . .
C1 C 0.0000 -0.0234(16) 0.2500 0.0442(17) Uani 1 2 d S . .
O1 O 0.0000 -0.2896(11) 0.2500 0.0588(14) Uani 1 2 d S . .
O2 O 0.12186(12) -0.0070(9) 0.63369(18) 0.0753(13) Uani 1 1 d . . .
H2 H 0.1115 -0.1226 0.6024 0.113 Uiso 1 1 calc R . .
N2 N 0.09106(15) 0.6107(10) 0.53319(19) 0.0594(13) Uani 1 1 d . . .
C6 C 0.03499(16) 0.3114(13) 0.4538(3) 0.0626(16) Uani 1 1 d . . .
H6 H 0.0084 0.2474 0.4365 0.075 Uiso 1 1 calc R . .
C3 C 0.05699(17) 0.2047(11) 0.4289(2) 0.0533(14) Uani 1 1 d . . .
C2 C 0.03860(19) -0.0110(12) 0.3730(3) 0.0720(18) Uani 1 1 d . . .
H2A H 0.0602 -0.1341 0.3781 0.086 Uiso 1 1 calc R . .
H2B H 0.0191 -0.1304 0.3754 0.086 Uiso 1 1 calc R . .
O3 O 0.05891(14) -0.0109(11) 0.6125(2) 0.0934(16) Uani 1 1 d . . .
C4 C 0.09623(19) 0.3075(13) 0.4582(3) 0.0643(16) Uani 1 1 d . . .
H4 H 0.1123 0.2427 0.4432 0.077 Uiso 1 1 calc R . .
C7 C 0.05302(18) 0.5128(13) 0.5042(3) 0.0653(16) Uani 1 1 d . . .
H7 H 0.0374 0.5861 0.5192 0.078 Uiso 1 1 calc R . .
C5 C 0.11186(18) 0.5039(13) 0.5090(3) 0.0678(17) Uani 1 1 d . . .
H5 H 0.1387 0.5673 0.5281 0.081 Uiso 1 1 calc R . .
C9 C 0.11031(17) 0.2825(13) 0.7019(3) 0.0660(16) Uani 1 1 d . . .
```

H9A H 0.1209 0.4496 0.6921 0.079 Uiso 1 1 calc R . .
H9B H 0.1331 0.1938 0.7427 0.079 Uiso 1 1 calc R . .
C12 C 0.1235(2) 0.4210(14) 0.8395(3) 0.0725(18) Uani 1 1 d . . .
C10 C 0.07773(17) 0.3797(14) 0.7147(3) 0.0731(18) Uani 1 1 d . . .
H10A H 0.0562 0.4842 0.6754 0.088 Uiso 1 1 calc R . .
H10B H 0.0652 0.2112 0.7201 0.088 Uiso 1 1 calc R . .
C11 C 0.09483(18) 0.5663(14) 0.7760(3) 0.0792(19) Uani 1 1 d . . .
H11A H 0.1088 0.7286 0.7717 0.095 Uiso 1 1 calc R . .
H11B H 0.0721 0.6409 0.7772 0.095 Uiso 1 1 calc R . .
C8 C 0.0939(2) 0.0761(13) 0.6451(3) 0.0641(16) Uani 1 1 d . . .
C13 C 0.14681(19) 0.3033(16) 0.8923(3) 0.0766(19) Uani 1 1 d . . .
C16 C 0.22432(18) -0.0718(15) 1.0720(3) 0.0763(19) Uani 1 1 d . . .
C14 C 0.17419(19) 0.1733(15) 0.9539(3) 0.0752(19) Uani 1 1 d . . .
C15 C 0.1967(2) 0.0609(16) 1.0076(4) 0.080(2) Uani 1 1 d . . .
C17 C 0.2118(2) -0.1295(17) 1.1150(3) 0.092(2) Uani 1 1 d . . .
H17 H 0.1854 -0.0775 1.1023 0.110 Uiso 1 1 calc R . .
C18 C 0.2625(2) -0.162(2) 1.0906(4) 0.122(3) Uani 1 1 d . . .
H18 H 0.2709 -0.1327 1.0615 0.147 Uiso 1 1 calc R . .
C19 C 0.2380(3) -0.263(2) 1.1761(4) 0.111(3) Uani 1 1 d . . .
H19 H 0.2297 -0.2995 1.2052 0.133 Uiso 1 1 calc R . .
C21 C 0.2771(2) -0.343(2) 1.1939(4) 0.126(3) Uani 1 1 d . . .
H21 H 0.2953 -0.4308 1.2354 0.151 Uiso 1 1 calc R . .
C20 C 0.2884(2) -0.294(3) 1.1515(4) 0.155(4) Uani 1 1 d . . .
H20 H 0.3144 -0.3505 1.1635 0.186 Uiso 1 1 calc R . .

loop_
 _atom_site_aniso_label
 _atom_site_aniso_U_11
 _atom_site_aniso_U_22
 _atom_site_aniso_U_33
 _atom_site_aniso_U_23
 _atom_site_aniso_U_13
 _atom_site_aniso_U_12
N1 0.082(3) 0.028(2) 0.042(3) 0.004(2) 0.031(2) 0.001(2)
C1 0.055(4) 0.035(5) 0.045(4) 0.000 0.030(4) 0.000
O1 0.088(4) 0.030(3) 0.058(3) 0.000 0.040(3) 0.000
O2 0.085(3) 0.074(3) 0.065(3) -0.013(2) 0.040(2) -0.007(2)
N2 0.076(3) 0.054(3) 0.044(3) -0.003(2) 0.031(3) -0.007(3)
C6 0.065(3) 0.059(4) 0.058(4) -0.002(3) 0.031(3) -0.005(3)
C3 0.070(4) 0.042(3) 0.038(3) 0.008(3) 0.025(3) 0.004(3)
C2 0.109(5) 0.038(4) 0.050(3) 0.002(3) 0.033(3) 0.005(3)
O3 0.082(3) 0.119(4) 0.081(3) -0.024(3) 0.047(3) -0.032(3)
C4 0.088(4) 0.053(4) 0.065(4) 0.005(3) 0.050(4) 0.009(3)
C7 0.074(4) 0.068(5) 0.060(4) -0.006(3) 0.041(3) -0.005(3)
C5 0.065(4) 0.064(4) 0.072(4) 0.000(3) 0.037(3) -0.010(3)
C9 0.086(4) 0.055(4) 0.056(3) 0.003(3) 0.040(3) -0.005(3)

```
C12 0.082(4) 0.082(5) 0.071(4) 0.005(4) 0.053(4) 0.018(4)
C10 0.071(3) 0.081(5) 0.059(4) 0.011(3) 0.031(3) 0.017(3)
C11 0.088(4) 0.078(5) 0.071(4) 0.007(4) 0.044(4) 0.022(4)
C8 0.079(4) 0.068(5) 0.050(4) 0.006(3) 0.040(3) -0.003(4)
C13 0.074(4) 0.106(6) 0.064(4) -0.004(4) 0.047(4) 0.000(4)
C16 0.064(4) 0.101(5) 0.054(4) 0.002(3) 0.027(3) -0.001(4)
C14 0.066(4) 0.096(5) 0.063(4) -0.004(4) 0.035(4) -0.001(4)
C15 0.069(4) 0.100(6) 0.066(4) -0.003(4) 0.035(4) -0.005(4)
C17 0.086(4) 0.127(7) 0.071(4) 0.005(4) 0.049(4) 0.009(4)
C18 0.069(4) 0.207(10) 0.085(5) 0.034(6) 0.039(4) 0.018(5)
C19 0.121(6) 0.145(8) 0.072(5) 0.020(5) 0.057(5) 0.014(6)
C21 0.089(6) 0.169(9) 0.088(6) 0.029(6) 0.030(5) 0.013(6)
C20 0.076(5) 0.283(14) 0.096(6) 0.064(8) 0.042(5) 0.043(7)

_geom_special_details
;
 All esds (except the esd in the dihedral angle between two l.s. planes)
 are estimated using the full covariance matrix.  The cell esds are taken
 into account individually in the estimation of esds in distances, angles
 and torsion angles; correlations between esds in cell parameters are only
 used when they are defined by crystal symmetry.  An approximate (isotropic)
 treatment of cell esds is used for estimating esds involving l.s. planes.
;

loop_
 _geom_bond_atom_site_label_1
 _geom_bond_atom_site_label_2
 _geom_bond_distance
 _geom_bond_site_symmetry_2
 _geom_bond_publ_flag
N1 C1 1.354(5) . ?
N1 C2 1.447(6) . ?
C1 O1 1.240(8) . ?
C1 N1 1.354(5) 2 ?
O2 C8 1.327(7) . ?
N2 C7 1.323(6) . ?
N2 C5 1.330(7) . ?
C6 C7 1.369(7) . ?
C6 C3 1.384(7) . ?
C3 C4 1.370(7) . ?
C3 C2 1.494(7) . ?
O3 C8 1.205(6) . ?
C4 C5 1.361(8) . ?
C9 C8 1.482(8) . ?
C9 C10 1.537(7) . ?
C12 C13 1.196(8) . ?
```

```
C12 C11 1.454(9) . ?
C10 C11 1.498(8) . ?
C13 C14 1.384(10) . ?
C16 C18 1.365(8) . ?
C16 C17 1.388(8) . ?
C16 C15 1.434(9) . ?
C14 C15 1.194(8) . ?
C17 C19 1.376(9) . ?
C18 C20 1.367(10) . ?
C19 C21 1.391(10) . ?
C21 C20 1.332(10) . ?

loop_
 _geom_angle_atom_site_label_1
 _geom_angle_atom_site_label_2
 _geom_angle_atom_site_label_3
 _geom_angle
 _geom_angle_site_symmetry_1
 _geom_angle_site_symmetry_3
 _geom_angle_publ_flag
C1 N1 C2 120.7(5) . . ?
O1 C1 N1 122.1(3) . . ?
O1 C1 N1 122.1(3) . 2 ?
N1 C1 N1 115.8(6) . 2 ?
C7 N2 C5 115.3(5) . . ?
C7 C6 C3 119.0(5) . . ?
C4 C3 C6 116.5(5) . . ?
C4 C3 C2 122.2(5) . . ?
C6 C3 C2 121.3(5) . . ?
N1 C2 C3 110.5(4) . . ?
C5 C4 C3 120.4(5) . . ?
N2 C7 C6 124.8(5) . . ?
N2 C5 C4 124.0(5) . . ?
C8 C9 C10 112.8(5) . . ?
C13 C12 C11 179.0(6) . . ?
C11 C10 C9 113.4(5) . . ?
C12 C11 C10 114.2(5) . . ?
O3 C8 O2 122.7(6) . . ?
O3 C8 C9 124.3(6) . . ?
O2 C8 C9 113.0(5) . . ?
C12 C13 C14 178.7(9) . . ?
C18 C16 C17 118.5(6) . . ?
C18 C16 C15 120.7(6) . . ?
C17 C16 C15 120.7(6) . . ?
C15 C14 C13 177.6(6) . . ?
C14 C15 C16 179.1(7) . . ?
```

C19 C17 C16 120.5(6) . . ?
C20 C18 C16 120.6(7) . . ?
C17 C19 C21 119.0(7) . . ?
C20 C21 C19 120.0(8) . . ?
C21 C20 C18 121.4(8) . . ?

_diffrn_measured_fraction_theta_max 0.884
_diffrn_reflns_theta_full 28.38
_diffrn_measured_fraction_theta_full 0.884
_refine_diff_density_max 0.479
_refine_diff_density_min -0.493
_refine_diff_density_rms 0.167

$(22c)_2$•3PyO

```
data_zl60t

_audit_creation_method           SHELXL-97
_chemical_name_systematic
;
 ?
;
_chemical_name_common            ?
_chemical_melting_point          ?
_chemical_formula_moiety         ?
_chemical_formula_sum
 'C42 H38 N4 O6'
_chemical_formula_weight         694.76

loop_
 _atom_type_symbol
 _atom_type_description
 _atom_type_scat_dispersion_real
 _atom_type_scat_dispersion_imag
 _atom_type_scat_source
'C'  'C'   0.0033   0.0016
 'International Tables Vol C Tables 4.2.6.8 and 6.1.1.4'
 'H'  'H'   0.0000   0.0000
 'International Tables Vol C Tables 4.2.6.8 and 6.1.1.4'
 'N'  'N'   0.0061   0.0033
 'International Tables Vol C Tables 4.2.6.8 and 6.1.1.4'
 'O'  'O'   0.0106   0.0060
 'International Tables Vol C Tables 4.2.6.8 and 6.1.1.4'

_symmetry_cell_setting           triclinic
_symmetry_space_group_name_H-M    P-1

loop_
 _symmetry_equiv_pos_as_xyz
 'x, y, z'
 '-x, -y, -z'

_cell_length_a                  4.989(3)
_cell_length_b                  12.643(6)
_cell_length_c                  15.886(8)
_cell_angle_alpha                110.483(9)
_cell_angle_beta                 95.245(9)
_cell_angle_gamma                98.538(11)
_cell_volume                    917.1(8)
```

```
_cell_formula_units_Z            1
_cell_measurement_temperature    273(2)
_cell_measurement_reflns_used    ?
_cell_measurement_theta_min      ?
_cell_measurement_theta_max      ?

_exptl_crystal_description       ?
_exptl_crystal_colour            ?
_exptl_crystal_size_max          ?
_exptl_crystal_size_mid          ?
_exptl_crystal_size_min          ?
_exptl_crystal_density_meas      ?
_exptl_crystal_density_diffrn    1.258
_exptl_crystal_density_method    'not measured'
_exptl_crystal_F_000             366
_exptl_absorpt_coefficient_mu    0.085
_exptl_absorpt_correction_type   ?
_exptl_absorpt_correction_T_min  ?
_exptl_absorpt_correction_T_max  ?
_exptl_absorpt_process_details   ?

_exptl_special_details
;
 ?
;

_diffrn_ambient_temperature      273(2)
_diffrn_radiation_wavelength     0.71073
_diffrn_radiation_type           MoK\a
_diffrn_radiation_source         'fine-focus sealed tube'
_diffrn_radiation_monochromator  graphite
_diffrn_measurement_device_type  ?
_diffrn_measurement_method       ?
_diffrn_detector_area_resol_mean ?
_diffrn_standards_number         ?
_diffrn_standards_interval_count ?
_diffrn_standards_interval_time  ?
_diffrn_standards_decay_%        ?
_diffrn_reflns_number            5696
_diffrn_reflns_av_R_equivalents  0.0775
_diffrn_reflns_av_sigmaI/netI    0.2428
_diffrn_reflns_limit_h_min       -6
_diffrn_reflns_limit_h_max       6
_diffrn_reflns_limit_k_min       -16
_diffrn_reflns_limit_k_max       12
_diffrn_reflns_limit_l_min       -18
```

```
_diffrn_reflns_limit_l_max       19
_diffrn_reflns_theta_min         1.39
_diffrn_reflns_theta_max         28.54
_reflns_number_total             3968
_reflns_number_gt                833
_reflns_threshold_expression     >2sigma(I)

_computing_data_collection       ?
_computing_cell_refinement       ?
_computing_data_reduction        ?
_computing_structure_solution    'SHELXS-97 (Sheldrick, 1990)'
_computing_structure_refinement  'SHELXL-97 (Sheldrick, 1997)'
_computing_molecular_graphics    ?
_computing_publication_material  ?

_refine_special_details
;
 Refinement of F^2^ against ALL reflections.  The weighted R-factor wR and
 goodness of fit S are based on F^2^, conventional R-factors R are based
 on F, with F set to zero for negative F^2^. The threshold expression of
 F^2^ > 2sigma(F^2^) is used only for calculating R-factors(gt) etc. and is
 not relevant to the choice of reflections for refinement.  R-factors based
 on F^2^ are statistically about twice as large as those based on F, and R-
 factors based on ALL data will be even larger.
;

_refine_ls_structure_factor_coef  Fsqd
_refine_ls_matrix_type           full
_refine_ls_weighting_scheme      calc
_refine_ls_weighting_details
 'calc w=1/[\s^2^(Fo^2^)+(0.1086P)^2^+0.0000P] where P=(Fo^2^+2Fc^2^)/3'
_atom_sites_solution_primary     direct
_atom_sites_solution_secondary   difmap
_atom_sites_solution_hydrogens   geom
_refine_ls_hydrogen_treatment    mixed
_refine_ls_extinction_method     SHELXL
_refine_ls_extinction_coef       0.013(6)
_refine_ls_extinction_expression
 'Fc^*^=kFc[1+0.001xFc^2^\l^3^/sin(2\q)]^-1/4^'
_refine_ls_number_reflns         3968
_refine_ls_number_parameters     236
_refine_ls_number_restraints     0
_refine_ls_R_factor_all          0.3088
_refine_ls_R_factor_gt           0.0904
_refine_ls_wR_factor_ref         0.3025
_refine_ls_wR_factor_gt          0.2470
```

```
_refine_ls_goodness_of_fit_ref    0.878
_refine_ls_restrained_S_all       0.878
_refine_ls_shift/su_max           0.004
_refine_ls_shift/su_mean          0.000

loop_
 _atom_site_label
 _atom_site_type_symbol
 _atom_site_fract_x
 _atom_site_fract_y
 _atom_site_fract_z
 _atom_site_U_iso_or_equiv
 _atom_site_adp_type
 _atom_site_occupancy
 _atom_site_symmetry_multiplicity
 _atom_site_calc_flag
 _atom_site_refinement_flags
 _atom_site_disorder_assembly
 _atom_site_disorder_group
O1 O 1.3225(11) 0.5622(5) 0.0773(3) 0.094(2) Uani 1 1 d . . .
N2 N 0.6601(13) 0.5979(6) 0.3878(4) 0.0827(19) Uani 1 1 d . . .
C7 C 0.7068(16) 0.6437(6) 0.3233(5) 0.079(2) Uani 1 1 d . . .
H7 H 0.6277 0.7062 0.3242 0.095 Uiso 1 1 calc R . .
C2 C 0.9095(16) 0.6622(5) 0.1921(4) 0.087(2) Uani 1 1 d . . .
H2A H 0.7922 0.7186 0.2001 0.104 Uiso 1 1 calc R . .
H2B H 1.0985 0.7026 0.2050 0.104 Uiso 1 1 calc R . .
C3 C 0.8639(16) 0.6026(6) 0.2572(4) 0.069(2) Uani 1 1 d . . .
C6 C 0.7762(17) 0.5112(8) 0.3863(5) 0.082(2) Uani 1 1 d . . .
H6 H 0.7486 0.4793 0.4301 0.098 Uiso 1 1 calc R . .
N1 N 0.8496(13) 0.5797(4) 0.0975(3) 0.084(2) Uani 1 1 d . . .
H1 H 0.6831 0.5544 0.0701 0.101 Uiso 1 1 calc R . .
C4 C 0.9860(16) 0.5130(7) 0.2585(5) 0.085(2) Uani 1 1 d . . .
H4 H 1.1007 0.4846 0.2165 0.102 Uiso 1 1 calc R . .
C5 C 0.9369(18) 0.4657(7) 0.3227(6) 0.095(3) Uani 1 1 d . . .
H5 H 1.0127 0.4029 0.3229 0.114 Uiso 1 1 calc R . .
C1 C 1.080(3) 0.5408(7) 0.0499(5) 0.102(3) Uani 1 1 d . . .
O2 O 0.6133(11) 1.3116(4) 0.4788(3) 0.0901(16) Uani 1 1 d . . .
H2 H 0.5302 1.3329 0.5220 0.135 Uiso 1 1 calc R . .
O3 O 0.7149(11) 1.1904(4) 0.5441(3) 0.1000(19) Uani 1 1 d . . .
C12 C 0.6325(16) 0.9370(6) 0.2872(5) 0.083(2) Uani 1 1 d . . .
C9 C 0.8819(15) 1.1848(6) 0.4055(4) 0.081(2) Uani 1 1 d . . .
H9A H 1.0276 1.2471 0.4092 0.097 Uiso 1 1 calc R . .
H9B H 0.7584 1.1653 0.3491 0.097 Uiso 1 1 calc R . .
C10 C 1.0067(16) 1.0817(7) 0.4010(5) 0.088(2) Uani 1 1 d . . .
H10A H 1.1291 1.0701 0.3559 0.105 Uiso 1 1 calc R . .
H10B H 1.1164 1.0983 0.4594 0.105 Uiso 1 1 calc R . .
```

C8 C 0.7283(16) 1.2273(7) 0.4826(5) 0.073(2) Uani 1 1 d . . .
C16 C 0.0359(19) 0.8308(7) -0.0255(5) 0.082(2) Uani 1 1 d . . .
C13 C 0.4990(16) 0.9099(6) 0.2158(5) 0.083(2) Uani 1 1 d . . .
C11 C 0.8008(17) 0.9713(7) 0.3776(5) 0.100(3) Uani 1 1 d . . .
H11A H 0.8972 0.9103 0.3783 0.120 Uiso 1 1 calc R . .
H11B H 0.6812 0.9813 0.4235 0.120 Uiso 1 1 calc R . .
C15 C 0.2022(16) 0.8576(6) 0.0596(5) 0.085(2) Uani 1 1 d . . .
C18 C -0.047(2) 0.8599(8) -0.1648(5) 0.104(3) Uani 1 1 d . . .
H18 H 0.0058 0.8972 -0.2035 0.125 Uiso 1 1 calc R . .
C17 C 0.1140(18) 0.8857(7) -0.0833(5) 0.101(3) Uani 1 1 d . . .
H17 H 0.2757 0.9403 -0.0667 0.121 Uiso 1 1 calc R . .
C14 C 0.3387(17) 0.8828(6) 0.1322(5) 0.087(2) Uani 1 1 d . . .
C19 C -0.284(3) 0.7794(10) -0.1899(6) 0.123(4) Uani 1 1 d . . .
H19 H -0.3928 0.7621 -0.2455 0.148 Uiso 1 1 calc R . .
C21 C -0.203(2) 0.7505(8) -0.0509(6) 0.108(3) Uani 1 1 d . . .
H21 H -0.2582 0.7135 -0.0122 0.129 Uiso 1 1 calc R . .
C20 C -0.3596(19) 0.7249(7) -0.1336(7) 0.112(3) Uani 1 1 d . . .
H20 H -0.5200 0.6695 -0.1512 0.135 Uiso 1 1 calc R . .

loop_
 _atom_site_aniso_label
 _atom_site_aniso_U_11
 _atom_site_aniso_U_22
 _atom_site_aniso_U_33
 _atom_site_aniso_U_23
 _atom_site_aniso_U_13
 _atom_site_aniso_U_12
O1 0.062(4) 0.126(5) 0.073(3) 0.023(3) -0.022(3) 0.006(3)
N2 0.089(5) 0.088(5) 0.070(4) 0.036(4) 0.009(3) -0.002(4)
C7 0.104(7) 0.057(5) 0.066(5) 0.021(4) 0.000(5) -0.003(4)
C2 0.121(7) 0.067(5) 0.055(4) 0.014(4) 0.013(4) -0.013(5)
C3 0.084(6) 0.059(5) 0.054(4) 0.012(4) 0.013(4) 0.006(4)
C6 0.091(7) 0.083(6) 0.072(5) 0.038(5) 0.006(5) -0.003(5)
N1 0.117(6) 0.073(4) 0.047(3) 0.012(3) 0.015(4) -0.002(4)
C4 0.106(7) 0.072(6) 0.063(5) 0.012(4) 0.008(4) 0.013(5)
C5 0.121(8) 0.084(6) 0.087(6) 0.038(5) 0.015(6) 0.026(5)
C1 0.177(10) 0.087(7) 0.057(5) 0.032(4) 0.038(7) 0.047(7)
O2 0.118(5) 0.086(4) 0.070(3) 0.033(3) 0.027(3) 0.016(3)
O3 0.127(5) 0.112(4) 0.061(3) 0.045(3) 0.005(3) -0.001(3)
C12 0.103(7) 0.062(5) 0.078(5) 0.027(4) -0.009(5) 0.005(4)
C9 0.079(6) 0.097(6) 0.061(5) 0.026(4) 0.007(4) 0.012(5)
C10 0.091(6) 0.098(6) 0.073(5) 0.032(4) -0.005(4) 0.020(6)
C8 0.075(6) 0.064(5) 0.070(5) 0.025(4) -0.009(4) -0.006(4)
C16 0.097(7) 0.082(6) 0.065(5) 0.026(4) 0.007(5) 0.023(5)
C13 0.095(6) 0.075(5) 0.070(5) 0.027(4) -0.003(5) 0.003(4)
C11 0.123(8) 0.087(6) 0.094(6) 0.047(5) -0.003(5) 0.011(6)

C15 0.092(7) 0.076(5) 0.077(5) 0.026(4) 0.004(5) 0.001(5)
C18 0.134(9) 0.114(8) 0.071(6) 0.039(5) 0.015(6) 0.036(7)
C17 0.115(7) 0.100(6) 0.078(6) 0.033(5) 0.008(5) 0.000(5)
C14 0.112(7) 0.068(5) 0.071(5) 0.021(4) 0.005(5) 0.007(5)
C19 0.157(11) 0.122(9) 0.085(7) 0.024(6) -0.013(7) 0.066(8)
C21 0.115(8) 0.100(7) 0.110(7) 0.046(5) -0.002(6) 0.021(6)
C20 0.104(8) 0.097(7) 0.116(8) 0.032(6) -0.028(6) 0.006(6)

_geom_special_details
;
All esds (except the esd in the dihedral angle between two l.s. planes)
are estimated using the full covariance matrix. The cell esds are taken
into account individually in the estimation of esds in distances, angles
and torsion angles; correlations between esds in cell parameters are only
used when they are defined by crystal symmetry. An approximate (isotropic)
treatment of cell esds is used for estimating esds involving l.s. planes.
;

loop_
_geom_bond_atom_site_label_1
_geom_bond_atom_site_label_2
_geom_bond_distance
_geom_bond_site_symmetry_2
_geom_bond_publ_flag
O1 C1 1.204(11) . ?
N2 C6 1.308(8) . ?
N2 C7 1.363(8) . ?
C7 C3 1.370(9) . ?
C2 N1 1.472(7) . ?
C2 C3 1.491(9) . ?
C3 C4 1.369(9) . ?
C6 C5 1.369(10) . ?
N1 C1 1.484(10) . ?
C4 C5 1.374(9) . ?
C1 C1 1.610(16) 2_765 ?
O2 C8 1.299(8) . ?
O3 C8 1.224(7) . ?
C12 C13 1.171(8) . ?
C12 C11 1.480(9) . ?
C9 C8 1.486(9) . ?
C9 C10 1.509(8) . ?
C10 C11 1.511(9) . ?
C16 C21 1.371(10) . ?
C16 C17 1.382(10) . ?
C16 C15 1.422(9) . ?
C13 C14 1.388(9) . ?

```
C15 C14 1.196(9) . ?
C18 C19 1.367(12) . ?
C18 C17 1.363(9) . ?
C19 C20 1.354(12) . ?
C21 C20 1.372(10) . ?

loop_
 _geom_angle_atom_site_label_1
 _geom_angle_atom_site_label_2
 _geom_angle_atom_site_label_3
 _geom_angle
 _geom_angle_site_symmetry_1
 _geom_angle_site_symmetry_3
 _geom_angle_publ_flag
C6 N2 C7 117.4(7) . . ?
N2 C7 C3 123.5(7) . . ?
N1 C2 C3 111.1(5) . . ?
C4 C3 C7 117.6(7) . . ?
C4 C3 C2 123.4(8) . . ?
C7 C3 C2 118.9(7) . . ?
N2 C6 C5 122.5(8) . . ?
C2 N1 C1 119.2(6) . . ?
C3 C4 C5 119.1(8) . . ?
C6 C5 C4 119.9(8) . . ?
O1 C1 N1 130.2(7) . . ?
O1 C1 C1 128.5(12) . 2_765 ?
N1 C1 C1 101.3(11) . 2_765 ?
C13 C12 C11 179.9(11) . . ?
C8 C9 C10 115.5(7) . . ?
C11 C10 C9 114.5(7) . . ?
O3 C8 O2 123.2(8) . . ?
O3 C8 C9 124.9(8) . . ?
O2 C8 C9 111.9(7) . . ?
C21 C16 C17 119.4(7) . . ?
C21 C16 C15 120.4(8) . . ?
C17 C16 C15 120.2(9) . . ?
C12 C13 C14 177.4(8) . . ?
C12 C11 C10 112.1(6) . . ?
C14 C15 C16 178.1(8) . . ?
C19 C18 C17 120.4(9) . . ?
C18 C17 C16 119.9(8) . . ?
C15 C14 C13 178.8(8) . . ?
C20 C19 C18 119.8(9) . . ?
C16 C21 C20 119.6(9) . . ?
C19 C20 C21 120.8(9) . . ?
```

```
_diffrn_measured_fraction_theta_max    0.850
_diffrn_reflns_theta_full              28.54
_diffrn_measured_fraction_theta_full   0.850
_refine_diff_density_max    0.375
_refine_diff_density_min   -0.206
_refine_diff_density_rms    0.052
```

$(22c)_2$•4PyO

```
data_zl59m

_audit_creation_method           SHELXL-97
_chemical_name_systematic
;
 ?
;
_chemical_name_common            ?
_chemical_melting_point          ?
_chemical_formula_moiety         ?
_chemical_formula_sum
 'C42 H38 N4 O6'
_chemical_formula_weight         694.76

loop_
 _atom_type_symbol
 _atom_type_description
 _atom_type_scat_dispersion_real
 _atom_type_scat_dispersion_imag
 _atom_type_scat_source
'C'  'C'   0.0033   0.0016
 'International Tables Vol C Tables 4.2.6.8 and 6.1.1.4'
 'H'  'H'   0.0000   0.0000
 'International Tables Vol C Tables 4.2.6.8 and 6.1.1.4'
 'N'  'N'   0.0061   0.0033
 'International Tables Vol C Tables 4.2.6.8 and 6.1.1.4'
 'O'  'O'   0.0106   0.0060
 'International Tables Vol C Tables 4.2.6.8 and 6.1.1.4'

_symmetry_cell_setting           Monoclinic
_symmetry_space_group_name_H-M    Pn

loop_
 _symmetry_equiv_pos_as_xyz
 'x, y, z'
 'x+1/2, -y, z+1/2'

_cell_length_a                   15.414(6)
_cell_length_b                   5.225(2)
_cell_length_c                   22.866(9)
_cell_angle_alpha                 90.00
_cell_angle_beta                  91.989(7)
_cell_angle_gamma                  90.00
_cell_volume                     1840.3(12)
```

```
_cell_formula_units_Z            2
_cell_measurement_temperature    273(2)
_cell_measurement_reflns_used    600
_cell_measurement_theta_min      2.64
_cell_measurement_theta_max      21.75

_exptl_crystal_description       ?
_exptl_crystal_colour            ?
_exptl_crystal_size_max          ?
_exptl_crystal_size_mid          ?
_exptl_crystal_size_min          ?
_exptl_crystal_density_meas      0
_exptl_crystal_density_diffrn    1.254
_exptl_crystal_density_method    'not measured'
_exptl_crystal_F_000             732
_exptl_absorpt_coefficient_mu    0.085
_exptl_absorpt_correction_type   none
_exptl_absorpt_correction_T_min  ?
_exptl_absorpt_correction_T_max  ?
_exptl_absorpt_process_details   ?

_exptl_special_details
;
 ?
;

_diffrn_ambient_temperature      273(2)
_diffrn_radiation_wavelength     0.71073
_diffrn_radiation_type           MoK\a
_diffrn_radiation_source         'fine-focus sealed tube'
_diffrn_radiation_monochromator  graphite
_diffrn_measurement_device_type  'CCD area detector'
_diffrn_measurement_method       'phi and omega scans'
_diffrn_detector_area_resol_mean  ?
_diffrn_standards_number         ?
_diffrn_standards_interval_count  ?
_diffrn_standards_interval_time  ?
_diffrn_standards_decay_%        ?
_diffrn_reflns_number            10496
_diffrn_reflns_av_R_equivalents  0.1903
_diffrn_reflns_av_sigmaI/netI    0.4544
_diffrn_reflns_limit_h_min       -20
_diffrn_reflns_limit_h_max       14
_diffrn_reflns_limit_k_min       -6
_diffrn_reflns_limit_k_max       7
_diffrn_reflns_limit_l_min       -30
```

```
_diffrn_reflns_limit_l_max       29
_diffrn_reflns_theta_min         1.62
_diffrn_reflns_theta_max         28.60
_reflns_number_total             6009
_reflns_number_gt                1377
_reflns_threshold_expression     >2sigma(I)

_computing_data_collection       'Bruker SMART'
_computing_cell_refinement       'Bruker SMART'
_computing_data_reduction        'Bruker SAINT'
_computing_structure_solution    'SHELXS-97 (Sheldrick, 1990)'
_computing_structure_refinement  'SHELXL-97 (Sheldrick, 1997)'
_computing_molecular_graphics    'Bruker SHELXTL'
_computing_publication_material  'Bruker SHELXTL'

_refine_special_details
;
Refinement of F^2^ against ALL reflections.  The weighted R-factor wR and
goodness of fit S are based on F^2^, conventional R-factors R are based
on F, with F set to zero for negative F^2^. The threshold expression of
F^2^ > 2sigma(F^2^) is used only for calculating R-factors(gt) etc. and is
not relevant to the choice of reflections for refinement.  R-factors based
on F^2^ are statistically about twice as large as those based on F, and R-
factors based on ALL data will be even larger.
;

_refine_ls_structure_factor_coef  Fsqd
_refine_ls_matrix_type           full
_refine_ls_weighting_scheme      calc
_refine_ls_weighting_details
'calc w=1/[\s^2^(Fo^2^)+(0.0793P)^2^+0.0000P] where P=(Fo^2^+2Fc^2^)/3'
_atom_sites_solution_primary     direct
_atom_sites_solution_secondary   difmap
_atom_sites_solution_hydrogens   geom
_refine_ls_hydrogen_treatment    mixed
_refine_ls_extinction_method     SHELXL
_refine_ls_extinction_coef       0.075(10)
_refine_ls_extinction_expression
'Fc^*^=kFc[1+0.001xFc^2^\l^3^/sin(2\q)]^-1/4^'
_refine_ls_abs_structure_details
'Flack H D (1983), Acta Cryst. A39, 876-881'
_refine_ls_abs_structure_Flack   4(6)
_refine_ls_number_reflns         6009
_refine_ls_number_parameters     470
_refine_ls_number_restraints     2
_refine_ls_R_factor_all          0.3576
```

```
_refine_ls_R_factor_gt           0.1138
_refine_ls_wR_factor_ref         0.3740
_refine_ls_wR_factor_gt          0.2363
_refine_ls_goodness_of_fit_ref   0.870
_refine_ls_restrained_S_all      0.869
_refine_ls_shift/su_max          0.400
_refine_ls_shift/su_mean         0.014

loop_
 _atom_site_label
 _atom_site_type_symbol
 _atom_site_fract_x
 _atom_site_fract_y
 _atom_site_fract_z
 _atom_site_U_iso_or_equiv
 _atom_site_adp_type
 _atom_site_occupancy
 _atom_site_symmetry_multiplicity
 _atom_site_calc_flag
 _atom_site_refinement_flags
 _atom_site_disorder_assembly
 _atom_site_disorder_group
C1 C 0.7197(11) 0.441(3) 0.6950(7) 0.069(5) Uani 1 1 d . . .
H1A H 0.7238 0.2668 0.7094 0.083 Uiso 1 1 calc R . .
H1B H 0.6773 0.5305 0.7177 0.083 Uiso 1 1 calc R . .
O1 O 1.2120(8) -0.419(2) 0.4134(5) 0.070(4) Uani 1 1 d . . .
H1 H 1.2508 -0.5216 0.4072 0.104 Uiso 1 1 calc R . .
O5 O 0.6845(10) 0.007(2) 0.6207(5) 0.075(4) Uani 1 1 d . . .
O6 O 0.6405(10) 0.501(2) 0.5195(5) 0.077(4) Uani 1 1 d . . .
C2 C 1.1117(12) 0.116(3) 0.3280(6) 0.057(5) Uani 1 1 d . . .
H2A H 1.1615 0.2263 0.3233 0.069 Uiso 1 1 calc R . .
H2B H 1.1030 0.0181 0.2922 0.069 Uiso 1 1 calc R . .
N1 N 0.9737(11) 0.779(3) 0.7162(6) 0.069(4) Uani 1 1 d . . .
O2 O 1.2525(9) -0.249(2) 0.3310(6) 0.081(4) Uani 1 1 d . . .
C3 C 1.2040(11) -0.257(4) 0.3686(10) 0.069(6) Uani 1 1 d . . .
C4 C 0.9286(13) 0.926(4) 0.1776(8) 0.075(6) Uani 1 1 d . . .
N4 N 0.3562(10) 0.300(3) 0.4097(7) 0.066(4) Uani 1 1 d . . .
C5 C 1.0329(11) 0.277(3) 0.3375(9) 0.079(6) Uani 1 1 d . . .
H5A H 0.9836 0.1652 0.3428 0.095 Uiso 1 1 calc R . .
H5B H 1.0421 0.3739 0.3734 0.095 Uiso 1 1 calc R . .
C6 C 1.0126(13) 0.448(4) 0.2921(10) 0.081(7) Uani 1 1 d . . .
C7 C 0.9556(12) 0.586(4) 0.6779(8) 0.068(5) Uani 1 1 d . . .
H7 H 0.9997 0.5289 0.6543 0.082 Uiso 1 1 calc R . .
C8 C 0.8892(14) 1.099(4) 0.1355(8) 0.067(5) Uani 1 1 d . . .
C9 C 0.9391(15) 1.276(4) 0.1096(8) 0.083(6) Uani 1 1 d . . .
H9 H 0.9981 1.2847 0.1195 0.100 Uiso 1 1 calc R . .
```

N2 N 0.6903(9) 0.438(3) 0.6336(5) 0.064(4) Uani 1 1 d . . .
H2 H 0.6791 0.5813 0.6166 0.077 Uiso 1 1 calc R . .
C10 C 0.9567(12) 0.780(3) 0.2132(8) 0.061(5) Uani 1 1 d . . .
C11 C 1.1303(13) -0.068(3) 0.3788(7) 0.064(5) Uani 1 1 d . . .
H11A H 1.0779 -0.1636 0.3862 0.077 Uiso 1 1 calc R . .
H11B H 1.1448 0.0316 0.4136 0.077 Uiso 1 1 calc R . .
C12 C 0.3747(14) 0.104(4) 0.4429(7) 0.060(5) Uani 1 1 d . . .
H12 H 0.3297 0.0147 0.4597 0.072 Uiso 1 1 calc R . .
C13 C 0.9053(12) 0.875(4) 0.7458(8) 0.065(5) Uani 1 1 d . . .
H13 H 0.9133 1.0141 0.7706 0.078 Uiso 1 1 calc R . .
C14 C 0.4606(14) 0.022(3) 0.4539(8) 0.064(5) Uani 1 1 d . . .
H14 H 0.4717 -0.1225 0.4766 0.077 Uiso 1 1 calc R . .
N3 N 0.6406(9) 0.067(3) 0.5059(5) 0.065(4) Uani 1 1 d . . .
H3 H 0.6417 -0.0818 0.5220 0.079 Uiso 1 1 calc R . .
C15 C 0.8156(19) 1.431(5) 0.0529(8) 0.095(8) Uani 1 1 d . . .
H15 H 0.7912 1.5487 0.0266 0.114 Uiso 1 1 calc R . .
C16 C 0.5096(15) 0.365(4) 0.3942(8) 0.087(6) Uani 1 1 d . . .
H16 H 0.5529 0.4578 0.3766 0.105 Uiso 1 1 calc R . .
C17 C 0.8058(11) 0.569(3) 0.7036(7) 0.059(5) Uani 1 1 d . . .
C18 C 0.4213(18) 0.419(4) 0.3864(8) 0.083(7) Uani 1 1 d . . .
H18 H 0.4070 0.5546 0.3616 0.100 Uiso 1 1 calc R . .
C19 C 0.8751(13) 0.469(3) 0.6720(8) 0.070(5) Uani 1 1 d . . .
H19 H 0.8670 0.3271 0.6478 0.083 Uiso 1 1 calc R . .
C20 C 0.6800(12) 0.225(4) 0.6028(7) 0.067(5) Uani 1 1 d . . .
C21 C 0.9874(12) 0.592(4) 0.2543(9) 0.066(5) Uani 1 1 d . . .
C22 C 0.6247(12) 0.086(3) 0.4412(6) 0.068(5) Uani 1 1 d . . .
H22A H 0.6377 -0.0750 0.4224 0.081 Uiso 1 1 calc R . .
H22B H 0.6609 0.2187 0.4250 0.081 Uiso 1 1 calc R . .
C23 C 0.7659(14) 1.243(4) 0.0765(8) 0.082(6) Uani 1 1 d . . .
H23 H 0.7080 1.2222 0.0646 0.098 Uiso 1 1 calc R . .
C24 C 0.9043(17) 1.443(4) 0.0692(9) 0.088(7) Uani 1 1 d . . .
H24 H 0.9395 1.5651 0.0524 0.106 Uiso 1 1 calc R . .
C25 C 0.6535(10) 0.279(3) 0.5403(7) 0.065(4) Uani 1 1 d . . .
C26 C 0.8048(17) 1.077(4) 0.1200(8) 0.084(6) Uani 1 1 d . . .
H26 H 0.7711 0.9539 0.1377 0.100 Uiso 1 1 calc R . .
C27 C 0.5266(14) 0.155(3) 0.4316(6) 0.065(5) Uani 1 1 d . . .
C28 C 0.8248(13) 0.764(3) 0.7387(8) 0.076(6) Uani 1 1 d . . .
H28 H 0.7802 0.8313 0.7603 0.091 Uiso 1 1 calc R . .
O4 O 0.6107(8) 1.910(2) 0.2091(4) 0.073(4) Uani 1 1 d . . .
H4 H 0.5708 2.0086 0.2157 0.109 Uiso 1 1 calc R . .
O3 O 0.5805(9) 1.770(3) 0.2977(6) 0.086(4) Uani 1 1 d . . .
C29 C 0.6916(13) 1.571(3) 0.2463(7) 0.062(5) Uani 1 1 d . . .
H29A H 0.7451 1.6613 0.2391 0.074 Uiso 1 1 calc R . .
H29B H 0.6769 1.4708 0.2115 0.074 Uiso 1 1 calc R . .
C30 C 0.6239(14) 1.756(4) 0.2545(9) 0.069(6) Uani 1 1 d . . .
C31 C 0.8662(13) 0.712(3) 0.4104(8) 0.067(5) Uani 1 1 d . . .

C32 C 0.7078(12) 1.388(4) 0.2973(7) 0.068(5) Uani 1 1 d . . .
H32A H 0.6575 1.2786 0.3016 0.082 Uiso 1 1 calc R . .
H32B H 0.7169 1.4844 0.3332 0.082 Uiso 1 1 calc R . .
C33 C 0.8941(15) 0.569(4) 0.4455(8) 0.078(6) Uani 1 1 d . . .
C34 C 0.7876(12) 1.224(3) 0.2862(7) 0.068(5) Uani 1 1 d . . .
H34A H 0.7772 1.1310 0.2499 0.082 Uiso 1 1 calc R . .
H34B H 0.8364 1.3373 0.2806 0.082 Uiso 1 1 calc R . .
C35 C 0.9320(14) 0.398(4) 0.4879(8) 0.068(5) Uani 1 1 d . . .
C36 C 0.8334(15) 0.877(4) 0.3691(9) 0.078(6) Uani 1 1 d . . .
C37 C 0.8130(14) 1.035(4) 0.3329(8) 0.068(6) Uani 1 1 d . . .
C38 C 1.0112(17) 0.065(4) 0.5670(8) 0.079(7) Uani 1 1 d . . .
H38 H 1.0373 -0.0413 0.5952 0.095 Uiso 1 1 calc R . .
C39 C 1.0236(14) 0.423(4) 0.5039(8) 0.076(6) Uani 1 1 d . . .
H39 H 1.0555 0.5556 0.4881 0.091 Uiso 1 1 calc R . .
C40 C 1.0633(16) 0.259(4) 0.5411(8) 0.092(7) Uani 1 1 d . . .
H40 H 1.1226 0.2707 0.5497 0.111 Uiso 1 1 calc R . .
C41 C 0.926(2) 0.027(4) 0.5527(9) 0.098(9) Uani 1 1 d . . .
H41 H 0.8943 -0.1006 0.5704 0.117 Uiso 1 1 calc R . .
C42 C 0.8876(13) 0.188(4) 0.5103(8) 0.077(6) Uani 1 1 d . . .
H42 H 0.8313 0.1543 0.4966 0.093 Uiso 1 1 calc R . .

loop_
 _atom_site_aniso_label
 _atom_site_aniso_U_11
 _atom_site_aniso_U_22
 _atom_site_aniso_U_33
 _atom_site_aniso_U_23
 _atom_site_aniso_U_13
 _atom_site_aniso_U_12
C1 0.064(12) 0.080(13) 0.063(10) -0.007(9) 0.004(8) -0.012(11)
O1 0.079(10) 0.055(8) 0.073(7) 0.015(7) -0.019(7) -0.001(8)
O5 0.095(11) 0.051(9) 0.078(8) 0.001(6) -0.024(7) 0.000(7)
O6 0.122(12) 0.030(7) 0.077(7) 0.000(6) -0.019(7) -0.005(7)
C2 0.083(14) 0.028(9) 0.060(10) 0.001(8) -0.005(9) 0.009(10)
N1 0.098(14) 0.038(9) 0.068(9) -0.011(8) -0.025(9) 0.003(9)
O2 0.085(10) 0.067(9) 0.090(9) 0.008(7) 0.010(8) 0.019(8)
C3 0.030(10) 0.075(15) 0.101(15) -0.005(14) 0.010(10) 0.009(11)
C4 0.062(14) 0.071(14) 0.092(15) 0.034(12) 0.005(11) 0.020(12)
N4 0.061(11) 0.053(10) 0.081(11) -0.015(9) -0.009(9) 0.006(9)
C5 0.046(12) 0.057(13) 0.136(16) 0.036(13) 0.022(11) 0.015(11)
C6 0.050(13) 0.045(12) 0.15(2) 0.040(13) 0.012(13) 0.008(11)
C7 0.048(12) 0.066(13) 0.090(13) 0.004(11) 0.002(10) -0.001(11)
C8 0.065(15) 0.046(12) 0.089(14) 0.021(10) 0.001(11) -0.014(12)
C9 0.118(19) 0.051(13) 0.081(13) -0.012(11) 0.006(12) -0.016(13)
N2 0.071(10) 0.063(10) 0.057(8) 0.003(8) -0.015(7) -0.004(8)
C10 0.068(13) 0.049(12) 0.065(11) 0.002(10) -0.003(9) 0.003(11)

C11 0.063(13) 0.048(10) 0.081(12) 0.023(10) -0.014(10) 0.014(10)
C12 0.079(16) 0.043(12) 0.058(10) 0.005(9) 0.001(9) -0.011(11)
C13 0.047(12) 0.066(13) 0.082(12) -0.020(10) 0.005(10) -0.017(11)
C14 0.073(16) 0.042(11) 0.076(12) 0.000(9) -0.018(11) -0.008(10)
N3 0.077(10) 0.058(9) 0.061(8) 0.005(8) -0.007(7) 0.011(8)
C15 0.13(2) 0.079(16) 0.074(13) -0.006(12) -0.017(14) 0.054(17)
C16 0.100(17) 0.075(14) 0.088(14) 0.023(12) 0.015(12) 0.020(13)
C17 0.059(12) 0.053(11) 0.062(10) -0.003(9) -0.017(9) -0.001(10)
C18 0.12(2) 0.065(14) 0.065(12) 0.008(11) 0.004(13) 0.003(16)
C19 0.058(14) 0.060(12) 0.090(13) -0.018(10) -0.001(10) -0.010(10)
C20 0.096(13) 0.050(12) 0.053(10) -0.004(9) -0.022(8) 0.006(10)
C21 0.049(12) 0.042(12) 0.107(14) 0.004(11) 0.010(10) 0.000(10)
C22 0.098(15) 0.056(10) 0.048(9) -0.009(8) -0.025(8) 0.011(11)
C23 0.065(13) 0.089(16) 0.092(15) 0.027(14) 0.001(11) 0.007(13)
C24 0.10(2) 0.060(14) 0.101(15) 0.020(12) -0.010(14) 0.003(14)
C25 0.054(10) 0.057(12) 0.085(12) 0.003(10) 0.005(8) 0.005(9)
C26 0.12(2) 0.061(13) 0.072(12) 0.017(11) 0.001(13) 0.012(15)
C27 0.095(16) 0.061(13) 0.039(9) -0.007(8) -0.014(9) 0.009(12)
C28 0.085(15) 0.062(13) 0.081(12) -0.017(10) -0.008(10) -0.008(11)
O4 0.074(9) 0.072(8) 0.072(8) 0.010(7) 0.003(7) 0.025(8)
O3 0.095(10) 0.078(10) 0.087(9) 0.017(8) 0.020(8) 0.034(8)
C29 0.068(13) 0.041(10) 0.076(11) -0.010(10) -0.003(10) 0.015(11)
C30 0.103(17) 0.041(11) 0.060(11) 0.015(11) -0.020(11) -0.001(12)
C31 0.090(15) 0.033(11) 0.076(12) 0.012(10) -0.012(11) 0.002(10)
C32 0.040(10) 0.082(14) 0.083(12) -0.005(11) -0.003(9) 0.015(11)
C33 0.106(19) 0.054(13) 0.075(13) -0.009(11) -0.007(12) -0.007(13)
C34 0.081(14) 0.066(14) 0.056(10) 0.007(10) -0.003(10) 0.006(11)
C35 0.084(17) 0.059(13) 0.060(11) -0.006(10) -0.005(11) 0.011(13)
C36 0.117(18) 0.044(12) 0.071(13) -0.003(11) -0.010(12) 0.013(12)
C37 0.067(14) 0.068(14) 0.069(12) -0.002(11) -0.003(10) -0.005(11)
C38 0.11(2) 0.069(15) 0.062(12) 0.008(10) -0.004(12) -0.016(14)
C39 0.069(15) 0.058(13) 0.100(14) 0.004(12) -0.004(12) 0.004(13)
C40 0.13(2) 0.067(14) 0.076(12) 0.006(12) -0.040(13) -0.006(16)
C41 0.16(3) 0.055(14) 0.078(14) 0.016(12) 0.026(16) 0.014(17)
C42 0.067(14) 0.067(14) 0.098(15) 0.001(12) 0.010(11) 0.015(12)

_geom_special_details
;
All esds (except the esd in the dihedral angle between two l.s. planes)
are estimated using the full covariance matrix. The cell esds are taken
into account individually in the estimation of esds in distances, angles
and torsion angles; correlations between esds in cell parameters are only
used when they are defined by crystal symmetry. An approximate (isotropic)
treatment of cell esds is used for estimating esds involving l.s. planes.
;

```
loop_
 _geom_bond_atom_site_label_1
 _geom_bond_atom_site_label_2
 _geom_bond_distance
 _geom_bond_site_symmetry_2
 _geom_bond_publ_flag
C1 N2 1.461(18) . ?
C1 C17 1.49(2) . ?
O1 C3 1.33(2) . ?
O5 C20 1.214(18) . ?
O6 C25 1.269(17) . ?
C2 C5 1.50(2) . ?
C2 C11 1.53(2) . ?
N1 C7 1.36(2) . ?
N1 C13 1.37(2) . ?
O2 C3 1.16(2) . ?
C3 C11 1.53(2) . ?
C4 C10 1.19(2) . ?
C4 C8 1.44(3) . ?
N4 C18 1.31(2) . ?
N4 C12 1.30(2) . ?
C5 C6 1.40(3) . ?
C6 C21 1.20(2) . ?
C7 C19 1.39(3) . ?
C8 C26 1.34(3) . ?
C8 C9 1.35(3) . ?
C9 C24 1.37(3) . ?
N2 C20 1.319(19) . ?
C10 C21 1.43(3) . ?
C12 C14 1.41(3) . ?
C13 C28 1.37(2) . ?
C14 C27 1.35(2) . ?
N3 C25 1.367(19) . ?
N3 C22 1.494(17) . ?
C15 C23 1.37(3) . ?
C15 C24 1.41(3) . ?
C16 C18 1.40(3) . ?
C16 C27 1.41(2) . ?
C17 C28 1.33(2) . ?
C17 C19 1.41(2) . ?
C20 C25 1.500(19) . ?
C22 C27 1.56(3) . ?
C23 C26 1.43(2) . ?
O4 C30 1.326(19) . ?
O3 C30 1.22(2) . ?
C29 C30 1.44(3) . ?
```

C29 C32 1.52(2) . ?
C31 C33 1.17(2) . ?
C31 C36 1.36(3) . ?
C32 C34 1.53(2) . ?
C33 C35 1.43(3) . ?
C34 C37 1.49(2) . ?
C35 C42 1.40(3) . ?
C35 C39 1.45(3) . ?
C36 C37 1.20(2) . ?
C38 C41 1.36(3) . ?
C38 C40 1.44(3) . ?
C39 C40 1.34(2) . ?
C41 C42 1.40(3) . ?

loop_
 _geom_angle_atom_site_label_1
 _geom_angle_atom_site_label_2
 _geom_angle_atom_site_label_3
 _geom_angle
 _geom_angle_site_symmetry_1
 _geom_angle_site_symmetry_3
 _geom_angle_publ_flag
N2 C1 C17 112.2(14) . . ?
C5 C2 C11 112.0(14) . . ?
C7 N1 C13 116.5(16) . . ?
O2 C3 O1 123.2(18) . . ?
O2 C3 C11 126(2) . . ?
O1 C3 C11 110.1(17) . . ?
C10 C4 C8 176(2) . . ?
C18 N4 C12 117.1(18) . . ?
C6 C5 C2 114.4(17) . . ?
C21 C6 C5 174(2) . . ?
N1 C7 C19 123.6(19) . . ?
C26 C8 C9 120(2) . . ?
C26 C8 C4 120.5(18) . . ?
C9 C8 C4 119(2) . . ?
C24 C9 C8 121(2) . . ?
C20 N2 C1 123.4(14) . . ?
C4 C10 C21 177(2) . . ?
C2 C11 C3 114.3(15) . . ?
N4 C12 C14 122.0(18) . . ?
N1 C13 C28 119.8(17) . . ?
C27 C14 C12 119.7(18) . . ?
C25 N3 C22 122.0(14) . . ?
C23 C15 C24 119(2) . . ?
C18 C16 C27 113(2) . . ?

C28 C17 C19 116.1(17) . . ?
C28 C17 C1 126.9(18) . . ?
C19 C17 C1 117.0(16) . . ?
N4 C18 C16 128(2) . . ?
C7 C19 C17 118.6(17) . . ?
O5 C20 N2 127.4(15) . . ?
O5 C20 C25 120.3(15) . . ?
N2 C20 C25 112.1(14) . . ?
C6 C21 C10 175(2) . . ?
N3 C22 C27 106.2(14) . . ?
C15 C23 C26 119(2) . . ?
C9 C24 C15 121(2) . . ?
O6 C25 N3 120.5(14) . . ?
O6 C25 C20 124.1(15) . . ?
N3 C25 C20 115.4(14) . . ?
C8 C26 C23 121(2) . . ?
C14 C27 C16 120(2) . . ?
C14 C27 C22 124.8(17) . . ?
C16 C27 C22 115(2) . . ?
C17 C28 C13 125(2) . . ?
C30 C29 C32 114.9(16) . . ?
O3 C30 O4 122(2) . . ?
O3 C30 C29 124.8(17) . . ?
O4 C30 C29 113.5(19) . . ?
C33 C31 C36 179(2) . . ?
C29 C32 C34 109.7(15) . . ?
C31 C33 C35 177(2) . . ?
C37 C34 C32 116.4(15) . . ?
C42 C35 C33 123.0(19) . . ?
C42 C35 C39 117.4(18) . . ?
C33 C35 C39 119(2) . . ?
C37 C36 C31 173(2) . . ?
C36 C37 C34 177.9(19) . . ?
C41 C38 C40 124(2) . . ?
C40 C39 C35 122(2) . . ?
C39 C40 C38 118(2) . . ?
C38 C41 C42 118(2) . . ?
C35 C42 C41 122(2) . . ?

_diffrn_measured_fraction_theta_max 0.878
_diffrn_reflns_theta_full 28.60
_diffrn_measured_fraction_theta_full 0.878
_refine_diff_density_max 0.390
_refine_diff_density_min -0.380
_refine_diff_density_rms 0.112

$(22d)_2$•4PyU

```
data_zl70m

_audit_creation_method           SHELXL-97
_chemical_name_systematic
;
 ?
;
_chemical_name_common            ?
_chemical_melting_point          ?
_chemical_formula_moiety         ?
_chemical_formula_sum
 'C43 H42 N4 O5'
_chemical_formula_weight         694.81

loop_
 _atom_type_symbol
 _atom_type_description
 _atom_type_scat_dispersion_real
 _atom_type_scat_dispersion_imag
 _atom_type_scat_source
'C'  'C'   0.0033   0.0016
 'International Tables Vol C Tables 4.2.6.8 and 6.1.1.4'
 'H'  'H'   0.0000   0.0000
 'International Tables Vol C Tables 4.2.6.8 and 6.1.1.4'
 'N'  'N'   0.0061   0.0033
 'International Tables Vol C Tables 4.2.6.8 and 6.1.1.4'
 'O'  'O'   0.0106   0.0060
 'International Tables Vol C Tables 4.2.6.8 and 6.1.1.4'

_symmetry_cell_setting           Monoclinic
_symmetry_space_group_name_H-M    Pc

loop_
 _symmetry_equiv_pos_as_xyz
 'x, y, z'
 'x, -y, z+1/2'

_cell_length_a                   12.736(3)
_cell_length_b                   4.6632(9)
_cell_length_c                   32.466(6)
_cell_angle_alpha                 90.00
_cell_angle_beta                  96.789(4)
_cell_angle_gamma                   90.00
_cell_volume                     1914.6(6)
```

```
_cell_formula_units_Z            2
_cell_measurement_temperature    273(2)
_cell_measurement_reflns_used    ?
_cell_measurement_theta_min      ?
_cell_measurement_theta_max      ?

_exptl_crystal_description       ?
_exptl_crystal_colour            ?
_exptl_crystal_size_max          ?
_exptl_crystal_size_mid          ?
_exptl_crystal_size_min          ?
_exptl_crystal_density_meas      0
_exptl_crystal_density_diffrn    1.205
_exptl_crystal_density_method    'not measured'
_exptl_crystal_F_000             736
_exptl_absorpt_coefficient_mu    0.080
_exptl_absorpt_correction_type   none
_exptl_absorpt_correction_T_min  ?
_exptl_absorpt_correction_T_max  ?
_exptl_absorpt_process_details   ?

_exptl_special_details
;
 ?
;

_diffrn_ambient_temperature      273(2)
_diffrn_radiation_wavelength     0.71073
_diffrn_radiation_type           MoK\a
_diffrn_radiation_source         'fine-focus sealed tube'
_diffrn_radiation_monochromator  graphite
_diffrn_measurement_device_type  'CCD area detector'
_diffrn_measurement_method       'phi and omega scans'
_diffrn_detector_area_resol_mean  ?
_diffrn_standards_number         ?
_diffrn_standards_interval_count  ?
_diffrn_standards_interval_time  ?
_diffrn_standards_decay_%        ?
_diffrn_reflns_number            10995
_diffrn_reflns_av_R_equivalents  0.0531
_diffrn_reflns_av_sigmaI/netI    0.1132
_diffrn_reflns_limit_h_min       -15
_diffrn_reflns_limit_h_max       16
_diffrn_reflns_limit_k_min       -6
_diffrn_reflns_limit_k_max       5
_diffrn_reflns_limit_l_min       -38
```

```
_diffrn_reflns_limit_l_max       40
_diffrn_reflns_theta_min         1.61
_diffrn_reflns_theta_max         28.47
_reflns_number_total             6448
_reflns_number_gt                2192
_reflns_threshold_expression     >2sigma(I)

_computing_data_collection       'Bruker SMART'
_computing_cell_refinement       'Bruker SMART'
_computing_data_reduction        'Bruker SAINT'
_computing_structure_solution    'SHELXS-97 (Sheldrick, 1990)'
_computing_structure_refinement  'SHELXL-97 (Sheldrick, 1997)'
_computing_molecular_graphics    'Bruker SHELXTL'
_computing_publication_material  'Bruker SHELXTL'

_refine_special_details
;
Refinement of F^2^ against ALL reflections.  The weighted R-factor wR and
goodness of fit S are based on F^2^, conventional R-factors R are based
on F, with F set to zero for negative F^2^. The threshold expression of
F^2^ > 2sigma(F^2^) is used only for calculating R-factors(gt) etc. and is
not relevant to the choice of reflections for refinement.  R-factors based
on F^2^ are statistically about twice as large as those based on F, and R-
factors based on ALL data will be even larger.
;

_refine_ls_structure_factor_coef  Fsqd
_refine_ls_matrix_type           full
_refine_ls_weighting_scheme      calc
_refine_ls_weighting_details
'calc w=1/[\s^2^(Fo^2^)+(0.0545P)^2^+0.0000P] where P=(Fo^2^+2Fc^2^)/3'
_atom_sites_solution_primary     direct
_atom_sites_solution_secondary   difmap
_atom_sites_solution_hydrogens   geom
_refine_ls_hydrogen_treatment    mixed
_refine_ls_extinction_method     none
_refine_ls_extinction_coef       ?
_refine_ls_abs_structure_details
'Flack H D (1983), Acta Cryst. A39, 876-881'
_refine_ls_abs_structure_Flack   1(3)
_refine_ls_number_reflns         6448
_refine_ls_number_parameters     469
_refine_ls_number_restraints     2
_refine_ls_R_factor_all          0.1720
_refine_ls_R_factor_gt           0.0492
_refine_ls_wR_factor_ref         0.1324
```

```
_refine_ls_wR_factor_gt          0.0996
_refine_ls_goodness_of_fit_ref   0.787
_refine_ls_restrained_S_all      0.787
_refine_ls_shift/su_max          0.063
_refine_ls_shift/su_mean         0.013

loop_
 _atom_site_label
 _atom_site_type_symbol
 _atom_site_fract_x
 _atom_site_fract_y
 _atom_site_fract_z
 _atom_site_U_iso_or_equiv
 _atom_site_adp_type
 _atom_site_occupancy
 _atom_site_symmetry_multiplicity
 _atom_site_calc_flag
 _atom_site_refinement_flags
 _atom_site_disorder_assembly
 _atom_site_disorder_group
O3 O 0.8424(6) -0.0773(5) 0.1316(3) 0.0583(7) Uani 1 1 d . . .
N3 N 0.7583(5) 0.3486(15) 0.1389(2) 0.0523(18) Uani 1 1 d . . .
H3 H 0.7610 0.5329 0.1389 0.063 Uiso 1 1 calc R . .
N1 N 1.2007(5) 0.8018(16) 0.0476(2) 0.0558(18) Uani 1 1 d . . .
O4 O 1.3734(5) 0.1524(15) 0.25483(18) 0.091(2) Uani 1 1 d . . .
H4 H 1.4051 0.0391 0.2415 0.136 Uiso 1 1 calc R . .
C9 C 0.5973(6) 0.4146(16) 0.1703(2) 0.044(2) Uani 1 1 d . . .
C1 C 0.8483(9) 0.1894(8) 0.1309(3) 0.0445(9) Uani 1 1 d . . .
O1 O 0.3116(4) 0.1515(14) 1.00708(18) 0.0782(19) Uani 1 1 d . . .
H1 H 0.2793 0.0402 1.0205 0.117 Uiso 1 1 calc R . .
N2 N 0.9293(6) 0.3390(16) 0.1254(2) 0.067(2) Uani 1 1 d . . .
H2 H 0.9242 0.5227 0.1263 0.080 Uiso 1 1 calc R . .
C11 C 0.4448(6) 0.688(2) 0.1772(3) 0.064(3) Uani 1 1 d . . .
H11 H 0.3775 0.7488 0.1667 0.077 Uiso 1 1 calc R . .
O5 O 1.2564(5) 0.1277(15) 0.1999(2) 0.082(2) Uani 1 1 d . . .
C30 C 0.4642(8) 0.431(2) 1.0080(3) 0.073(3) Uani 1 1 d . . .
H30A H 0.4222 0.6020 1.0014 0.088 Uiso 1 1 calc R . .
H30B H 0.4762 0.3419 0.9819 0.088 Uiso 1 1 calc R . .
C8 C 0.6622(6) 0.2072(19) 0.1473(3) 0.059(2) Uani 1 1 d . . .
H8A H 0.6791 0.0376 0.1641 0.071 Uiso 1 1 calc R . .
H8B H 0.6219 0.1483 0.1215 0.071 Uiso 1 1 calc R . .
N4 N 0.4873(5) 0.7868(17) 0.2159(2) 0.0591(19) Uani 1 1 d . . .
C13 C 0.5839(7) 0.699(2) 0.2300(3) 0.064(3) Uani 1 1 d . . .
H13 H 0.6148 0.7672 0.2555 0.077 Uiso 1 1 calc R . .
C12 C 0.6408(6) 0.510(2) 0.2083(3) 0.056(2) Uani 1 1 d . . .
H12 H 0.7077 0.4491 0.2194 0.067 Uiso 1 1 calc R . .
```

C3 C 1.0883(6) 0.4156(17) 0.0918(3) 0.051(2) Uani 1 1 d . . .
C22 C 0.7038(8) 1.355(2) 0.3220(3) 0.080(3) Uani 1 1 d . . .
C10 C 0.4966(6) 0.507(2) 0.1543(3) 0.055(2) Uani 1 1 d . . .
H10 H 0.4658 0.4455 0.1284 0.066 Uiso 1 1 calc R . .
C32 C 0.6415(7) 0.6881(18) 1.0061(2) 0.060(2) Uani 1 1 d . . .
H32A H 0.6053 0.8620 0.9961 0.073 Uiso 1 1 calc R . .
H32B H 0.6548 0.5765 0.9820 0.073 Uiso 1 1 calc R . .
C5 C 1.1063(7) 0.704(2) 0.0327(2) 0.064(3) Uani 1 1 d . . .
H5 H 1.0777 0.7659 0.0066 0.077 Uiso 1 1 calc R . .
C19 C 0.8788(7) 0.934(2) 0.2605(3) 0.078(3) Uani 1 1 d . . .
C20 C 0.8230(9) 1.057(3) 0.2813(3) 0.086(3) Uani 1 1 d . . .
C29 C 0.4032(7) 0.234(2) 1.0304(3) 0.064(3) Uani 1 1 d . . .
C36 C 0.9310(7) 1.224(2) 0.9581(3) 0.081(3) Uani 1 1 d . . .
C2 C 1.0304(6) 0.2139(18) 0.1178(3) 0.057(2) Uani 1 1 d . . .
H2A H 1.0182 0.0323 0.1034 0.068 Uiso 1 1 calc R . .
H2B H 1.0733 0.1778 0.1440 0.068 Uiso 1 1 calc R . .
O2 O 0.4265(5) 0.1427(15) 1.0648(2) 0.085(2) Uani 1 1 d . . .
C4 C 1.0491(6) 0.522(2) 0.0526(3) 0.061(2) Uani 1 1 d . . .
H4A H 0.9826 0.4647 0.0404 0.073 Uiso 1 1 calc R . .
C31 C 0.5687(7) 0.519(2) 1.0301(3) 0.068(3) Uani 1 1 d . . .
H31A H 0.6058 0.3473 1.0404 0.081 Uiso 1 1 calc R . .
H31B H 0.5555 0.6323 1.0541 0.081 Uiso 1 1 calc R . .
C6 C 1.1850(7) 0.508(2) 0.1063(3) 0.070(3) Uani 1 1 d . . .
H6 H 1.2171 0.4453 0.1319 0.084 Uiso 1 1 calc R . .
C18 C 0.9450(8) 0.748(2) 0.2351(3) 0.095(3) Uani 1 1 d . . .
H18A H 0.9537 0.8448 0.2093 0.114 Uiso 1 1 calc R . .
H18B H 0.9086 0.5686 0.2285 0.114 Uiso 1 1 calc R . .
C24 C 0.6756(10) 1.669(3) 0.3809(4) 0.109(4) Uani 1 1 d . . .
H24 H 0.7470 1.6470 0.3904 0.131 Uiso 1 1 calc R . .
C23 C 0.6400(8) 1.518(2) 0.3487(3) 0.073(3) Uani 1 1 d . . .
C17 C 1.0536(7) 0.687(2) 0.2587(3) 0.088(3) Uani 1 1 d . . .
H17A H 1.0904 0.8656 0.2659 0.106 Uiso 1 1 calc R . .
H17B H 1.0460 0.5835 0.2841 0.106 Uiso 1 1 calc R . .
C38 C 1.0532(9) 1.512(2) 0.9168(3) 0.082(3) Uani 1 1 d . . .
C7 C 1.2384(7) 0.702(2) 0.0824(3) 0.070(3) Uani 1 1 d . . .
H7 H 1.3060 0.7609 0.0932 0.084 Uiso 1 1 calc R . .
C21 C 0.7627(8) 1.207(2) 0.3038(3) 0.076(3) Uani 1 1 d . . .
C41 C 1.1838(12) 1.832(3) 0.8741(4) 0.115(5) Uani 1 1 d . . .
H41 H 1.2283 1.9518 0.8612 0.138 Uiso 1 1 calc R . .
C14 C 1.2884(6) 0.224(2) 0.2339(3) 0.059(2) Uani 1 1 d . . .
C16 C 1.1152(7) 0.509(2) 0.2308(3) 0.073(3) Uani 1 1 d . . .
H16A H 1.1258 0.6157 0.2060 0.088 Uiso 1 1 calc R . .
H16B H 1.0772 0.3340 0.2227 0.088 Uiso 1 1 calc R . .
C28 C 0.5247(9) 1.517(2) 0.3372(3) 0.092(3) Uani 1 1 d . . .
H28 H 0.4923 1.4109 0.3150 0.111 Uiso 1 1 calc R . .
C37 C 0.9831(8) 1.346(2) 0.9374(3) 0.080(3) Uani 1 1 d . . .

C15 C 1.2224(7) 0.438(2) 0.2559(3) 0.072(3) Uani 1 1 d . . .
H15A H 1.2624 0.6144 0.2610 0.086 Uiso 1 1 calc R . .
H15B H 1.2099 0.3598 0.2826 0.086 Uiso 1 1 calc R . .
C42 C 1.2236(9) 1.671(3) 0.9063(4) 0.102(4) Uani 1 1 d . . .
H42 H 1.2962 1.6651 0.9141 0.122 Uiso 1 1 calc R . .
C34 C 0.8155(8) 0.928(2) 1.0049(3) 0.082(3) Uani 1 1 d . . .
C35 C 0.8640(7) 1.065(2) 0.9833(3) 0.078(3) Uani 1 1 d . . .
C33 C 0.7474(7) 0.771(2) 1.0297(3) 0.075(3) Uani 1 1 d . . .
H33A H 0.7348 0.8882 1.0533 0.090 Uiso 1 1 calc R . .
H33B H 0.7836 0.5987 1.0402 0.090 Uiso 1 1 calc R . .
C25 C 0.6211(12) 1.852(3) 0.4020(4) 0.116(4) Uani 1 1 d . . .
H25 H 0.6557 1.9777 0.4213 0.139 Uiso 1 1 calc R . .
C43 C 1.1556(8) 1.513(3) 0.9280(3) 0.108(4) Uani 1 1 d . . .
H43 H 1.1833 1.4056 0.9508 0.129 Uiso 1 1 calc R . .
C39 C 1.0064(9) 1.689(3) 0.8826(3) 0.089(3) Uani 1 1 d . . .
H39 H 0.9338 1.7124 0.8761 0.107 Uiso 1 1 calc R . .
C40 C 1.0809(12) 1.823(3) 0.8602(3) 0.122(5) Uani 1 1 d . . .
H40 H 1.0577 1.9075 0.8348 0.147 Uiso 1 1 calc R . .
C27 C 0.4678(10) 1.686(4) 0.3617(5) 0.139(6) Uani 1 1 d . . .
H27 H 0.3946 1.6878 0.3557 0.167 Uiso 1 1 calc R . .
C26 C 0.5118(15) 1.850(3) 0.3942(4) 0.134(5) Uani 1 1 d . . .
H26 H 0.4701 1.9555 0.4103 0.161 Uiso 1 1 calc R . .

loop_
 _atom_site_aniso_label
 _atom_site_aniso_U_11
 _atom_site_aniso_U_22
 _atom_site_aniso_U_33
 _atom_site_aniso_U_23
 _atom_site_aniso_U_13
 _atom_site_aniso_U_12
O3 0.0528(14) 0.0299(14) 0.0958(18) -0.010(4) 0.0241(12) 0.010(4)
N3 0.042(4) 0.030(4) 0.091(5) 0.008(3) 0.032(3) 0.006(3)
N1 0.046(4) 0.064(5) 0.057(4) 0.003(4) 0.001(3) -0.001(4)
O4 0.079(5) 0.119(6) 0.071(4) -0.037(4) -0.003(4) 0.037(4)
C9 0.039(5) 0.040(5) 0.053(5) -0.004(4) 0.009(4) -0.013(4)
C1 0.048(2) 0.034(2) 0.055(2) -0.004(5) 0.0160(18) 0.013(5)
O1 0.062(4) 0.090(5) 0.081(4) 0.006(4) -0.002(3) -0.017(4)
N2 0.056(5) 0.033(4) 0.119(6) -0.001(4) 0.042(4) 0.002(4)
C11 0.037(4) 0.091(7) 0.060(5) -0.022(5) -0.013(4) 0.005(5)
O5 0.071(4) 0.107(6) 0.065(4) -0.023(4) -0.003(3) 0.028(4)
C30 0.084(7) 0.061(7) 0.079(7) -0.012(5) 0.029(5) -0.006(5)
C8 0.040(5) 0.056(6) 0.085(6) 0.004(5) 0.025(4) -0.006(4)
N4 0.047(4) 0.074(5) 0.057(4) -0.013(4) 0.011(4) 0.002(4)
C13 0.046(5) 0.071(7) 0.068(6) -0.011(5) -0.020(4) -0.005(5)
C12 0.036(4) 0.064(6) 0.067(6) -0.008(5) 0.011(4) 0.003(4)

C3 0.041(5) 0.043(6) 0.073(6) -0.019(4) 0.020(5) -0.009(4)
C22 0.077(7) 0.071(7) 0.094(7) 0.008(5) 0.022(6) 0.009(6)
C10 0.043(5) 0.060(6) 0.062(5) -0.019(4) 0.010(4) -0.007(4)
C32 0.063(6) 0.060(6) 0.056(5) 0.000(4) -0.001(4) 0.011(4)
C5 0.055(5) 0.098(7) 0.044(5) -0.006(5) 0.023(4) -0.011(5)
C19 0.045(5) 0.105(8) 0.083(7) -0.014(6) 0.005(5) 0.027(5)
C20 0.084(7) 0.098(9) 0.082(7) 0.022(6) 0.025(6) -0.003(7)
C29 0.068(7) 0.056(6) 0.067(7) -0.013(5) 0.006(6) 0.006(5)
C36 0.062(6) 0.114(8) 0.061(6) 0.017(6) -0.014(5) -0.029(6)
C2 0.057(5) 0.038(5) 0.079(6) -0.006(4) 0.023(4) -0.001(4)
O2 0.081(4) 0.104(6) 0.070(5) 0.004(4) 0.007(4) -0.019(4)
C4 0.043(5) 0.079(7) 0.057(6) -0.022(5) -0.005(4) -0.016(5)
C31 0.073(6) 0.064(6) 0.066(6) -0.002(5) 0.004(5) -0.015(5)
C6 0.063(6) 0.082(7) 0.062(6) 0.005(5) -0.008(5) -0.022(5)
C18 0.080(7) 0.110(8) 0.090(7) -0.049(6) -0.006(5) 0.016(6)
C24 0.110(9) 0.111(10) 0.101(9) -0.029(8) -0.010(7) 0.012(8)
C23 0.073(6) 0.069(6) 0.083(7) 0.022(5) 0.036(5) 0.012(5)
C17 0.065(6) 0.100(8) 0.104(7) -0.018(6) 0.028(5) 0.035(5)
C38 0.077(7) 0.106(8) 0.058(6) 0.015(5) -0.012(5) -0.012(7)
C7 0.040(5) 0.074(7) 0.096(7) 0.003(6) 0.005(5) -0.016(5)
C21 0.074(6) 0.069(6) 0.091(7) 0.000(5) 0.029(5) -0.001(5)
C41 0.134(11) 0.133(11) 0.088(9) 0.002(7) 0.050(8) -0.073(9)
C14 0.042(5) 0.082(6) 0.053(6) -0.015(5) 0.005(4) 0.022(5)
C16 0.061(6) 0.072(7) 0.087(7) -0.015(5) 0.017(5) 0.007(5)
C28 0.078(7) 0.094(8) 0.104(8) -0.013(6) 0.005(6) -0.012(6)
C37 0.072(6) 0.124(9) 0.042(5) 0.016(5) -0.005(5) -0.016(6)
C15 0.052(5) 0.079(7) 0.082(6) -0.023(5) 0.000(5) 0.019(5)
C42 0.088(8) 0.134(11) 0.090(8) -0.011(7) 0.036(6) -0.025(7)
C34 0.076(7) 0.090(8) 0.077(7) 0.008(6) -0.006(5) 0.021(6)
C35 0.050(5) 0.091(8) 0.089(7) 0.035(5) -0.015(5) -0.024(5)
C33 0.063(6) 0.072(6) 0.090(7) -0.014(5) 0.008(5) -0.015(5)
C25 0.132(10) 0.105(9) 0.106(9) -0.006(6) -0.007(7) 0.043(8)
C43 0.075(7) 0.182(11) 0.068(6) -0.007(6) 0.017(6) -0.023(7)
C39 0.088(7) 0.111(9) 0.069(7) 0.005(6) 0.014(5) -0.021(7)
C40 0.148(11) 0.154(11) 0.069(7) 0.033(7) 0.027(7) -0.026(9)
C27 0.080(9) 0.182(16) 0.162(14) -0.007(11) 0.038(9) 0.039(9)
C26 0.178(14) 0.141(12) 0.085(8) 0.001(7) 0.019(9) 0.044(11)

_geom_special_details
;
All esds (except the esd in the dihedral angle between two l.s. planes)
are estimated using the full covariance matrix. The cell esds are taken
into account individually in the estimation of esds in distances, angles
and torsion angles; correlations between esds in cell parameters are only
used when they are defined by crystal symmetry. An approximate (isotropic)
treatment of cell esds is used for estimating esds involving l.s. planes.

;

loop_
 _geom_bond_atom_site_label_1
 _geom_bond_atom_site_label_2
 _geom_bond_distance
 _geom_bond_site_symmetry_2
 _geom_bond_publ_flag
O3 C1 1.246(4) . ?
N3 C1 1.415(10) . ?
N3 C8 1.445(10) . ?
N1 C7 1.264(11) . ?
N1 C5 1.324(10) . ?
O4 C14 1.252(9) . ?
C9 C12 1.366(11) . ?
C9 C10 1.394(10) . ?
C9 C8 1.523(11) . ?
C1 N2 1.275(11) . ?
O1 C29 1.368(11) . ?
N2 C2 1.461(10) . ?
C11 C10 1.348(11) . ?
C11 N4 1.387(10) . ?
O5 C14 1.218(10) . ?
C30 C29 1.452(13) . ?
C30 C31 1.494(12) . ?
N4 C13 1.325(10) . ?
C13 C12 1.385(12) . ?
C3 C6 1.336(11) . ?
C3 C4 1.401(11) . ?
C3 C2 1.512(11) . ?
C22 C21 1.223(13) . ?
C22 C23 1.469(14) . ?
C32 C31 1.503(12) . ?
C32 C33 1.520(12) . ?
C5 C4 1.334(12) . ?
C19 C20 1.185(13) . ?
C19 C18 1.518(13) . ?
C20 C21 1.321(15) . ?
C29 O2 1.201(10) . ?
C36 C37 1.149(13) . ?
C36 C35 1.453(15) . ?
C6 C7 1.417(12) . ?
C18 C17 1.526(13) . ?
C24 C23 1.295(15) . ?
C24 C25 1.339(15) . ?
C23 C28 1.471(14) . ?

C17 C16 1.515(12) . ?
C38 C43 1.312(14) . ?
C38 C37 1.410(14) . ?
C38 C39 1.456(15) . ?
C41 C42 1.336(18) . ?
C41 C40 1.335(17) . ?
C14 C15 1.536(12) . ?
C16 C15 1.540(12) . ?
C28 C27 1.382(17) . ?
C42 C43 1.391(15) . ?
C34 C35 1.176(13) . ?
C34 C33 1.450(15) . ?
C25 C26 1.385(18) . ?
C39 C40 1.407(15) . ?
C27 C26 1.37(2) . ?

loop_
 _geom_angle_atom_site_label_1
 _geom_angle_atom_site_label_2
 _geom_angle_atom_site_label_3
 _geom_angle
 _geom_angle_site_symmetry_1
 _geom_angle_site_symmetry_3
 _geom_angle_publ_flag
C1 N3 C8 121.2(6) . . ?
C7 N1 C5 115.6(8) . . ?
C12 C9 C10 119.6(8) . . ?
C12 C9 C8 117.6(7) . . ?
C10 C9 C8 122.9(7) . . ?
O3 C1 N2 126.8(9) . . ?
O3 C1 N3 117.9(9) . . ?
N2 C1 N3 115.1(3) . . ?
C1 N2 C2 123.3(7) . . ?
C10 C11 N4 123.1(8) . . ?
C29 C30 C31 115.6(9) . . ?
N3 C8 C9 108.9(6) . . ?
C13 N4 C11 117.1(7) . . ?
N4 C13 C12 122.9(8) . . ?
C9 C12 C13 119.0(8) . . ?
C6 C3 C4 114.8(8) . . ?
C6 C3 C2 119.7(9) . . ?
C4 C3 C2 125.5(8) . . ?
C21 C22 C23 172.8(11) . . ?
C11 C10 C9 118.4(8) . . ?
C31 C32 C33 115.9(7) . . ?
N1 C5 C4 124.6(9) . . ?

C20 C19 C18 174.0(11) . . ?
C19 C20 C21 176.8(12) . . ?
O2 C29 O1 121.1(9) . . ?
O2 C29 C30 127.0(9) . . ?
O1 C29 C30 111.9(9) . . ?
C37 C36 C35 178.5(11) . . ?
N2 C2 C3 110.1(7) . . ?
C5 C4 C3 120.5(8) . . ?
C30 C31 C32 117.6(8) . . ?
C3 C6 C7 119.8(9) . . ?
C19 C18 C17 111.2(8) . . ?
C23 C24 C25 127.2(13) . . ?
C24 C23 C22 126.2(11) . . ?
C24 C23 C28 116.8(10) . . ?
C22 C23 C28 117.0(10) . . ?
C16 C17 C18 107.7(8) . . ?
C43 C38 C37 122.4(10) . . ?
C43 C38 C39 120.9(11) . . ?
C37 C38 C39 116.7(9) . . ?
N1 C7 C6 124.6(8) . . ?
C22 C21 C20 175.5(12) . . ?
C42 C41 C40 120.9(11) . . ?
O5 C14 O4 124.7(8) . . ?
O5 C14 C15 121.3(8) . . ?
O4 C14 C15 114.0(8) . . ?
C17 C16 C15 106.9(8) . . ?
C27 C28 C23 115.3(11) . . ?
C36 C37 C38 172.5(11) . . ?
C14 C15 C16 113.1(8) . . ?
C41 C42 C43 119.5(12) . . ?
C35 C34 C33 174.9(10) . . ?
C34 C35 C36 175.7(10) . . ?
C34 C33 C32 113.7(9) . . ?
C24 C25 C26 118.2(14) . . ?
C38 C43 C42 121.3(12) . . ?
C40 C39 C38 113.9(11) . . ?
C41 C40 C39 122.3(11) . . ?
C26 C27 C28 124.5(13) . . ?
C27 C26 C25 117.1(14) . . ?

_diffrn_measured_fraction_theta_max 0.891
_diffrn_reflns_theta_full 28.47
_diffrn_measured_fraction_theta_full 0.891
_refine_diff_density_max 0.131
_refine_diff_density_min -0.135
_refine_diff_density_rms 0.033

$(22d)_2$•4PyO

```
data_zl69m

_audit_creation_method           SHELXL-97
_chemical_name_systematic
;
 ?
;
_chemical_name_common            ?
_chemical_melting_point          ?
_chemical_formula_moiety         ?
_chemical_formula_sum
 'C44 H42 N4 O6'
_chemical_formula_weight         722.82

loop_
 _atom_type_symbol
 _atom_type_description
 _atom_type_scat_dispersion_real
 _atom_type_scat_dispersion_imag
 _atom_type_scat_source
 'C'  'C'   0.0033   0.0016
 'International Tables Vol C Tables 4.2.6.8 and 6.1.1.4'
 'H'  'H'   0.0000   0.0000
 'International Tables Vol C Tables 4.2.6.8 and 6.1.1.4'
 'N'  'N'   0.0061   0.0033
 'International Tables Vol C Tables 4.2.6.8 and 6.1.1.4'
 'O'  'O'   0.0106   0.0060
 'International Tables Vol C Tables 4.2.6.8 and 6.1.1.4'

_symmetry_cell_setting           Triclinic
_symmetry_space_group_name_H-M    P-1

loop_
 _symmetry_equiv_pos_as_xyz
 'x, y, z'
 '-x, -y, -z'

_cell_length_a                  5.075(2)
_cell_length_b                  12.376(5)
_cell_length_c                  15.589(6)
_cell_angle_alpha                86.892(7)
_cell_angle_beta                 81.822(7)
_cell_angle_gamma                   82.493(8)
_cell_volume                    960.2(7)
```

```
_cell_formula_units_Z            1
_cell_measurement_temperature    293(2)
_cell_measurement_reflns_used    ?
_cell_measurement_theta_min      ?
_cell_measurement_theta_max      ?

_exptl_crystal_description       ?
_exptl_crystal_colour            ?
_exptl_crystal_size_max          ?
_exptl_crystal_size_mid          ?
_exptl_crystal_size_min          ?
_exptl_crystal_density_meas      ?
_exptl_crystal_density_diffrn    1.250
_exptl_crystal_density_method    'not measured'
_exptl_crystal_F_000             382
_exptl_absorpt_coefficient_mu    0.084
_exptl_absorpt_correction_type   none
_exptl_absorpt_correction_T_min  ?
_exptl_absorpt_correction_T_max  ?
_exptl_absorpt_process_details   ?

_exptl_special_details
;
 ?
;

_diffrn_ambient_temperature      293(2)
_diffrn_radiation_wavelength     0.71073
_diffrn_radiation_type           MoK\a
_diffrn_radiation_source         'fine-focus sealed tube'
_diffrn_radiation_monochromator  graphite
_diffrn_measurement_device_type  'CCD area detector'
_diffrn_measurement_method       'phi and omega scans'
_diffrn_detector_area_resol_mean  ?
_diffrn_standards_number         ?
_diffrn_standards_interval_count  ?
_diffrn_standards_interval_time  ?
_diffrn_standards_decay_%        ?
_diffrn_reflns_number            5659
_diffrn_reflns_av_R_equivalents  0.0384
_diffrn_reflns_av_sigmaI/netI    0.1424
_diffrn_reflns_limit_h_min       -6
_diffrn_reflns_limit_h_max       6
_diffrn_reflns_limit_k_min       -12
_diffrn_reflns_limit_k_max       16
_diffrn_reflns_limit_l_min       -17
```

```
_diffrn_reflns_limit_l_max       19
_diffrn_reflns_theta_min         1.32
_diffrn_reflns_theta_max         28.46
_reflns_number_total             4078
_reflns_number_gt                1301
_reflns_threshold_expression     >2sigma(I)

_computing_data_collection       'Bruker SMART'
_computing_cell_refinement       'Bruker SMART'
_computing_data_reduction        'Bruker SHELXTL'
_computing_structure_solution    'SHELXS-97 (Sheldrick, 1990)'
_computing_structure_refinement  'SHELXL-97 (Sheldrick, 1997)'
_computing_molecular_graphics    'Bruker SHELXTL'
_computing_publication_material  'Bruker SHELXTL'

_refine_special_details
;
 Refinement of F^2^ against ALL reflections.  The weighted R-factor wR and
 goodness of fit S are based on F^2^, conventional R-factors R are based
 on F, with F set to zero for negative F^2^. The threshold expression of
 F^2^ > 2sigma(F^2^) is used only for calculating R-factors(gt) etc. and is
 not relevant to the choice of reflections for refinement.  R-factors based
 on F^2^ are statistically about twice as large as those based on F, and R-
 factors based on ALL data will be even larger.
;

_refine_ls_structure_factor_coef  Fsqd
_refine_ls_matrix_type           full
_refine_ls_weighting_scheme      calc
_refine_ls_weighting_details
 'calc w=1/[\s^2^(Fo^2^)+(0.2000P)^2^+0.0000P] where P=(Fo^2^+2Fc^2^)/3'
_atom_sites_solution_primary     direct
_atom_sites_solution_secondary   difmap
_atom_sites_solution_hydrogens   geom
_refine_ls_hydrogen_treatment    mixed
_refine_ls_extinction_method     none
_refine_ls_extinction_coef       ?
_refine_ls_number_reflns         4078
_refine_ls_number_parameters     244
_refine_ls_number_restraints     0
_refine_ls_R_factor_all          0.1962
_refine_ls_R_factor_gt           0.0710
_refine_ls_wR_factor_ref         0.2735
_refine_ls_wR_factor_gt          0.2040
_refine_ls_goodness_of_fit_ref   0.654
_refine_ls_restrained_S_all      0.654
```

```
_refine_ls_shift/su_max          0.000
_refine_ls_shift/su_mean         0.000

loop_
 _atom_site_label
 _atom_site_type_symbol
 _atom_site_fract_x
 _atom_site_fract_y
 _atom_site_fract_z
 _atom_site_U_iso_or_equiv
 _atom_site_adp_type
 _atom_site_occupancy
 _atom_site_symmetry_multiplicity
 _atom_site_calc_flag
 _atom_site_refinement_flags
 _atom_site_disorder_assembly
 _atom_site_disorder_group
O1 O 1.2999(5) 0.4129(2) 0.4918(2) 0.0648(9) Uani 1 1 d . . .
N1 N 0.8860(6) 0.3768(2) 0.4792(2) 0.0495(9) Uani 1 1 d . . .
H1 H 0.7224 0.4041 0.4766 0.059 Uiso 1 1 calc R . .
O2 O 1.1940(6) 0.8886(2) 0.3469(2) 0.0777(10) Uani 1 1 d . . .
C1 C 1.0603(8) 0.4417(3) 0.4920(2) 0.0456(9) Uani 1 1 d . . .
O3 O 1.2057(7) 0.9969(3) 0.2296(2) 0.0792(10) Uani 1 1 d . . .
H3 H 1.3005 1.0280 0.2561 0.119 Uiso 1 1 calc R . .
N2 N 0.4977(7) 0.1081(3) 0.3131(2) 0.0583(9) Uani 1 1 d . . .
C2 C 0.9599(8) 0.2613(3) 0.4695(3) 0.0603(11) Uani 1 1 d . . .
H2A H 0.9410 0.2253 0.5264 0.072 Uiso 1 1 calc R . .
H2B H 1.1476 0.2485 0.4451 0.072 Uiso 1 1 calc R . .
C3 C 0.7976(7) 0.2103(3) 0.4131(3) 0.0475(10) Uani 1 1 d . . .
C10 C 0.8554(9) 0.7555(3) 0.2875(3) 0.0641(12) Uani 1 1 d . . .
H10A H 0.7425 0.7816 0.3396 0.077 Uiso 1 1 calc R . .
H10B H 1.0095 0.7092 0.3050 0.077 Uiso 1 1 calc R . .
C4 C 0.7348(8) 0.1067(3) 0.4343(3) 0.0581(11) Uani 1 1 d . . .
H4 H 0.7913 0.0691 0.4831 0.070 Uiso 1 1 calc R . .
C17 C -0.0893(9) 0.3079(4) 0.0782(3) 0.0622(12) Uani 1 1 d . . .
C9 C 0.9500(9) 0.8510(3) 0.2343(3) 0.0627(12) Uani 1 1 d . . .
H9A H 1.0471 0.8251 0.1796 0.075 Uiso 1 1 calc R . .
H9B H 0.7946 0.9003 0.2215 0.075 Uiso 1 1 calc R . .
C16 C 0.0553(9) 0.3688(4) 0.1262(3) 0.0685(12) Uani 1 1 d . . .
C15 C 0.1711(9) 0.4217(4) 0.1665(3) 0.0678(13) Uani 1 1 d . . .
C8 C 1.1265(8) 0.9132(3) 0.2764(3) 0.0562(11) Uani 1 1 d . . .
C5 C 0.5886(9) 0.0595(3) 0.3830(3) 0.0613(12) Uani 1 1 d . . .
H5 H 0.5502 -0.0111 0.3980 0.074 Uiso 1 1 calc R . .
C13 C 0.4405(9) 0.5302(4) 0.2498(3) 0.0695(13) Uani 1 1 d . . .
C7 C 0.7071(9) 0.2612(3) 0.3412(3) 0.0606(12) Uani 1 1 d . . .
H7 H 0.7453 0.3314 0.3246 0.073 Uiso 1 1 calc R . .
```

C11 C 0.6994(9) 0.6885(3) 0.2390(3) 0.0626(12) Uani 1 1 d . . .
H11A H 0.8140 0.6606 0.1878 0.075 Uiso 1 1 calc R . .
H11B H 0.5483 0.7352 0.2200 0.075 Uiso 1 1 calc R . .
C14 C 0.3163(9) 0.4798(4) 0.2114(3) 0.0671(13) Uani 1 1 d . . .
C6 C 0.5593(9) 0.2082(4) 0.2935(3) 0.0654(12) Uani 1 1 d . . .
H6 H 0.4990 0.2446 0.2448 0.078 Uiso 1 1 calc R . .
C12 C 0.5968(9) 0.5934(4) 0.2941(3) 0.0726(13) Uani 1 1 d . . .
H12A H 0.7487 0.5459 0.3117 0.087 Uiso 1 1 calc R . .
H12B H 0.4871 0.6215 0.3462 0.087 Uiso 1 1 calc R . .
C22 C -0.2388(10) 0.3582(4) 0.0174(3) 0.0828(15) Uani 1 1 d . . .
H22 H -0.2456 0.4331 0.0065 0.099 Uiso 1 1 calc R . .
C19 C -0.2231(14) 0.1365(5) 0.0471(5) 0.110(2) Uani 1 1 d . . .
H19 H -0.2179 0.0614 0.0567 0.132 Uiso 1 1 calc R . .
C20 C -0.3756(13) 0.1909(7) -0.0122(4) 0.111(2) Uani 1 1 d . . .
H20 H -0.4775 0.1525 -0.0419 0.133 Uiso 1 1 calc R . .
C18 C -0.0782(11) 0.1961(4) 0.0921(3) 0.0857(15) Uani 1 1 d . . .
H18 H 0.0273 0.1607 0.1318 0.103 Uiso 1 1 calc R . .
C21 C -0.3778(12) 0.2983(6) -0.0272(4) 0.1023(19) Uani 1 1 d . . .
H21 H -0.4762 0.3330 -0.0690 0.123 Uiso 1 1 calc R . .

loop_
 _atom_site_aniso_label
 _atom_site_aniso_U_11
 _atom_site_aniso_U_22
 _atom_site_aniso_U_33
 _atom_site_aniso_U_23
 _atom_site_aniso_U_13
 _atom_site_aniso_U_12
O1 0.0371(17) 0.0643(19) 0.098(2) -0.0309(16) -0.0144(14) -0.0064(13)
N1 0.0384(18) 0.0426(19) 0.070(2) -0.0161(15) -0.0107(15) -0.0054(14)
O2 0.097(2) 0.069(2) 0.080(2) 0.0045(17) -0.0400(19) -0.0326(18)
C1 0.039(2) 0.051(2) 0.050(2) -0.0120(18) -0.0070(17) -0.0148(18)
O3 0.105(3) 0.074(2) 0.072(2) 0.0010(17) -0.0346(18) -0.0374(19)
N2 0.066(2) 0.055(2) 0.059(2) -0.0116(17) -0.0139(18) -0.0143(18)
C2 0.055(3) 0.052(3) 0.079(3) -0.012(2) -0.022(2) -0.008(2)
C3 0.045(2) 0.042(2) 0.056(2) -0.0100(18) -0.0060(18) -0.0067(18)
C10 0.068(3) 0.064(3) 0.067(3) -0.018(2) -0.028(2) -0.006(2)
C4 0.069(3) 0.044(2) 0.065(3) 0.000(2) -0.021(2) -0.010(2)
C17 0.066(3) 0.074(3) 0.051(3) -0.009(2) -0.008(2) -0.022(2)
C9 0.069(3) 0.062(3) 0.062(3) -0.014(2) -0.022(2) -0.011(2)
C16 0.068(3) 0.071(3) 0.069(3) -0.004(2) -0.012(2) -0.018(3)
C15 0.073(3) 0.065(3) 0.070(3) -0.006(2) -0.019(3) -0.016(3)
C8 0.058(3) 0.053(3) 0.061(3) -0.012(2) -0.016(2) -0.005(2)
C5 0.073(3) 0.045(2) 0.072(3) -0.008(2) -0.016(2) -0.021(2)
C13 0.075(3) 0.062(3) 0.077(3) -0.002(2) -0.023(3) -0.015(3)
C7 0.082(3) 0.047(2) 0.057(3) 0.000(2) -0.008(2) -0.023(2)

C11 0.067(3) 0.057(3) 0.070(3) -0.016(2) -0.021(2) -0.010(2)
C14 0.070(3) 0.062(3) 0.074(3) -0.007(2) -0.019(3) -0.016(2)
C6 0.083(3) 0.061(3) 0.057(3) -0.001(2) -0.017(2) -0.020(2)
C12 0.078(3) 0.071(3) 0.080(3) -0.005(3) -0.032(3) -0.026(3)
C22 0.096(4) 0.097(4) 0.063(3) -0.007(3) -0.022(3) -0.024(3)
C19 0.147(6) 0.086(4) 0.103(5) -0.025(4) 0.004(4) -0.053(4)
C20 0.116(5) 0.151(7) 0.080(4) -0.045(4) 0.001(4) -0.066(5)
C18 0.106(4) 0.075(4) 0.080(4) -0.011(3) -0.011(3) -0.025(3)
C21 0.100(4) 0.140(6) 0.076(4) -0.018(4) -0.026(3) -0.029(4)

_geom_special_details
;
All esds (except the esd in the dihedral angle between two l.s. planes)
are estimated using the full covariance matrix. The cell esds are taken
into account individually in the estimation of esds in distances, angles
and torsion angles; correlations between esds in cell parameters are only
used when they are defined by crystal symmetry. An approximate (isotropic)
treatment of cell esds is used for estimating esds involving l.s. planes.
;

loop_
_geom_bond_atom_site_label_1
_geom_bond_atom_site_label_2
_geom_bond_distance
_geom_bond_site_symmetry_2
_geom_bond_publ_flag
O1 C1 1.221(4) . ?
N1 C1 1.311(4) . ?
N1 C2 1.440(5) . ?
O2 C8 1.209(5) . ?
C1 C1 1.512(7) 2_766 ?
O3 C8 1.308(5) . ?
N2 C5 1.327(5) . ?
N2 C6 1.327(5) . ?
C2 C3 1.501(5) . ?
C3 C7 1.362(5) . ?
C3 C4 1.372(5) . ?
C10 C9 1.498(6) . ?
C10 C11 1.515(5) . ?
C4 C5 1.365(5) . ?
C17 C22 1.371(6) . ?
C17 C18 1.384(6) . ?
C17 C16 1.423(6) . ?
C9 C8 1.493(6) . ?
C16 C15 1.191(6) . ?
C15 C14 1.375(6) . ?

C13 C14 1.181(6) . ?
C13 C12 1.447(6) . ?
C7 C6 1.373(6) . ?
C11 C12 1.522(6) . ?
C22 C21 1.365(7) . ?
C19 C20 1.381(9) . ?
C19 C18 1.386(8) . ?
C20 C21 1.336(8) . ?

loop_
 _geom_angle_atom_site_label_1
 _geom_angle_atom_site_label_2
 _geom_angle_atom_site_label_3
 _geom_angle
 _geom_angle_site_symmetry_1
 _geom_angle_site_symmetry_3
 _geom_angle_publ_flag
C1 N1 C2 122.1(3) . . ?
O1 C1 N1 124.4(3) . . ?
O1 C1 C1 121.4(4) . 2_766 ?
N1 C1 C1 114.1(4) . 2_766 ?
C5 N2 C6 116.0(4) . . ?
N1 C2 C3 114.5(3) . . ?
C7 C3 C4 117.5(4) . . ?
C7 C3 C2 123.6(4) . . ?
C4 C3 C2 118.9(4) . . ?
C9 C10 C11 112.7(4) . . ?
C3 C4 C5 119.3(4) . . ?
C22 C17 C18 119.0(4) . . ?
C22 C17 C16 121.0(4) . . ?
C18 C17 C16 120.1(5) . . ?
C8 C9 C10 114.6(4) . . ?
C15 C16 C17 178.4(5) . . ?
C16 C15 C14 177.2(6) . . ?
O2 C8 O3 122.5(4) . . ?
O2 C8 C9 123.6(4) . . ?
O3 C8 C9 113.9(4) . . ?
N2 C5 C4 124.1(4) . . ?
C14 C13 C12 178.0(5) . . ?
C3 C7 C6 119.6(4) . . ?
C10 C11 C12 112.6(4) . . ?
C13 C14 C15 179.7(6) . . ?
N2 C6 C7 123.5(4) . . ?
C13 C12 C11 113.6(4) . . ?
C17 C22 C21 120.0(5) . . ?
C20 C19 C18 118.6(6) . . ?

C21 C20 C19 120.6(6) . . ?
C17 C18 C19 120.4(6) . . ?
C20 C21 C22 121.5(6) . . ?

_diffrn_measured_fraction_theta_max 0.844
_diffrn_reflns_theta_full 28.46
_diffrn_measured_fraction_theta_full 0.844
_refine_diff_density_max 0.253
_refine_diff_density_min -0.264
_refine_diff_density_rms 0.063

61a

```
data_zl78m

_audit_creation_method           SHELXL-97
_chemical_name_systematic
;
 ?
;
_chemical_name_common            ?
_chemical_melting_point          ?
_chemical_formula_moiety         ?
_chemical_formula_sum
 'C13 H5 F5 O2'
_chemical_formula_weight         288.17

loop_
 _atom_type_symbol
 _atom_type_description
 _atom_type_scat_dispersion_real
 _atom_type_scat_dispersion_imag
 _atom_type_scat_source
'C'  'C'   0.0033   0.0016
 'International Tables Vol C Tables 4.2.6.8 and 6.1.1.4'
'H'  'H'   0.0000   0.0000
 'International Tables Vol C Tables 4.2.6.8 and 6.1.1.4'
'O'  'O'   0.0106   0.0060
 'International Tables Vol C Tables 4.2.6.8 and 6.1.1.4'
'F'  'F'   0.0171   0.0103
 'International Tables Vol C Tables 4.2.6.8 and 6.1.1.4'

_symmetry_cell_setting           Monoclinic
_symmetry_space_group_name_H-M    P21/n

loop_
 _symmetry_equiv_pos_as_xyz
 'x, y, z'
 '-x+1/2, y+1/2, -z+1/2'
 '-x, -y, -z'
 'x-1/2, -y-1/2, z-1/2'

_cell_length_a                   5.216(3)
_cell_length_b                   5.780(3)
_cell_length_c                   39.74(2)
_cell_angle_alpha                 90.00
_cell_angle_beta                  92.340(10)
```

```
_cell_angle_gamma                90.00
_cell_volume                     1197.0(11)
_cell_formula_units_Z            4
_cell_measurement_temperature    273(2)
_cell_measurement_reflns_used    ?
_cell_measurement_theta_min      ?
_cell_measurement_theta_max      ?

_exptl_crystal_description       ?
_exptl_crystal_colour            ?
_exptl_crystal_size_max          ?
_exptl_crystal_size_mid          ?
_exptl_crystal_size_min          ?
_exptl_crystal_density_meas      0
_exptl_crystal_density_diffrn    1.599
_exptl_crystal_density_method    'not measured'
_exptl_crystal_F_000             576
_exptl_absorpt_coefficient_mu    0.159
_exptl_absorpt_correction_type   none
_exptl_absorpt_correction_T_min  ?
_exptl_absorpt_correction_T_max  ?
_exptl_absorpt_process_details   ?

_exptl_special_details
;
 ?
;

_diffrn_ambient_temperature      273(2)
_diffrn_radiation_wavelength     0.71073
_diffrn_radiation_type           MoK\a
_diffrn_radiation_source         'fine-focus sealed tube'
_diffrn_radiation_monochromator  graphite
_diffrn_measurement_device_type  'CCD area detector'
_diffrn_measurement_method       'phi and omega scans'
_diffrn_detector_area_resol_mean  ?
_diffrn_standards_number         ?
_diffrn_standards_interval_count  ?
_diffrn_standards_interval_time  ?
_diffrn_standards_decay_%        ?
_diffrn_reflns_number            6917
_diffrn_reflns_av_R_equivalents  0.0973
_diffrn_reflns_av_sigmaI/netI    0.2076
_diffrn_reflns_limit_h_min       -6
_diffrn_reflns_limit_h_max       6
_diffrn_reflns_limit_k_min       -7
```

```
_diffrn_reflns_limit_k_max       7
_diffrn_reflns_limit_l_min       -39
_diffrn_reflns_limit_l_max       53
_diffrn_reflns_theta_min         1.03
_diffrn_reflns_theta_max         28.61
_reflns_number_total             2713
_reflns_number_gt                645
_reflns_threshold_expression     >2sigma(I)

_computing_data_collection       'Bruker SMART'
_computing_cell_refinement       'Bruker SMART'
_computing_data_reduction        'Bruker SAINT'
_computing_structure_solution    'SHELXS-97 (Sheldrick, 1990)'
_computing_structure_refinement   'SHELXL-97 (Sheldrick, 1997)'
_computing_molecular_graphics    'Bruker SHELXTL'
_computing_publication_material   'Bruker SHELXTL'

_refine_special_details
;
 Refinement of F^2^ against ALL reflections.  The weighted R-factor wR and
 goodness of fit S are based on F^2^, conventional R-factors R are based
 on F, with F set to zero for negative F^2^. The threshold expression of
 F^2^ > 2sigma(F^2^) is used only for calculating R-factors(gt) etc. and is
 not relevant to the choice of reflections for refinement.  R-factors based
 on F^2^ are statistically about twice as large as those based on F, and R-
 factors based on ALL data will be even larger.
;

_refine_ls_structure_factor_coef  Fsqd
_refine_ls_matrix_type           full
_refine_ls_weighting_scheme      calc
_refine_ls_weighting_details
 'calc w=1/[\s^2^(Fo^2^)+(0.1008P)^2^+0.0000P] where P=(Fo^2^+2Fc^2^)/3'
_atom_sites_solution_primary     direct
_atom_sites_solution_secondary    difmap
_atom_sites_solution_hydrogens    geom
_refine_ls_hydrogen_treatment    mixed
_refine_ls_extinction_method     none
_refine_ls_extinction_coef       ?
_refine_ls_number_reflns         2713
_refine_ls_number_parameters     181
_refine_ls_number_restraints     0
_refine_ls_R_factor_all          0.2419
_refine_ls_R_factor_gt           0.0509
_refine_ls_wR_factor_ref         0.2141
_refine_ls_wR_factor_gt          0.1278
```

```
_refine_ls_goodness_of_fit_ref    0.710
_refine_ls_restrained_S_all       0.710
_refine_ls_shift/su_max           0.000
_refine_ls_shift/su_mean          0.000

loop_
 _atom_site_label
 _atom_site_type_symbol
 _atom_site_fract_x
 _atom_site_fract_y
 _atom_site_fract_z
 _atom_site_U_iso_or_equiv
 _atom_site_adp_type
 _atom_site_occupancy
 _atom_site_symmetry_multiplicity
 _atom_site_calc_flag
 _atom_site_refinement_flags
 _atom_site_disorder_assembly
 _atom_site_disorder_group
O1 O -0.2881(7) 0.2065(6) 0.00714(9) 0.0828(12) Uani 1 1 d . . .
O2 O -0.3348(7) -0.1088(6) 0.03769(9) 0.0886(12) Uani 1 1 d . . .
H2 H -0.4483 -0.1363 0.0234 0.133 Uiso 1 1 calc R . .
F3 F 1.6502(6) 0.8142(6) 0.22626(8) 0.1083(12) Uani 1 1 d . . .
C11 C 1.4555(9) 0.7618(11) 0.20446(13) 0.0694(16) Uani 1 1 d . . .
C2 C -0.0148(8) 0.1508(8) 0.05654(11) 0.0619(14) Uani 1 1 d . . .
H2A H 0.1174 0.0328 0.0563 0.074 Uiso 1 1 calc R . .
H2B H -0.0844 0.1526 0.0788 0.074 Uiso 1 1 calc R . .
F1 F 0.9859(6) 0.3147(6) 0.19280(9) 0.1100(12) Uani 1 1 d . . .
F2 F 1.3768(7) 0.4278(7) 0.23563(8) 0.1218(13) Uani 1 1 d . . .
C8 C 1.0491(9) 0.6439(9) 0.15993(12) 0.0588(14) Uani 1 1 d . . .
C4 C 0.3086(9) 0.4415(9) 0.07407(12) 0.0650(15) Uani 1 1 d . . .
F5 F 1.1412(7) 0.9824(6) 0.13006(8) 0.1167(13) Uani 1 1 d . . .
F4 F 1.5312(7) 1.0919(6) 0.17318(9) 0.1212(14) Uani 1 1 d . . .
C5 C 0.4807(10) 0.4829(9) 0.09441(12) 0.0698(15) Uani 1 1 d . . .
C13 C 1.1944(10) 0.8431(10) 0.15628(13) 0.0671(15) Uani 1 1 d . . .
C6 C 0.6750(9) 0.5400(9) 0.11702(12) 0.0656(15) Uani 1 1 d . . .
C9 C 1.1211(10) 0.5093(10) 0.18724(13) 0.0675(15) Uani 1 1 d . . .
C3 C 0.1033(9) 0.3846(8) 0.04943(12) 0.0702(15) Uani 1 1 d . . .
H3A H 0.1713 0.3833 0.0271 0.084 Uiso 1 1 calc R . .
H3B H -0.0286 0.5028 0.0499 0.084 Uiso 1 1 calc R . .
C7 C 0.8454(10) 0.5869(9) 0.13640(12) 0.0669(15) Uani 1 1 d . . .
C1 C -0.2254(9) 0.0906(10) 0.03087(14) 0.0595(14) Uani 1 1 d . . .
C10 C 1.3153(10) 0.5669(11) 0.20925(12) 0.0709(16) Uani 1 1 d . . .
C12 C 1.3941(10) 0.8984(10) 0.17804(15) 0.0744(16) Uani 1 1 d . . .

loop_
```

```
 _atom_site_aniso_label
 _atom_site_aniso_U_11
 _atom_site_aniso_U_22
 _atom_site_aniso_U_33
 _atom_site_aniso_U_23
 _atom_site_aniso_U_13
 _atom_site_aniso_U_12
O1 0.081(3) 0.093(3) 0.071(3) 0.021(2) -0.037(2) -0.031(2)
O2 0.089(3) 0.086(3) 0.087(3) 0.021(2) -0.047(2) -0.028(2)
F3 0.077(2) 0.154(3) 0.089(2) -0.022(2) -0.0413(19) -0.019(2)
C11 0.045(3) 0.107(5) 0.055(4) -0.018(4) -0.022(3) -0.015(3)
C2 0.054(3) 0.074(4) 0.056(3) -0.005(3) -0.025(3) -0.007(3)
F1 0.105(3) 0.102(2) 0.121(3) 0.023(2) -0.029(2) -0.041(2)
F2 0.113(3) 0.152(3) 0.097(2) 0.041(2) -0.043(2) -0.012(2)
C8 0.051(3) 0.068(4) 0.056(3) -0.010(3) -0.017(3) -0.009(3)
C4 0.054(3) 0.081(4) 0.059(3) 0.002(3) -0.007(3) -0.015(3)
F5 0.123(3) 0.119(3) 0.105(2) 0.040(2) -0.042(2) -0.026(2)
F4 0.114(3) 0.104(2) 0.142(3) 0.007(2) -0.037(2) -0.057(2)
C5 0.055(3) 0.092(4) 0.061(3) -0.005(3) -0.016(3) -0.015(3)
C13 0.068(4) 0.074(4) 0.058(4) 0.003(3) -0.020(3) -0.010(3)
C6 0.050(3) 0.084(4) 0.063(3) -0.012(3) -0.006(3) -0.015(3)
C9 0.058(3) 0.069(4) 0.075(4) -0.006(3) -0.017(3) -0.020(3)
C3 0.064(3) 0.081(4) 0.064(3) -0.002(3) -0.028(3) -0.017(3)
C7 0.054(3) 0.082(4) 0.064(3) -0.012(3) -0.011(3) -0.010(3)
C1 0.043(3) 0.070(4) 0.064(4) -0.003(3) -0.015(3) -0.009(3)
C10 0.065(4) 0.090(4) 0.055(3) 0.013(3) -0.023(3) -0.004(3)
C12 0.062(4) 0.076(4) 0.083(4) -0.007(4) -0.016(3) -0.023(3)

_geom_special_details
;
 All esds (except the esd in the dihedral angle between two l.s. planes)
 are estimated using the full covariance matrix.  The cell esds are taken
 into account individually in the estimation of esds in distances, angles
 and torsion angles; correlations between esds in cell parameters are only
 used when they are defined by crystal symmetry.  An approximate (isotropic)
 treatment of cell esds is used for estimating esds involving l.s. planes.
;

loop_
 _geom_bond_atom_site_label_1
 _geom_bond_atom_site_label_2
 _geom_bond_distance
 _geom_bond_site_symmetry_2
 _geom_bond_publ_flag
O1 C1 1.191(5) . ?
O2 C1 1.319(5) . ?
```

```
F3 C11 1.343(5) . ?
C11 C12 1.342(7) . ?
C11 C10 1.360(7) . ?
C2 C1 1.509(6) . ?
C2 C3 1.517(6) . ?
F1 C9 1.351(5) . ?
F2 C10 1.349(5) . ?
C8 C9 1.375(6) . ?
C8 C13 1.389(6) . ?
C8 C7 1.425(6) . ?
C4 C5 1.207(6) . ?
C4 C3 1.459(6) . ?
F5 C13 1.337(5) . ?
F4 C12 1.346(6) . ?
C5 C6 1.367(6) . ?
C13 C12 1.364(6) . ?
C6 C7 1.183(6) . ?
C9 C10 1.353(6) . ?

loop_
 _geom_angle_atom_site_label_1
 _geom_angle_atom_site_label_2
 _geom_angle_atom_site_label_3
 _geom_angle
 _geom_angle_site_symmetry_1
 _geom_angle_site_symmetry_3
 _geom_angle_publ_flag
C12 C11 F3 121.5(6) . . ?
C12 C11 C10 119.0(5) . . ?
F3 C11 C10 119.5(5) . . ?
C1 C2 C3 111.7(4) . . ?
C9 C8 C13 114.8(5) . . ?
C9 C8 C7 124.0(5) . . ?
C13 C8 C7 121.2(5) . . ?
C5 C4 C3 178.3(6) . . ?
C4 C5 C6 177.4(6) . . ?
F5 C13 C12 118.8(5) . . ?
F5 C13 C8 118.9(5) . . ?
C12 C13 C8 122.3(5) . . ?
C7 C6 C5 179.0(6) . . ?
F1 C9 C10 118.8(5) . . ?
F1 C9 C8 118.2(4) . . ?
C10 C9 C8 123.0(5) . . ?
C4 C3 C2 111.6(4) . . ?
C6 C7 C8 179.5(6) . . ?
O1 C1 O2 123.1(4) . . ?
```

O1 C1 C2 125.1(5) . . ?
O2 C1 C2 111.8(5) . . ?
F2 C10 C9 120.2(5) . . ?
F2 C10 C11 119.4(5) . . ?
C9 C10 C11 120.4(5) . . ?
C11 C12 F4 119.3(5) . . ?
C11 C12 C13 120.6(5) . . ?
F4 C12 C13 120.0(5) . . ?

_diffrn_measured_fraction_theta_max 0.887
_diffrn_reflns_theta_full 28.61
_diffrn_measured_fraction_theta_full 0.887
_refine_diff_density_max 0.320
_refine_diff_density_min -0.359
_refine_diff_density_rms 0.135

$(66bH)_2OG•2CH_3OH$

```
data_zl46m

_audit_creation_method           SHELXL-97
_chemical_name_systematic
;
 ?
;
_chemical_name_common            ?
_chemical_melting_point          ?
_chemical_formula_moiety         ?
_chemical_formula_sum
 'C13.33 H20 N2.67 O5.33'
_chemical_formula_weight         302.99

loop_
 _atom_type_symbol
 _atom_type_description
 _atom_type_scat_dispersion_real
 _atom_type_scat_dispersion_imag
 _atom_type_scat_source
 'C'  'C'   0.0033   0.0016
 'International Tables Vol C Tables 4.2.6.8 and 6.1.1.4'
 'H'  'H'   0.0000   0.0000
 'International Tables Vol C Tables 4.2.6.8 and 6.1.1.4'
 'N'  'N'   0.0061   0.0033
 'International Tables Vol C Tables 4.2.6.8 and 6.1.1.4'
 'O'  'O'   0.0106   0.0060
 'International Tables Vol C Tables 4.2.6.8 and 6.1.1.4'

_symmetry_cell_setting           Triclinic
_symmetry_space_group_name_H-M    P-1

loop_
 _symmetry_equiv_pos_as_xyz
 'x, y, z'
 '-x, -y, -z'

_cell_length_a                   7.8337(13)
_cell_length_b                   11.785(2)
_cell_length_c                   13.783(2)
_cell_angle_alpha                 105.734(3)
_cell_angle_beta                 92.531(3)
_cell_angle_gamma                   92.469(3)
_cell_volume                     1221.6(4)
```

```
_cell_formula_units_Z            3
_cell_measurement_temperature    273(2)
_cell_measurement_reflns_used    1597
_cell_measurement_theta_min      2.95
_cell_measurement_theta_max      25.79

_exptl_crystal_description       ?
_exptl_crystal_colour            ?
_exptl_crystal_size_max          ?
_exptl_crystal_size_mid          ?
_exptl_crystal_size_min          ?
_exptl_crystal_density_meas      0
_exptl_crystal_density_diffrn    1.236
_exptl_crystal_density_method    'not measured'
_exptl_crystal_F_000             484
_exptl_absorpt_coefficient_mu    0.096
_exptl_absorpt_correction_type   none
_exptl_absorpt_correction_T_min  ?
_exptl_absorpt_correction_T_max  ?
_exptl_absorpt_process_details   ?

_exptl_special_details
;
?
;

_diffrn_ambient_temperature      273(2)
_diffrn_radiation_wavelength     0.71073
_diffrn_radiation_type           MoK\a
_diffrn_radiation_source         'fine-focus sealed tube'
_diffrn_radiation_monochromator  graphite
_diffrn_measurement_device_type  'CCD area detector'
_diffrn_measurement_method       'phi and omega scans'
_diffrn_detector_area_resol_mean ?
_diffrn_standards_number         ?
_diffrn_standards_interval_count ?
_diffrn_standards_interval_time  ?
_diffrn_standards_decay_%        ?
_diffrn_reflns_number            7304
_diffrn_reflns_av_R_equivalents  0.0568
_diffrn_reflns_av_sigmaI/netI    0.1988
_diffrn_reflns_limit_h_min       -10
_diffrn_reflns_limit_h_max       10
_diffrn_reflns_limit_k_min       -8
_diffrn_reflns_limit_k_max       15
_diffrn_reflns_limit_l_min       -18
```

```
_diffrn_reflns_limit_l_max       18
_diffrn_reflns_theta_min         1.54
_diffrn_reflns_theta_max         28.59
_reflns_number_total             5258
_reflns_number_gt                2987
_reflns_threshold_expression     >2sigma(I)

_computing_data_collection       'Bruker SMART'
_computing_cell_refinement       'Bruker SMART'
_computing_data_reduction        'Bruker SAINT'
_computing_structure_solution    'SHELXS-97 (Sheldrick, 1990)'
_computing_structure_refinement  'SHELXL-97 (Sheldrick, 1997)'
_computing_molecular_graphics    'Bruker SHELXTL'
_computing_publication_material  'Bruker SHELXTL'

_refine_special_details
;
Refinement of F^2^ against ALL reflections.  The weighted R-factor wR and
goodness of fit S are based on F^2^, conventional R-factors R are based
on F, with F set to zero for negative F^2^. The threshold expression of
F^2^ > 2sigma(F^2^) is used only for calculating R-factors(gt) etc. and is
not relevant to the choice of reflections for refinement.  R-factors based
on F^2^ are statistically about twice as large as those based on F, and R-
factors based on ALL data will be even larger.
;

_refine_ls_structure_factor_coef  Fsqd
_refine_ls_matrix_type           full
_refine_ls_weighting_scheme      calc
_refine_ls_weighting_details
'calc w=1/[\s^2^(Fo^2^)+(0.0000P)^2^+0.1301P] where P=(Fo^2^+2Fc^2^)/3'
_atom_sites_solution_primary     direct
_atom_sites_solution_secondary   difmap
_atom_sites_solution_hydrogens   geom
_refine_ls_hydrogen_treatment    mixed
_refine_ls_extinction_method     none
_refine_ls_extinction_coef       ?
_refine_ls_number_reflns         5258
_refine_ls_number_parameters     295
_refine_ls_number_restraints     0
_refine_ls_R_factor_all          0.1449
_refine_ls_R_factor_gt           0.0942
_refine_ls_wR_factor_ref         0.2900
_refine_ls_wR_factor_gt          0.2275
_refine_ls_goodness_of_fit_ref   1.043
_refine_ls_restrained_S_all      1.043
```

```
_refine_ls_shift/su_max          0.004
_refine_ls_shift/su_mean         0.000

loop_
 _atom_site_label
 _atom_site_type_symbol
 _atom_site_fract_x
 _atom_site_fract_y
 _atom_site_fract_z
 _atom_site_U_iso_or_equiv
 _atom_site_adp_type
 _atom_site_occupancy
 _atom_site_symmetry_multiplicity
 _atom_site_calc_flag
 _atom_site_refinement_flags
 _atom_site_disorder_assembly
 _atom_site_disorder_group
O1 O 1.0713(2) 1.02534(17) 0.64295(13) 0.0488(5) Uani 1 1 d . . .
O4 O 0.5601(2) -0.03434(17) 0.85675(14) 0.0503(5) Uani 1 1 d . . .
O3 O 1.1966(3) 0.99037(19) 0.94323(15) 0.0601(6) Uani 1 1 d . . .
O6 O 0.6993(2) 0.0156(2) 0.56690(15) 0.0589(6) Uani 1 1 d . . .
O2 O 1.0062(3) 1.14954(18) 0.78663(16) 0.0673(7) Uani 1 1 d . . .
N1 N 0.4331(3) 0.0344(2) 0.62570(17) 0.0476(6) Uani 1 1 d . . .
H1 H 0.3260 0.0356 0.6096 0.057 Uiso 1 1 calc R . .
C1 C 1.0410(4) 0.9881(2) 0.9485(2) 0.0437(7) Uani 1 1 d . . .
C4 C 0.5427(4) 0.0129(2) 0.5525(2) 0.0443(7) Uani 1 1 d . . .
N2 N 0.9281(3) 0.9670(2) 0.87127(16) 0.0490(6) Uani 1 1 d . . .
H2 H 0.8209 0.9678 0.8822 0.059 Uiso 1 1 calc R . .
N3 N 0.5003(3) 0.8317(2) 0.98930(18) 0.0557(7) Uani 1 1 d . . .
H3A H 0.5899 0.7904 0.9971 0.084 Uiso 1 1 calc R . .
H3B H 0.4978 0.8943 1.0425 0.084 Uiso 1 1 calc R . .
H3C H 0.5092 0.8555 0.9336 0.084 Uiso 1 1 calc R . .
O5 O 0.4659(4) -0.15239(19) 0.70920(17) 0.0763(8) Uani 1 1 d . . .
N4 N -0.0069(3) 0.1717(2) 0.52160(18) 0.0552(7) Uani 1 1 d . . .
H4A H -0.0038 0.1429 0.5750 0.083 Uiso 1 1 calc R . .
H4B H -0.0142 0.1124 0.4653 0.083 Uiso 1 1 calc R . .
H4C H -0.0976 0.2150 0.5230 0.083 Uiso 1 1 calc R . .
C2 C 0.9794(4) 0.9424(3) 0.7688(2) 0.0477(7) Uani 1 1 d . . .
H2A H 0.8880 0.8948 0.7245 0.057 Uiso 1 1 calc R . .
H2B H 1.0790 0.8954 0.7628 0.057 Uiso 1 1 calc R . .
C6 C 0.5031(3) -0.0544(2) 0.7661(2) 0.0424(7) Uani 1 1 d . . .
C3 C 1.0217(3) 1.0499(2) 0.7317(2) 0.0416(7) Uani 1 1 d . . .
C5 C 0.4864(4) 0.0555(2) 0.7300(2) 0.0463(7) Uani 1 1 d . . .
H5A H 0.4048 0.1046 0.7704 0.056 Uiso 1 1 calc R . .
H5B H 0.5962 0.0998 0.7422 0.056 Uiso 1 1 calc R . .
C15 C 0.4185(5) 0.5801(3) 0.8460(3) 0.0671(10) Uani 1 1 d . . .
```

C9 C 0.0778(5) 0.4259(3) 0.6556(3) 0.0669(10) Uani 1 1 d . . .
C11 C -0.1309(5) 0.5907(3) 0.6989(3) 0.0711(10) Uani 1 1 d . . .
C18 C 0.7213(6) 0.3377(3) 0.7846(3) 0.0857(12) Uani 1 1 d . . .
H18 H 0.7992 0.2789 0.7708 0.103 Uiso 1 1 calc R . .
C17 C 0.6223(5) 0.4124(3) 0.8021(3) 0.0695(10) Uani 1 1 d . . .
C13 C 0.3410(5) 0.7566(3) 0.9803(3) 0.0668(10) Uani 1 1 d . . .
H13A H 0.2460 0.8067 0.9992 0.080 Uiso 1 1 calc R . .
H13B H 0.3509 0.7083 1.0269 0.080 Uiso 1 1 calc R . .
C14 C 0.3033(5) 0.6766(3) 0.8735(3) 0.0731(10) Uani 1 1 d . . .
H14A H 0.1865 0.6436 0.8675 0.088 Uiso 1 1 calc R . .
H14B H 0.3122 0.7239 0.8260 0.088 Uiso 1 1 calc R . .
C16 C 0.5126(5) 0.5011(3) 0.8261(3) 0.0669(9) Uani 1 1 d . . .
C10 C -0.0174(5) 0.5038(3) 0.6757(3) 0.0657(9) Uani 1 1 d . . .
C7 C 0.1496(5) 0.2457(3) 0.5240(3) 0.0667(10) Uani 1 1 d . . .
H7A H 0.1347 0.2913 0.4756 0.080 Uiso 1 1 calc R . .
H7B H 0.2440 0.1954 0.5042 0.080 Uiso 1 1 calc R . .
C12 C -0.2326(6) 0.6629(3) 0.7158(3) 0.0848(12) Uani 1 1 d . . .
H12 H -0.3131 0.7200 0.7292 0.102 Uiso 1 1 calc R . .
C8 C 0.1935(5) 0.3297(3) 0.6287(3) 0.0719(10) Uani 1 1 d . . .
H8A H 0.1894 0.2852 0.6784 0.086 Uiso 1 1 calc R . .
H8B H 0.3095 0.3629 0.6310 0.086 Uiso 1 1 calc R . .
O7 O 0.3173(5) 0.7369(2) 0.5277(3) 0.1186(14) Uani 1 1 d . . .
H7 H 0.3563 0.7801 0.5820 0.178 Uiso 1 1 calc R . .
C20 C 0.3615(6) 0.6254(4) 0.5192(4) 0.1123(18) Uani 1 1 d . . .
H20A H 0.4639 0.6269 0.5605 0.168 Uiso 1 1 calc R . .
H20B H 0.3814 0.5874 0.4500 0.168 Uiso 1 1 calc R . .
H20C H 0.2706 0.5826 0.5409 0.168 Uiso 1 1 calc R . .
O8 O 0.1975(5) 0.2669(3) 0.9565(3) 0.1310(16) Uani 1 1 d . . .
H8 H 0.1402 0.2235 0.9085 0.196 Uiso 1 1 calc R . .
C19 C 0.1457(6) 0.3773(4) 0.9740(4) 0.1173(19) Uani 1 1 d . . .
H19A H 0.1155 0.4049 1.0428 0.176 Uiso 1 1 calc R . .
H19B H 0.0479 0.3779 0.9297 0.176 Uiso 1 1 calc R . .
H19C H 0.2367 0.4281 0.9619 0.176 Uiso 1 1 calc R . .

loop_
 _atom_site_aniso_label
 _atom_site_aniso_U_11
 _atom_site_aniso_U_22
 _atom_site_aniso_U_33
 _atom_site_aniso_U_23
 _atom_site_aniso_U_13
 _atom_site_aniso_U_12
O1 0.0502(12) 0.0605(12) 0.0442(11) 0.0273(9) 0.0106(9) 0.0060(9)
O4 0.0502(13) 0.0642(13) 0.0440(11) 0.0264(9) 0.0052(9) 0.0094(9)
O3 0.0437(14) 0.0881(16) 0.0593(13) 0.0349(12) 0.0173(10) 0.0117(11)
O6 0.0381(13) 0.0865(16) 0.0593(13) 0.0305(11) 0.0053(9) 0.0113(10)

O2 0.1020(19) 0.0462(13) 0.0585(13) 0.0195(11) 0.0118(12) 0.0174(12)
N1 0.0416(14) 0.0633(15) 0.0479(13) 0.0302(11) 0.0080(11) 0.0115(11)
C1 0.0466(18) 0.0467(16) 0.0483(16) 0.0288(12) 0.0112(12) 0.0078(12)
C4 0.0457(18) 0.0490(16) 0.0473(16) 0.0266(12) 0.0065(13) 0.0106(12)
N2 0.0449(15) 0.0668(16) 0.0436(13) 0.0273(11) 0.0117(11) 0.0051(11)
N3 0.0767(19) 0.0485(14) 0.0501(14) 0.0255(11) 0.0061(13) 0.0123(13)
O5 0.124(2) 0.0467(13) 0.0591(14) 0.0183(11) -0.0163(14) 0.0140(13)
N4 0.0755(18) 0.0447(14) 0.0525(15) 0.0238(11) 0.0079(13) 0.0105(12)
C2 0.0570(18) 0.0506(16) 0.0435(15) 0.0247(13) 0.0116(13) 0.0049(13)
C6 0.0421(16) 0.0483(16) 0.0416(15) 0.0181(12) 0.0083(12) 0.0104(12)
C3 0.0415(16) 0.0474(16) 0.0420(15) 0.0214(12) 0.0025(11) 0.0089(11)
C5 0.0546(18) 0.0494(16) 0.0408(15) 0.0203(12) 0.0069(12) 0.0111(13)
C15 0.077(3) 0.0497(19) 0.075(2) 0.0186(17) 0.0051(19) 0.0011(17)
C9 0.081(3) 0.0462(19) 0.074(2) 0.0186(16) 0.0012(19) -0.0028(17)
C11 0.090(3) 0.0454(19) 0.083(3) 0.0238(17) 0.018(2) 0.0041(18)
C18 0.103(3) 0.057(2) 0.107(3) 0.034(2) 0.034(3) 0.008(2)
C17 0.085(3) 0.047(2) 0.081(2) 0.0240(17) 0.016(2) 0.0063(18)
C13 0.079(2) 0.056(2) 0.078(2) 0.0351(17) 0.0184(19) 0.0132(17)
C14 0.075(3) 0.059(2) 0.088(3) 0.0244(19) -0.004(2) 0.0077(18)
C16 0.078(3) 0.049(2) 0.075(2) 0.0193(17) 0.0058(19) -0.0006(18)
C10 0.078(2) 0.0449(19) 0.075(2) 0.0177(16) 0.0073(19) -0.0007(17)
C7 0.078(2) 0.055(2) 0.078(2) 0.0331(17) 0.0233(19) 0.0145(17)
C12 0.101(3) 0.051(2) 0.110(3) 0.030(2) 0.032(3) 0.009(2)
C8 0.071(2) 0.058(2) 0.090(3) 0.0248(19) 0.002(2) 0.0034(17)
O7 0.156(3) 0.0677(18) 0.114(2) 0.0018(17) -0.064(2) 0.0371(19)
C20 0.119(4) 0.065(3) 0.141(4) 0.012(3) -0.032(3) 0.018(3)
O8 0.152(3) 0.0663(19) 0.151(3) -0.0018(19) -0.072(3) 0.038(2)
C19 0.116(4) 0.062(3) 0.157(5) 0.006(3) -0.031(3) 0.020(3)

_geom_special_details
;
All esds (except the esd in the dihedral angle between two l.s. planes)
are estimated using the full covariance matrix. The cell esds are taken
into account individually in the estimation of esds in distances, angles
and torsion angles; correlations between esds in cell parameters are only
used when they are defined by crystal symmetry. An approximate (isotropic)
treatment of cell esds is used for estimating esds involving l.s. planes.
;

loop_
_geom_bond_atom_site_label_1
_geom_bond_atom_site_label_2
_geom_bond_distance
_geom_bond_site_symmetry_2
_geom_bond_publ_flag
O1 C3 1.261(3) . ?

```
O4 C6 1.264(3) . ?
O3 C1 1.224(3) . ?
O6 C4 1.232(3) . ?
O2 C3 1.227(3) . ?
N1 C4 1.333(4) . ?
N1 C5 1.431(3) . ?
C1 N2 1.316(4) . ?
C1 C1 1.545(5) 2_777 ?
C4 C4 1.514(5) 2_656 ?
N2 C2 1.442(3) . ?
N3 C13 1.479(4) . ?
O5 C6 1.222(3) . ?
N4 C7 1.467(4) . ?
C2 C3 1.519(4) . ?
C6 C5 1.517(4) . ?
C15 C16 1.194(5) . ?
C15 C14 1.462(5) . ?
C9 C10 1.190(5) . ?
C9 C8 1.461(5) . ?
C11 C12 1.175(5) . ?
C11 C10 1.367(5) . ?
C18 C17 1.181(5) . ?
C17 C16 1.362(5) . ?
C13 C14 1.526(5) . ?
C7 C8 1.527(5) . ?
O7 C20 1.349(5) . ?
O8 C19 1.341(4) . ?

loop_
 _geom_angle_atom_site_label_1
 _geom_angle_atom_site_label_2
 _geom_angle_atom_site_label_3
 _geom_angle
 _geom_angle_site_symmetry_1
 _geom_angle_site_symmetry_3
 _geom_angle_publ_flag
C4 N1 C5 122.6(2) . . ?
O3 C1 N2 125.5(3) . . ?
O3 C1 C1 121.1(3) . 2_777 ?
N2 C1 C1 113.4(3) . 2_777 ?
O6 C4 N1 124.4(3) . . ?
O6 C4 C4 122.0(3) . 2_656 ?
N1 C4 C4 113.6(3) . 2_656 ?
C1 N2 C2 121.8(3) . . ?
N2 C2 C3 115.6(2) . . ?
O5 C6 O4 124.9(3) . . ?
```

O5 C6 C5 120.8(3) . . ?
O4 C6 C5 114.2(2) . . ?
O2 C3 O1 125.8(3) . . ?
O2 C3 C2 120.2(2) . . ?
O1 C3 C2 113.9(2) . . ?
N1 C5 C6 115.2(2) . . ?
C16 C15 C14 178.3(4) . . ?
C10 C9 C8 178.8(4) . . ?
C12 C11 C10 177.4(5) . . ?
C18 C17 C16 177.4(5) . . ?
N3 C13 C14 112.2(3) . . ?
C15 C14 C13 113.5(3) . . ?
C15 C16 C17 178.6(4) . . ?
C9 C10 C11 178.2(4) . . ?
N4 C7 C8 112.0(3) . . ?
C9 C8 C7 113.1(3) . . ?

_diffrn_measured_fraction_theta_max 0.841
_diffrn_reflns_theta_full 28.59
_diffrn_measured_fraction_theta_full 0.841
_refine_diff_density_max 0.538
_refine_diff_density_min -0.266
_refine_diff_density_rms 0.082

$(66dH)_2OG$ monomer

```
data_zl45t1

_audit_creation_method            SHELXL-97
_chemical_name_systematic
;
 ?
;
_chemical_name_common             ?
_chemical_melting_point           ?
_chemical_formula_moiety          ?
_chemical_formula_sum
 'C22 H30 N4 O6'
_chemical_formula_weight          446.50

loop_
 _atom_type_symbol
 _atom_type_description
 _atom_type_scat_dispersion_real
 _atom_type_scat_dispersion_imag
 _atom_type_scat_source
 'C'  'C'   0.0033   0.0016
 'International Tables Vol C Tables 4.2.6.8 and 6.1.1.4'
 'H'  'H'   0.0000   0.0000
 'International Tables Vol C Tables 4.2.6.8 and 6.1.1.4'
 'N'  'N'   0.0061   0.0033
 'International Tables Vol C Tables 4.2.6.8 and 6.1.1.4'
 'O'  'O'   0.0106   0.0060
 'International Tables Vol C Tables 4.2.6.8 and 6.1.1.4'

_symmetry_cell_setting            Monoclinic
_symmetry_space_group_name_H-M    P21/c

loop_
 _symmetry_equiv_pos_as_xyz
 'x, y, z'
 '-x, y+1/2, -z+1/2'
 '-x, -y, -z'
 'x, -y-1/2, z-1/2'

_cell_length_a                    16.982(6)
_cell_length_b                    4.7894(17)
_cell_length_c                    14.272(5)
_cell_angle_alpha                 90.00
_cell_angle_beta                  93.746(5)
```

```
_cell_angle_gamma                90.00
_cell_volume                     1158.3(7)
_cell_formula_units_Z            2
_cell_measurement_temperature    273(2)
_cell_measurement_reflns_used    ?
_cell_measurement_theta_min      ?
_cell_measurement_theta_max      ?

_exptl_crystal_description       ?
_exptl_crystal_colour            ?
_exptl_crystal_size_max          ?
_exptl_crystal_size_mid          ?
_exptl_crystal_size_min          ?
_exptl_crystal_density_meas      0
_exptl_crystal_density_diffrn    1.280
_exptl_crystal_density_method    'not measured'
_exptl_crystal_F_000             476
_exptl_absorpt_coefficient_mu    0.094
_exptl_absorpt_correction_type   none
_exptl_absorpt_correction_T_min  ?
_exptl_absorpt_correction_T_max  ?
_exptl_absorpt_process_details   ?

_exptl_special_details
;
 ?
;

_diffrn_ambient_temperature      273(2)
_diffrn_radiation_wavelength     0.71073
_diffrn_radiation_type           MoK\a
_diffrn_radiation_source         'fine-focus sealed tube'
_diffrn_radiation_monochromator  graphite
_diffrn_measurement_device_type  'CCD area detector'
_diffrn_measurement_method       'phi and omega scans'
_diffrn_detector_area_resol_mean  ?
_diffrn_standards_number         ?
_diffrn_standards_interval_count  ?
_diffrn_standards_interval_time  ?
_diffrn_standards_decay_%        ?
_diffrn_reflns_number            6674
_diffrn_reflns_av_R_equivalents  0.1602
_diffrn_reflns_av_sigmaI/netI    0.4369
_diffrn_reflns_limit_h_min       -22
_diffrn_reflns_limit_h_max       21
_diffrn_reflns_limit_k_min       -3
```

```
_diffrn_reflns_limit_k_max       6
_diffrn_reflns_limit_l_min       -18
_diffrn_reflns_limit_l_max       19
_diffrn_reflns_theta_min         1.20
_diffrn_reflns_theta_max         28.66
_reflns_number_total             2650
_reflns_number_gt                489
_reflns_threshold_expression     >2sigma(I)

_computing_data_collection       'Bruker SMART'
_computing_cell_refinement       'Bruker SMART'
_computing_data_reduction        'Bruker SAINT'
_computing_structure_solution    'SHELXS-97 (Sheldrick, 1990)'
_computing_structure_refinement   'SHELXL-97 (Sheldrick, 1997)'
_computing_molecular_graphics    'Bruker SHELXTL'
_computing_publication_material   'Bruker SHELXTL'

_refine_special_details
;
 Refinement of F^2^ against ALL reflections.  The weighted R-factor wR and
 goodness of fit S are based on F^2^, conventional R-factors R are based
 on F, with F set to zero for negative F^2^. The threshold expression of
 F^2^ > 2sigma(F^2^) is used only for calculating R-factors(gt) etc. and is
 not relevant to the choice of reflections for refinement.  R-factors based
 on F^2^ are statistically about twice as large as those based on F, and R-
 factors based on ALL data will be even larger.
;

_refine_ls_structure_factor_coef  Fsqd
_refine_ls_matrix_type           full
_refine_ls_weighting_scheme      calc
_refine_ls_weighting_details
 'calc w=1/[\s^2^(Fo^2^)+(0.0947P)^2^+0.0000P] where P=(Fo^2^+2Fc^2^)/3'
_atom_sites_solution_primary     direct
_atom_sites_solution_secondary    difmap
_atom_sites_solution_hydrogens    geom
_refine_ls_hydrogen_treatment    mixed
_refine_ls_extinction_method     none
_refine_ls_extinction_coef       ?
_refine_ls_number_reflns         2650
_refine_ls_number_parameters     146
_refine_ls_number_restraints     0
_refine_ls_R_factor_all          0.3125
_refine_ls_R_factor_gt           0.0532
_refine_ls_wR_factor_ref         0.2392
_refine_ls_wR_factor_gt          0.1305
```

```
_refine_ls_goodness_of_fit_ref    0.696
_refine_ls_restrained_S_all       0.696
_refine_ls_shift/su_max           0.000
_refine_ls_shift/su_mean          0.000

loop_
 _atom_site_label
 _atom_site_type_symbol
 _atom_site_fract_x
 _atom_site_fract_y
 _atom_site_fract_z
 _atom_site_U_iso_or_equiv
 _atom_site_adp_type
 _atom_site_occupancy
 _atom_site_symmetry_multiplicity
 _atom_site_calc_flag
 _atom_site_refinement_flags
 _atom_site_disorder_assembly
 _atom_site_disorder_group
O2 O 0.1610(2) 0.4107(9) 0.2497(3) 0.0591(13) Uani 1 1 d . . .
N1 N 0.0634(3) -0.0526(10) 0.4068(3) 0.0452(13) Uani 1 1 d . . .
H1 H 0.0871 -0.1969 0.4308 0.054 Uiso 1 1 calc R . .
O3 O 0.1550(2) 0.4199(9) 0.4056(3) 0.0527(12) Uani 1 1 d . . .
C1 C 0.0069(4) 0.0643(14) 0.4524(4) 0.0418(15) Uani 1 1 d . . .
C2 C 0.0873(3) 0.0539(13) 0.3168(4) 0.0446(16) Uani 1 1 d . . .
H2A H 0.0403 0.0980 0.2773 0.054 Uiso 1 1 calc R . .
H2B H 0.1154 -0.0922 0.2858 0.054 Uiso 1 1 calc R . .
O1 O -0.0316(2) 0.2706(10) 0.4230(3) 0.0597(14) Uani 1 1 d . . .
C3 C 0.1394(3) 0.3123(13) 0.3251(5) 0.0458(17) Uani 1 1 d . . .
N2 N 0.1706(3) 0.4237(10) 0.5964(3) 0.0500(14) Uani 1 1 d . . .
H2C H 0.1719 0.3298 0.5427 0.075 Uiso 1 1 calc R . .
H2D H 0.1276 0.5305 0.5946 0.075 Uiso 1 1 calc R . .
H2E H 0.1694 0.3039 0.6439 0.075 Uiso 1 1 calc R . .
C6 C 0.3895(4) 0.6265(13) 0.6193(4) 0.0577(19) Uani 1 1 d . . .
H6A H 0.3872 0.7401 0.6753 0.069 Uiso 1 1 calc R . .
H6B H 0.3886 0.7509 0.5656 0.069 Uiso 1 1 calc R . .
C8 C 0.5351(4) 0.6496(17) 0.6276(4) 0.063(2) Uani 1 1 d . . .
C5 C 0.3175(3) 0.4384(14) 0.6104(4) 0.0540(18) Uani 1 1 d . . .
H5A H 0.3181 0.3314 0.5527 0.065 Uiso 1 1 calc R . .
H5B H 0.3194 0.3080 0.6625 0.065 Uiso 1 1 calc R . .
C7 C 0.4664(4) 0.4623(15) 0.6248(4) 0.064(2) Uani 1 1 d . . .
H7A H 0.4691 0.3465 0.6807 0.076 Uiso 1 1 calc R . .
H7B H 0.4675 0.3404 0.5706 0.076 Uiso 1 1 calc R . .
C4 C 0.2426(3) 0.6040(14) 0.6097(4) 0.0560(18) Uani 1 1 d . . .
H4A H 0.2411 0.7042 0.6686 0.067 Uiso 1 1 calc R . .
H4B H 0.2421 0.7407 0.5595 0.067 Uiso 1 1 calc R . .
```

C10 C 0.6496(4) 0.9942(17) 0.6304(4) 0.060(2) Uani 1 1 d . . .
C9 C 0.5879(4) 0.8097(17) 0.6279(5) 0.062(2) Uani 1 1 d . . .
C11 C 0.7005(5) 1.1602(17) 0.6308(5) 0.073(2) Uani 1 1 d . . .
H11 H 0.7409 1.2916 0.6311 0.087 Uiso 1 1 calc R . .

loop_
 _atom_site_aniso_label
 _atom_site_aniso_U_11
 _atom_site_aniso_U_22
 _atom_site_aniso_U_33
 _atom_site_aniso_U_23
 _atom_site_aniso_U_13
 _atom_site_aniso_U_12
O2 0.093(3) 0.049(3) 0.038(2) 0.003(2) 0.026(2) -0.012(3)
N1 0.054(3) 0.039(3) 0.044(3) 0.007(3) 0.015(3) 0.011(3)
O3 0.068(3) 0.050(3) 0.040(3) -0.008(2) 0.008(2) -0.006(2)
C1 0.044(4) 0.039(4) 0.043(4) -0.006(4) 0.013(3) -0.004(4)
C2 0.055(4) 0.041(4) 0.039(3) 0.006(3) 0.011(3) 0.001(4)
O1 0.061(3) 0.066(3) 0.054(3) 0.013(3) 0.015(2) 0.019(3)
C3 0.052(4) 0.038(4) 0.048(4) -0.002(4) 0.008(4) 0.002(3)
N2 0.050(3) 0.061(4) 0.040(3) 0.010(3) 0.007(2) 0.007(3)
C6 0.059(5) 0.058(5) 0.057(4) -0.002(4) 0.004(3) -0.009(4)
C8 0.063(6) 0.082(7) 0.044(4) 0.001(4) 0.003(4) 0.003(5)
C5 0.048(4) 0.065(5) 0.051(4) 0.003(4) 0.010(3) 0.004(4)
C7 0.059(5) 0.079(6) 0.053(4) -0.005(4) 0.005(3) 0.001(5)
C4 0.058(4) 0.063(5) 0.046(4) -0.002(4) 0.004(3) 0.000(4)
C10 0.059(5) 0.072(6) 0.052(4) 0.002(4) 0.009(4) -0.002(5)
C9 0.058(5) 0.080(6) 0.050(4) -0.007(4) 0.007(4) 0.002(5)
C11 0.072(6) 0.083(7) 0.063(5) 0.010(5) 0.004(4) 0.004(5)

_geom_special_details
;
 All esds (except the esd in the dihedral angle between two l.s. planes)
 are estimated using the full covariance matrix. The cell esds are taken
 into account individually in the estimation of esds in distances, angles
 and torsion angles; correlations between esds in cell parameters are only
 used when they are defined by crystal symmetry. An approximate (isotropic)
 treatment of cell esds is used for estimating esds involving l.s. planes.
;

loop_
 _geom_bond_atom_site_label_1
 _geom_bond_atom_site_label_2
 _geom_bond_distance
 _geom_bond_site_symmetry_2
 _geom_bond_publ_flag

O2 C3 1.252(6) . ?
N1 C1 1.319(7) . ?
N1 C2 1.463(6) . ?
O3 C3 1.272(6) . ?
C1 O1 1.243(6) . ?
C1 C1 1.523(11) 3_556 ?
C2 C3 1.522(8) . ?
N2 C4 1.499(7) . ?
C6 C5 1.517(8) . ?
C6 C7 1.522(8) . ?
C8 C9 1.180(9) . ?
C8 C7 1.470(9) . ?
C5 C4 1.498(7) . ?
C10 C11 1.175(9) . ?
C10 C9 1.369(10) . ?

loop_
 _geom_angle_atom_site_label_1
 _geom_angle_atom_site_label_2
 _geom_angle_atom_site_label_3
 _geom_angle
 _geom_angle_site_symmetry_1
 _geom_angle_site_symmetry_3
 _geom_angle_publ_flag
C1 N1 C2 122.5(5) . . ?
O1 C1 N1 123.7(5) . . ?
O1 C1 C1 120.9(7) . 3_556 ?
N1 C1 C1 115.4(8) . 3_556 ?
N1 C2 C3 114.1(5) . . ?
O2 C3 O3 124.7(6) . . ?
O2 C3 C2 116.2(6) . . ?
O3 C3 C2 119.0(6) . . ?
C5 C6 C7 112.4(5) . . ?
C9 C8 C7 176.8(8) . . ?
C4 C5 C6 111.4(6) . . ?
C8 C7 C6 111.3(6) . . ?
N2 C4 C5 112.4(5) . . ?
C11 C10 C9 177.3(8) . . ?
C8 C9 C10 178.7(8) . . ?

_diffrn_measured_fraction_theta_max 0.885
_diffrn_reflns_theta_full 28.66
_diffrn_measured_fraction_theta_full 0.885
_refine_diff_density_max 0.243
_refine_diff_density_min -0.243
_refine_diff_density_rms 0.077

$(66dH)_2OG$ polymer

```
data_zl45fm1

_audit_creation_method           SHELXL-97
_chemical_name_systematic
;
 ?
;
_chemical_name_common             ?
_chemical_melting_point          ?
_chemical_formula_moiety          ?
_chemical_formula_sum
 'C22 H30 N4 O6'
_chemical_formula_weight          446.50

loop_
 _atom_type_symbol
 _atom_type_description
 _atom_type_scat_dispersion_real
 _atom_type_scat_dispersion_imag
 _atom_type_scat_source
'C'  'C'   0.0033   0.0016
 'International Tables Vol C Tables 4.2.6.8 and 6.1.1.4'
'H'  'H'   0.0000   0.0000
 'International Tables Vol C Tables 4.2.6.8 and 6.1.1.4'
'N'  'N'   0.0061   0.0033
 'International Tables Vol C Tables 4.2.6.8 and 6.1.1.4'
'O'  'O'   0.0106   0.0060
 'International Tables Vol C Tables 4.2.6.8 and 6.1.1.4'

_symmetry_cell_setting            Monoclinic
_symmetry_space_group_name_H-M    P21/c

loop_
 _symmetry_equiv_pos_as_xyz
 'x, y, z'
 '-x, y+1/2, -z+1/2'
 '-x, -y, -z'
 'x, -y-1/2, z-1/2'

_cell_length_a                 15.926(6)
_cell_length_b                 4.8354(19)
_cell_length_c                 14.234(6)
_cell_angle_alpha               90.00
_cell_angle_beta                93.704(9)
```

```
_cell_angle_gamma                90.00
_cell_volume                     1093.8(7)
_cell_formula_units_Z            2
_cell_measurement_temperature    273(2)
_cell_measurement_reflns_used    254
_cell_measurement_theta_min      2.56
_cell_measurement_theta_max      21.97

_exptl_crystal_description       ?
_exptl_crystal_colour            ?
_exptl_crystal_size_max          ?
_exptl_crystal_size_mid          ?
_exptl_crystal_size_min          ?
_exptl_crystal_density_meas      0
_exptl_crystal_density_diffrn    1.356
_exptl_crystal_density_method    'not measured'
_exptl_crystal_F_000             476
_exptl_absorpt_coefficient_mu    0.100
_exptl_absorpt_correction_type   none
_exptl_absorpt_correction_T_min  ?
_exptl_absorpt_correction_T_max  ?
_exptl_absorpt_process_details   ?

_exptl_special_details
;
 ?
;

_diffrn_ambient_temperature      273(2)
_diffrn_radiation_wavelength     0.71073
_diffrn_radiation_type           MoK\a
_diffrn_radiation_source         'fine-focus sealed tube'
_diffrn_radiation_monochromator  graphite
_diffrn_measurement_device_type  'CCD area detector'
_diffrn_measurement_method       'phi and omega scans'
_diffrn_detector_area_resol_mean  ?
_diffrn_standards_number         ?
_diffrn_standards_interval_count  ?
_diffrn_standards_interval_time  ?
_diffrn_standards_decay_%        ?
_diffrn_reflns_number            6410
_diffrn_reflns_av_R_equivalents  0.2330
_diffrn_reflns_av_sigmaI/netI    0.3806
_diffrn_reflns_limit_h_min       -20
_diffrn_reflns_limit_h_max       20
_diffrn_reflns_limit_k_min       -5
```

```
_diffrn_reflns_limit_k_max       6
_diffrn_reflns_limit_l_min       -19
_diffrn_reflns_limit_l_max       16
_diffrn_reflns_theta_min         1.28
_diffrn_reflns_theta_max         28.50
_reflns_number_total             2501
_reflns_number_gt                552
_reflns_threshold_expression     >2sigma(I)

_computing_data_collection       'Bruker SMART'
_computing_cell_refinement       'Bruker SMART'
_computing_data_reduction        'Bruker SAINT'
_computing_structure_solution    'SHELXS-97 (Sheldrick, 1990)'
_computing_structure_refinement   'SHELXL-97 (Sheldrick, 1997)'
_computing_molecular_graphics    'Bruker SHELXTL'
_computing_publication_material   'Bruker SHELXTL'

_refine_special_details
;
 Refinement of F^2^ against ALL reflections.  The weighted R-factor wR and
 goodness of fit S are based on F^2^, conventional R-factors R are based
 on F, with F set to zero for negative F^2^. The threshold expression of
 F^2^ > 2sigma(F^2^) is used only for calculating R-factors(gt) etc. and is
 not relevant to the choice of reflections for refinement.  R-factors based
 on F^2^ are statistically about twice as large as those based on F, and R-
 factors based on ALL data will be even larger.
;

_refine_ls_structure_factor_coef  Fsqd
_refine_ls_matrix_type           full
_refine_ls_weighting_scheme      calc
_refine_ls_weighting_details
 'calc w=1/[\s^2^(Fo^2^)+(0.0701P)^2^+0.0000P] where P=(Fo^2^+2Fc^2^)/3'
_atom_sites_solution_primary     direct
_atom_sites_solution_secondary    difmap
_atom_sites_solution_hydrogens    geom
_refine_ls_hydrogen_treatment    mixed
_refine_ls_extinction_method     none
_refine_ls_extinction_coef       ?
_refine_ls_number_reflns         2501
_refine_ls_number_parameters     146
_refine_ls_number_restraints     0
_refine_ls_R_factor_all          0.3438
_refine_ls_R_factor_gt           0.0764
_refine_ls_wR_factor_ref         0.2213
_refine_ls_wR_factor_gt          0.1420
```

```
_refine_ls_goodness_of_fit_ref    0.817
_refine_ls_restrained_S_all       0.817
_refine_ls_shift/su_max           0.000
_refine_ls_shift/su_mean          0.000

loop_
 _atom_site_label
 _atom_site_type_symbol
 _atom_site_fract_x
 _atom_site_fract_y
 _atom_site_fract_z
 _atom_site_U_iso_or_equiv
 _atom_site_adp_type
 _atom_site_occupancy
 _atom_site_symmetry_multiplicity
 _atom_site_calc_flag
 _atom_site_refinement_flags
 _atom_site_disorder_assembly
 _atom_site_disorder_group
O1 O 0.1690(3) 0.5744(9) 0.9075(3) 0.0544(13) Uani 1 1 d . . .
O2 O 0.1746(3) 0.5920(9) 0.7513(3) 0.0561(13) Uani 1 1 d . . .
N2 N 0.1786(3) 0.9433(10) 0.6006(3) 0.0516(16) Uani 1 1 d . . .
H2A H 0.1771 0.8492 0.5468 0.077 Uiso 1 1 calc R . .
H2B H 0.1357 1.0614 0.5994 0.077 Uiso 1 1 calc R . .
H2C H 0.1749 0.8263 0.6484 0.077 Uiso 1 1 calc R . .
C4 C 0.2594(4) 1.0994(14) 0.6127(4) 0.0509(19) Uani 1 1 d . . .
H4A H 0.2617 1.1985 0.6721 0.061 Uiso 1 1 calc R . .
H4B H 0.2622 1.2338 0.5624 0.061 Uiso 1 1 calc R . .
O3 O -0.0315(3) 0.7332(10) 0.9218(3) 0.0595(15) Uani 1 1 d . . .
N1 N 0.0716(3) 1.0481(11) 0.9100(3) 0.0467(15) Uani 1 1 d . . .
H1 H 0.0967 1.1886 0.9360 0.056 Uiso 1 1 calc R . .
C7 C 0.4882(4) 0.8328(15) 0.6240(4) 0.064(2) Uani 1 1 d . . .
H7A H 0.4807 0.7118 0.6772 0.077 Uiso 1 1 calc R . .
H7B H 0.4793 0.7215 0.5676 0.077 Uiso 1 1 calc R . .
C3 C 0.1521(4) 0.6859(14) 0.8288(5) 0.0430(18) Uani 1 1 d . . .
C1 C 0.0088(4) 0.9311(15) 0.9527(4) 0.0409(16) Uani 1 1 d . . .
C6 C 0.4188(4) 1.0490(14) 0.6224(4) 0.0499(18) Uani 1 1 d . . .
H6A H 0.4249 1.1757 0.5704 0.060 Uiso 1 1 calc R . .
H6B H 0.4231 1.1545 0.6805 0.060 Uiso 1 1 calc R . .
C5 C 0.3329(4) 0.9063(14) 0.6113(4) 0.0521(19) Uani 1 1 d . . .
H5A H 0.3292 0.8056 0.5522 0.063 Uiso 1 1 calc R . .
H5B H 0.3292 0.7727 0.6617 0.063 Uiso 1 1 calc R . .
C2 C 0.0993(4) 0.9468(14) 0.8208(4) 0.0459(18) Uani 1 1 d . . .
H2D H 0.1318 1.0907 0.7925 0.055 Uiso 1 1 calc R . .
H2E H 0.0501 0.9111 0.7787 0.055 Uiso 1 1 calc R . .
C11 C 0.6412(4) 0.7278(17) 0.6331(4) 0.0499(19) Uani 1 1 d . . .
```

H11 H 0.6974 0.7816 0.6359 0.060 Uiso 1 1 calc R . .
C8 C 0.5790(4) 0.9262(19) 0.6300(4) 0.0539(19) Uani 1 1 d . . .
C9 C 0.6006(4) 1.2134(19) 0.6315(4) 0.051(2) Uani 1 1 d . . .
C13 C 0.6209(4) 1.4483(19) 0.6322(4) 0.0499(19) Uani 1 1 d . . .

loop_
 _atom_site_aniso_label
 _atom_site_aniso_U_11
 _atom_site_aniso_U_22
 _atom_site_aniso_U_33
 _atom_site_aniso_U_23
 _atom_site_aniso_U_13
 _atom_site_aniso_U_12
O1 0.069(3) 0.064(3) 0.031(3) 0.006(2) 0.008(2) 0.002(3)
O2 0.086(3) 0.052(3) 0.032(3) 0.003(2) 0.015(2) 0.013(3)
N2 0.050(3) 0.076(4) 0.029(3) 0.004(3) 0.000(3) 0.015(3)
C4 0.045(4) 0.059(5) 0.049(4) 0.001(4) -0.001(3) 0.002(4)
O3 0.067(3) 0.066(4) 0.046(3) -0.020(3) 0.011(2) -0.031(3)
N1 0.059(3) 0.041(4) 0.042(3) -0.014(3) 0.019(3) -0.006(3)
C7 0.062(5) 0.067(6) 0.063(5) -0.004(4) 0.003(4) 0.001(5)
C3 0.045(5) 0.043(5) 0.043(4) -0.005(4) 0.012(4) -0.011(4)
C1 0.045(4) 0.043(5) 0.036(4) 0.007(4) 0.010(3) 0.007(4)
C6 0.057(4) 0.056(5) 0.037(4) -0.003(3) 0.005(3) -0.015(4)
C5 0.051(4) 0.065(5) 0.041(4) 0.007(4) 0.006(3) 0.005(4)
C2 0.059(4) 0.050(5) 0.031(4) 0.001(3) 0.020(3) 0.004(4)
C11 0.039(4) 0.068(6) 0.042(4) 0.003(4) 0.004(3) -0.002(5)
C8 0.051(5) 0.071(6) 0.039(4) 0.009(4) -0.001(3) -0.007(5)
C9 0.056(5) 0.054(6) 0.042(4) 0.003(4) -0.001(3) -0.003(5)
C13 0.059(5) 0.050(5) 0.042(4) -0.005(4) 0.010(3) 0.002(5)

_geom_special_details
;
 All esds (except the esd in the dihedral angle between two l.s. planes)
 are estimated using the full covariance matrix. The cell esds are taken
 into account individually in the estimation of esds in distances, angles
 and torsion angles; correlations between esds in cell parameters are only
 used when they are defined by crystal symmetry. An approximate (isotropic)
 treatment of cell esds is used for estimating esds involving l.s. planes.
;

loop_
 _geom_bond_atom_site_label_1
 _geom_bond_atom_site_label_2
 _geom_bond_distance
 _geom_bond_site_symmetry_2
 _geom_bond_publ_flag

O1 C3 1.257(7) . ?
O2 C3 1.266(6) . ?
N2 C4 1.492(7) . ?
C4 C5 1.499(8) . ?
O3 C1 1.218(7) . ?
N1 C1 1.329(7) . ?
N1 C2 1.455(6) . ?
C7 C8 1.511(8) . ?
C7 C6 1.520(8) . ?
C3 C2 1.516(8) . ?
C1 C1 1.546(12) 3_577 ?
C6 C5 1.531(7) . ?
C11 C8 1.378(9) . ?
C11 C13 1.390(9) 1_545 ?
C8 C9 1.430(9) . ?
C9 C13 1.181(9) . ?
C13 C11 1.390(9) 1_565 ?

loop_
 _geom_angle_atom_site_label_1
 _geom_angle_atom_site_label_2
 _geom_angle_atom_site_label_3
 _geom_angle
 _geom_angle_site_symmetry_1
 _geom_angle_site_symmetry_3
 _geom_angle_publ_flag
N2 C4 C5 110.6(5) . . ?
C1 N1 C2 122.3(5) . . ?
C8 C7 C6 119.1(6) . . ?
O1 C3 O2 124.5(6) . . ?
O1 C3 C2 120.6(6) . . ?
O2 C3 C2 114.8(6) . . ?
O3 C1 N1 124.3(6) . . ?
O3 C1 C1 122.1(8) . 3_577 ?
N1 C1 C1 113.6(8) . 3_577 ?
C7 C6 C5 109.6(5) . . ?
C4 C5 C6 114.3(6) . . ?
N1 C2 C3 114.4(5) . . ?
C8 C11 C13 120.7(7) . 1_545 ?
C11 C8 C9 120.2(6) . . ?
C11 C8 C7 118.5(7) . . ?
C9 C8 C7 121.3(7) . . ?
C13 C9 C8 178.0(8) . . ?
C9 C13 C11 177.5(8) . 1_565 ?

_diffrn_measured_fraction_theta_max   0.899

```
_diffrn_reflns_theta_full              28.50
_diffrn_measured_fraction_theta_full   0.899
_refine_diff_density_max    0.217
_refine_diff_density_min   -0.255
_refine_diff_density_rms    0.060
```

70•4PyO polymer

```
data_zl52m

_audit_creation_method           SHELXL-97
_chemical_name_systematic
;
 ?
;
_chemical_name_common            ?
_chemical_melting_point          ?
_chemical_formula_moiety         ?
_chemical_formula_sum
 'C24 H24 N4 O6'
_chemical_formula_weight         464.47

loop_
 _atom_type_symbol
 _atom_type_description
 _atom_type_scat_dispersion_real
 _atom_type_scat_dispersion_imag
 _atom_type_scat_source
'C'  'C'   0.0033   0.0016
 'International Tables Vol C Tables 4.2.6.8 and 6.1.1.4'
 'H'  'H'   0.0000   0.0000
 'International Tables Vol C Tables 4.2.6.8 and 6.1.1.4'
 'N'  'N'   0.0061   0.0033
 'International Tables Vol C Tables 4.2.6.8 and 6.1.1.4'
 'O'  'O'   0.0106   0.0060
 'International Tables Vol C Tables 4.2.6.8 and 6.1.1.4'

_symmetry_cell_setting           Triclinic
_symmetry_space_group_name_H-M    P-1

loop_
 _symmetry_equiv_pos_as_xyz
 'x, y, z'
 '-x, -y, -z'

_cell_length_a                  4.824(7)
_cell_length_b                  9.085(12)
_cell_length_c                  12.724(18)
_cell_angle_alpha                108.78(3)
_cell_angle_beta                 96.71(3)
_cell_angle_gamma                   96.19(3)
_cell_volume                    518.0(12)
```

```
_cell_formula_units_Z            1
_cell_measurement_temperature    273(2)
_cell_measurement_reflns_used    167
_cell_measurement_theta_min      2.40
_cell_measurement_theta_max      20.07

_exptl_crystal_description       ?
_exptl_crystal_colour            ?
_exptl_crystal_size_max          ?
_exptl_crystal_size_mid          ?
_exptl_crystal_size_min          ?
_exptl_crystal_density_meas      0
_exptl_crystal_density_diffrn    1.489
_exptl_crystal_density_method    'not measured'
_exptl_crystal_F_000             244
_exptl_absorpt_coefficient_mu    0.109
_exptl_absorpt_correction_type   none
_exptl_absorpt_correction_T_min  ?
_exptl_absorpt_correction_T_max  ?
_exptl_absorpt_process_details   ?

_exptl_special_details
;
 ?
;

_diffrn_ambient_temperature      273(2)
_diffrn_radiation_wavelength     0.71073
_diffrn_radiation_type           MoK\a
_diffrn_radiation_source         'fine-focus sealed tube'
_diffrn_radiation_monochromator  graphite
_diffrn_measurement_device_type  'CCD area detector'
_diffrn_measurement_method       'phi and omega scans'
_diffrn_detector_area_resol_mean  ?
_diffrn_standards_number         ?
_diffrn_standards_interval_count  ?
_diffrn_standards_interval_time  ?
_diffrn_standards_decay_%        ?
_diffrn_reflns_number            2738
_diffrn_reflns_av_R_equivalents  0.1430
_diffrn_reflns_av_sigmaI/netI    0.5519
_diffrn_reflns_limit_h_min       -5
_diffrn_reflns_limit_h_max       6
_diffrn_reflns_limit_k_min       -11
_diffrn_reflns_limit_k_max       11
_diffrn_reflns_limit_l_min       -16
```

```
_diffrn_reflns_limit_l_max       13
_diffrn_reflns_theta_min         1.71
_diffrn_reflns_theta_max         28.50
_reflns_number_total             2174
_reflns_number_gt                454
_reflns_threshold_expression     >2sigma(I)

_computing_data_collection       'Bruker SMART'
_computing_cell_refinement       'Bruker SMART'
_computing_data_reduction        'Bruker SAINT'
_computing_structure_solution    'SHELXS-97 (Sheldrick, 1990)'
_computing_structure_refinement  'SHELXL-97 (Sheldrick, 1997)'
_computing_molecular_graphics    'Bruker SHELXTL'
_computing_publication_material  'Bruker SHELXTL'

_refine_special_details
;
Refinement of F^2^ against ALL reflections.  The weighted R-factor wR and
goodness of fit S are based on F^2^, conventional R-factors R are based
on F, with F set to zero for negative F^2^. The threshold expression of
F^2^ > 2sigma(F^2^) is used only for calculating R-factors(gt) etc. and is
not relevant to the choice of reflections for refinement.  R-factors based
on F^2^ are statistically about twice as large as those based on F, and R-
factors based on ALL data will be even larger.
;

_refine_ls_structure_factor_coef  Fsqd
_refine_ls_matrix_type           full
_refine_ls_weighting_scheme      calc
_refine_ls_weighting_details
'calc w=1/[\s^2^(Fo^2^)+(0.2000P)^2^+0.0000P] where P=(Fo^2^+2Fc^2^)/3'
_atom_sites_solution_primary     direct
_atom_sites_solution_secondary   difmap
_atom_sites_solution_hydrogens   geom
_refine_ls_hydrogen_treatment    mixed
_refine_ls_extinction_method     none
_refine_ls_extinction_coef       ?
_refine_ls_number_reflns         2174
_refine_ls_number_parameters     154
_refine_ls_number_restraints     0
_refine_ls_R_factor_all          0.3983
_refine_ls_R_factor_gt           0.1421
_refine_ls_wR_factor_ref         0.4463
_refine_ls_wR_factor_gt          0.3546
_refine_ls_goodness_of_fit_ref   0.874
_refine_ls_restrained_S_all      0.874
```

```
_refine_ls_shift/su_max          0.000
_refine_ls_shift/su_mean         0.000

loop_
 _atom_site_label
 _atom_site_type_symbol
 _atom_site_fract_x
 _atom_site_fract_y
 _atom_site_fract_z
 _atom_site_U_iso_or_equiv
 _atom_site_adp_type
 _atom_site_occupancy
 _atom_site_symmetry_multiplicity
 _atom_site_calc_flag
 _atom_site_refinement_flags
 _atom_site_disorder_assembly
 _atom_site_disorder_group
O1 O 0.2606(18) 0.4722(11) 0.0840(7) 0.066(3) Uani 1 1 d . . .
C11 C 0.898(2) 0.0245(13) 0.9704(10) 0.037(3) Uani 1 1 d . . .
C10 C 0.970(2) 0.0941(14) 0.8862(10) 0.047(3) Uani 1 1 d . . .
H10A H 1.0882 0.0295 0.8405 0.057 Uiso 1 1 calc R . .
H10B H 1.0813 0.1971 0.9252 0.057 Uiso 1 1 calc R . .
N2 N 0.721(2) 0.4359(11) 0.0913(8) 0.050(3) Uani 1 1 d . . .
H2 H 0.8683 0.4436 0.0604 0.060 Uiso 1 1 calc R . .
O2 O 0.366(2) -0.0169(12) 0.6620(8) 0.084(3) Uani 1 1 d . . .
H11 H 0.2938 -0.1013 0.6141 0.126 Uiso 1 1 calc R . .
O3 O 0.6521(19) -0.1604(12) 0.7092(8) 0.070(3) Uani 1 1 d . . .
N1 N 1.133(2) 0.7501(14) 0.4878(10) 0.065(3) Uani 1 1 d . . .
C3 C 0.872(3) 0.5198(17) 0.2932(11) 0.053(3) Uani 1 1 d . . .
C12 C 0.623(2) 0.0040(14) 0.9918(10) 0.044(3) Uani 1 1 d . . .
C9 C 0.726(2) 0.1126(14) 0.8095(10) 0.051(3) Uani 1 1 d . . .
H9A H 0.5869 0.1582 0.8540 0.062 Uiso 1 1 calc R . .
H9B H 0.7926 0.1856 0.7732 0.062 Uiso 1 1 calc R . .
C8 C 0.588(3) -0.0371(18) 0.7219(11) 0.053(4) Uani 1 1 d . . .
C7 C 1.105(3) 0.4947(16) 0.3561(13) 0.063(4) Uani 1 1 d . . .
H7 H 1.1805 0.4016 0.3344 0.075 Uiso 1 1 calc R . .
C1 C 0.484(3) 0.4709(16) 0.0477(11) 0.059(4) Uani 1 1 d . . .
C4 C 0.793(3) 0.6565(16) 0.3251(12) 0.065(4) Uani 1 1 d . . .
H4 H 0.6470 0.6781 0.2805 0.077 Uiso 1 1 calc R . .
C5 C 0.919(3) 0.7677(16) 0.4218(12) 0.066(4) Uani 1 1 d . . .
H5 H 0.8496 0.8629 0.4434 0.079 Uiso 1 1 calc R . .
C2 C 0.742(3) 0.3856(14) 0.1878(10) 0.055(4) Uani 1 1 d . . .
H2A H 0.8559 0.3020 0.1765 0.066 Uiso 1 1 calc R . .
H2B H 0.5547 0.3442 0.1961 0.066 Uiso 1 1 calc R . .
C6 C 1.216(3) 0.618(2) 0.4534(13) 0.088(5) Uani 1 1 d . . .
H6 H 1.3682 0.6030 0.4985 0.105 Uiso 1 1 calc R . .
```

```
loop_
 _atom_site_aniso_label
 _atom_site_aniso_U_11
 _atom_site_aniso_U_22
 _atom_site_aniso_U_33
 _atom_site_aniso_U_23
 _atom_site_aniso_U_13
 _atom_site_aniso_U_12
O1 0.038(5) 0.110(8) 0.060(6) 0.030(6) 0.033(5) 0.025(5)
C11 0.017(6) 0.056(8) 0.041(7) 0.015(6) 0.018(5) 0.007(5)
C10 0.022(6) 0.069(9) 0.056(9) 0.024(8) 0.011(6) 0.013(6)
N2 0.048(7) 0.069(7) 0.041(6) 0.026(6) 0.015(5) 0.017(5)
O2 0.071(7) 0.112(8) 0.064(7) 0.027(6) -0.013(6) 0.019(6)
O3 0.060(6) 0.064(6) 0.077(7) 0.015(6) -0.007(5) 0.023(5)
N1 0.058(8) 0.080(9) 0.062(9) 0.023(8) 0.014(7) 0.028(7)
C3 0.045(8) 0.065(10) 0.053(9) 0.023(8) 0.020(7) 0.014(7)
C12 0.032(6) 0.061(8) 0.039(7) 0.009(6) 0.014(6) 0.020(6)
C9 0.042(7) 0.062(9) 0.053(9) 0.024(8) 0.008(6) 0.010(6)
C8 0.034(8) 0.075(11) 0.050(9) 0.016(9) 0.017(7) 0.012(8)
C7 0.057(9) 0.061(10) 0.071(11) 0.016(9) 0.018(8) 0.029(8)
C1 0.049(8) 0.072(10) 0.055(10) 0.020(8) 0.005(8) 0.011(7)
C4 0.068(10) 0.043(9) 0.074(11) 0.013(8) -0.005(8) 0.014(8)
C5 0.067(10) 0.057(10) 0.062(11) -0.002(8) 0.008(8) 0.028(8)
C2 0.064(9) 0.057(9) 0.039(8) 0.010(7) 0.007(7) 0.007(7)
C6 0.070(11) 0.119(15) 0.063(12) 0.019(11) -0.002(9) 0.019(11)

_geom_special_details
;
 All esds (except the esd in the dihedral angle between two l.s. planes)
 are estimated using the full covariance matrix.  The cell esds are taken
 into account individually in the estimation of esds in distances, angles
 and torsion angles; correlations between esds in cell parameters are only
 used when they are defined by crystal symmetry.  An approximate (isotropic)
 treatment of cell esds is used for estimating esds involving l.s. planes.
;

loop_
 _geom_bond_atom_site_label_1
 _geom_bond_atom_site_label_2
 _geom_bond_distance
 _geom_bond_site_symmetry_2
 _geom_bond_publ_flag
O1 C1 1.220(14) . ?
C11 C11 1.367(19) 2_757 ?
C11 C12 1.389(13) . ?
```

C11 C10 1.463(14) . ?
C10 C9 1.498(13) . ?
N2 C1 1.325(14) . ?
N2 C2 1.438(13) . ?
O2 C8 1.306(14) . ?
O3 C8 1.160(14) . ?
N1 C6 1.261(17) . ?
N1 C5 1.311(15) . ?
C3 C4 1.291(16) . ?
C3 C7 1.385(16) . ?
C3 C2 1.504(17) . ?
C12 C12 1.23(2) 2_657 ?
C9 C8 1.479(17) . ?
C7 C6 1.379(19) . ?
C1 C1 1.49(3) 2_665 ?
C4 C5 1.340(17) . ?

loop_
 _geom_angle_atom_site_label_1
 _geom_angle_atom_site_label_2
 _geom_angle_atom_site_label_3
 _geom_angle
 _geom_angle_site_symmetry_1
 _geom_angle_site_symmetry_3
 _geom_angle_publ_flag
C11 C11 C12 117.9(13) 2_757 . ?
C11 C11 C10 120.5(12) 2_757 . ?
C12 C11 C10 121.6(10) . . ?
C11 C10 C9 116.3(10) . . ?
C1 N2 C2 123.0(11) . . ?
C6 N1 C5 114.7(14) . . ?
C4 C3 C7 118.5(14) . . ?
C4 C3 C2 125.2(12) . . ?
C7 C3 C2 116.2(13) . . ?
C12 C12 C11 175.0(17) 2_657 . ?
C8 C9 C10 113.5(11) . . ?
O3 C8 O2 122.1(14) . . ?
O3 C8 C9 126.5(13) . . ?
O2 C8 C9 111.3(13) . . ?
C6 C7 C3 114.8(13) . . ?
O1 C1 N2 126.5(12) . . ?
O1 C1 C1 119.6(16) . 2_665 ?
N2 C1 C1 113.6(16) . 2_665 ?
C3 C4 C5 120.8(13) . . ?
N1 C5 C4 123.8(13) . . ?
N2 C2 C3 111.1(10) . . ?

N1 C6 C7 127.0(15) . . ?

_diffrn_measured_fraction_theta_max 0.824
_diffrn_reflns_theta_full 28.50
_diffrn_measured_fraction_theta_full 0.824
_refine_diff_density_max 0.396
_refine_diff_density_min -0.491
_refine_diff_density_rms 0.106